University of Nevada Reno

1-G SHAKE TABLE EXPERIMENTAL EVALUATION OF BUILDING SETTLEMENTS FOUNDED ON LIQUEFIABLE SOILS

A thesis submitted in partial fulfillment of
the requirements for the degree of Master of Science
in Civil and Environmental Engineering

by

Joseph A.W. Toth

Dr. Ramin Motamed / Thesis Advisor

December, 2016

University of Nevada, Reno

THE GRADUATE SCHOOL

We recommend that the thesis
prepared under our supervision by

Joseph A.W. Toth

Entitled

1-G SHAKE TABLE EXPERIMENTAL EVALUATION OF BUILDING SETTLEMENTS FOUNDED ON LIQUEFIABLE SOILS

be accepted in partial fulfillment of the
requirements for the degree of

MASTER OF SCIENCE

Ramin Motamed, Ph.D., Advisor

Raj Siddharthan, Ph.D., Committee Member

John G. Anderson, Ph.D., Graduate School Representative

David W Zeh, Ph.D., Graduate Dean, Graduate School

December, 2016

Abstract

Post-disaster reconnaissance of areas affected by recent earthquakes in Japan and New Zealand has documented extensive damage to buildings with shallow foundations resulting from liquefaction-induced settlement. Current practices in predicting degree of liquefaction-induced settlement are based on semi-empirical relationships for free-field conditions and do not consider external loadings from structures. However, field observations have noted that liquefaction settlement from buildings can be considerably greater than the semi-empirical estimations.

The controlling mechanisms of liquefaction settlement under load are not well understood and are currently being investigated by researchers within the Geo-seismic community. Our research is based on a series of 1-g shake table experiments using a transparent soil box to reproduce liquefaction-induced building settlements. Settlements were evaluated using a scaled model of a building foundation representative of a lightly loaded single to double story building. Experimental testing included use of manually induced shaking, implementation of an eccentric-mass shaker and use of a biaxial large scale shake table. Comprehensive parametric study was carried out to establish the effects of several parameters on free-field and building settlements such as building width, relative density, ground motion duration and thickness of liquefiable layer. Experiments included use of accelerometers, pore water pressure sensors and linear variable differential transformers (LVDT) to monitor behavior in both free-field and model building footprints during induction of liquefaction. A comprehensive parametric study was conducted evaluating the influence of key parameters. Results of this study suggest the following on liquefaction settlement behavior. Increases in foundation width showed decreases in settlement. Increases in relative density of soil also showed decreases in settlement. Increases in ground motion duration lead to increases in settlement. Increases in thickness of liquefiable layer lead to increases in settlement. Free-field settlement was predicted using two common methods in practice and compared with the settlements measured directly in our experiments. These predictions are shown to be lower than measurements observed for building foundations and also slightly over-predict settlements observed in the free-field. Results of these studies are also compared with previous centrifuge, shake table and field observations normalized for width of foundation and thickness of liquefiable layer and are generally in good agreement. Lastly, a brief discussion is presented suggesting the use of helical piles as a mitigation strategy in reducing the building settlements of structures founded over liquefiable soils.

The width of the soil container used in experimentation restricted use of larger model foundation diameters. Current model diameters used in experimentation suggest that prototype foundations are more typical of isolated piers and footings rather than mat foundations when considering laws of similitude. Additionally, soil model grain size characteristics are representative of a coarse sand to fine grained gravel.

Dedication

Dedicated to the memory of Helen Georgina Roney

Acknowledgements

I would like to acknowledge Bob Fehling of VersaGrade Inc. for providing the background geotechnical information which served as the starting point of my physical model and was the basis of all my research.

Dr. Ramin Motamed, Assistant Professor at the University of Nevada, Reno, Department of Civil and Environmental Engineering. Thank you for your guidance and instruction throughout this project.

Katy Cottingham, Andrew Walker and Rick Mitchells at the offices of Golder Associates Inc. located in Redmond, Washington and Anchorage, Alaska. Your encouragement, mentorship and support has played a large role in my professional development as an engineer.

This project would not have been possible without the following people in the Department of Civil and Environmental Engineering at the University of Nevada, Reno. Murugaiyah Piratheepan, Laboratory Manager and Research Scientist through the Western Regional Superpave Center, Pavement Engineering and Science Program. Murugaiyah kindly accommodated our project needs by providing use of their ovens located in the aggregate laboratory. Mark Lattin, Development Technician. Mark assisted us greatly in setting up our instrumentation. Patrick LaPlace, Chad and Todd Lyttle at the Earthquake

Engineering Laboratory at the University of Nevada, Reno for their time and services in using the biaxial shake table.

Lastly, to everyone who assisted me with operating the camera during experimentation, recording measurements, running the instrument software and especially helping to construct, deconstruct and dry the sand in preparation for the next experiment.

Table of Contents

LIST OF TABLES

LIST OF FIGURES

Chapter 1 Introduction

1.1 General Introduction

Recent earthquakes in New Zealand and Japan have documented extensive settlement and damage to buildings and residential structures resulting from the effects of liquefaction. Depending on the type of foundation, settlement can translate damage to the superstructure of the building. The Canterbury Earthquake Sequence (2010-2011) saw as many as 20,000 residential homes damaged from poor ground conditions that were susceptible to liquefaction (Henderson 2013). Almost half of those structures were deemed a total loss. The Great Tohoku Earthquake of 2011 produced similar effects to structures. Field reconnaissance of the areas affected by these earthquakes noted several observations in regards to performance of foundation types and degree of settlement. In Christchurch, certain foundation types performed better in terms of damage not translating to the superstructure, while other foundation types settled and resulted in large differential displacements and damage to the building superstructure.

Until recently, liquefaction-induced settlement has been estimated for free-field conditions, meaning a liquefiable area not subject to the influence of external loadings such as buildings. Methods to develop these estimates provide a general range of probable settlement in liquefaction susceptible soils. Estimates have been proposed by Tokimatsu and Seed (1987), Ishihara and Yoshimine

(1992). However, it has always been understood that structures founded over liquefiable soils will typically show greater settlement than predicted using the free-field settlement estimates. Current standards of practice in estimating probable liquefaction-induced settlements are solely based on volumetric strains. These volumetric strains are a result of dissipation of excess pore water pressures and assume that the majority of settlement occurs in post-liquefaction. Numerous experimental studies have been conducted in an effort to improve the methods that predict liquefaction-induced building settlement. These studies included centrifuge and 1-g shake table tests to monitor behavior of settlement during development of soil liquefaction. Additionally, previous research has focused on isolating the mechanisms controlling the settlement to gain further insights on the behavior and relationships of governing liquefaction settlement. Field observations of building foundation settlement and research have illustrated that liquefaction settlement tends to decrease with increasing foundation width. However, further research is needed to better isolate and define other factors that influence and contribute to the settlement of such structures within liquefiable soils.

1.2 Problem Description

Current practices used to predict liquefaction-induced building settlement are based on semi-empirical relationships in the free-field. The controlling mechanisms of liquefaction-induced building settlement are not well understood. Research focused on identifying the controlling mechanisms and influence of parameters such as foundation width, relative density of soil, thickness of liquefiable layer and ground motion duration on liquefaction settlement will provide additional insight on this issue. Improved understandings and better insights on liquefaction-induced building settlement will ultimately lead to better design procedures and mitigations for foundations residing over liquefaction susceptible soils. Additionally, these insights will also lead to improved semi-empirical methods in predicting liquefaction settlements.

1.3 Scope

A comprehensive parametric study was conducted to evaluate liquefaction-induced settlement for a series of model structures founded over liquefiable soils. However, before commencement of any experimentation, a thorough review of previous research and literature concerning the effects of liquefaction-induced settlement was conducted and used as a guide to narrow our experimental focus. Review of these previous studies allowed us to identify parameters that were well understood as well as parameters that could benefit from additional research. Our literature review also included field reconnaissance reports of previous earthquakes that documented extensively the effects of liquefaction on structures. Review of previous research and field observations assisted in refining our experimental models to draw focus to specific fundamental parameters contributing to liquefaction such as ground accelerations and excess pore water pressures.

Each model structure was representative of a typical one-to-two story building. The models consisted of circular “rigid shallow” foundations of various diameters, each applying a similar contact pressure on the soil model. The study also evaluated the efficacy of helical piles as a mitigation strategy for underpinning of these foundations in liquefiable soils. In total, 56 experiments were conducted on a scaled model with liquefiable soil conditions. Liquefaction was induced using a 1-g shaking table for each experiment. The experiments were carried out in four phases. Phase 1, the initial phase, was used mainly to gain an understanding of how best to construct each model and implement instrumentation. Phase 2, continued to refine and calibrate the models, however it included pressure sensors to measure pore water pressure and one linear variable differential transformer (LVDT) to observe settlement for our model buildings. Phase 3 testing was more of the production phase. In Phase 3, the model included all instrumentation and model buildings. These results were used to conduct the majority of our parametric study. Phase 4 tested our soil model on a large scale shake table equipped with hydraulic actuators. In addition, it also used a realistic input motion for the 1979 El Centro Earthquake. Results of Phases 2 through 4 were compared to previous experimental studies and field observations that have focused on defining the relationship between width of foundations and magnitude of settlement during instances of liquefaction.

Chapter 2 Literature Review

Although devastating and oftentimes tragic, earthquake events provide the opportunity for observation of both the mechanisms of earthquake induced failures as well as the performance of structures and their various types of foundations. Often these observations lead practitioners to new insights on soil structure interactions, soil mechanics and new designs or mitigation strategies towards preventing future catastrophes. Commonly, these insights are observed and then evaluated through means of experimental studies, where researchers draw inferences based on the outcomes of those experiments with the ultimate goal of deriving new understandings and building upon the standards of practice in engineering design.

The following sections will explore in detail some of the more recent field observations of past earthquake events that are providing greater insight into the controlling mechanisms of liquefaction and their subsequent damage. These observations, coupled with recent experiments into the behavior of structures founded on liquefiable soils are intent on furthering the understanding of the behavior and improving the standards of practice used in designing structures in such environments.

2.1 Observations from Past Earthquakes

Recent large magnitude earthquakes have caused significant damage both in Japan and New Zealand. These earthquakes were centered near large population centers with structures and appurtenances ranging from lightly loaded to larger multi-story buildings. Immediately after each event, researchers mobilized to document the damage and effects resulting from these catastrophic events. Both the March 11, 2011 M9.0 earthquake centered off the northeastern coast of Japan and the 2010-2011 Canterbury earthquake sequence centered off the New Zealand coast near Christchurch were equally devastating. Unfortunately, these events also provided the opportunity for observations on the performance of many foundation types subjected to these events.

March 11, 2011 Tohoku Earthquake

The March 11th event in Japan was centered approximately 200 miles northeast of Tokyo Bay. The magnitude 9.0 earthquake was responsible for generating a catastrophic tsunami that inundated the coastlines. The long duration event was also responsible for causing severe liquefaction. In fact, the areas of highest liquefaction-induced damage within the Tokyo Bay and surrounding areas were identified as those constructed over reclaimed soils (Ashford et al. 2011, Yasuda et al. 2012). According to Yasuda 2012, a great deal of land has been reclaimed in the Tokyo Bay area since the seventeenth century. More recently in the 1960’s, Tokyo began dredging marine sediments from the bay and reclaiming them to accommodate growth in industry and increase land for residential property. Figure 2-1 presents a typical schematic of the dredging operation that was employed for land reclamation. In the figure it can be clearly seen that the dredged marine sediments were re-deposited below the sea level (ground water table). As a result, the soils were largely loose, unconsolidated and saturated based on the nature of their deposition. Yasuda also noted that historically, land reclamation had occurred in the original estuaries along the Tokyo Bay region.

Composition of the dredged fill soils from Tokyo Bay were characterized as being mostly a sandy soil, however it was also noted that at times the fill material did contain a higher fines content. Subsurface characterization of the Tokyo Bay area after the March 11th event identified that the reclaimed soils in the Urayasu District were as much as 6-9 meters in thickness below the groundwater table and contained SPT N-values ranging from 2-8 blows (Yasuda et al. 2012). It was further identified that although the fill soils with higher fines contents should have been less susceptible to liquefaction, the long duration of the seismic event was likely a contributing factor.

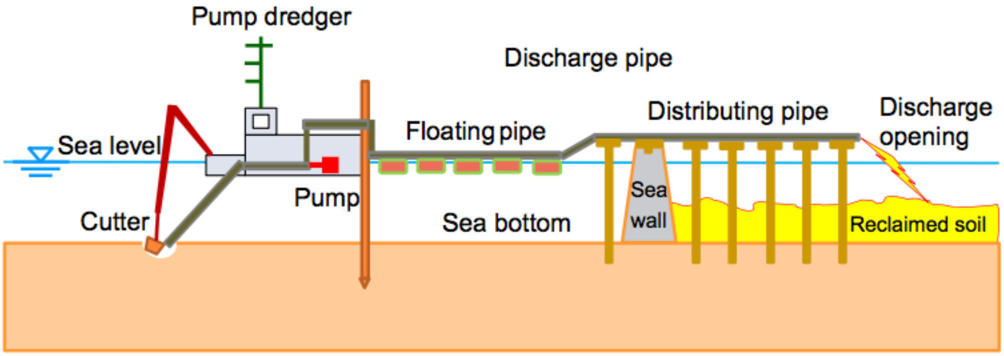

Figure 2-1: Typical Schematic of Dredging Operations for Reclaimed Soils (Yasuda et al. 2012)

According to Yasuda et al. 2012, as many as 27,000 structures within the Tohoku and Kanto regions of Japan were damaged as a result of liquefaction.

Performance of these structures varied considerably based on their foundation type and whether ground improvement methods had been implemented. Ashford et al. 2011 observed that many light residential and commercial structures experienced a large degree of settlement and tilting. These structures were typically founded on a rigid mat foundation with deep grade beams and also noted that damage usually did not translate to the super structure despite the large degree of tilting and settlement. Figure 2-2 presents the typical damage incurred as a result of liquefaction-induced settlement. The figure shows two buildings with an adjacent sidewalk. It is apparent that one building has experienced minimal settlement and the other has experienced significant settlement and appears to be tilting. The building that experienced the large degree of settlement is founded on a mat-type foundation while the other is supported by a pile foundation system. Liquefaction-induced damages were also observed to have impacted buried utilities and lifelines as well as levee structures and many other appurtenances of infrastructure.

Figure 2-2: Liquefaction-Induced Building Settlement in Uraysu, Japan (Ashford et al. 2011 and Bray 2016)

During the field reconnaissance after the March 11th event both Yasuda et al. 2012, and Ashord et al. 2011 observed foundations that had previously employed ground improvement methods. Ground improvement methods have been employed within the Tokyo Bay region as a liquefaction countermeasure since the 1980’s. These methods consist of vibratory sand compaction piles SCP), non-vibratory SCP, gravel drains and lattice-type deep mixing (Yasuda et al. 2012). Reconnaissance of the areas that implemented ground improvement methods typically showed good performance and minimal damage (Ashford et al. 2011, Yasuda et al. 2012).

2010-2011 Canterbury Earthquake Sequence

The Canterbury earthquake sequence also provided good grounds to observe the performance of structures and foundations subjected to the effects of liquefaction-induced settlement. Between September 2010 through December 2011, New Zealand was affected by a series of strong motions that triggered localized to widespread, minor to severe liquefaction in the Canterbury region (Bray et al. 2015, Henderson 2013, van Ballegooy et al. 2014). Reconnaissance of the affected areas identified that the Central Business District (CBD) of downtown Christchurch experienced the most significant damage resulting from liquefaction. Furthermore, it was observed that liquefaction-induced damage produced varying effects on buildings with different structural and foundation systems (Bray et al. 2015). Four types of foundations were identified on lightly loaded structures in the heavily affected area, (1) concrete perimeter with short piers, (2) concrete slab on grade, (3) RibRaft slabs and (4) driven pile foundations (Henderson 2013). Figure 2-3 presents an aerial view of Christchurch region and the corresponding ground surface observations of liquefaction-induced damage resulting from the February 22nd, 2011 event. The areas of highest liquefaction damage can be seen within and around the channels and flood plains of the Avon River. Subsurface conditions throughout the CBD and Christchurch can be characterized as having highly variable, alternating deposits of sands and gravels with overbank deposits of silty soils (Bray et al., 2015). The water table throughout the area is relatively shallow, 1-3 meters below the ground surface (Bray et al. 2015).

Approximately 20,000 homes were identified to have experienced some degree of damage and approximately 7,000 of those homes were deemed uninhabitable due to the severity of the damage incurred (Henderson 2013). Reconnaissance teams performed detailed inspections of these homes and areas subjected to the effects of liquefaction. These detailed inspections focused on level of subsidence, degree of tilting and any noticeable damage incurred to the foundation and superstructure (Henderson 2013).

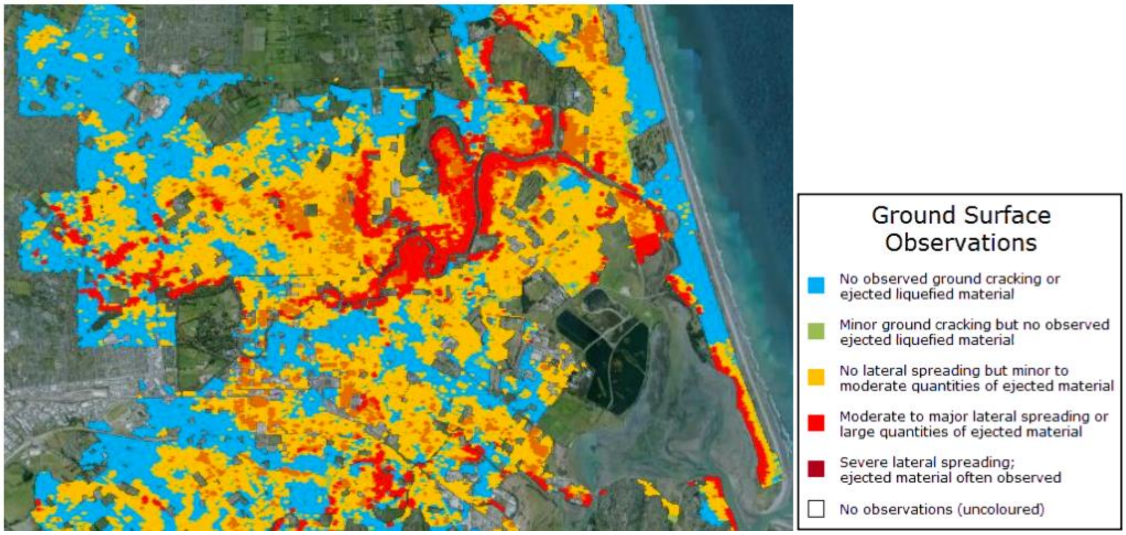

Figure 2-3: Severity of Liquefaction-Induced Damage within Christchurch after February 22, 2011 Event. (Henderson 2013)

In addition, these inspections led to the development of a qualitative system of seven groupings that defined the severity of damage to foundations and structures, ultimately defining a “red zone”, where reconstruction of damaged structures was no longer feasible. These groupings also included three “technical land categories” to assist in repair and reconstruction; where each category is based on severity and potential for future liquefaction-induced damage effecting performance of foundations (van Ballegooy 2014). In the case of van Ballegooy et al. 2014, the field reconnaissance was conducted to assist in insurance compensation purposes given the scale of homes effected by liquefaction-induced damage. Figure 2-4 presents the liquefaction-induced damage resulting from the February 22, 2011 event. Considerable amounts of sediment ejecta can be seen in addition to the water inundation of homes resulting from liquefaction.

Figure 2-4: Liquefaction-Induced Damage Christchurch (van Ballegooy 2014)

2.2 Prior Experimental Studies

Liu and Dobry (1997)

Liu and Dobry (1997) conducted 8 centrifugal tests that investigated the seismic response of shallow foundations on liquefiable soil. Two series of experiments were conducted that evaluated the settlement of shallow foundations subjected to soil liquefaction; Series C focused on varying the depth of compaction of soil beneath the model foundation while Series G investigated the effects of soil permeability on seismic response. Series C utilized vibrocompaction methods to vary the depth of compaction for five model tests (C0 through C4). Test C0 served as a base model for the case of zero compaction. Series G focused on effects of different cohesionless grain sizes by employing a glycol solution in the centrifuge to model permeability of a finer grained soil. Three tests were performed for Series G (G0, G55 and G85). Each suffix for Series G represents the percentage of glycol present in solution for the centrifuge model. Series C testing was completed using a model footing, representative of a shallow foundation that induced a prototype dimensions and contact pressure of approximately 4.56 m and 100 kPa respectively. Series G testing was completed using a model footing, representative of a shallow foundation that induced a prototype dimensions and contact pressure of approximately 2.85 m and 122 kPa respectively. Liu and Dobry (1997) concluded in Series C that as the compaction depth increased, so did the acceleration of the building footing during shaking. With increased compaction and footing acceleration, the settlement of the building decreased as well. Series G showed that with decreasing grain size, or decreasing permeability, the dissipation of excess pore water pressure increases. Series G also suggest that with decreasing soil permeability in sands, post-liquefaction settlement is likely to increase. The data for each series were validated by comparing the results to the bounds presented in Figure 2-5. Figure 2-5 presents two plots, the first plot is the data set from two historic earthquakes (1964 Niigata and 1990 Luzon) where liquefaction-induced settlement was prevalent. Each event allowed researchers to document first-hand the degree of settlement for varying widths of foundations. The data resulted in the two bounded curves and is commonly used today to compare liquefaction-induced settlement data. The curves suggest based on observations that settlement is proportional to the foundation width. The second plot in Figure 2-5 presents the results of both the Series C and G experiments. Series C data clearly shows that with increasing compaction of soils and reduction in thickness of liquefiable layer, the settlement is decreased. Series G shows that results without ground improvement fall within the bounds of previous observations.

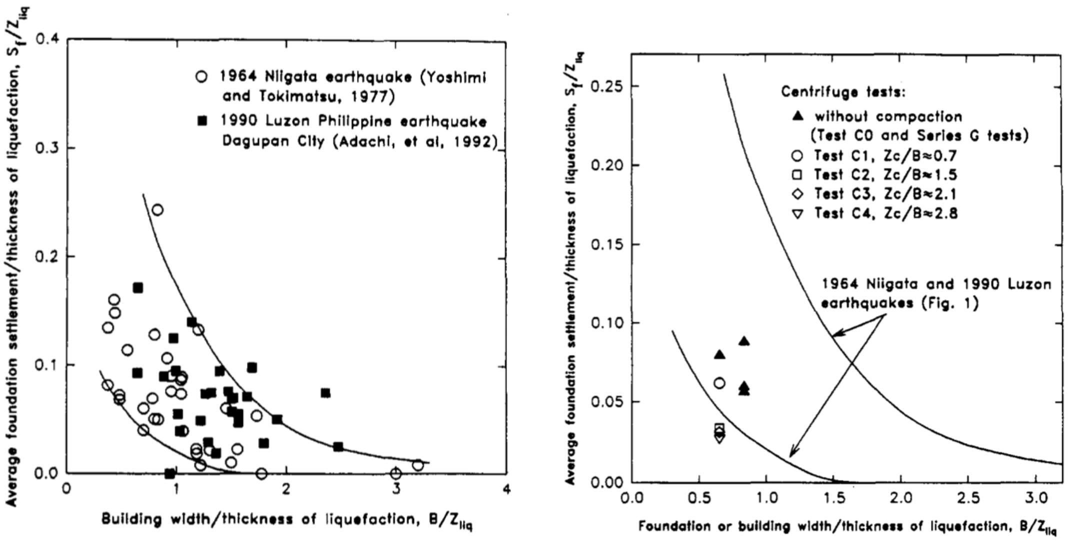

Figure 2-5: Normalized Settlement versus Normalized Building Width for Centrifuge Testing (Liu and Dobry 1997)

<u>Dashti et al. (2010a)</u>

Current state of practice in estimating liquefaction-induced settlement is to use procedures that evaluate postliquefaction settlement in the free-field environment. However, recent earthquakes have shown that seismically induced settlement for buildings on shallow foundations can be considerably larger. Dashti et al. (2010a) have identified the need to identify the key mechanisms involved in liquefaction-induced building settlement. A series of centrifuge experiments evaluating model buildings on shallow foundations seated over a layered liquefiable stratum were performed to identify those key mechanisms. Each test included three model foundations A, B and C. Model foundation A represented a two-story structure, Model B represented a two-story structure with wider footprint and Model C represented a four-story structure. Contact pressures for Models A, B and C ranged from 80, 80 and 130 kPa respectively.

Dashti et al. (2010a) indicated through the results of the centrifuge testing that building settlement is not directly proportional to the thickness of the liquefiable layer. Additionally, the results show that the majority of settlement occurs during strong shaking with minimal settlement occurring as a result of postliquefaction excess pore water pressure dissipation. Past investigations of the relationship between building settlement and liquefaction have identified other important factors such as intensity of shaking, relative density of soils, thickness of liquefiable deposits and contact pressure of the structure in question. Commonly, these parameters, excepting contact pressure, are used in the 1D free-field liquefaction settlement procedures proposed by Tokimatsu and Seed (1987); Ishihara and Yoshimine (1992). Dashti et al. (2010a), however, point out that these procedures ignore the partial drainage that occurs during strong shaking and important deviatoric strain mechanisms. It was observed during testing that partial drainage existed both horizontally and vertically away from each model building in response to the increased pore pressures, while each model footing generated a soil-structure cyclic response in both inertial forces and pore water pressure. Bray et al. (2014) also noted that settlement of the building occurred linearly with duration of shaking and dramatically decreased upon cessation of shaking. Significant settlements were also observed in the free-field during shaking suggesting partial drainage. Lastly, Dashti et al. (2010a) concluded that for each scenario in centrifuge testing, static and dynamic deviatoric-induced movements in combination with sedimentation and localized volumetric strains due to partial drainage during earthquake shaking were responsible for most of settlements measured in the experiments. Similar inferences can be assumed for the case of free-field settlement excluding the influence of static and deviatoric-induced movements. In Figure 2-6, Dashti et al. (2010a) expand on the previous results from the Liu and Dobry case study in an attempt to validate their data. Normalized results in this plot do not show good agreement with the Lui and Dobry centrifuge tests. It should be noted that the contact pressure for the Dashti experiments were quite large, on the order of 80 and 130kPa which is not characteristic of a shallow lightly loaded foundation.

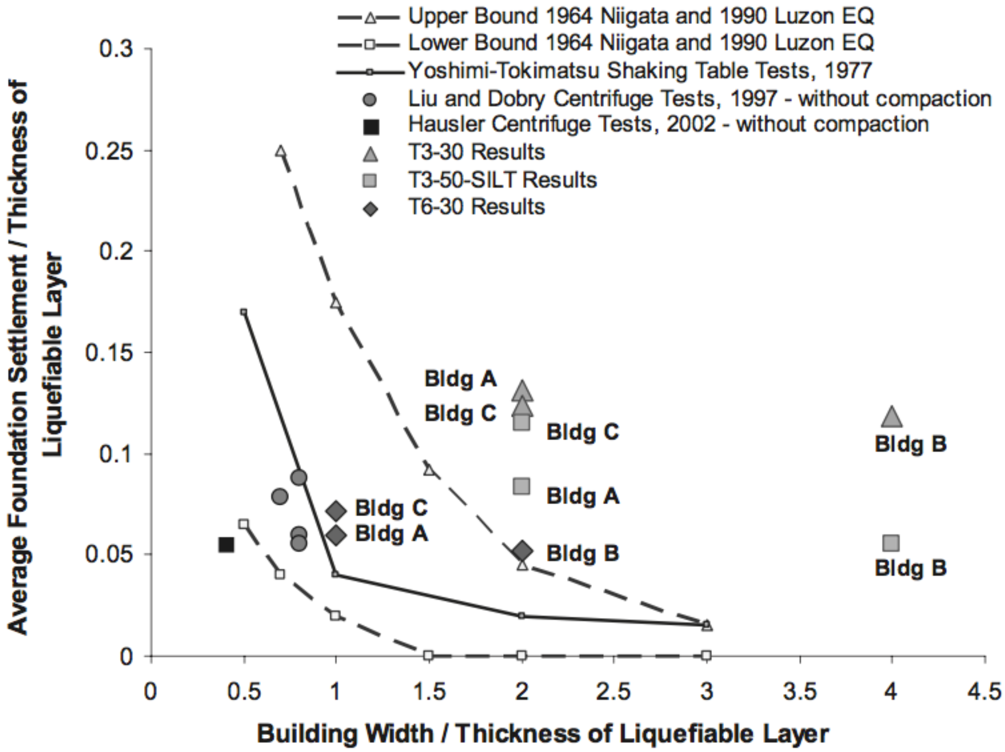

Figure 2-6: Normalized Foundation Settlements of Dashti Centrifuge Experiments (Dashti et al. 2010a)

Dashti et al. (2010b)

Dashti et al. (2010b) further elaborates on their previously published research. The author further iterates that estimating postliquefaction settlement in the free-field is not an appropriate measure to evaluate settlement of buildings founded over liquefiable soils. Dashti et al. (2010a) performed centrifuge experiments to identify controlling mechanisms governing seismically-induced settlement of buildings with rigid mat foundations over thin layers of liquefiable soils. To further understand the controlling mechanisms of settlement, specific mitigation techniques were employed on each model in an attempt to isolate selective parameters. Dashti et al. (2010b) observed that denser liquefiable soils lead to increased stiffness and thus decrease likelihood of bearing failure. However, an increase in relative density of liquefiable soil, also leads to an increase in demand on the structure, thus promoting ratcheting of the soil-structure. Ratcheting can be described as an accumulation of strain during each cycle during strong ground motion. Results of these experiments have revealed that the initiation, rate and amount of liquefaction-induced building settlement follow the rate of ground shaking intensity. The shaking intensity rate (SIR) can be measured as the slope of the arias intensity at its strongest time of shaking. Dashti et al. (2010b) surmise that the SIR along with other key parameters may be useful in developing a framework for estimating liquefaction-induced building settlement. Specific mitigation strategies were implemented in each model to reduce influence of certain key parameters while isolating others. Latex water barriers were installed on some model perimeters to reduce horizontal flow of water while more rigid structural walls were used to reduce effects of shear-induced deformations and volumetric strains. Each subsurface remediation reduced overall settlement of the model building.

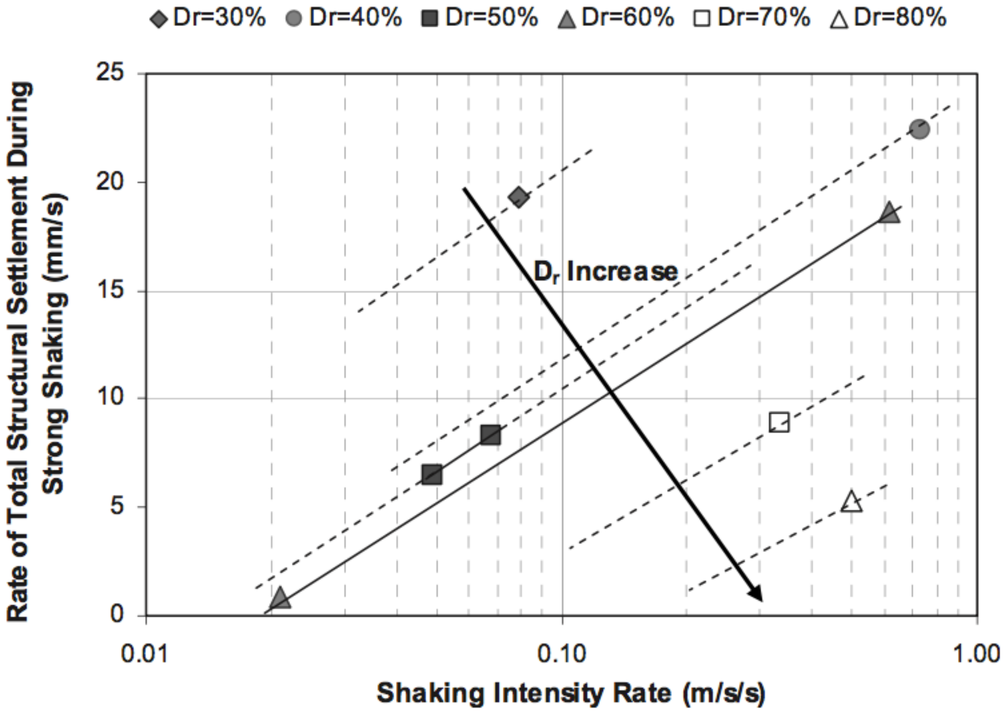

Figure 2-7: Comparison of Settlement Rate to Shaking Intensity Rate with Increasing Relative Density (Dashti et al. 2010b)

<u>Bray and Dashti (2014)</u>

Liquefaction-induced ground displacement has contributed greatly to differential movements of buildings founded in liquefiable soils during earthquakes. Settlement based damage has been observed in buildings that experience punching, tilting and lateral sliding as a result of bearing failure. Bray and Dashti (2014) have observed in previous centrifuge experiments that much of the building movement occurs during earthquake strong shaking. Bray and Dashti

(2014) further clarify that shear-induced movements resulting from shaking-induced ratcheting of the buildings into the softened soil and volumetric-induced movements due to localized drainage in response to high transient hydraulic gradients during shaking are important effects that are not captured in most design procedures. More specifically, importance of each mechanism are dependent upon earthquake motions, the liquefiable soil and structure. These mechanisms are further dependent upon the shaking intensity rate (SIR) of the ground motion. Sediment ejecta, resulting from dissipation of excess pore water pressure, tended to have more of an influence on building settlement when founded over shallow thin deposits of liquefiable material. Bray and Dashti (2014) have identified that the dominant mechanisms for many cases of liquefaction-induced settlement are, sediment ejecta, foundation ratcheting, bearing failure due to soil strength loss and localized volumetric strains resulting from transient hydraulic gradients. Building settlement was also observed to increase significantly after Ru $\approx$ 1 with minor contributions in consolidation-induced volumetric strain after shaking had ceased. Lastly, Bray and Dashti (2014) reassert that current engineering practices use an empirical based solution to estimate liquefaction-induced settlement for free-field conditions. The empirical approach does not take into consideration other dominant key parameters that contribute to liquefaction settlement of structures during seismic loading events. Although a simplified approach currently does not exist, Bray and Dashti (2014) provide recommendations to help guide the engineer in performance-based engineering assessment. Bray and Dashti (2014) recommend performing a wellcalibrated, nonlinear, effective stress, dynamic analysis to provide further insight into the problem and has been implemented with reasonably well results using the UBCSAND model within FLAC-2D. Figure 2-8 presents the Liquefaction-induced displacement mechanisms typically of a structure during seismic events. These movements contribute to development of deviatoric and volumetric strains.

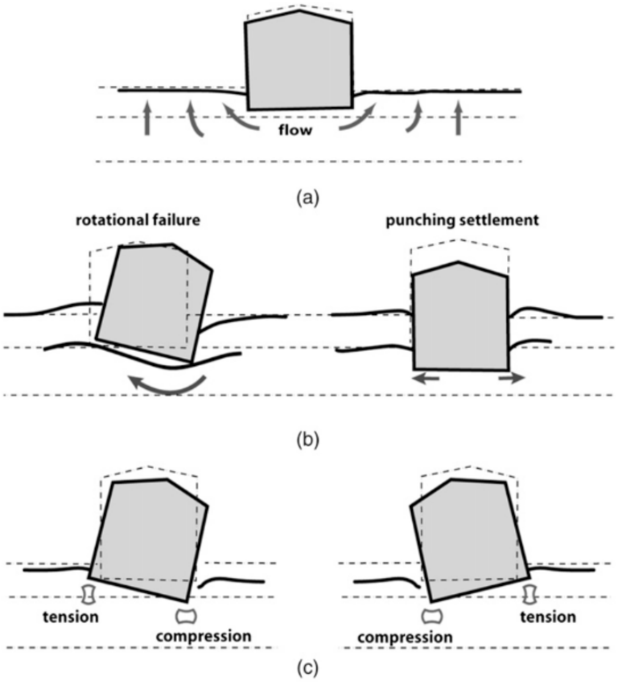

Figure 2-8: Liquefaction-Induced Displacement Mechanisms (Bray and Dashti 2014)

<u>Rasouli et al. (2015)</u>

Liquefaction-induced settlement of lightly loaded structures, such as residential properties, in liquefaction prone areas is very common. To date, cost-effective solutions in mitigation of these settlements is not very prevalent. Rasouli et al. (2015) performed a series of 1-g shake table experiments that investigated the performance of sheetpile walls as a potential mitigation strategy in reducing settlements experienced from the effects of liquefaction. It was believed that by restricting the lateral displacement of liquefiable soils during earthquake events, the overall settlement of structures founded within the perimeter of those sheetpile walls could be reduced.

The study focused specifically on four scenarios of evaluation; (1) Baseline (no mitigation employed), (2) Full embedment of sheetpiles in a non-liquefiable bearing layer, (3) Staggered embedment of sheetpiles into non-liquefiable bearing layer and (4) Half-length embedment of sheetpiles terminating in liquefiable soils. In addition, evaluations were conducted that compared degree of settlement resulting from different depths of ground water table (shallow vs. deep). Rasouli et al. observed that in all cases that lower groundwater table, or non-liquefiable surface layer, the ultimate settlement is reduced. Sheetpiles with non-liquefiable surficial layers tend to increase the fixity of the sheetpile system and protect the foundation against settlement (Rasouli et al. 2015). Continuous sheetpiles were observed to delay the generation of excess pore water pressure ultimately offsetting the initiation of liquefaction-induced settlement. Rasouli et al. (2015) surmised that this is beneficial for cases of weaker shaking. Cases of staggered embedment of sheetpile systems into bearing stratum also showed a delay in generation of excess pore water pressure. However, the staggered approach did not restrict lateral movement of liquefiable soil and in some cases was observed to increase the degree of settlement. Cases of half-length embedment of sheetpile walls into the subsurface showed no reduction in liquefaction-induced settlement. Lastly, Rasouli et al. (2015) touch on the subject of post-liquefaction settlement in structures. It was observed during some evaluations that thin pockets of water developed within the liquefiable stratum beneath the foundation as a result of the large excess pore water pressures. As the pressures dissipated after cessation of shaking the settlement of the model structure continued.

2.3 Current Practices in Estimating Liquefaction Induced Free-Field Settlements

According to Kramer (1996) the tendency of sands to densify when subjected to earthquake loading is well documented. The process of densification, or settlement, frequently causes distress to structures and foundations. However, reasonably approximate estimations of this settlement have proven to be complex. Several semi-empirical methods have been developed to evaluate settlement of sands subjected to earthquake loadings (Tokimatsu and Seed 1987; Ishihara and Yoshimine 1992). These semi-empirical methods are derived largely from theory in liquefaction susceptibility based on the relationship between cyclic stress and cyclic resistance ratios. Theory and practice of evaluating liquefaction resistance has more recently been discussed by leading practitioners, providing new recommendations and updates to current standards of practice (Youd et al. 2001; Idriss and Boulanger 2004).

Tokimatsu and Seed (1987)

Tokimatsu and Seed propose a simplified approach in evaluating settlement of saturated and unsaturated sands subjected to earthquake loading. This simplified method of analysis considers the cyclic stress ratio and maximum shear strain to be the primary controlling factors of liquefaction-induced settlement for saturated sands. Additionally, the relative density of the soil or standard penetration value (N-value) along with earthquake magnitude also contribute to the degree of settlement. Tokimatsu and Seed present observed settlements at 6 sites and compare those observations with the predictions using their simplified approach. Results of these observations compare well with the predictive chart presented in Figure 2-9. Tokimatsu and Seed noted that, under static conditions, this predictive analysis can pose error on the order of 25-50%. They further point out that this method becomes less reliable when considering more complex soil conditions associated with earthquake loadings. Use of this method can be considered a first case approximation in evaluating settlement of saturated sands based on volumetric deformations.

The following equations (2.1 through 2.4) are used when evaluating the settlement for clean saturated sands in conjunction with Figure 2-9. Figure 2.9 is an empirical chart that relates the cyclic stress ratio and corrected standard blow counts to a corresponding volumetric strain.

Cyclic Shear Stress

$$\tau cyc = 0.65 * \left(\frac{amax}{g}\right) * \sigma o * rd \quad (2.1)$$

a_{max} = Maximum horizontal acceleration at the ground surface

σ_o = Total overburden stress at target depth

r_d = Stress reduction factor

Cyclic Shear Stress Ratio

$$CSR = \frac{\tau cyc}{\sigma o'} \qquad (2.2)$$

$\sigma_{o'}$ = Effective overburden stress at target depth

SPT N-Value – Normalized to an effective overburden pressure of 1 tsf and effective drill rod energy equal to 60%.

$$(N1)60 = CER * CN * N \qquad (2.3)$$

C_{ER} = Correction factor for drill rod energy during SPT.

C_N = Correction factor for effective overburden pressure.

Free-Field Settlement

$$\Delta H \ = \ \varepsilon v\ (\%) * H \qquad (2.4)$$

ε_v = Volumetric Strain (%)

H = Thickness of Liquefiable Layer

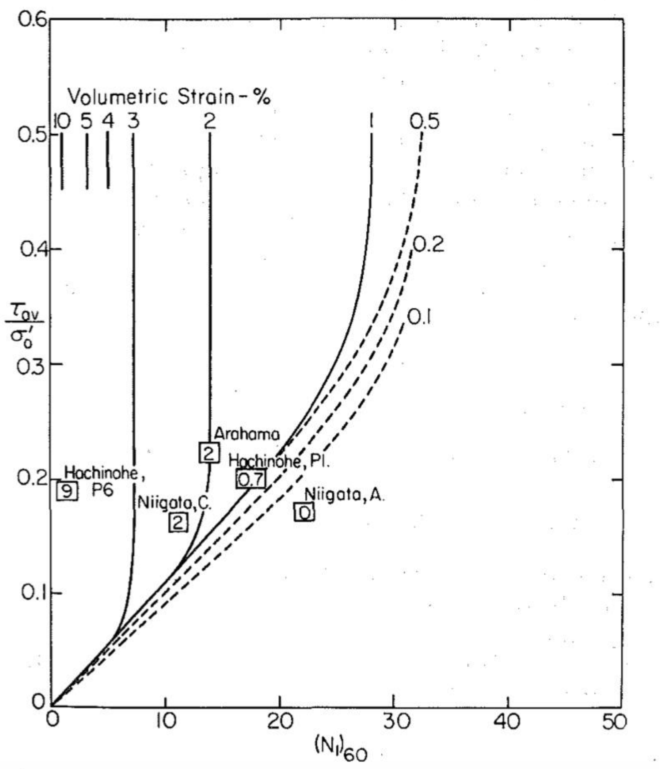

Figure 2-9: Volumetric Strain for Clean Saturated Sands (Tokimatsu and Seed, 1987)

Ishihara and Yoshimine (1992)

Ishihara and Yoshimine (1992) evaluated laboratory data on sands tested using a simple shear apparatus. The results of this evaluation were used to generate a series of curves defining volumetric strains resulting from the dissipation of pore water pressures. Ishihara and Yoshimine (1992) further correlated these volumetric strains to the relative density of sand and factor of safety against liquefaction. Similar to the original methodology presented by Tokimatsu and Seed (1987), Ishihara and Yoshimine (1992) augmented the methodology to include the factor of safety. According to Ishihara and Yoshimine (1992), the factor of safety considered using the maximum shear strain is a key parameter in identifying changes in volumetric strain. These volumetric strains and their corresponding relationships with relative density can be used to estimate the probable liquefaction induced settlement for a given site by integrating the volume changes for each subsurface layer. Ishihara and Yoshimine (1992) used the proposed methodology to compare estimated liquefaction induced settlement for sites damaged during the 1964 Niigata earthquake. They conclude that the methodology enables an approximate estimate of liquefaction-induced settlements resulting from postliquefaction volumetric strains.

The following equations (2.5 through 2.10) are used when evaluating the settlement for clean saturated sands in conjunction with Figure 2-10.

Cyclic Shear Stress

$$\tau cyc = 0.65 * \left(\frac{amax}{g}\right) * \sigma o * rd \qquad (2.5)$$

a_{max} = Maximum horizontal acceleration at the ground surface

σ_o = Total overburden stress at target depth

r_d = Stress reduction factor

Cyclic Shear Stress Ratio

$$CSR = \frac{\tau cyc}{\sigma o'} \qquad (2.6)$$

$\sigma_{o'}$ = Effective overburden stress at target depth

Cyclic Shear Stress Ratio (Liquefaction)

$$CSRL = CSRM7.5\ (MCF) \qquad (2.7)$$

$CSR_{M7.5}$ – CSR from equation 2.6, representative of a M7.5 event.

MCF – Magnitude Correction Factor = 1.0

Factor of Safety (Liquefaction)

$$FSL = \frac{\tau cyc,L}{\tau cyc} \qquad (2.8)$$

$\tau cyc, L$ = $CSR_L * \sigma_{o'}$

SPT N-Value – Normalized to an effective overburden pressure of 1 tsf and effective drill rod energy equal to 60%.

$$(N1)60 = CER * CN * N \qquad (2.9)$$

C_{ER} = Correction factor for drill rod energy during SPT.

C_N = Correction factor for effective overburden pressure.

Free-Field Settlement

$$\Delta H\ =\ \varepsilon v\ (\%) * H \qquad (2.10)$$

ε_v = Volumetric Strain (%)

H = Thickness of Liquefiable Layer

Figure 2-10 is an empirical chart based on similar correlations to Tokimatsu and Seed. However, Figure 2-10 uses the cyclic stress ratio to estimate the factor of safety against liquefaction and relates it to the corrected standard blow count, relative density of soil or tip stress using (CPT) to derive an estimate volumetric strain.

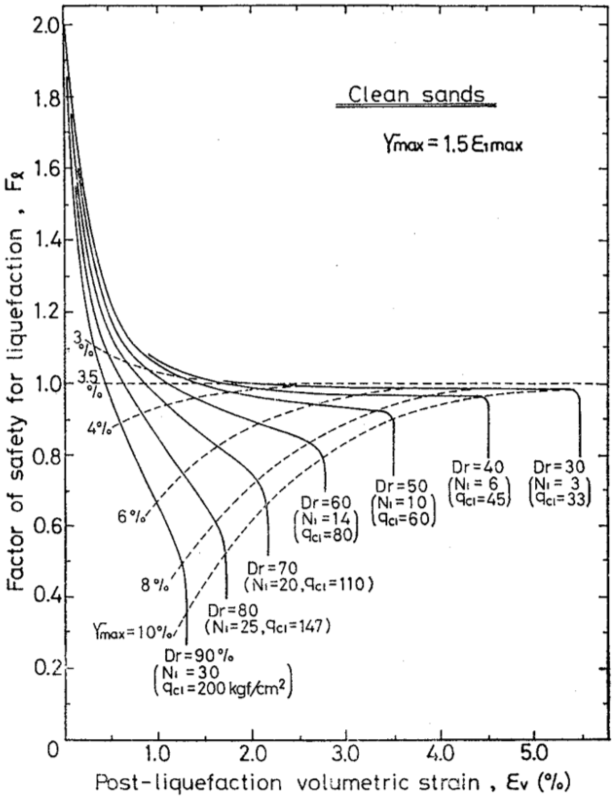

Figure 2-10: Volumetric Strain as a Function of Factor of Safety (Ishihara and Yoshimine, 1992)

Youd et al. 2001

Standard practice for evaluating liquefaction resistance of soils has commonly employed a “simplified approach” originally investigated and proposed by Seed and Idriss (1971). Youd and Seed stated that the largely empirical method has not undergone any general peer review nor updates to the procedure. A sponsored workshop was conducted in 1996 by the National Center for Earthquake Engineering Research (NCEER) to discuss developments and implement improvements to the simplified approach. Recommendations were developed for the following topics. (a) criteria based on standard penetration tests, (b) criteria based on cone penetration tests, (c) criteria based on shear wave velocity measurements, (d) use of the becker penetration test for gravelly soil, (e) magnitude scaling factors, (f) correction factors for overburden pressures and sloping ground, (g) input values for earthquake magnitude and peak acceleration.

The workshop participants proposed the following equations for determining the mean stress reduction factor when evaluating the cyclic stress ratio (CSR). The following equations (2.11 and 2.12) are recommended for noncritical and routine practice.

Stress Reduction Factors

$$rd = 1.0 - 0.00765z\ (for\ \leq\ 9.15m) \tag{2.11}$$

$$rd = 1.174 - 0.0267z\ (for\ 9.15m\ < z \leq 23m) \tag{2.12}$$

z = depth below ground surface in meters.

In regards to the CSR, the workshop also proposed an updated plot for clean sands for a Magnitude 7.5 earthquake. The following plot presented in Figure 2-11, recommended limiting the low end of the CSR at 0.05 for lower values of $(N_1)_{60.}$ Additionally, they also provide recommendations to updating the estimation of $(N_1)_{60}$ through a series of corrections that account for hammer energy ratio, borehole diameter, rod length and sampler corrections. Most importantly there is also a correction factor for overburden stress. The following equation presents the proposed correction factors.

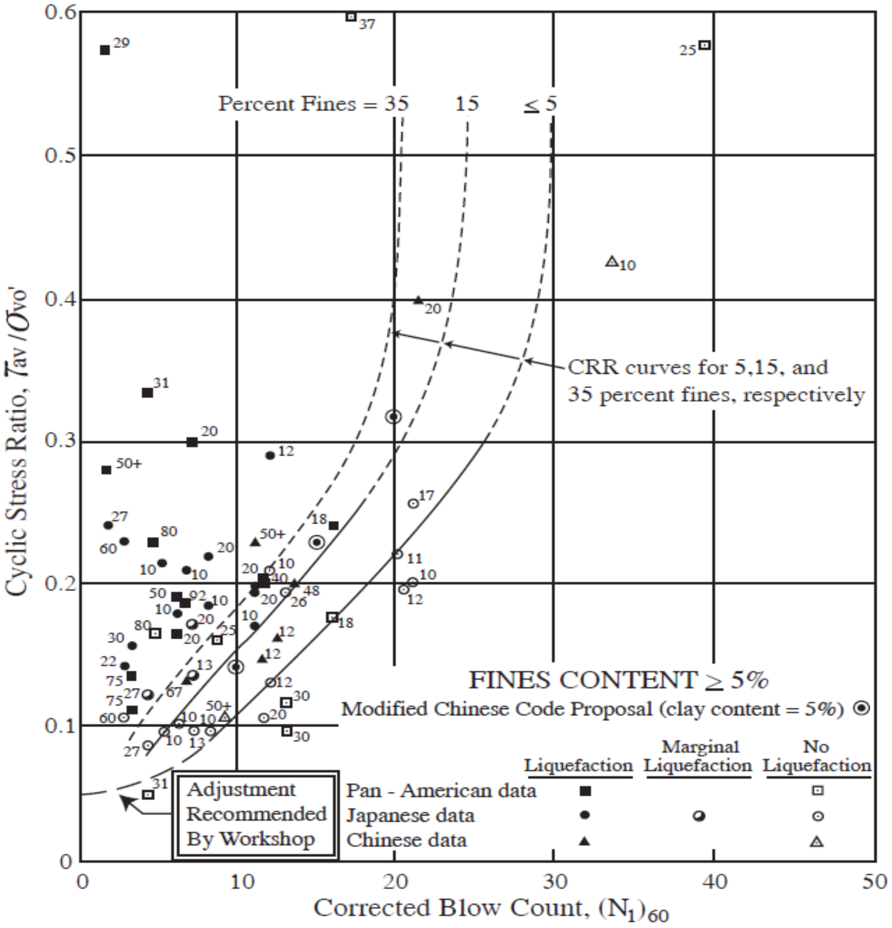

Figure 2-11: SPT Clean-Sand Base Curve for Evaluating Cyclic Stress Ratio (Youd et al., 2001)

SPT N-Value – Normalized to an effective overburden pressure of 1 tsf and effective drill rod energy equal to 60%.

$$(\mathrm{N1})60 = Nm * CN * CE * CB * CR * CS \qquad (2.13)$$

N_M = Measured standard penetration resistance

C_N = Correction factor to normalize N_M to common reference overburden stress.

C_E = Correction factor for hammer energy ratio.

$C_{\mathbf{B}}$ = Correction factor for borehole diameter

C_R = Correction factor for rod length

C_S = Correction for SPT samplers with or without liners

The magnitude scaling factor is also an important factor when evaluating the liquefaction resistance of soils. The simplified methods and recommendations discussed in Youd et al. 2001 were intended to put qualitative measures for an earthquake representative of a M7.5 event. The recommended revised Magnitude Scaling Factors based on the moment magnitude are presented in Figure 2-12.

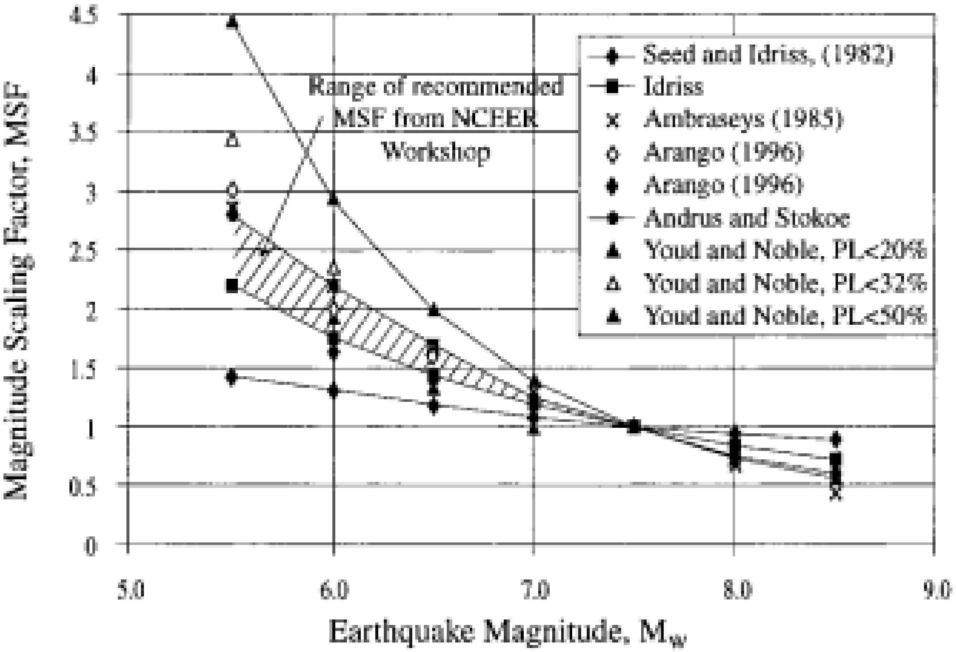

Figure 2-12: Recommended Magnitude Scaling Factors (MSF) (Youd et al., 2001)

2.4 Shake Table Testing Model Similitude

According to Kramer (1996), shake table testing has been used in geotechnical research for quite some time. Shake table testing allows for the model to be viewed from many perspectives during testing and can be constructed for many different sizes. Depending on the facilities available, shake tables can be so large that they allow for testing of soils and structures in prototype “actual” scale. However, this is not very common and therefore testing usually requires evaluations be completed on a scaled model with soil conditions at much lower in-situ stress levels. As a result, correction procedures have been developed to aid in the interpretation of shaking table test results (Kramer 1996). These correction procedures applied are known as the law of similitude.

The laws of similitude govern the scaling of specific parameters for a model whose corresponding dynamic behavior the model is trying to reproduce (Towhata 2008). The law provides basic scaling factors that consider geometry, stresses and strains for both soils and structures as well as dynamic behavior. Iai (1989) developed a theoretical consideration for similitude for shaking table tests of saturated soil-structure-fluid systems in the 1-g gravitational field. This theory was based on the basic equations that govern the equilibrium and the mass balance of soil skeleton, pore water and structures. Table 2-1 presents the scaling factors considered in our experimental evaluation using a 1-g shake table. Similitude for 1-g shake table tests assumed the special case as presented in Iai (1989) where the scaling factor for density of testing medium was assumed to be equal to 1. This is a reasonable assumption for soils.

Table 2-1: Similitude for 1-g Shake Table Tests (Adapted from Iai, 1989)

Parameter	**Item**	**Scaling Factors**
x	Length	λ
ρ	Density of Saturated Soil	1*
ε	Strain of Soil	$\lambda^{0.5}$
t	Time	$\lambda^{0.75}$
σ	Total and Effective Stress	λ
p	Pore-Water Pressure	λ
ü	Acceleration of Soil or Structure	1
EI	Flexural Rigidity	$\lambda^{3.5}$
EA	Longitudinal Rigidity	$\lambda^{1.5}$

Lastly, consideration is being given towards the density of the soils utilized in shake table testing. Table 2-1 assumes that the density of the soil has a scale factor equal to one, meaning that the model and prototype densities are equal. However, discussion has arisen if testing would be more accurate to prototype conditions by considering the shape of the stress-strain curve and dilatancy in model tests under low-effective stresses rather than assuming equal soil density (Towhata 2008). The brittleness index is a quantitative measure of the difference between peak and residual shear stress in relation to the peak shear stress. Research has identified through ring shear testing that confining stress plays an important role when choosing an appropriate relative density between prototype and model scales. The following Figure 2-13 presents the results of an experimental study that evaluated strength softening of soils. According to

Towhata (2008) the results of the study concluded that strength softening is a result of pore water pressure and soil dilatancy. Towhata further defines that soil dilatancy is influenced by both stress and density. Therefore consideration should be given when using 1-g shake table models of a scaled size because the stresses will not be representative.

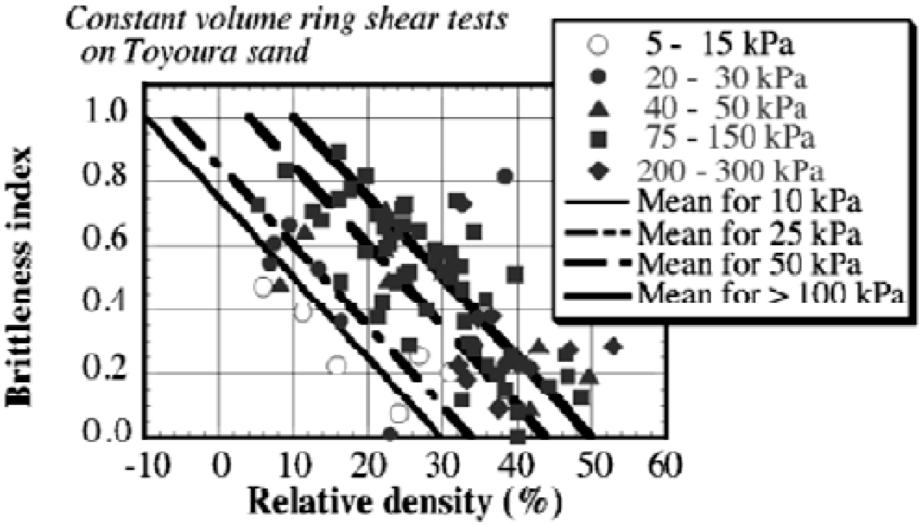

Figure 2-13: Combination of Relative Density and Effective Stress Level (Towhata, 2008)

Chapter 3 Test Procedures and Materials

3.1 Soil Container

Each experiment utilized a transparent soil box fitting the dimensions of 6.7 feet x 2.1 feet x 2.7 feet (length - width - height). The box was constructed of 1-inch thick lexan and reinforced along the corners by a rigid steel frame. Two valves were installed near the base of the box, allowing for saturation of the soil medium prior to testing. The inside base of the soil box contained 1-inch thick spacers and a perforated 0.25-inch thick acrylic sheet. The perforated acrylic sheet assisted in allowing the soil medium to be drained upon completion of each test. The inside of the soil container was fit with thin sheets of plexiglass. A grid pattern was marked on each plexiglass sheet with the dimensions of 5 by 10-cm and was used to make observations in settlement of the surface and placement of instrumentation. Lastly, the inside ends of the soil container were fit with 3-inch thick high density foam pads to reduce boundary effects during experimentation. Figures 3-1 presents the soil tank with corresponding dimensions utilized for experimental evaluations.

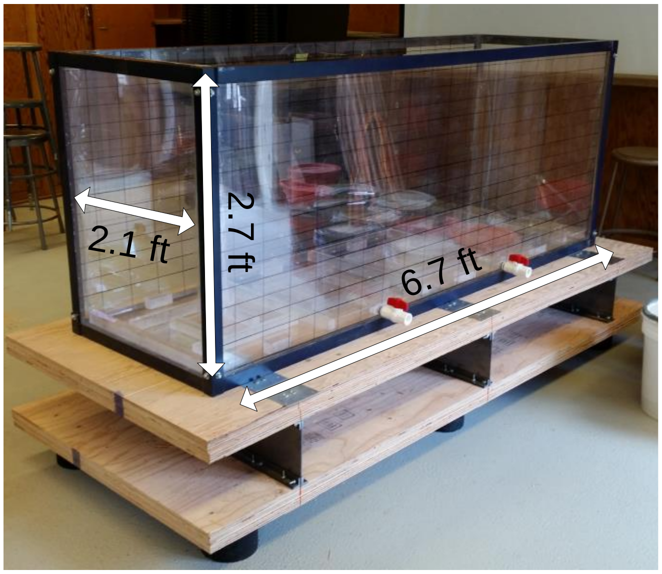

Figure 3-1: Soil Tank Dimensions

Figure 3-2 presented below shows our soil model consisting of two 1-foot thick layers of sand (non-liquefiable and liquefiable).

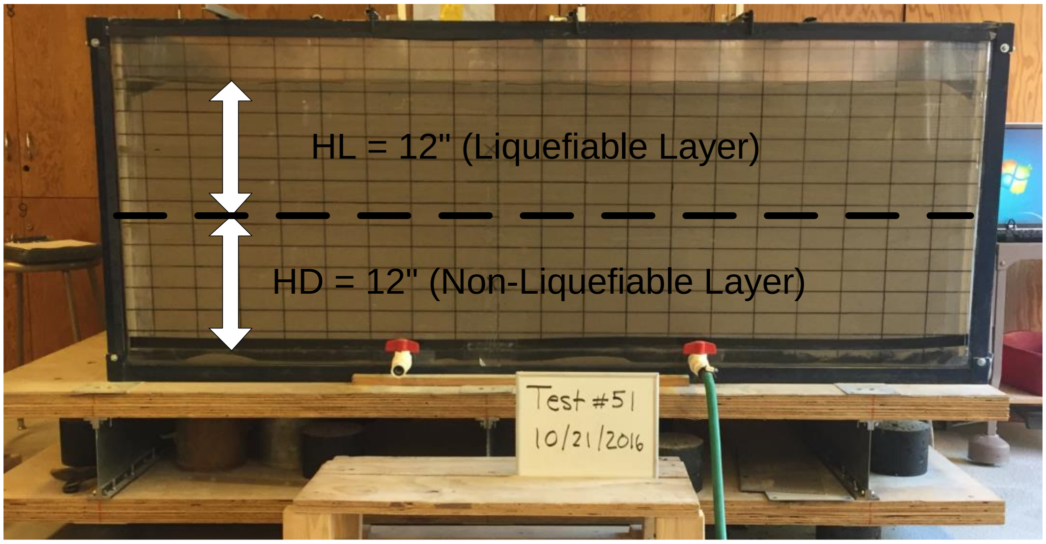

Figure 3-2: Soil Tank used in Experimental Evaluations

3.2 Shake Table Fabrication

A simple constructed shake table was utilized to perform the majority of our experimental evaluations. The table consisted of two 2-inch thick pieces of plywood separated by three equally spaced vertical support members (VSM) constructed of steel. The outer VSM were 1/16-inch in thickness and the center VSM was 1/8-inch thickness. The table was designed to seat the soil container with input motion being induced by displacing the top half of the table in relation to the bottom half of the table. The table was designed for approximately 1-inch of displacement and produce a frequency of 5-6 Hz. Configuration of the shake table and fabrication are presented in the following Figures 3-3 and 3-4. Figure 3-3 presents the bottom half of the shake table and VSM used to support the top half of the table.

Figure 3-3: Fabrication of Shake Table

Figure 3-4: Construction of top half of Shake Table

3.3 Shake Table Evaluations

Throughout the course of our research, three separate methods of shaking were employed to apply input-motions to the soil container. The first method utilized a simple 1-g manual shaking table. The second method, in an attempt to induce more consistent input motions, incorporated an eccentric-mass shaker to the shake table. The third method was performed using the facilities at the Earthquake Engineering Laboratory located at the University of Nevada, Reno.

3.3.1 Manual Shaking

Displacement or input shaking motion was implemented by inducing a horizontal force on the soil container for a specified duration. Repeatability of generating identical input acceleration characteristics between experiments presented challenges when applying shaking through means of manual shaking.

3.3.2 Eccentric Mass Shaker

In an effort to produce more consistent input motions for the experimental evaluations, an eccentric-mass shaker was installed on the shake table. An eccentric-mass shaker consists of a series of counter-rotating weights that are able to induce motions ranging from purely horizontal direction to purely vertical direction. The University of Nevada, Department of Civil and Environmental Engineering purchased the eccentric-mass shaker from ANCO in 1991. It is a Model # MK-12.2-49 and produces a maximum eccentricity of 49 lb-in over a range of 0 – 40 Hz. The mass shaker is capable of producing a maximum allowable force of 8,000 lbs. Figure 3-5 presents the inner workings of the eccentric-mass shaker. The counter rotating weights and shafts are protected by a thick aluminum housing and have been adjusted to induce a purely horizontal force.

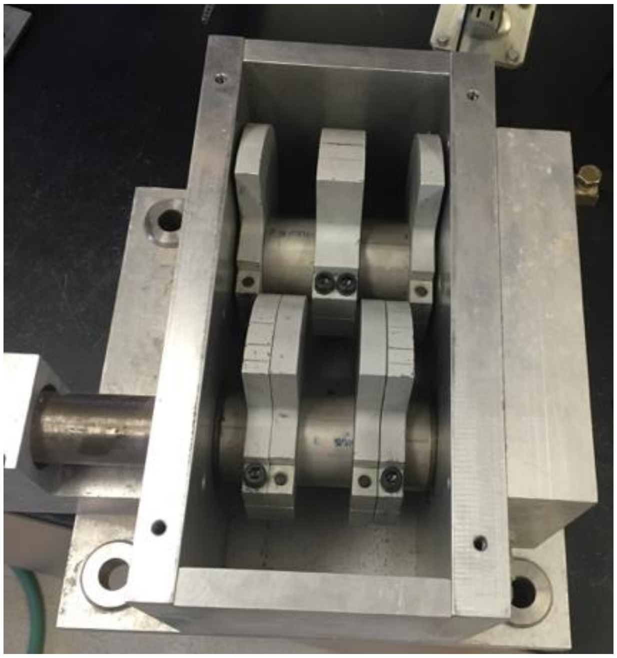

Figure 3-5: ANCO Eccentric-Mass Shaker

The intent in utilizing the eccentric-mass shaker was to produce more consistent input motions and thus reliable experimental results. Upon implementation, it was noted that the mass shaker was unable to induce liquefaction in the soil container at full capacity (2 feet of soil as presented in Figure 3-1). Therefore, the soil model was reduced by half to be able to induce liquefaction. As a result the soil model consisted of two 0.5 foot thick liquefiable and non-liquefiable layers.

3.3.3 Earthquake Engineering Laboratory (EEL)

The University of Nevada, Reno is home to one the largest full scale earthquake simulation laboratories in the world. The new building was opened in the summer of 2014 and includes a 10,000 square foot facility that hosts three-biaxial shake tables and one 6-degree-of-freedom-shake table (http://www.unr.edu/cceer/facilities-and-equipment/earthquake-laboratory). One experimental evaluation was completed using one of the biaxial shake tables located in the EEL and is presented in Figure 3-6. Each biaxial table has the dimensions of 14 feet x 14.5 feet and is capable of displacing a 50-ton payload to a peak acceleration of 1g. Each table is operated by a series of hydraulic actuators with operating frequencies ranging from 0 – 50 Hz.

Figure 3-6: Biaxial Shake Table with Soil Container Located in EEL.

3.4 Liquefaction Testing Medium

The experimental evaluation utilized a fine to medium grained, poorly graded sand as our testing medium ($D_{50} \approx 0.32$mm, $C_u \approx 1.75$, $C_c \approx 1.04$, $e_{min} \approx 0.73$, $e_{max} \approx 1.01$). The locally sourced material, Sierra Silica #60 Mesh, was purchased from Basalite located in Sparks, Nevada. Figure 3-7 presents the dry material ready for placement in the soil container. Figure 3-8 presents the average grain size characteristics of Sierra Silica #60Mesh.

Figure 3-7: Sierra Silica #60 Mesh in Storage Container

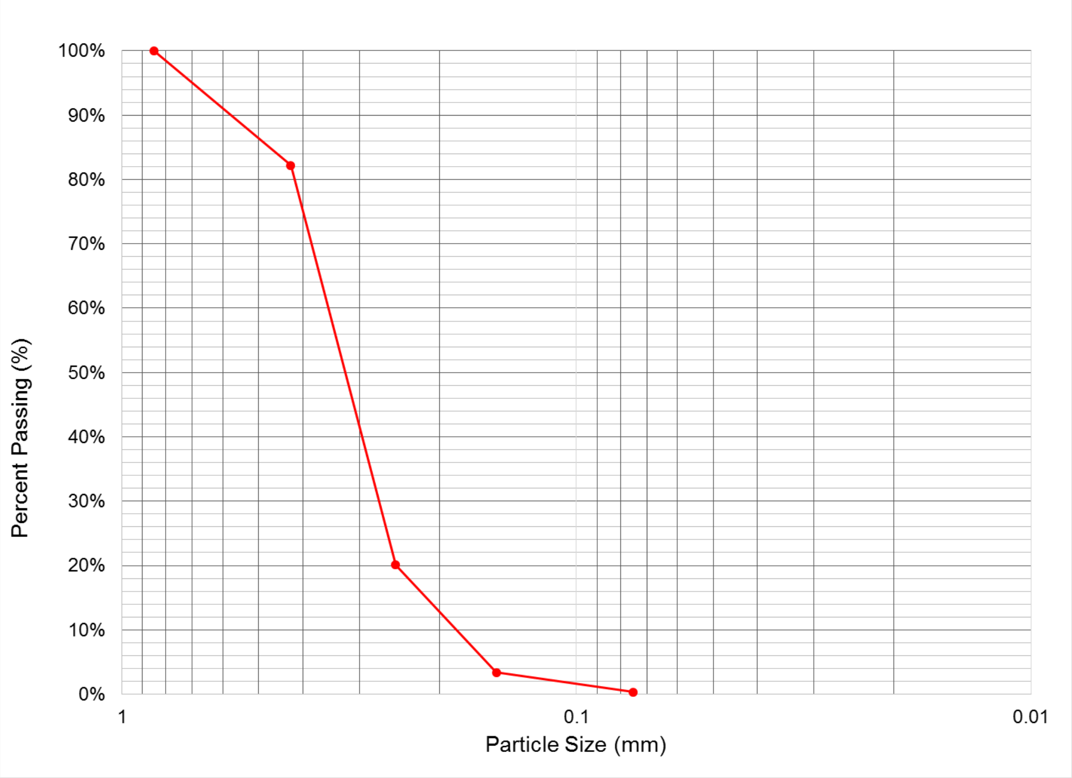

Figure 3-8: Average Grain-Size Distribution of Sierra Silica #60 Mesh

3.5 Construction of Liquefaction Evaluation Model

Each test was prepared by first constructing a moisture conditioned non-liquefiable layer. The non-liquefiable layer was conditioned to 5% moisture and then compacted in lifts within the base of the transparent soil box to a uniform thickness of 1.0 foot as presented in Figure 3-9.

Figure 3-9: Preparation of Non-Liquefiable Layer

Saturation of the non-liquefiable layer was then completed through use of a spigot located at the base of the soil box. Water was slowly introduced into the box, thus saturating the soil from the bottom up. Saturation continued until a sufficient height of standing water resided over the non-liquefiable layer, typically 0.5 feet or half the model liquefiable stratum thickness. The liquefiable layer was then constructed by means of dry pluviation. The sand was poured over a fine mesh screen situated over the transparent box assisting in uniform deposition and complete saturation of the liquefiable layer through the standing water. The phreatic surface, in each test, was located at the surface of the liquefiable layer. Figure 3-10 presents the soil model with the dense layer constructed and saturation completed and prior to construction of the liquefiable layer by means of pluviation through water.

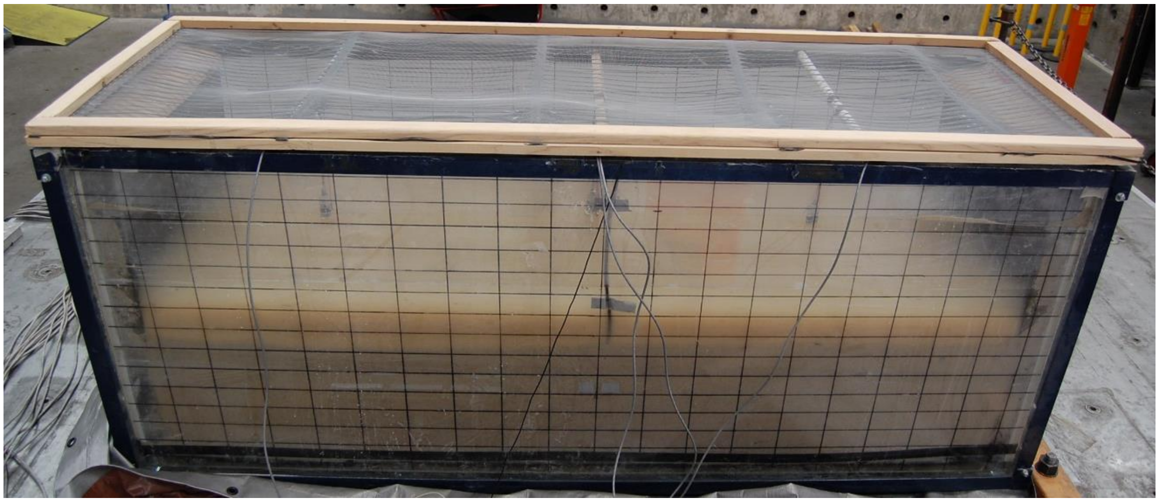

Figure 3-10: Soil Tank with Prepared Saturated Dense Layer Prior to Placement of Liquefiable Layer.

3.6 Instrumentation

Each experiment utilized a combination of instrumentation to assess behavior in ground acceleration, generation of excess pore water pressures and settlement behavior of model buildings. Table 3-1 summarizes the type, model number and quantity of instrumentation used during the final configuration of the experimental evaluations. Input and model accelerations were measured using a single-axis accelerometer capable of accelerations of up to 4g. Porewater pressure was measured using a pressure sensor cell modified to withstand submersed conditions. The pressure cell was housed in a plastic cylinder and waterproofed using a clear silicon glue. As an additional precaution, each sensor was then inserted into a thin membrane finger-cot. Displacement of model structures during testing was measured using a LVDT and is capable of measuring displacements up to approximately 4 inches. Figures 3-11 through 3-13 present the instrumentation used in the experimental evaluations and summarized in Table 3-1.

Table 3-1: Instrumentation used in Experimental Evaluation

Instrument Type	**Make**	**Model No.**	**Quantity**
Accelerometers	Memsic	CXL04GP1	6
LVDT	Novotechnik	TR-0100	3
Pressure Cells	Baystar Electrument	BH19MM	4

Figure 3-11: Memsic Accelerometers used in Experimental Evaluations.

Figure 3-12: Pressure Sensor Cells used in Experimental Evaluations.

Figure 3-13: Typical LVDT used in Experimental Evaluations.

The following schematic presented in Figure 3-14 shows the orientation of each instrument for each experimental configuration. The schematic includes two distinct soil layers differentiated by relative density and two model footings on either end with the free-field condition located at the center.

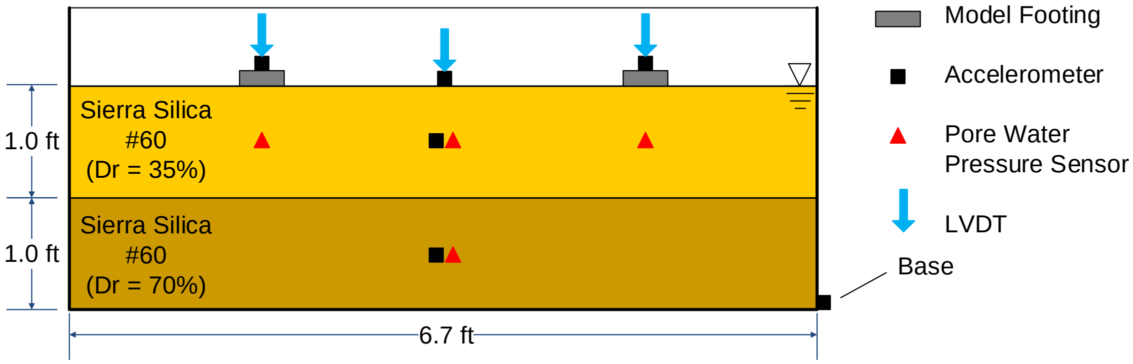

Figure 3-14: Schematic of Soil Profile and Instrumentation Layout

3.6 Foundation Models

3.6.1 Model Rigid Shallow Foundations

The model structures used in each experiment consisted of circular concrete footings of an equivalent approximate contact pressure of 12.5 psf. Model contact pressures were based on the average loading combinations (dead and live load) for a single family residence of approximately 125psf (Perko, 2009). Further discussion on scale of the model contact pressure was discussed in chapter 2 under similitude and further in Chapter 4. These footings represented the model buildings for two scenarios (1) unsupported rigid mat foundation (2) rigid mat foundation supported on helical piles. Figure 3-15 presents the range in foundation model sizes utilized in the experiments. Foundation model sizes included in the experimental evaluations were 3, 4.5, 6, 8 and 10-inch in diameter. The models supported by helical piles are aligned along the bottom portion of the figure. To maintain consistent measurement of building settlement, each model was marked to note north, east, south and west corners. In addition, one model was embedded with steel spacers which allowed each model to be supported on helical piles which are discussed in the following section. One accelerometer was secured to each footing in addition to a frictionless plate used to accommodate the needle on the displacement transducer.

Figure 3-15: Foundation Models Utilized in the Experiments

3.6.2 Model Helical Pile Foundations

Some experiments evaluated settlement of model structures founded on helical piles. Helical piles consist of a slender shaft and contain a helix at the tip. These piles are advanced into the ground by application of torque to a target depth, usually a more competent bearing layer. Figure 3-16 presents the model helical piles used in our experiments. Each helix was constructed using a 3-dimensional (3D) printer located at the University of Nevada, De La Mare Library. Use of a 3D printer ensured fabrication of true helices. These helices were secured to a solid aluminum shaft using a heavy grade clear epoxy capable of withstanding saturated conditions. Each helical pier was advanced to target depth into the model subsurface using a drill set to a nominal torque setting. The model footing with steel sleeves could then be placed over the aluminum shafts. Small rubber O-rings were placed over each shaft and used to secure the model structure to each shaft. Each helical pile was 22 inches in length to accommodate different bearing depths based on liquefiable layer thickness and was equipped with a single 1.2-inch diameter helix at the tip.

Figure 3-16: Model Helical Pile Foundations Utilized in the Experiments

3.6.3 Model Similitude

Our model was configured using the similitude laws defined by Iai (1989) and presented in Chapter 2. Each experiment assumed a scaled factor of similitude equal to 10. Our scaled model factors are presented below in Table 3-2.

Table 3-2: Similitude Laws for 1-g Shake Table Tests (λ = 10, scaling ratio in this study)

Variable		**Model**	**Prototype**
Length	**x**	$^{1}/_{\lambda}$	1
Density of Soil/Water	**ρ**	1	1
Strain of Soil	**ε**	$^{1}/_{\lambda\ 0.5}$	1
Time	**t**	$^{1}/_{\lambda\ 0.75}$	1
Total and Effective Stress	**σ** **σ'**	$^{1}/_{\lambda}$	1
Pore-Water pressure	**p**	$^{1}/_{\lambda}$	1
Acceleration	**ü**	1	1
Flexural Rigidity	**EI**	$^{1}/_{\lambda\ 3.5}$	1
Longitudinal Rigidity	**EA**	$^{1}/_{\lambda\ 1.5}$	1

Table 3-3 presents the similitude for material properties used to construct the helical piles and implemented in the experimental evaluations. Solid aluminum rods were chosen in lieu of aluminum tubing to more closely match flexural and longitudinal rigidity in similitude.

Table 3-3: Material Properties of Helical Pile Foundation

Material	Aluminum
Height (in)	22
Diameter (in)	0.375
E (ksi)	10,000
I (in^4)	0.00097

Material properties for the helices on each helical pile are not presented. Specific material properties of the plastic used to print each 3D helix were not known and thus similitude could not be determined.

3.6.4 Model Static Bearing Capacity

Bearing capacity was determined for our benchmark model foundation. The benchmark foundation was 6-inches in diameter. Our calculation used the following equation 3.1 suggested by Meyerhof in determination of the general bearing capacity (Das 2015).

$$q_u = c'(Nc)Fcs(Fcd)Fci + q(Nq)Fqs(Fqd)Fqi + \left(\frac{1}{2}\right)\gamma(B)N\gamma(F\gamma s)F\gamma d(F\gamma i) \tag{3.1}$$

c’ = cohesion
q’ = effective stress at the level of the bottom of the foundation
γ = unit weight of soil
B = width of foundation (or diameter for a circular foundation)
Fcs, Fqs, Fγs = foundation shape factors
Fcd, Fqd, Fγd = foundation depth factors
Fci, Fqi, Fγi = foundation inclination factors
Nc, Nq, Nγ = bearing capacity factors

Our calculation assumed the footing was founded directly on the ground surface with no depth of embedment. It also assumed that the water table was located at the surface. An angle of internal friction for the cohesionless sand in our model was assumed to be 30 degrees.

The ultimate static bearing capacity of our benchmark model was determined to be approximately 180 psf. A factor of safety of 3 was used to determine an allowable bearing capacity. The allowable bearing capacity is 60 psf, which is greater than our model footing contact pressure.

3.7 Experimental Testing Input Motions

In addition to all instrumentation, all testing was documented by means of photographs and video. Initial and final conditions of each test included photos in profile and plan view as well as video in profile and plan view.

3.7.1 Manual Shaking

Experimental evaluations #1 through 9 and #30 through 52 were conducted using input motions generated by means of manual shaking. Each experiment completed using methods of manual shaking had a predominant frequency that ranged between 3-4 Hz.

3.7.2 Eccentric Mass Shaker

Experimental evaluations #10 through 29 were conducted using input motions generated by the eccentric mass shaker. Each experiment completed using the eccentric-mass shaker had a predominant frequency that ranged between 4-5 Hz.

3.7.3 Earthquake Engineering Laboratory (EEL)

Experimental evaluation #53 was conducted using input motions generated by the biaxial shake table located in the EEL. The biaxial shake table utilized a historic earthquake record, commonly used in seismic testing and evaluations. We used the El Centro 1979 record and scaled it to 0.25g. It is important to note that because we only performed one test on the biaxial shake table, we were not able to calibrate the table to achieve a perfectly scale input motion. As a result our input motion was slightly larger.

Chapter 4 Experimental Program

4.1 Model Configuration and Preparation

Our initial model configuration was derived from a project located in South Lake Tahoe, Nevada (Figure 4-1). Project specific information was provided by the local foundation design company VersaGrade (a subsidiary of RamJack) and is located in Sparks, Nevada. The Landing Resort and Spa (formerly the Edge Resort and Spa) was undergoing facility upgrades and facility improvements to existing structures. These upgrades consisted of construction of a new one-to-two story resort administration building and an additional two story maintenance building. In the project geotechnical report, completed by HEM Consulting, LLC., liquefaction susceptible soils were identified within the project footprint. Subsurface investigations noted considerable clean deposits of loose coarse grained sand with a relatively shallow water table (approximately 2.5ft below ground surface). Using the boring logs and subsurface conditions encountered, we created a generalized geologic profile. The profile was used to identify a probable “worst case condition” of liquefaction susceptibility consisting of a loose, saturated ten-foot thick deposit of coarse sands. As a result, our model configuration adopted a basic profile consisting of similar conditions, however for simplicity the water table was located at the ground surface. For simplicity we assumed a ten-foot thick liquefiable layer over an equal non-liquefiable layer. Figure 4-2 presents the configuration of our soil model used for 1-g shake table testing. The model utilized a scaled factor of 10 for our experiments. Each experiment was constructed and prepared as described in Chapter 3.

Figure 4-1: Location of "The Landing Resort" Adjacent to Beach in South Lake Tahoe, NV (Google Earth, 2016).

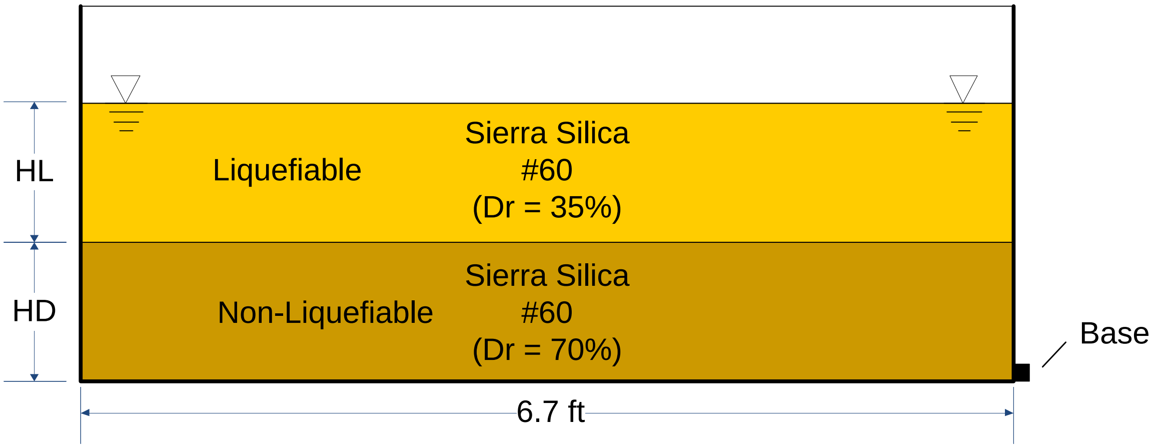

Figure 4-2: Profile View of Soil Model Configuration for 1-g Shake Table Testing

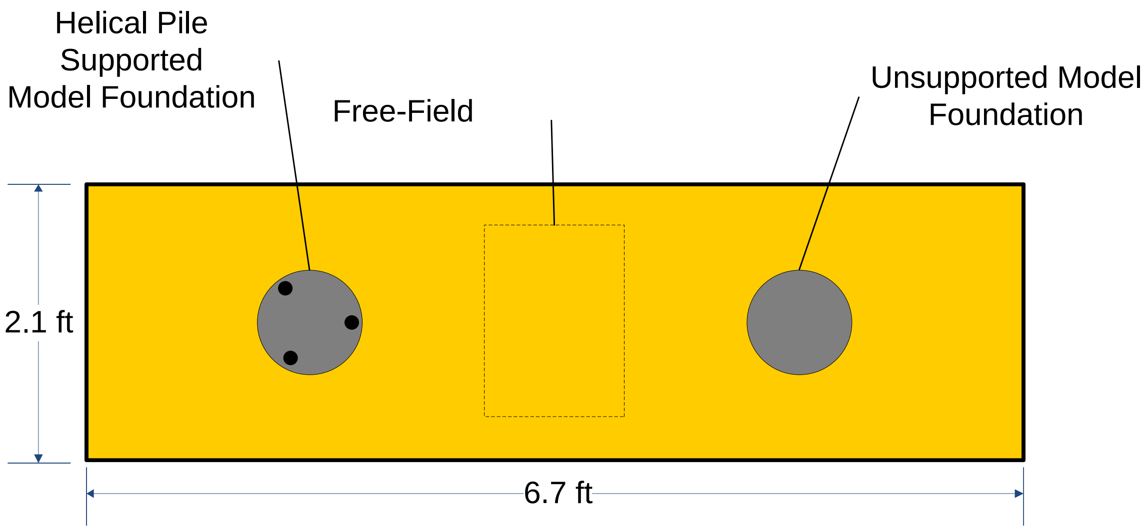

Figure 4-3: Plan View of Soil Model Configuration for 1-g Shake Table Testing

4.2 Phase 1 - Initial Testing and Model Calibration

Initial testing and model calibration consisted first of determining the properties of the Sierra Silica #60 Mesh and selecting relative densities that were representative of loose and dense sands for our liquefiable and non-liquefiable soils. Typically, liquefaction susceptibility increases as the relative density decreases in granular (cohesionless) soils.

For our liquefiable soil, we chose a target relative density of 35% and for our non-liquefiable soil we chose a target relative density of 70%. Table 4-1 presents the general variation of relative density compared to denseness of soils. Based on Table 4-1, our liquefiable layer ranged from loose to medium and our non-liquefiable layer was considered dense.

Table 4-1: Denseness of Granular Soil (Das 2015)

Relative Density, Dr (%)	Description
0-15	Very Loose
15-35	Loose
35-65	Medium
65-85	Dense
85-100	Very Dense

Relative Density

$$Dr\ (\%) = \frac{emax - e}{emax - emin} \qquad (4.1)$$

Dry Unit Weight

$$\gamma d = \frac{Gs * \gamma w}{1 + e} \qquad (4.2)$$

Saturated Unit Weight

$$\gamma sat = \frac{(Gs + e) * \gamma w}{1 + e} \qquad (4.3)$$

Equation 4-1 was used to determine the approximate void ratio of our testing medium for each target relative density of 35% and 70%. For our calculations we utilized the e_{max} and e_{min} presented in Chapter 3. Each corresponding void ratio could then be used to determine the dry unit weight of each model layer within the configuration (equation 4.2). Equation 4.3 was utilized when calculating the effective stress parameters to use for estimation of pore pressure ratios (Ru) equation 4.4.

Pore Pressure Ratio

$$\mathrm{Ru} = \frac{\sigma'(excess\_pwp)}{\sigma'} \qquad (4.4)$$

Table 4-2 presents the estimated void ratio, relative density, saturated and dry unit weights of sand utilized to construct the model layers.

Table 4-2: Soil Model Properties

Relative Density (D_r)	**Void Ratio (e)**	**γ_{sat} (pcf)**	**γ_d (pcf)**
25%	0.940	115.47	85.24
35%	0.912	116.25	86.58
45%	0.884	117.05	87.77
55%	0.856	117.87	89.09
70%	0.814	119.16	91.16

Note: Relative Densities and subsequent void ratios based on e_{max} = 1.01 and e_{min} = 0.73.

Our initial model evaluations #1 through 9, were conducted to develop experimental methods that were both consistent and repeatable. Each model evaluation consisted of a one-foot thick non-liquefiable layer overlain by a one-foot thick liquefiable layer. Only accelerometers were utilized during the first series of tests. The first series of tests included rough model buildings and excluded the use of helical piles. Figure 4-4 is a typical representation of our series of calibration models (Tests 1 through 9). The figure includes a model building (background) and free-field area (forefront), each equipped with an accelerometer.

The initial phase of our testing posed three significant challenges to overcome. The first became evident during the saturation portion of constructing the liquefiable layer. As water inundated the soil tank, the water began to creep between the lexan walls and rub sheets creating a large void of water between the rub sheet and lexan wall. When shaking commenced, the void collapsed, thus generating the large cracks in the soil surface as seen in Figure 4-4. This issue was remedied by placing multiple rows of clear double sided tape in between the lexan walls and rub sheets. The second issue observed were large deformations generated on either side of the soil tank. These deformations were a result of boundary effects generated by the direction of excitation and lack of damping at either end of the tank. These effects can also be seen in Figure 4-4. The boundary effects were reduced by placing 3-inch thick high density foam pads along the entire space of the soil tank at each end (Figure 4-5). Lastly, the gridlines observed on the soil tank in profile were intended to use as guides in creating a visual representation of the soil profile as it deformed during seismic induced liquefaction. Numerous attempts were made to create those grids within the soil profile using a colored sand of the same gradation. It was nearly impossible to place the colored sand below the water table in a clean orderly fashion thus matching the existing gridlines or baselines. All attempts to locate a matching colored sand or produce a colored sand of equal gradation fell short of the goal. Attempts at implementing colored sand delineators are presented in Figure 4-6. As a result, only the surface of the model was noted, before and after testing, depicting degree of settlement using dry erase markers.

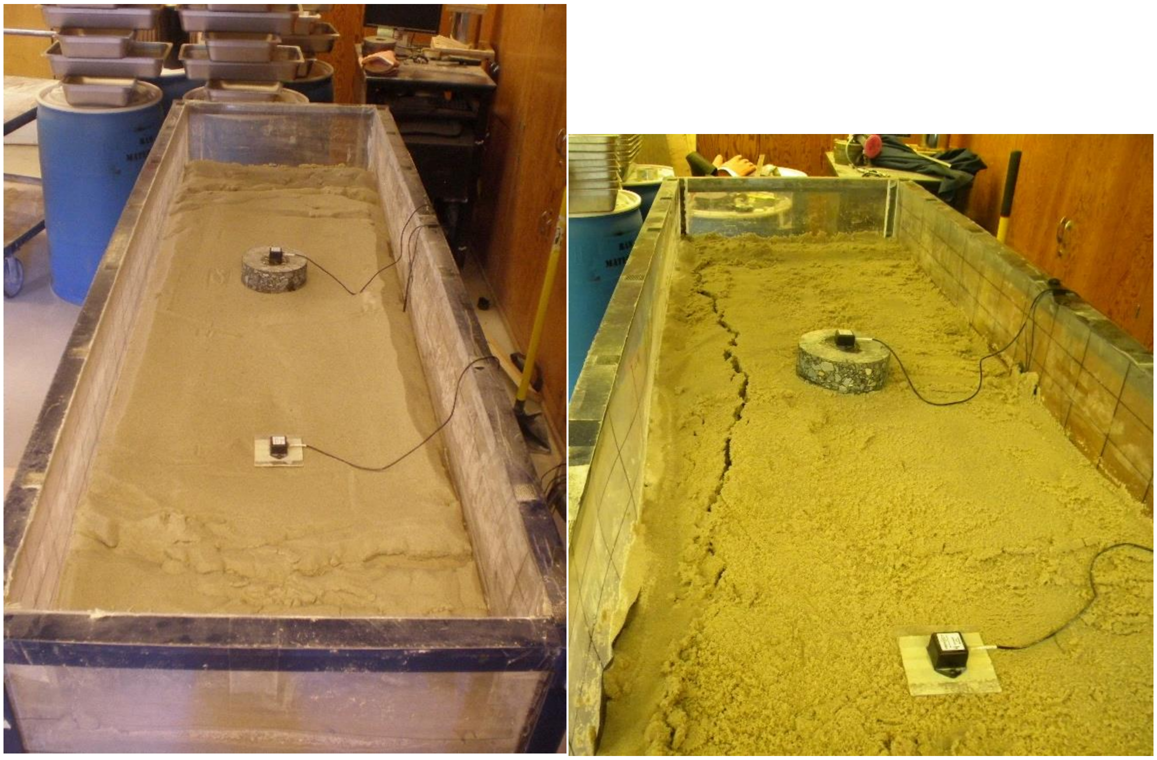

Figure 4-4: Phase 1 Boundary Effect Model Deformations

Figure 4-5: High Density Foam for Boundary Effect Reduction

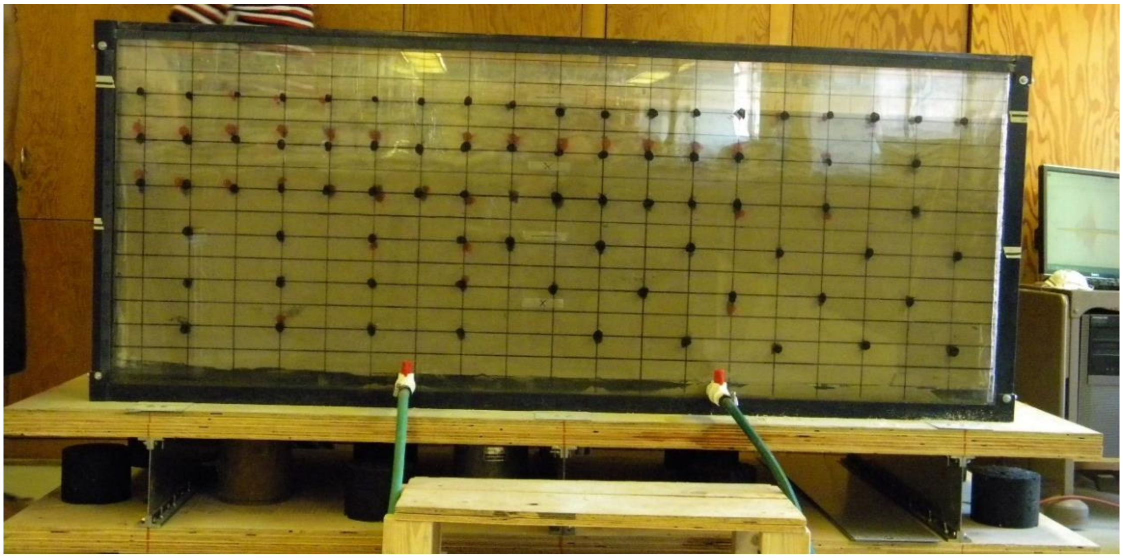

Figure 4-6: Phase 1 Typical Soil Tank Profile with Colored Sand Delineators

Figures 4-7 through 4-8 present the typical measured soil model accelerations and liquefaction-induced settlement for Phase 1 testing. Each experiment included accelerometers at the base of the model, center of each layer (liquefiable and non-liquefiable) as well as the surface (model building and free-field.) Each record is labeled according to their respective soil model depth.

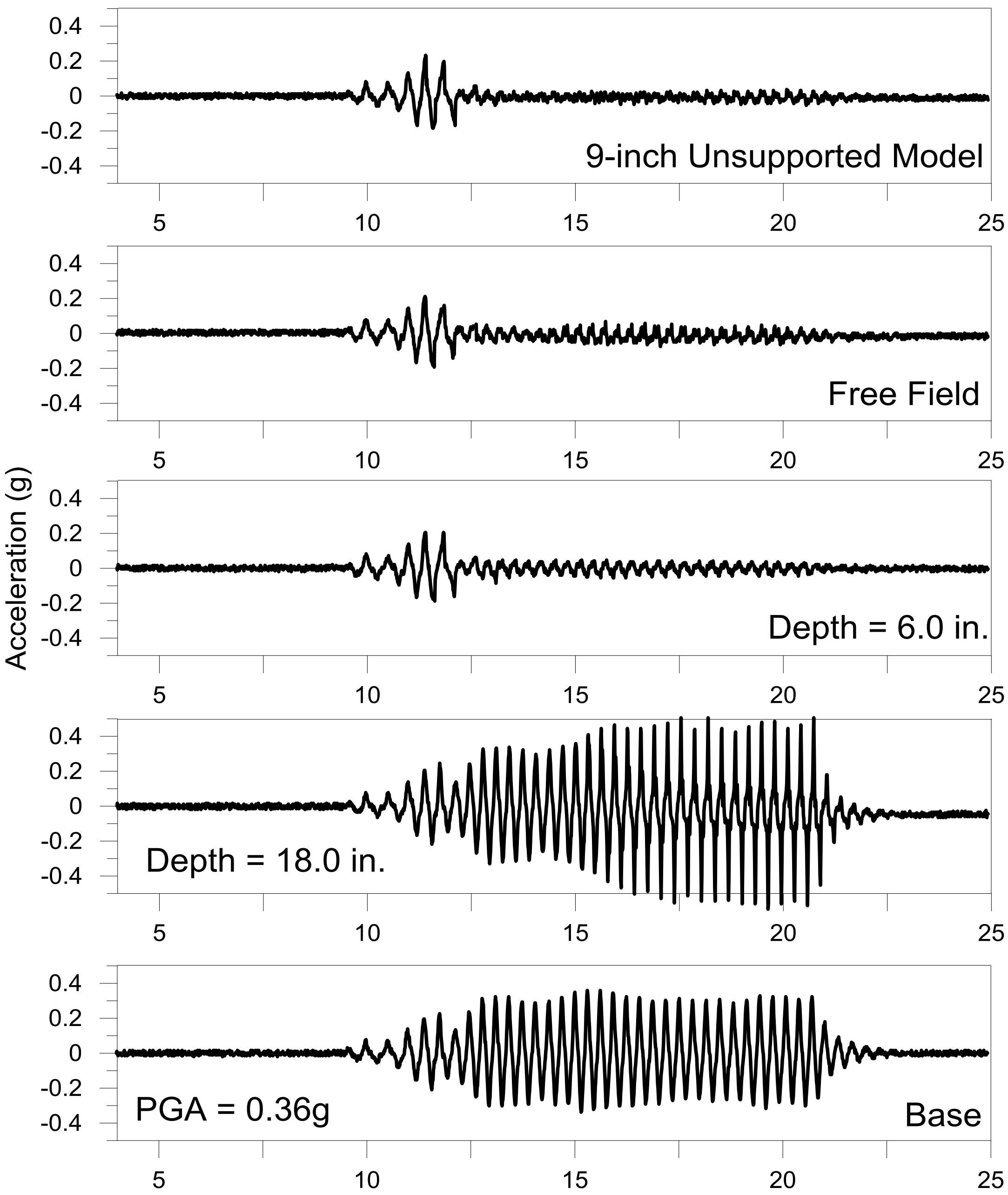

Figure 4-7: Test #9 – Soil Model Accelerations

The hand measured surficial settlements are presented below in Figure 4-8. Each experiment included manual measurement of the settlement using a fixed reference point to the surface of the soil model. Measurements were made using a grid pattern across the plan of the soil model before model excitation and post-liquefaction.

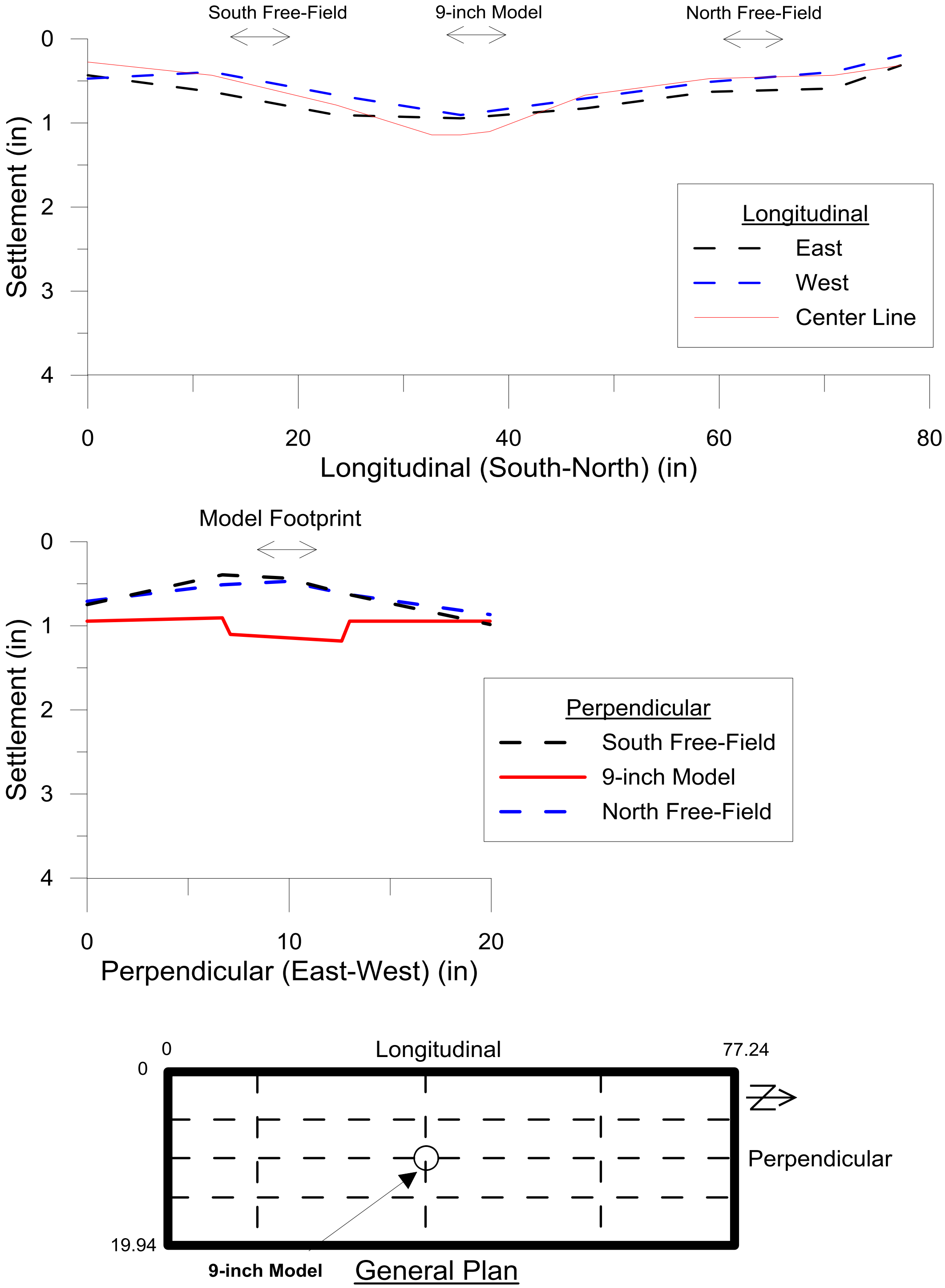

Figure 4-8: Test #9 – Observed Soil Model Settlement (Manually Measured)

Table 4-3 is a summary of the Phase 1 testing and includes basic model information regarding configuration parameters of each model. Appendix A presents plots of measured data for all experiments. A more comprehensive summary Table of all experiments is presented in Appendix B.

Table 4-3: Summary of Phase 1 Experimental Program

Test	**Date**	**Base PGA**	**Relative Density of Liquefiable**	**HL / HD**	**Foundation Diameter**	**Accelerometers**	**Pressure Sensors**	**LVDT**
#	**(m/d/yr)**	**(g)**	**(D_r)**	**(ft)**	**(ft)**	**No.**	**No.**	**No.**
1	8/12/15	0.23	35	1/1	0.75	--	--	--
2	8/20/15	0.22	35	1/1	0.75	--	--	--
3	8/25/15	0.44	35	1/1	--	--	--	--
4	9/4/15	0.03	35	1/1	--	--	--	--
5	9/18/15	0.36	35	1/1	0.5	4	--	--
6	9/25/15	0.40	35	1/1	0.5	5	--	--
7	10/2/15	0.44	35	1/1	0.5	5	--	--
8	10/7/15	0.38	35	1/1	0.5	5	--	--
9	10/30/15	0.36	35	1/1	0.75	5	--	--

4.3 Phase 2 - Eccentric Mass Vibrator Testing

Eccentric Mass Vibrator Testing was utilized in an effort to produce consistent repeatable results. However, limitations in the peak horizontal force the shaker could induce prevented us from conducting experiments using thicker 1 foot liquefiable and non-liquefiable layers. As a result, we decreased the thickness of the model layers to 0.5 foot in thickness. Testing included the use of model buildings more representative of a 1-2 story home and began to incorporate the use of a pressure sensor to monitor behavior of pore water pressure. Helical piles were not utilized during this series of testing. Figures 4-9 and 4-10 presents a typical model profile of our evaluations that utilized an eccentric mass shaker. Note the high density foam pads on each end of the soil tank to reduce boundary effects. All testing was performed using layers that were 0.5-feet in thickness. Locations of buried instrumentation are marked on the face of the soil tank and are denoted using the symbol “x” while horizontal lines symbolize both the non-liquefiable and liquefiable layers. Figure 4-9 shows a similar model configuration to Phase 1 with one model structure and accelerometer to monitor behavior in the free-field. Note the strings across the top portion of the soil tank in Figure 4-10. These strings were used in every model configuration and served as the grid pattern for manual measurement of liquefaction-induced settlement.

Figure 4-11 presents the measured soil model accelerations and includes the pore pressure ratio at the center of the liquefiable layer in the free-field environment. Figure 4-12 presents the results of the hand measured liquefaction-induced settlements for both free-field and model building foundation. Figure 4-13 presents the estimated spectral accelerations determined from filtered data using the Seismic analysis software Seismosignal. Tests 10 through 29 were performed using an eccentric-mass shaker and a summary of each configuration is presented in Table 4-4.

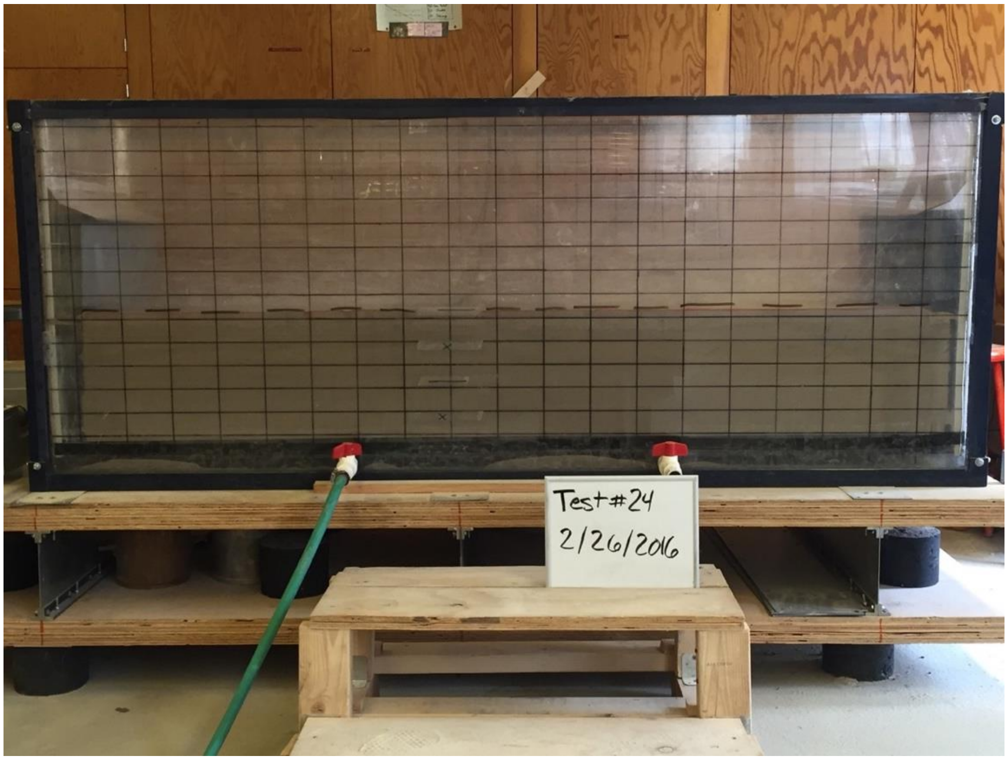

Figure 4-9: Test #24 Prior to Shaking

Figure 4-10: Test #24 prior to Shaking

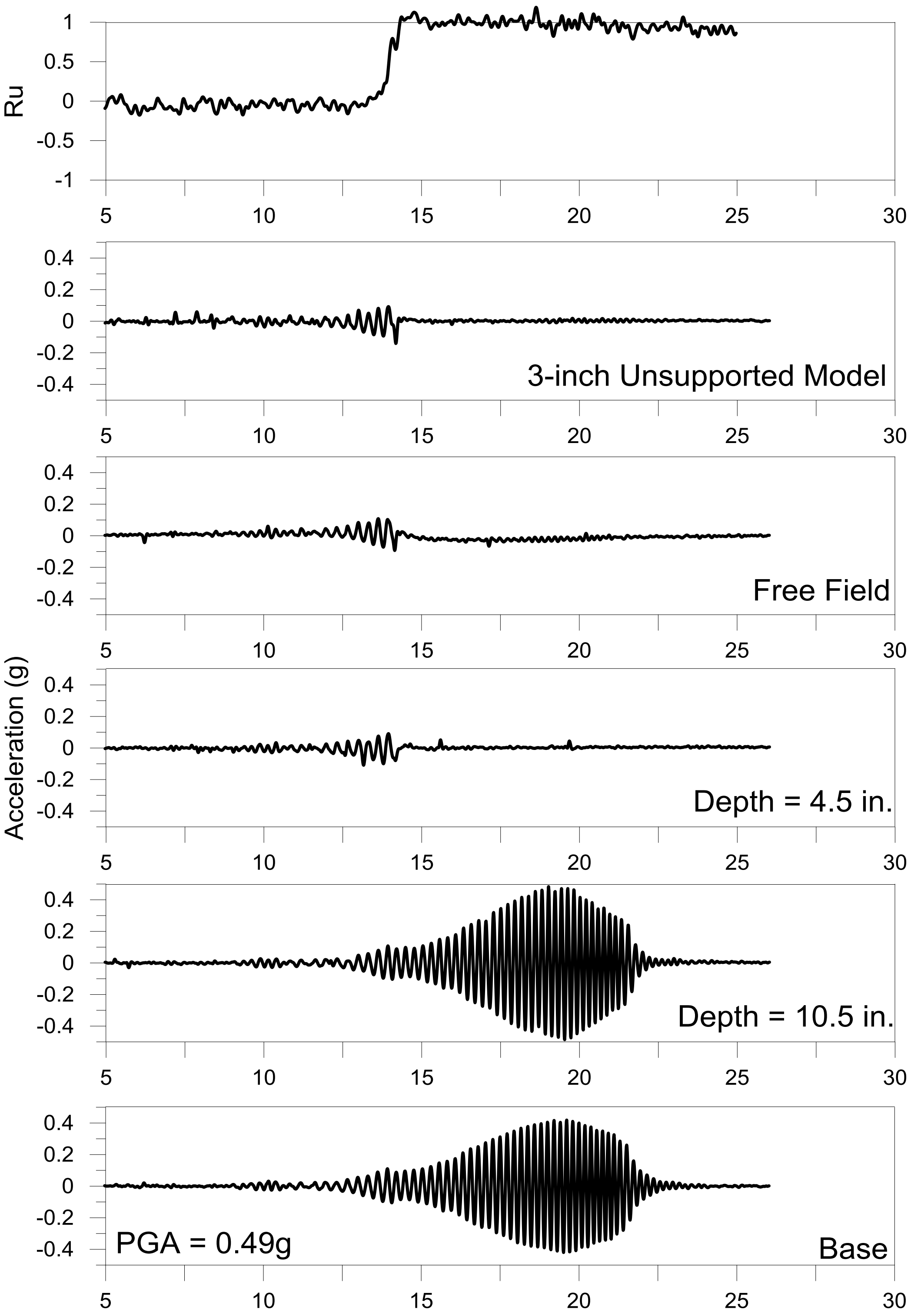

Figure 4-11: Test #27 – Soil Model Accelerations and Pore Pressure Ratio.

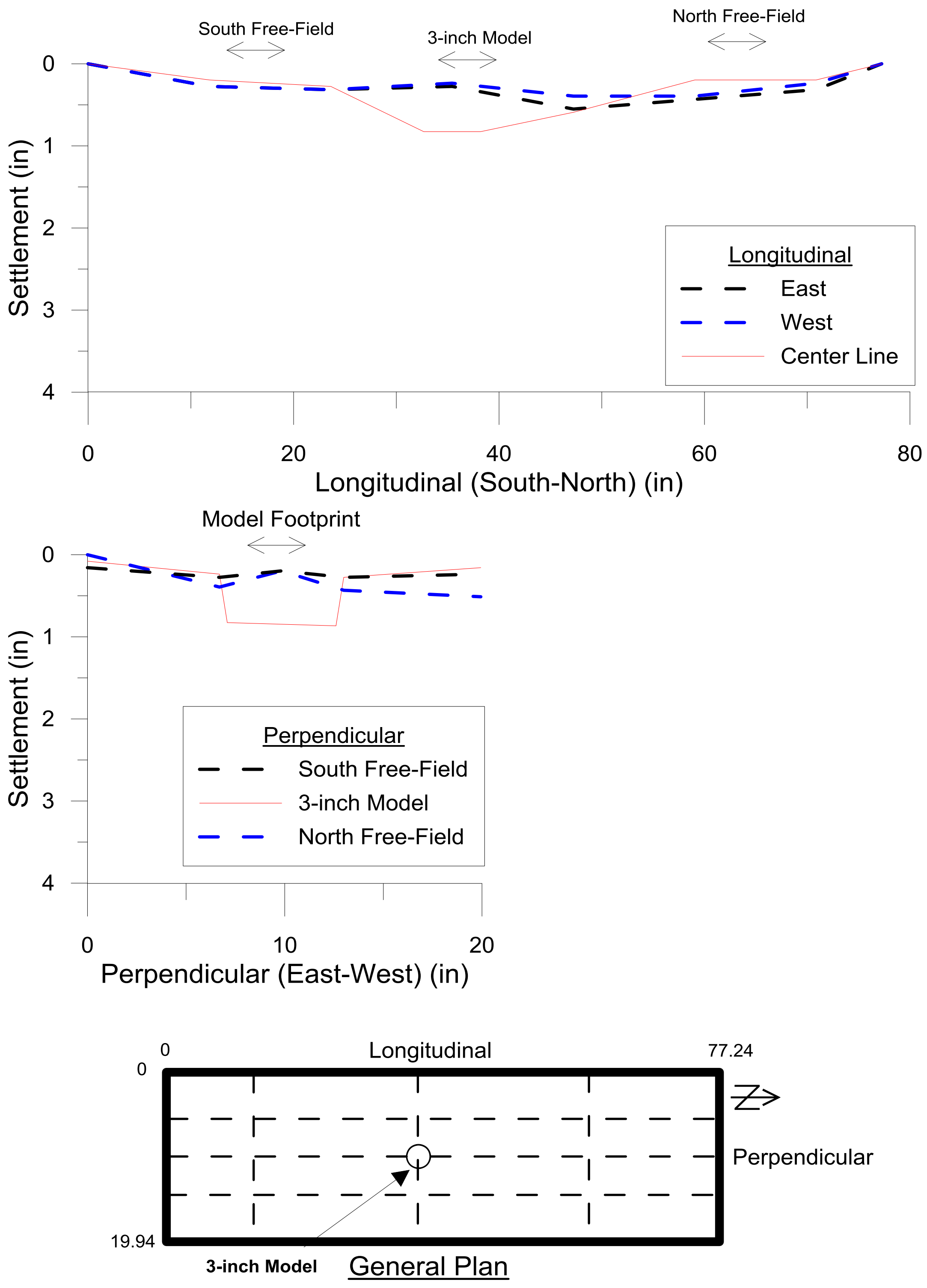

Figure 4-12: Test #27 – Observed Soil Model Settlement (Manually Measured)

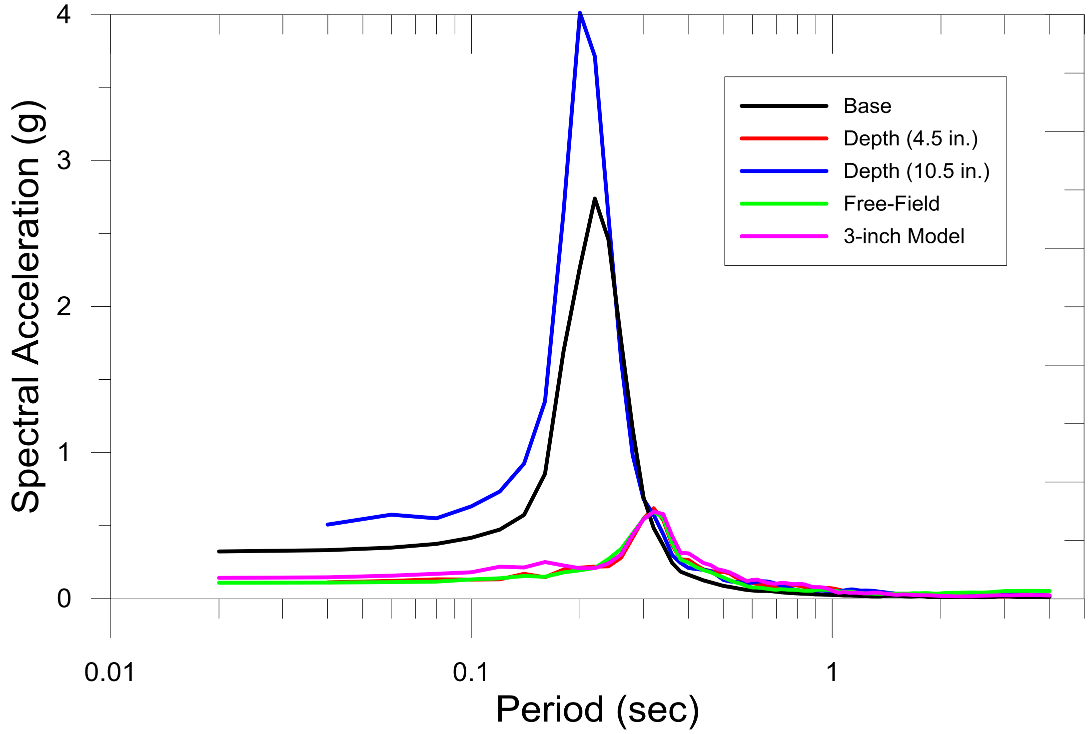

Figure 4-13: Test #27 – Estimated Spectral Accelerations

Table 4-4: Summary of Phase 2 Experimental Program

Test	Date	Base PGA	Relative Density of Liquefiable	HL / HD	Foundation Diameter	Accelerometers	Pressure Sensors	LVDT
#	**(m/d/yr)**	**(g)**	**(D_r)**	**(ft)**	**(ft)**	**No.**	**No.**	**No.**
10	11/6/15	0.31	35	1 / 1	0.5	5	--	--
11	11/13/15	0.30	35	0.5 / 0.5	0.5	5	--	--
12	11/20/15	0.33	35	0.5 / 0.5	0.5	5	--	--
13	12/1/15	0.30	35	0.5 / 0.5	0.5	5	1	--
14	12/8/15	0.20	35	0.5 / 0.5	0.5	5	1	--
15	12/11/15	0.16	35	0.5 / 0.5	0.5	5	--	--
16	12/15/15	0.17	35	0.5 / 0.5	0.5	5	--	--
17	12/18/15	0.17	35	0.5 / 0.5	0.5	5	--	--
18	1/5/16	0.39	35	0.5 / 0.5	0.5	5	--	--
19	1/8/16	0.37	35	0.5 / 0.5	0.5	5	--	--
19.1	1/22/16	0.36	35	0.5 / 0.5	0.5	5	--	--
19.2	2/5/16	0.34	35	0.5 / 0.5	0.5	5	1	--
20	1/12/16	0.36	35	0.5 / 0.5	0.5	5	--	--
21	1/14/16	0.37	35	0.5 / 0.5	0.5	5	--	--
22	1/20/16	0.34	35	0.5 / 0.5	0.67	5	--	--
22	2/12/16	0.34	35	0.5 / 0.5	0.67	5	1	--
23	2/19/16	0.33	35	0.5 / 0.5	0.83	5	1	--
24	2/26/16	0.34	35	0.5 / 0.5	1	5	1	--
25	3/1/16	0.33	35	0.5 / 0.5	0.25	5	1	--
26	3/9/16	0.37	35	0.5 / 0.5	0.375	5	1	--
27	3/16/16	0.49	35	0.75 / 0.25	0.25	5	1	--
28	3/18/16	0.44	35	0.75 / 0.25	0.375	5	1	--
29	3/24/16	0.5	35	0.75 / 0.25	0.5	5	1	--

4.4 Phase 3 - Manual Shaking Testing Results

Because of the limitations of the eccentric-mass shaker, testing reverted back to using the manual shaking method. This series of testing incorporated the final suite of instrumentation that included the use of 6-accelerometers, 4-pressure sensor cells and 3-LVDT’s as defined in the previous Chapter in Table 3-1. In addition, this series of testing utilized two model buildings; one unsupported rigid shallow foundation and one rigid shallow foundation supported on three-helical piles. Each model foundation was approximately equal in contact pressure. Tests #30 to 47 were performed using the helical pile and unsupported foundation configuration. Once it was established that helical piles provided a significant reduction in liquefaction-induced settlement, the use of helical piles was discontinued. The remaining Tests #47 through 52 were completed using unsupported model foundations of varying diameter. These tests were completed to better establish the relationship that foundation width has on degree of settlement. Figure 4-14 shows the final configuration of foundation models and instrumentation prior to testing for Phase 3. Figures 4-15 and 4-16 show the typical settlement observed during liquefaction evaluations. Figure 4-17 presents the soil model accelerations for Phase 3 experiments. Phase 3 include accelerometers on each model building foundation including the free-field environment. Figure 4-18 presents the pore pressure ratios located at the center of the non-liquefiable layer, and center of liquefiable layer located beneath each model building foundation and free-field environment. Figure 4-19 presents the estimate spectral accelerations and recorded model building settlement from LVDT’s. Figure 4-20 presents the manually measured settlements. Table 4-5 provides a summary of all Phase 3 experiments.

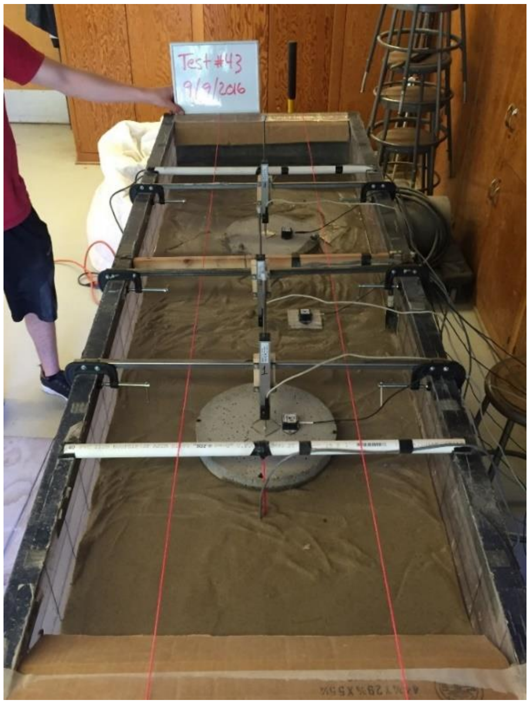

Figure 4-14: Test #43 Prior to Shaking

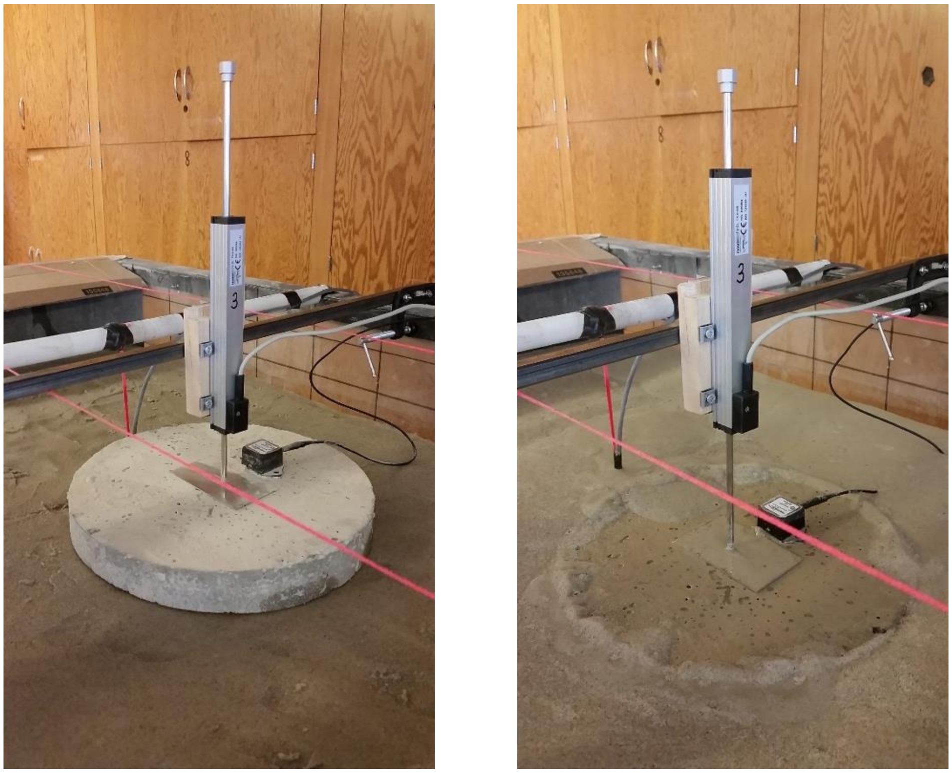

(a)

(b)

Figure 4-15: Test #52 Depiction of Settlement Resulting from Liquefaction (a) before and (b) after shaking.

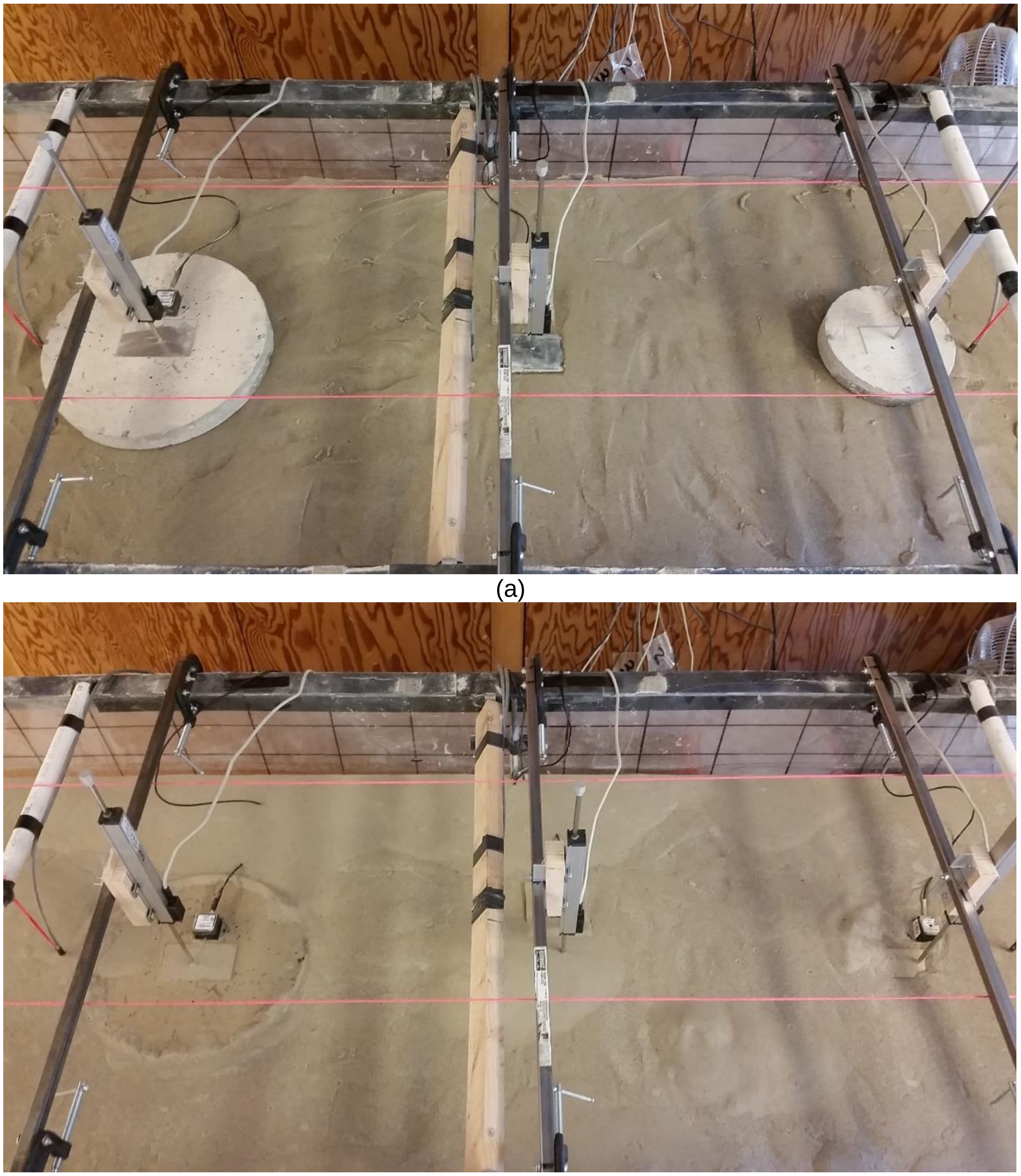

(a)

(b)

Figure 4-16: Test #52 Plan View of Settlement Resulting from Liquefaction for both Model Foundations (a) before and (b) after shaking.

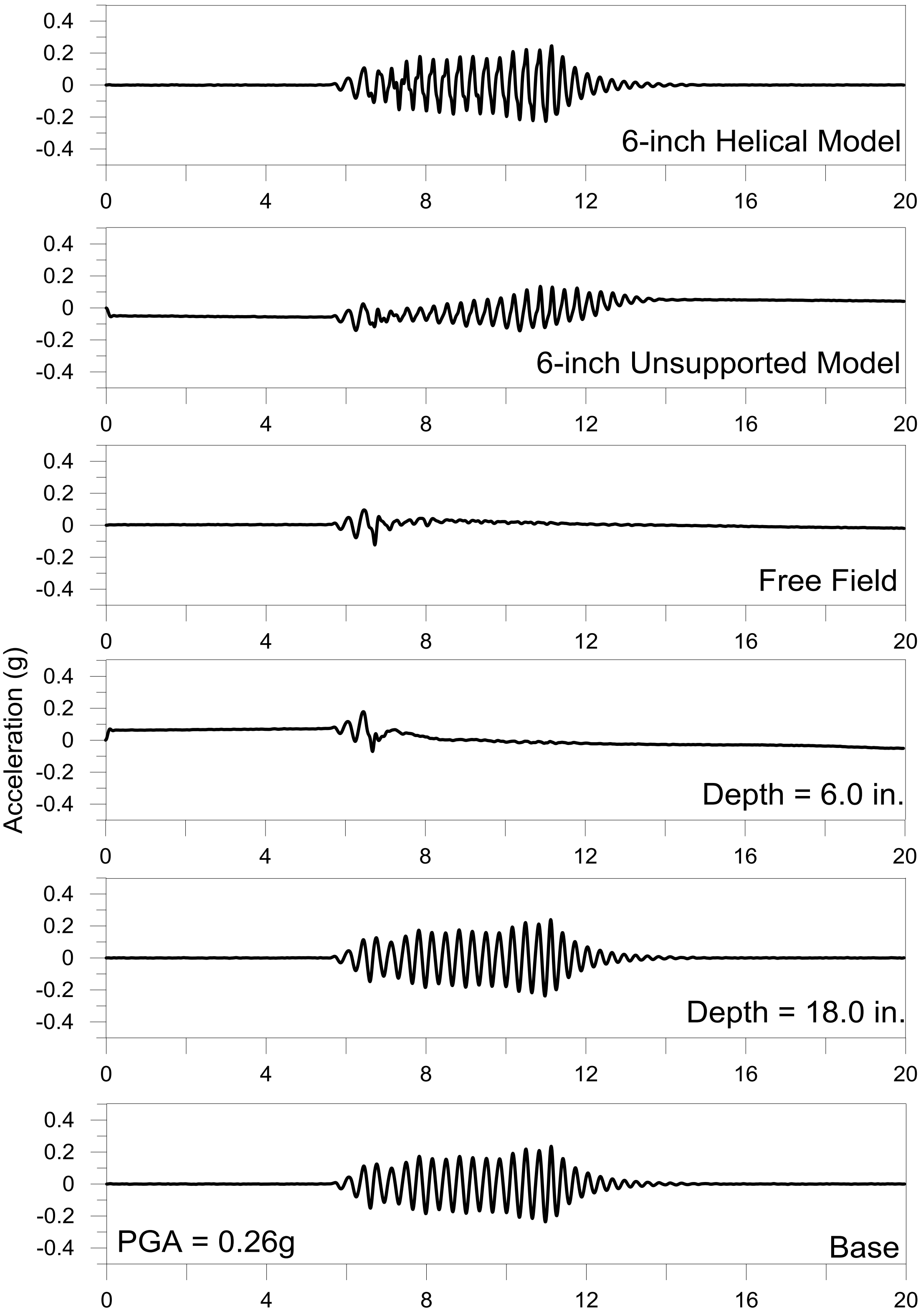

Figure 4-17: Test #38 – Soil Model Accelerations

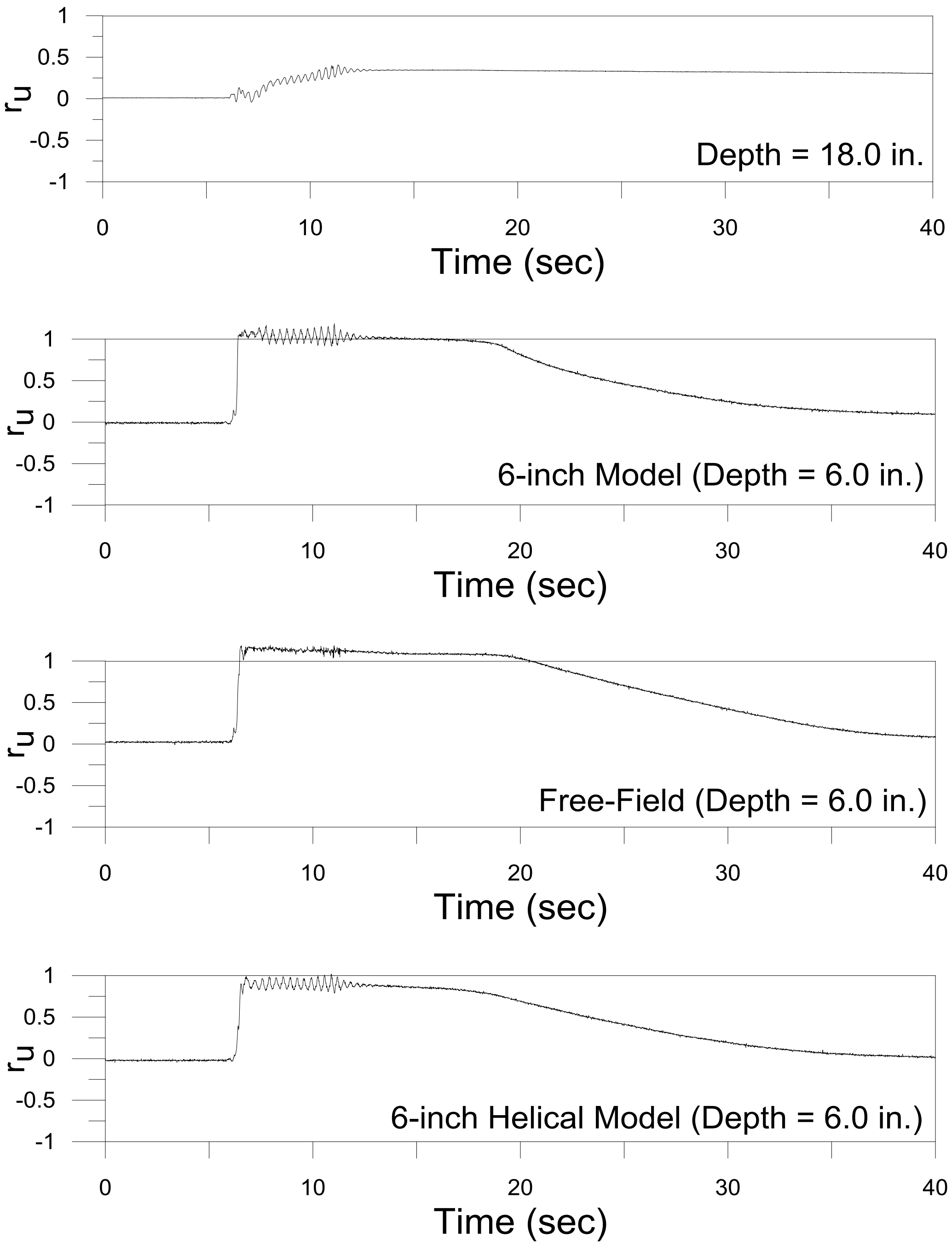

Figure 4-18: Test #38 – Observed Pore Pressure Ratios

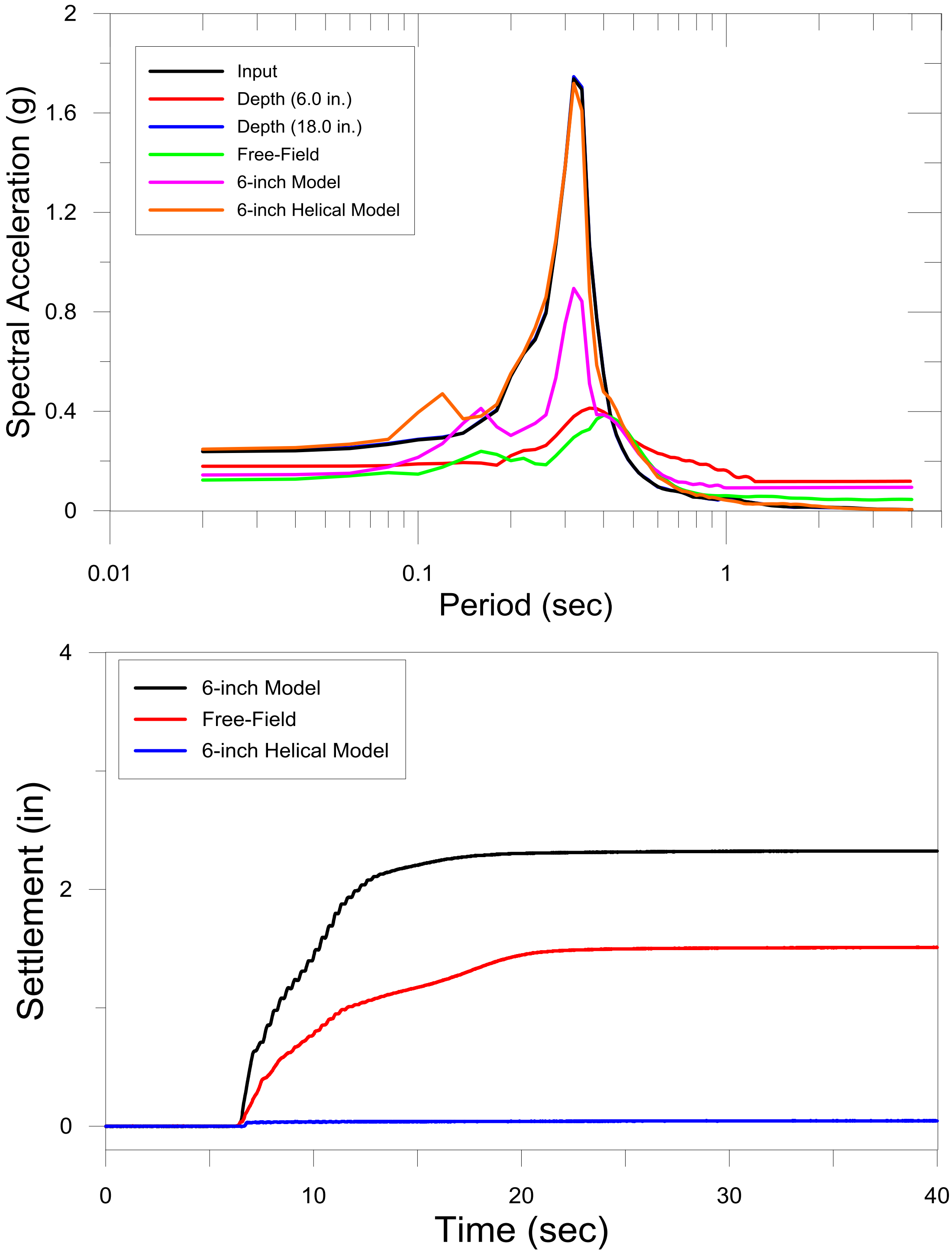

Figure 4-19: Test #38 – Estimated Model Spectra and Measured LVDT.

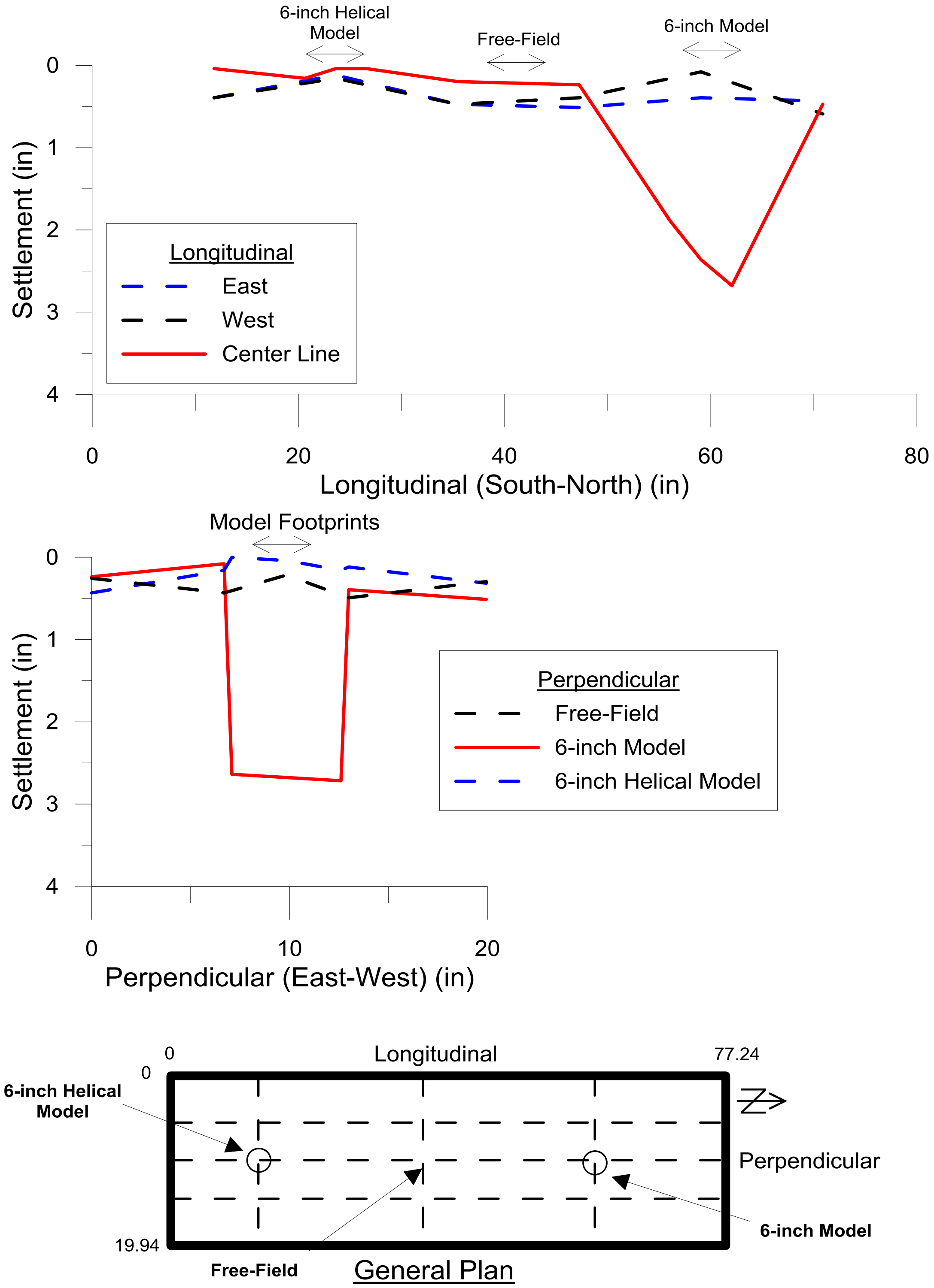

Figure 4-20: Test #38 – Observed Soil Model Settlement (Manually Measured)

Table 4-5: Summary of Phase 3 Experimental Program

Test	Date	Base PGA	Relative Density of Liquefiable	HL / HD	Foundation Diameter	Accelerometers	Pressure Sensors	LVDT
#	(m/d/yr)	(g)	(D_r)	(ft)	(ft)	No.	No.	No.
30	4/1/16	0.3	35	1 / 1	0.25	5	1	--
31	4/20/16	-	35	1 / 1	0.5	6	1	--
32	5/12/16	0.33	35	1 / 1	0.5	6	1	--
33	6/15/16	0.18	35	1 / 1	0.5	6	1	--
34	6/22/16	0.26	35	1 / 1	0.5	6	1	1
35	7/1/16	0.14	35	1 / 1	0.5	6	4	3
36	7/15/16	0.25	35	1 / 1	0.5	6	4	3
37	7/22/16	0.2	35	1 / 1	0.5	6	4	3
38	7/27/16	0.26	35	1 / 1	0.5	6	4	3
39	8/4/16	0.29	35	1 / 1	0.75	6	4	3
40	8/9/16	0.279	35	1 / 1	0.25	6	4	3
41	8/17/16	0.335	35	1 / 1	0.36	6	4	3
42	8/27/16	0.276	35	1 / 1	0.67	6	4	3
43	9/9/16	0.259	35	1 / 1	0.83	6	4	3
44	9/16/16	0.234	25	1 / 1	0.5	6	4	3
45	9/19/16	0.298	45	1 / 1	0.5	6	4	3
46	9/23/16	0.318	55	1 / 1	0.5	6	4	3
47	9/26/16	0.356	35	1.25 / 0.75	0.5	6	4	3
48	9/30/16	0.306	35	1.5 / 0.5	0.5 / 0.83	6	4	3
49	10/5/16	0.393	35	1.67 / 0.33	0.5 / 0.83	6	4	3
50	10/14/16	0.248	35	1 / 1	0.5 / 0.83	6	4	3
51	10/21/16	0.254	35	1 / 1	0.5 / 0.83	6	4	3
52	10/24/16	0.205	35	1 / 1	0.5 / 0.83	6	4	3

4.5 Phase 4 - EEL Validation (El Centro Input Record)

The final experiment was conducted on the biaxial shake table located in the EEL. Special care was taken to protect the large hydraulic actuators on the shake table from sand particulates by draping plastic sheeting over the areas where the actuators were exposed. The soil tank was lifted to the table surface and secured using dunnage that was anchored to the table surface. All instrumentation was channeled using the data acquisition system provided by the EEL. The model and placement of instrumentation was constructed using the same configuration as Tests #47 through 52. The EEL equipped the soil tank with GoPro cameras located at each condition representing foundations and free-field environment. An additional camera was placed at a distance away from the shake table to record performance of all the foundations in profile during excitation. Figure 4-21 presents Test #53 on the biaxial shake table prior to excitation. Figure 4-22 is a plan view of test #53 showing model building foundations situated on top of the liquefiable layer before testing.

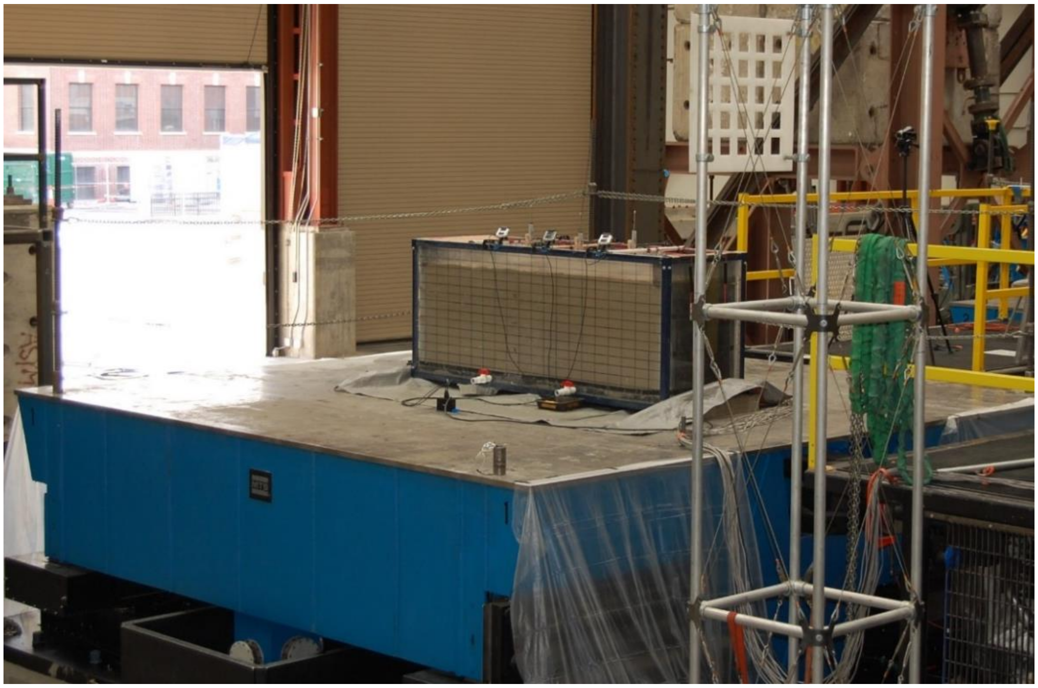

Figure 4-21: Test #53 Positioned on Biaxial Shaking Table

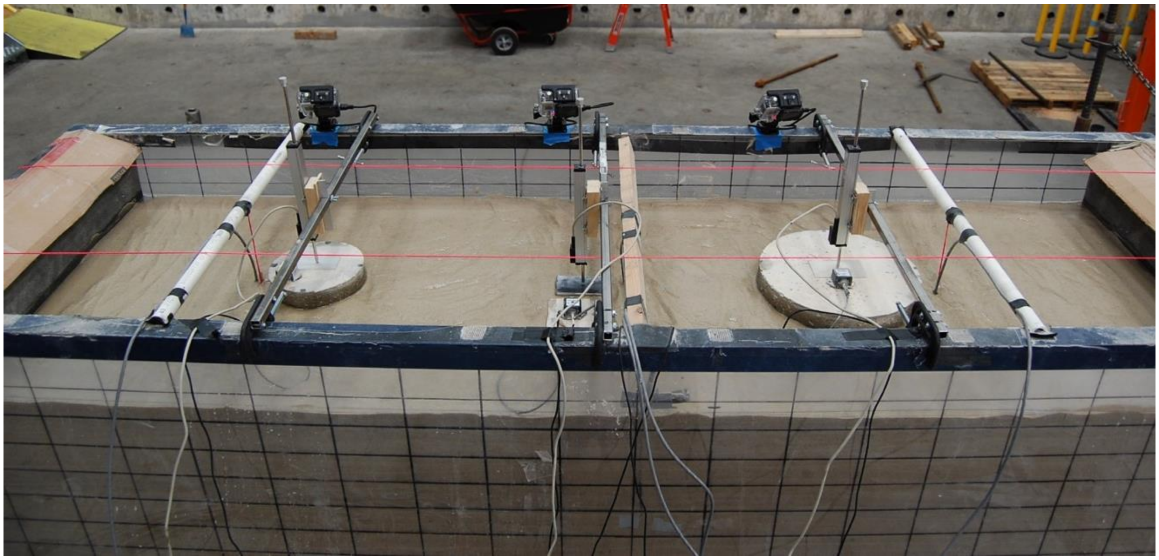

Figure 4-22: Test #53 Prior to Shaking

Figures 4-23 through 4-26 present the typical measured and observed recording similar to those presented for Phase 3 testing. Because of the characteristics of the input motion, including the ground motion duration, settlement was considerably greater than those observed during Phase 3 evaluations. Settlements recorded using the LVDT's do not present an accurate record of settlement. Settlement was so great during model excitation that the model building foundations settled beyond the limits of the LVDT's. In addition, at the beginning of ground motion input, the LVDT pin lost contact with the platform used to monitor free-field settlement and subsequently provided an exaggerated degree of settlement as shown in Figure 4-25. A summary of the model configuration is presented in Table 4-6.

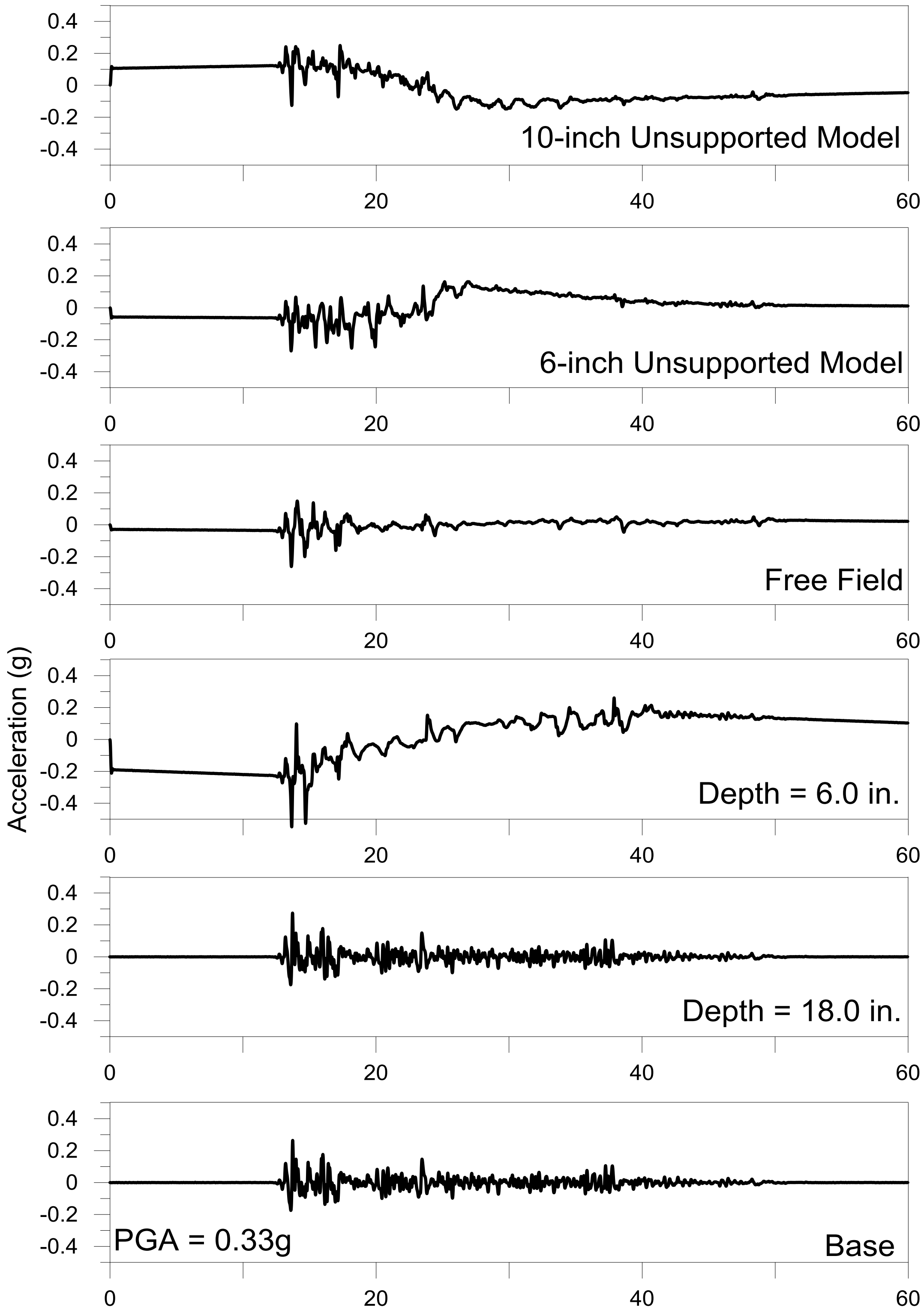

Figure 4-23: Test #53 – Soil Model Accelerations

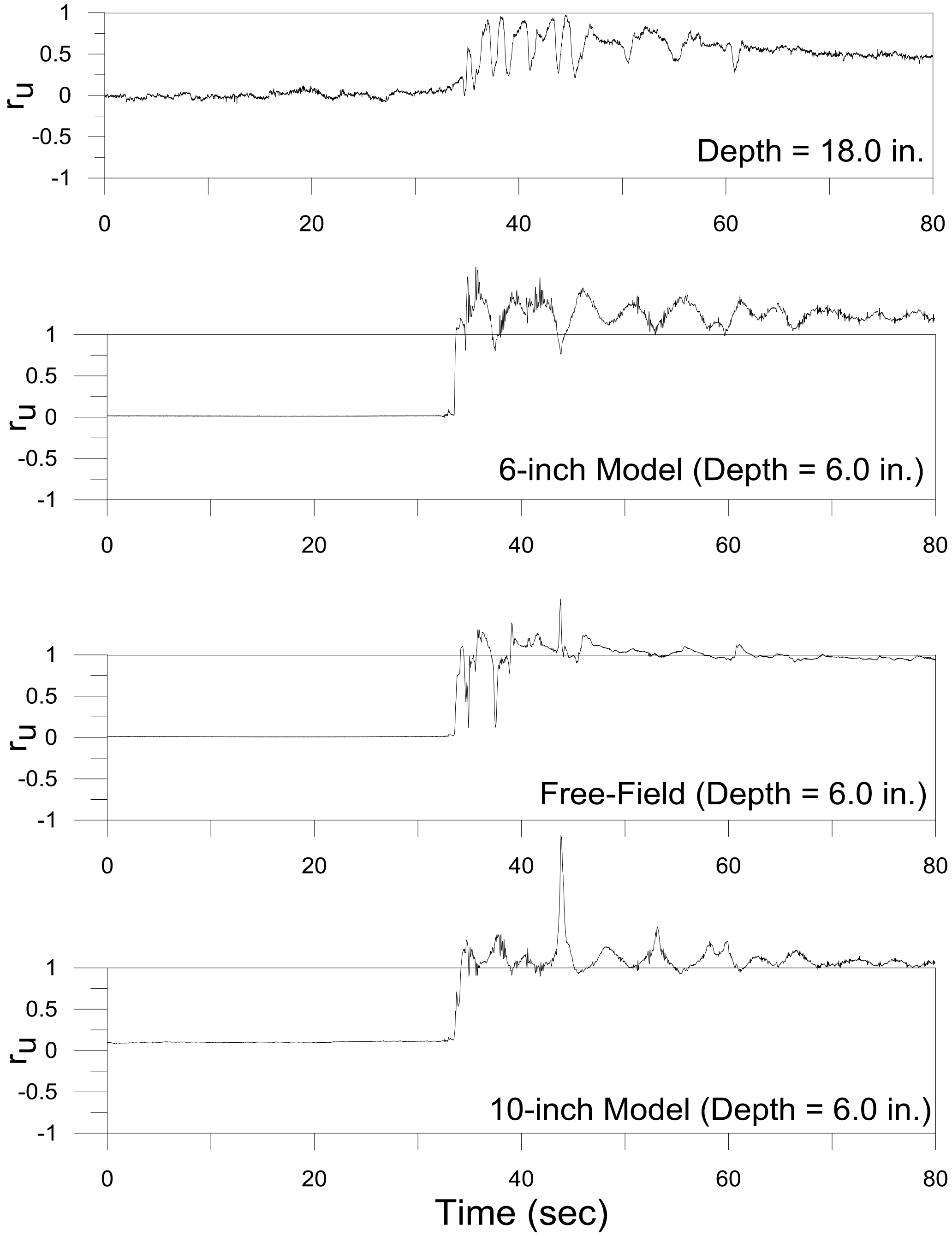

Figure 4-24: Test #53 – Observed Pore Pressure Ratios

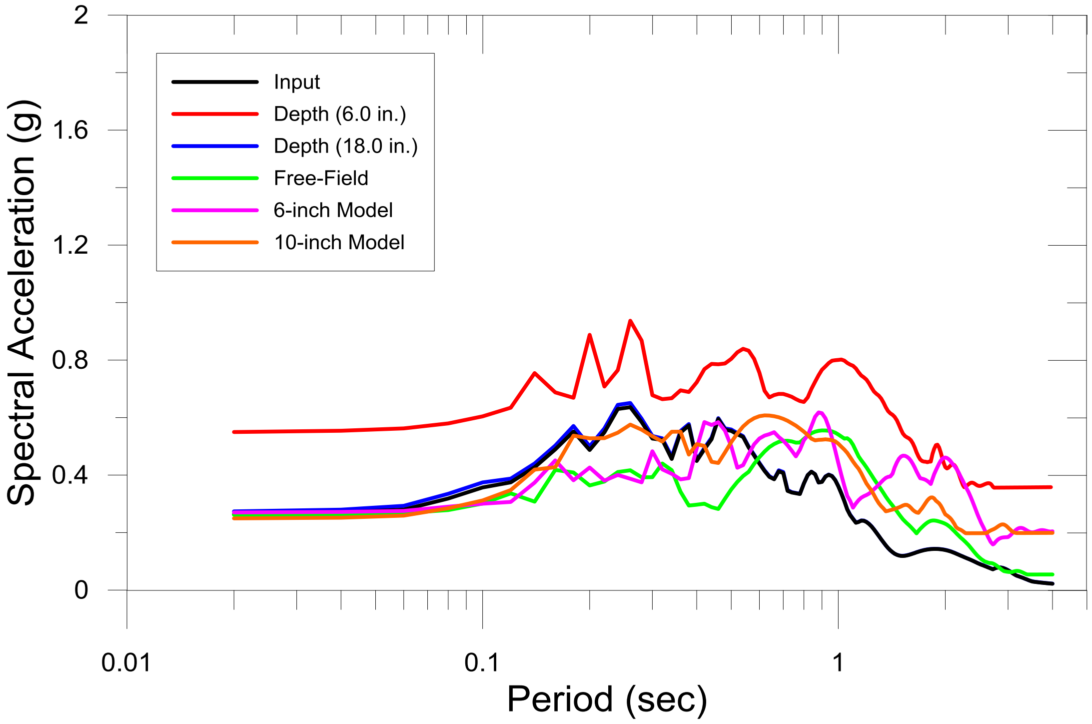

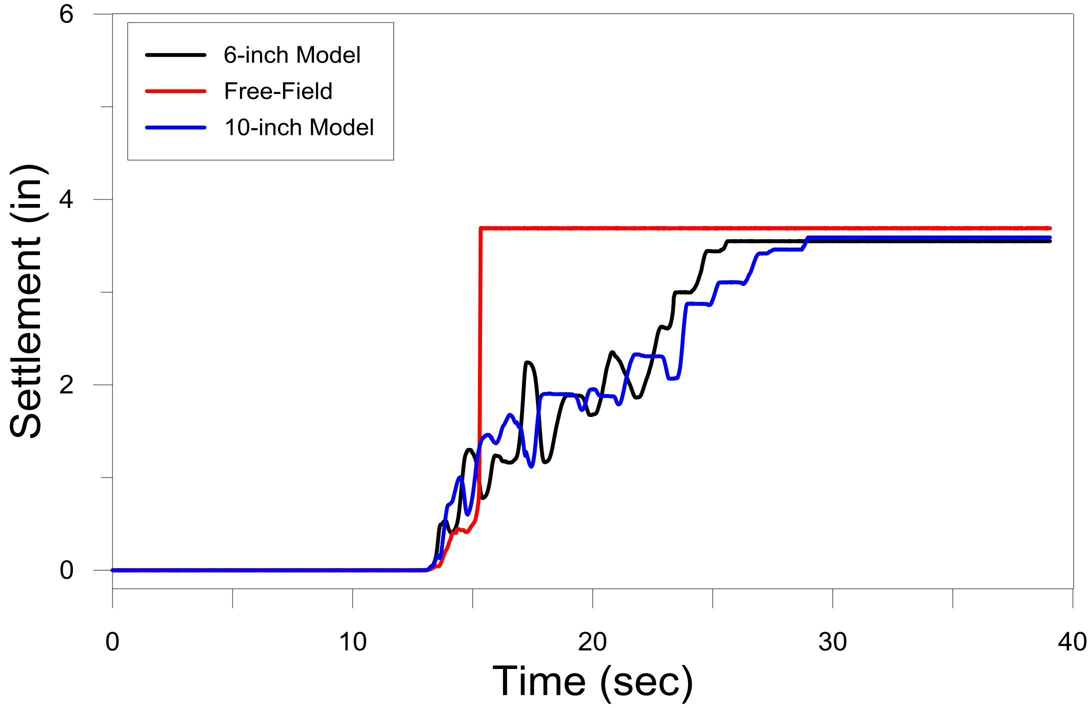

Figure 4-25: Test #53 – Estimated Model Spectra and Measured LVDT.

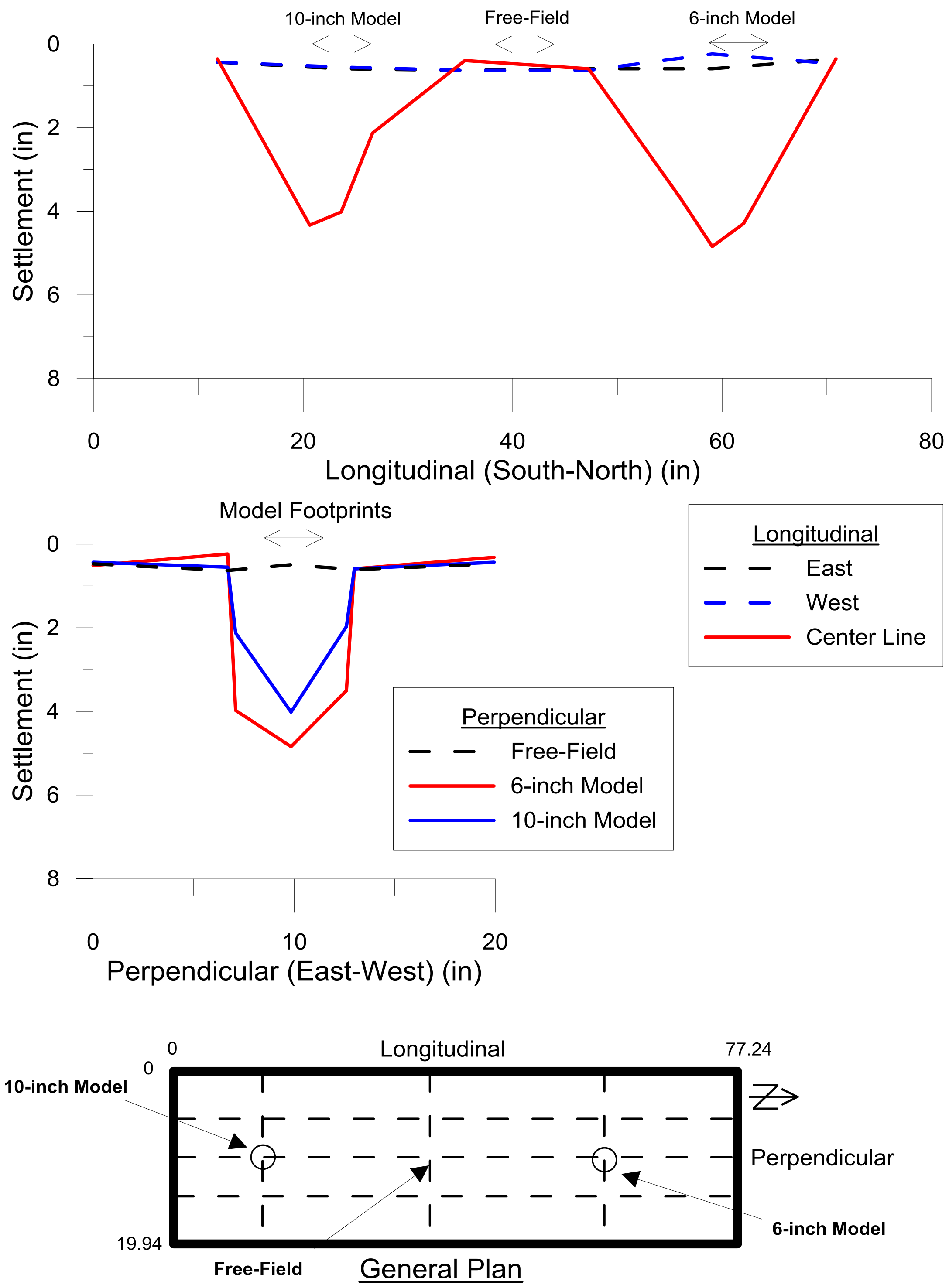

Figure 4-26: Test #53 – Observed Soil Model Settlement (Manually Measured)

Table 4-6: Summary of Phase 4 Experimental Program

Test	Date	Base PGA	Relative Density of Liquefiable	HL / HD	Foundation Diameter	Accelerometers	Pressure Sensors	LVDT
#	**(m/d/yr)**	**(g)**	**(D_r)**	**(ft)**	**(ft)**	**No.**	**No.**	**No.**
53	10/31/16	0.33	35	1 / 1	0.5 / 0.83	6	4	3

4.6 Semi-Empirical Estimation of Liquefaction-Induced Settlement

As discussed in Chapter 2, semi-empirical methods are often used to evaluate the settlement of saturated clean sands in the free-field environment. There are currently no methods that exist to provide an accurate estimation of liquefaction-induced building settlement. Each experiment in Phases 3 and 4 recorded the settlement of each model structure and free-field environment using LVDT's. In addition, to the LVDT's manual measurements were also recorded to document degree of settlement. These measurements were conducted by recording the initial height of the model surface from a known reference point and also immediately after testing. Figure 4-27 depicts the methods used to manually measure the settlement of the model surface for each test in Phases 3 and 4.

Using the semi-empirical methods discussed in Chapter 2 (Tokimatsu and Seed; Ishihara and Yoshimine), estimations of the theoretical settlement were calculated and compared to the actual values measured using the LVDT's.

Figure 4-28 presents a comparison of semi-empirical liquefaction settlement estimates with the average measured settlement in the free-field.

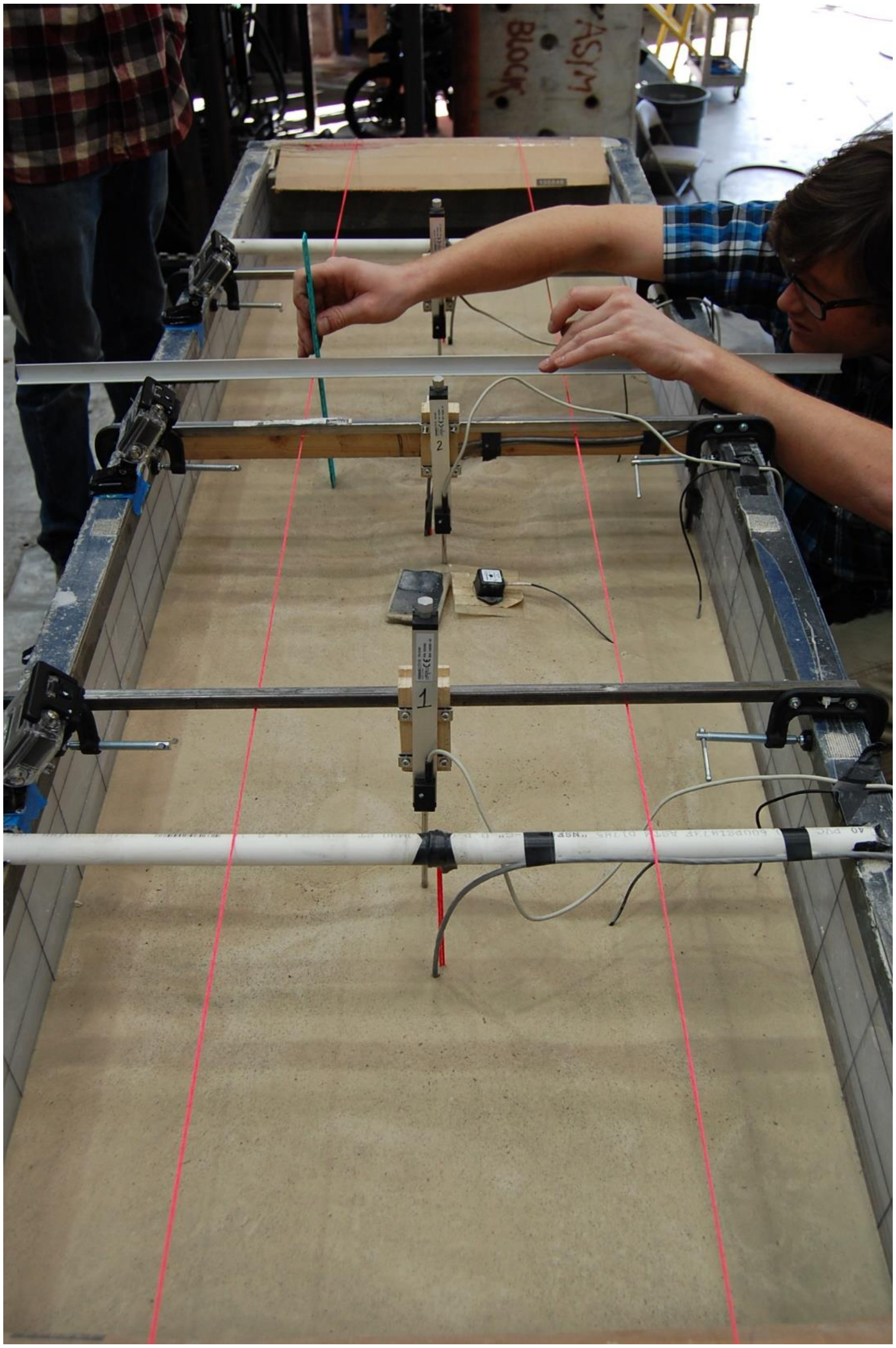

Figure 4-27: Typical Measurement of Settlement upon Completion of Shake Table Testing

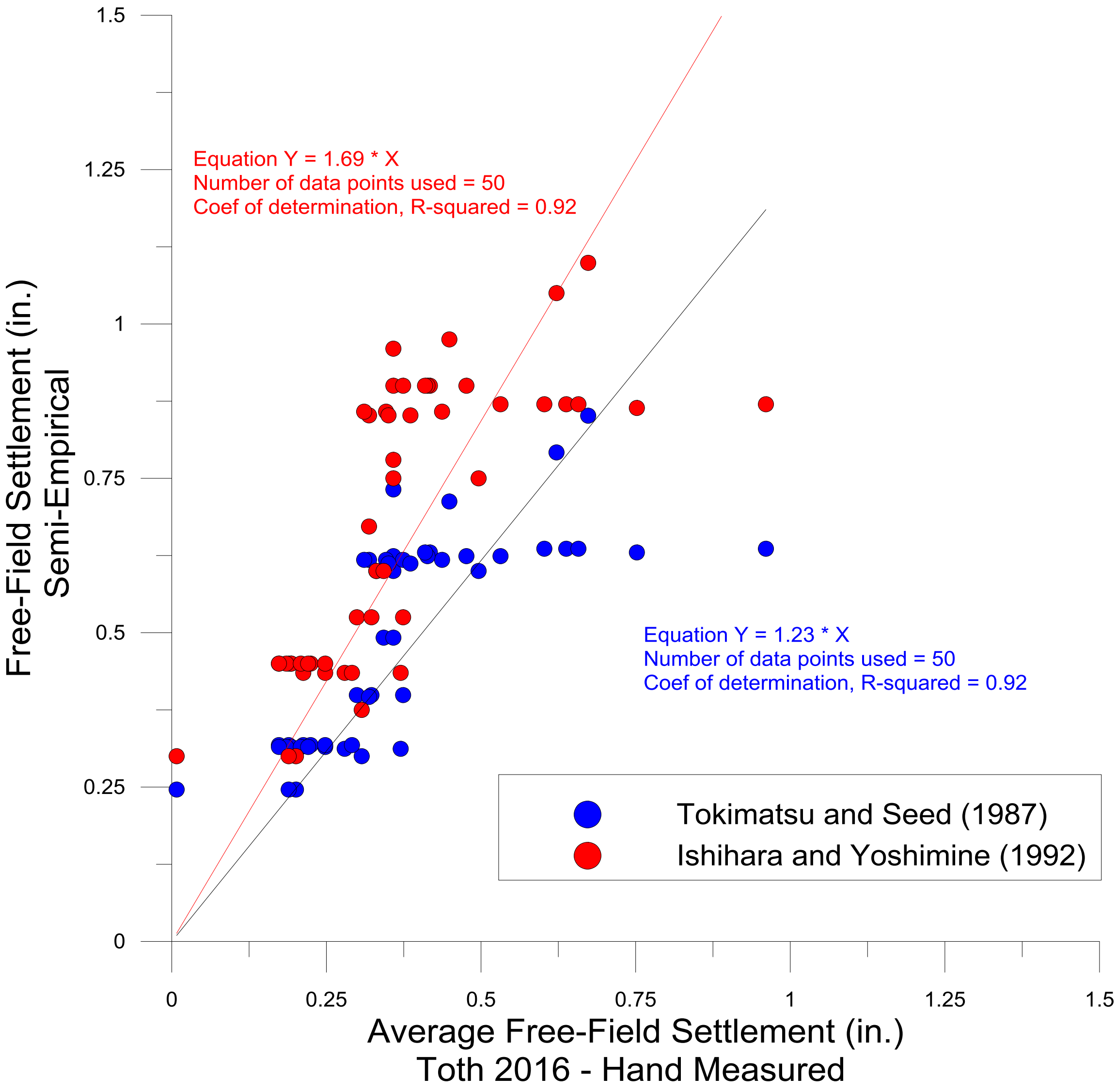

Figure 4-28: Comparison of Semi-Empirical Estimates of Liquefaction Settlement to Average Measured Settlement for Free-Field.

A comparison of our results of hand measured settlement values versus the LVDT measurements for free-field conditions are presented in Figure 4-29. Recorded values observed using the LVDT show that the hand measured values are not in agreeance with the LVDT readings. During experimentation, it was noted that the LVDT influenced the values because of the spring loaded pin that measured the subsequent deformation.

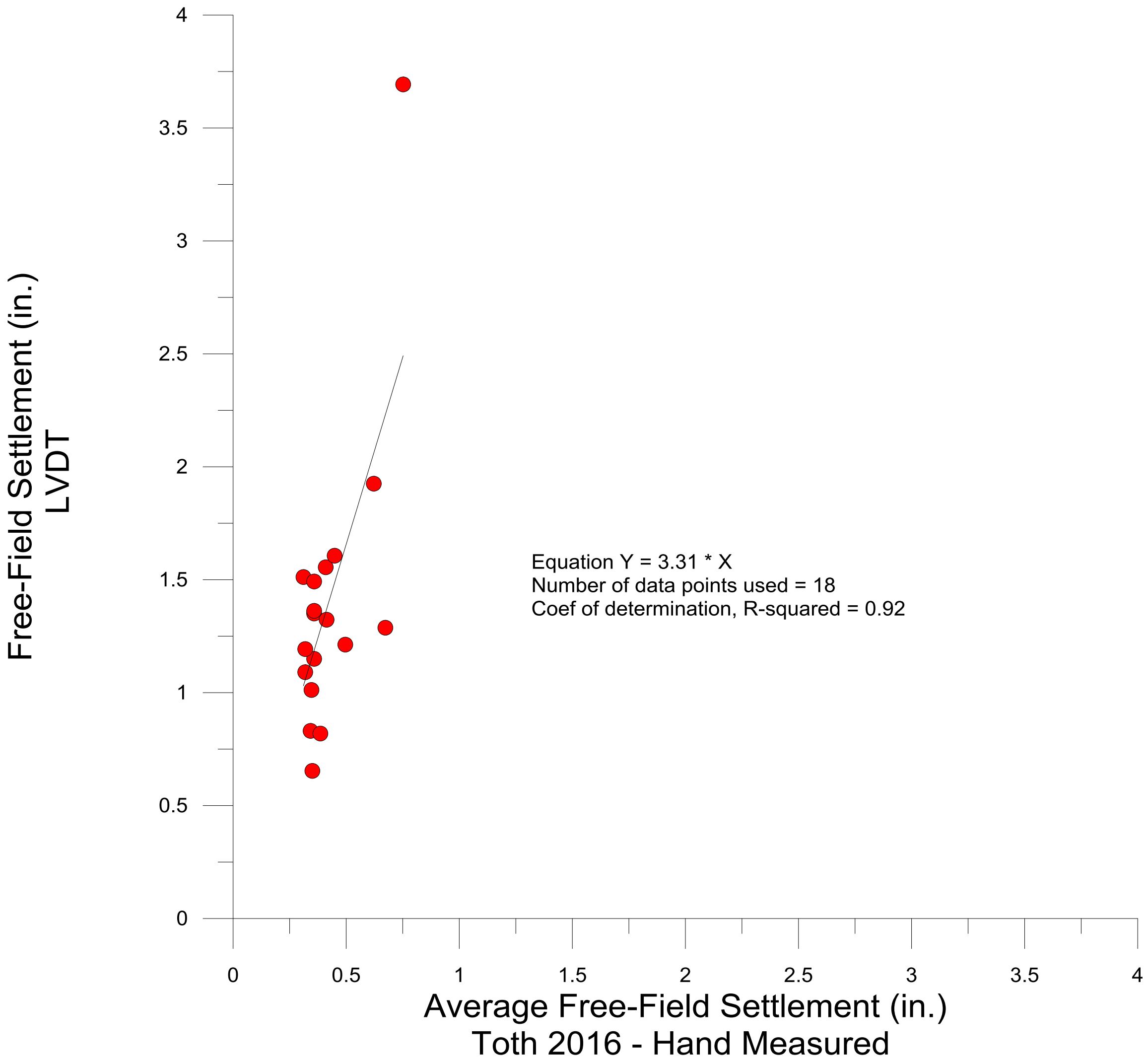

Figure 4-29: Comparison of Semi-Empirical Estimates of Liquefaction Settlement to Average Measured Settlement for Free-Field.

4.7 Results and Findings from Parametric Study

The results presented in the following section represent data from benchmark evaluations during our testing. Our series of evaluations considered a range of foundation diameters as well as variations in shaking duration, relative density and thickness of the liquefiable stratum.

4.7.2 Influence of Relative Density

Figures 4-30 and 4-31 present the measured benchmark settlements for both the Free-Field and 6-inch diameter Foundation condition over a range of increasing relative density of the liquefiable soil layer. Each scenario clearly shows that as relative density increases, the measured settlement for a nominal 12-inch thick liquefiable layer decreases. The settlement in the free-field appears more gradual, while the settlement for the benchmark foundation decreases at a greater rate.

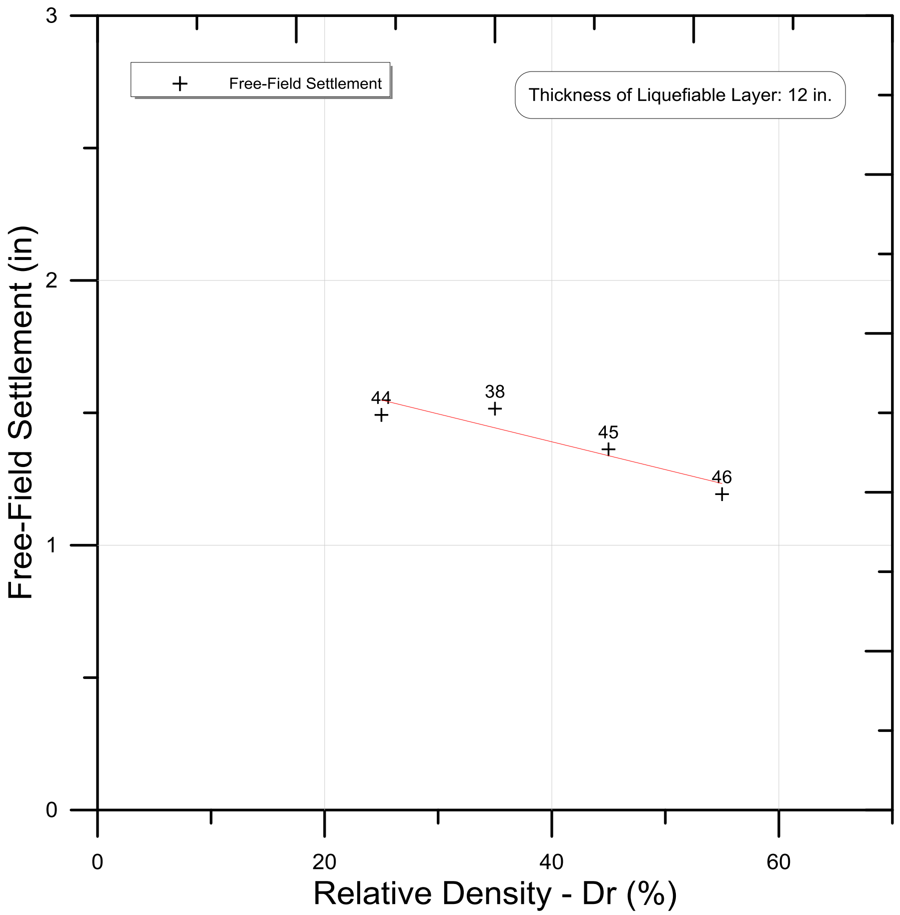

Figure 4-30: Comparison of Relative Density of Liquefiable Soil and Measured Settlement in Free-Field.

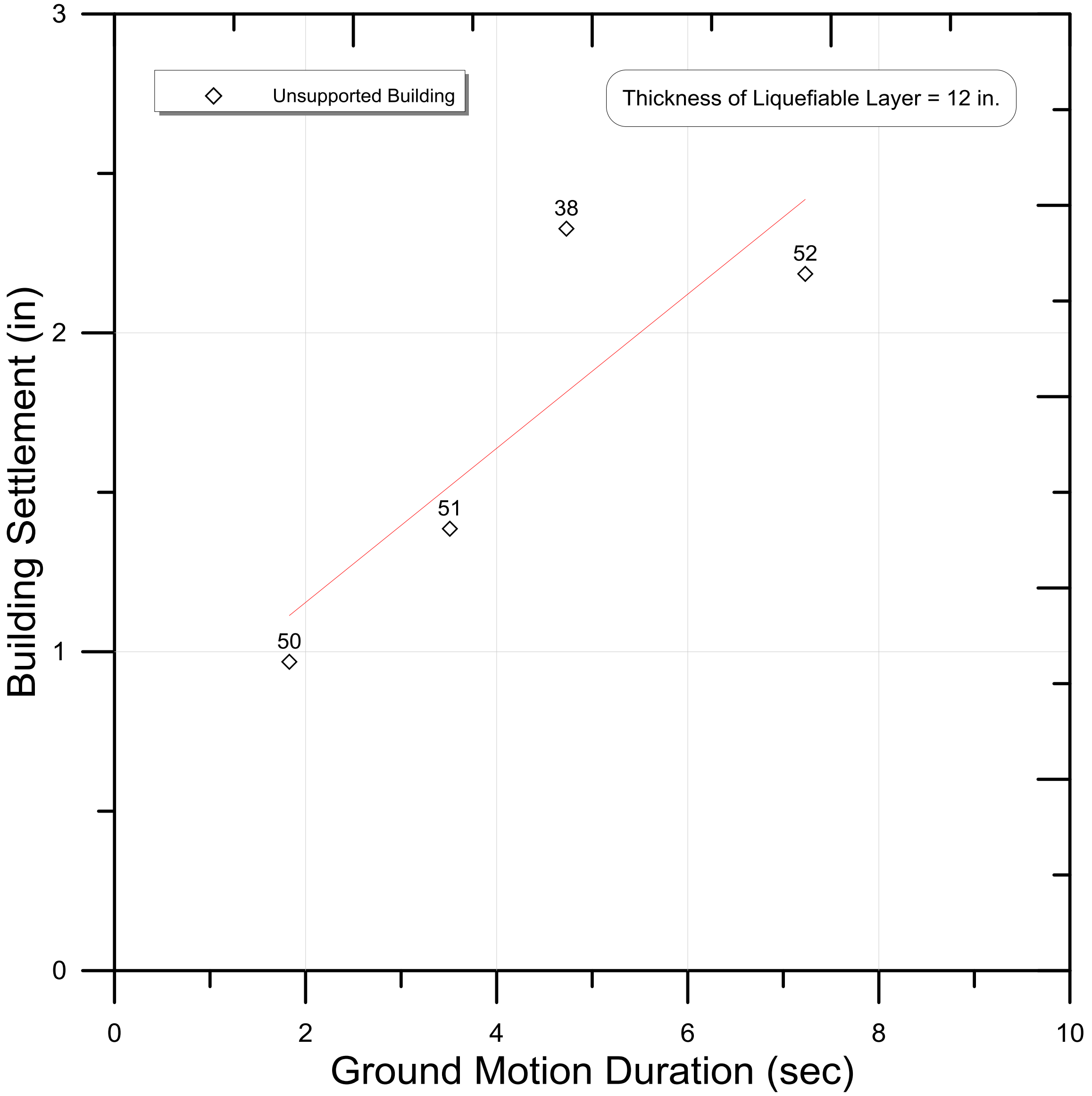

Figure 4-31: Comparison of Relative Density of Liquefiable Soil and Measured Settlement for 6-inch Diameter Foundation.

4.7.3 Influence of Foundation Diameter

Figure 4-32 presents the measured settlements over a range of building foundation diameters. For these benchmark evaluations, the relative density was maintained constant at 35% with a liquefiable layer thickness of 12-inches. The figure suggests that liquefaction-induced settlement decreases with increasing foundation diameter. Dashti et al. (2010a, 2010b) have previously stated that a linear relationship between observed settlement and foundation diameter does not exist, suggesting that there are greater factors influencing the behavior of the settlement. Our results do suggest a linear relationship in settlement behavior in regards to foundation width as well as normalized widths and liquefiable layer thicknesses.

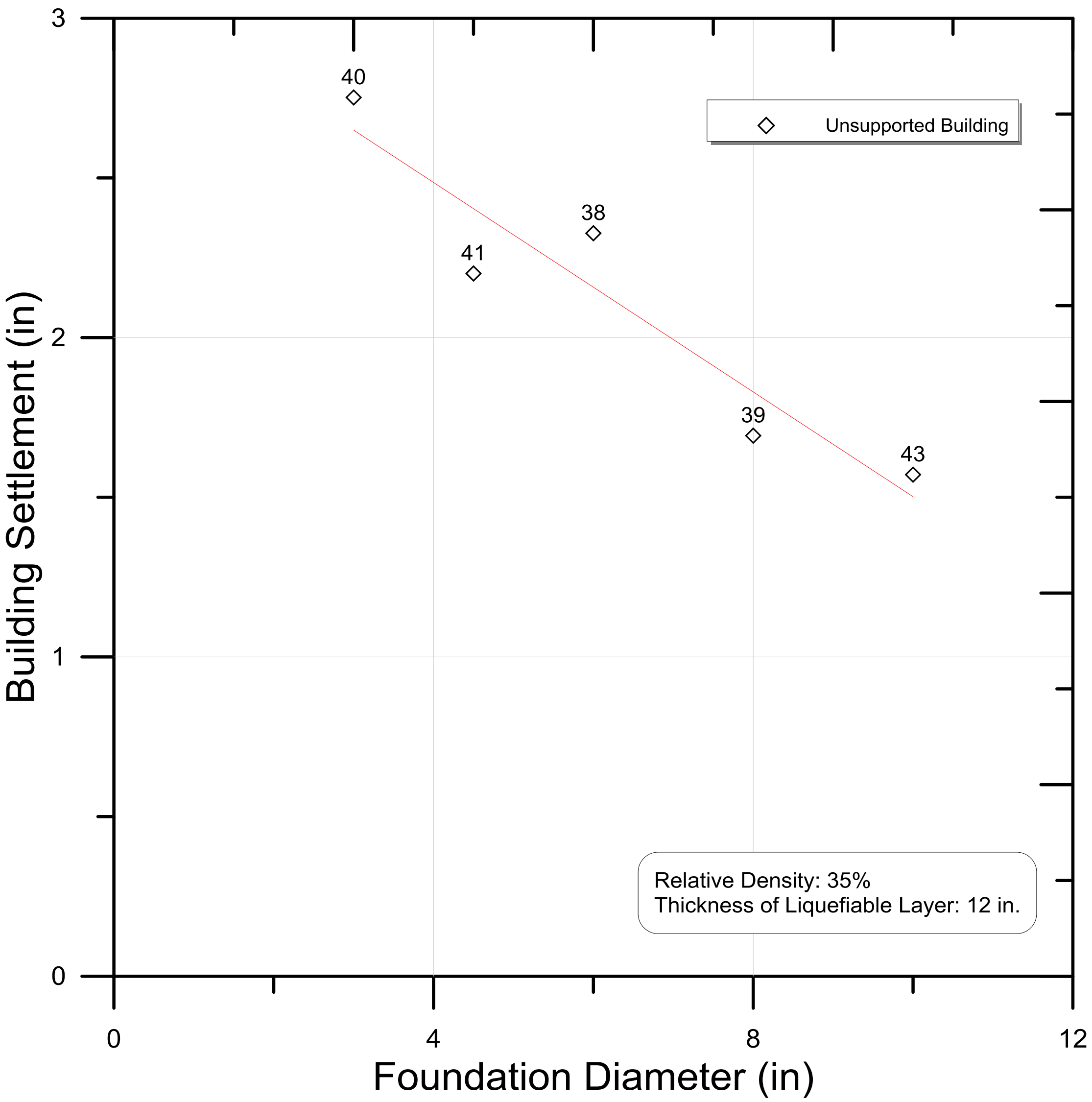

Figure 4-32: Comparison of Foundation Diameter and Measured Settlement.

4.7.4 Influence of Ground Motion Duration

Figures 4-33 and 4-34 present the measured settlement compared to shaking duration. For these benchmark evaluations, the relative density was maintained constant at 35% with a liquefiable layer thickness of 12-inches. The shaking duration was varied between 2, 4, 6 and 8 seconds. The values plotted represent the significant duration of shaking for each evaluation. The significant duration was estimated using the duration of strong motion for the base acceleration data for the time interval at which 5% and 95% of the recorded strong motion (Kramer, 1996) It is apparent that liquefaction-induced settlement increases with increasing shaking duration for both cases in the free-field and building foundation. Building settlement is observed to increase at a greater rate.

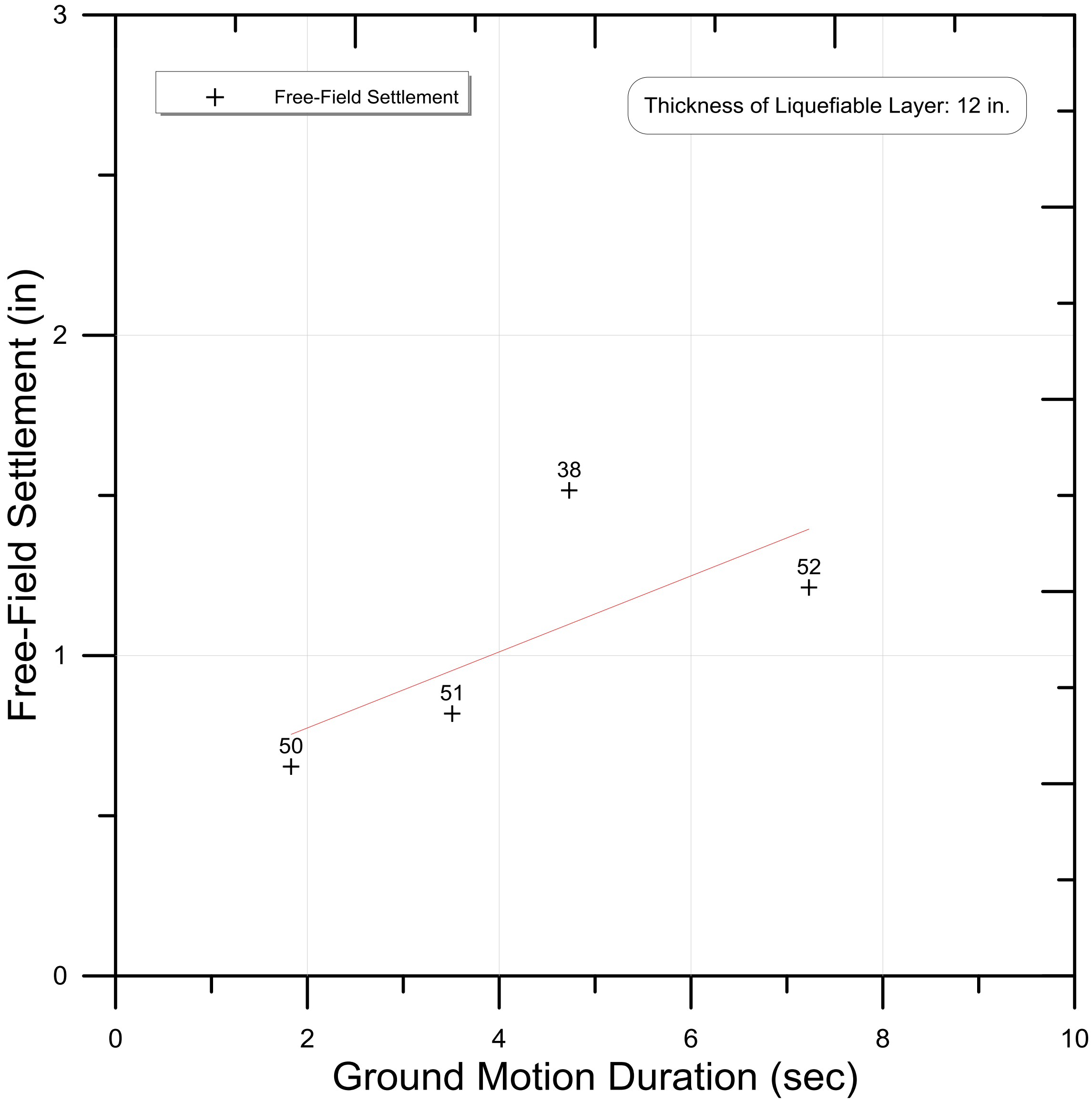

Figure 4-33: Comparison of Ground Motion Duration and Measured Settlement in Free-Field.

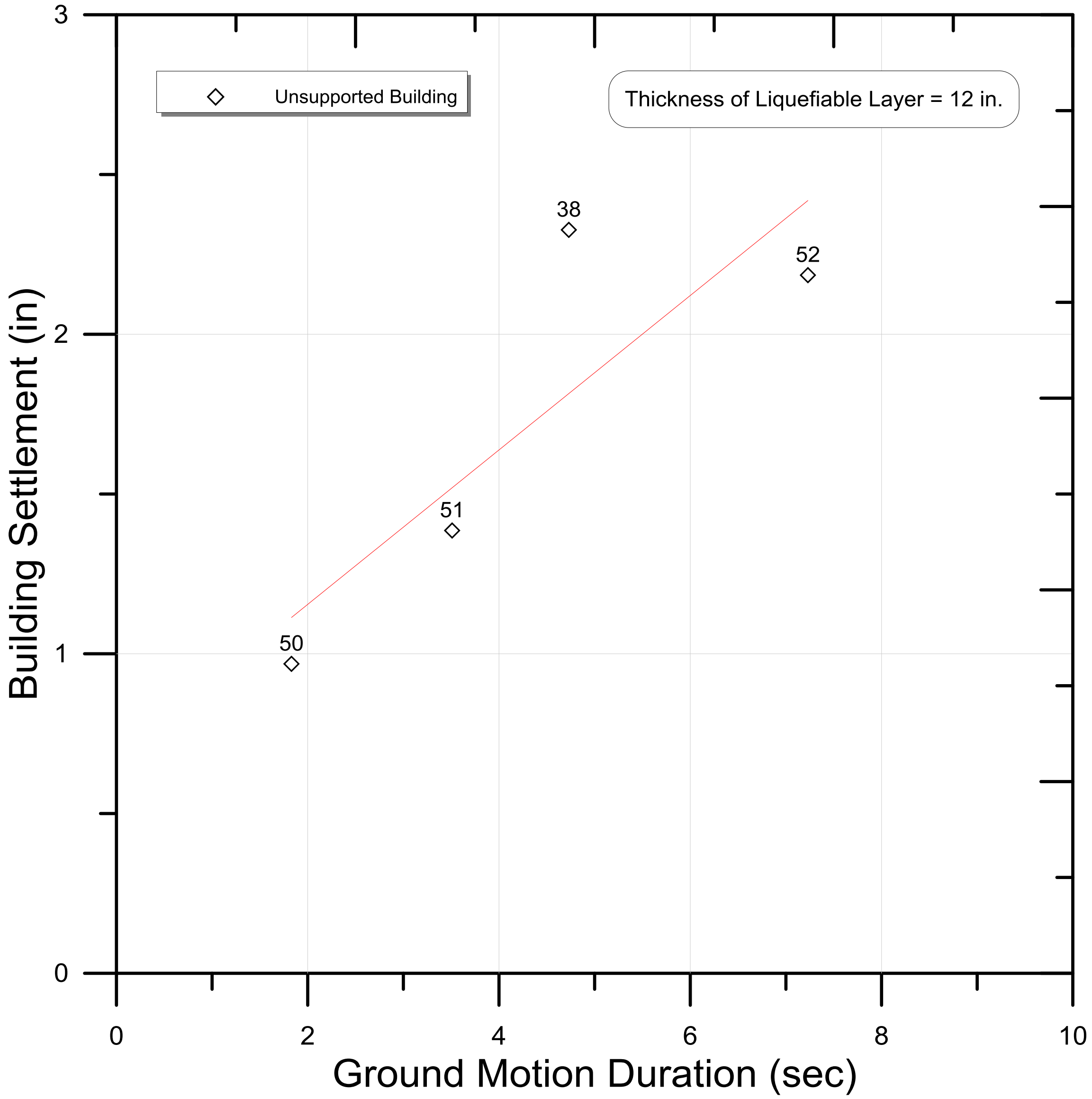

Figure 4-34: Comparison of Ground Motion Duration and Measured Settlement for 6-inch Building Foundation.

4.7.5 Influence of Thickness of Liquefiable Layer

Figures 4-35 and 4-36 present measured settlement in comparison to thickness of liquefiable layer. For these benchmark evaluations, the relative density was maintained constant at 35% and the liquefiable layer thickness was varied from

12-inches to 18-inches. Observed settlements are plotted for each case representing free-field, 6-inch and 10-inch building foundations. Most notable, it is observed that settlement increases with increases thickness of liquefiable layer. Also, it can be seen that increasing foundation diameters show reduced settlements and increase at roughly the same rate with increasing liquefiable layer thickness.

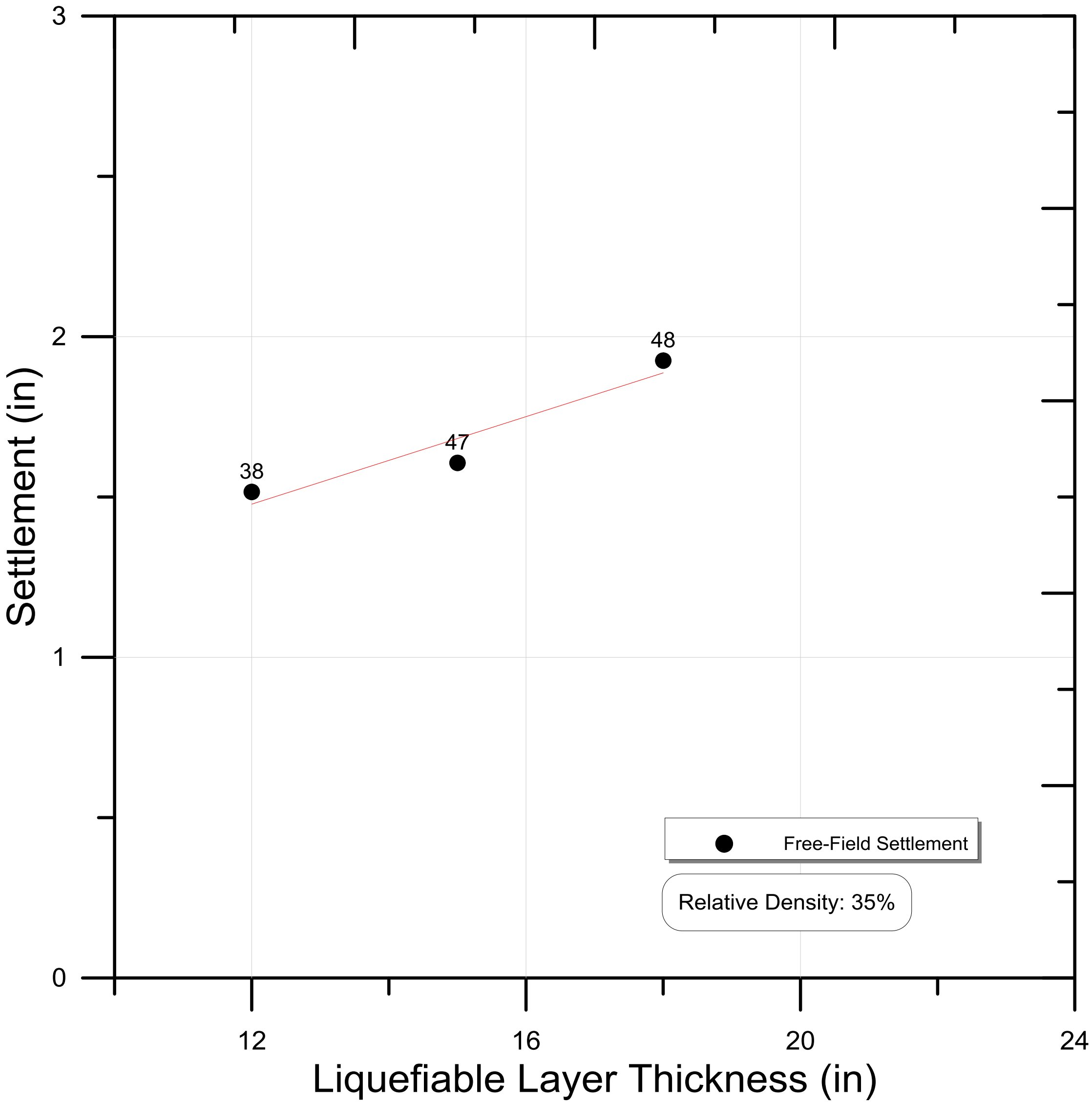

Figure 4-35: Comparison of Liquefiable Layer Thickness and Measured Settlement for Free-Field.

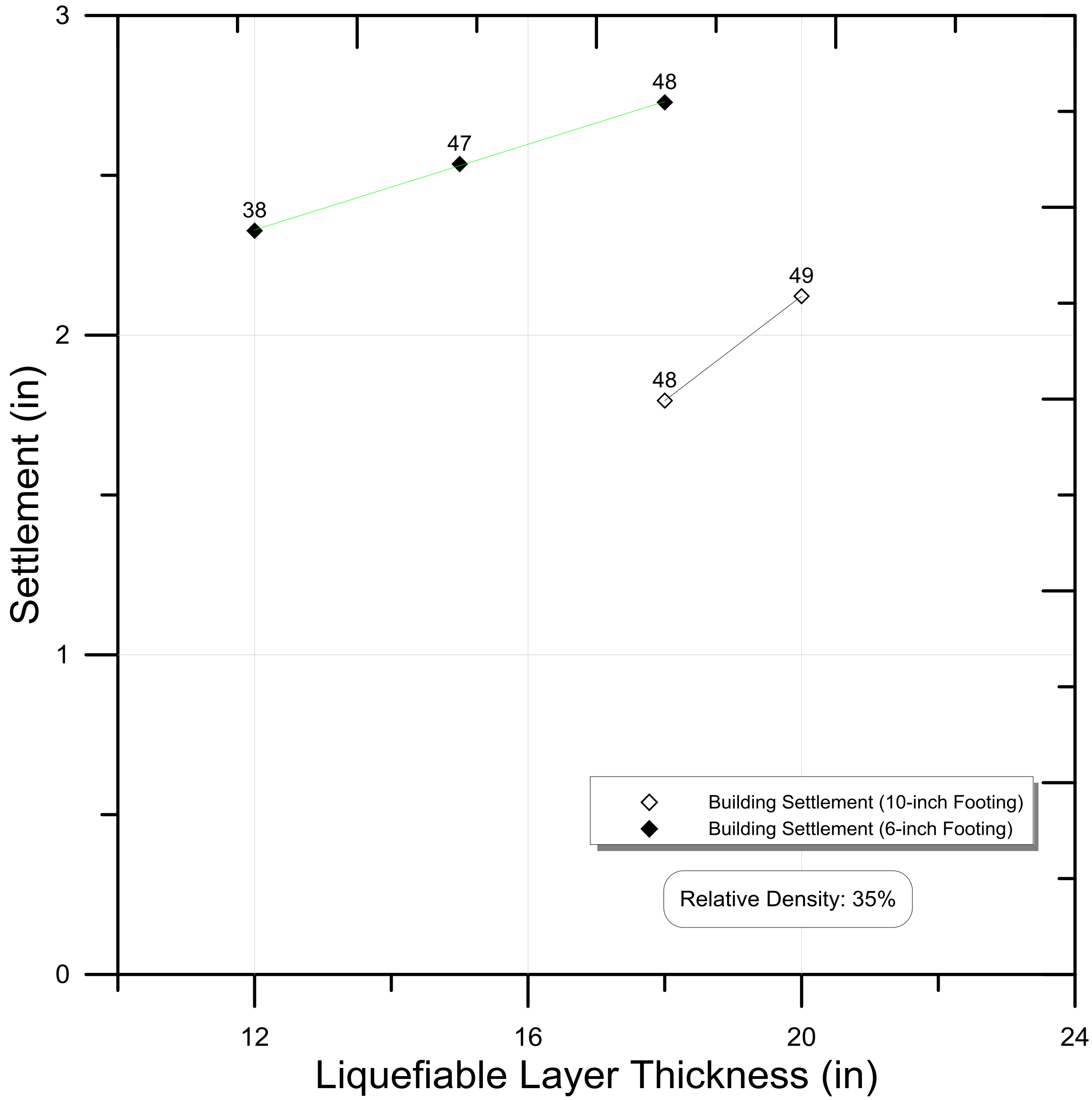

Figure 4-36: Comparison of Liquefiable Layer Thickness and Measured Settlement for 6-inch and 10-inch Building Foundation.

4.7.6 Normalized Settlement

Figures 4-37 and 4-38 present our results in comparison to previous studies of liquefaction-induced settlement for shallow foundations. The plot provides a normalized comparison of foundation settlement in regards to building width. This plot was previously presented in Dashti et al. (2010b) and Bray and Dashti (2014) and has been updated to include the results of our experiments. The updated plot is comprised of a series of field observations, centrifuge and shake table studies. The upper and lower bound plots are also based on previous field observations as described in Chapter 2. Liu/Dobry, Hausler, and Dashti plots are based on results from centrifuge testing while the Yoshimi results are based on shake table testing. Results show a similar scatter of data for normalized foundation settlements based on overall sources provided in the plot. It should be noted however, that the Liu/Dobry and Dashti data represent points for foundations of considerable contact pressure (approximately 2000 psf). Our data represented points for foundations with contact pressures closer to 125 psf and are more representative of a lightly loaded 1-to-2 story structure. In addition, the plot also shows that for our evaluations comprising the use of helical piles, a dramatic reduction in settlement is observed.

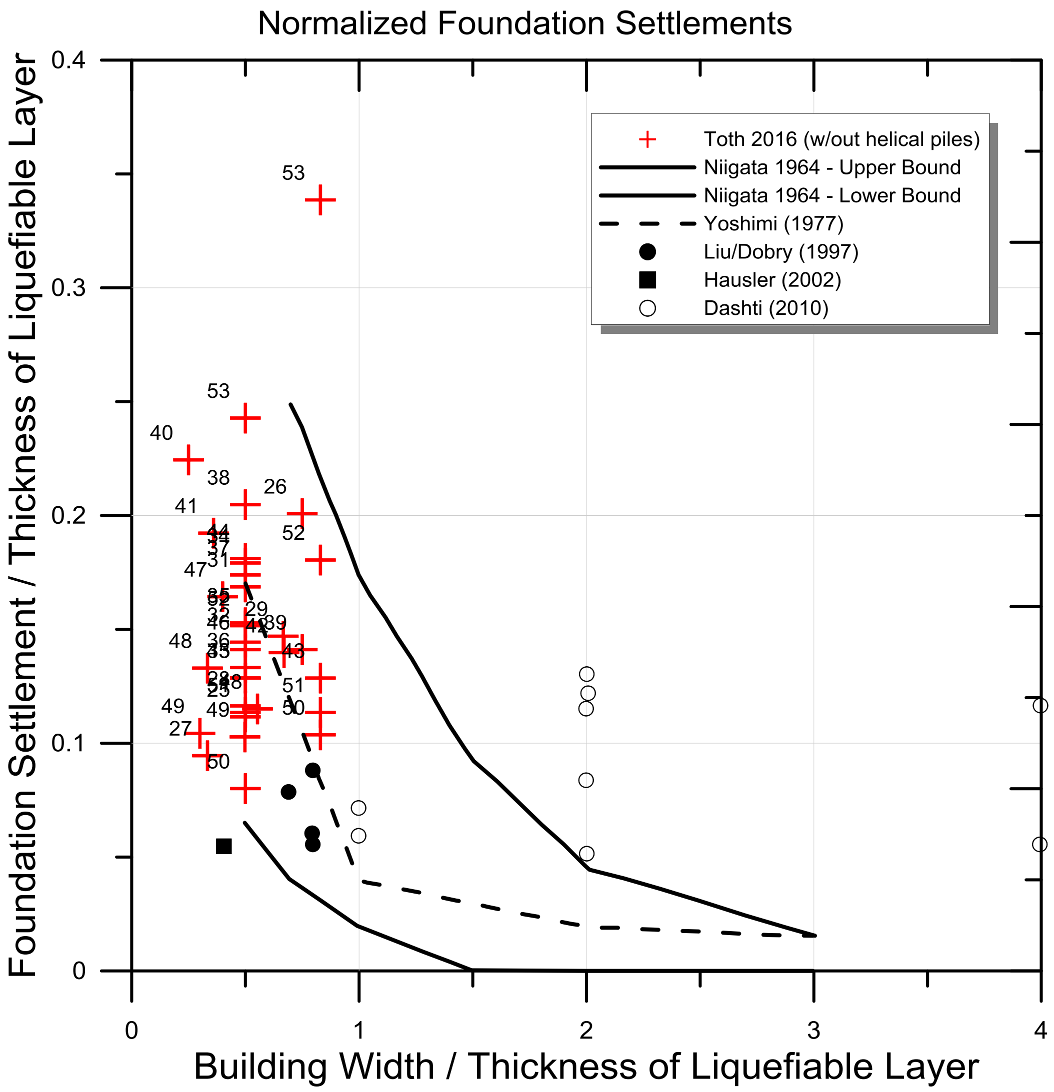

Figure 4-37: Comparison of Unsupported Foundations with Previous Research (Adapted from Dashti et al. 2010b)

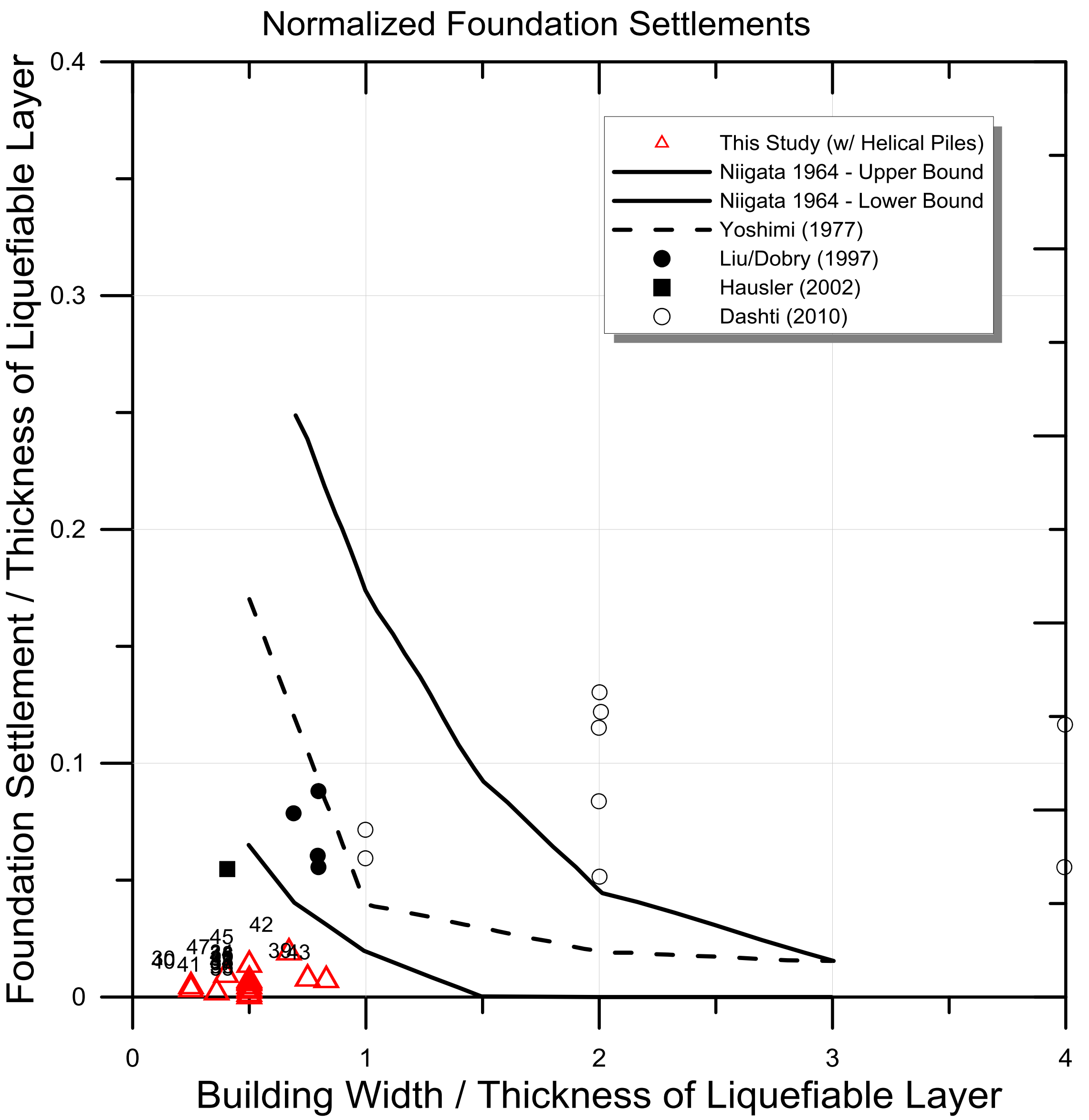

Figure 4-38: Comparison of Helical Pile Supported Foundations with Previous Research (Adapted from Dashti et al. 2010b)

<u>4.7.7 Comparison of Hand Measurements versus LVDT</u>

Settlements for our experiments were plotted comparing free-field with building settlement using both hand measured values and LVDT. Figure 4-39(a) presents the comparison of those results. Hand measured values comparing free-field to building settlements suggest that buildings experience settlement on order approximately 4.6 times greater than in the free-field. Measured values for LVDT show an increase in settlement on the order of 1.6 times greater. Measured values using the LVDT show a greater range in free-field values, suggesting that the LVDT had considerable influence on the degree of free-field settlement measured using LVDT’s. Figure 4-39(b) presents a proposed correction factor that could be applied to the results of the LVDT. The figure presents the hand measured free-field settlement values in relation to the ratio of the free-field measurements of hand and LVDT measurements. It was our observation that the spring within the lever pin of the LVDT exaggerated the settlement measured in the free-field. By applying the average of the ratio presented in Figure 4-39(b) to the LVDT values, the exaggeration effect of the spring should be accounted for and thus removed. We estimated an average ratio of approximately 0.33.

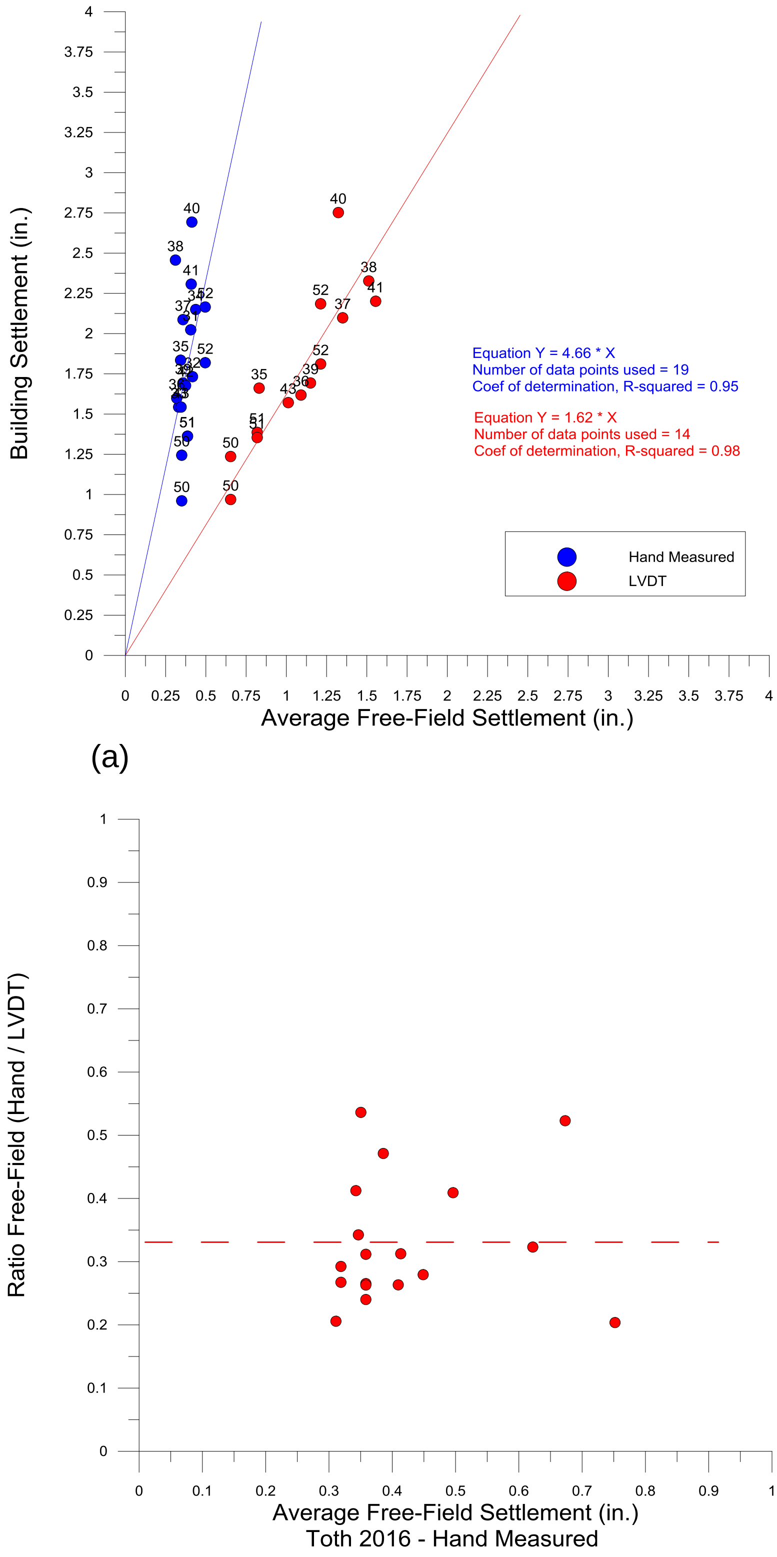

(a)

(b)

Figure 4-39: (a) Comparison of Free-Field and Building Settlement for Hand Measured and LVDT. (b) Average Proposed Correction Factor for LVDT Measurements in Free-Field.

To further investigate the influence of LVDT’s on measured Free-Field settlement, a comparison of measured free-field values and building footprint values were individually plotted using the hand measured and LVDT results. Figure 4-40 is a comparison of hand measured and LVDT values for the free-field. Figure 4-41 is a comparison of hand measured and LVDT values for the building footprint. It is clearly observed in Figure 4-41, that hand measured and LVDT values for the building footprint have an excellent correlation, suggesting consistency in the measured values. However, Figure 4-40 does not show that strong of a correlation. In the free-field case the implementation of the LVDT influenced our results, because of the downward force created by the spring loaded pin. At the moment of liquefaction when the soil lost its strength, the spring loaded pin tended to push the base plate further into the soil.

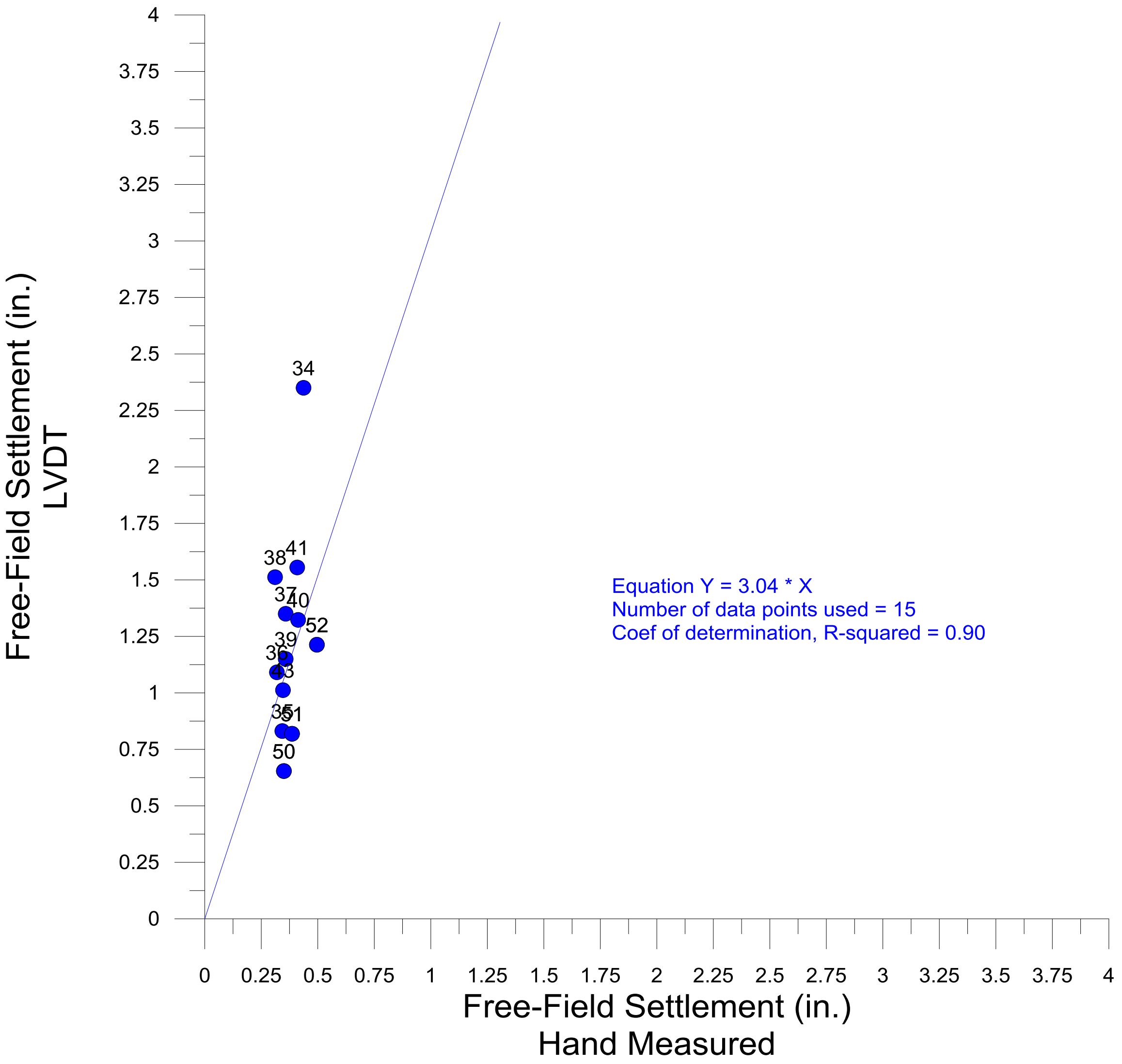

Figure 4-40: Comparison of Hand Measured Values vs LVDT for Free-Field

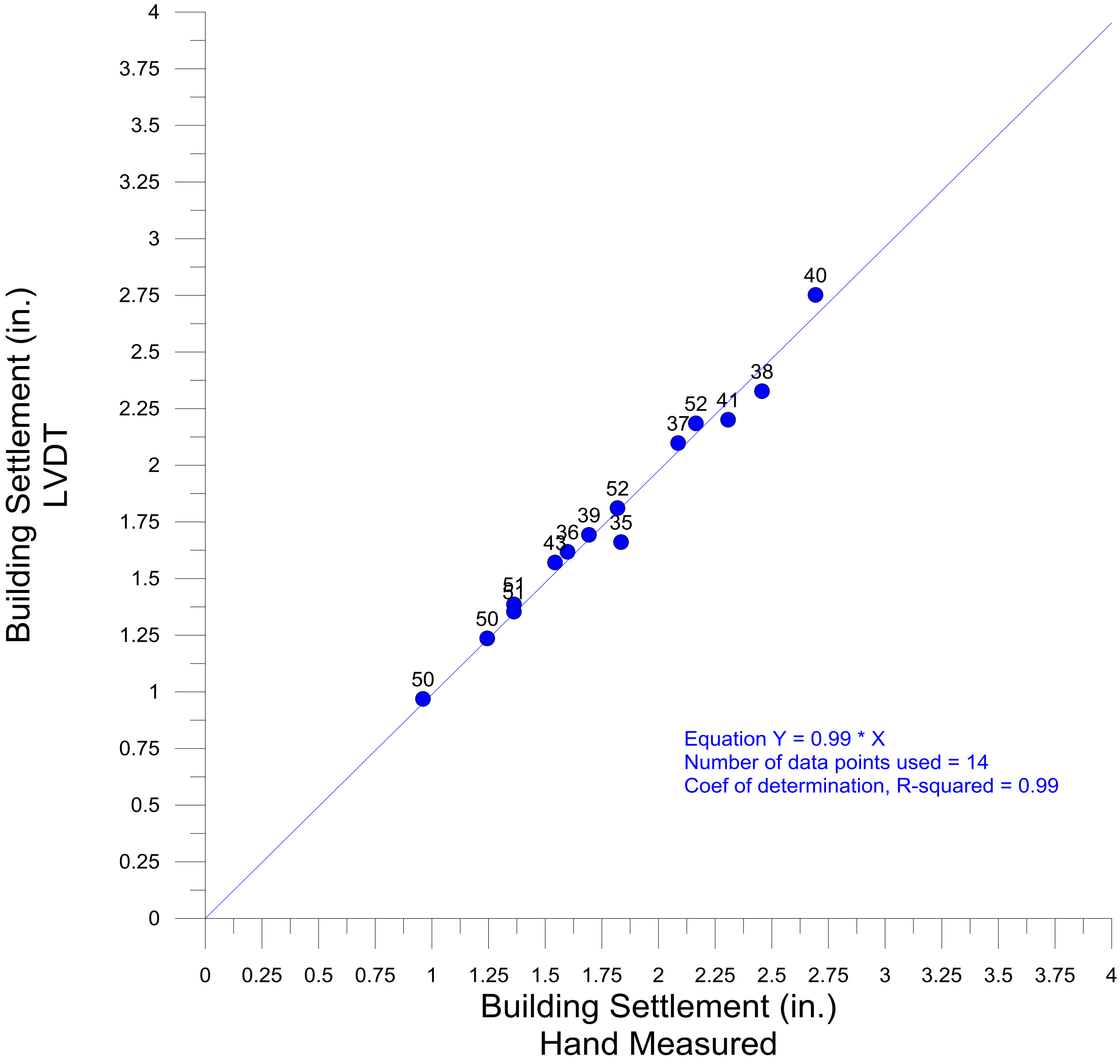

Figure 4-41: Comparison of Hand Measured Values vs LVDT for Building Footprint

4.7.8 Limitations in Scaled Model

Our experiments had certain limitations in regards to model scale. The soil used in each experiment was determined through laboratory testing to be a fine to medium grained, poorly graded sand. The sand had a D_{50} equal to approximately 0.3mm. D_{50} represents the corresponding particle size at 50% passing. When considering similitude for our model soil type and applying a similitude factor of

10, the D_{50} grain size in prototype becomes roughly 3mm in particle diameter. This suggest that our soil grain size characteristics in prototype are more representative of a coarse grained sand and possible fine grained gravel.

The dimensions of the soil container used to construct our soil model was limited in lateral extents with dimensions of only 2.1 feet in width. This restricted our experiments in using larger foundation models which would be more representative of a mat foundation. Considering similitude for the dimensions of the model foundations we used, our prototype mat foundation diameters would be more representative of isolated piers and footings. Prototype foundations dimensions based on our model diameters range from 2.5 ft to 8.3 ft.

Limitations were also present in regards to the influence of the footing over the depth of the layers within the soil model. Consideration was given to ensure that model diameters chosen, had a zone of influence that terminated within the soil model. The zone of influence was determined using Schmertmann’s method assuming a circular foundation with L/B ratio equal to 1. The maximum zone of influence was calculated by multiplying the diameter of the footing by 2.

Chapter 5 Conclusions and Recommendations

Field observations based on post-earthquake reconnaissance of structures founded over liquefiable soils has provided a trove of data on their performance. Major seismic events in both New Zealand and Japan have shown the high severity and large scale of damage resulting from liquefaction-induced settlement. The Canterbury Earthquake Sequence of 2010-2011 damaged as many as 20,000 homes resulting in enormous recovery costs. In order to limit the scale of damage generated by these events, new understandings and insights on the performance of these foundations would provide considerable benefit and possibly a reduction in costs to mitigate existing structures and to implement new design guidelines for future structures in areas susceptible to the effects of liquefaction.

Current standards of practice are used to estimate settlement of saturated liquefiable soils in the free-field environment. However, these procedures have not been able to account for settlement of structures founded over these soils. As a result, estimation of liquefaction-induced settlement can be considered a large approximation with sizeable uncertainty. In addition, these procedures assume settlement to occur as a result of volumetric strain in post-liquefaction pore-pressure dissipation. Recent centrifugal testing conducted to evaluate liquefaction-induced settlement has identified that very little settlement occurs in the post-liquefaction state and rather the majority of building and free-field settlements occur during strong ground motion events. Researchers have also identified other key parameters that influence the settlement of these structures. Dashti et al.(2010a and 2010b), surmise based on results of their centrifugal testing that deviatoric strains resulting from ratcheting of building foundations and the shaking intensity rate of the strong ground motion may be a large contributing factor to settlement.

5.1 Summary of Findings

A comprehensive parametric study was conducted to evaluate liquefaction-induced settlement over a range of parameters. These parameters included the following

a. Relative Density of Liquefiable Layer
b. Foundation Diameter
c. Ground Motion Duration
d. Thickness of Liquefiable Layer

The study was conducted using a simple 1-g shaking table to induce strong ground motions. The experimental evaluations utilized accelerometers to monitor excitation of each soil layer and model structure, pore-pressure sensors to monitor increases in pore-water pressure within each soil layer and beneath each foundation and LVDT's to monitor subsequent settlement of both model structures and free-field environment.

Generally, we observed that in each experiment, settlement of the model building was greater than the free-field environment. In conjunction with previous field reconnaissance observations and research of foundations subjected to liquefaction, current procedures used to predict liquefaction settlement are inadequate.

Influence of Relative Density

Results of benchmark testing were able to identify that liquefaction-induced settlement decreases with increasing soil relative density. It can be also be inferred that building settlement decreases at a greater rate with increasing soil relative density.

Influence of Foundation Diameter

Results have shown that liquefaction-induced settlement decreases with increasing foundation diameter. An approximate 45% reduction in settlement was observed between a 7.62cm foundation versus a 25.4cm foundation.

Influence of Ground Motion Duration

Results have also shown that longer ground motion durations tend to increase liquefaction-induced settlement. The increase in settlement is likely a result of increasing excess pore-water pressures with longer ground motion durations. It was observed during experimentation that the model foundations tilted and swayed when subjected to strong motions. This tilting and swaying can be interpreted as ratcheting of the soil-structure. This effect was likely responsible for the increase in settlement.

Influence of Thickness of Liquefiable Layer

Results of benchmark testing have shown that liquefaction-induced settlement increases with increasing liquefiable layer thickness in both the free-field environment and for model structures.

Normalized Foundation Settlement

Results of Phase 2 through 4 experimental evaluations were normalized in relation to the thickness of liquefiable layer. These results are compared to a previous research comprised of field observations, centrifuge and 1-g shake table evaluations. Overall, our data fit the curves bounded by upper and lower bound Niigata event and also show general agreement with Liu/Dobry, Hausler and a few of the points included by Dashti. Tests 19 through 24 can be seen extending beyond the upper bound of the Niigata event. It is believed that these points are outliers based on the soil model configuration of those experimental evaluations. Test 19 through 24 were performed using a half-scale soil model configuration of 15.24cm in thickness for both the liquefiable and non-liquefiable layers. The foundation diameters ranged from 15.24 to 25.4cm and subsequently created a strain influence factor that extended beyond the soil profile of the model. As a result, the settlements were exaggerated in those cases. It is likely that a similar situation existed for Dashti 2010a.

Our results for cases that implemented helical piles as an underpinning mitigation for rigid shallow foundations were also normalized and plotted in comparison to previous the research. The helical piles show a tight cluster and obvious reduction in liquefaction-induced settlement.

Lastly, the grain size distribution presented limitations within our model when considering the laws of similitude. Based on similitude laws, our soil model was more representative of a coarse grained sand to fine gravel in prototype.
The soil container dimensions also presented limitations when considering the width of the model mat foundation.

5.2 Recommendations for Future Research

To continue to improve on our existing experiments and build upon past research we recommend additional experiments. Benchmark testing allowed us to establish a general relationship on settlement of liquefiable soils over influence of parameters such as relative density, foundation diameter, strong motion duration and thickness of liquefiable deposit. To better define the relationship it is important to conduct additional benchmark testing using the same parameters. Doing so would provide confidence in the parametric relationships through repeatability.

Our soil model assumed continuous horizontal liquefiable stratums. Future testing should include spatial variability of liquefiable soil layer on settlement.

Due to time constraints in physical modelling, our parametric study was not able to consider the influence of inertial forces on liquefaction-induced settlement. We recommend conducting experiments that vary the weight of a benchmark model foundation diameter to draw inferences on settlement behavior.

Field reconnaissance and experimental studies have identified that for liquefiable soils that contain a non-liquefiable crust, the initiation of liquefaction is oftentimes delayed, resulting in reduced settlements. Future experiments should evaluate liquefaction settlement with soil models that include a crust of non-liquefiable soil, exhibiting cohesion. Additionally, experiments should evaluate the degree of settlement of with variation in the water table.

Lastly, future experimental studies should include testing on a larger or full-scale shake table using models in prototype or closer to prototype scale.

Chapter 6 References

1. Ashford, S.A., Boulanger, R.W., Donahue, J.L., & Stewart, J.P. "Geotechnical Quick Report on the Kanto Plain during the March 11, 2011, Off Pacific Coast of Tohoku Earthquake, Japan. GEER Association Report No. GEER-025a, 2011, pp. 1-20.

2. Bray, J.D. "Liquefaction-Induced Building Settlement." Geotechnical Extreme Events Reconnaissance (GEER) – Turning Disaster Into Knowledge, 4 November 2016, Faculty Club, U.C. Berkely, CA.

3. Bray, J.D. and Dashti, S. "Liquefaction-induced Building Movements." *Bulletin of Earthquake Engineering,* vol. 12, 2014, pp. 1129-1156.

4. Bray, J.D., Markham, C., and Cubrinovski, M., "Liquefaction Assessments in the Central Business District of Christchurch, New Zealand." *6th International Conference on Earthquake Geotechnical Engineering,* 2015, pp. 1-22.

5. Das, Braja M. "Principles of Foundation Engineering – 8th Edition." Cengage, 2015.

6. Dashti, S., Bray, J.D., Pestana, J. M., Riemer, M., and Wilson, D. "Mechanisms of Seismically Induced Settlement of Buildings with Shallow

Foundations." *Journal of Geotechnical and Geoenvironmental Engineering,* vol. 136, 2010a, pp.151-164.

7. Dashti, S., Bray, J.D., Pestana, J. M., Riemer, M., and Wilson, D. "Centrifuge Testing to Evaluate and Mitigate Liquefaction-Induced Building Settlement Mechanisms." *Journal of Geotechnical and Geoenvironmental Engineering,* vol. 136, 2010b, pp. 918-929.

8. "Earthquake Engineering Laboratory." University of Nevada, Reno. 30, October. 2016, http://www.unr.edu/cceer/facilities-and-equipment/earthquake-laboratory.

9. Henderson, D. "The Performance of House Foundations in the Cantebury Earthquakes." (Master's thesis). University of Canterbury, 2013, pp. 1-448. http://ir.canterbury.ac.nz/handle/10092/8741.

10. Iai, S. "Similitude for Shaking Table Tests on Soil-Structures-Fluid Model in 1g Gravitational Field." *Soils and Foundations,* vol. 29, 1989, pp. 105-118.

11. Idriss, I.M., Boulanger R.W. "Semi-Empirical Procedures for Evaluating Liquefaction Potential During Earthquakes." Soil Dynamics and Earthquake Engineering, vol. 26, 2006, pp. 32-56.

12. Ishihara K, Yoshimine, M. “Evaluation of Settlements in Deposits Following Liquefaction during Earthquakes.” Soils and Foundations, vol. 32(1), 1992, pp. 173-188.

13. Kramer, Steven L. “Geotechnical Earthquake Engineering.” Pearson, 1996.

14. Liu, L and Dobry, R., “Seismic Response of Shallow Foundation on Liquefiable Sand.” *Journal of Geotechnical and Geoenvironmental Engineering,* vol. 123, 1997, pp. 557-567.

15. Marin, H.E., “Geotechnical Investigation Report: The Edge Resort and Spa Project – Southeast Corner of Lakeshore Boulevard and Stateline Avenue, South Lake Tahoe in Eldorado County, California.” HEM Consulting LLC, dated November 16, 2012, pp. 1-32.

16. Perko, Howard A. “Helical Piles – A Practical Guide to Design and Installation.” John Wiley & Sons Inc, 2009.

17. Rasouli, R., Towhata, I., and Hayashida, T. “Mitigation of Seismic Settlement of Light Surface Structures by Installation of Sheet-Pile Walls Around the Foundation.” *Soil Dynamics and Earthquake Engineering,* vol. 72, 2015, pp. 108-118.

18. "The Landing Resort, Stateline, Nevada." 38.960938ºlat, -119.0949266ºlong. Google Earth, April, 2015. Accessed December 5, 2016.

19. Tokimatsu, K., and Seed, B. "Evaluation of Settlements in Sands Due to Earthquake Shaking." *Journal of Geotechnical Engineering,* vol. 113(8), 1987, pp. 861-878.

20. Towhata, Ikuo. "Geotechnical Earthquake Engineering." Springer, 2008.

21. Van Ballegooy, S., Malan, P., Lacrosse, V., Jacka, M.E., Cubrinovski, M., Bray, J.D., O'Rourke, T.D., Crawford, S.A., and Cowan, H. "Assessment of Liquefaction-Induced Land Damage for Residential Christchurch." Earthquake Spectra*,* vol. 30(1), 2014, pp. 31-55.

22. Yasuda, S., Harada, K., Ishikawa, K., and Kanemaru, Y. "Characteristics of Liquefaction in Tokyo Bay Area by the 2011 Great East Japan Earthquake." *Soils and Foundations,* vol. 52(5), 2012, pp. 793-810.

23. Youd, T.L., and Idriss, I.M. "Liquefaction Resistance of Soils: Summary Report from the 1996 NCEER and 1998 NCEER/NSF Workshops on Evaluation of Liquefaction Resistance of Soils." Journal of Geotechnical and Geoenvironmental Engineering. vol. 127, 2001, pp. 297-313.

Appendix A – Experimental Results

Test #1 (August 12, 2015)

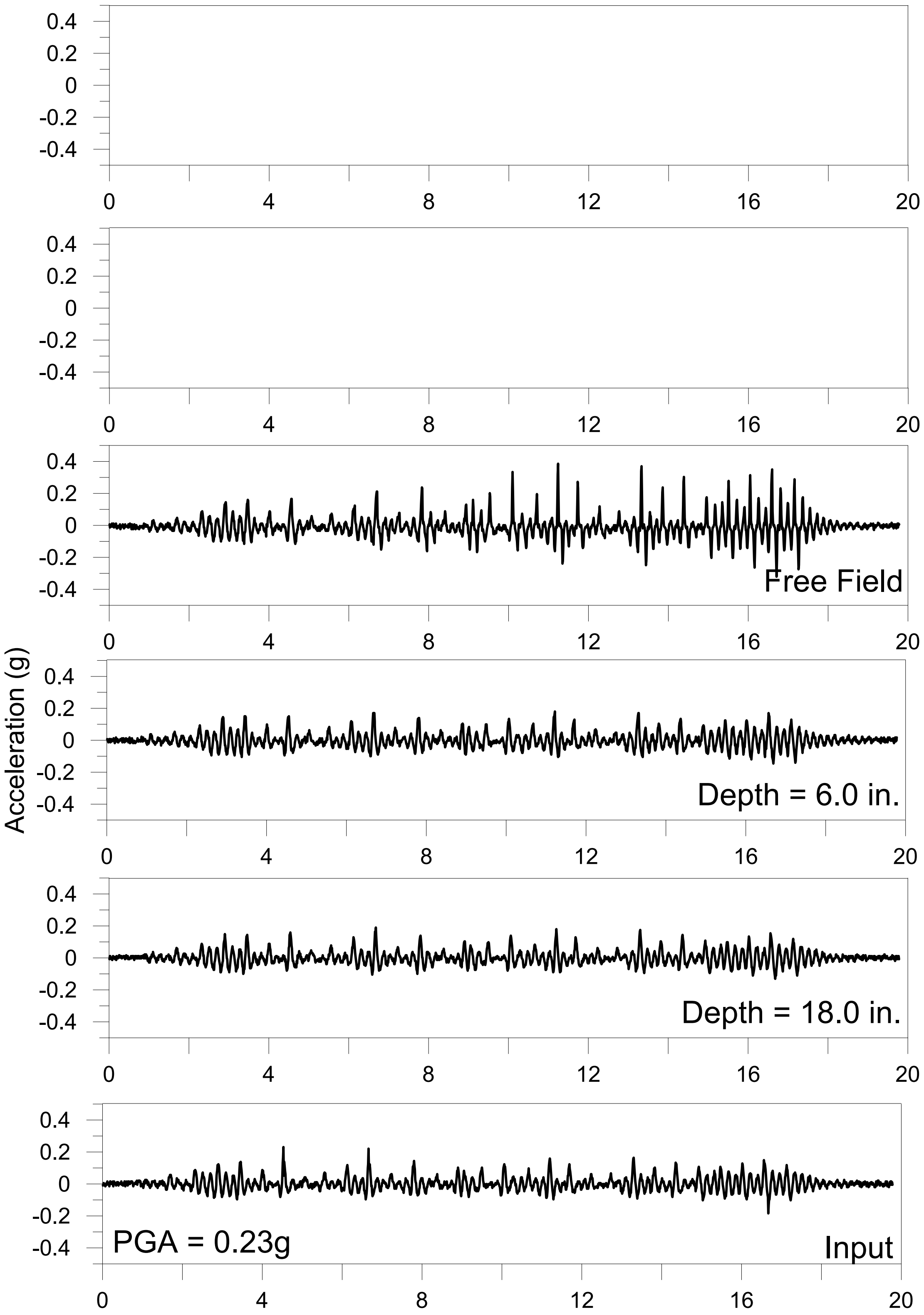

Test #2 (August 20, 2015)

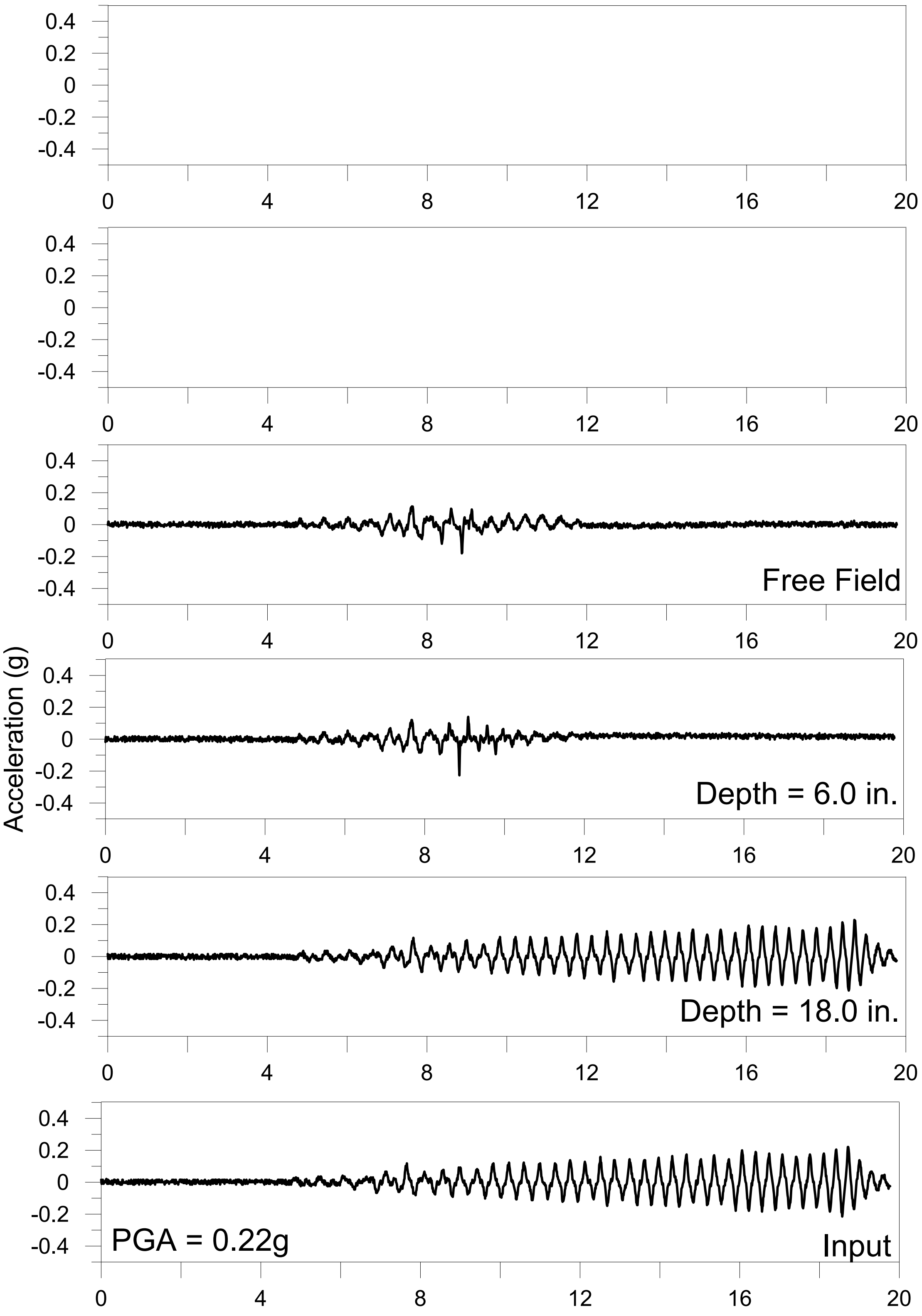

Test #3 (August 25, 2015)

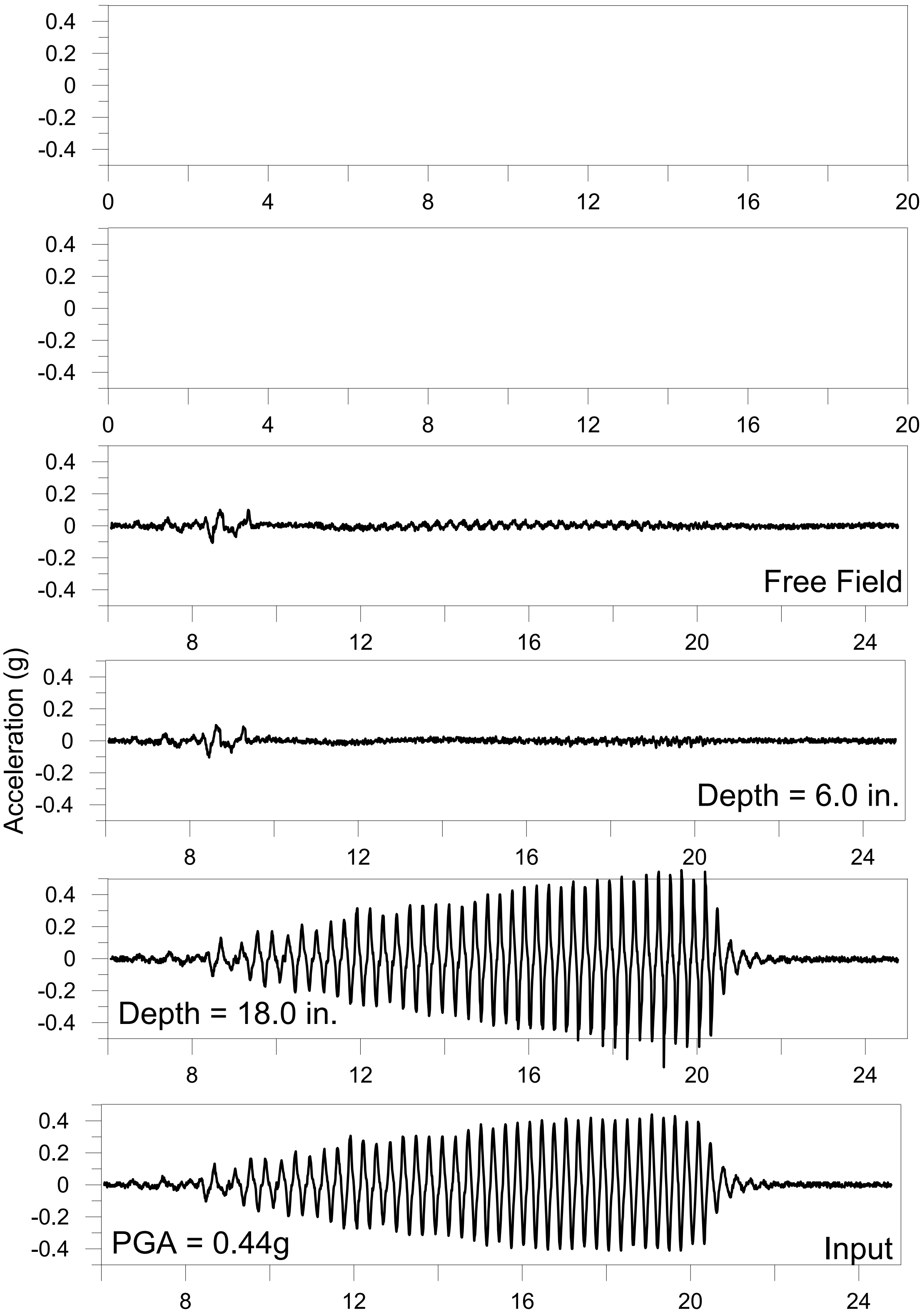

Test #4 (September 4, 2015)

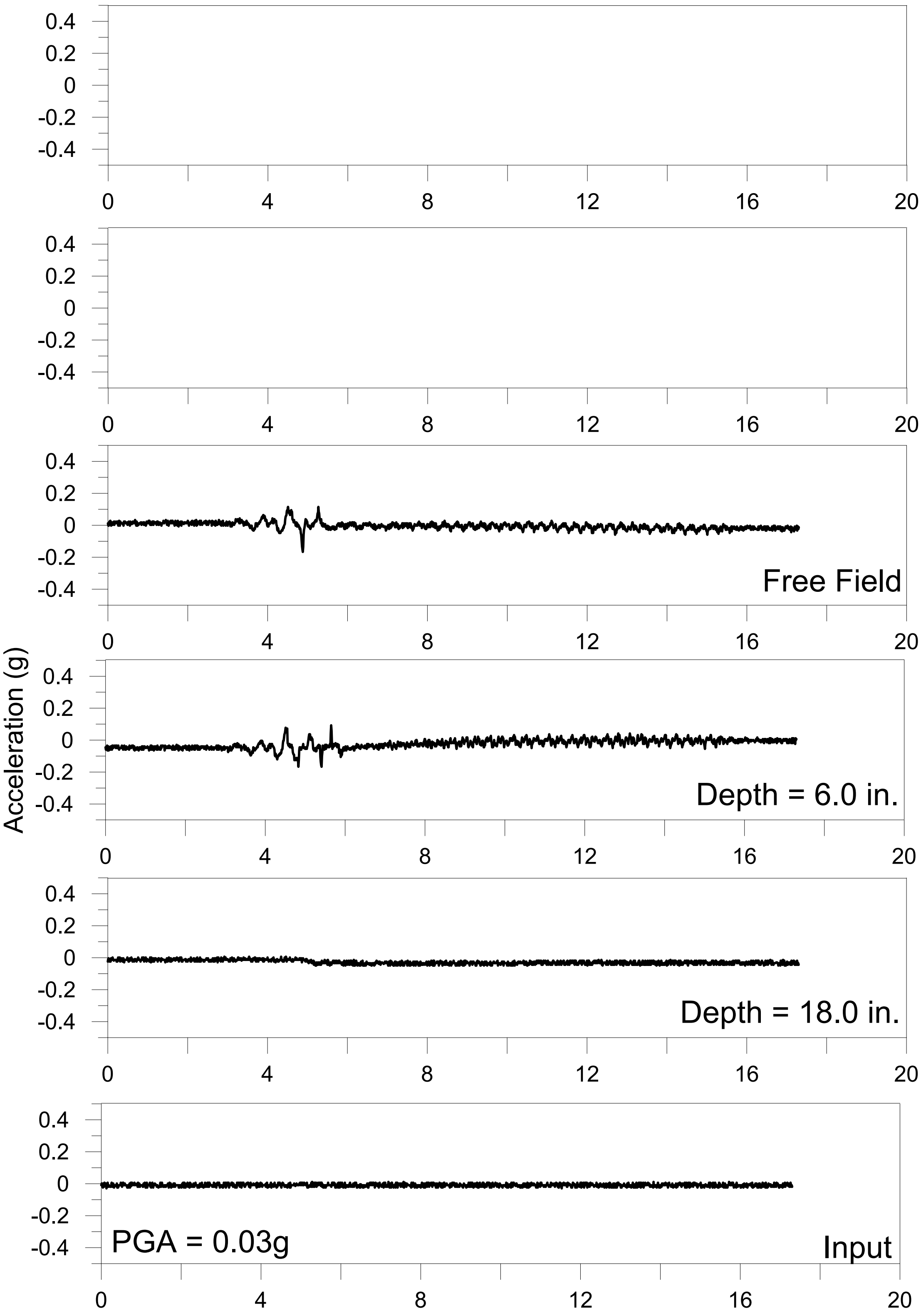

Test #5 (September 18, 2015)

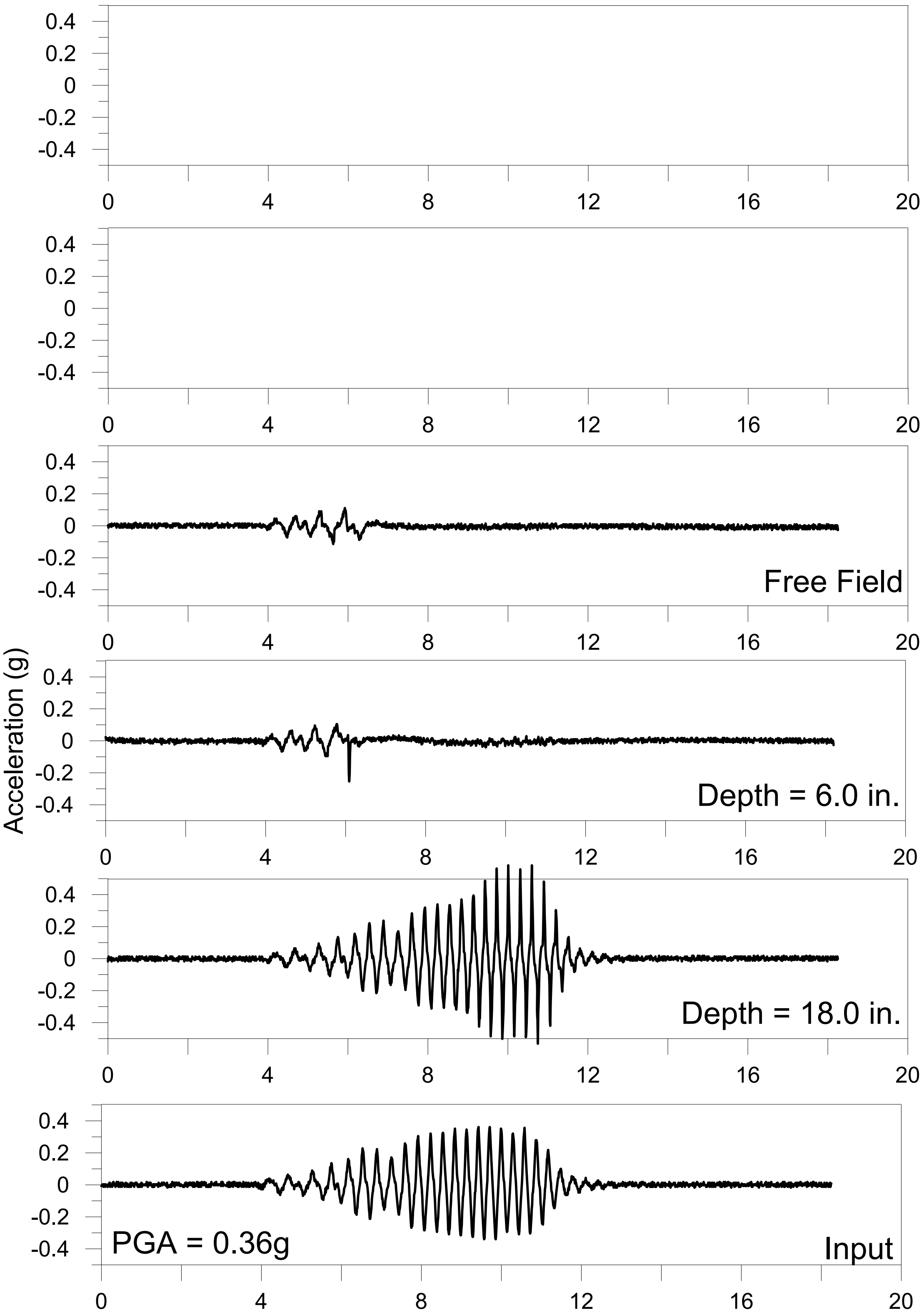

Test #6 (September 25, 2015)

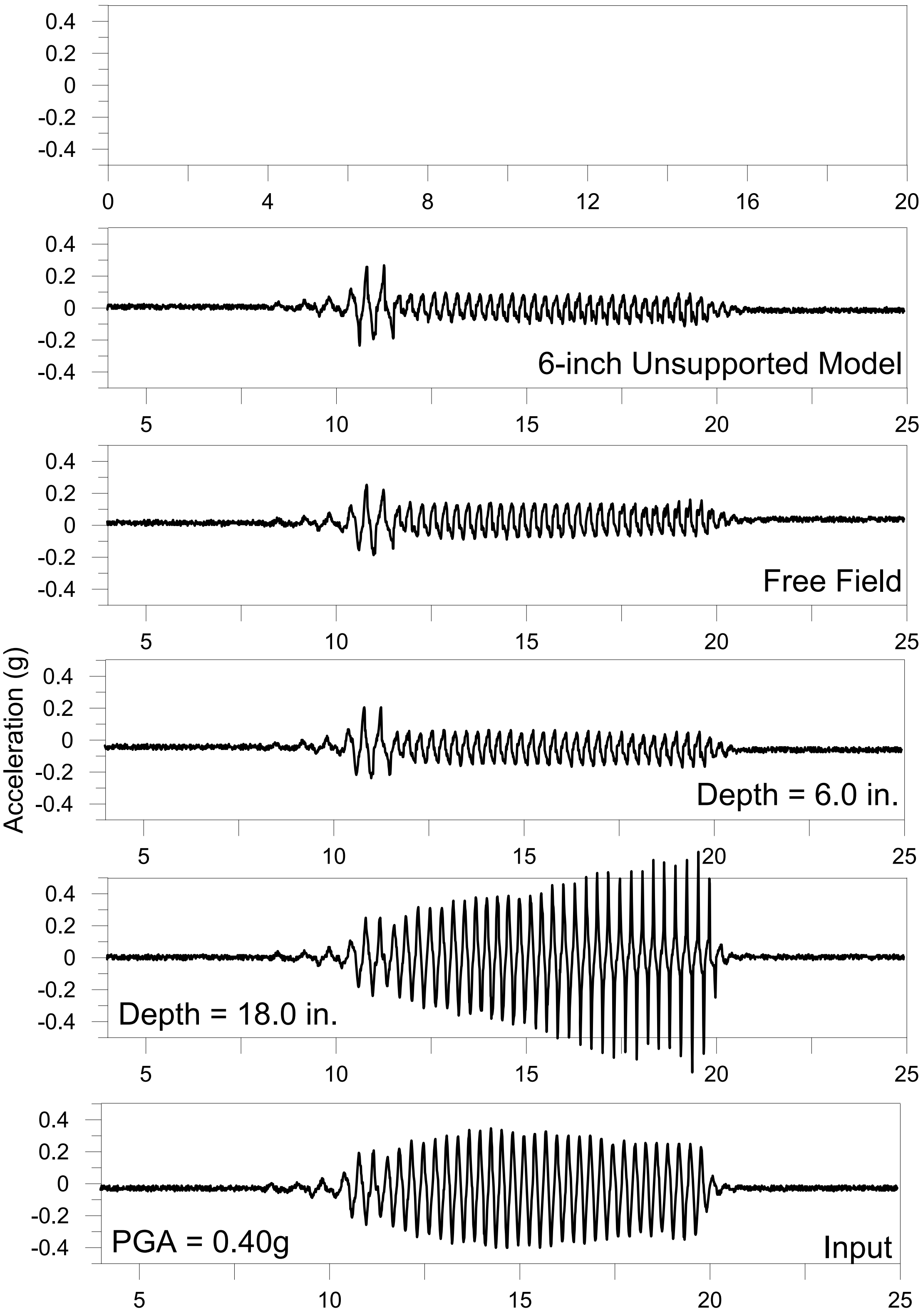

Test # 6: Settlement (cm)
9/25/2015
PGA: 0.40g

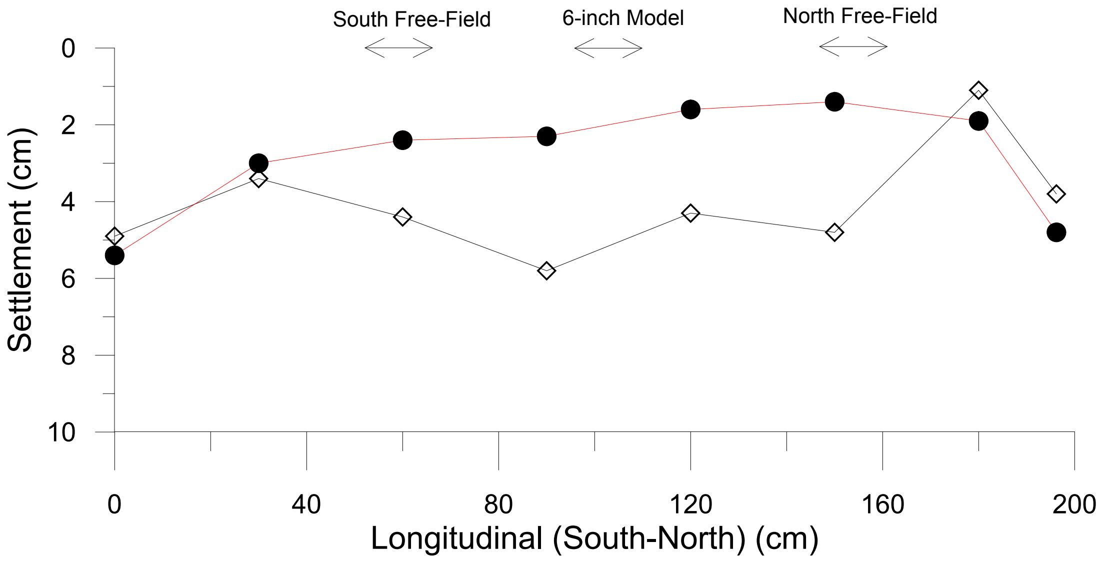

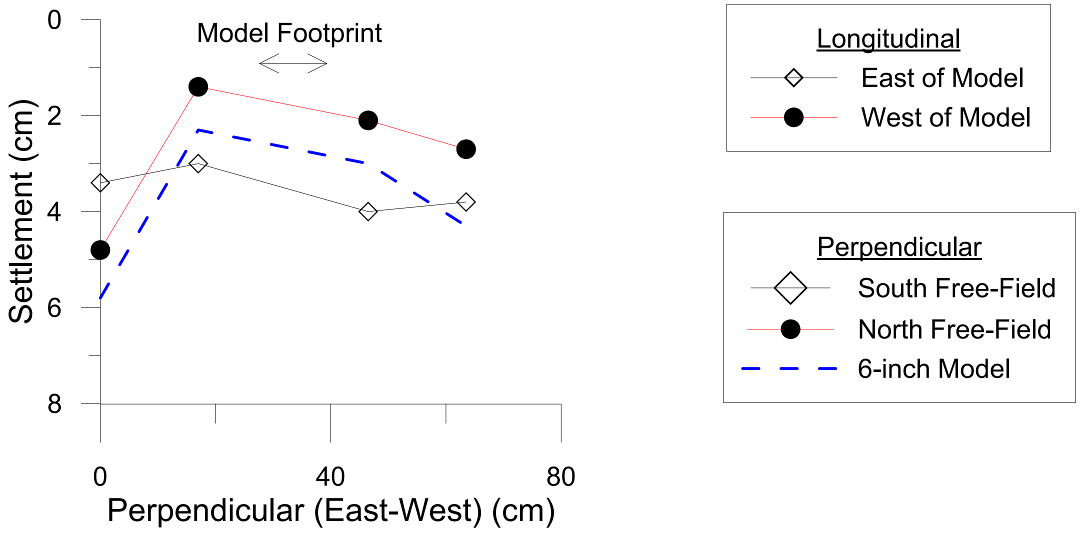

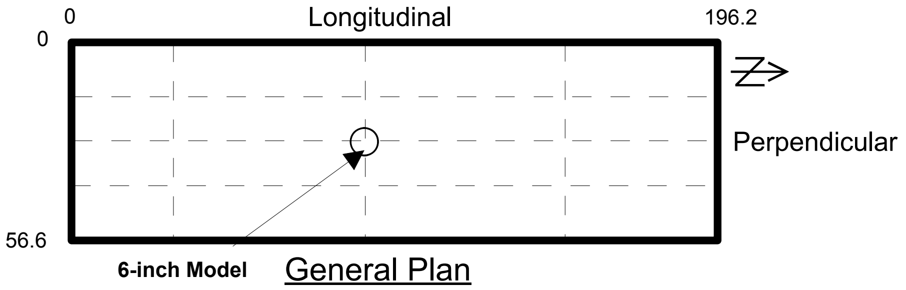

Test #7 (October 2, 2015)

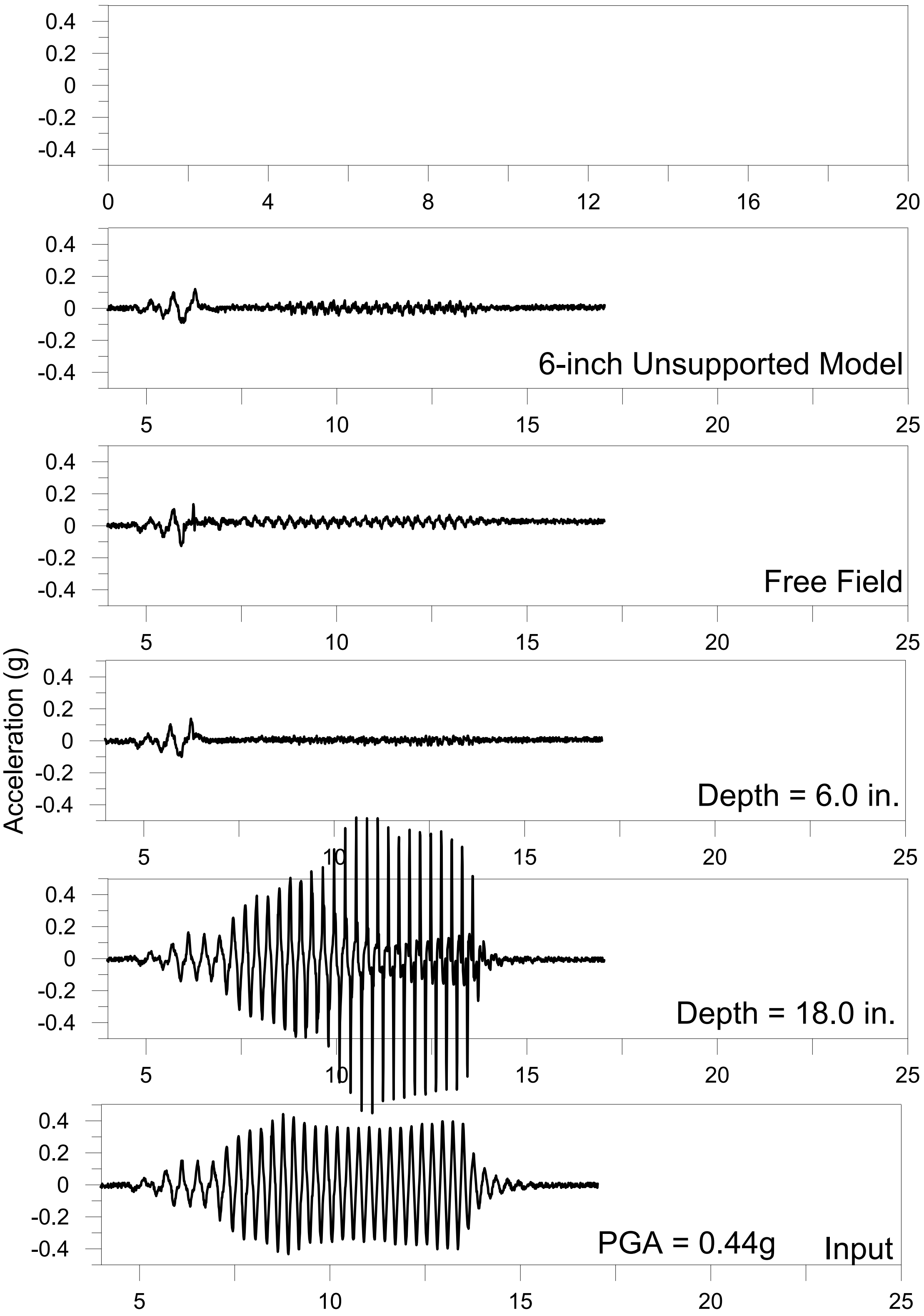

Test # 7: Settlement (cm)
10/2/2015
PGA: 0.44g

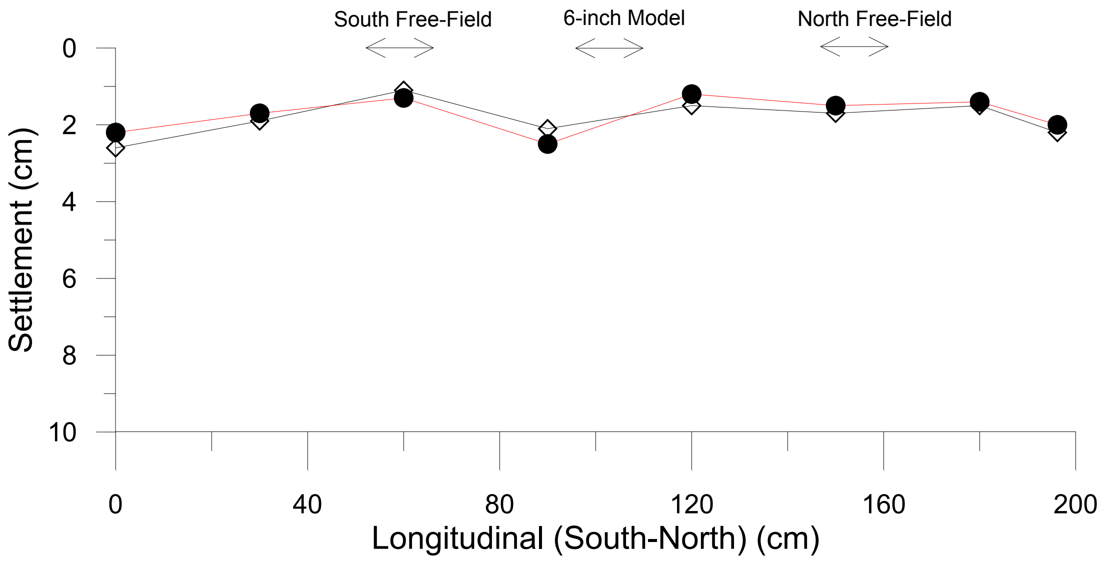

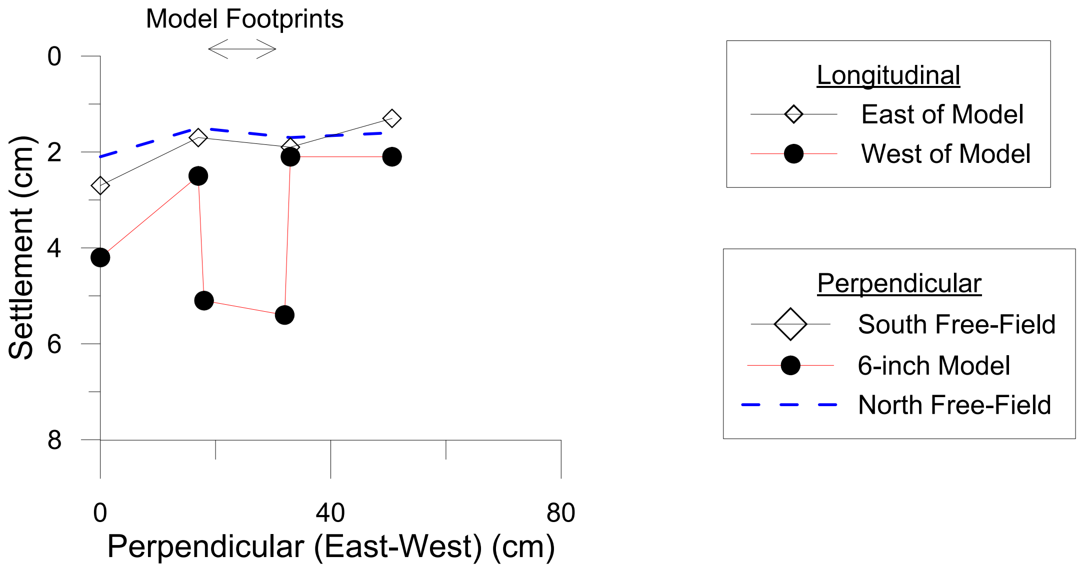

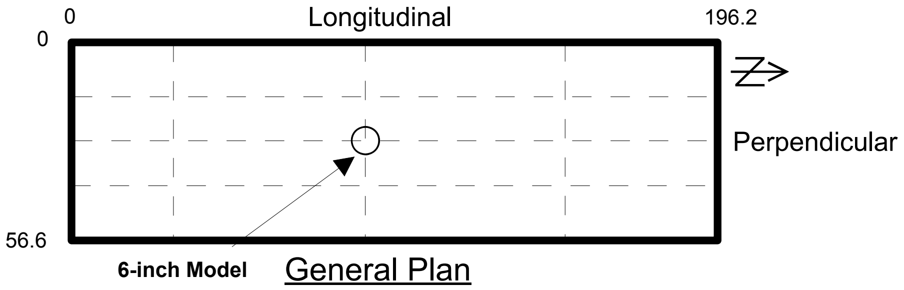

Test #8 (October 7, 2015)

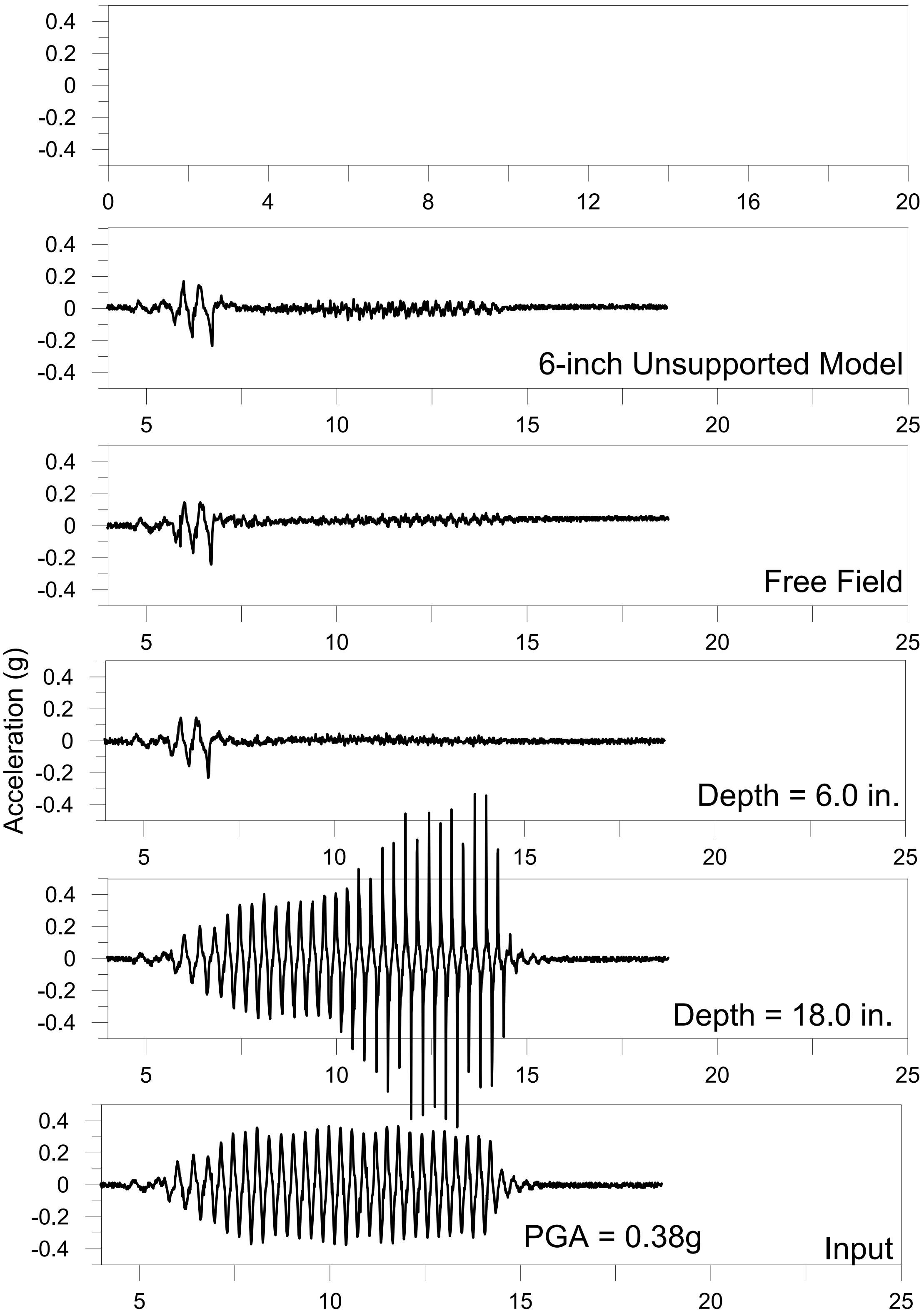

Test # 8: Settlement (cm)
10/7/2015
PGA: 0.38g

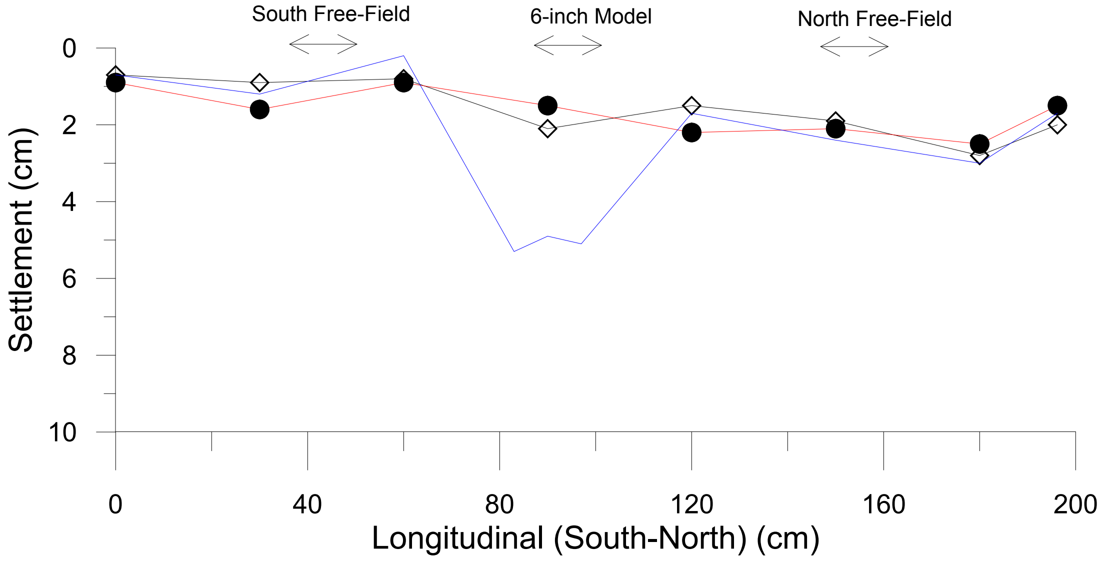

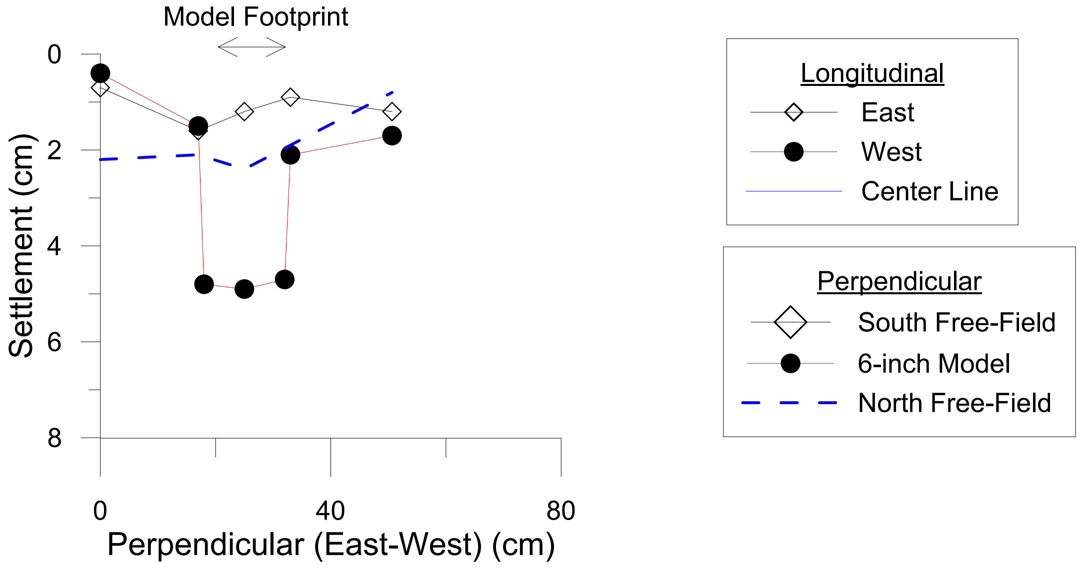

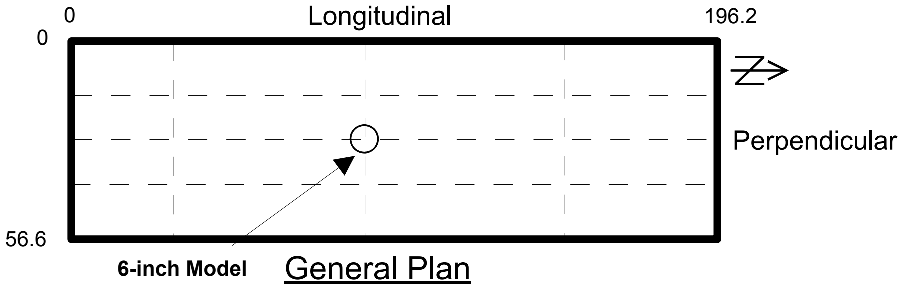

General Plan

Test #9 (October 30, 2015)

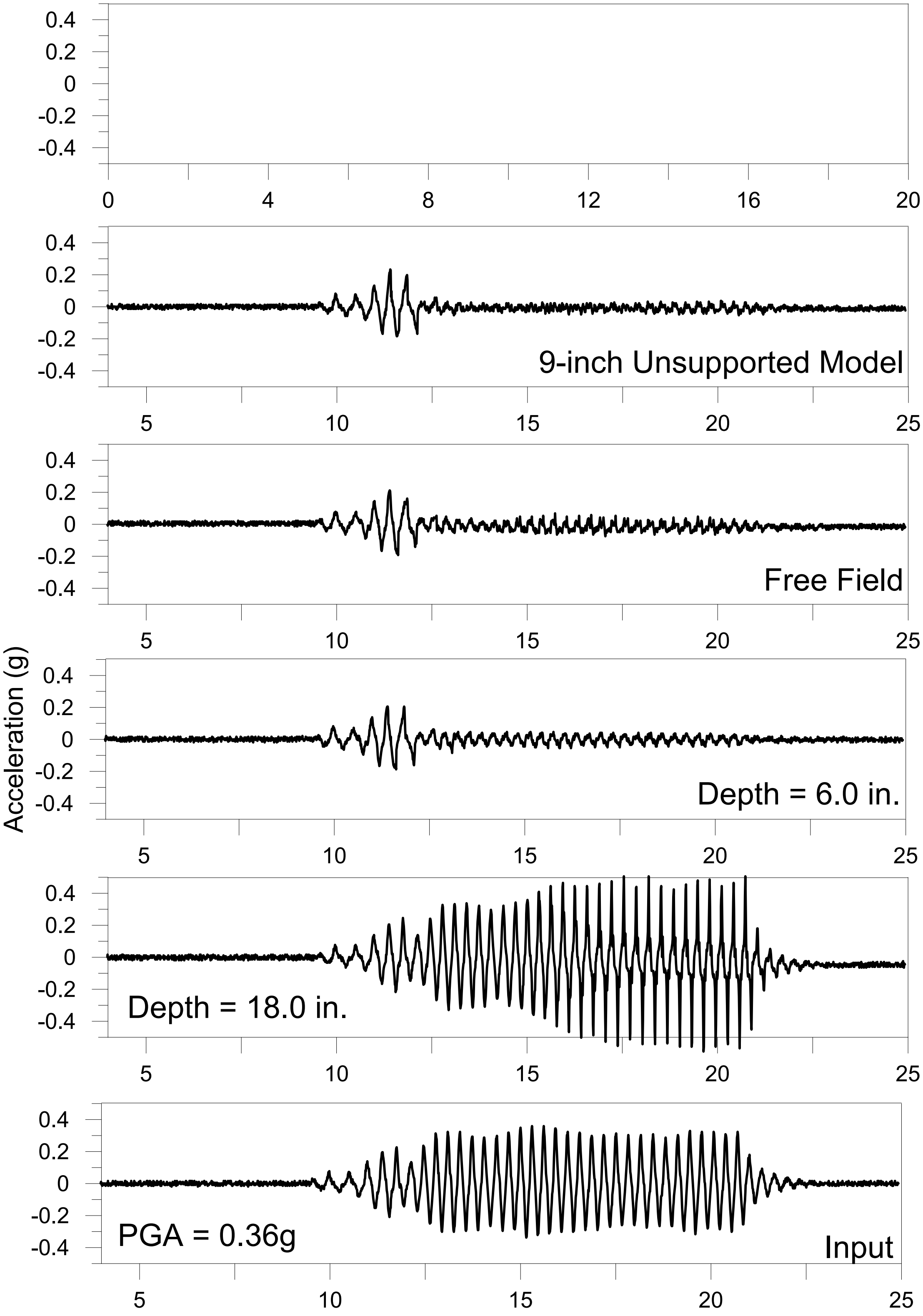

Test # 9: Settlement (cm)
10/30/2015
PGA: 0.36g

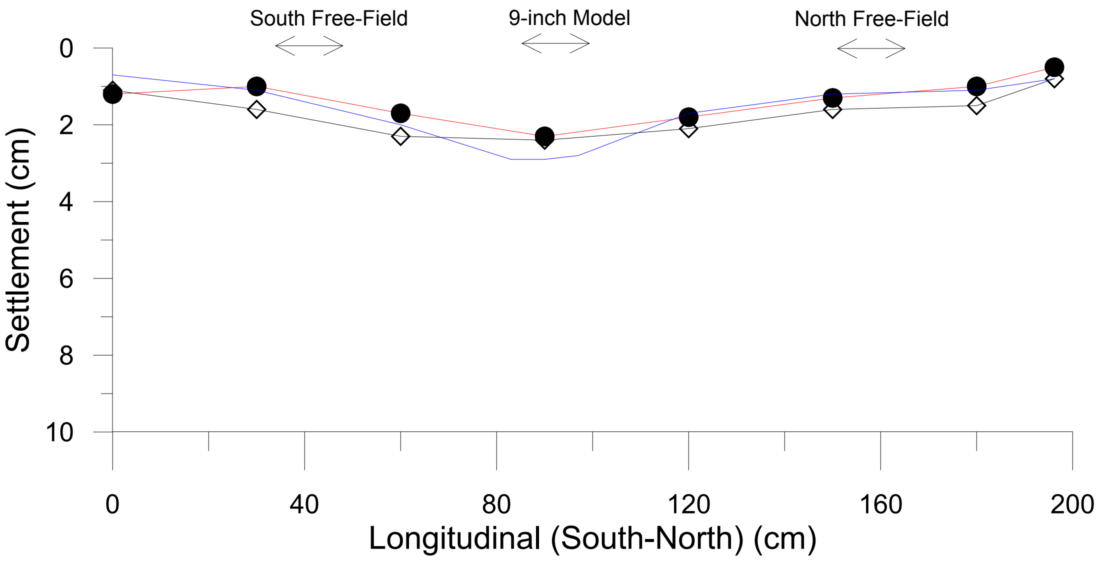

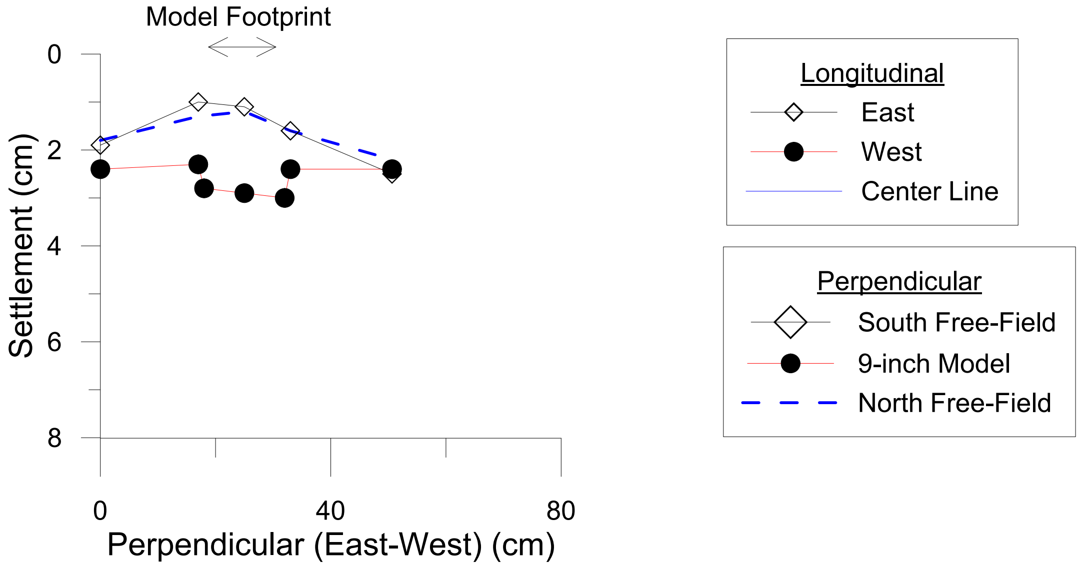

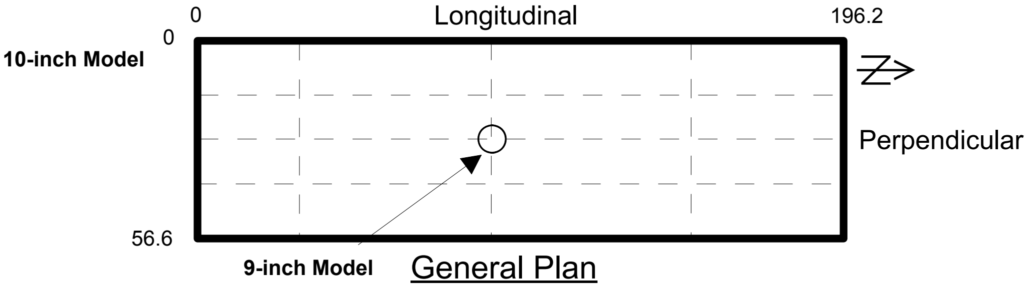

Test #10 (November 6, 2015)

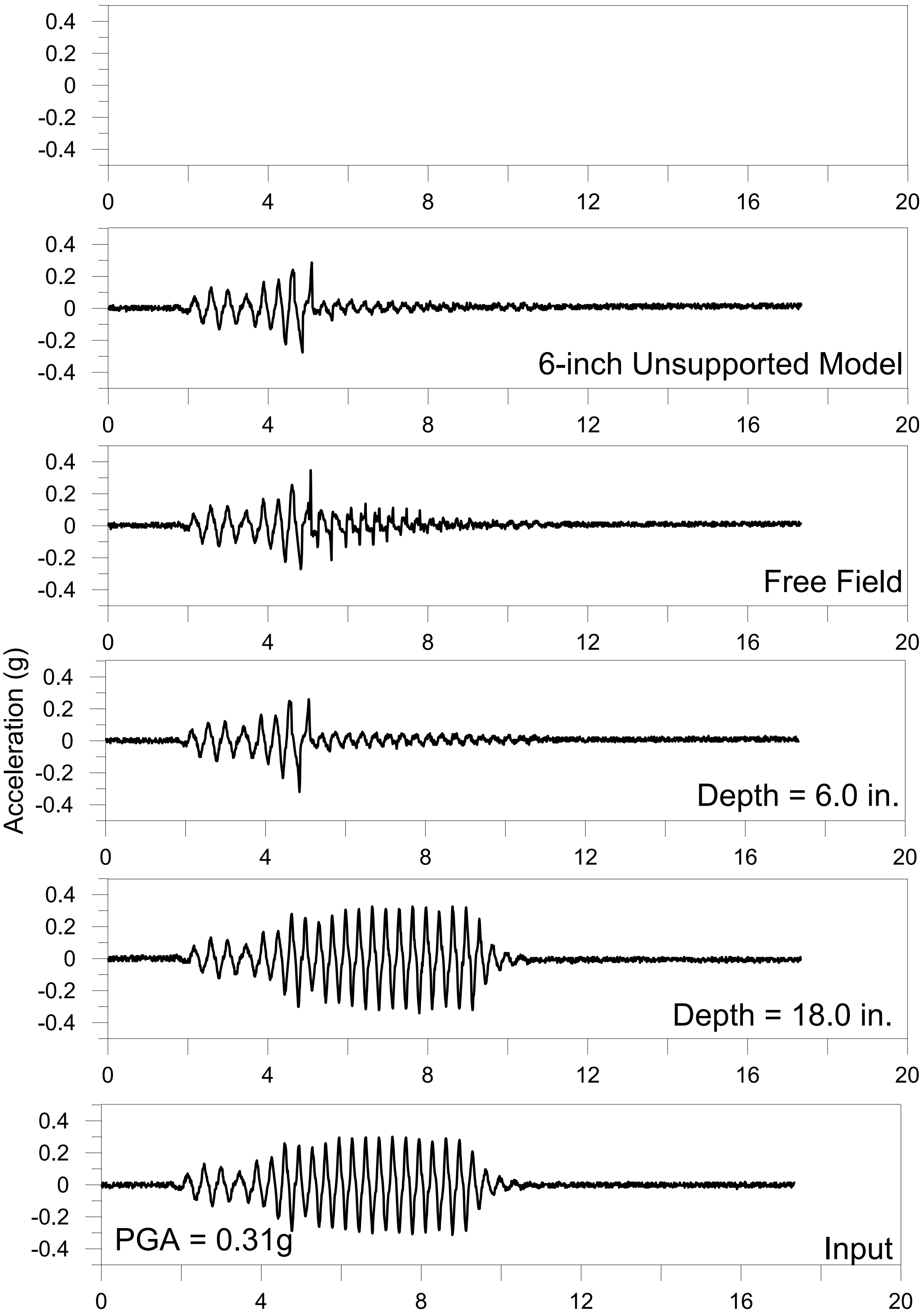

Test # 10: Settlement (cm)
11/6/2015
PGA: 0.31g

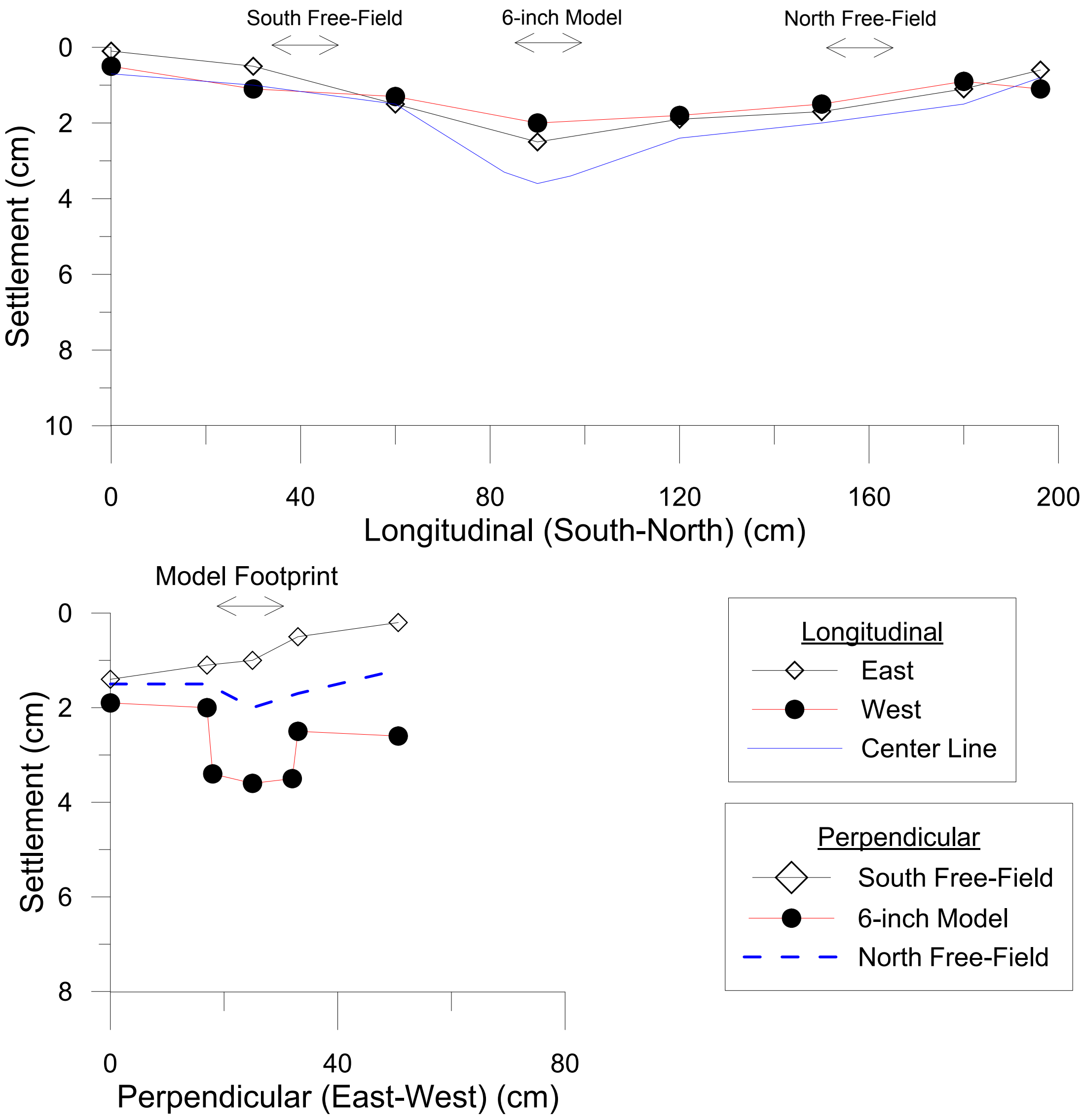

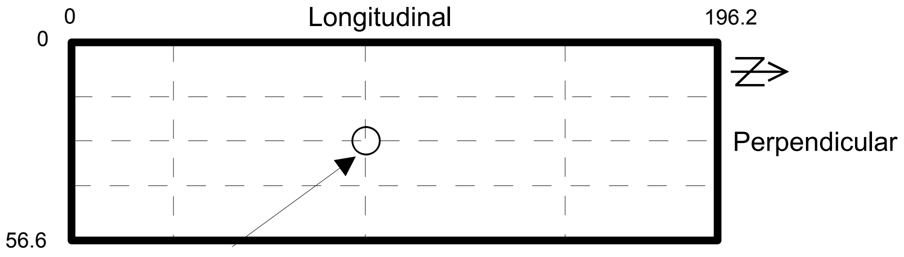

General Plan

Test #11 (November 13, 2015)

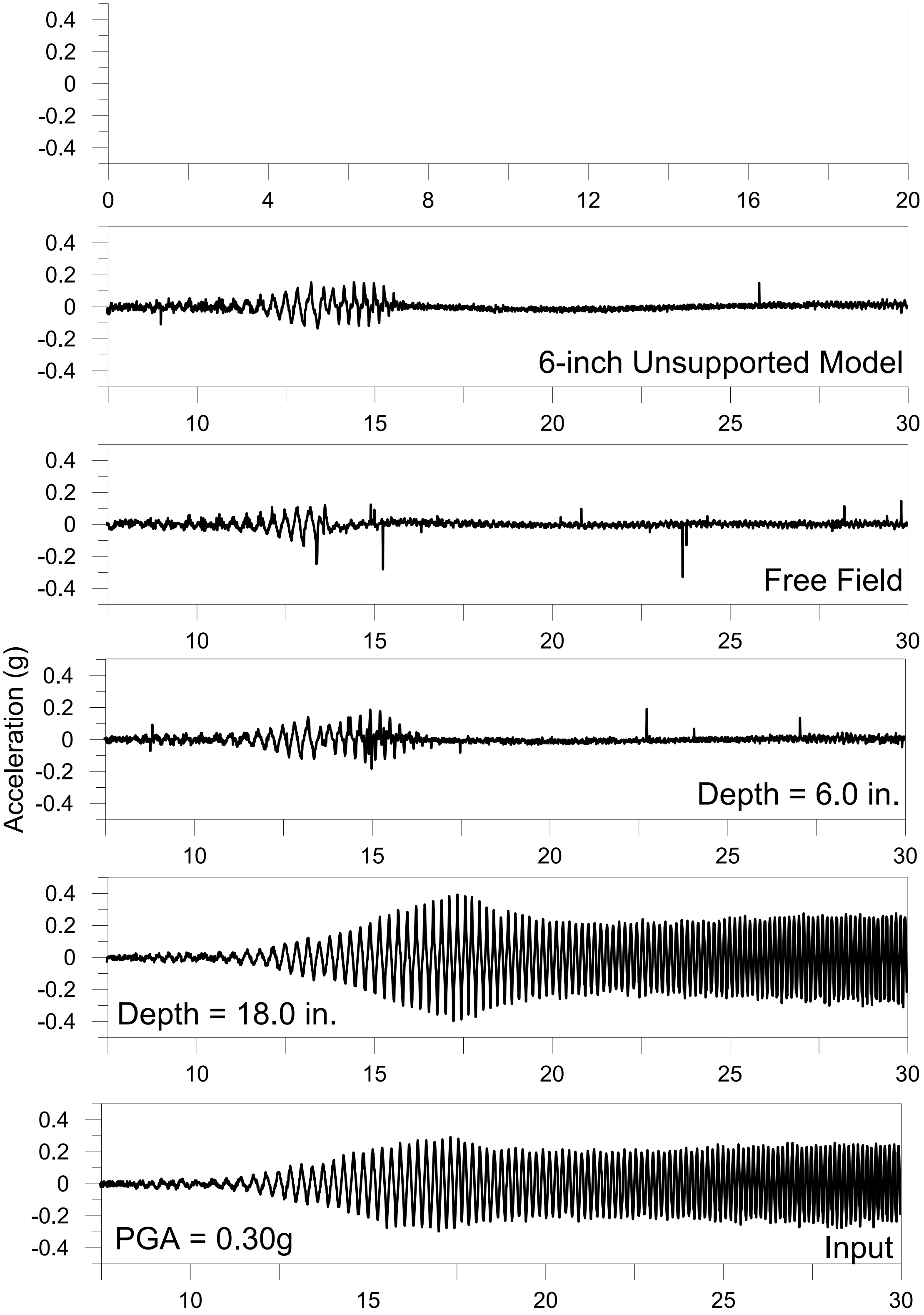

Test # 11: Settlement (cm)
11/13/2015
PGA: 0.30g

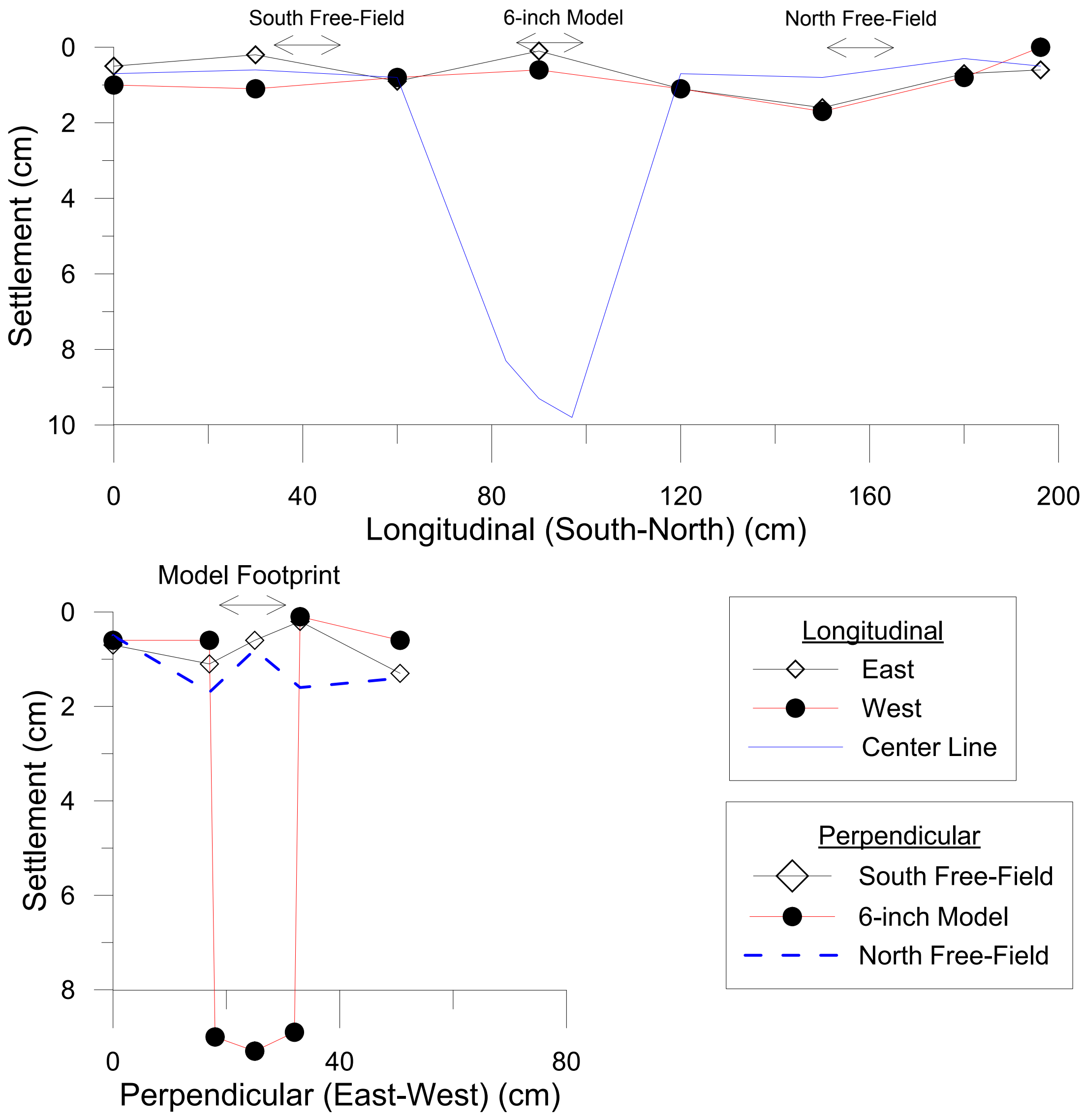

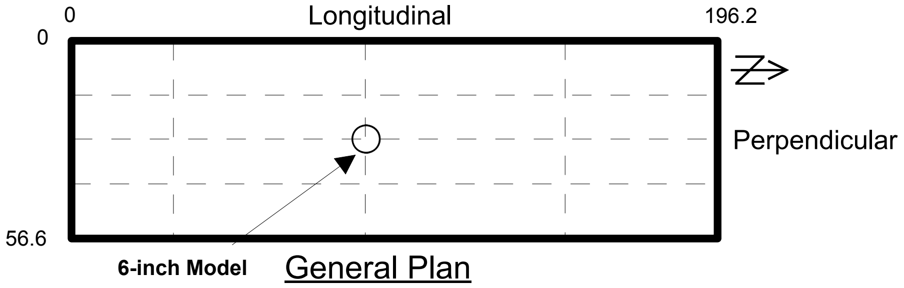

Test #12 (November 20, 2015)

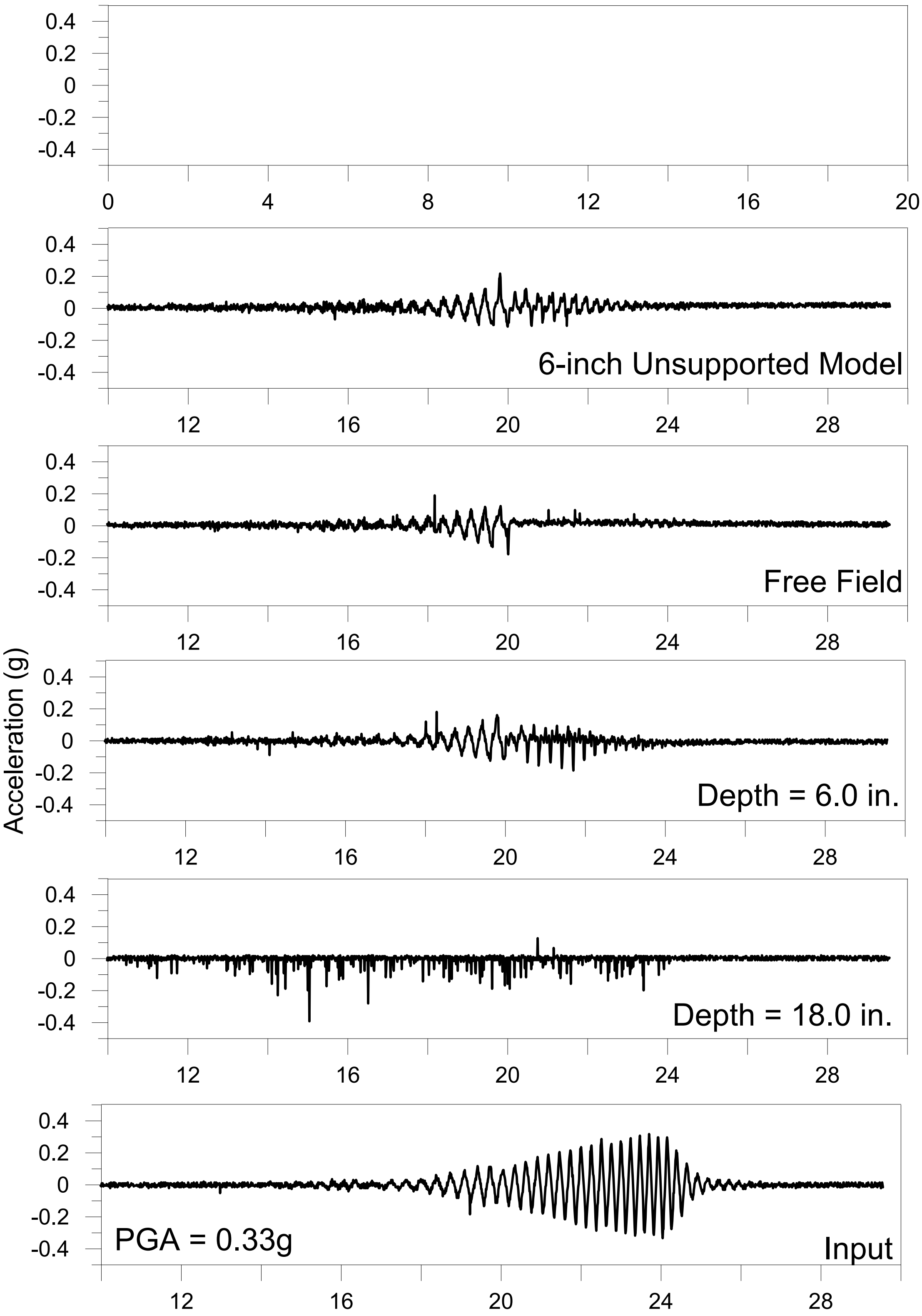

Test # 12: Settlement (cm)
11/20/2015
PGA: 0.33g

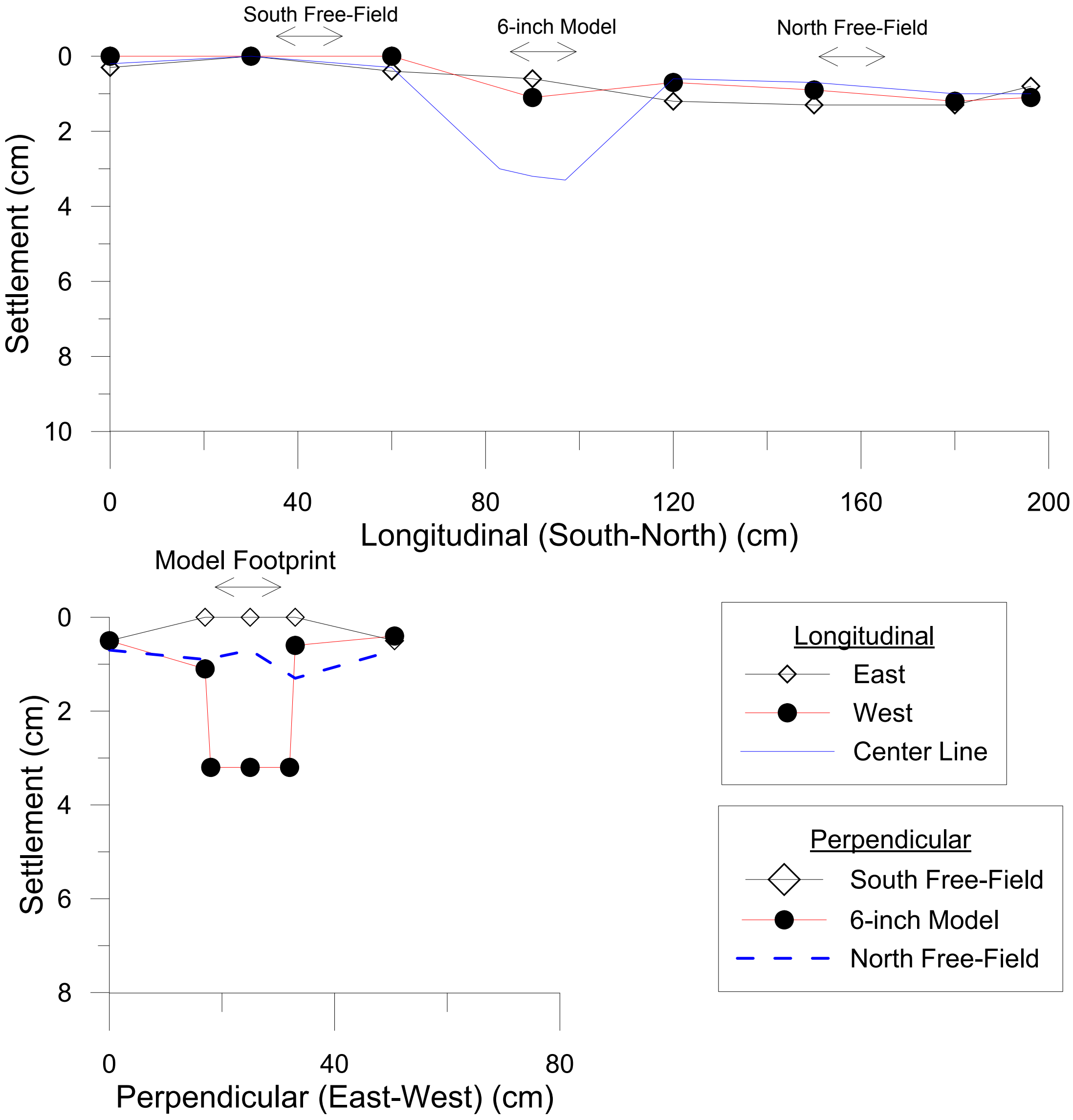

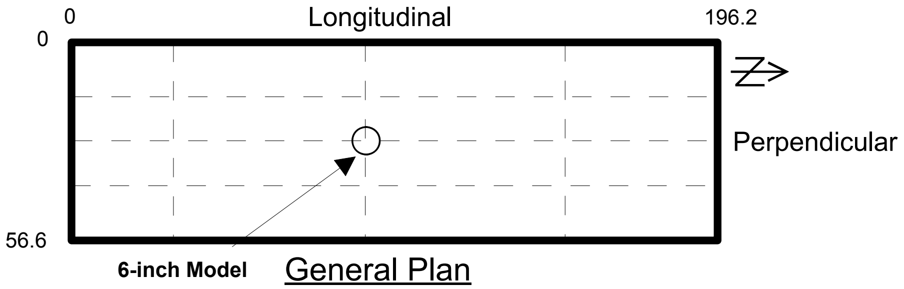

General Plan

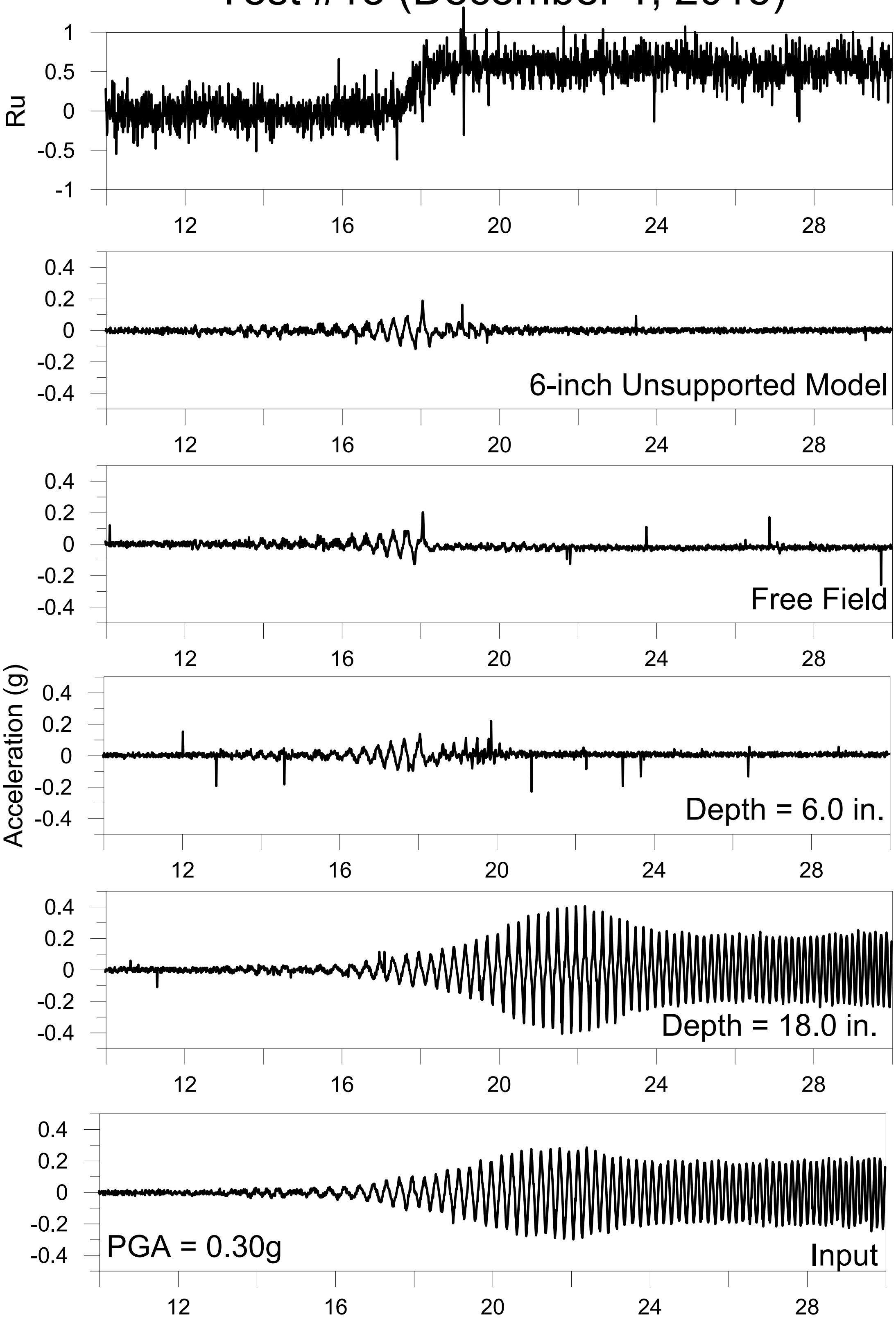

Test #13 (December 1, 2015)

Test # 13: Settlement (cm)
12/1/2015
PGA: 0.30g

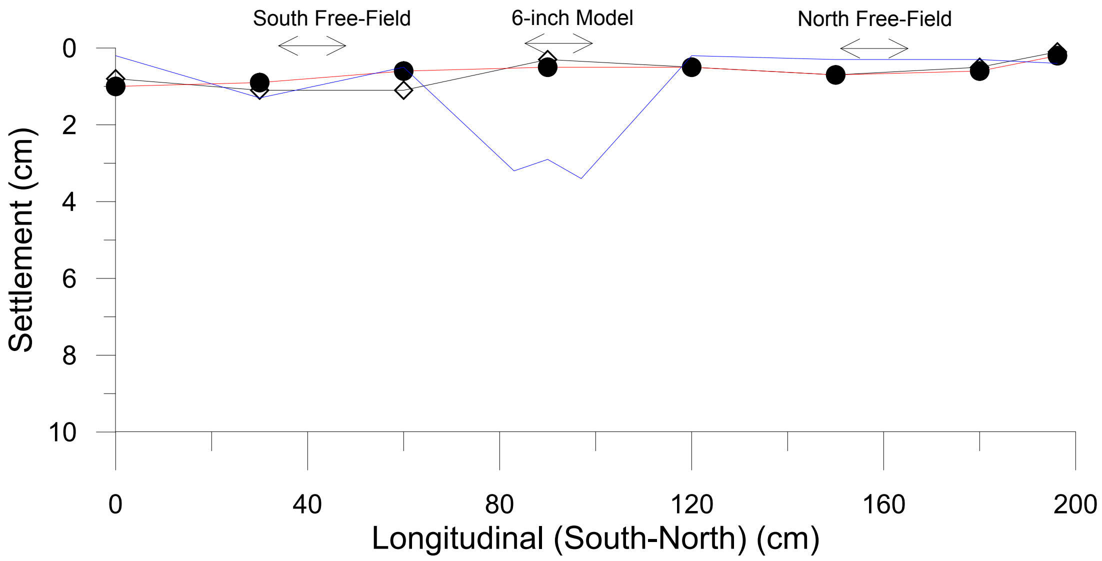

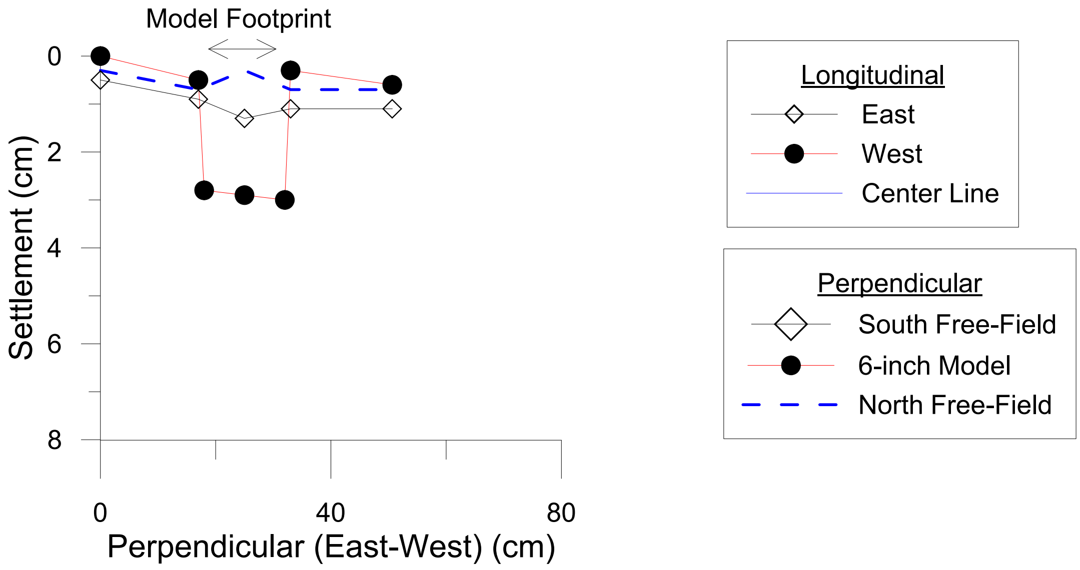

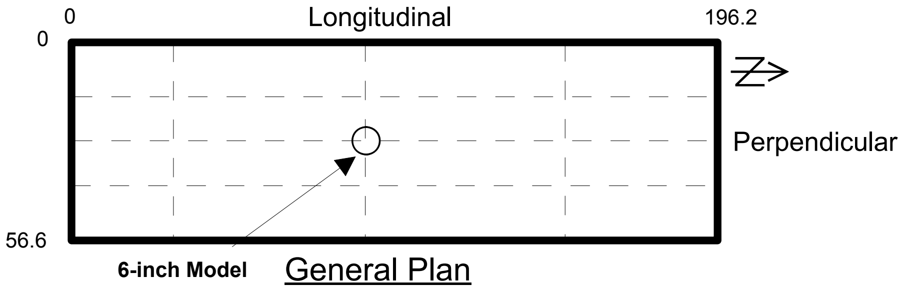

Test #14 (December 8, 2015)

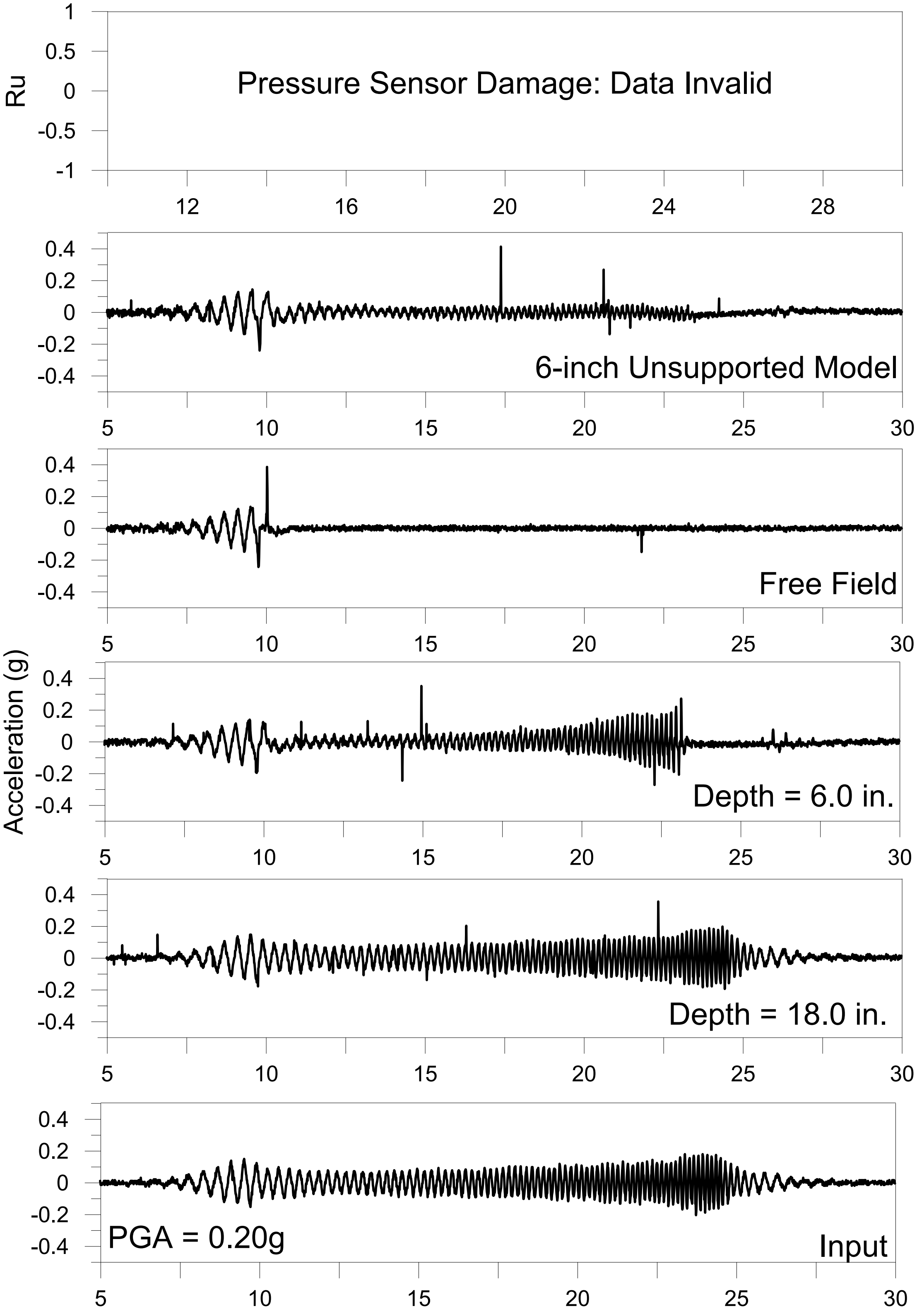

Test # 14: Settlement (cm)
12/8/2015
PGA: 0.20g

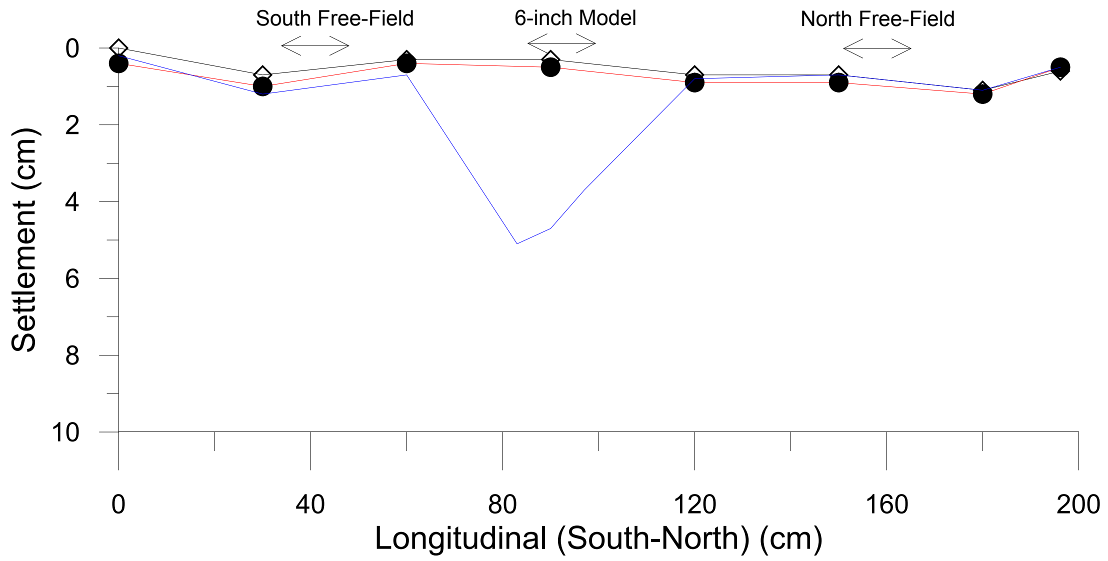

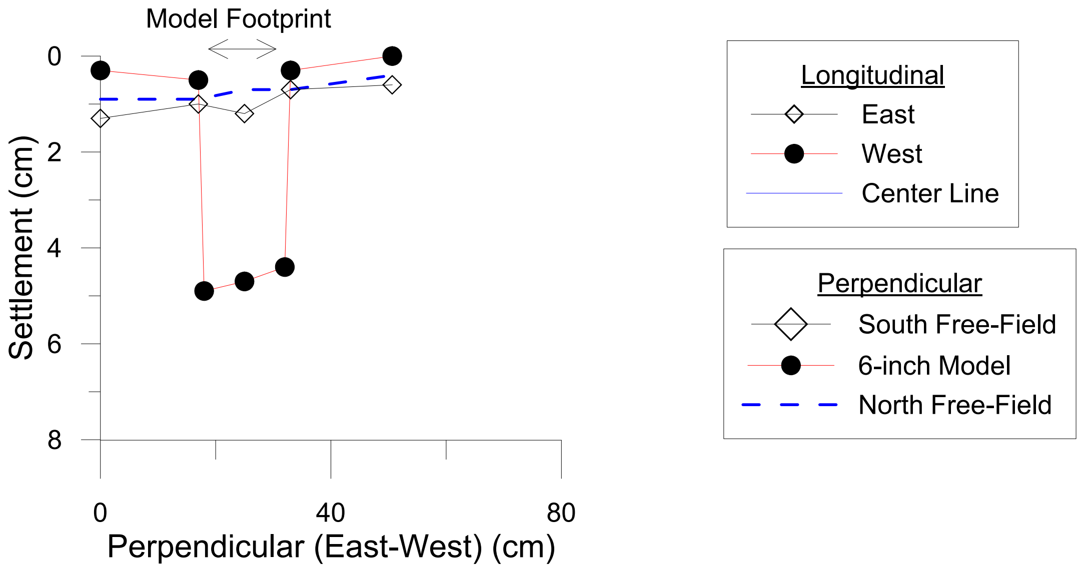

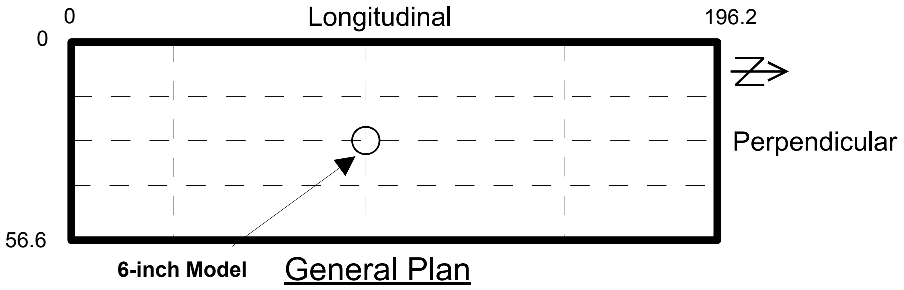

Test #15 (December 11, 2015)

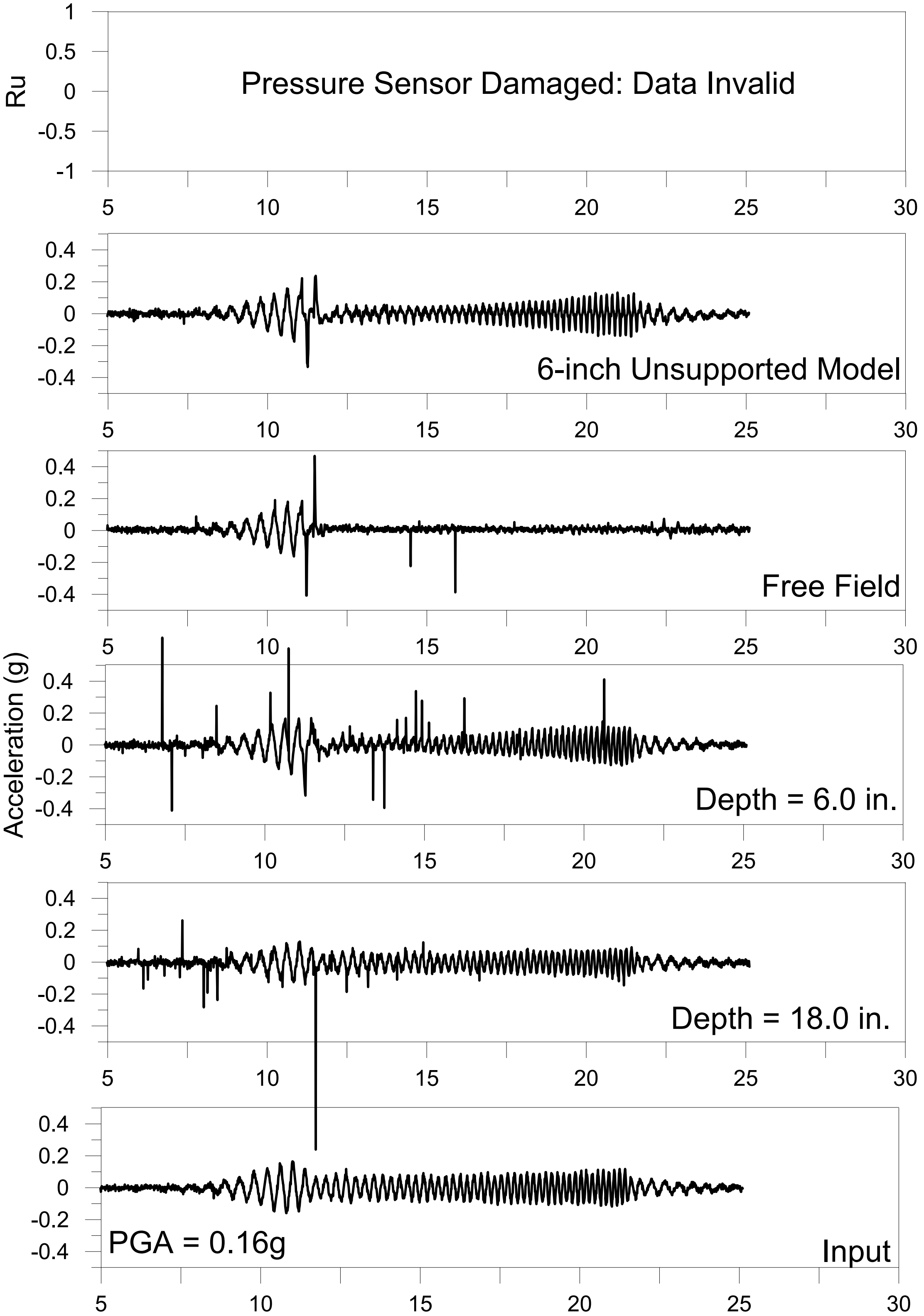

Test # 15: Settlement (cm)
12/11/2015
PGA: 0.16g

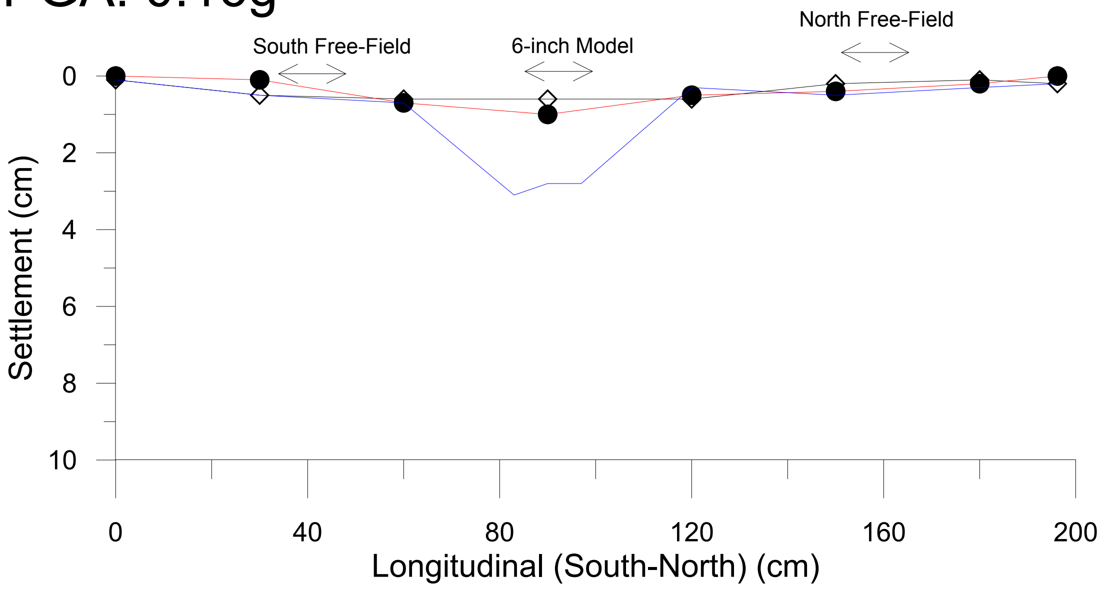

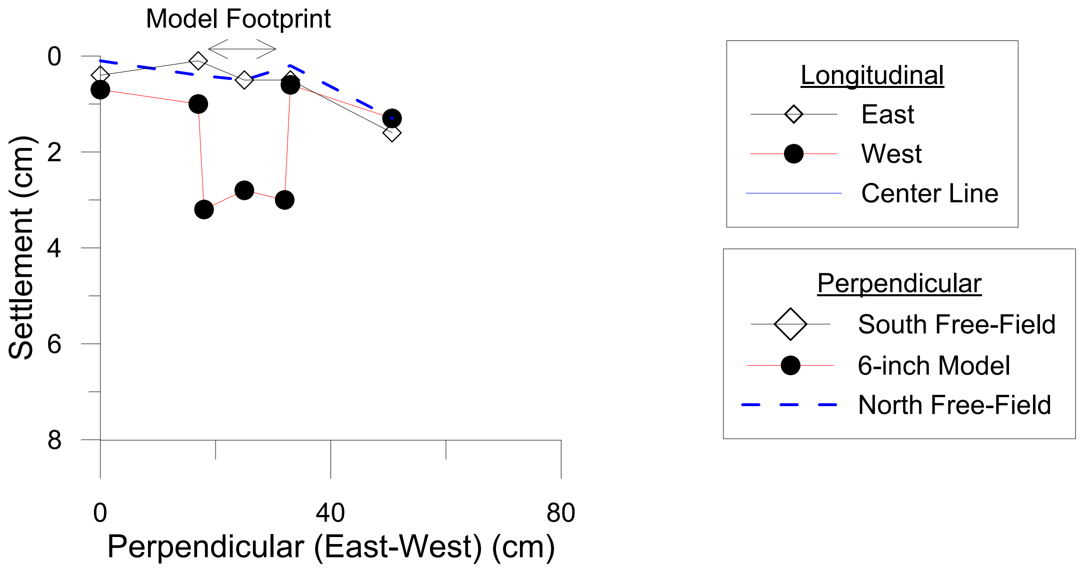

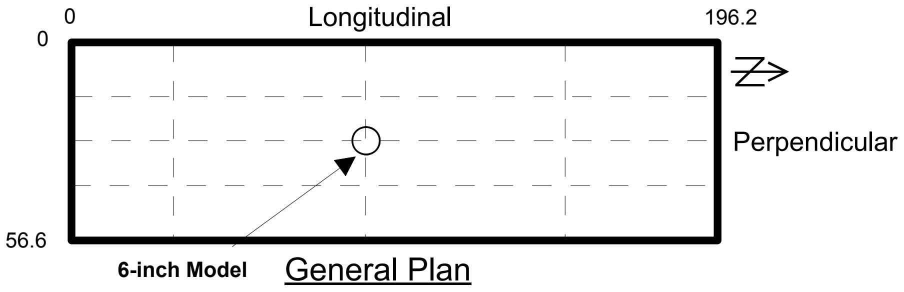

Test #16 (December 15, 2015)

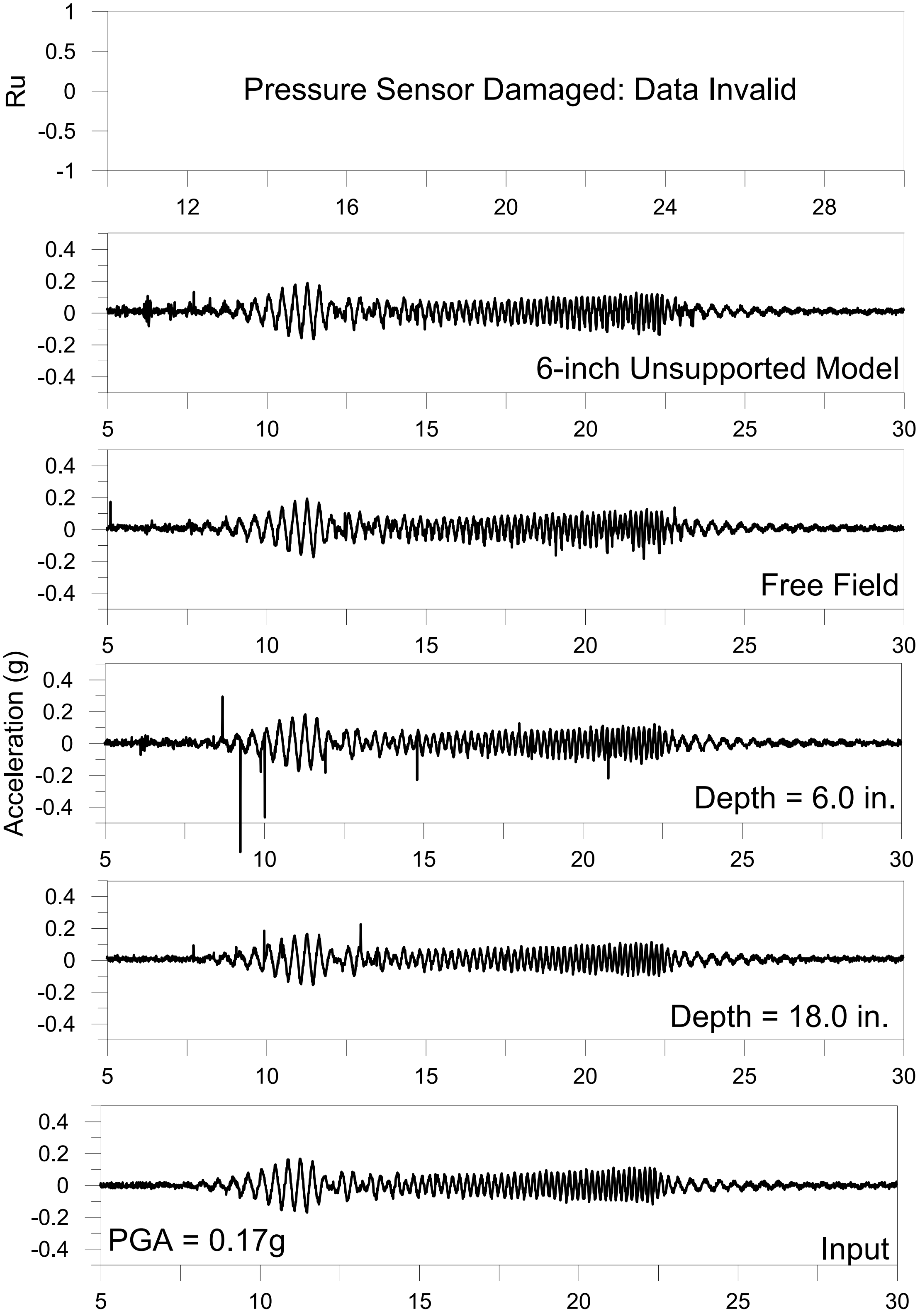

Test # 16: Settlement (cm)
12/15/2015
PGA: 0.17g

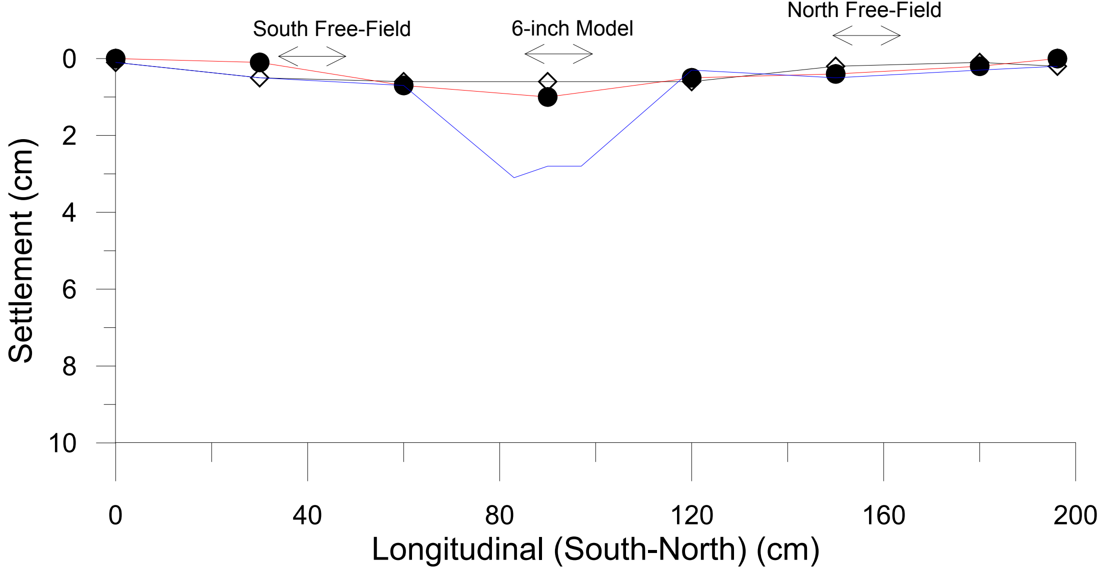

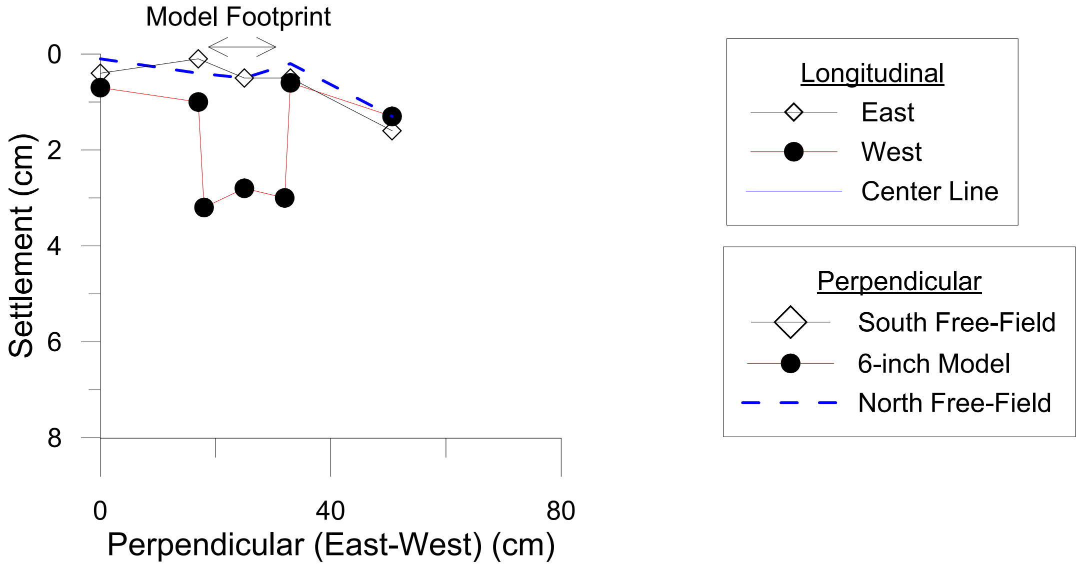

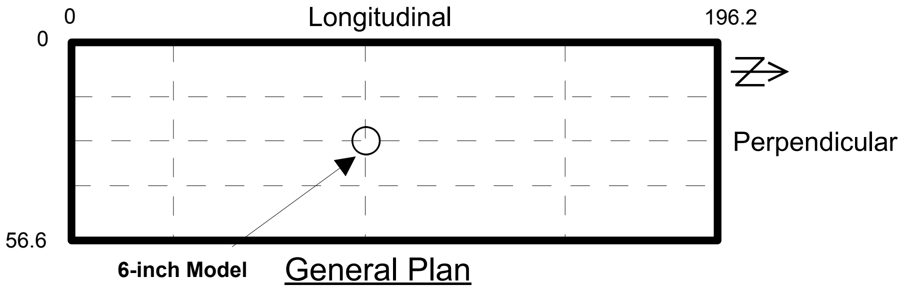

Test #17 (December 18, 2015)

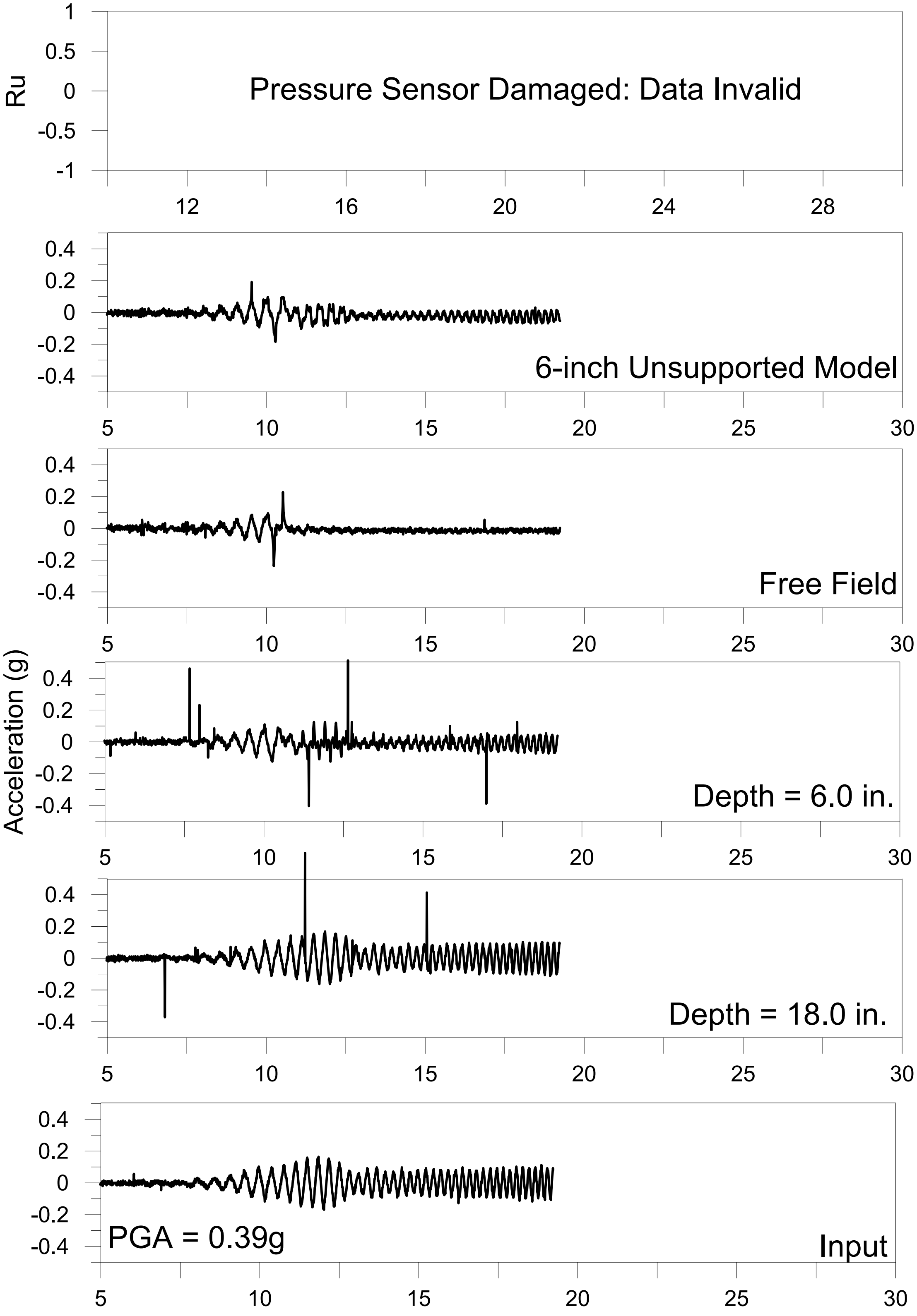

Test # 17: Settlement (cm)
11/6/2015
PGA: 0.31g

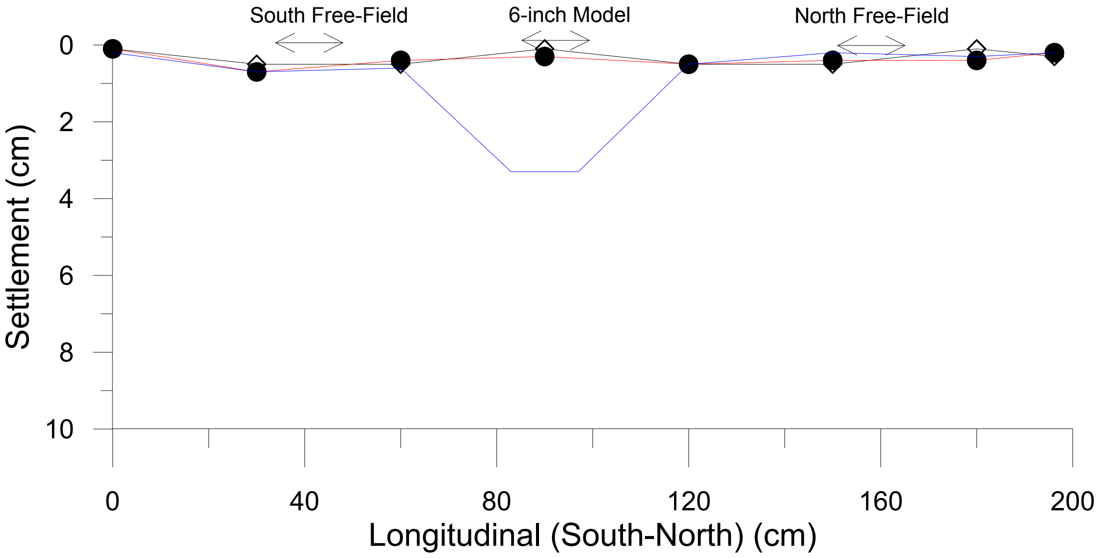

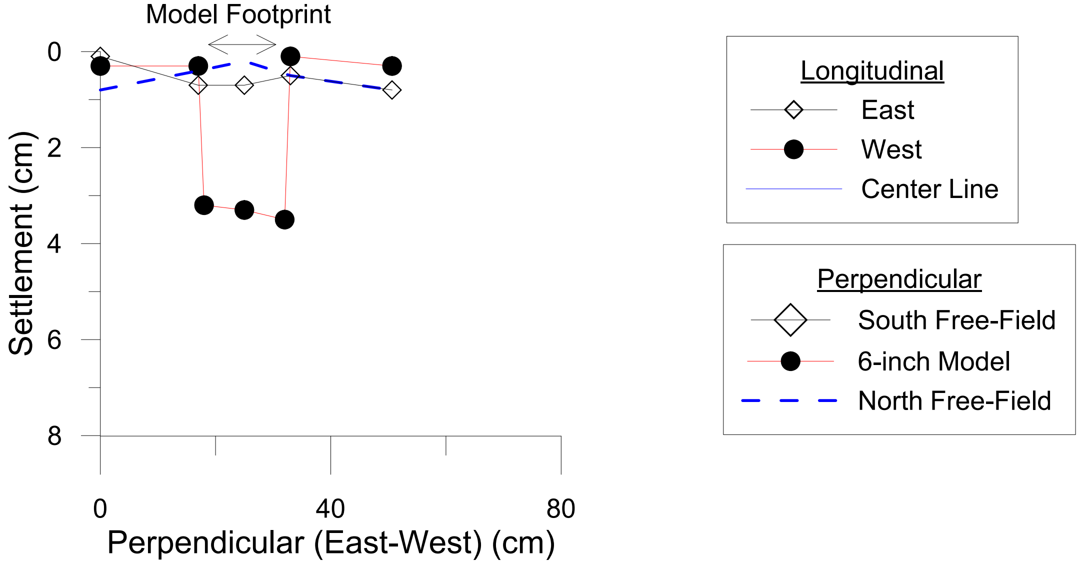

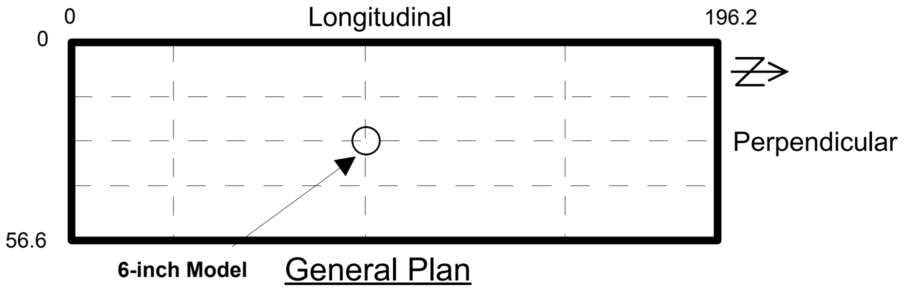

General Plan

Test #18 (January 1, 2016)

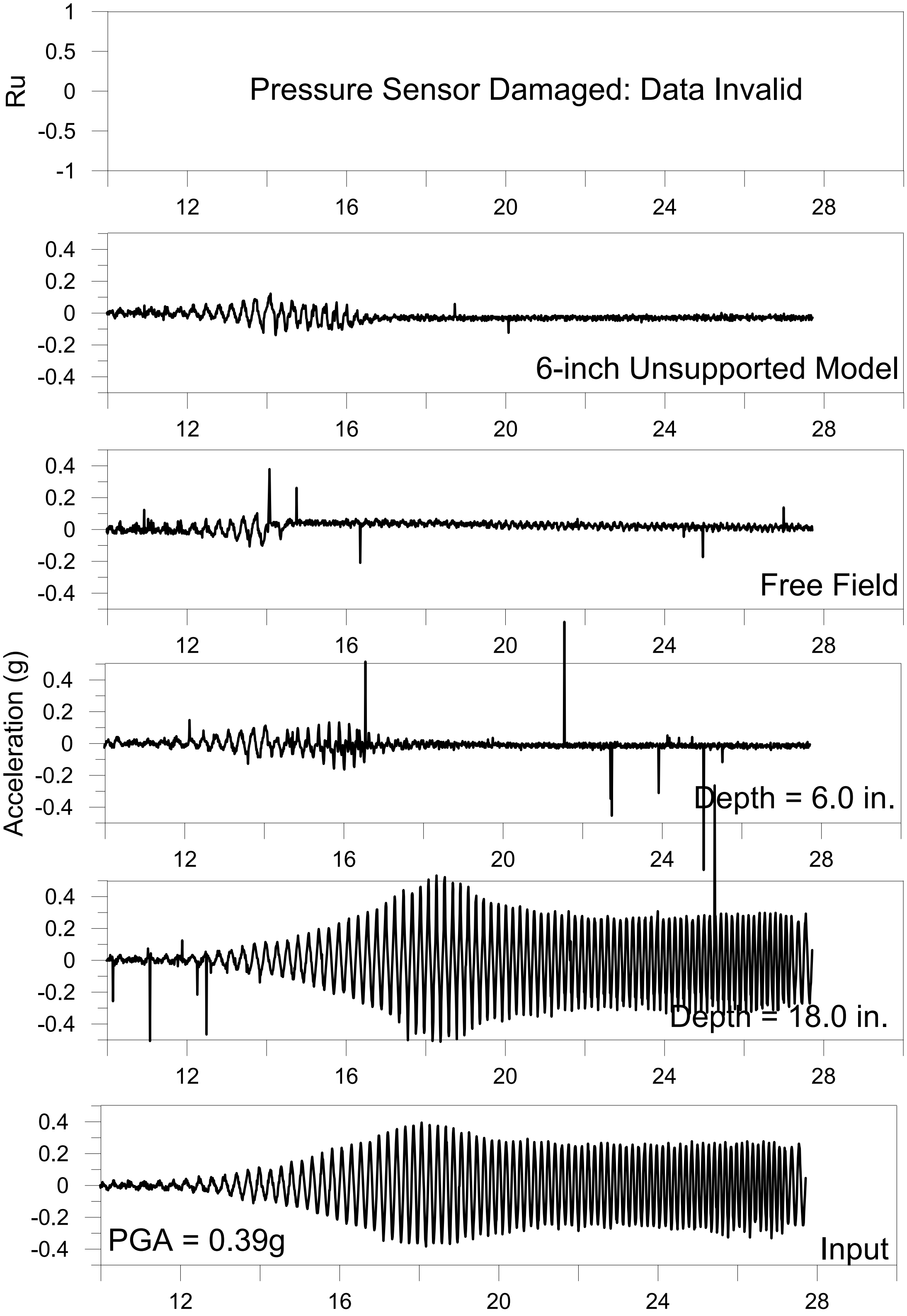

Test # 18: Settlement (cm)
1/1/2016
PGA: 0.39g

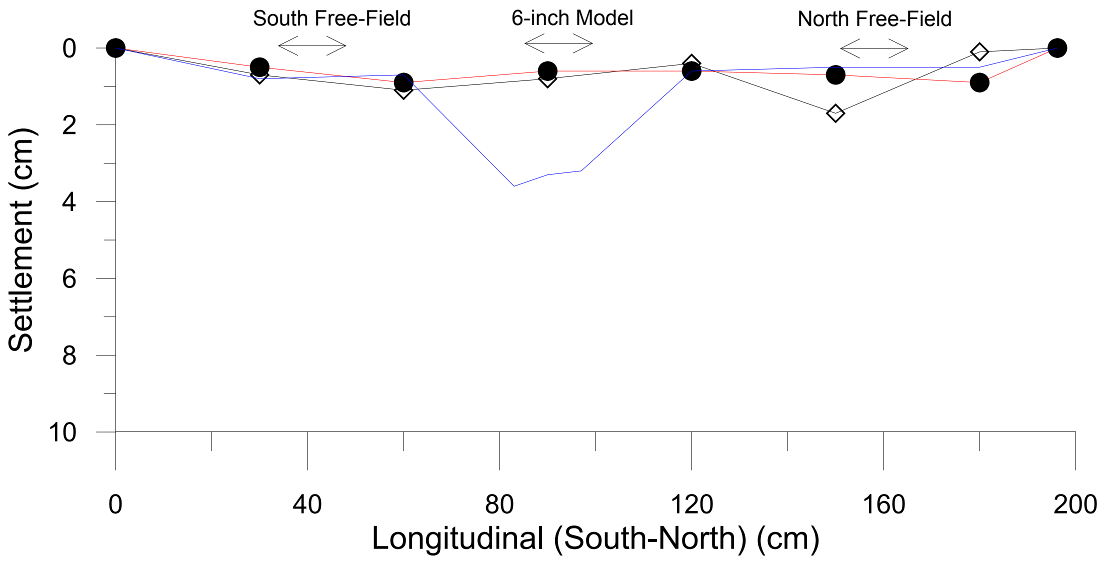

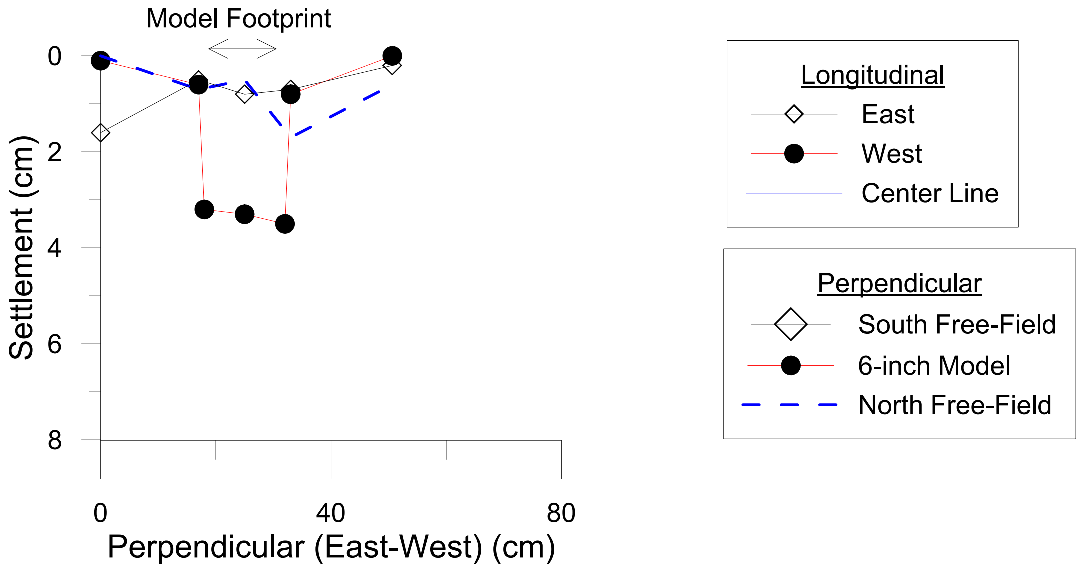

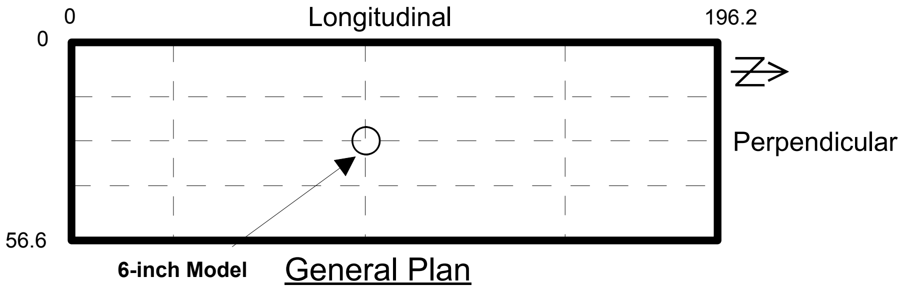

Test #19 (January 8, 2015)

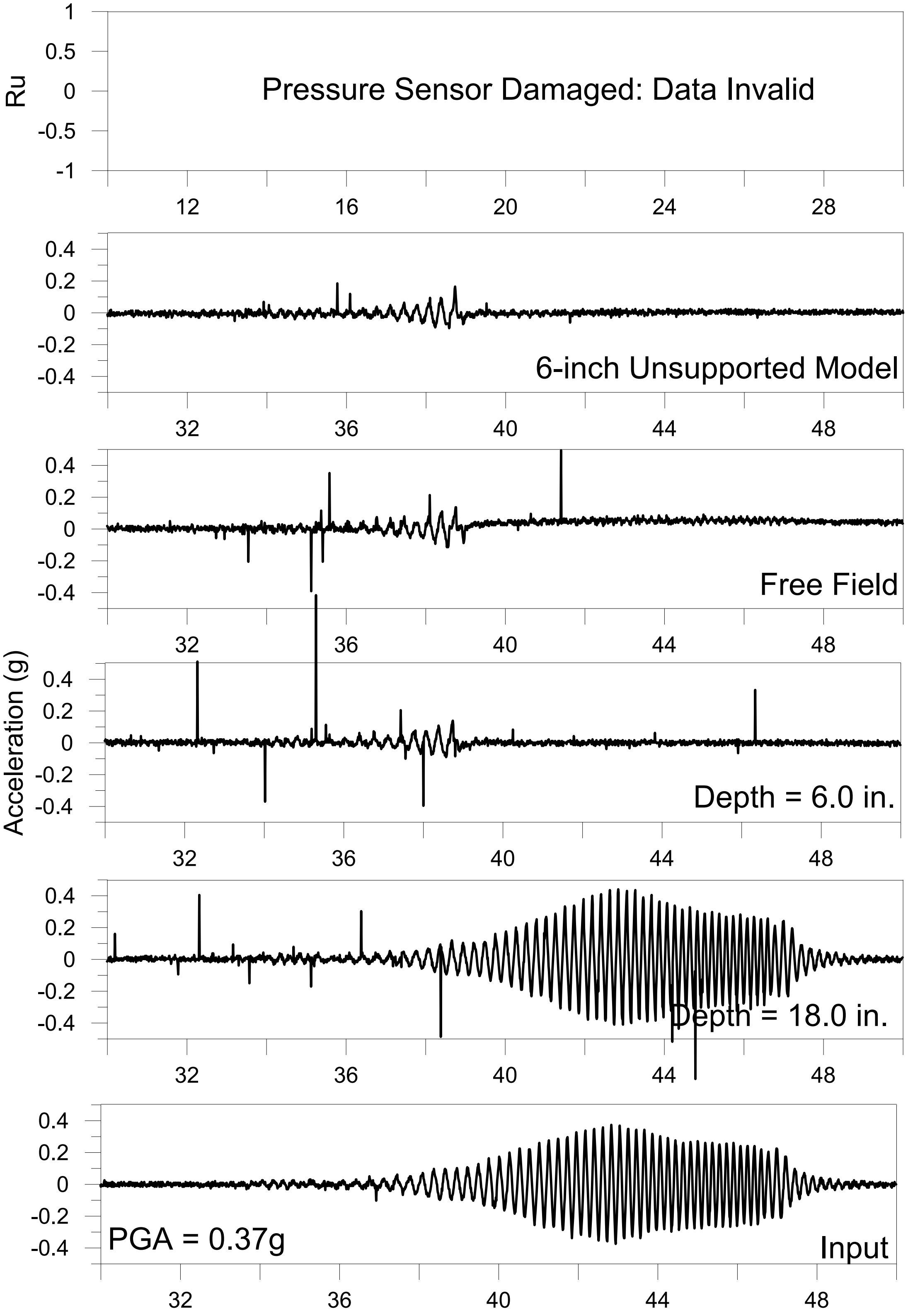

Test # 19: Settlement (cm)
1/8/2016
PGA: 0.37g

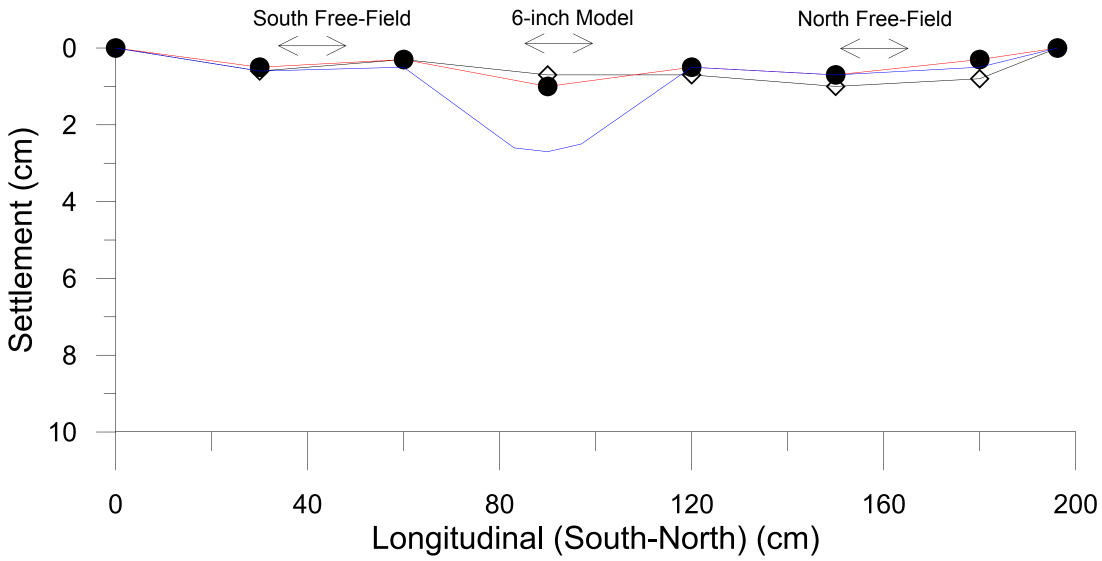

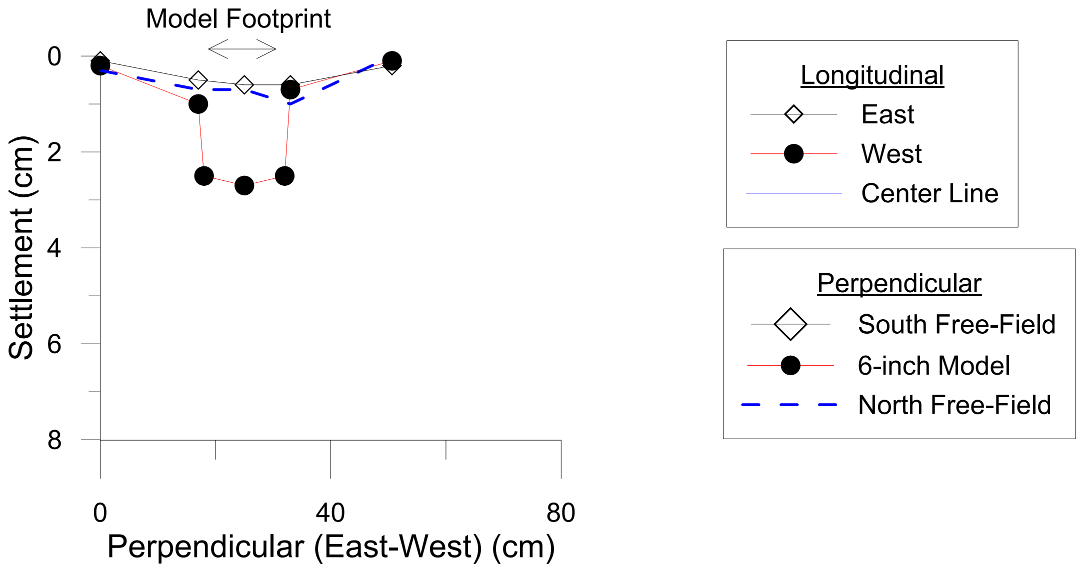

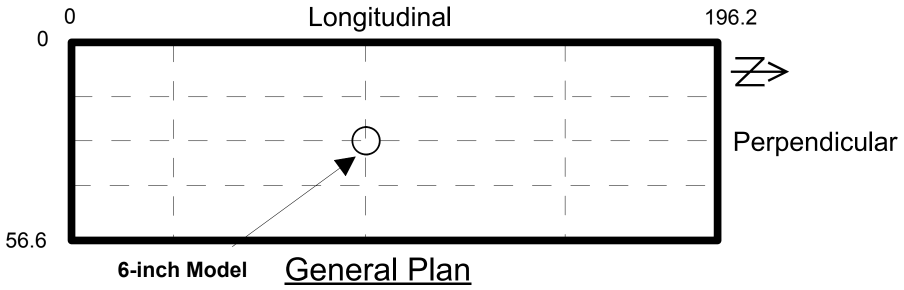

Test #19.1 (January 22, 2016)

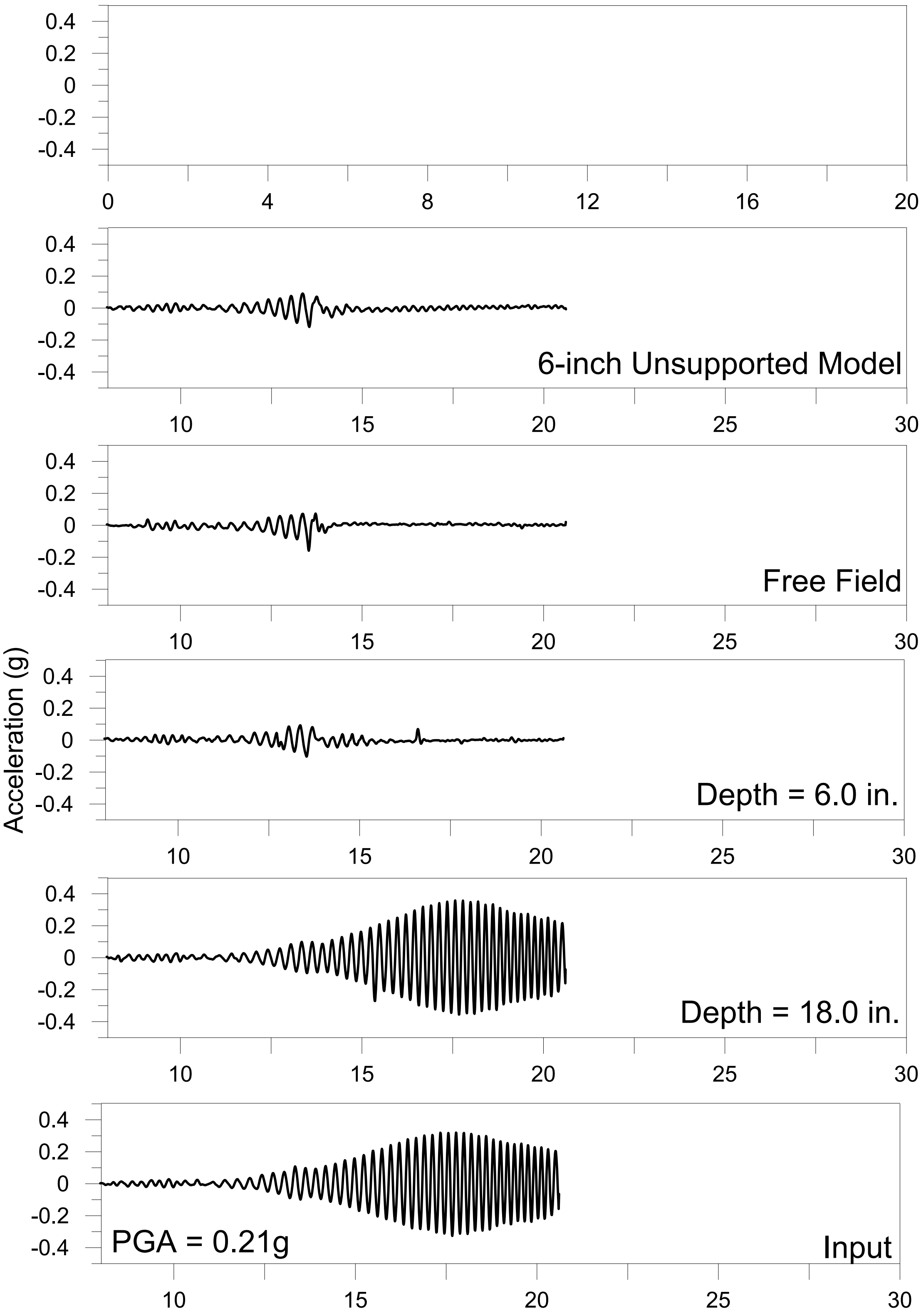

Test # 19.1: Settlement (cm)
1/22/2015
PGA: 0.36g

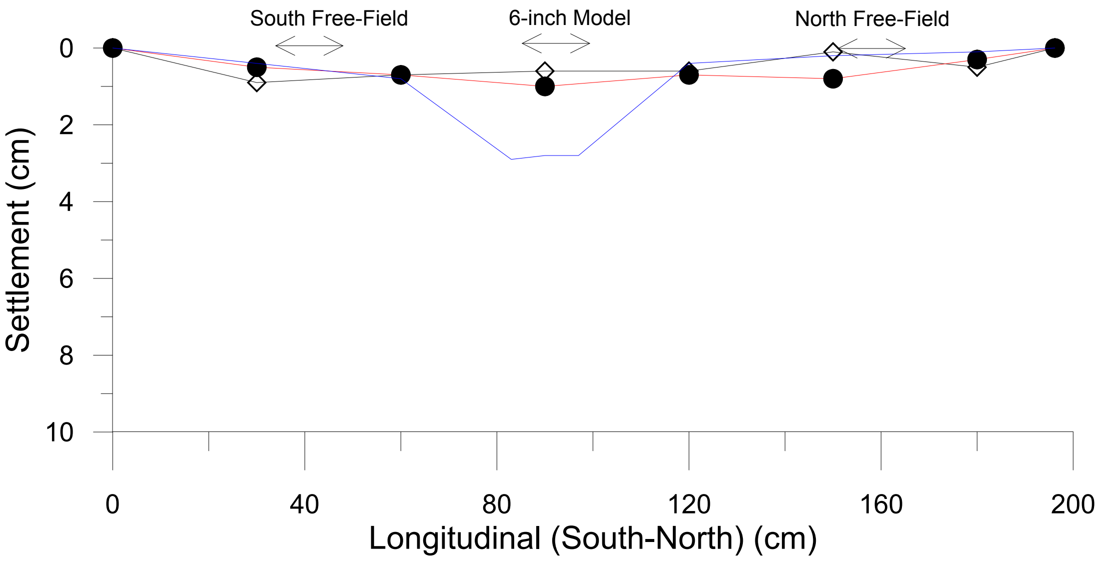

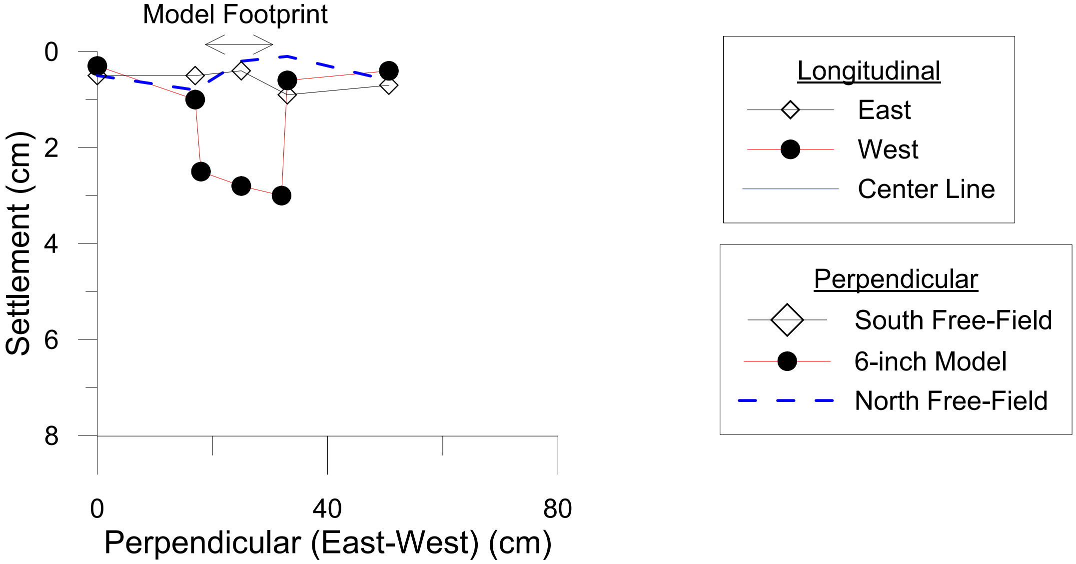

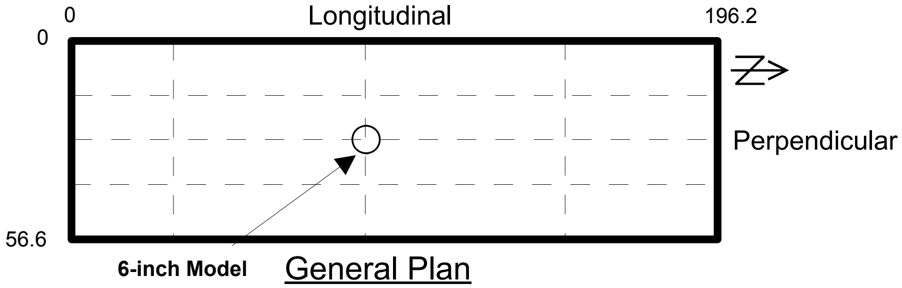

Test # 19.1: Ground Motion Characteristics
1/22/2016
PGA: 0.36g

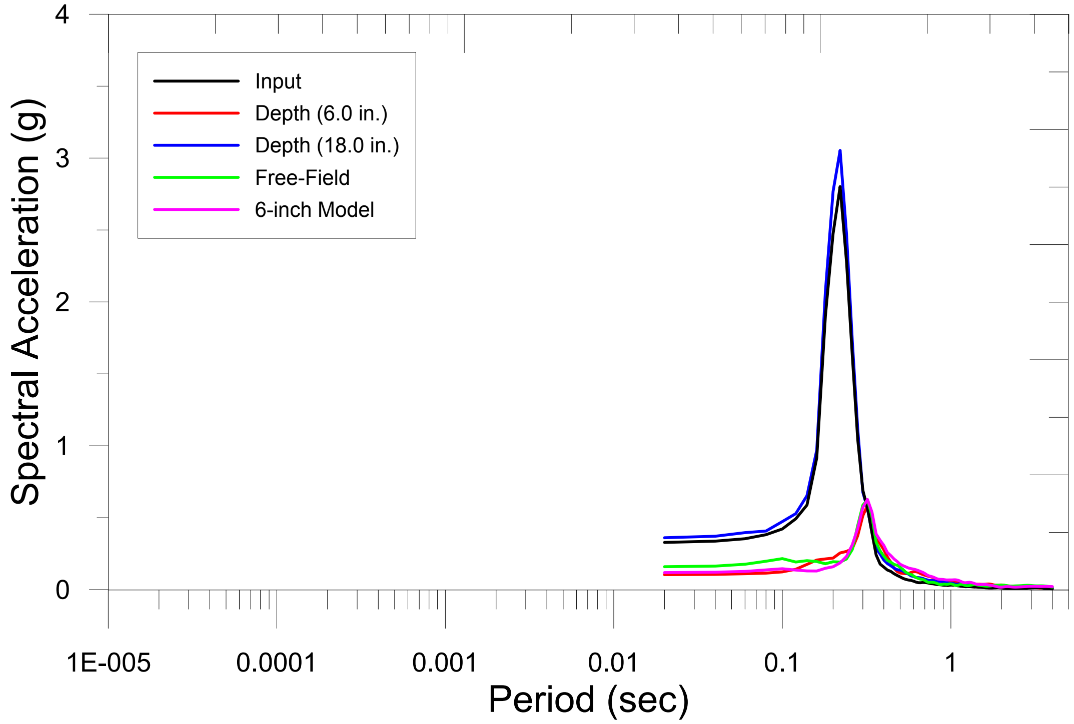

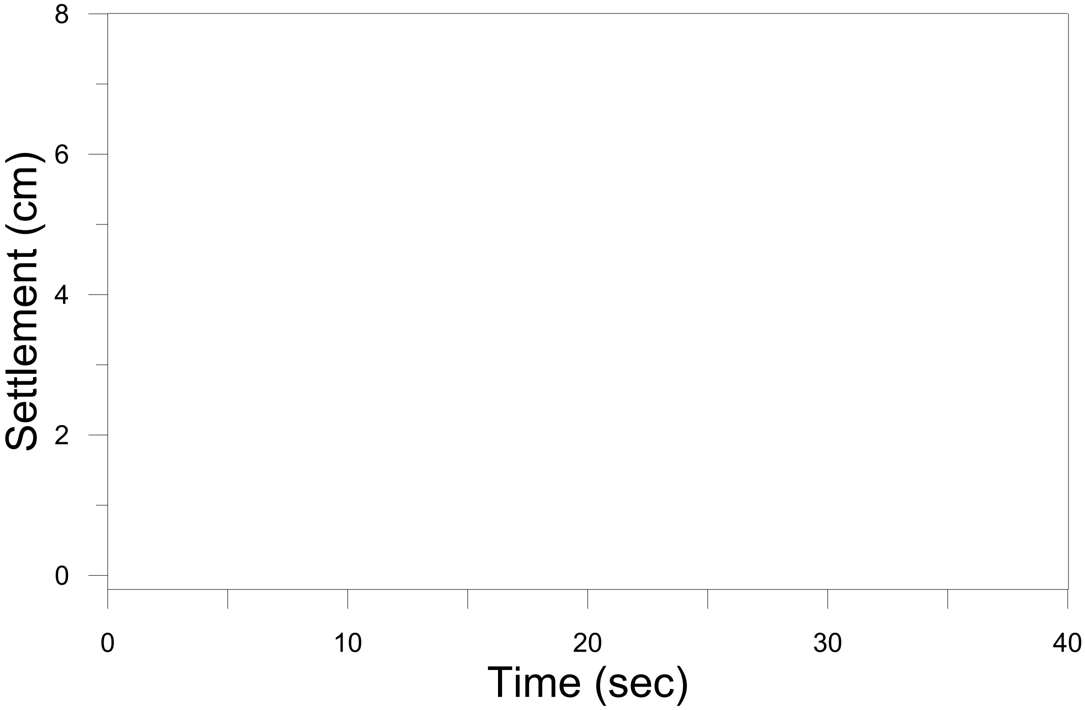

Test #19.2 (February 5, 2016)

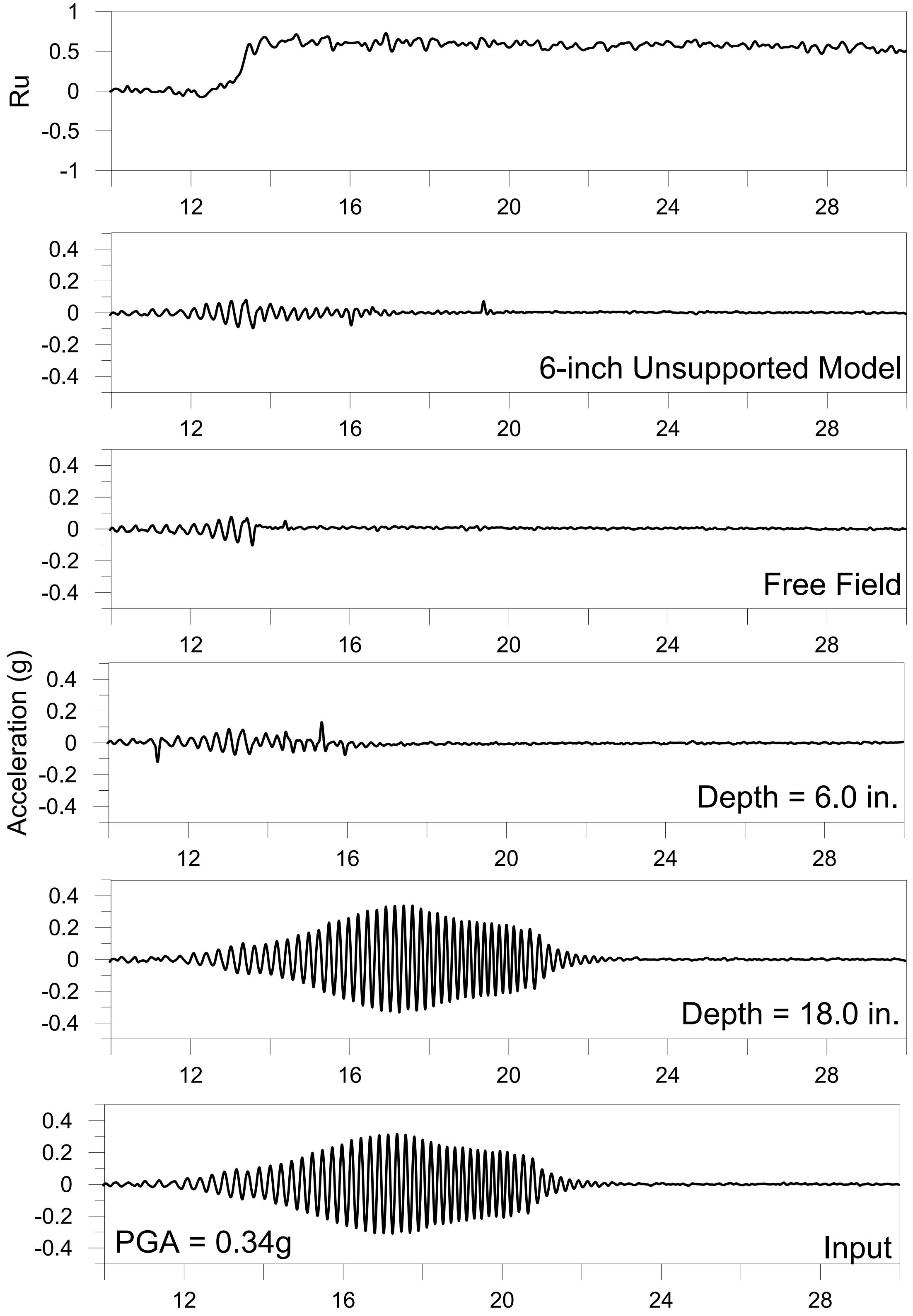

Test # 19.2: Settlement (cm)
2/5/2015
PGA: 0.34g

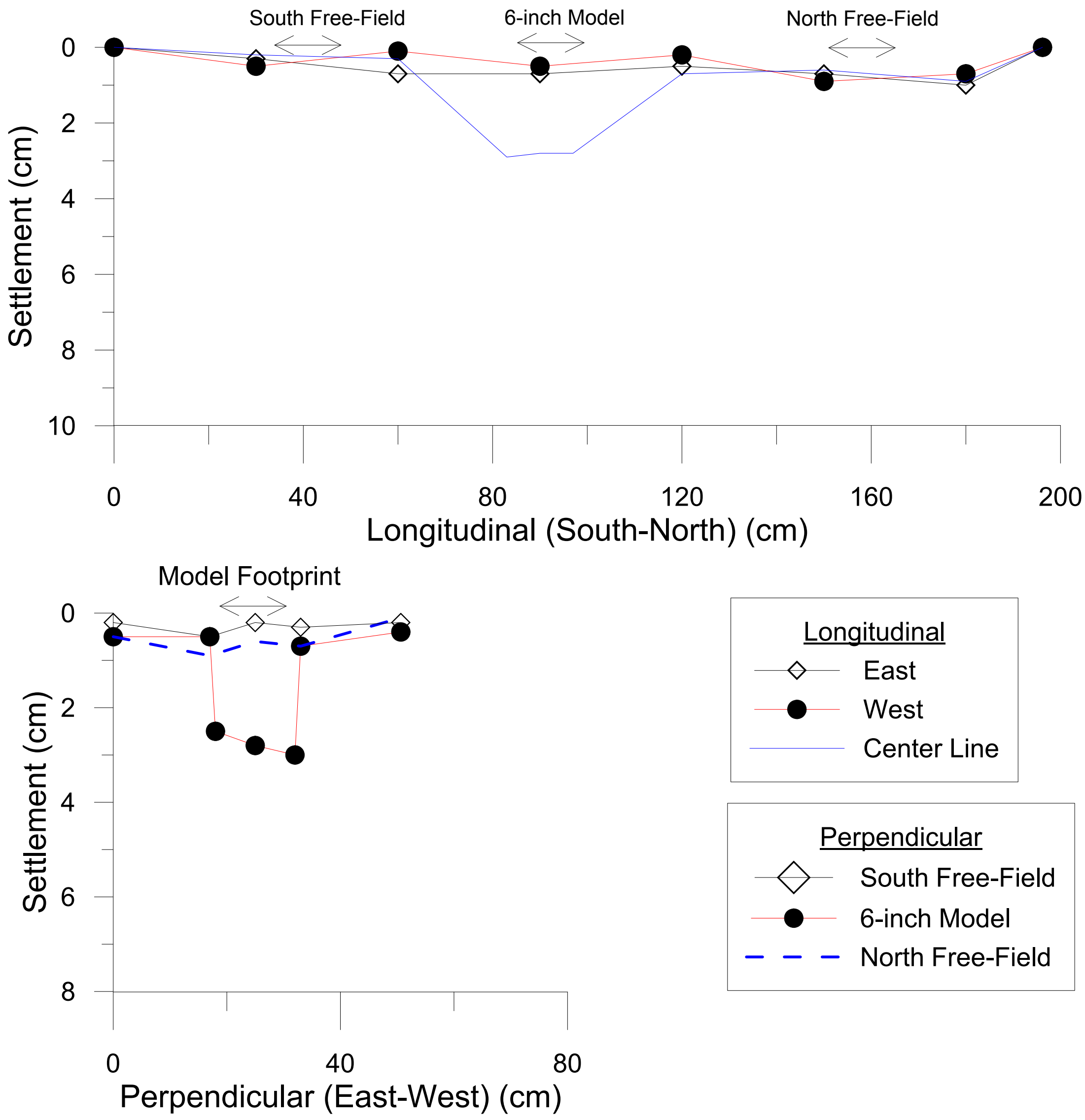

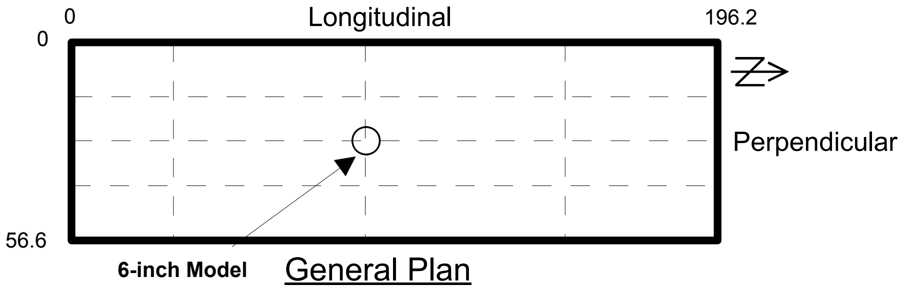

Test # 19.2: Ground Motion Characteristics
2/5/2016
PGA: 0.34g

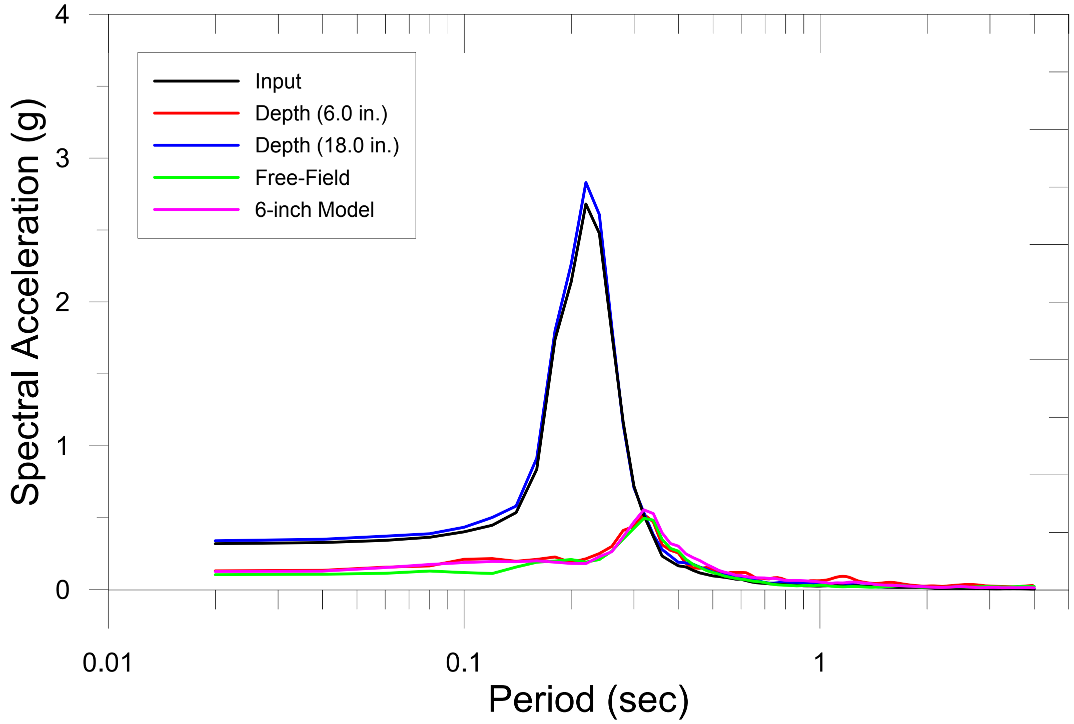

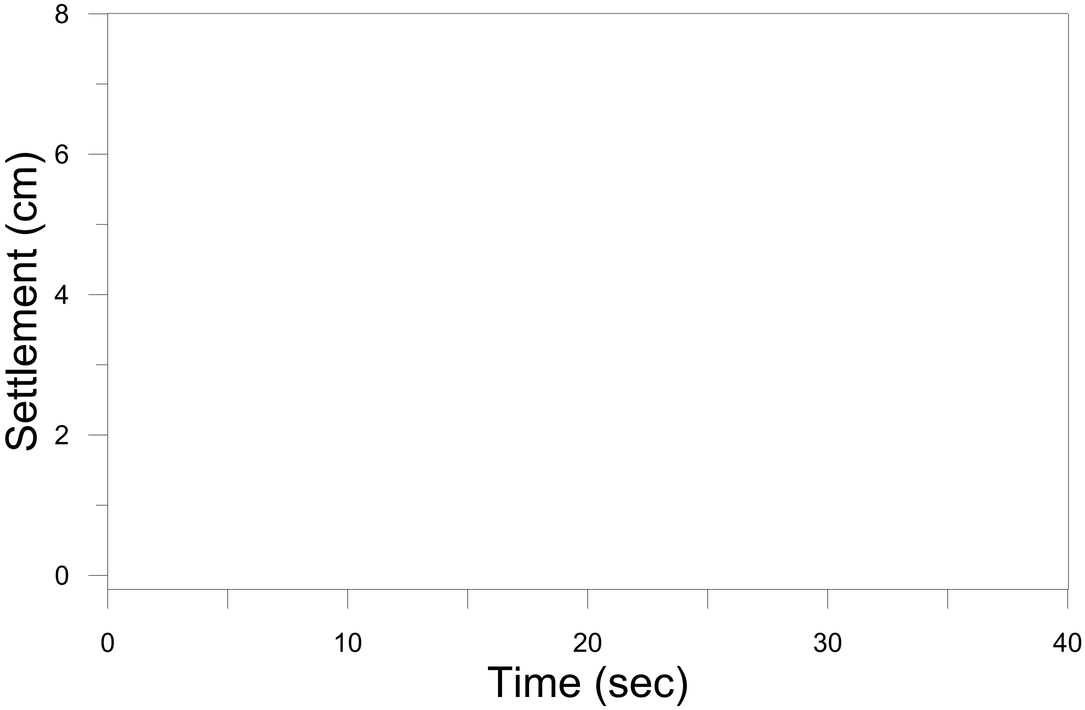

Test #20 (January 12, 2016)

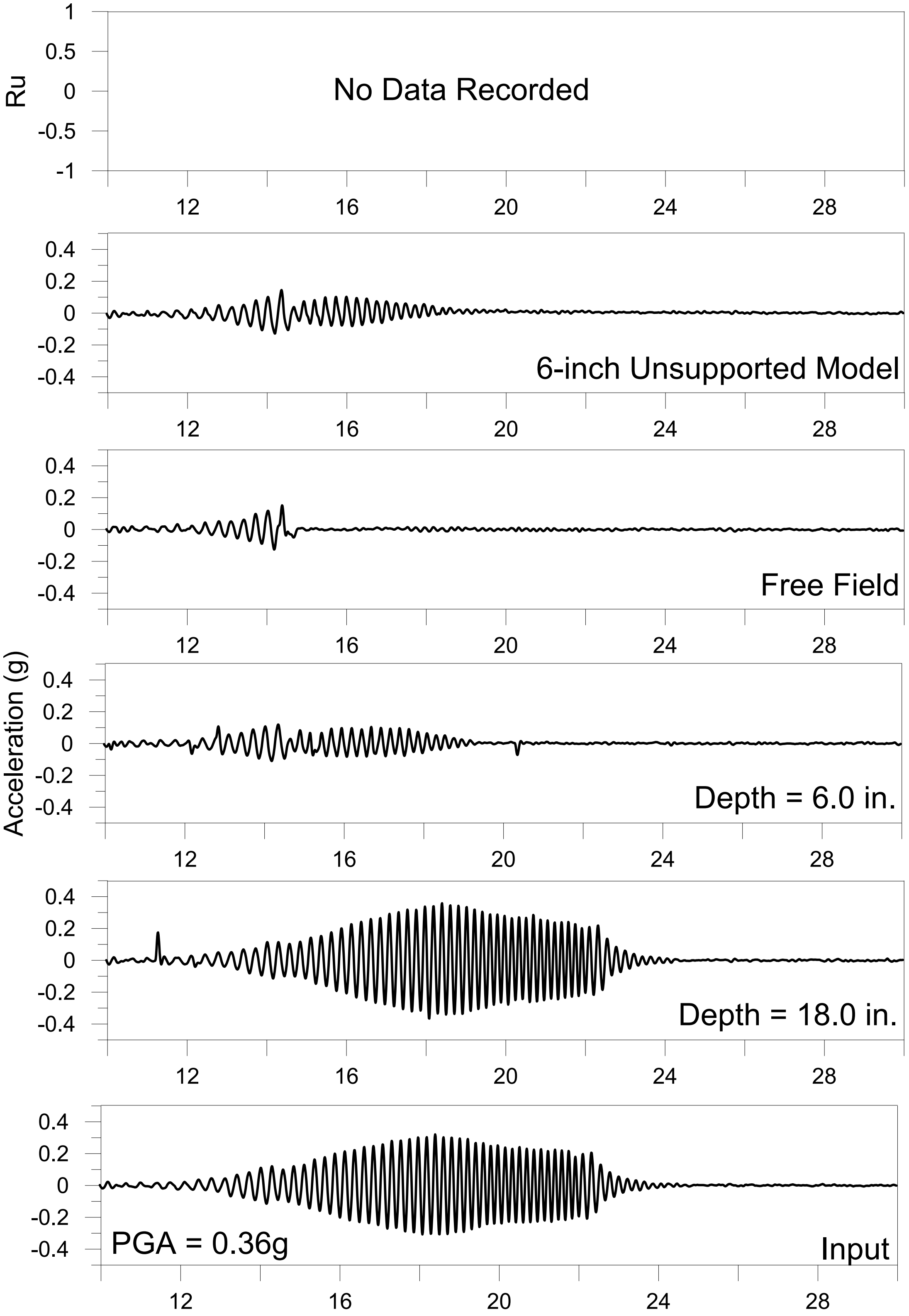

Test # 20: Settlement (cm)
1/12/2015
PGA: 0.36g

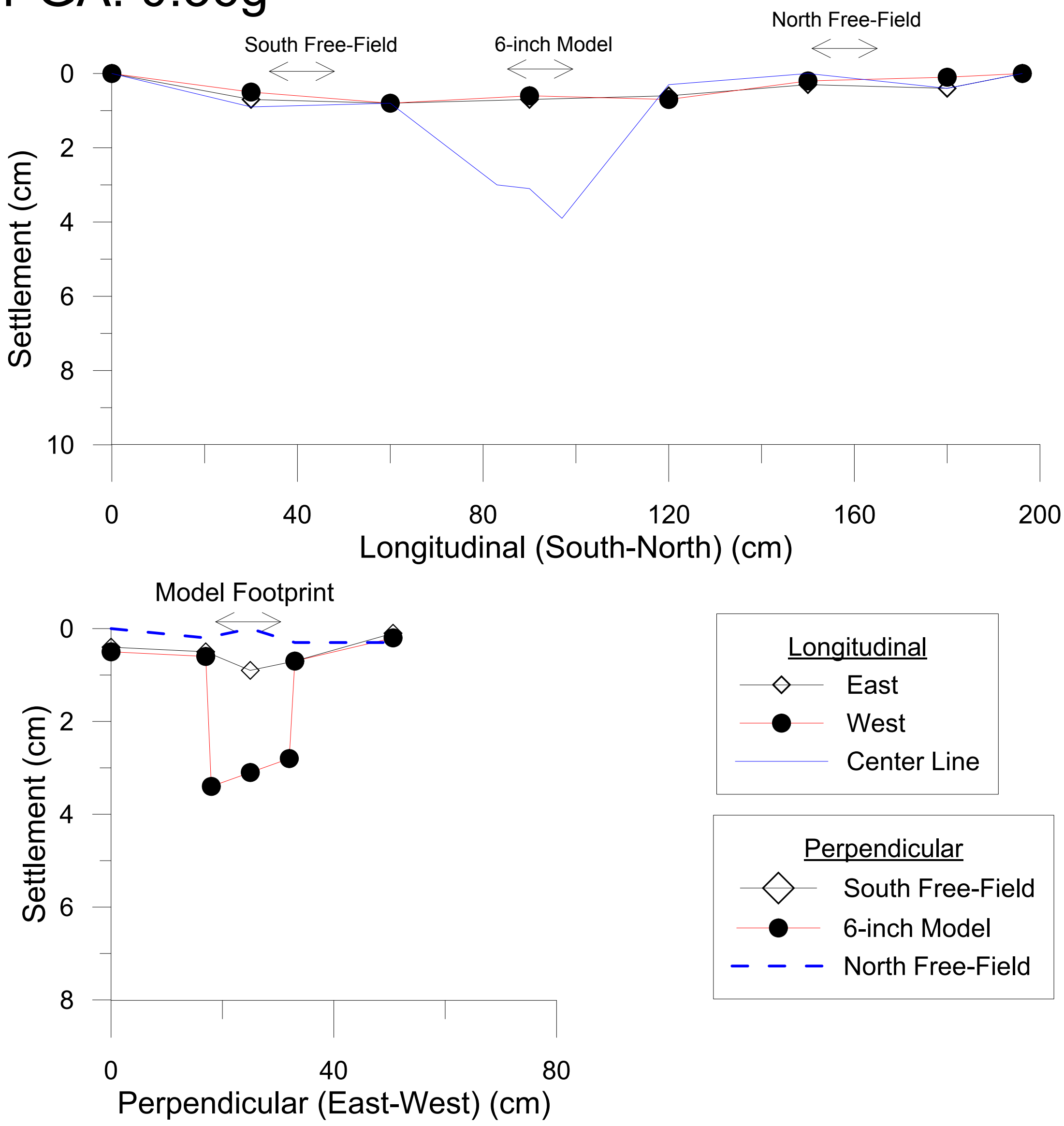

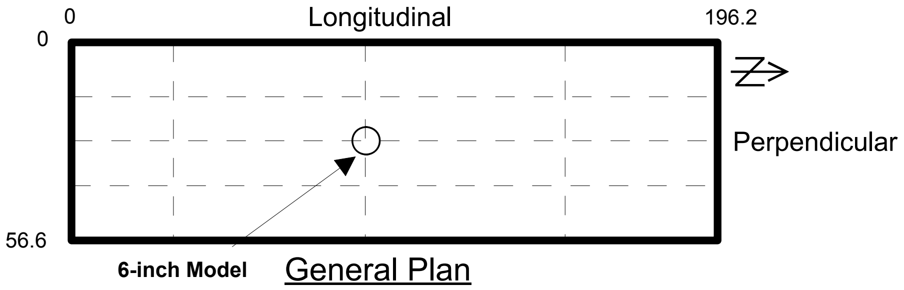

General Plan

Test # 20: Ground Motion Characteristics
1/12/2016
PGA: 0.36g

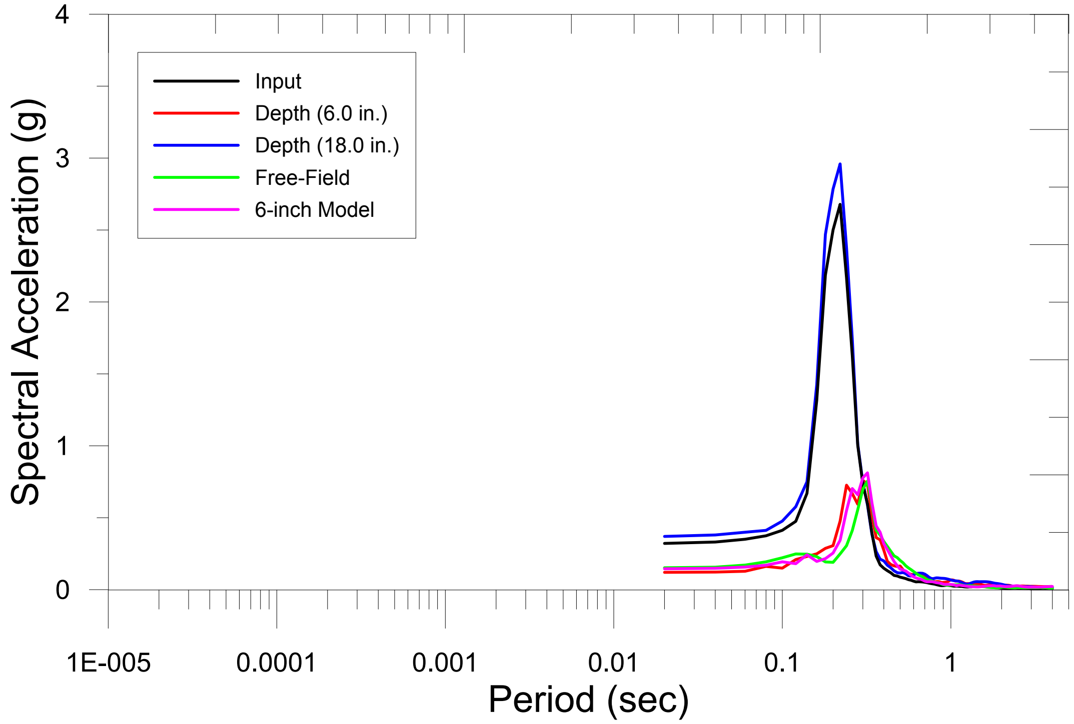

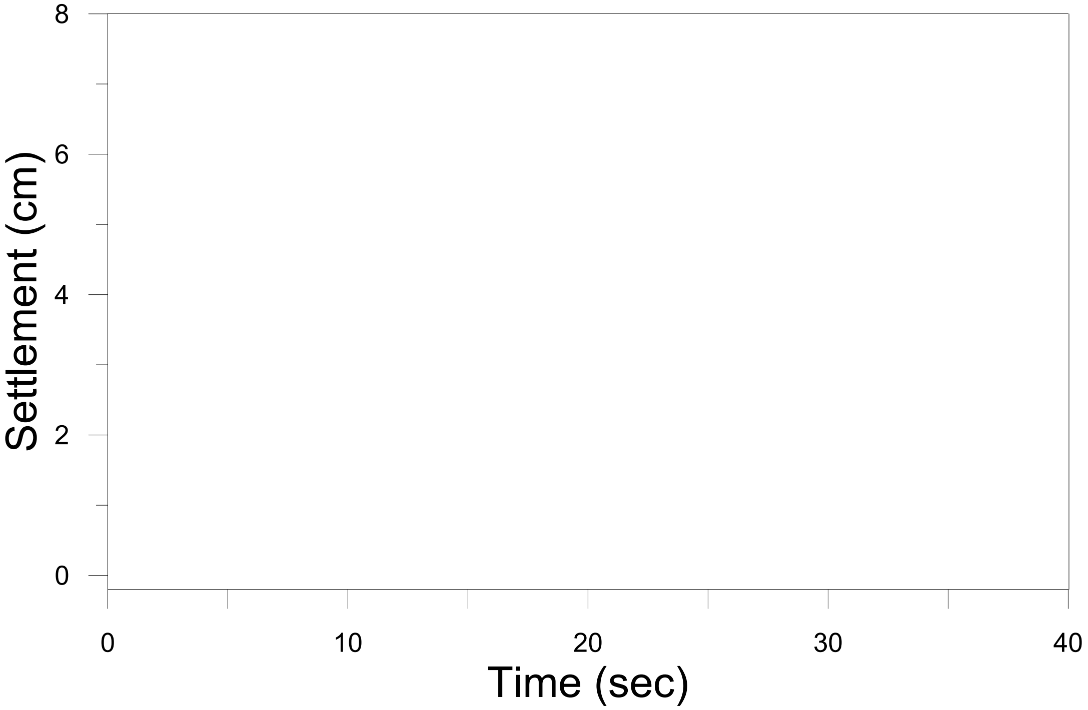

Test #21 (January 15, 2016)

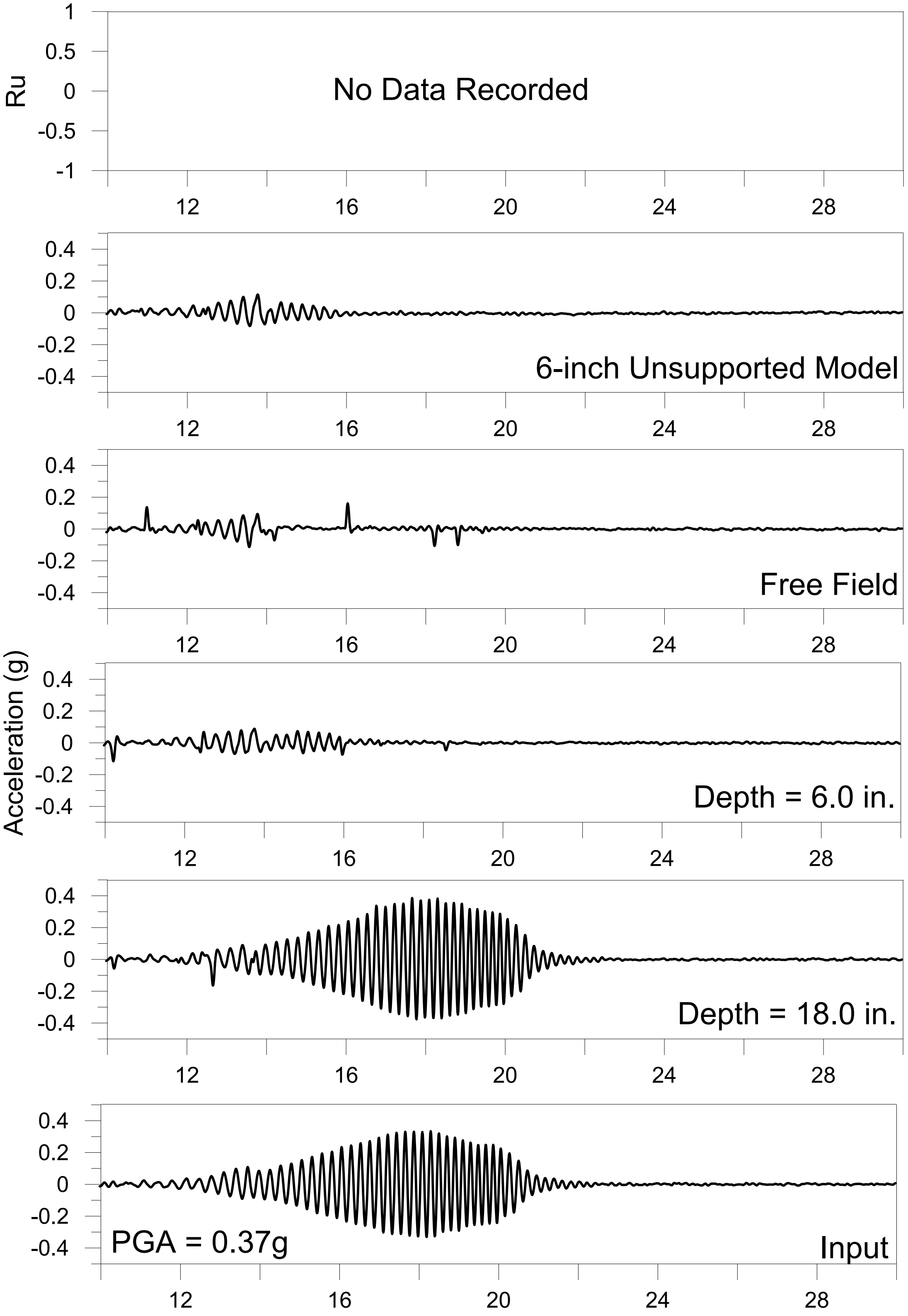

Test # 21: Settlement (cm)
1/15/2015
PGA: 0.37g

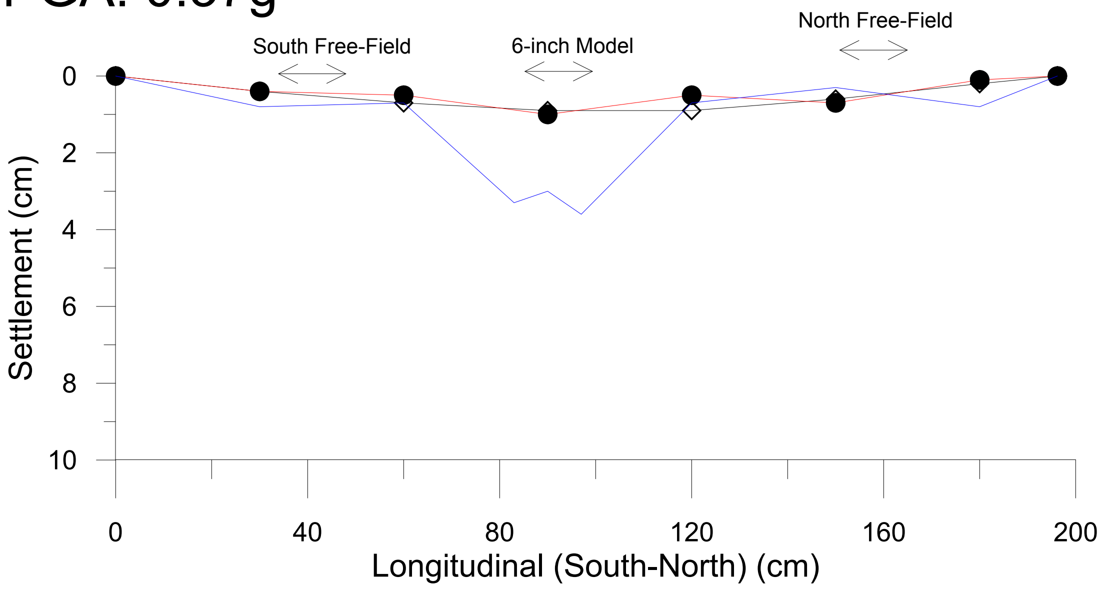

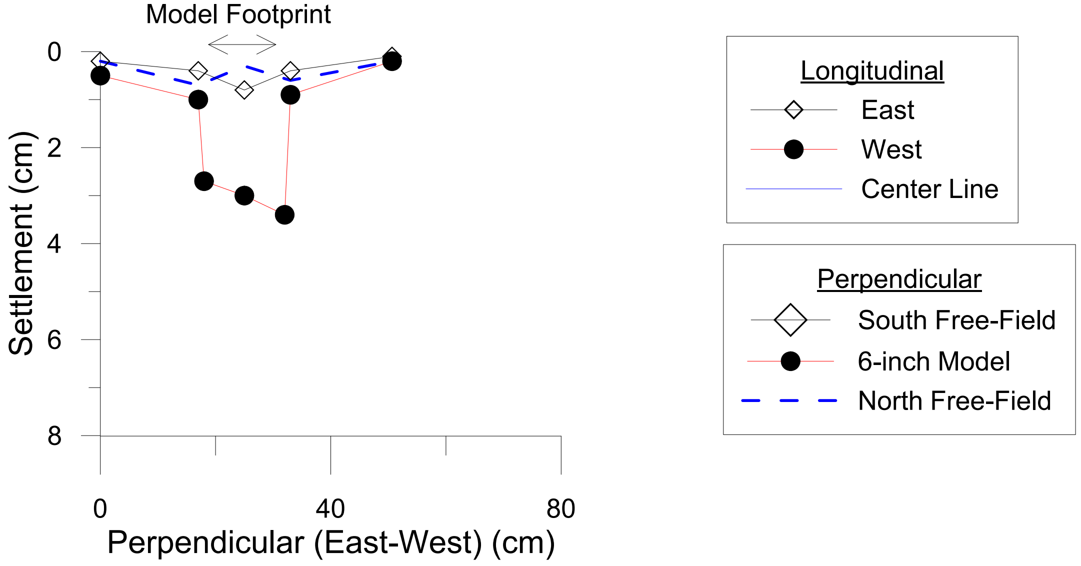

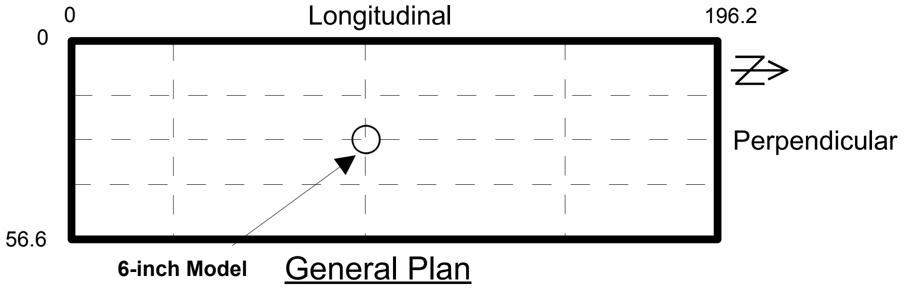

General Plan

Test # 21: Ground Motion Characteristics
1/15/2016
PGA: 0.37g

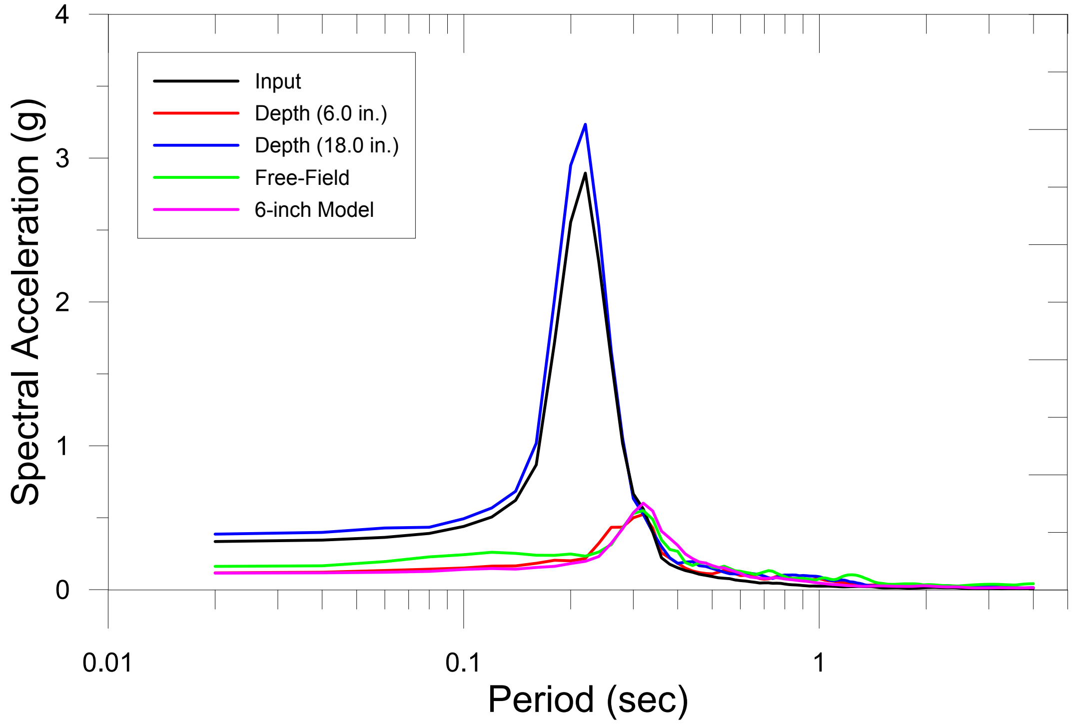

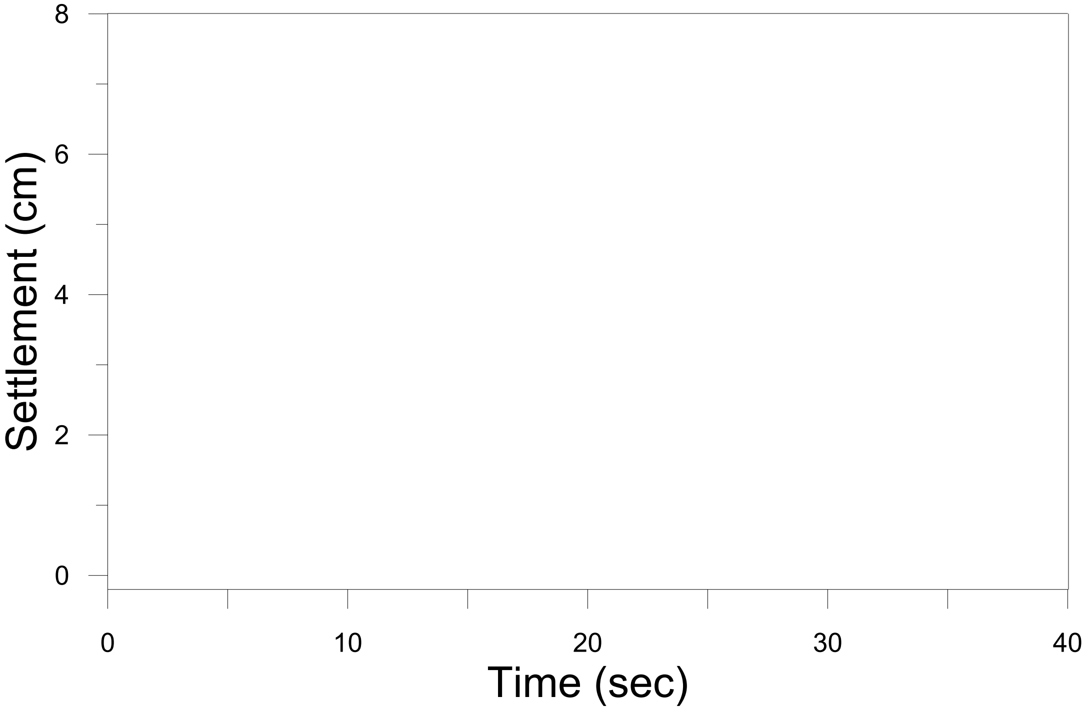

Test #22 (January 20, 2016)

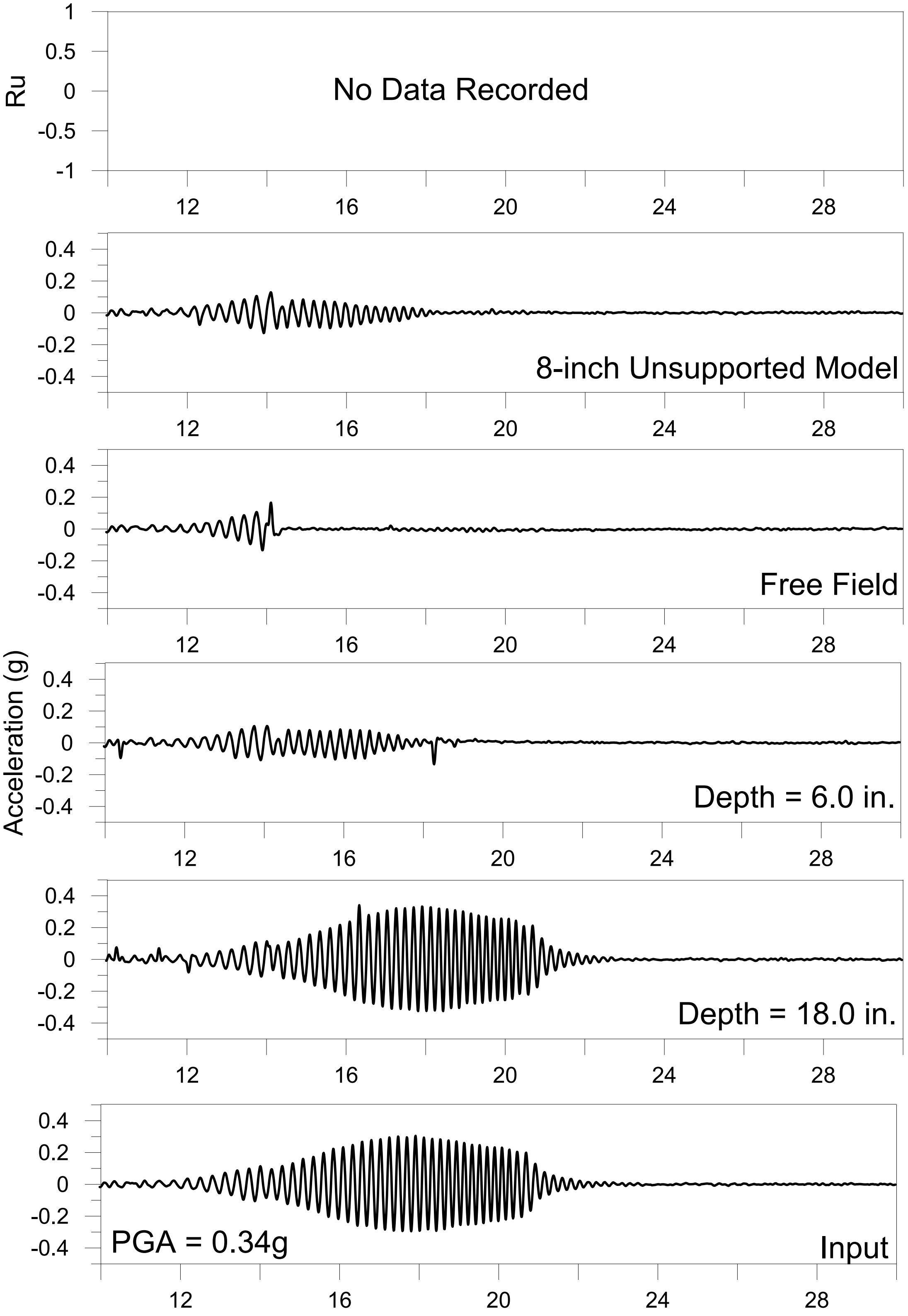

Test # 22: Settlement (cm)
1/20/2015
PGA: 0.34g

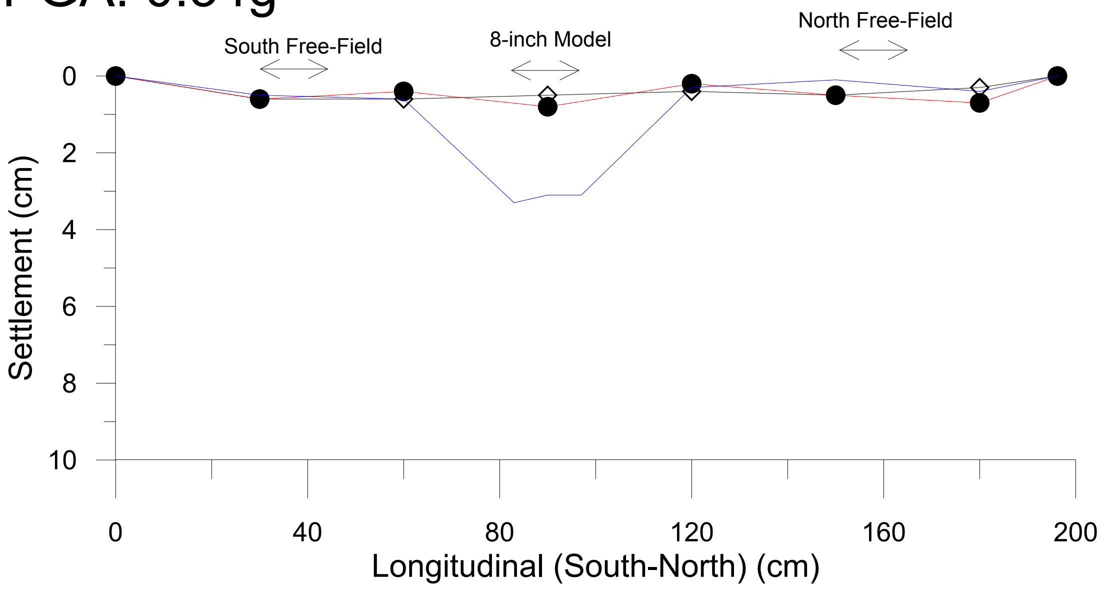

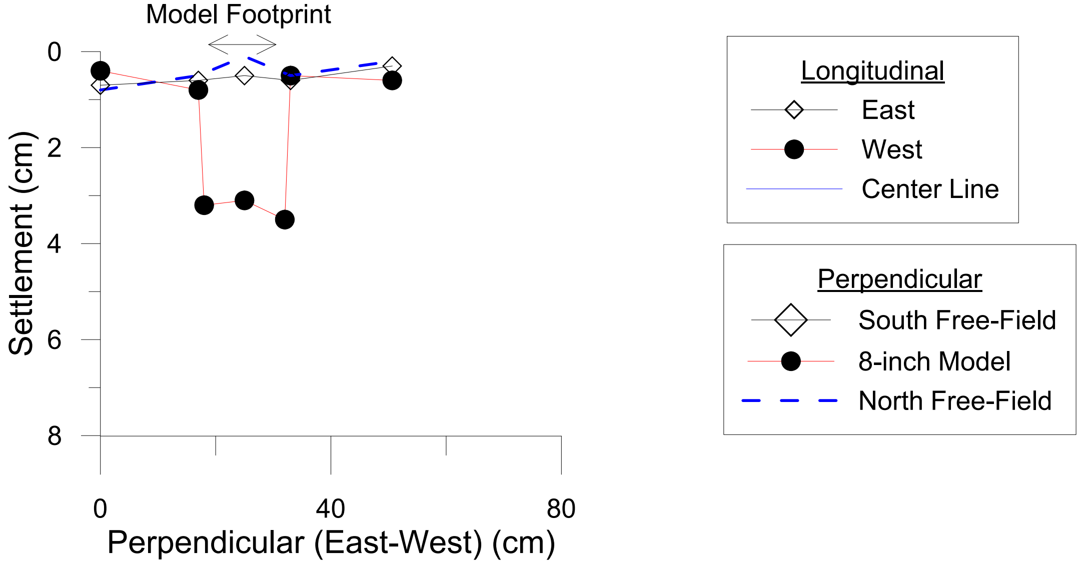

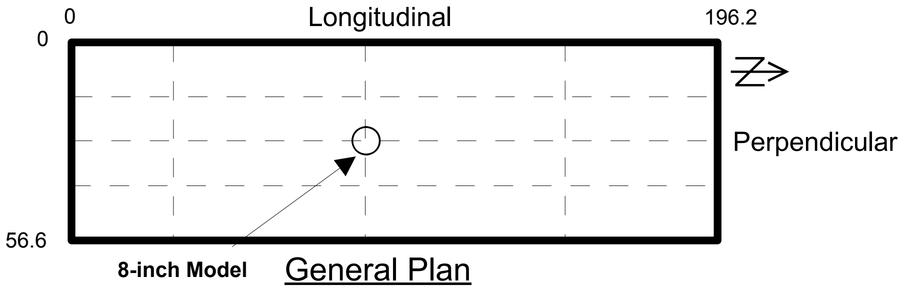

Test # 22: Ground Motion Characteristics
1/20/2016
PGA: 0.34g

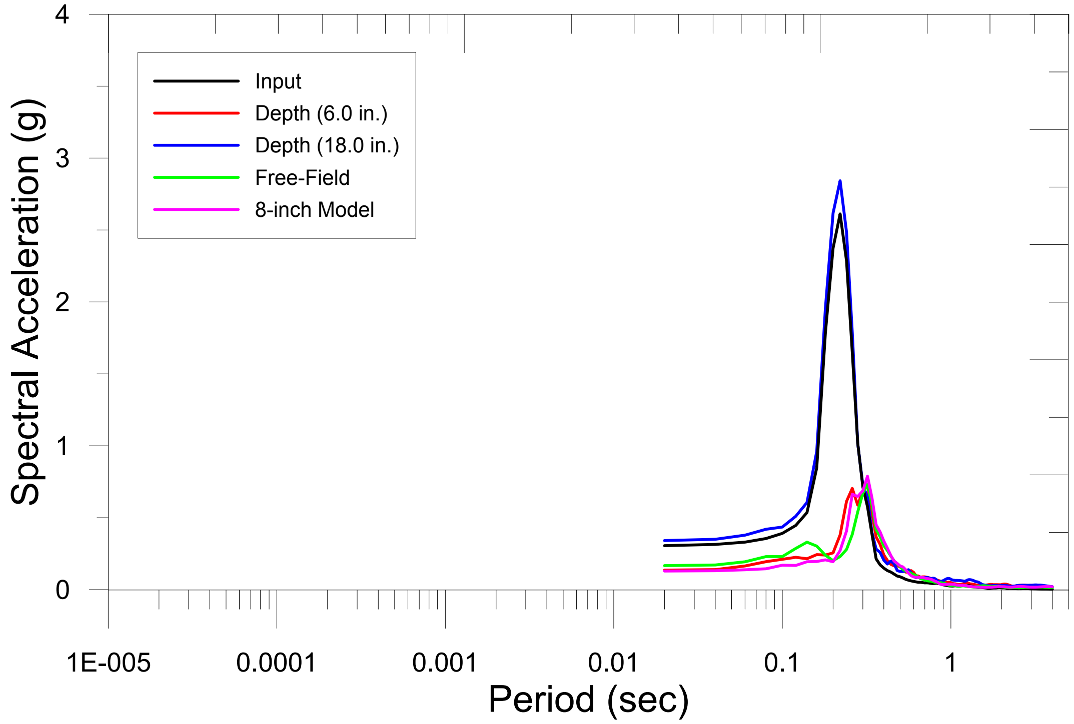

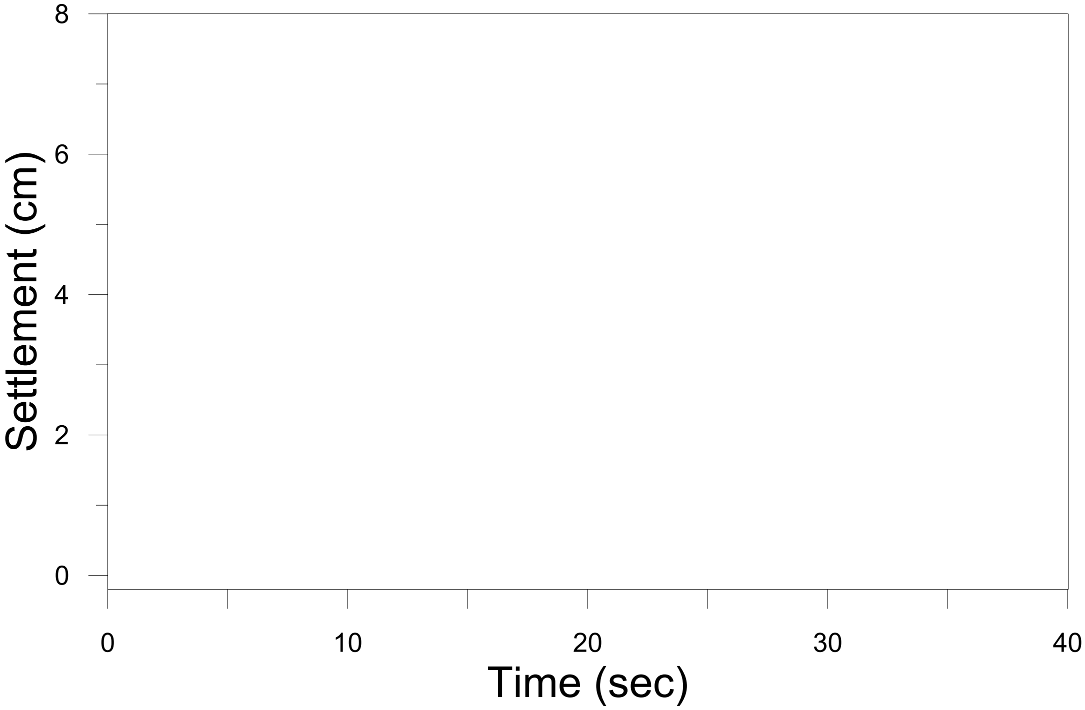

Test # 22.1: Settlement (cm)
2/12/2015
PGA: 0.34g

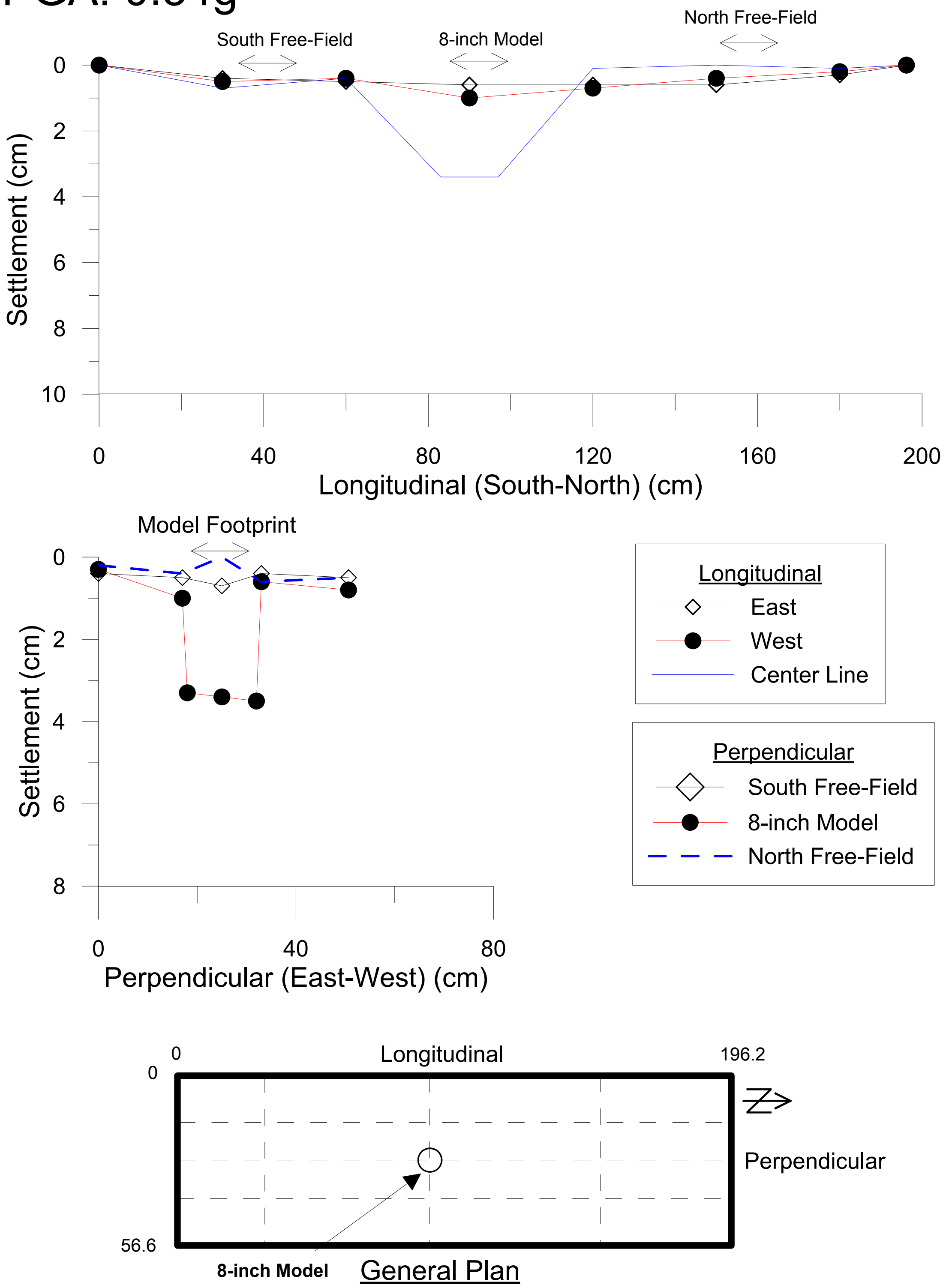

Test # 22.1: Ground Motion Characteristics
2/12/2016
PGA: 0.34g

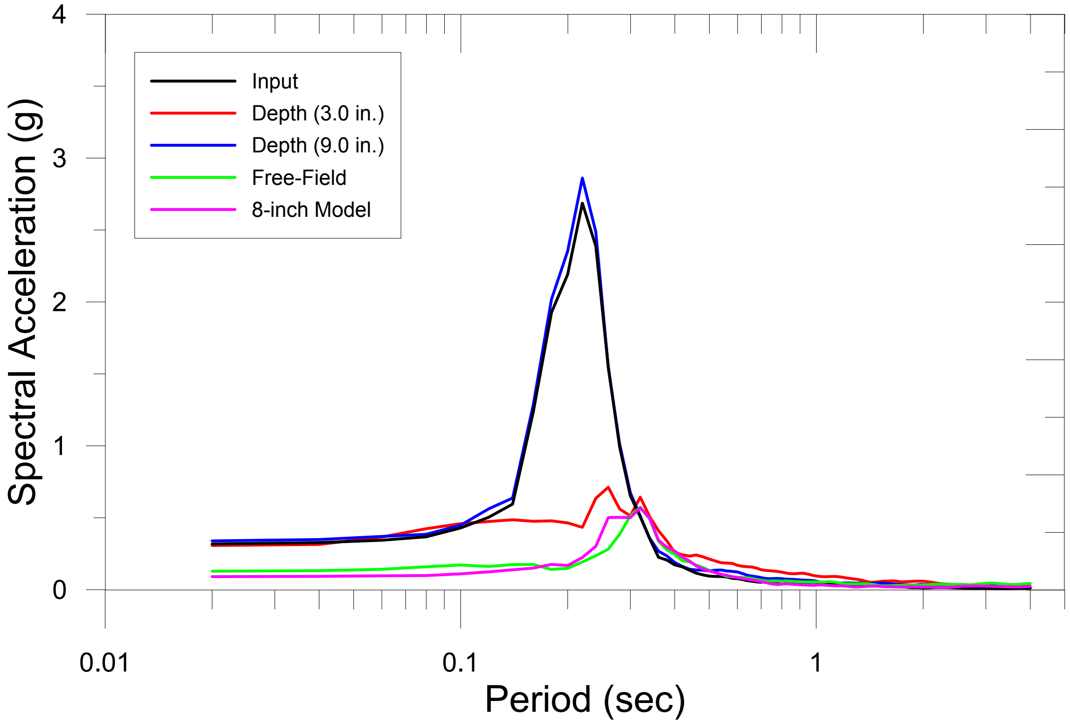

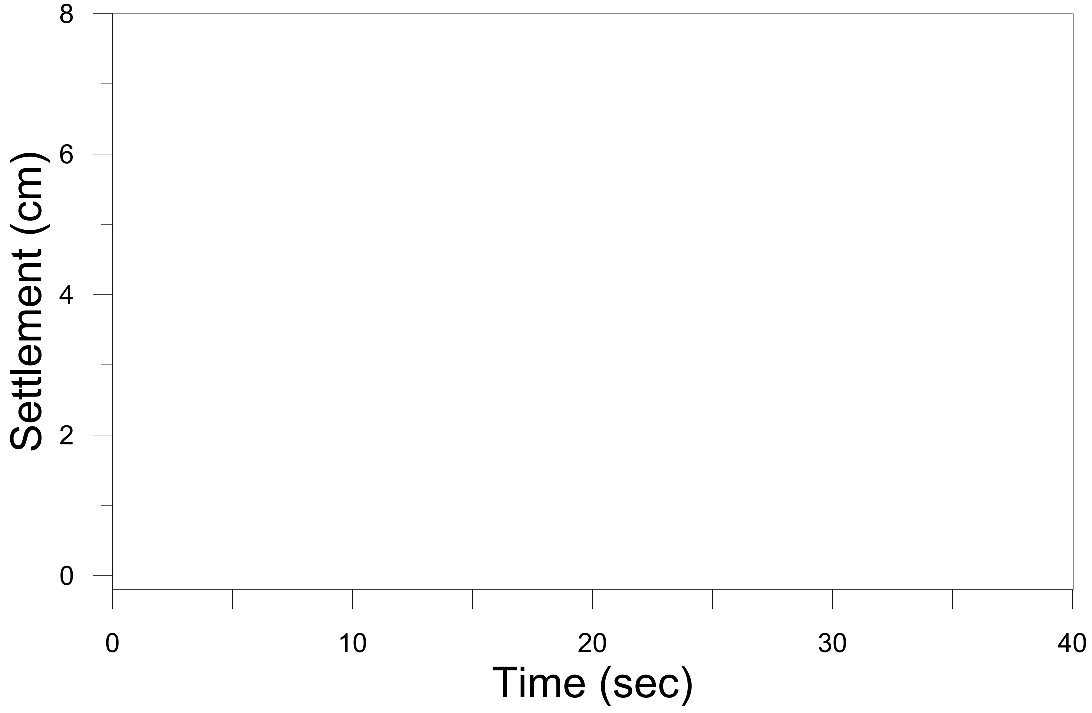

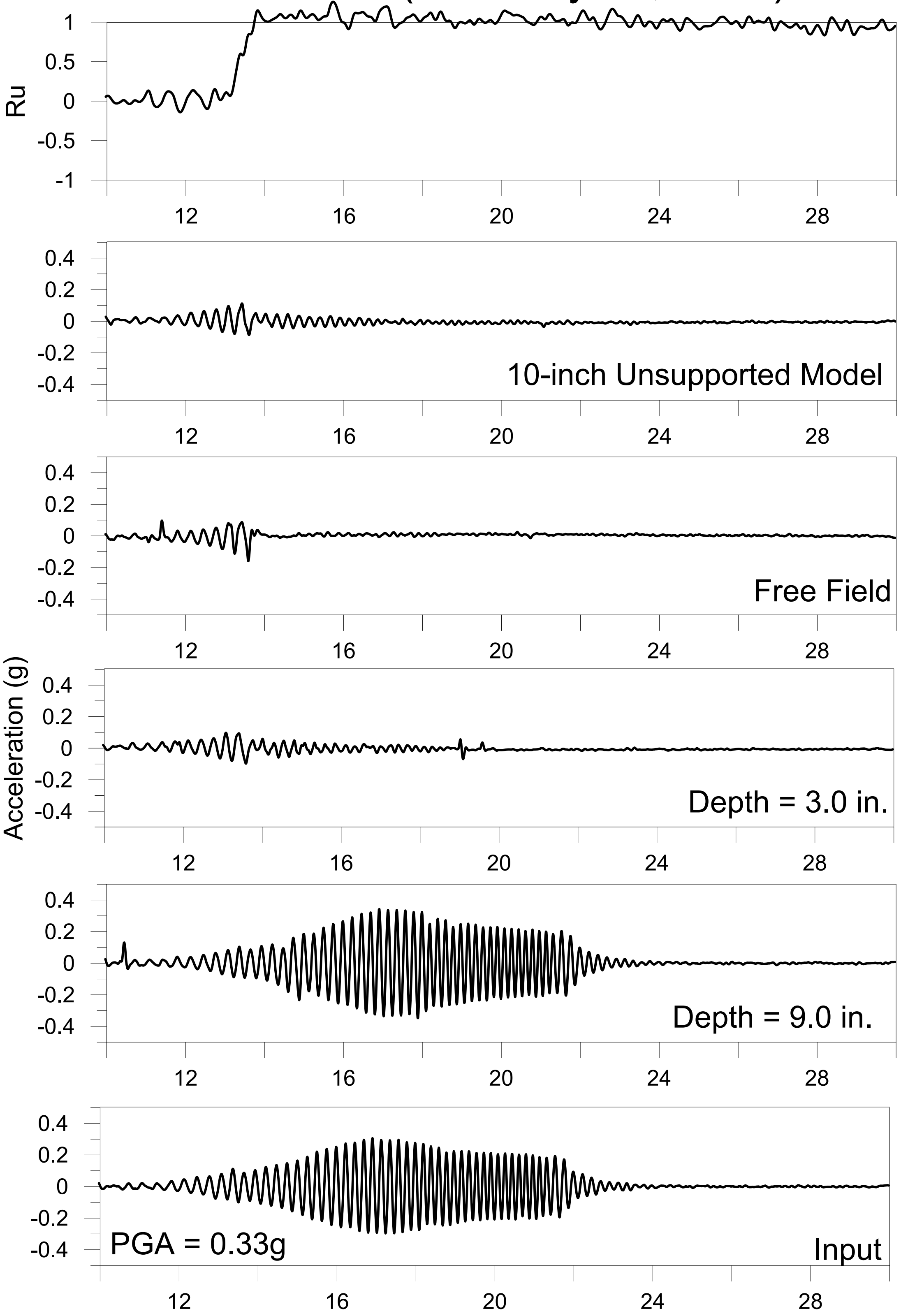

Test #23 (February 19, 2016)

Test # 23: Settlement (cm)
2/19/2015
PGA: 0.33g

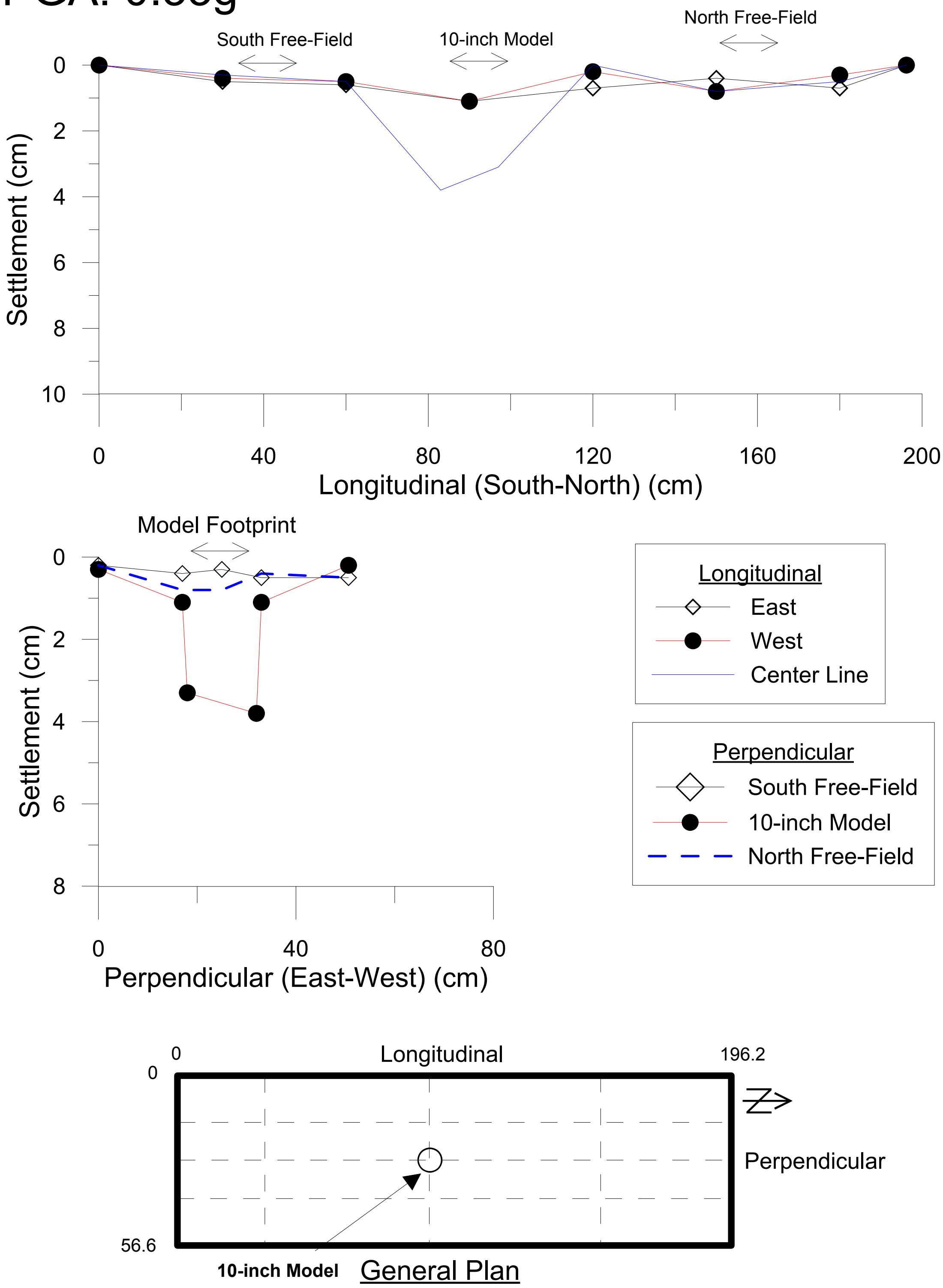

Test # 23: Ground Motion Characteristics
2/19/2016
PGA: 0.33g

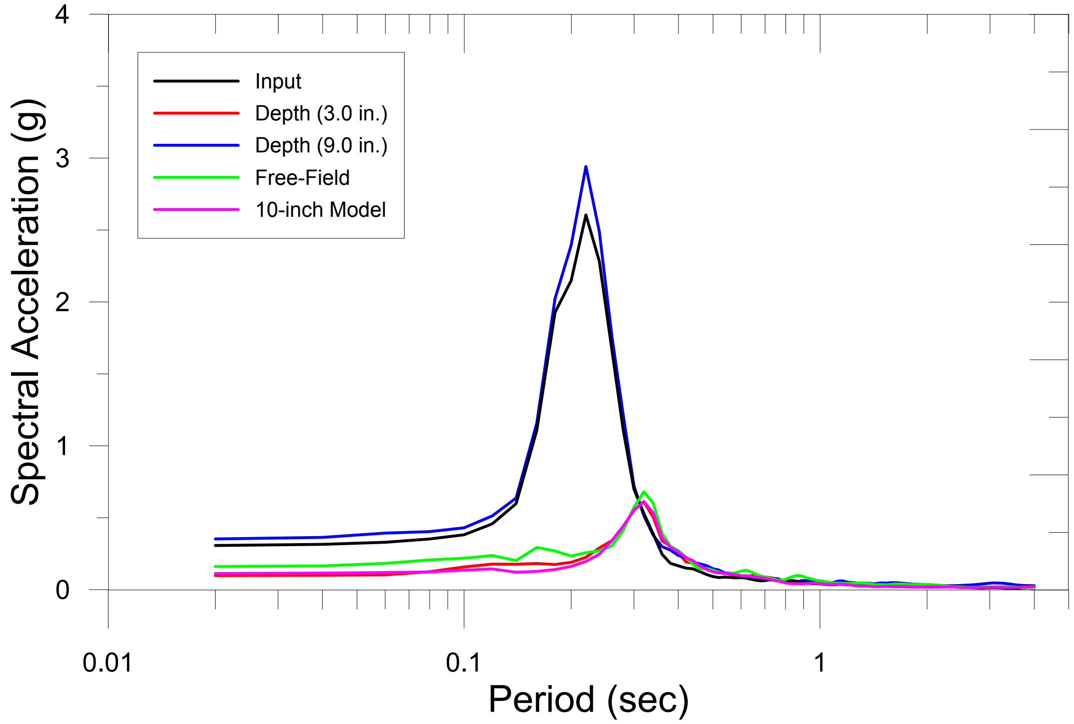

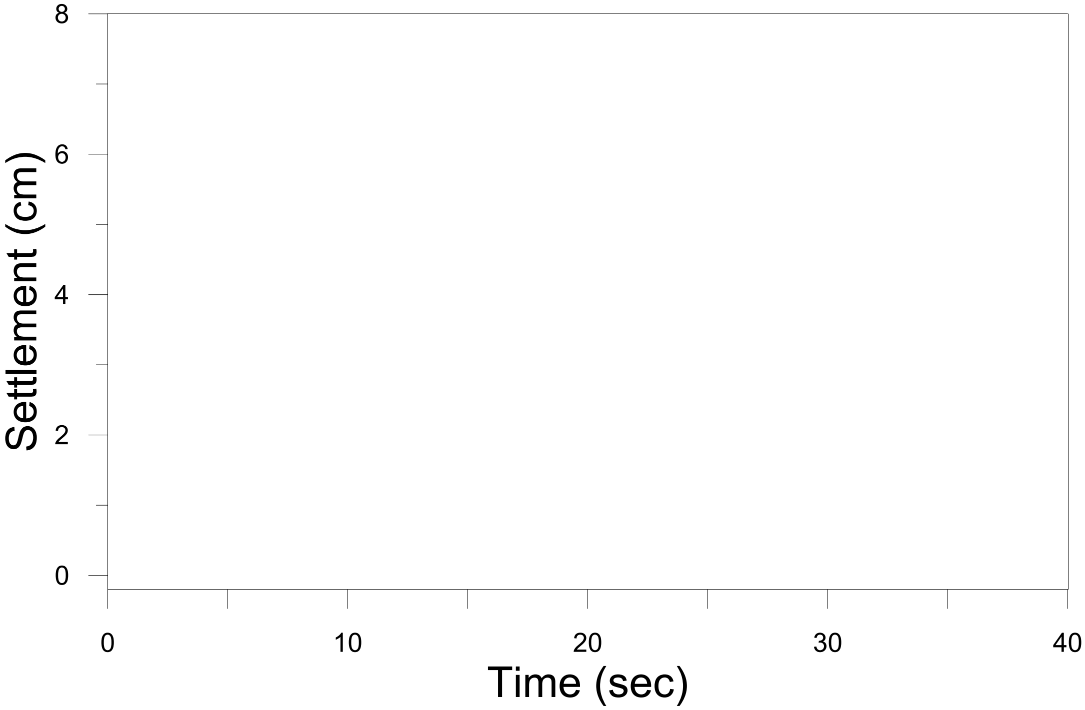

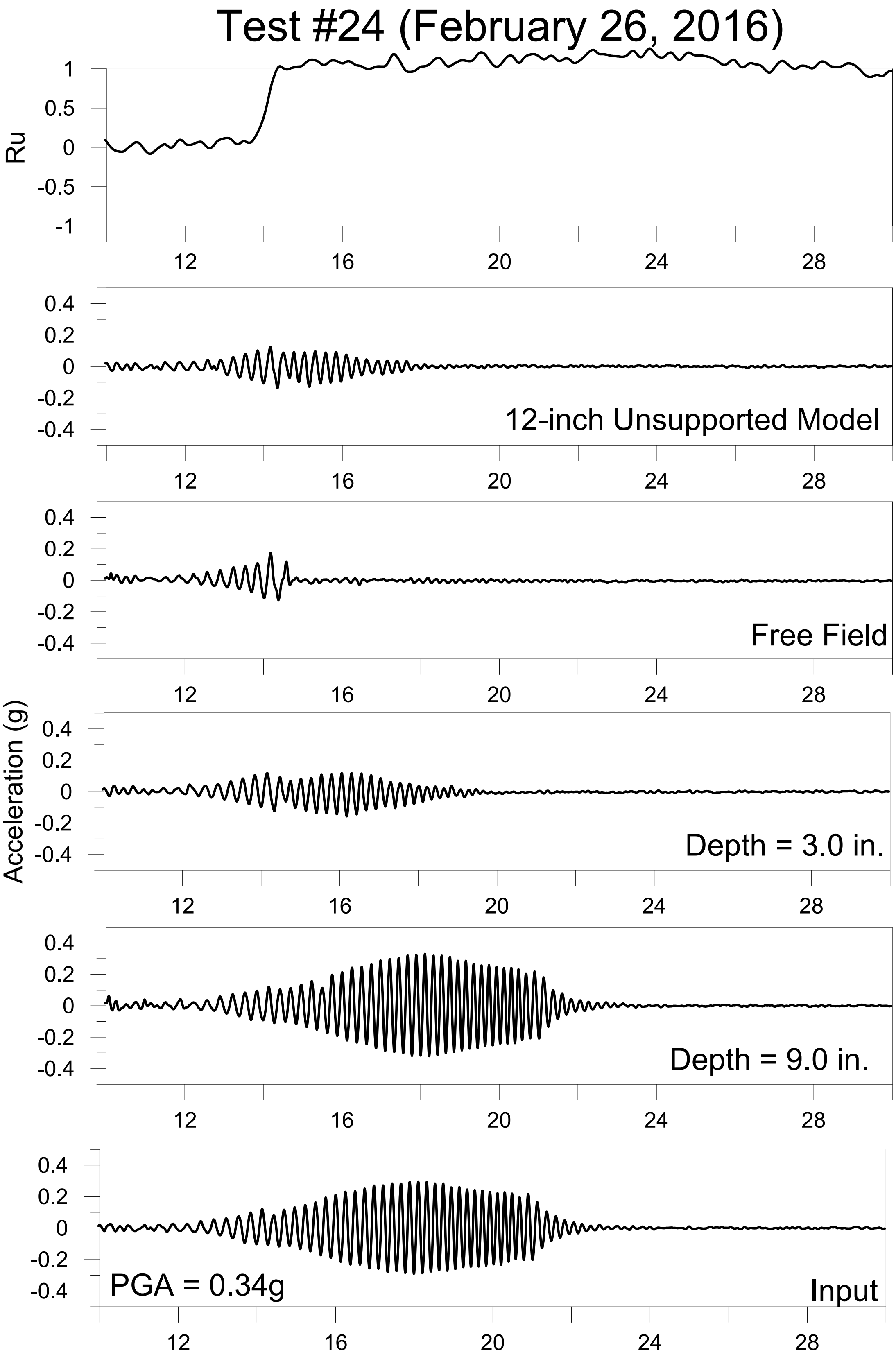
Test #24 (February 26, 2016)
Ru
1
0.5
0
-0.5
-1
12
16
20
24
28
Acceleration (g)
0.4
0.2
0
-0.2
-0.4
12-inch Unsupported Model
Free Field
Depth = 3.0 in.
Depth = 9.0 in.
PGA = 0.34g
Input

Test # 24: Settlement (cm)
2/26/2015
PGA: 0.34g

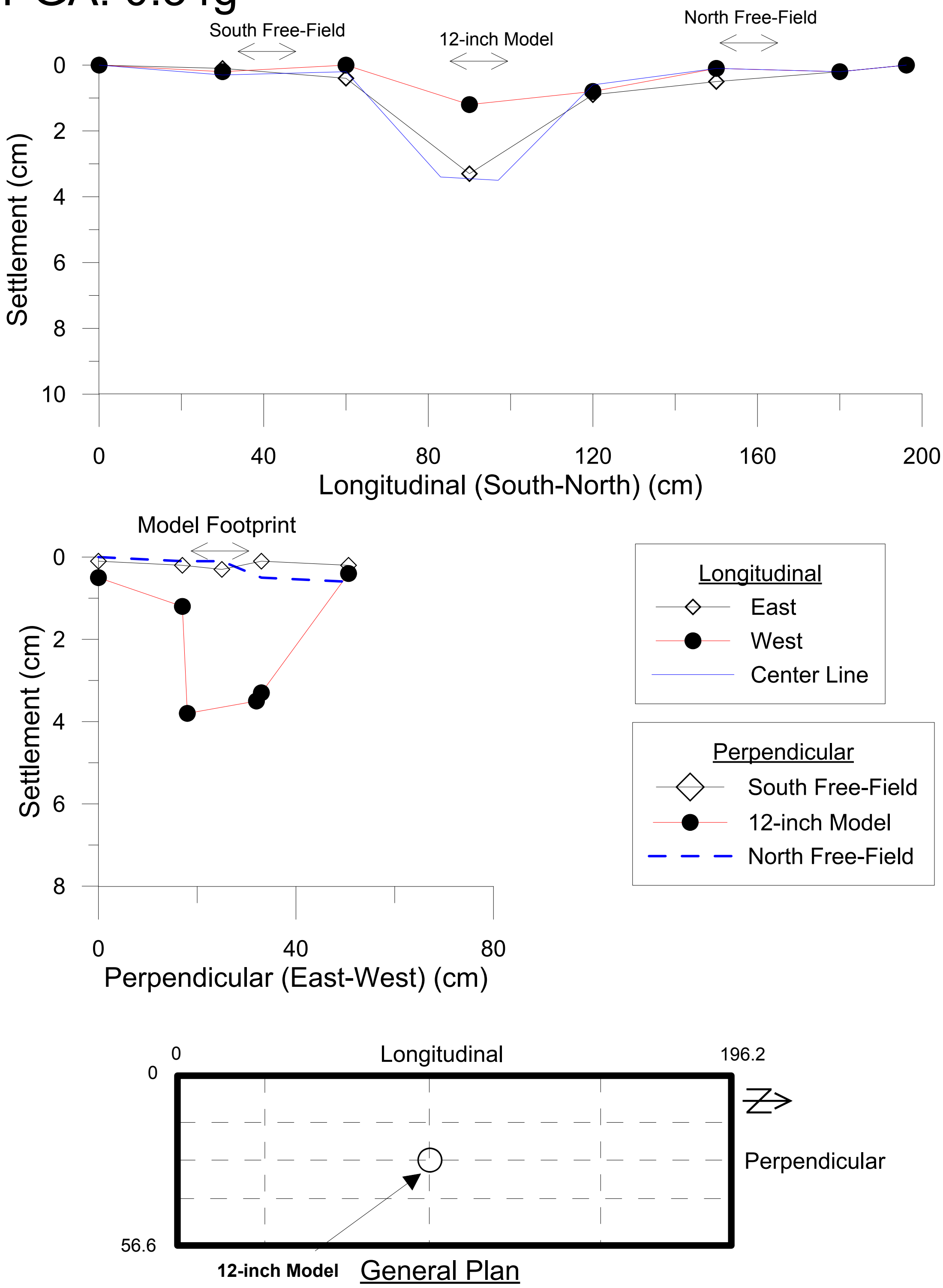

Test # 24: Ground Motion Characteristics
2/26/2016
PGA: 0.34g

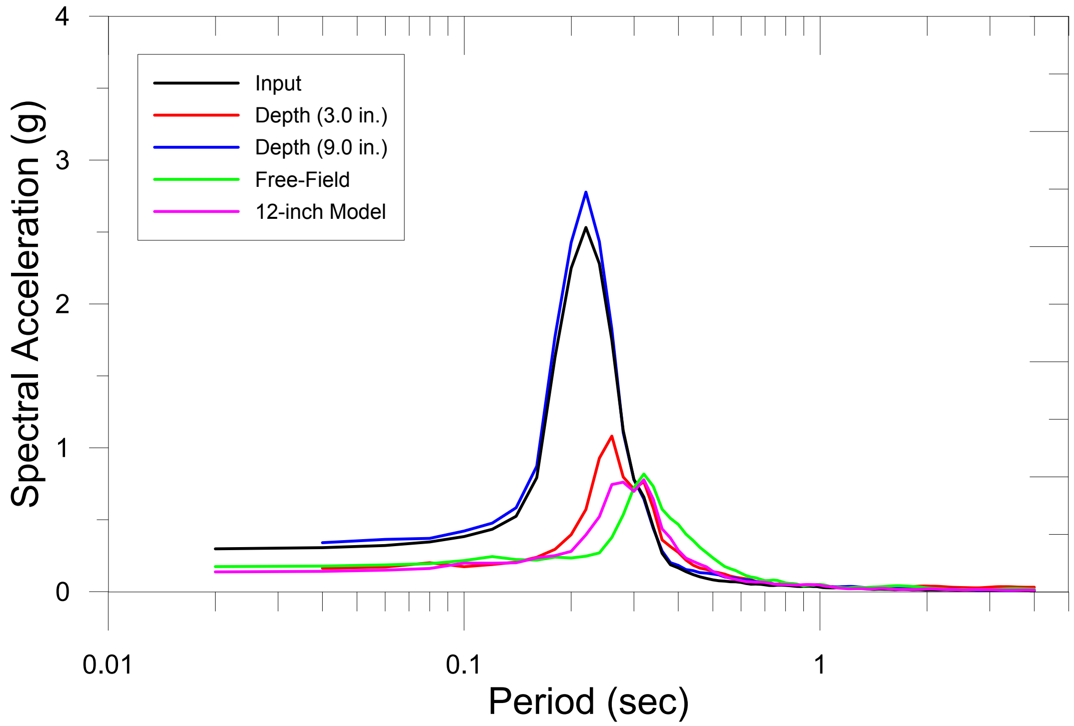

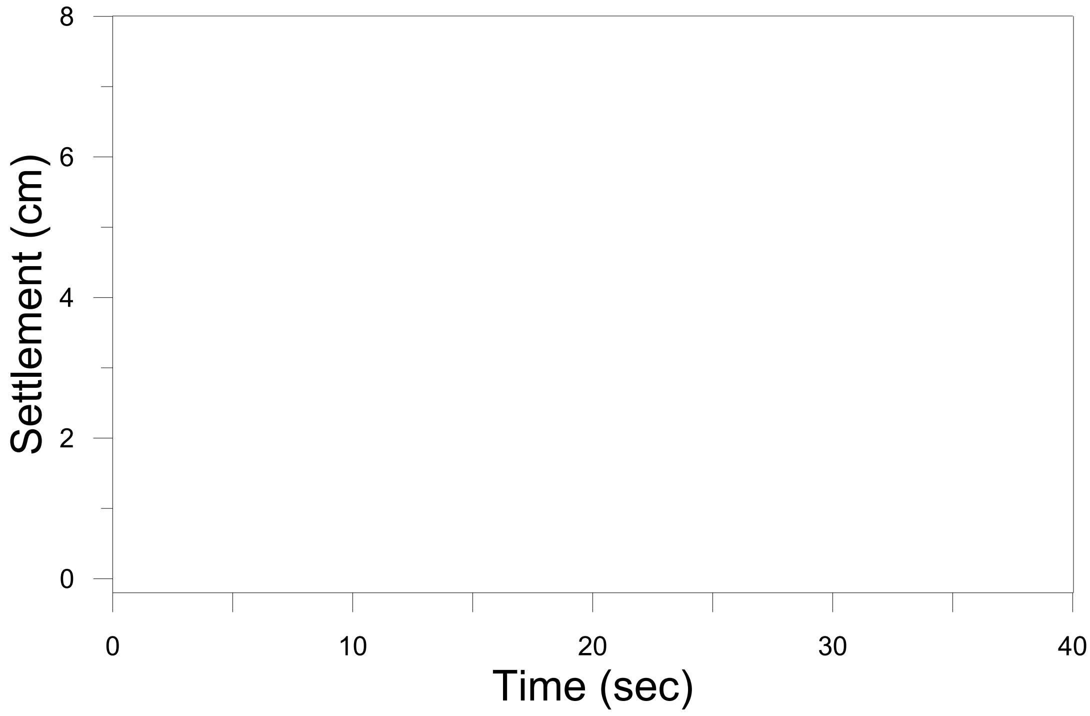

Test #25 (March 1, 2016)

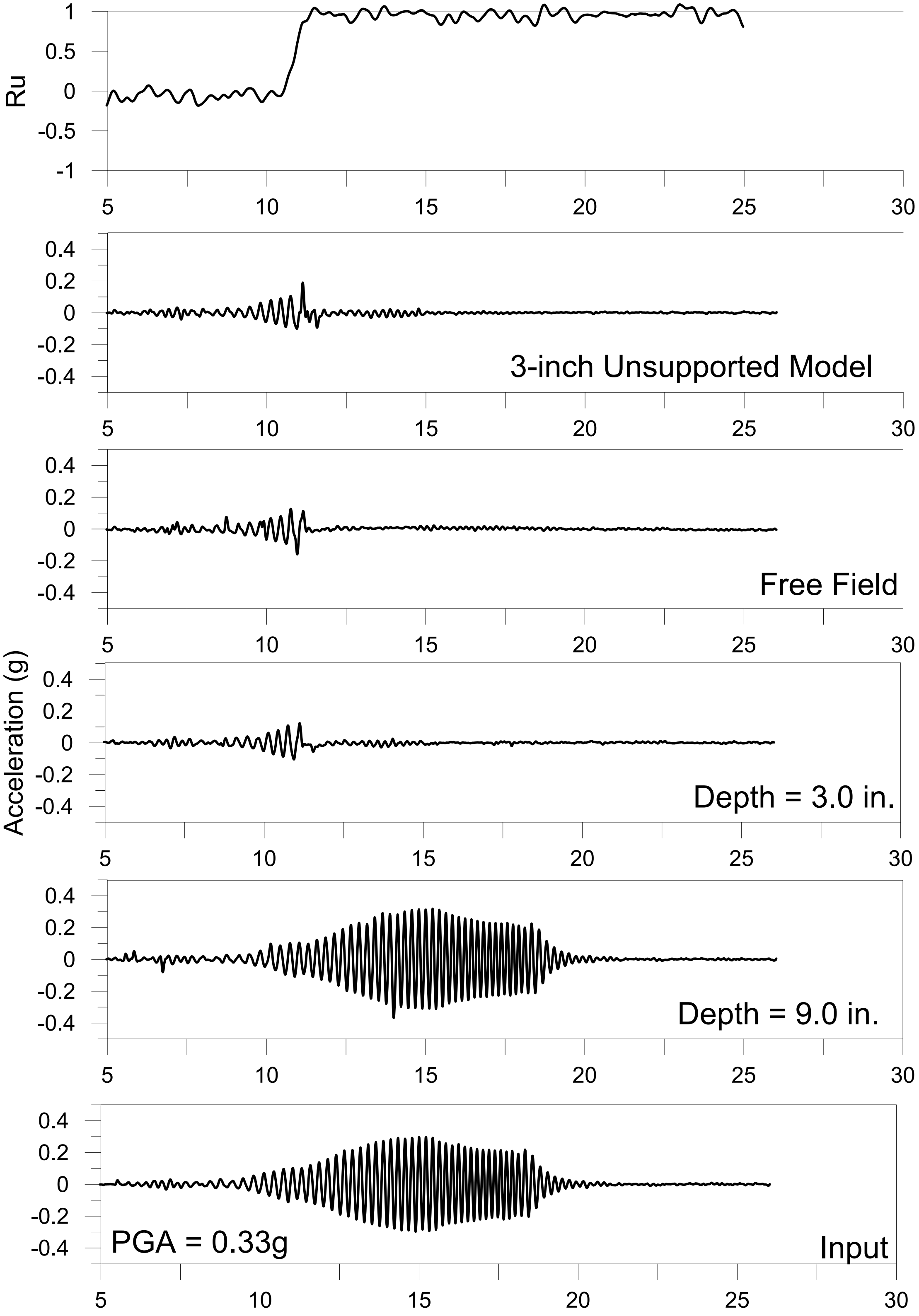

Test # 25: Settlement (cm)
3/1/2015
PGA: 0.33g

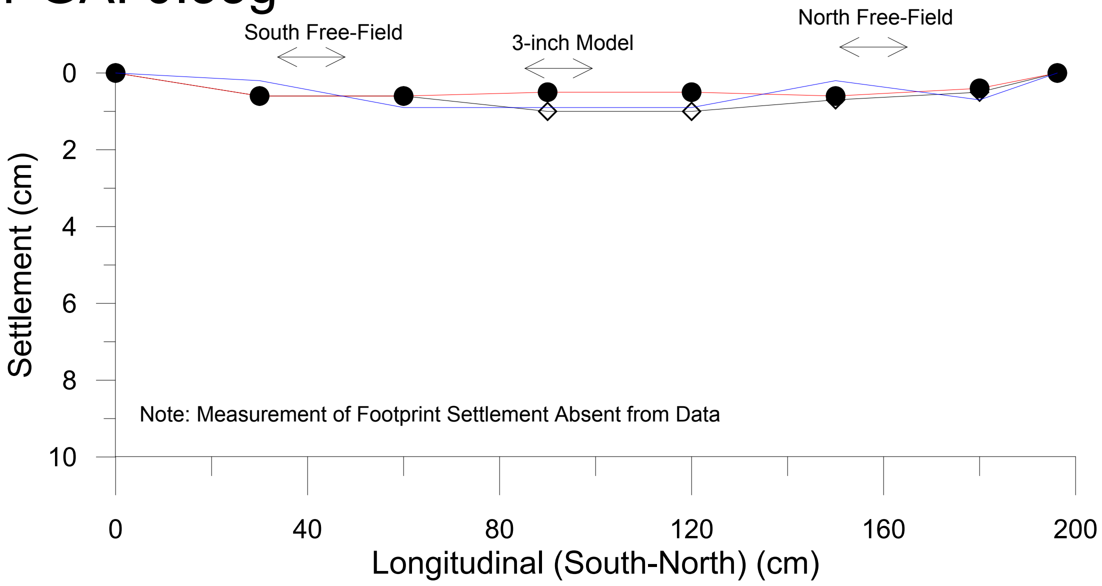

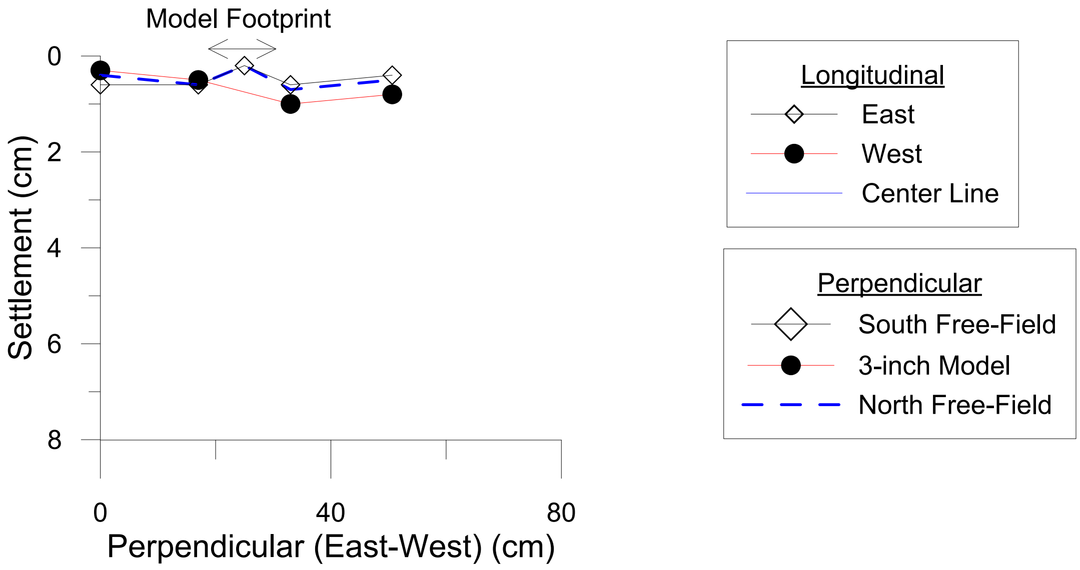

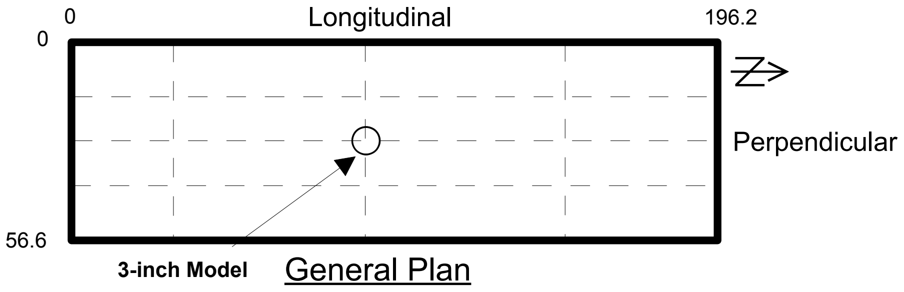

Test # 25: Ground Motion Characteristics
3/1/2016
PGA: 0.33g

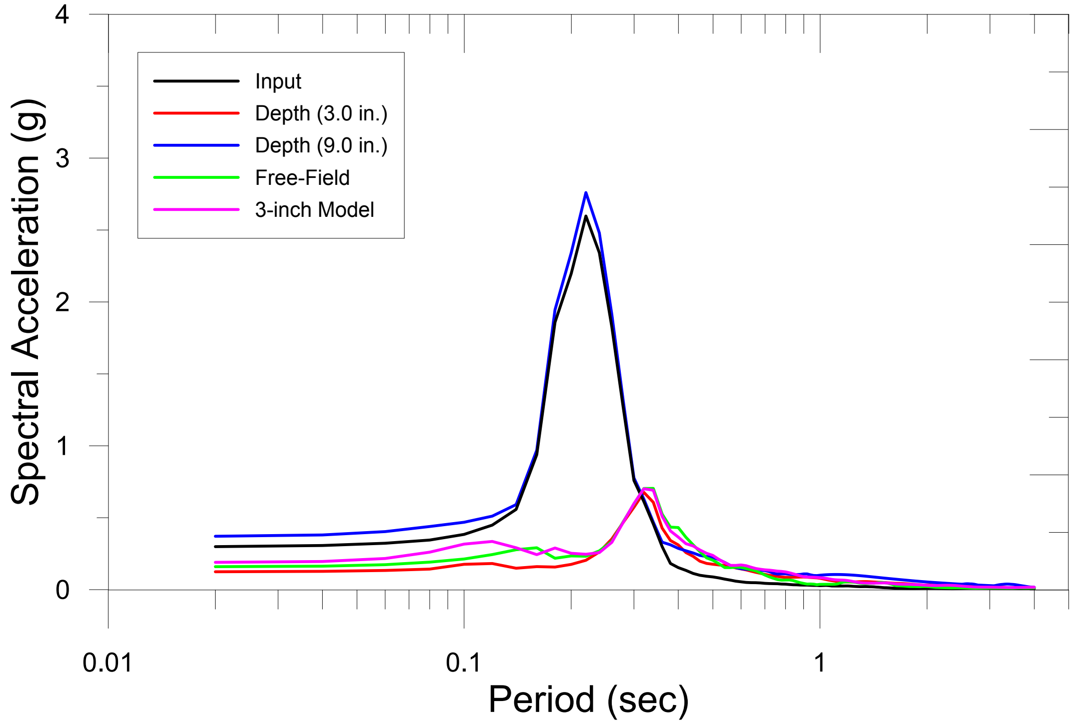

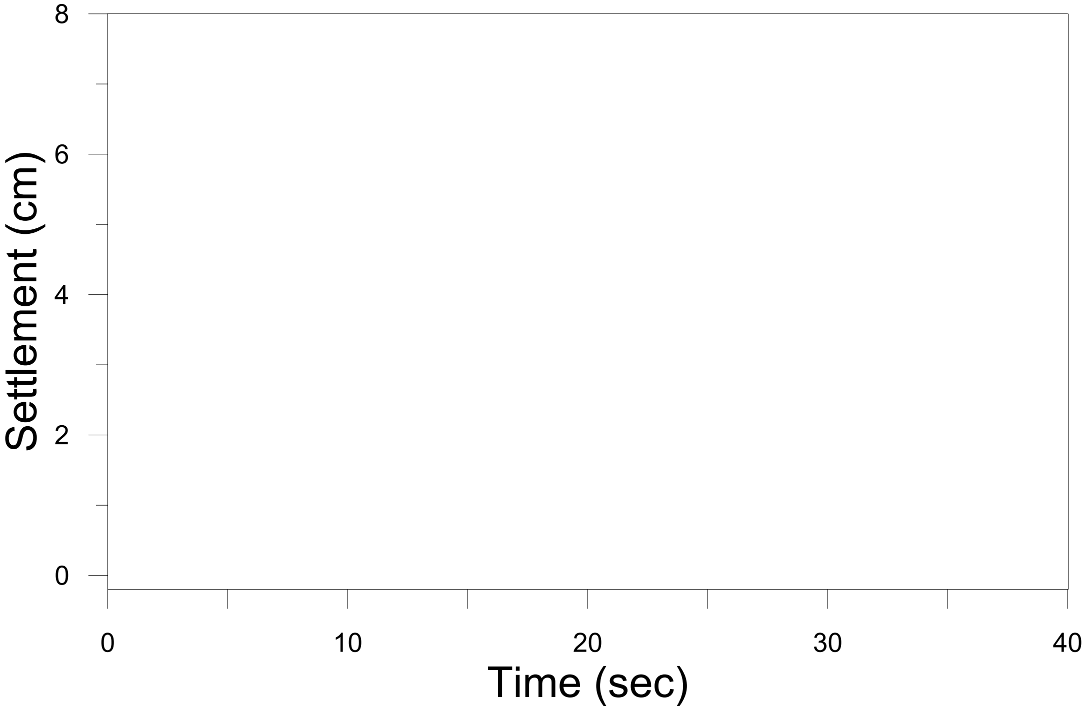

Test #26 (March 9, 2016)

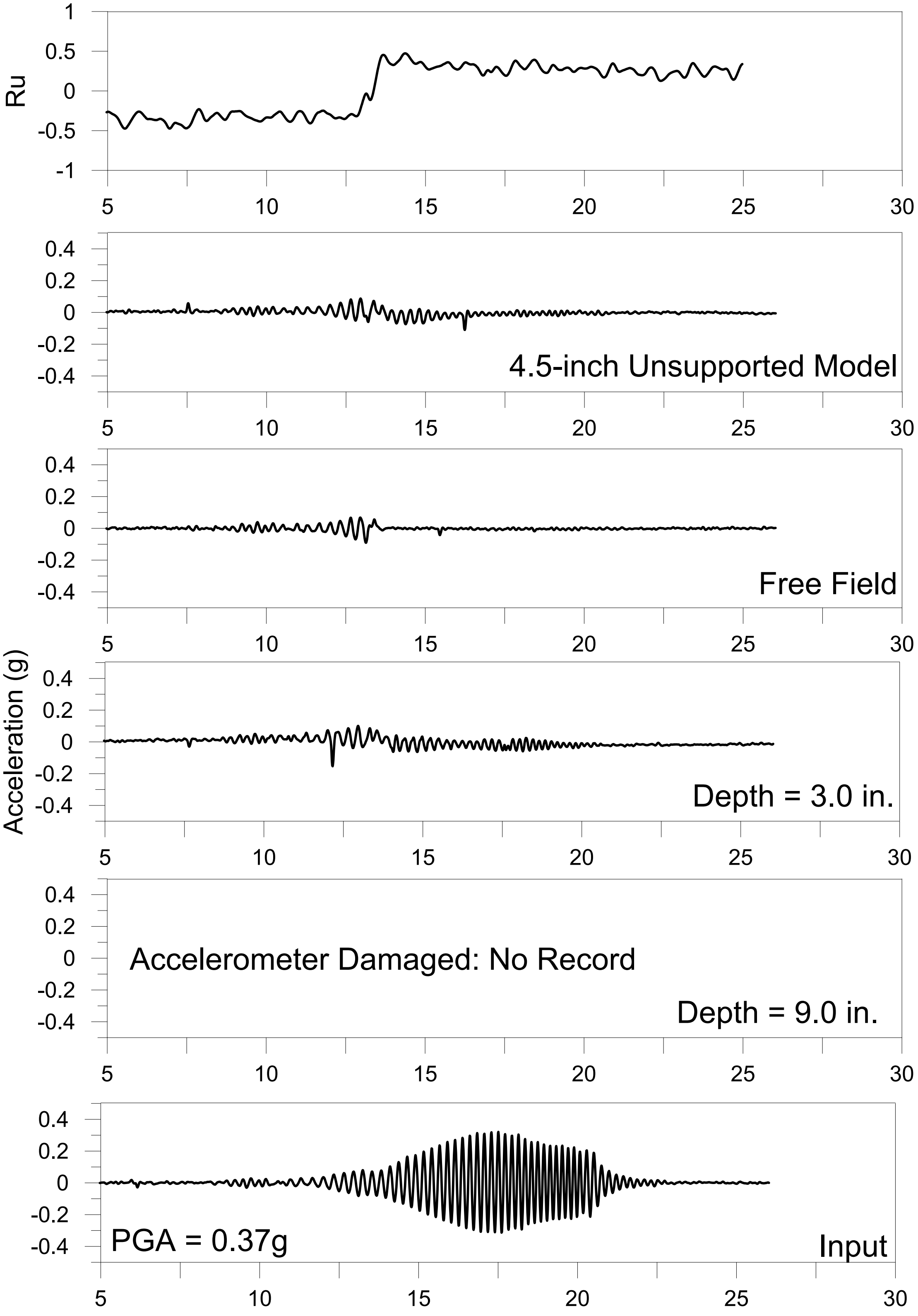

Test # 26: Settlement (cm)
3/9/2015
PGA: 0.37g

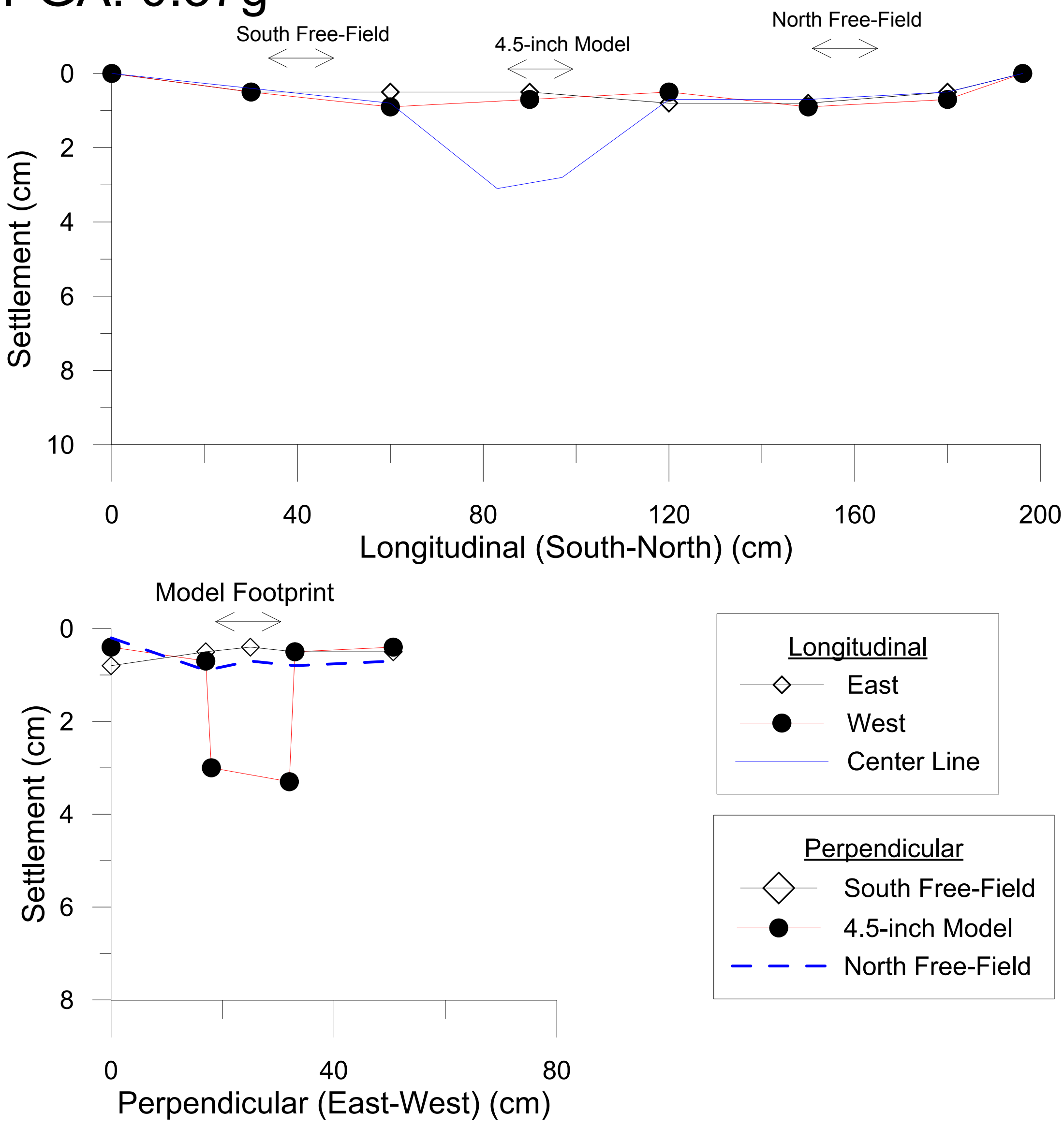

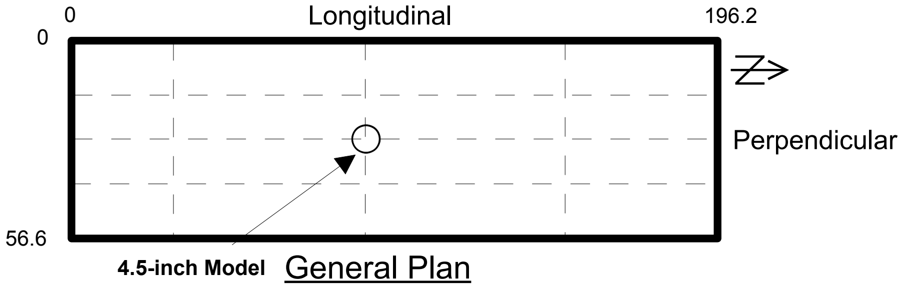

General Plan

Test # 26: Ground Motion Characteristics 3/9/2016 PGA: 0.37g

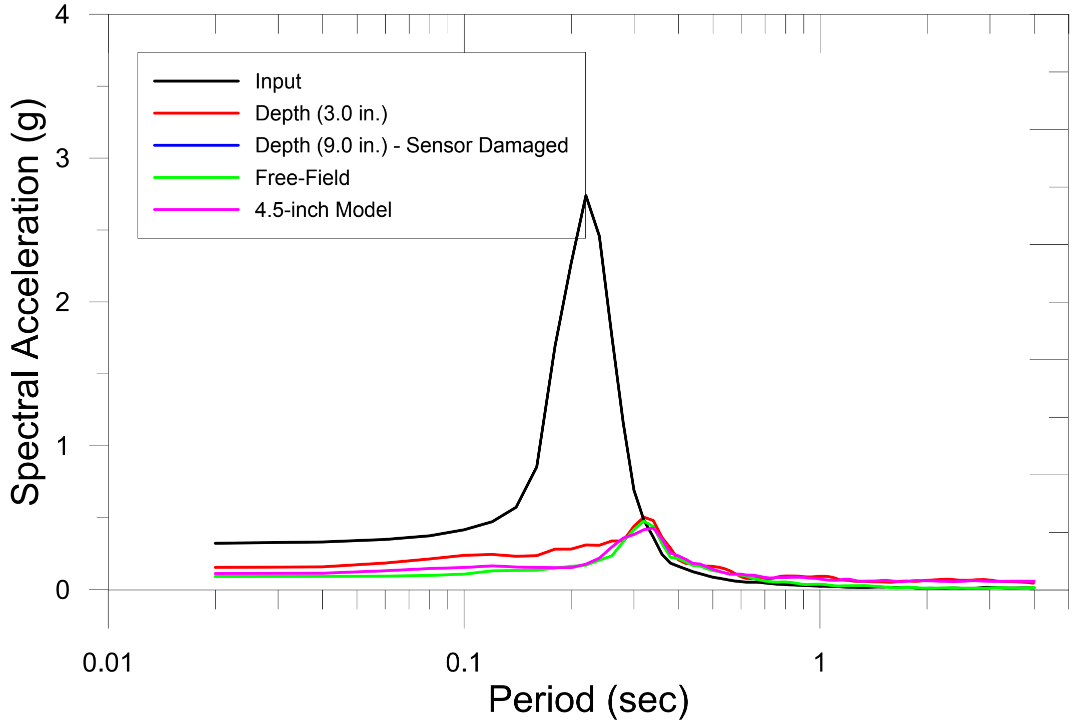

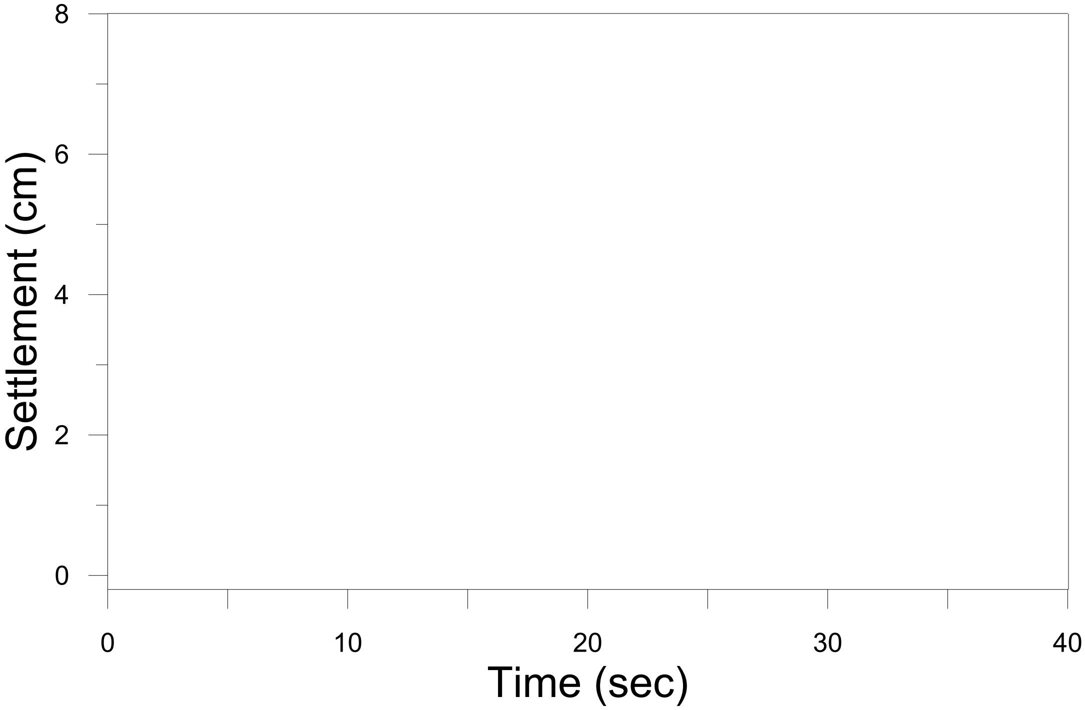

Test #27 (March 16, 2016)

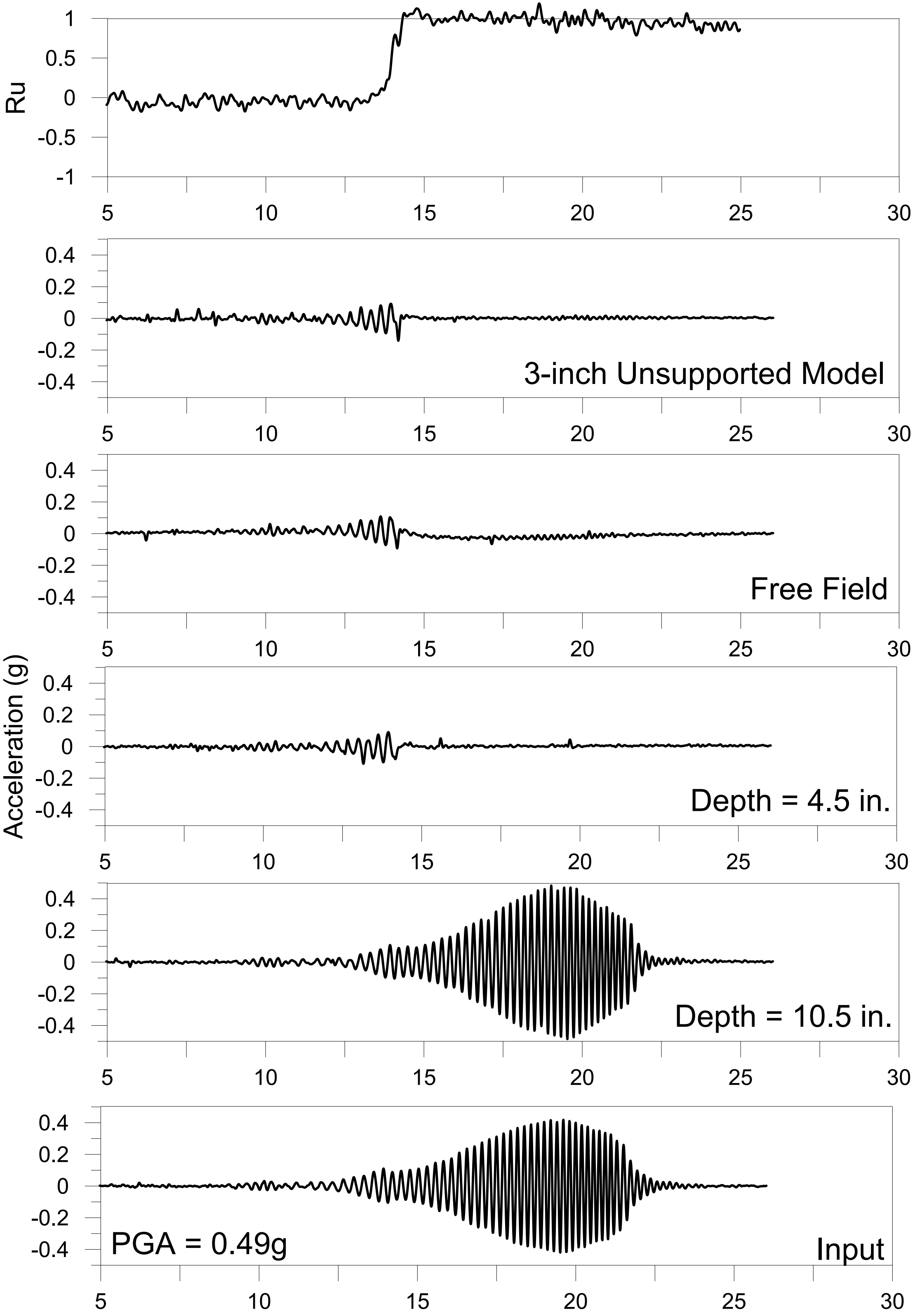

Test # 27: Settlement (cm)
3/16/2015
PGA: 0.49g

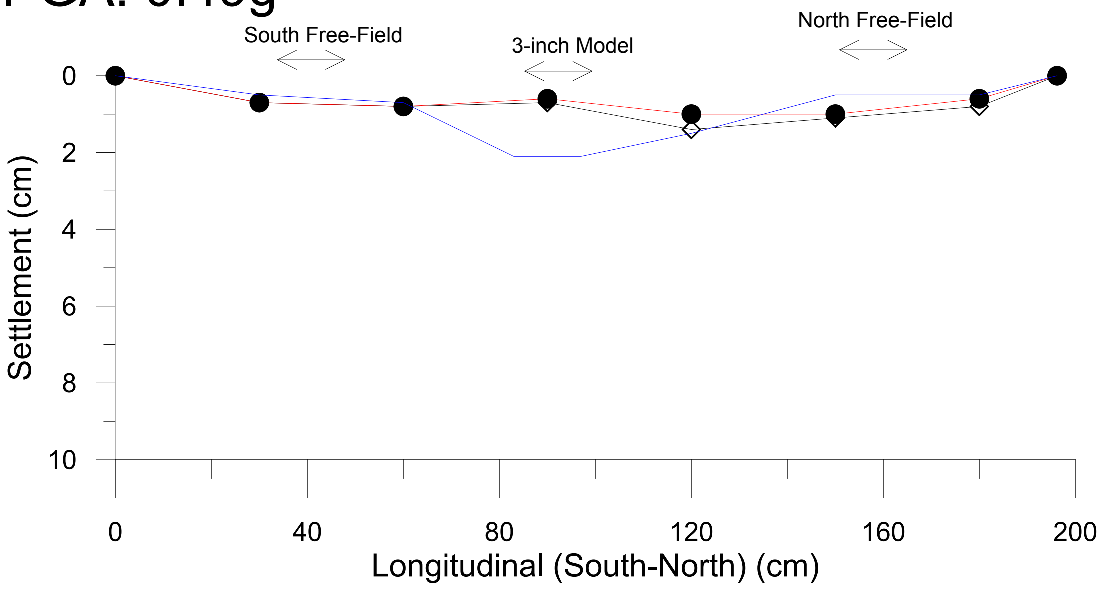

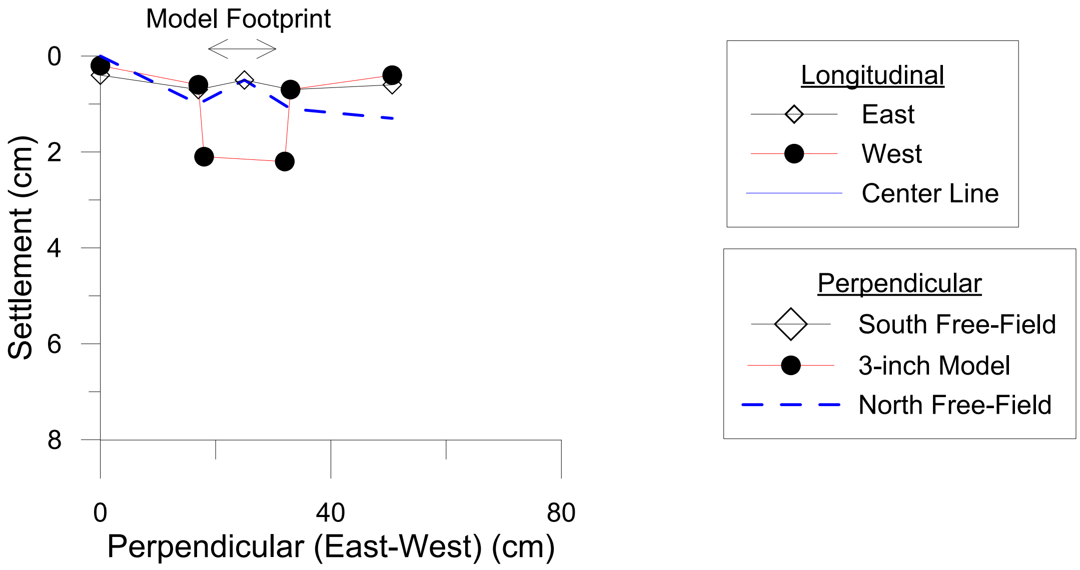

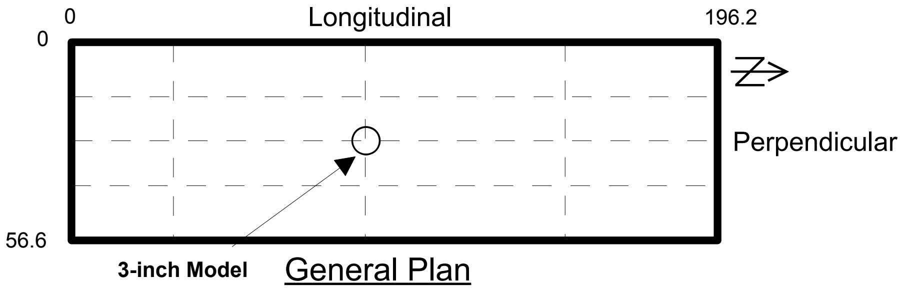

Test # 27: Ground Motion Characteristics
3/16/2016
PGA: 0.49g

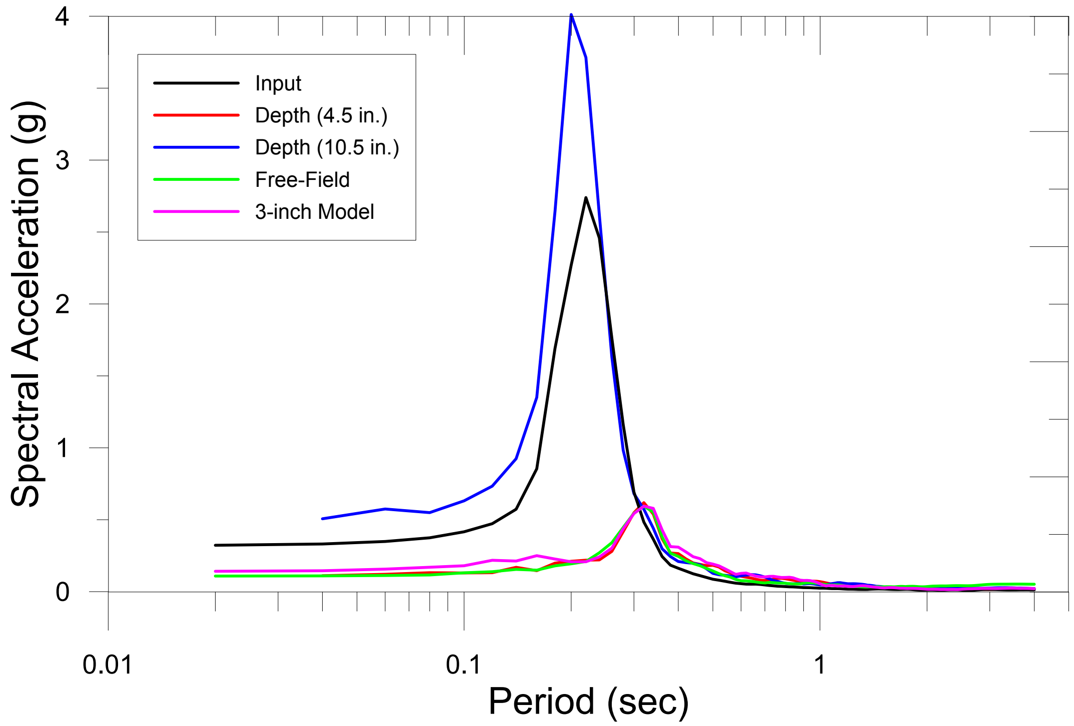

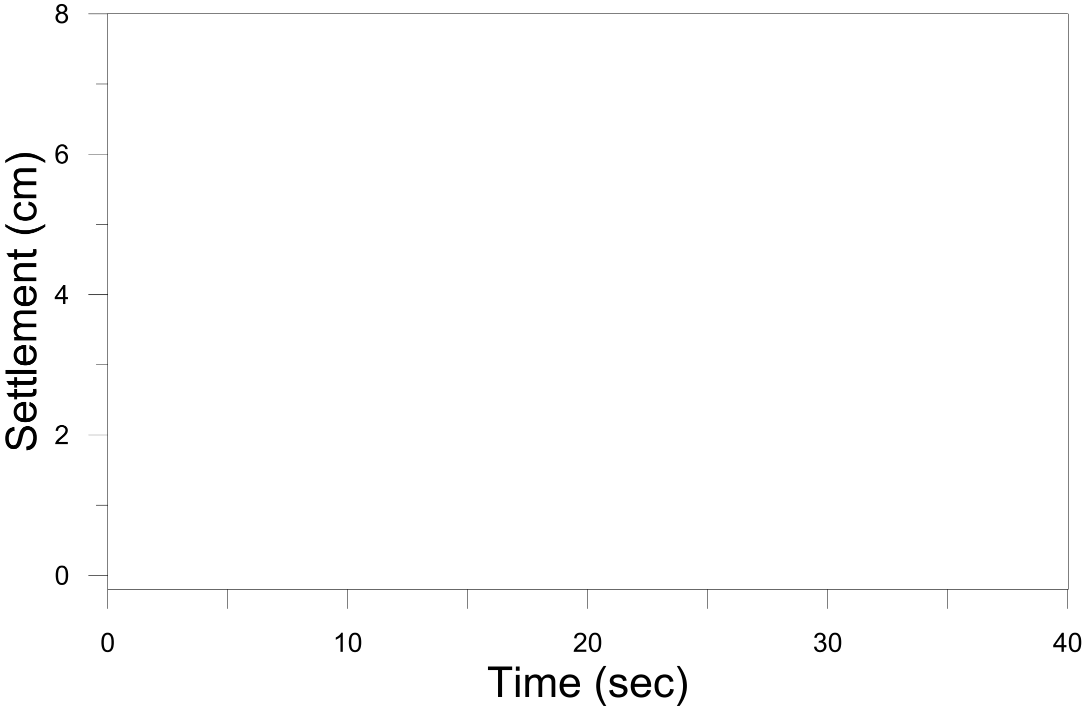

Test #28 (March 18, 2016)

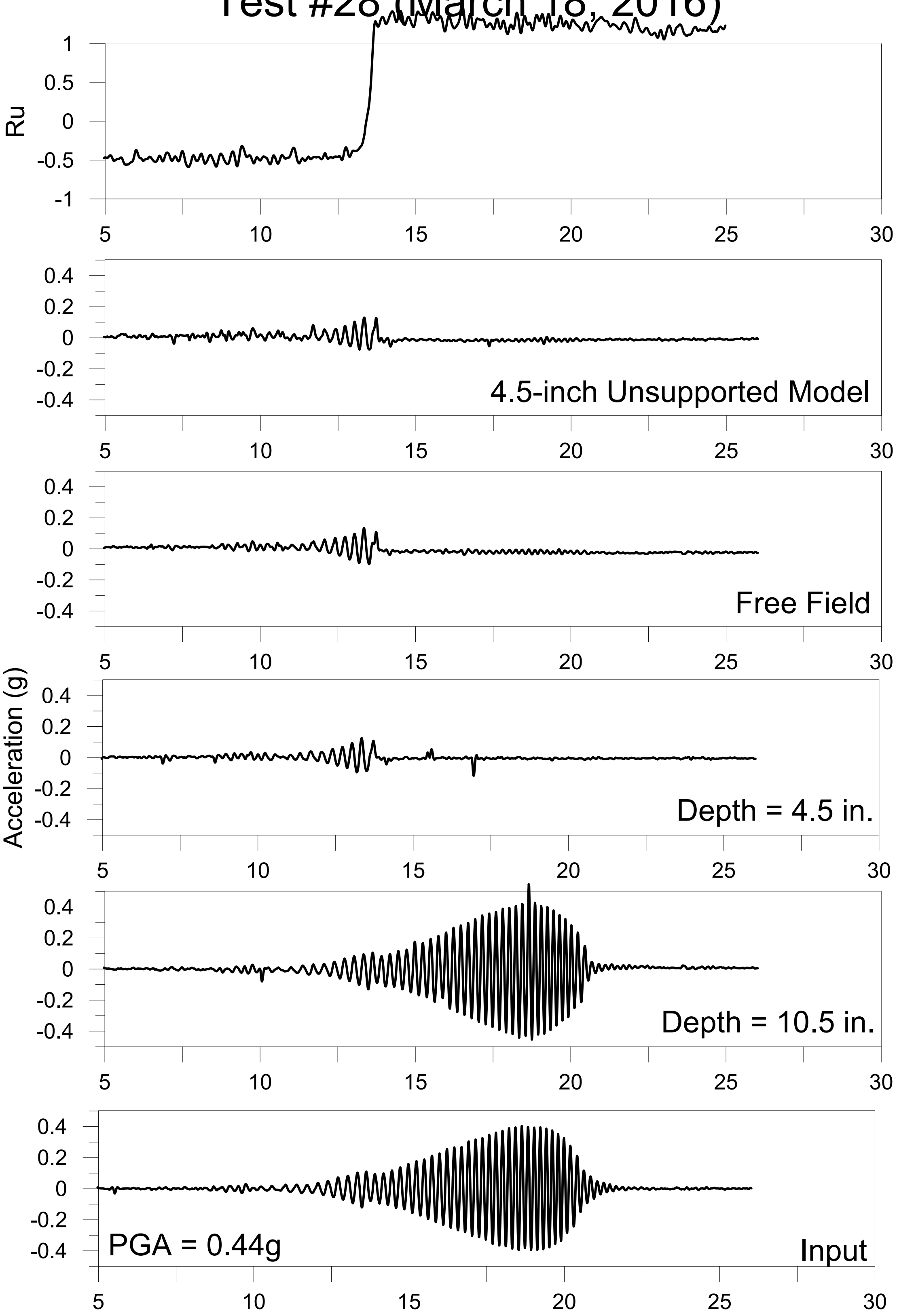

Test # 28: Settlement (cm)
3/18/2015
PGA: 0.44g

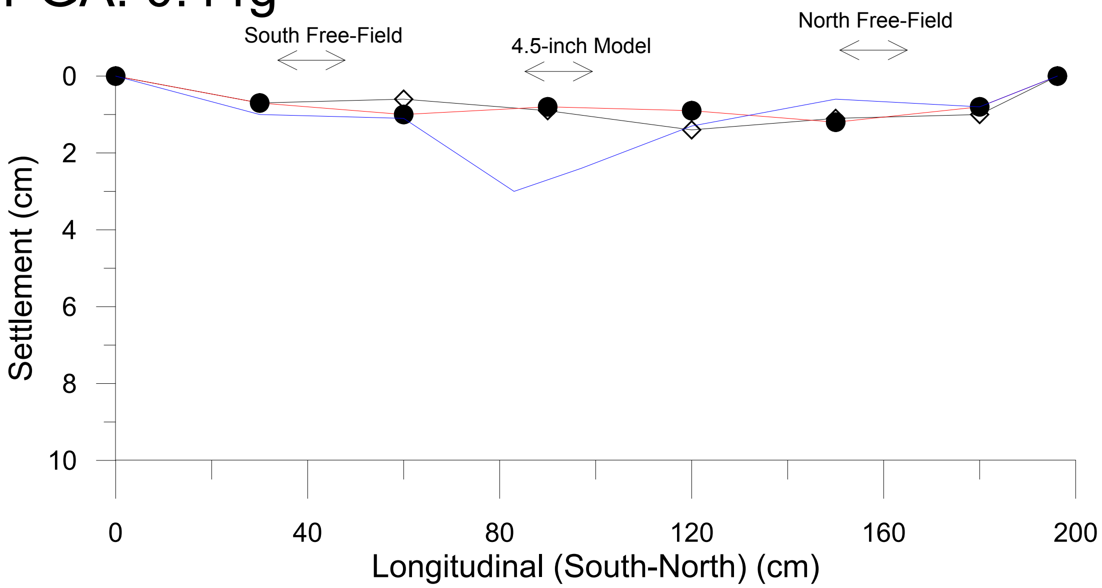

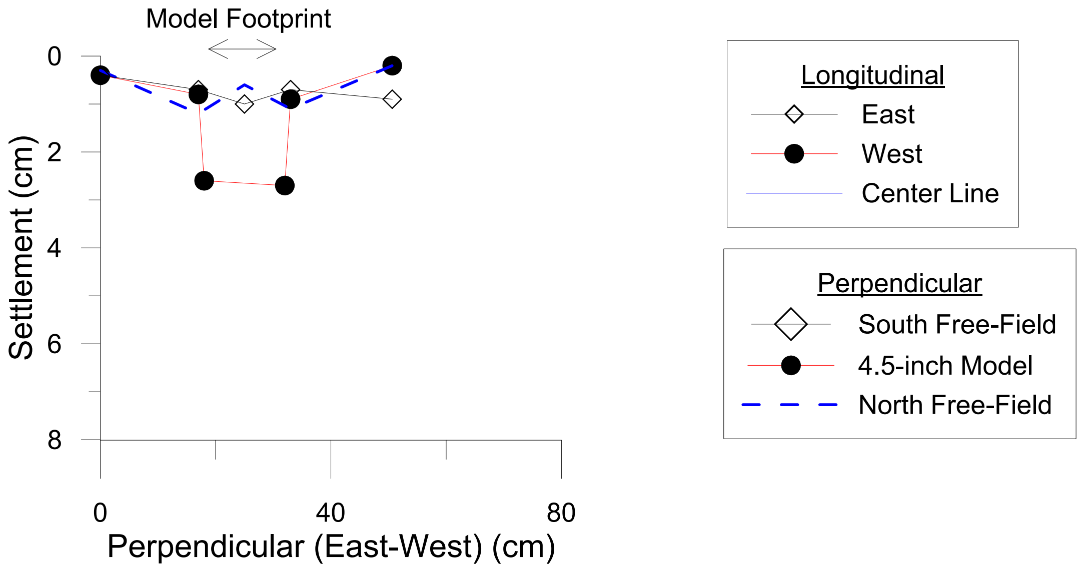

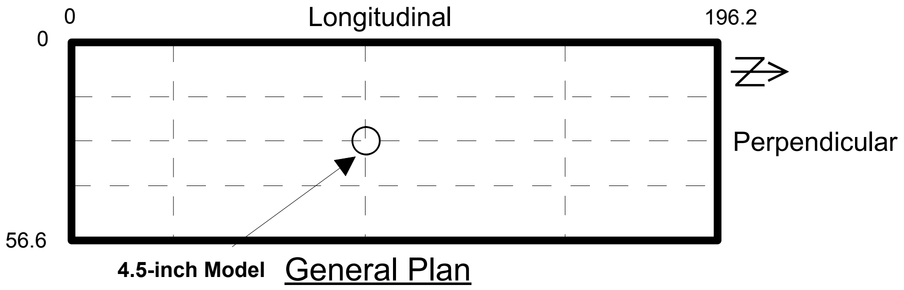

Test # 28: Ground Motion Characteristics
3/18/2016
PGA: 0.44g

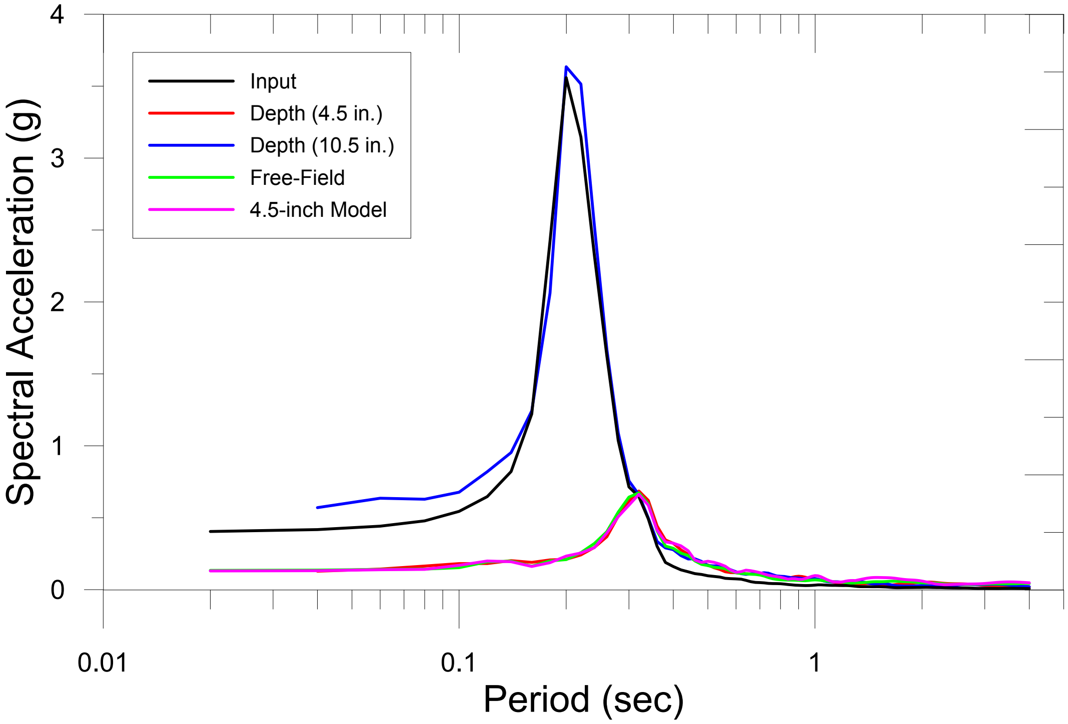

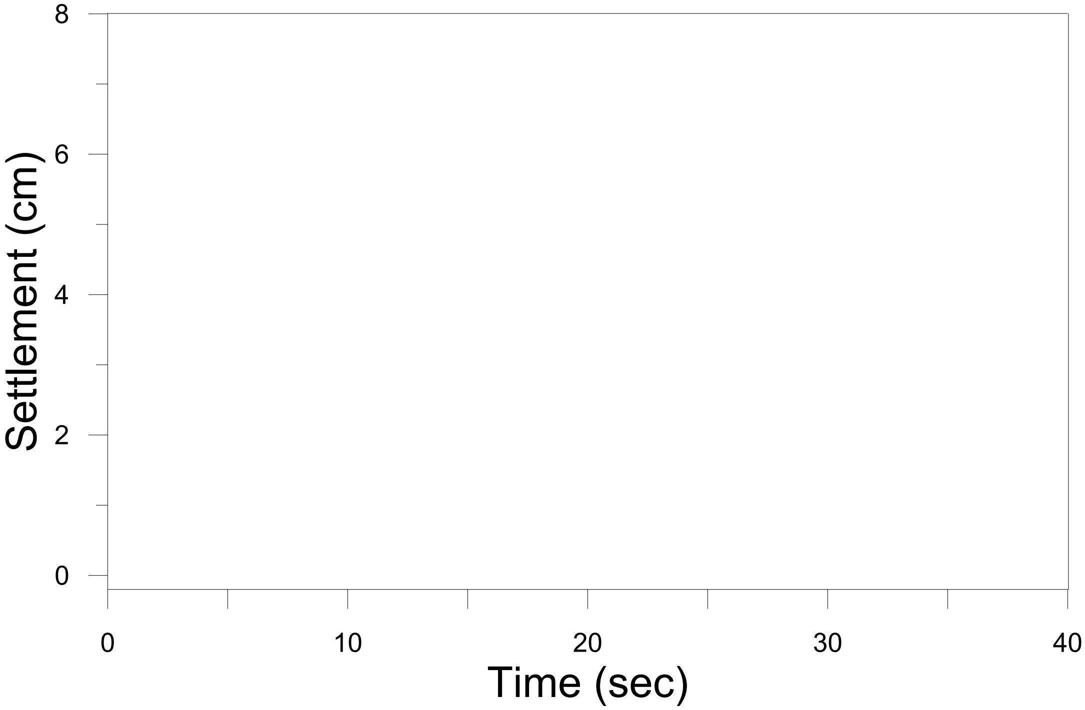

Test #29 (March 24, 2016)

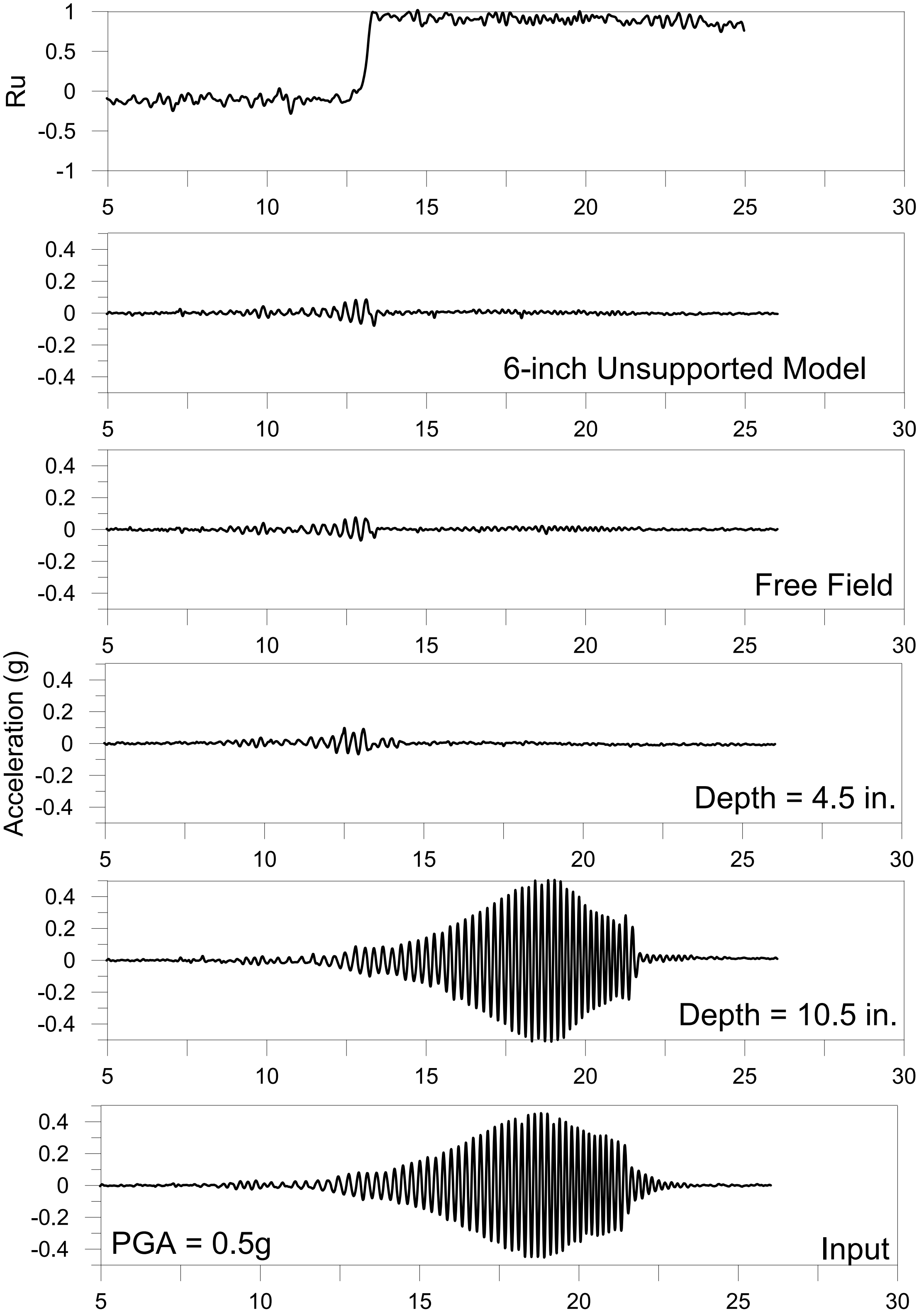

Test # 29: Settlement (cm)
3/24/2015
PGA: 0.50g

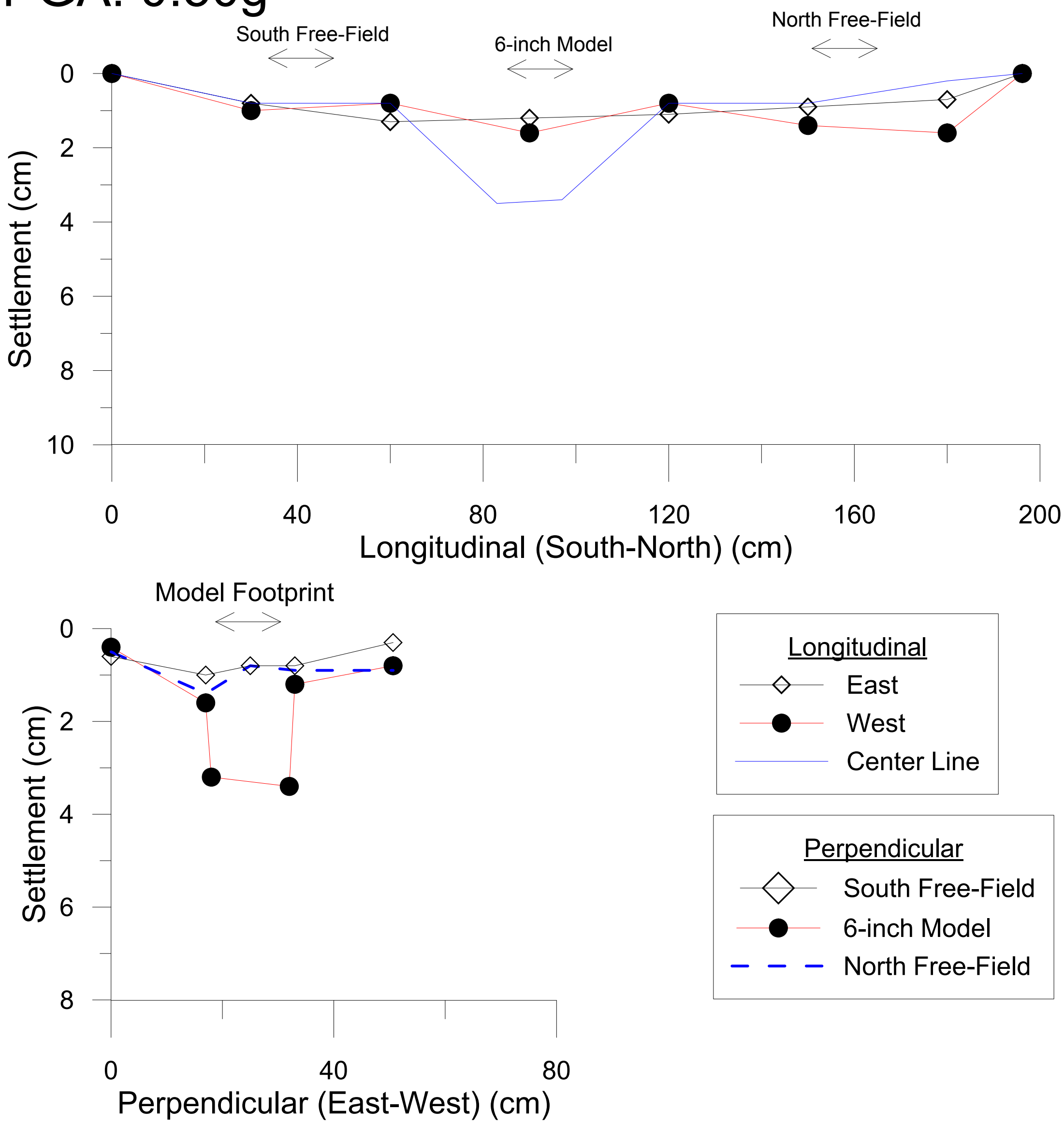

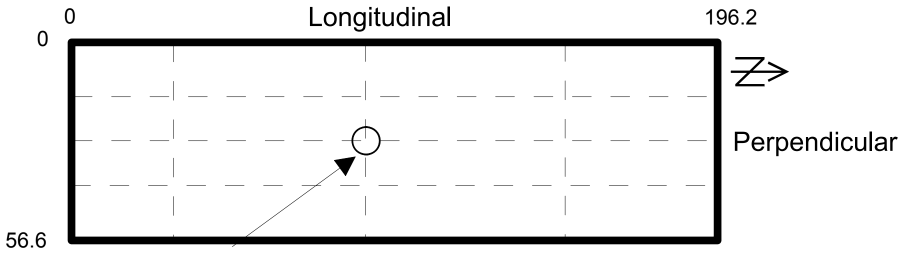

General Plan

Test # 29: Ground Motion Characteristics
3/24/2016
PGA: 0.50g

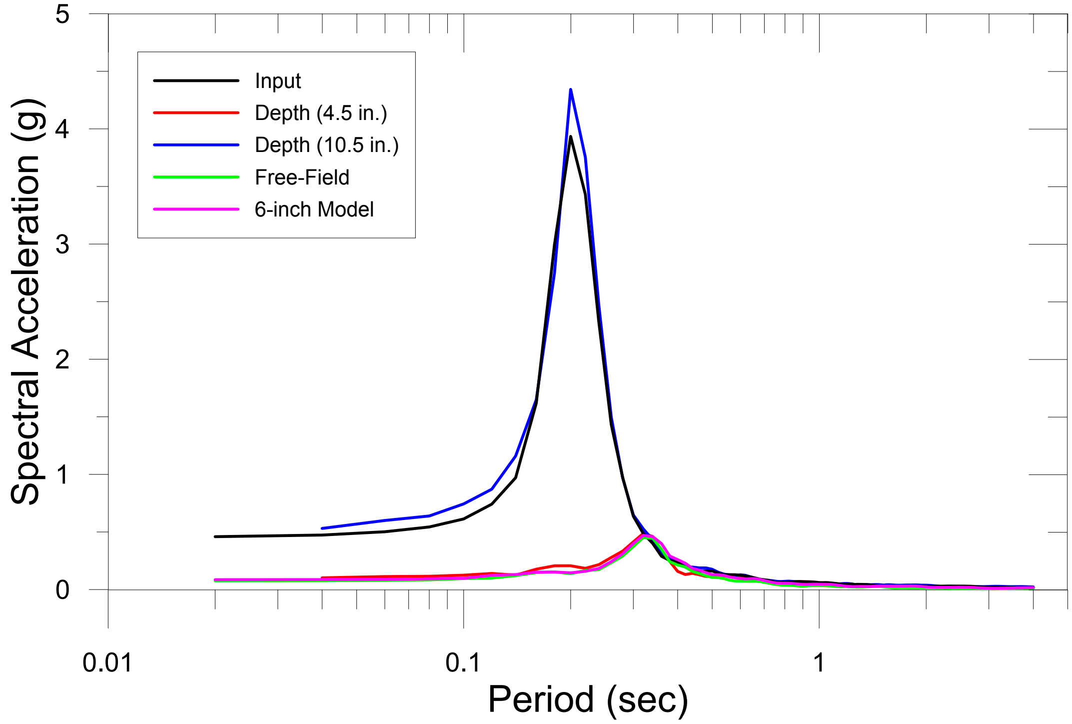

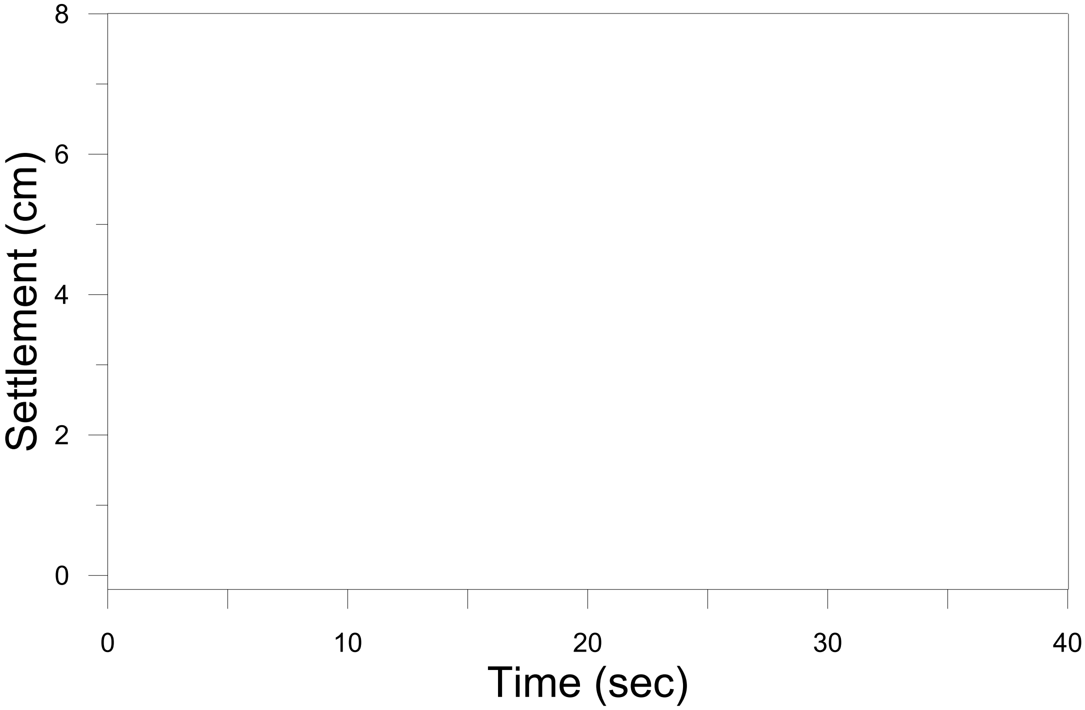

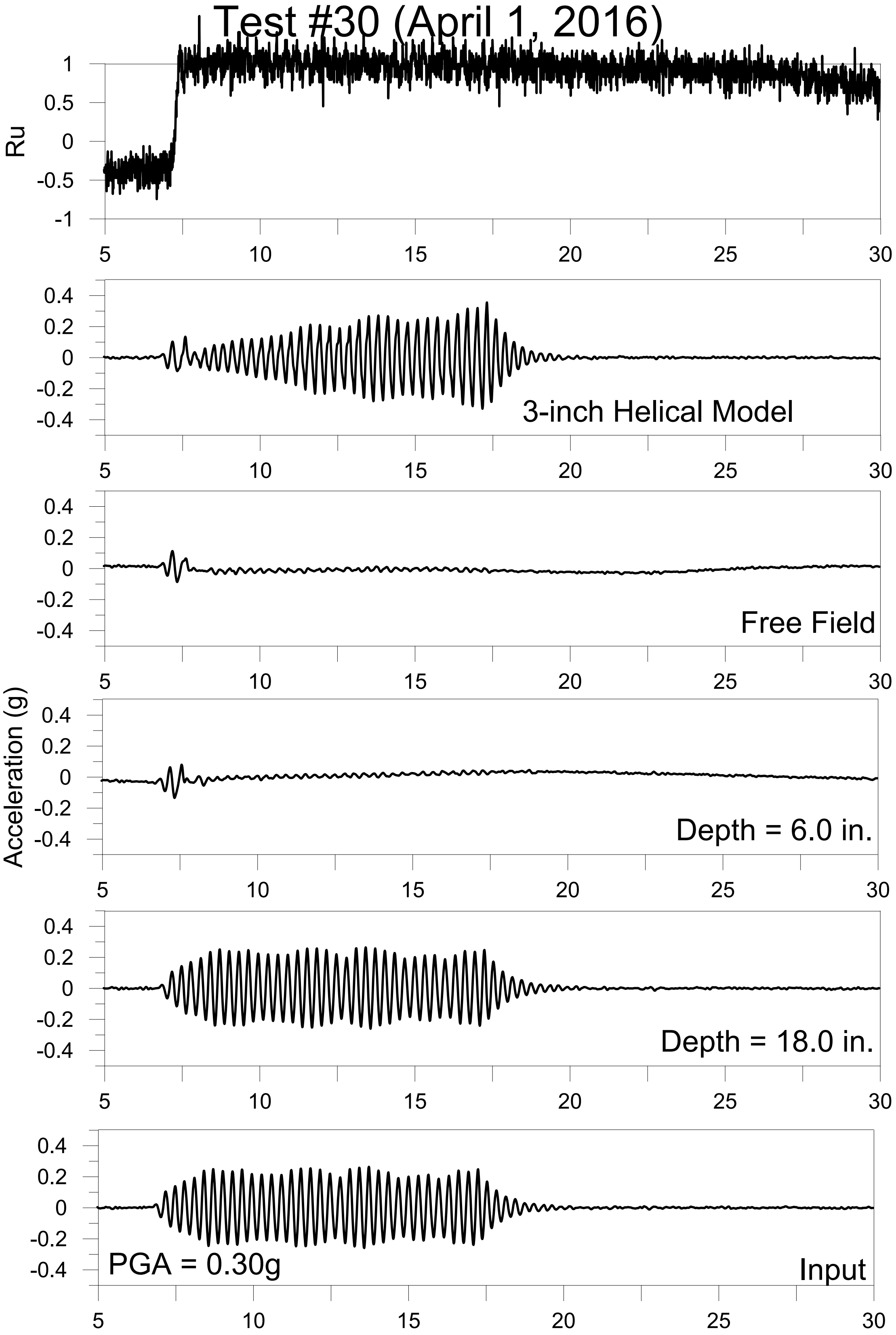
Test #30 (April 1, 2016)
Ru
1
0.5
0
-0.5
-1
5
10
15
20
25
30
3-inch Helical Model
Free Field
Acceleration (g)
Depth = 6.0 in.
Depth = 18.0 in.
PGA = 0.30g
Input
0.4
0.2
0
-0.2
-0.4

Test #34 (June 22, 2016)

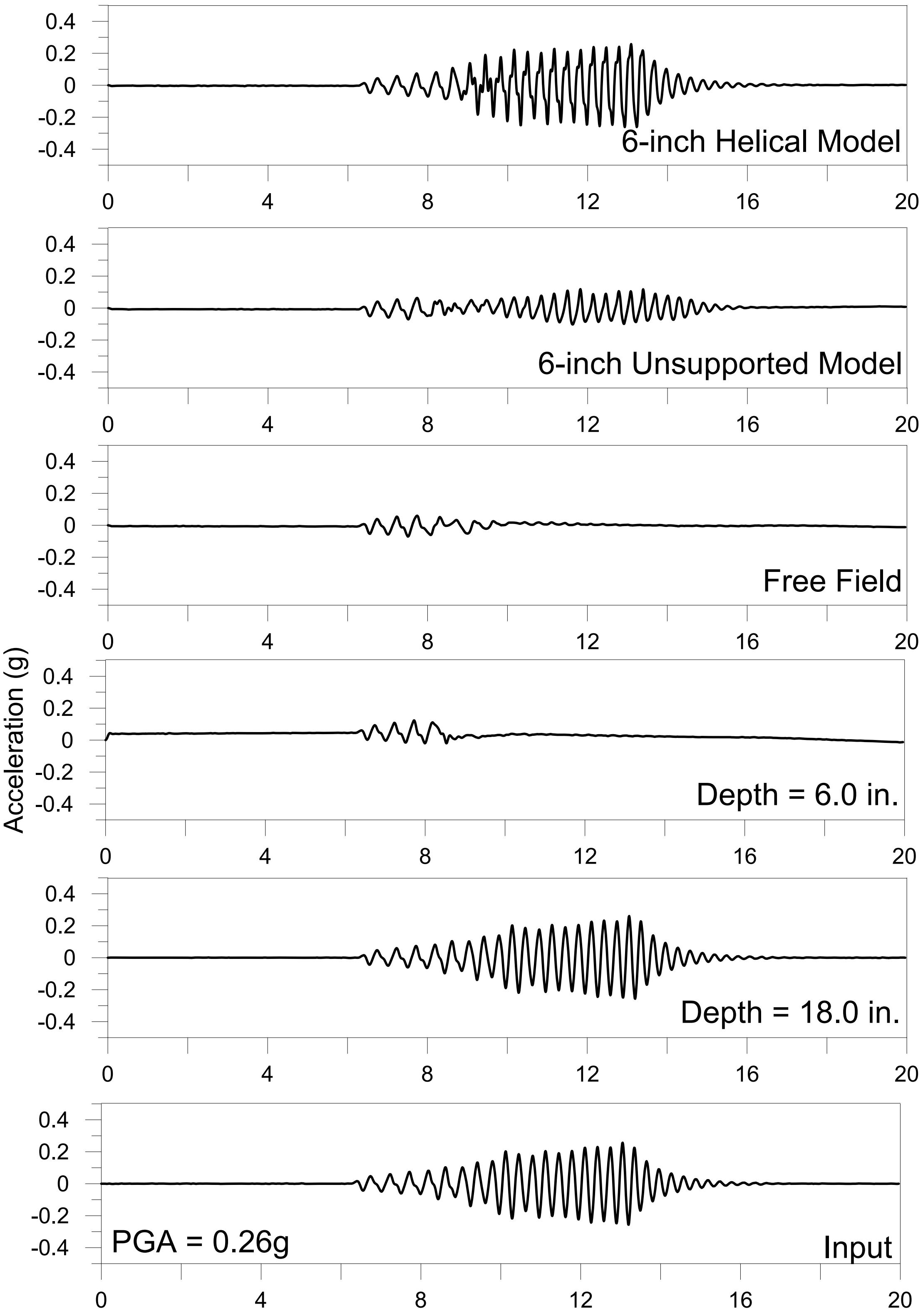

Test #34 (June 22, 2016)

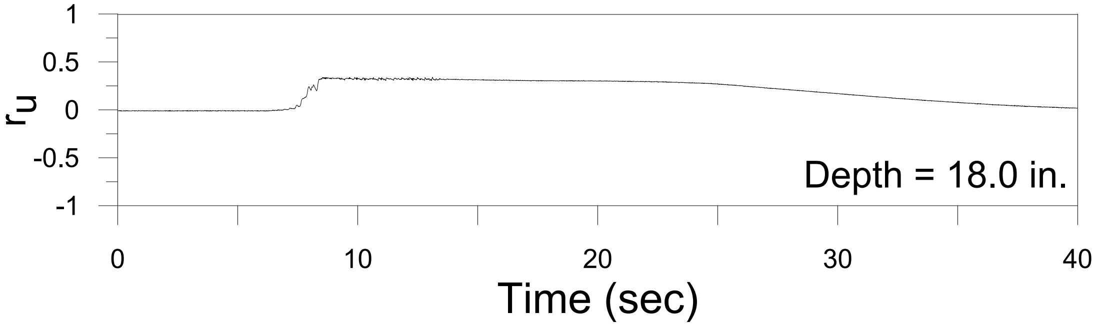

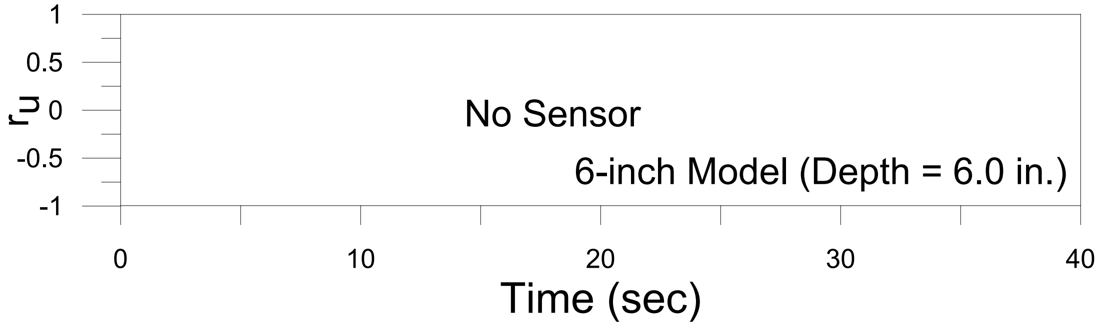

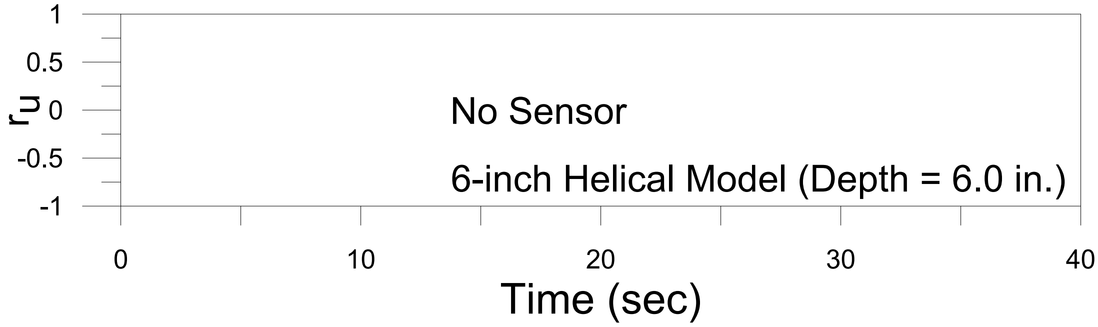

PGA = 0.26g

Test # 34: Settlement (cm)
6/22/2016
PGA: 0.26g

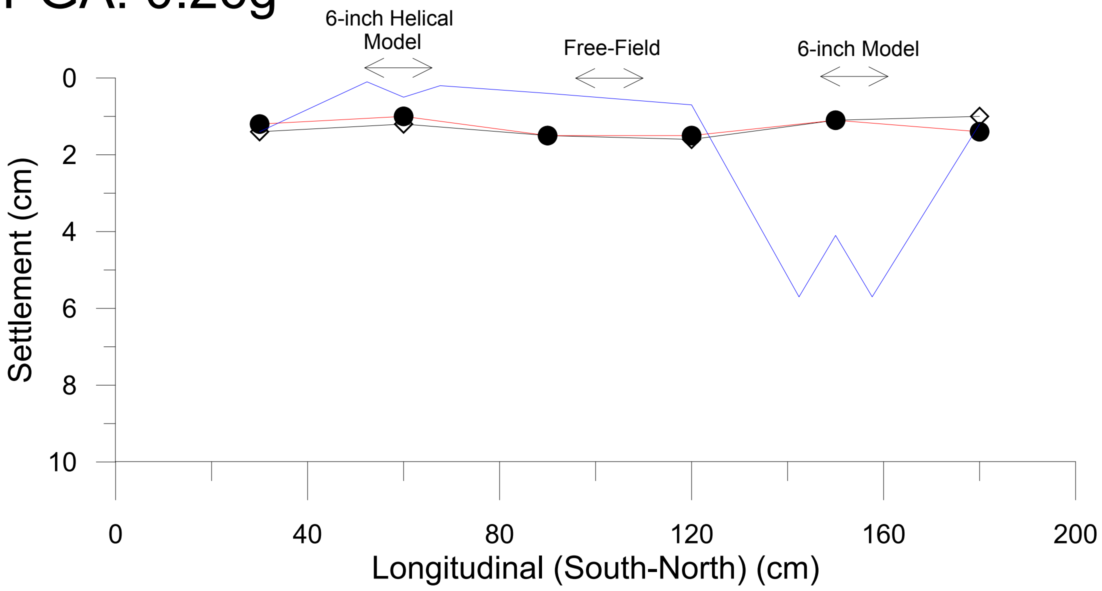

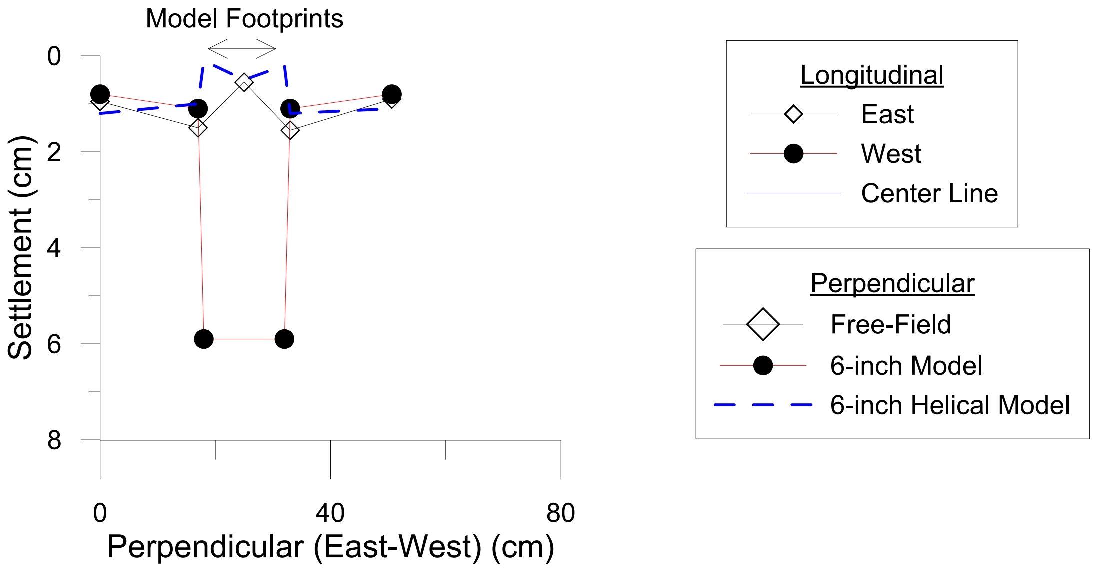

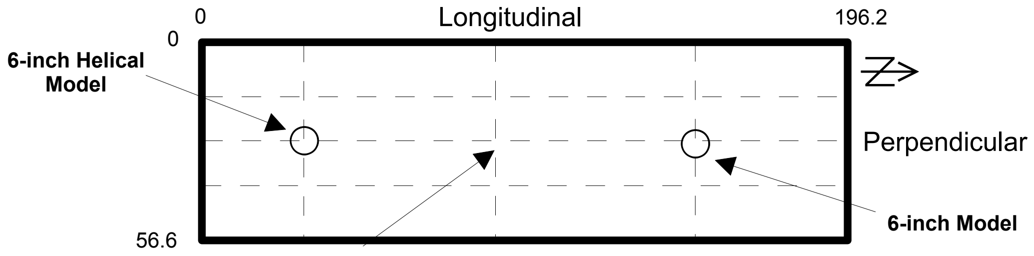

General Plan

Test # 34: Ground Motion Characteristics
6/22/2016
PGA: 0.26g

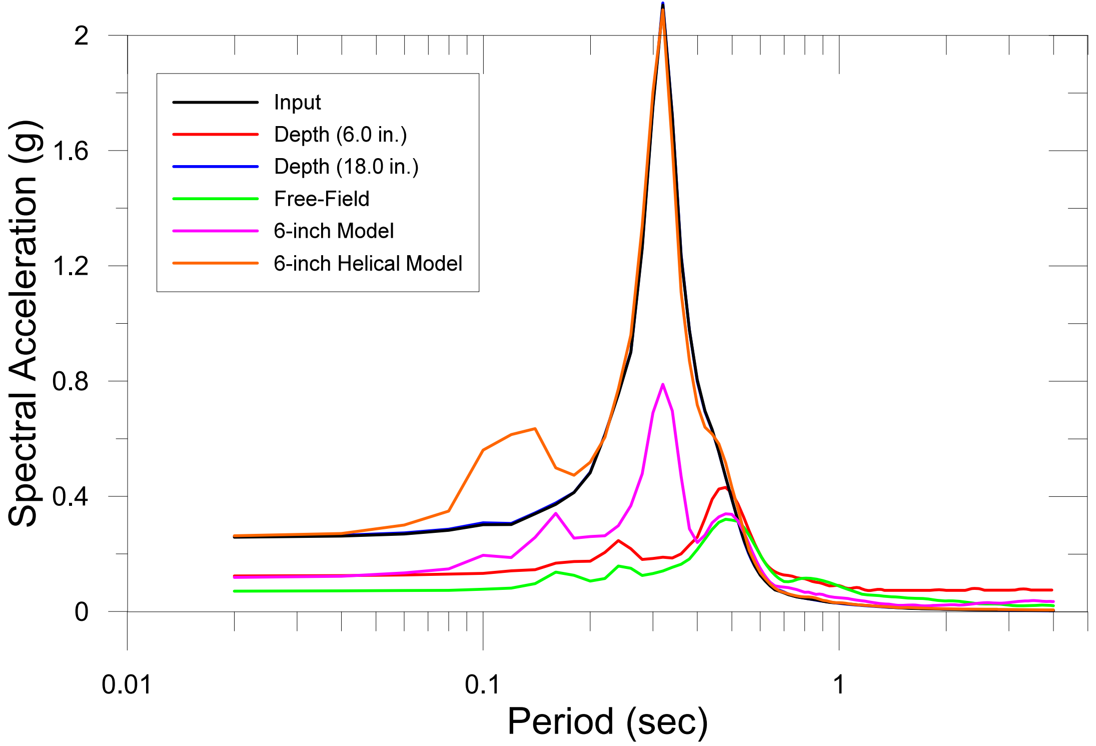

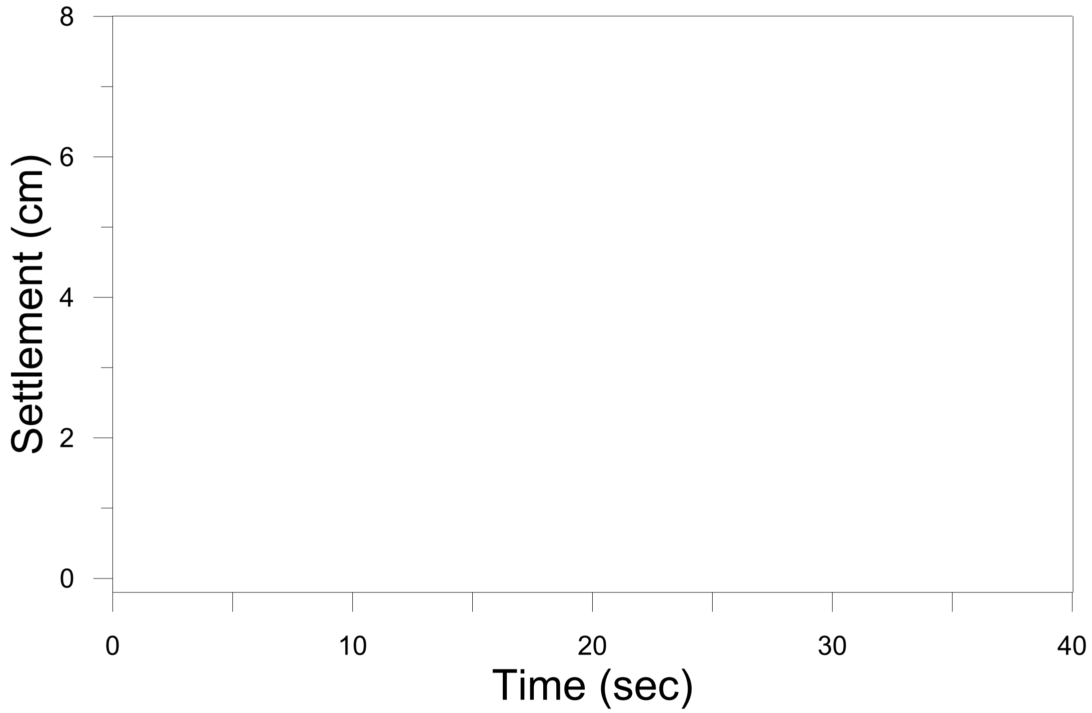

Test #35 (July 1, 2016)

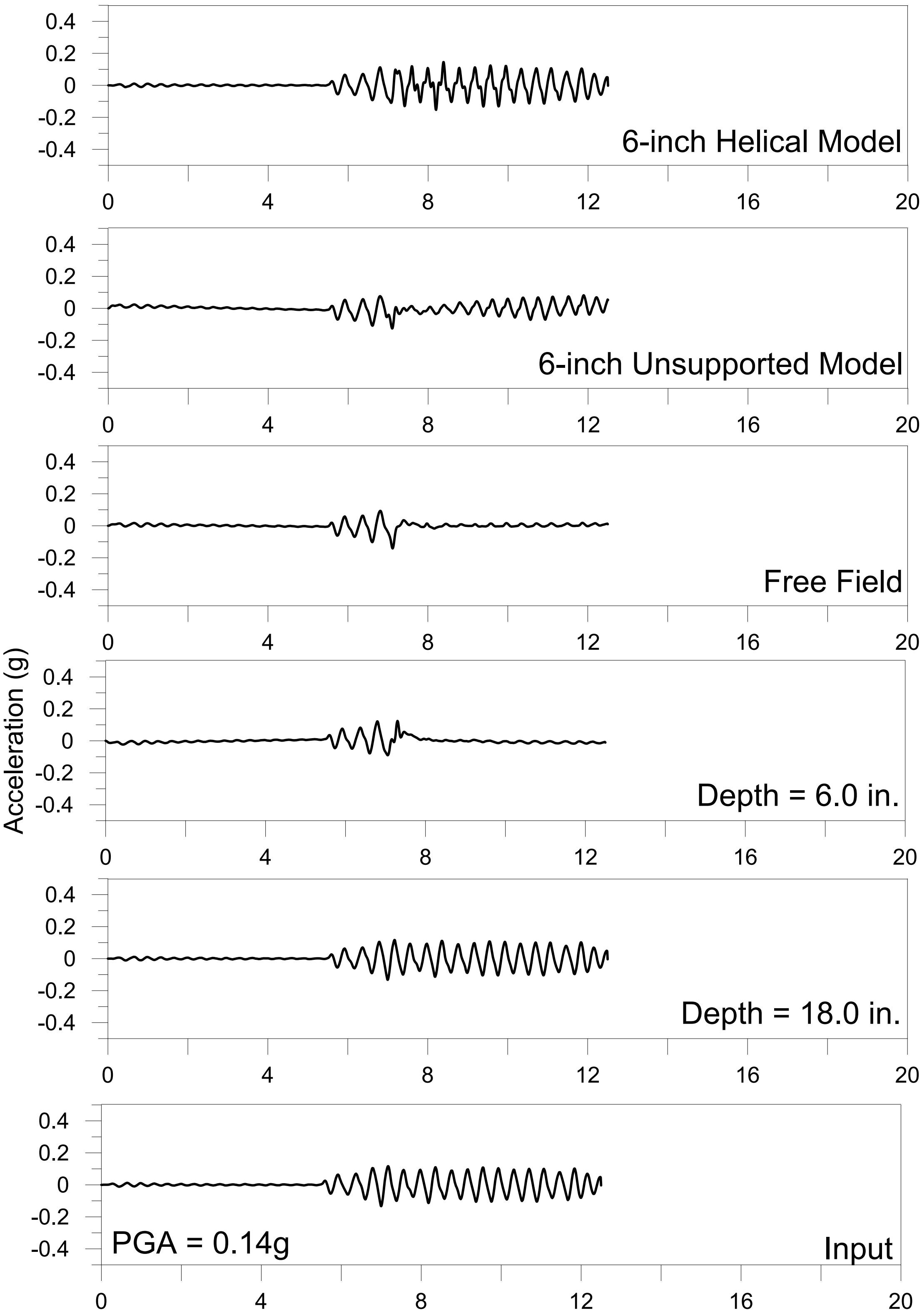

Test #35 (July 1, 2016)

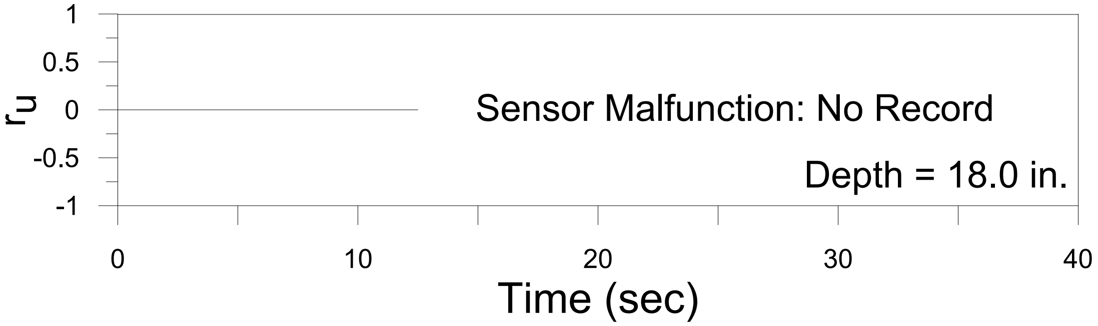

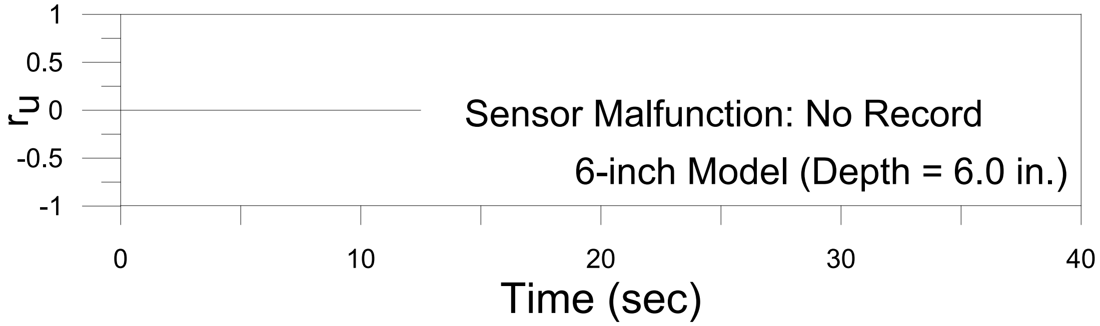

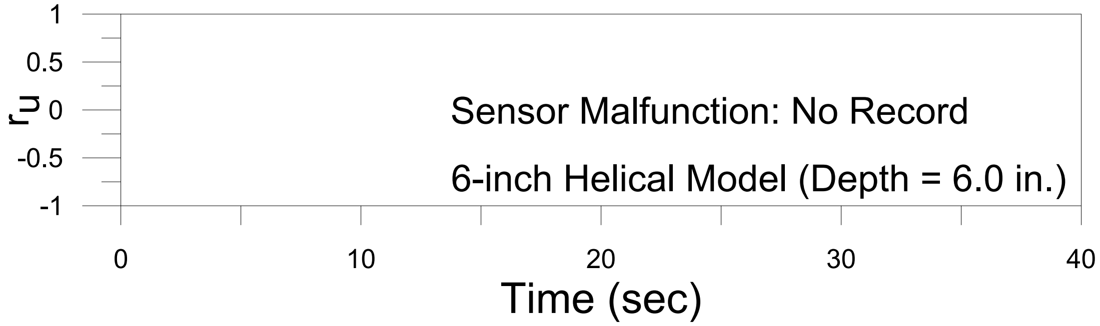

PGA = 0.14g

Test # 35: Ground Motion Characteristics
7/1/2016
PGA: 0.14g

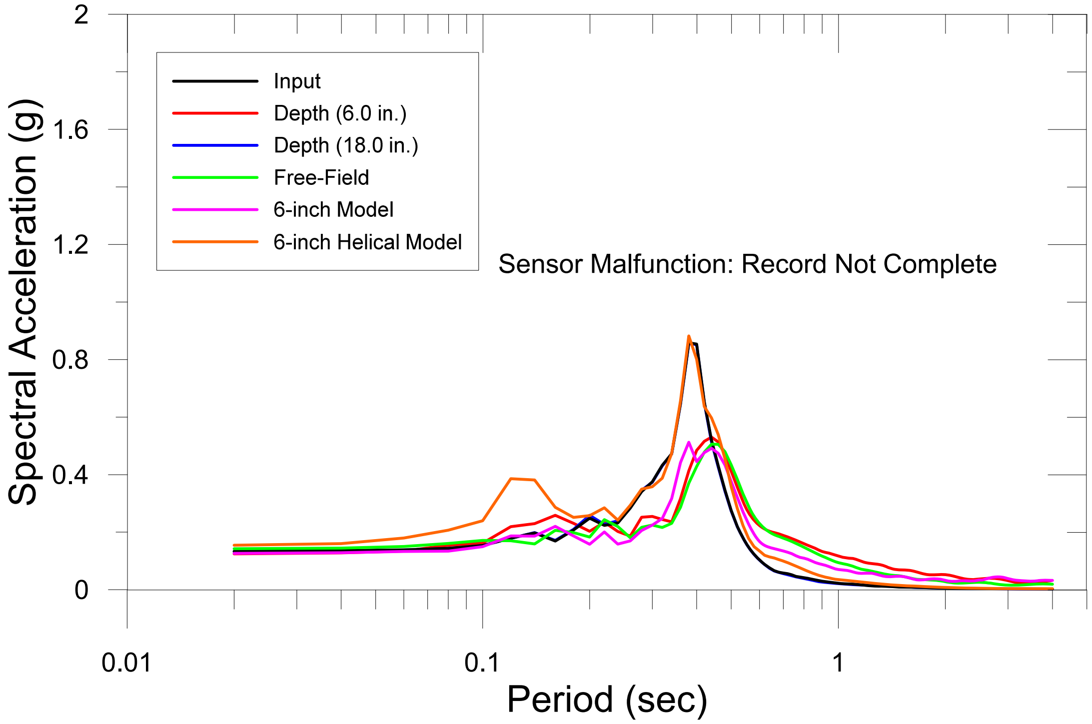

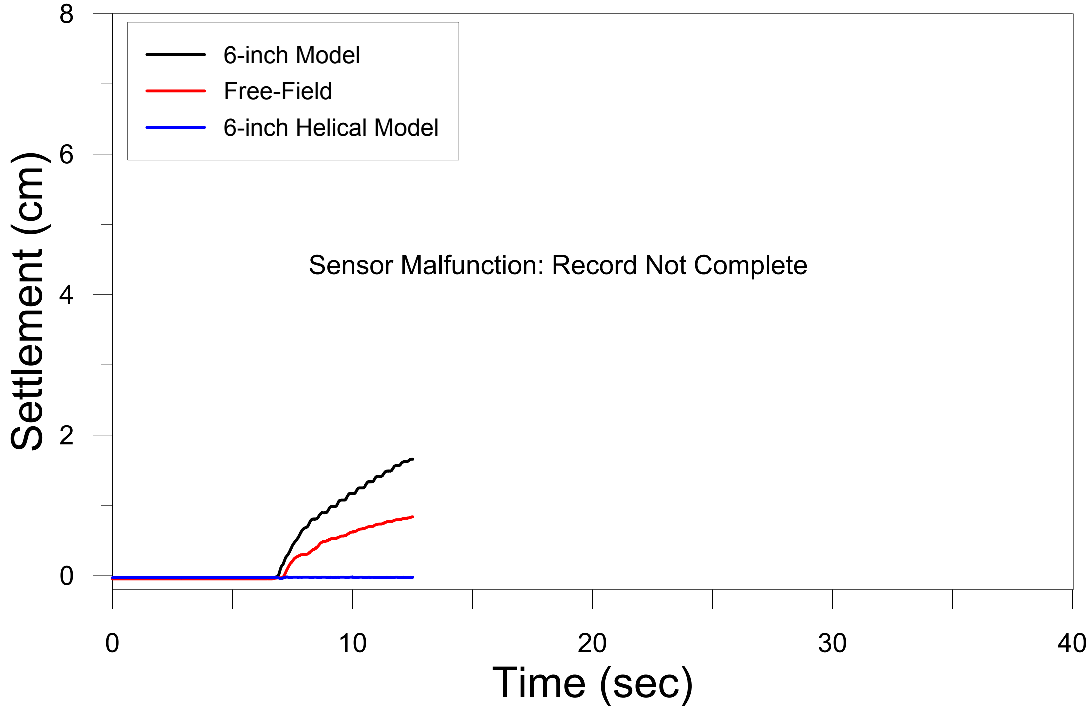

Test # 35: Settlement (cm)
7/1/2016
PGA: 0.14g

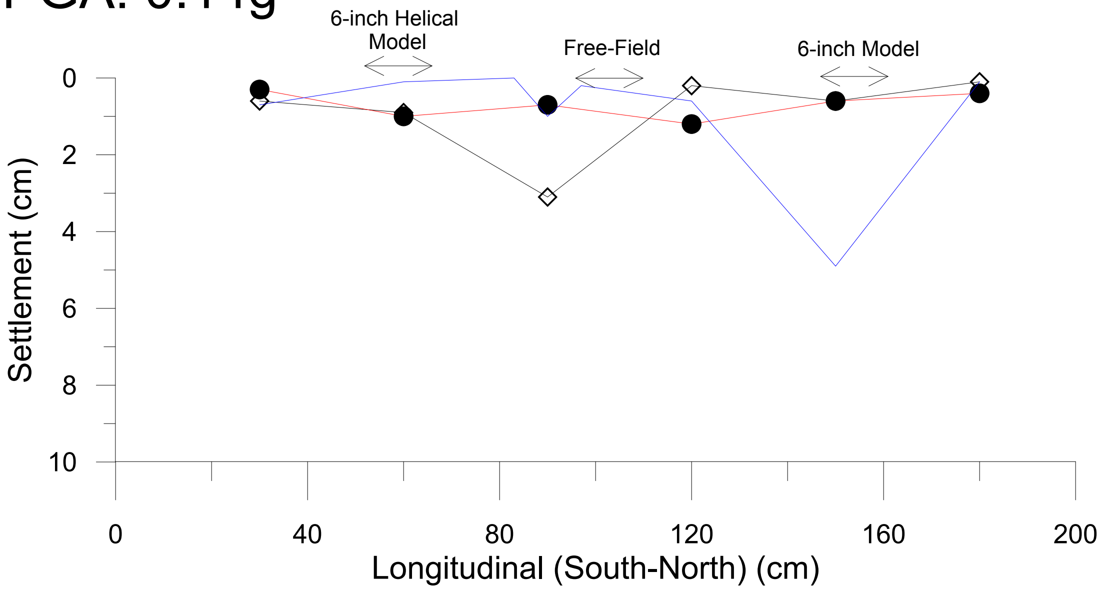

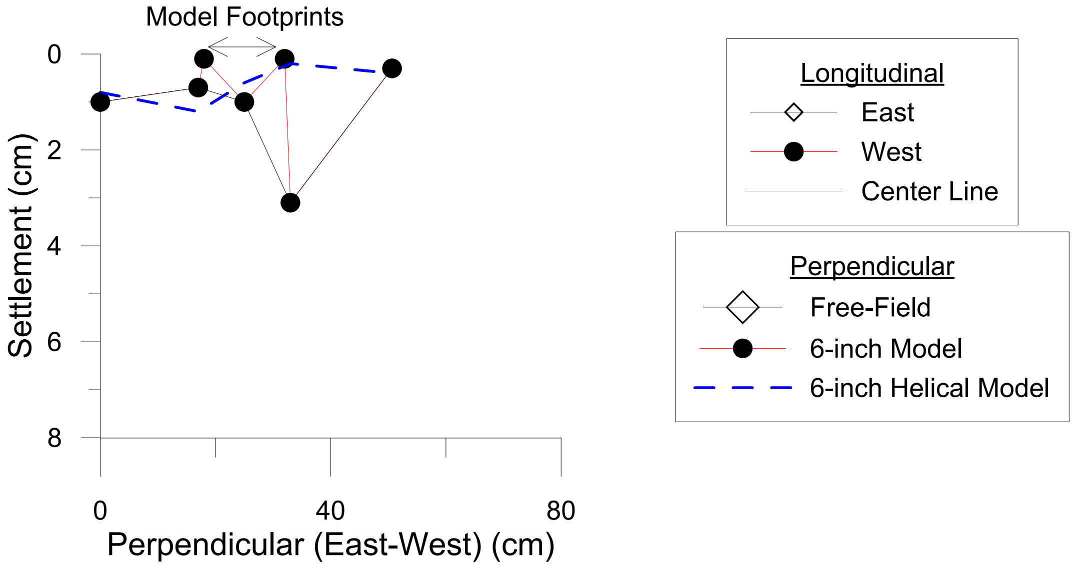

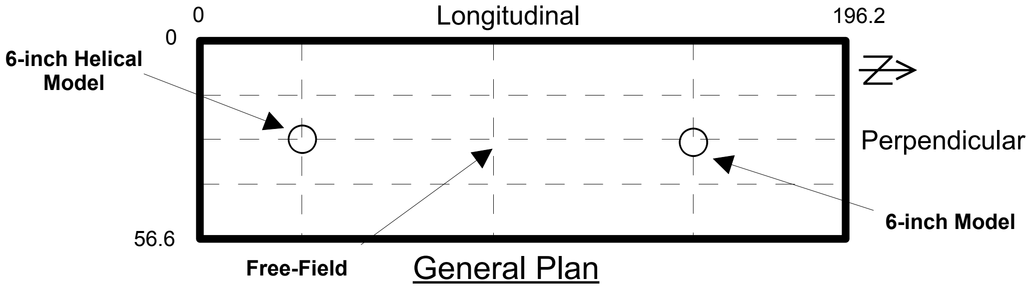

General Plan

Test #36 (July 15, 2016)

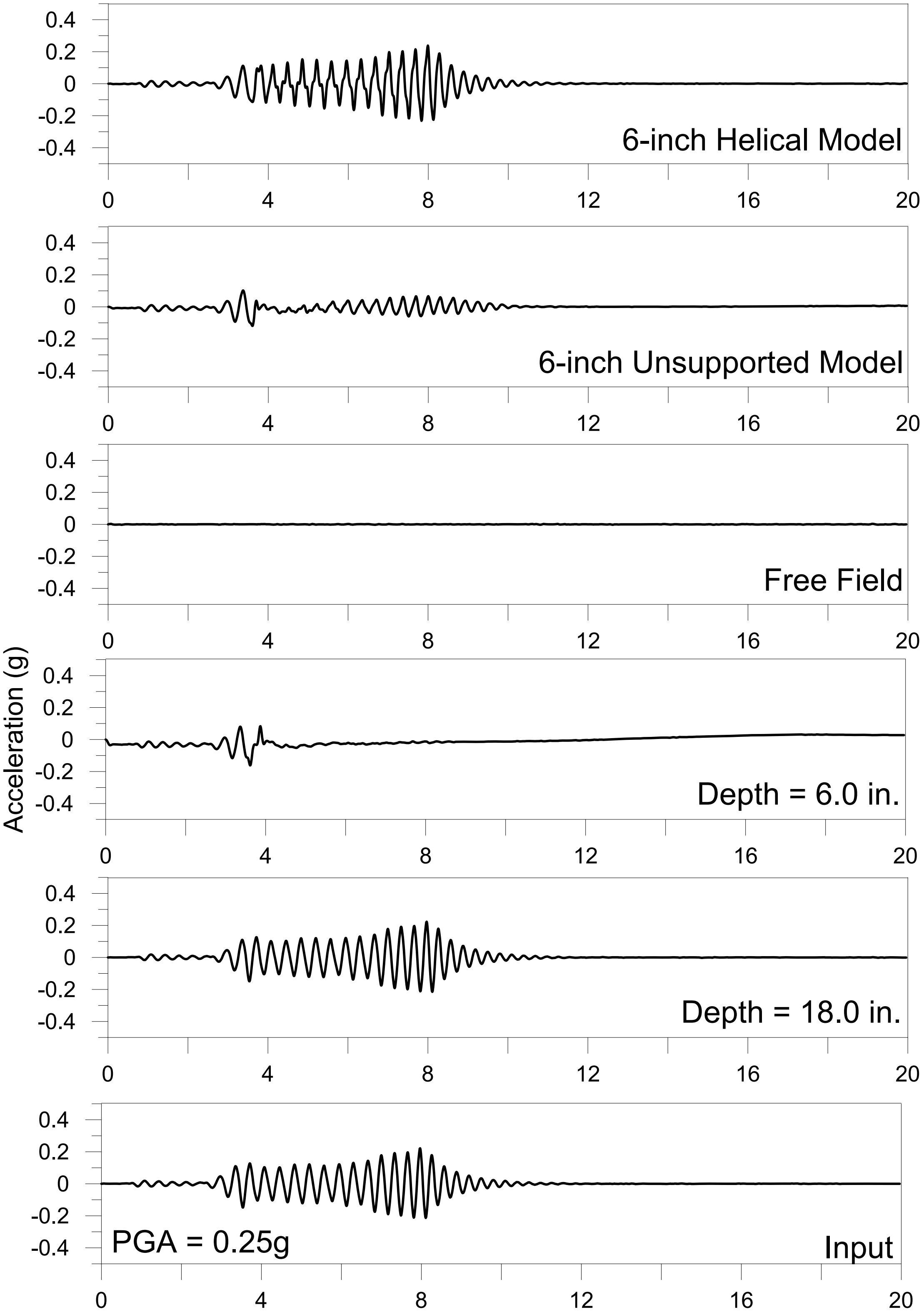

Test #36 (July 15, 2016)

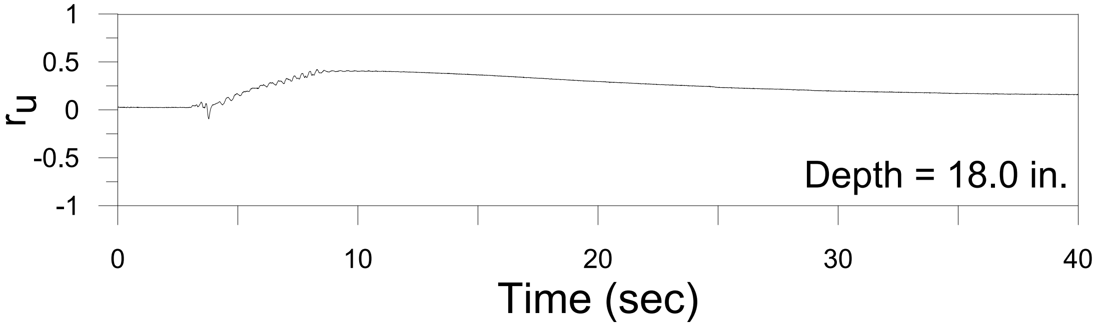

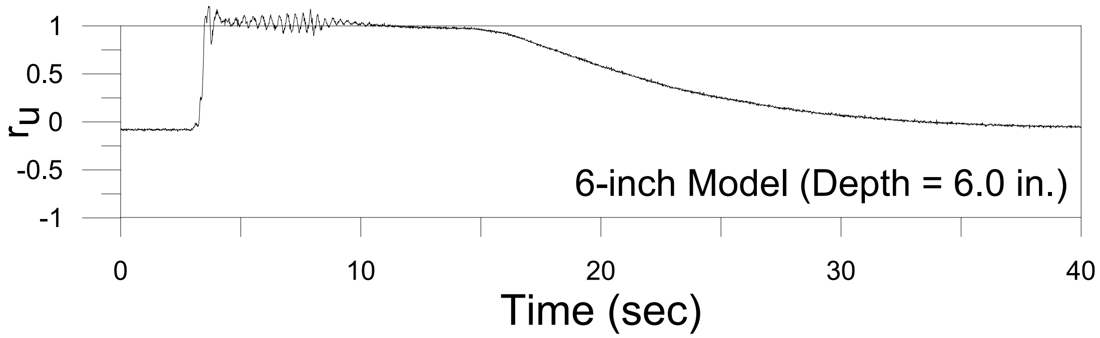

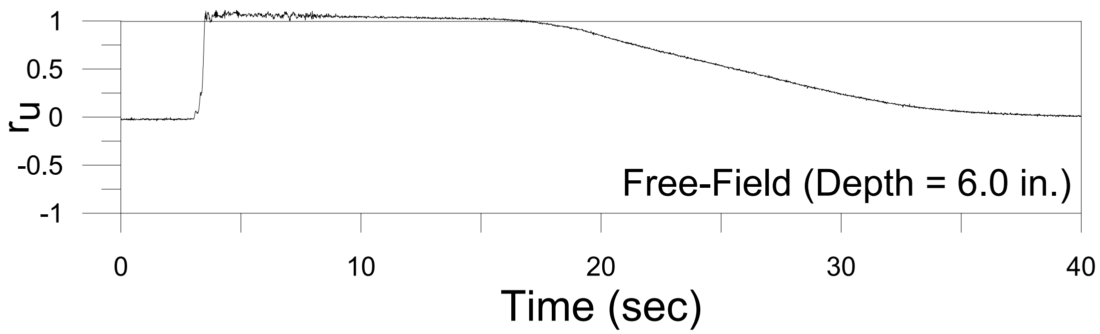

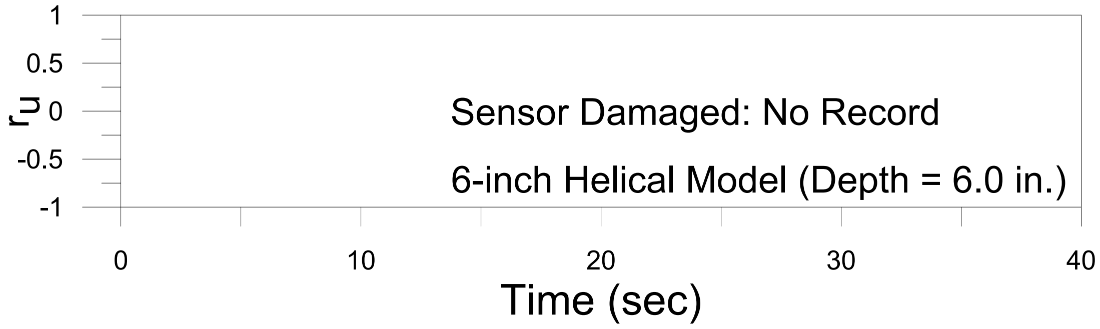

PGA = 0.25g

Test # 36: Ground Motion Characteristics
7/15/2016
PGA: 0.25g

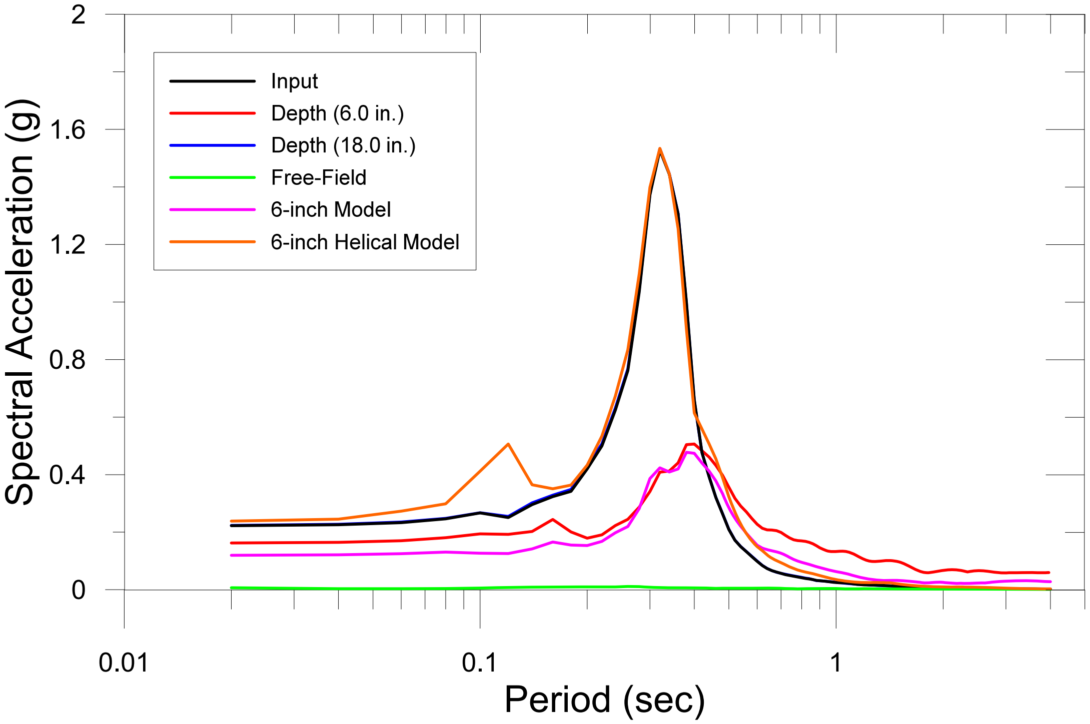

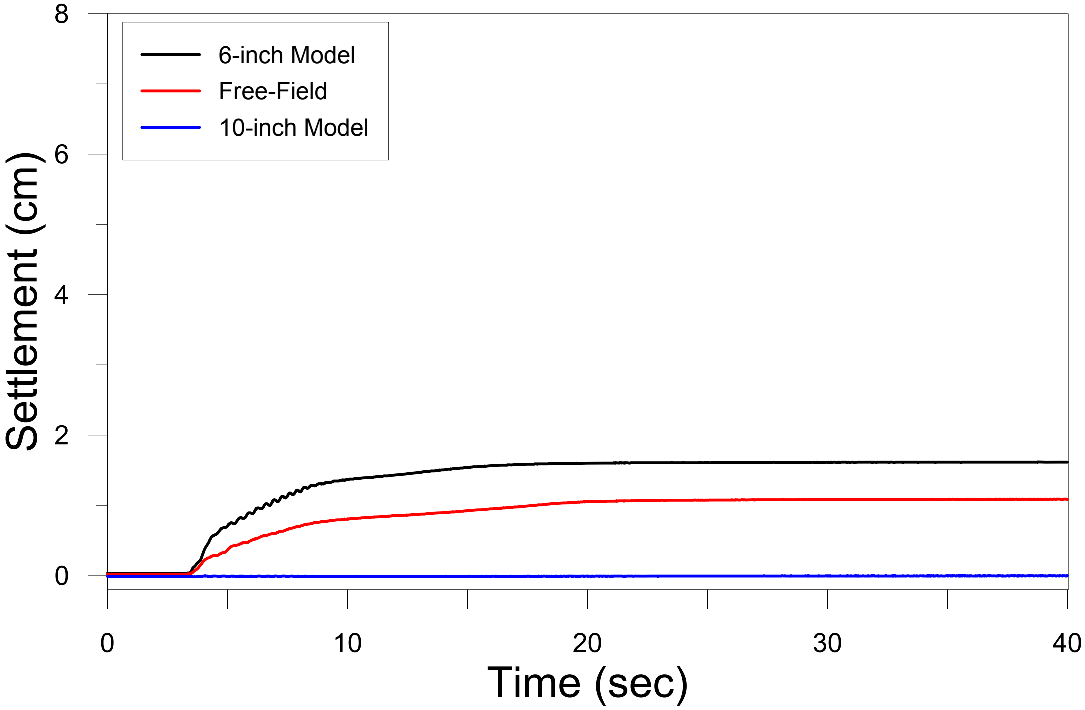

Test # 36: Settlement (cm)
7/15/2016
PGA: 0.25g

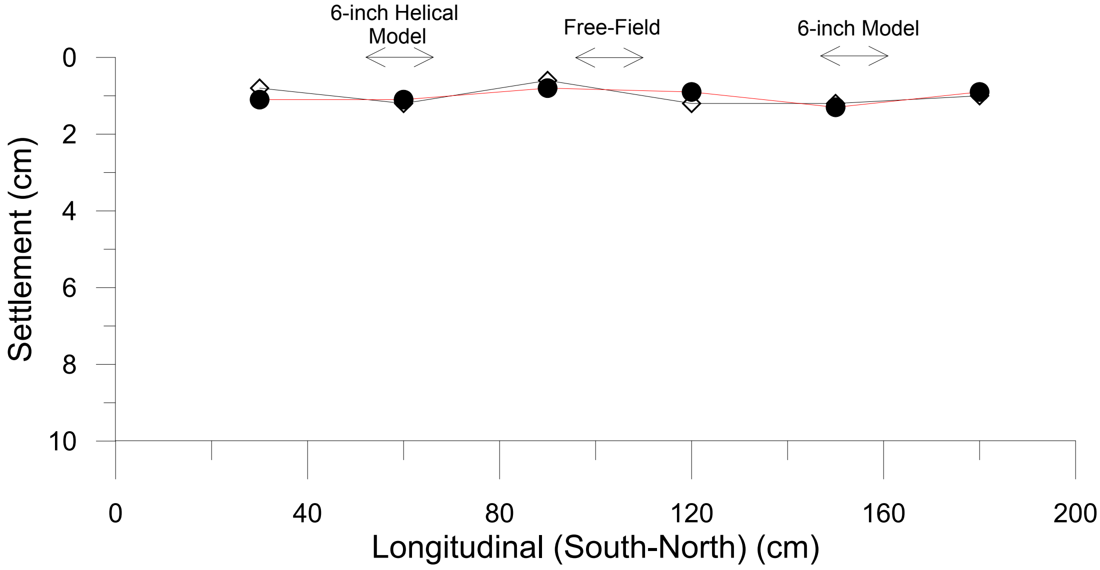

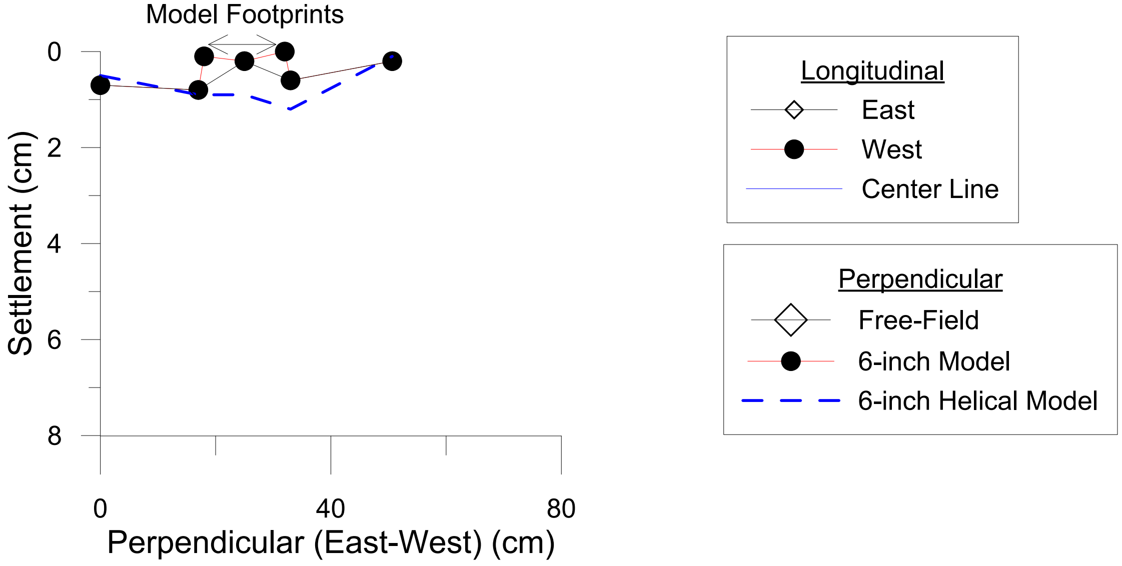

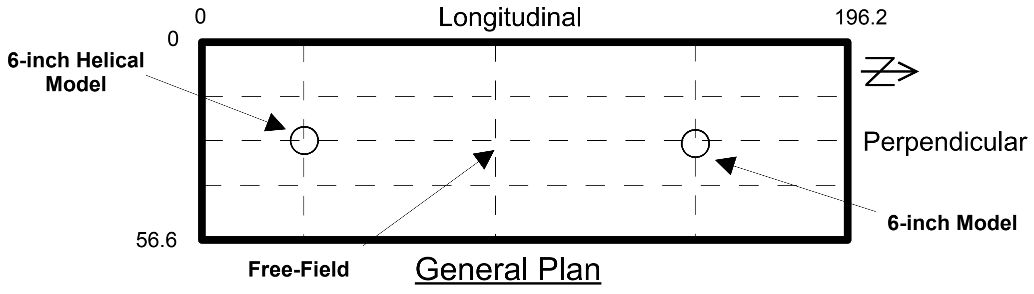

General Plan

Test #37 (July 22, 2016)

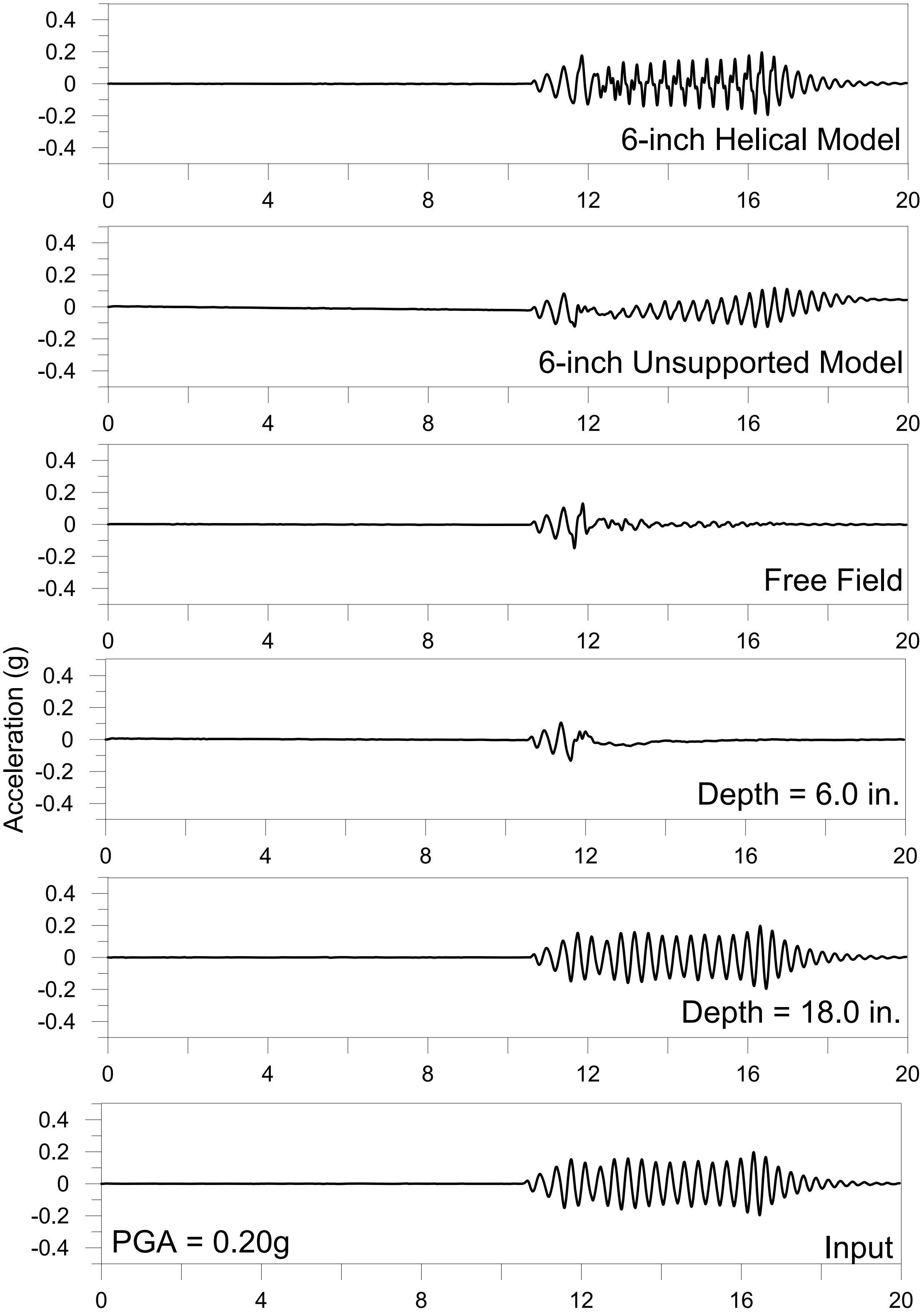

Test #37 (July 22, 2016)

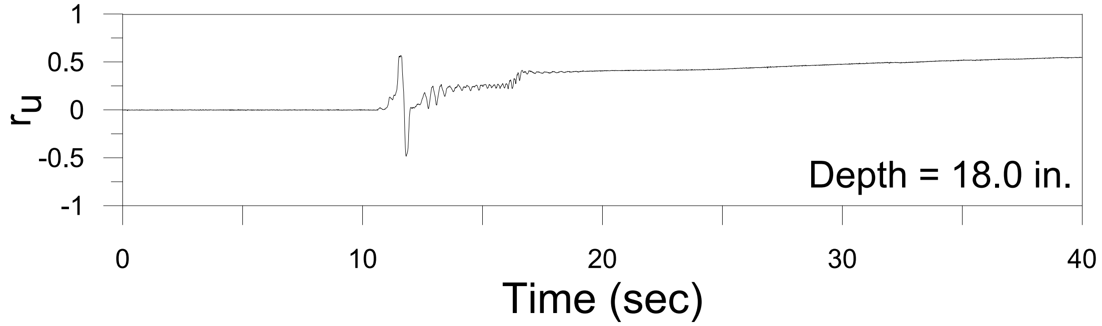

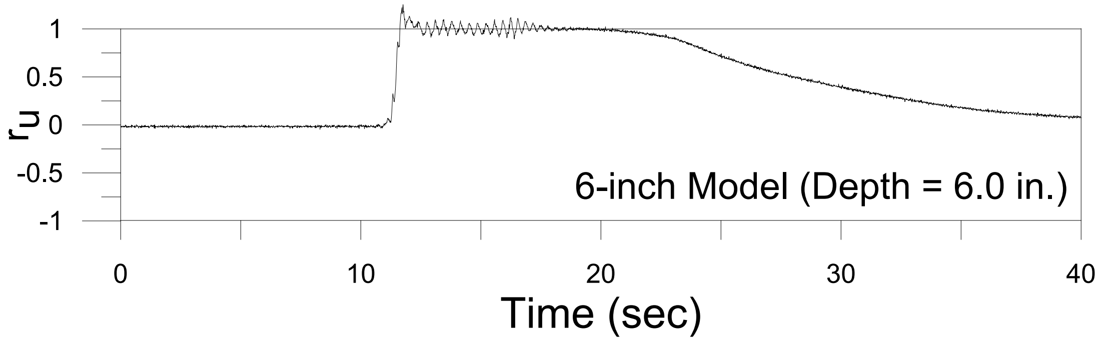

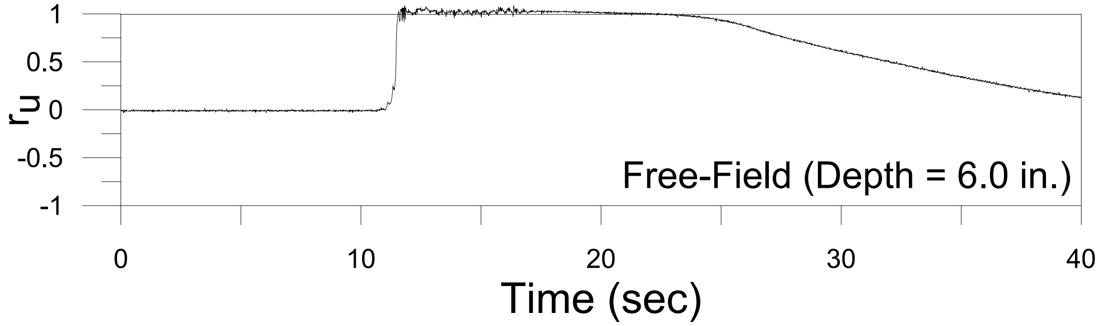

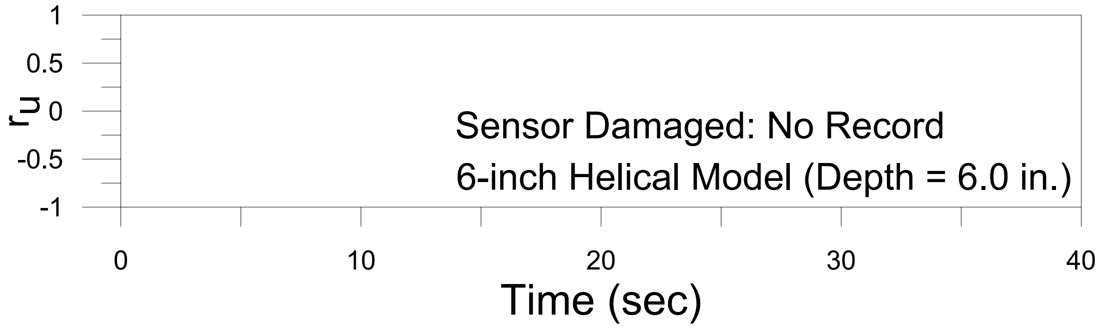

PGA = 0.20g

Test # 37: Ground Motion Characteristics
7/22/2016
PGA: 0.20g

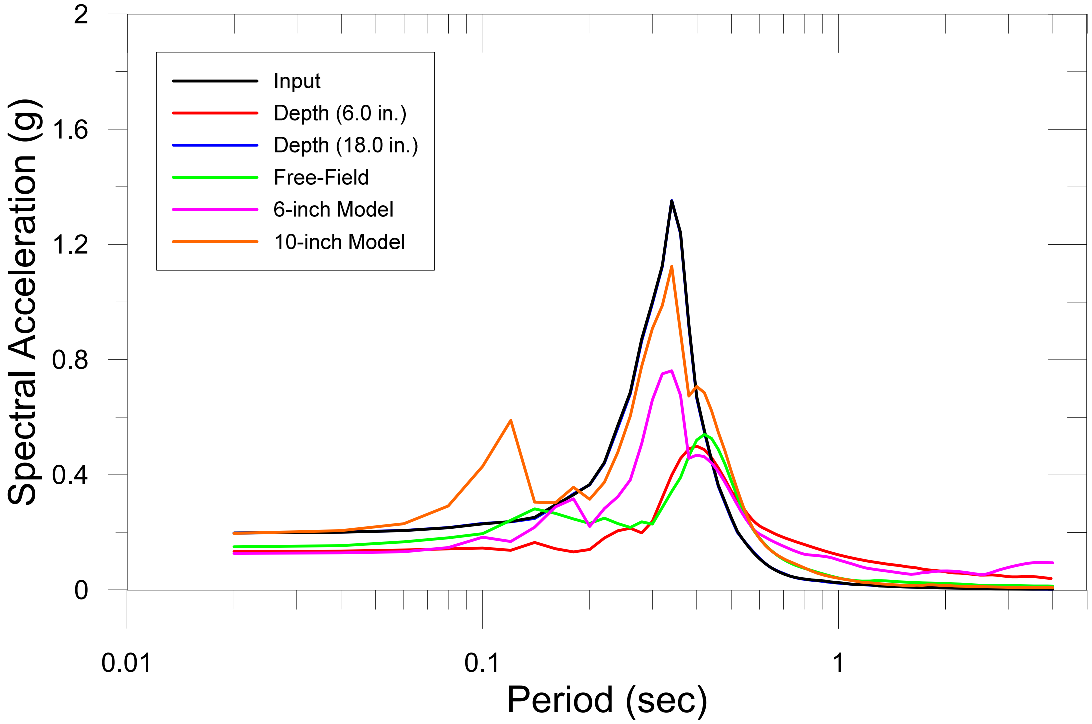

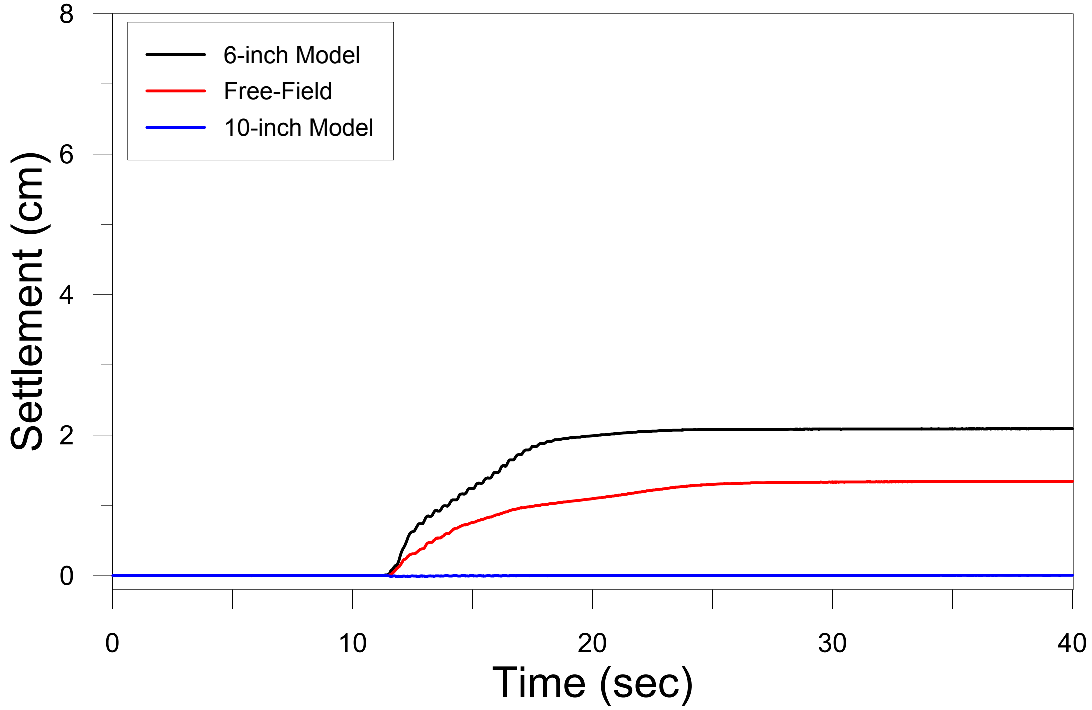

Test # 37: Settlement (cm)
7/22/2016
PGA: 0.20g

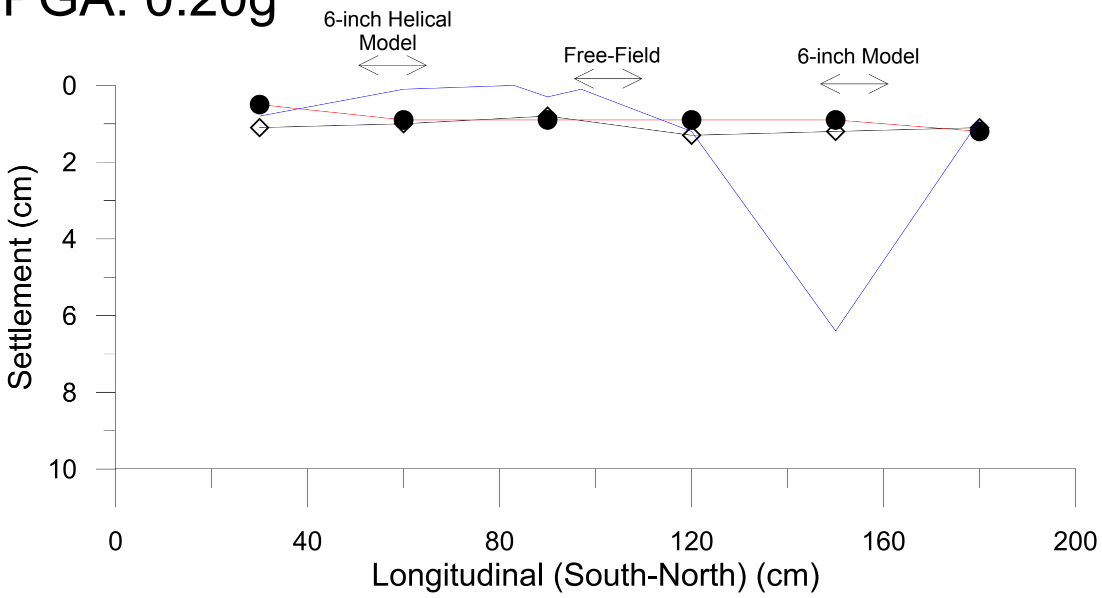

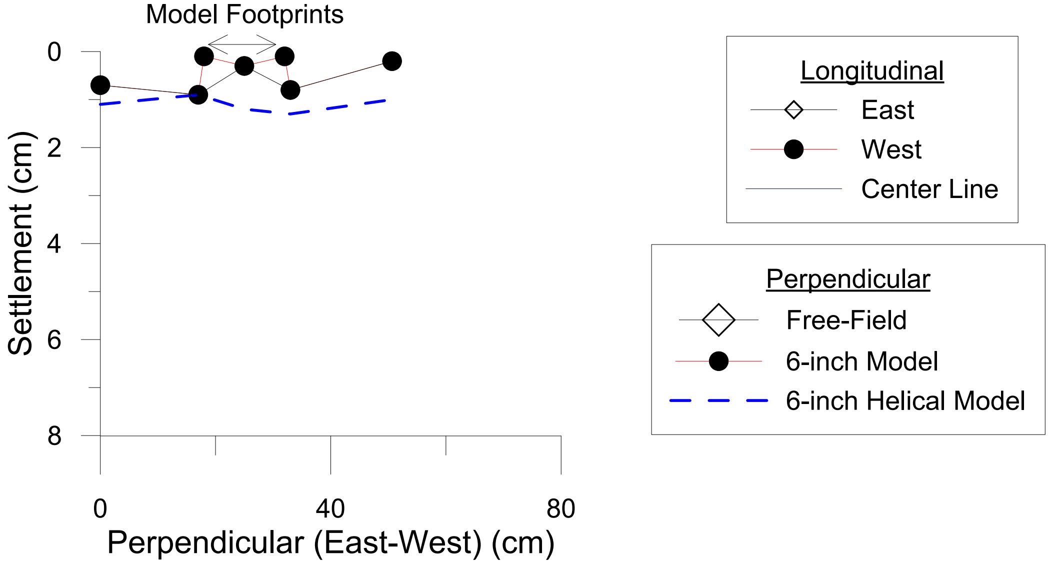

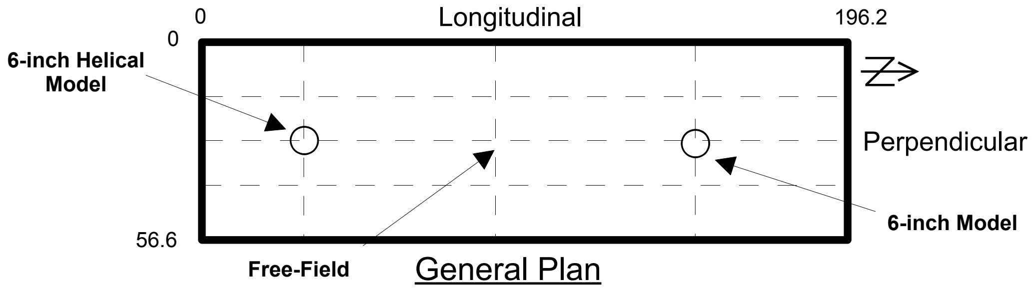

Test #38 (July 27, 2016)

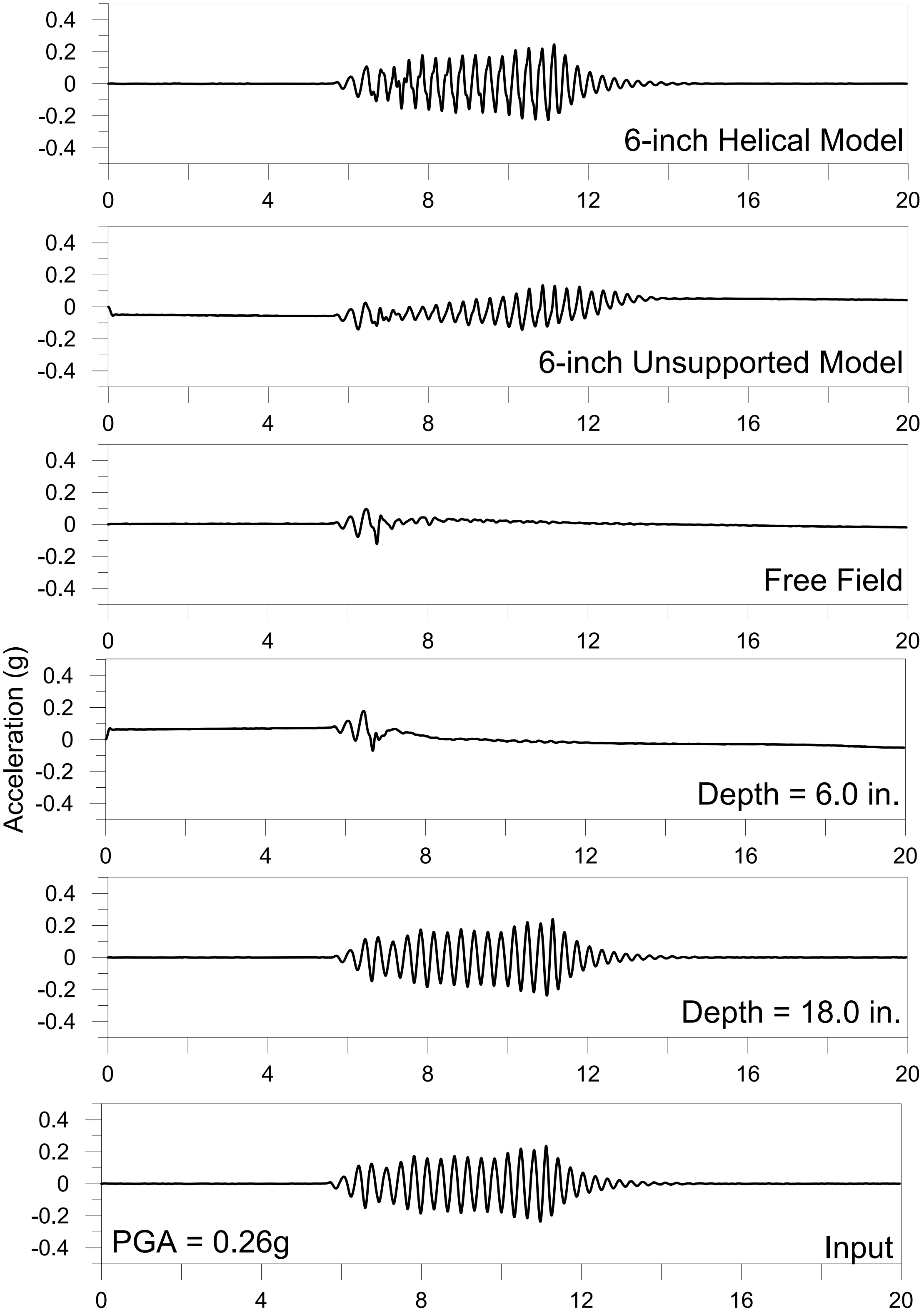

Test #38 (July 22, 2016)

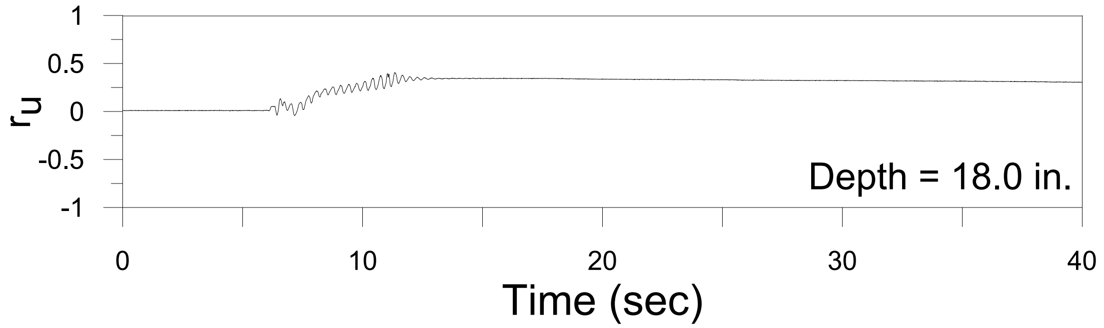

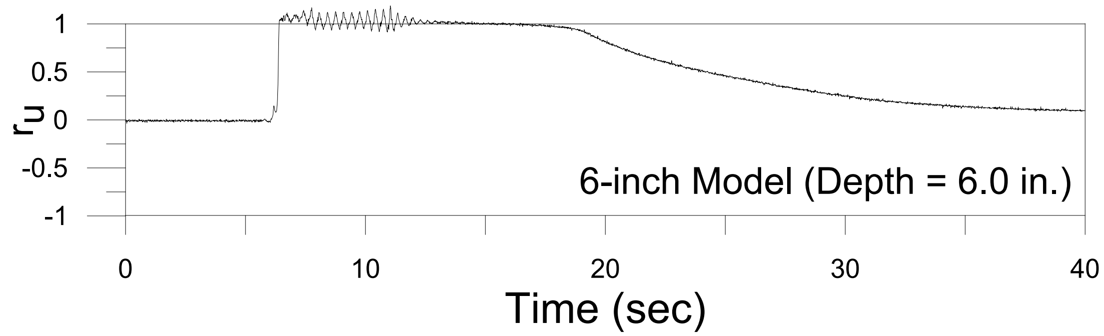

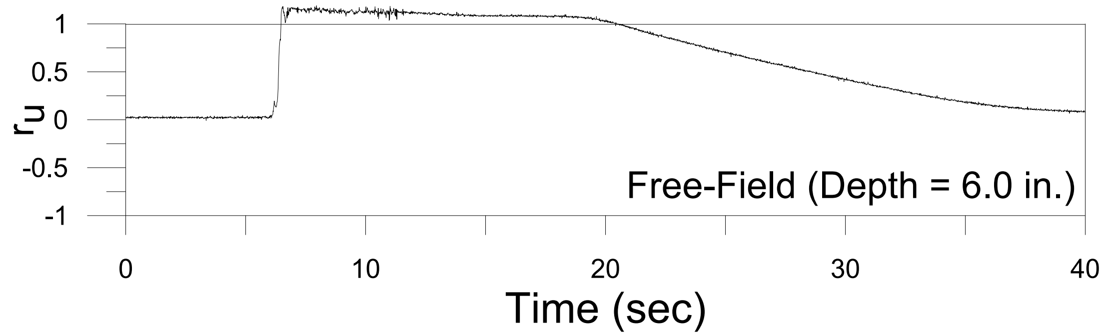

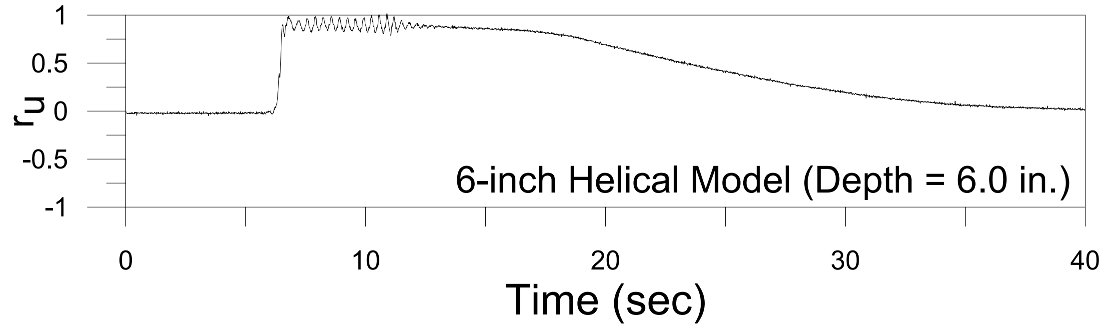

PGA = 0.26g

Test # 38: Ground Motion Characteristics
7/27/2016
PGA: 0.26g

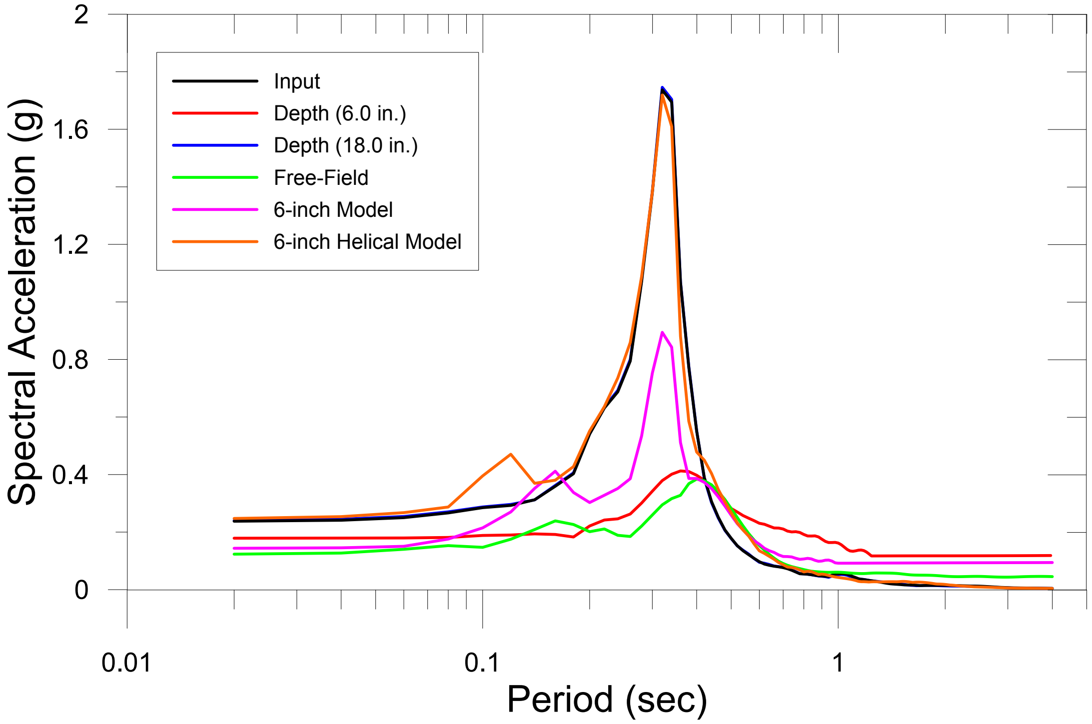

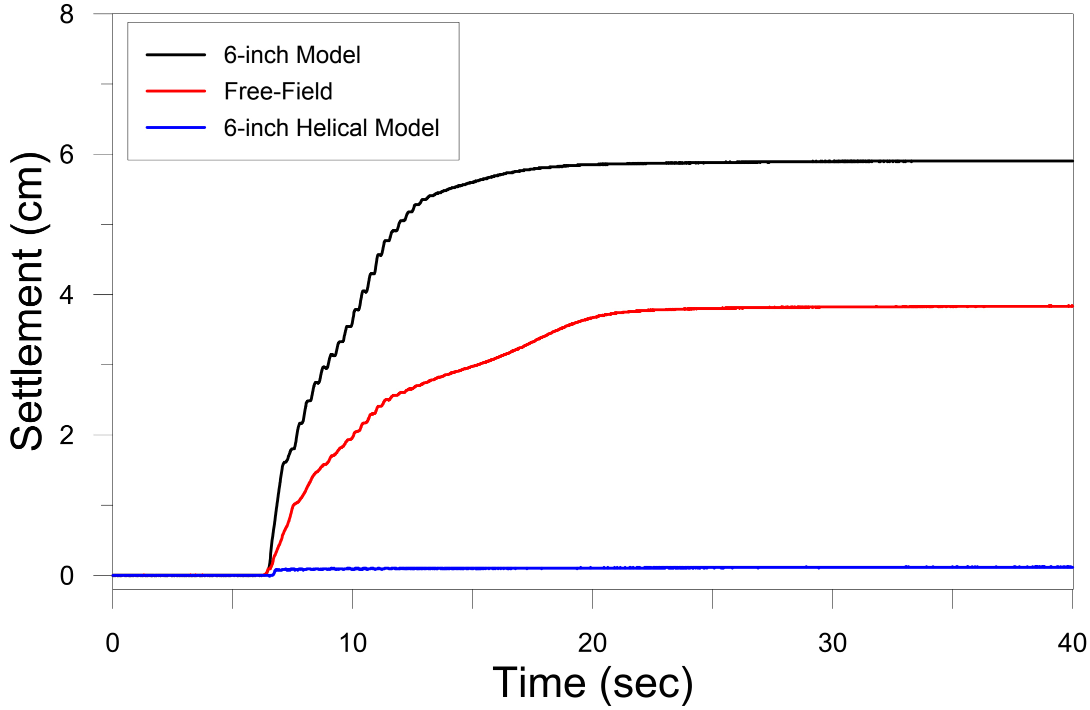

Test # 38: Settlement (cm)
7/27/2016
PGA: 0.26g

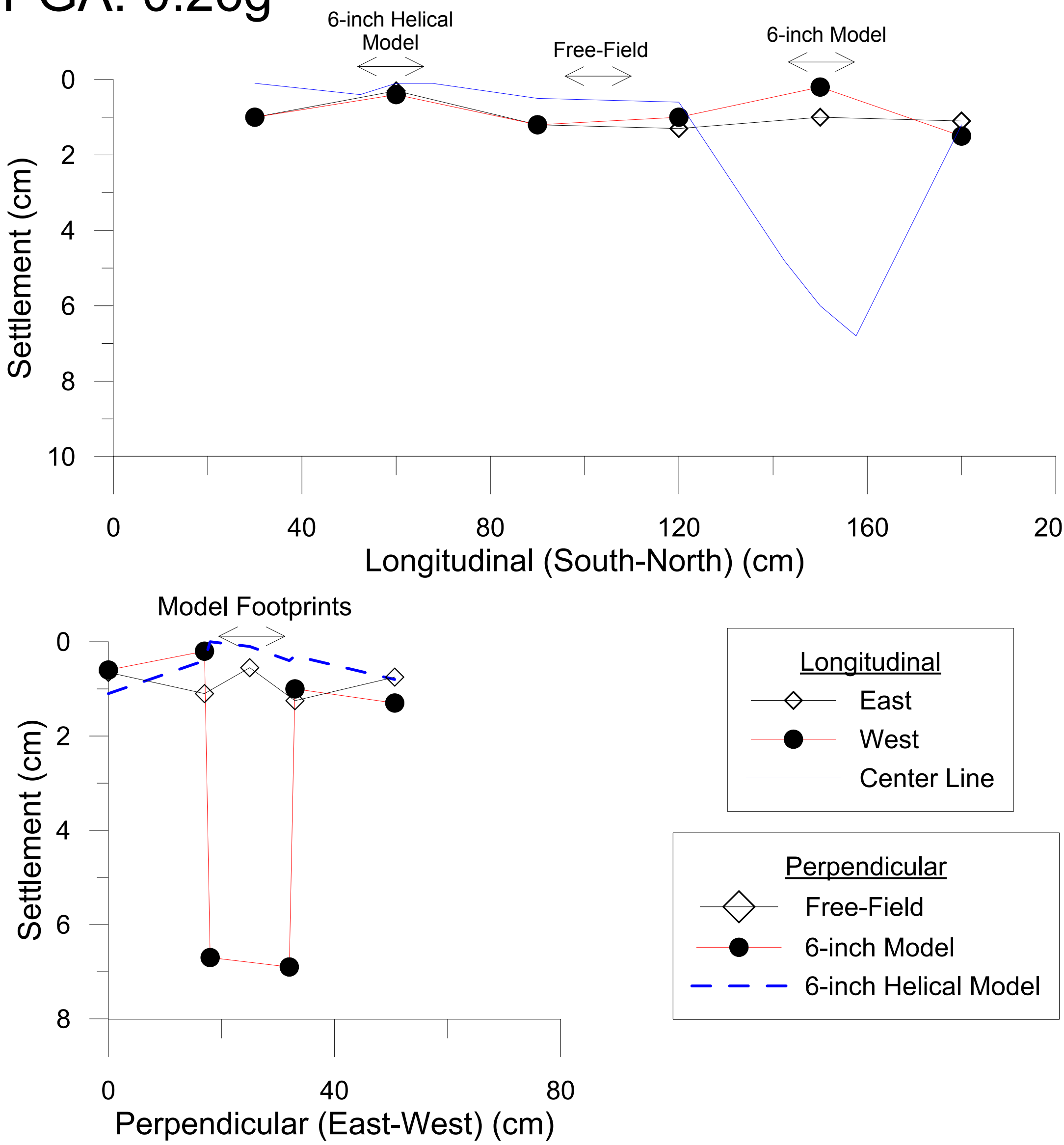

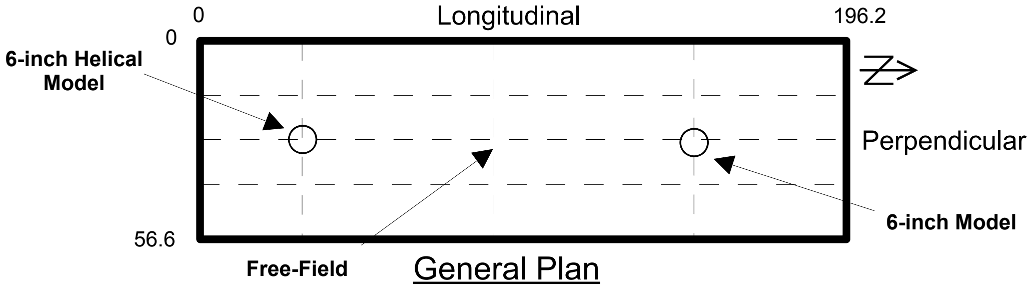

General Plan

Test #39 (August 4, 2016)

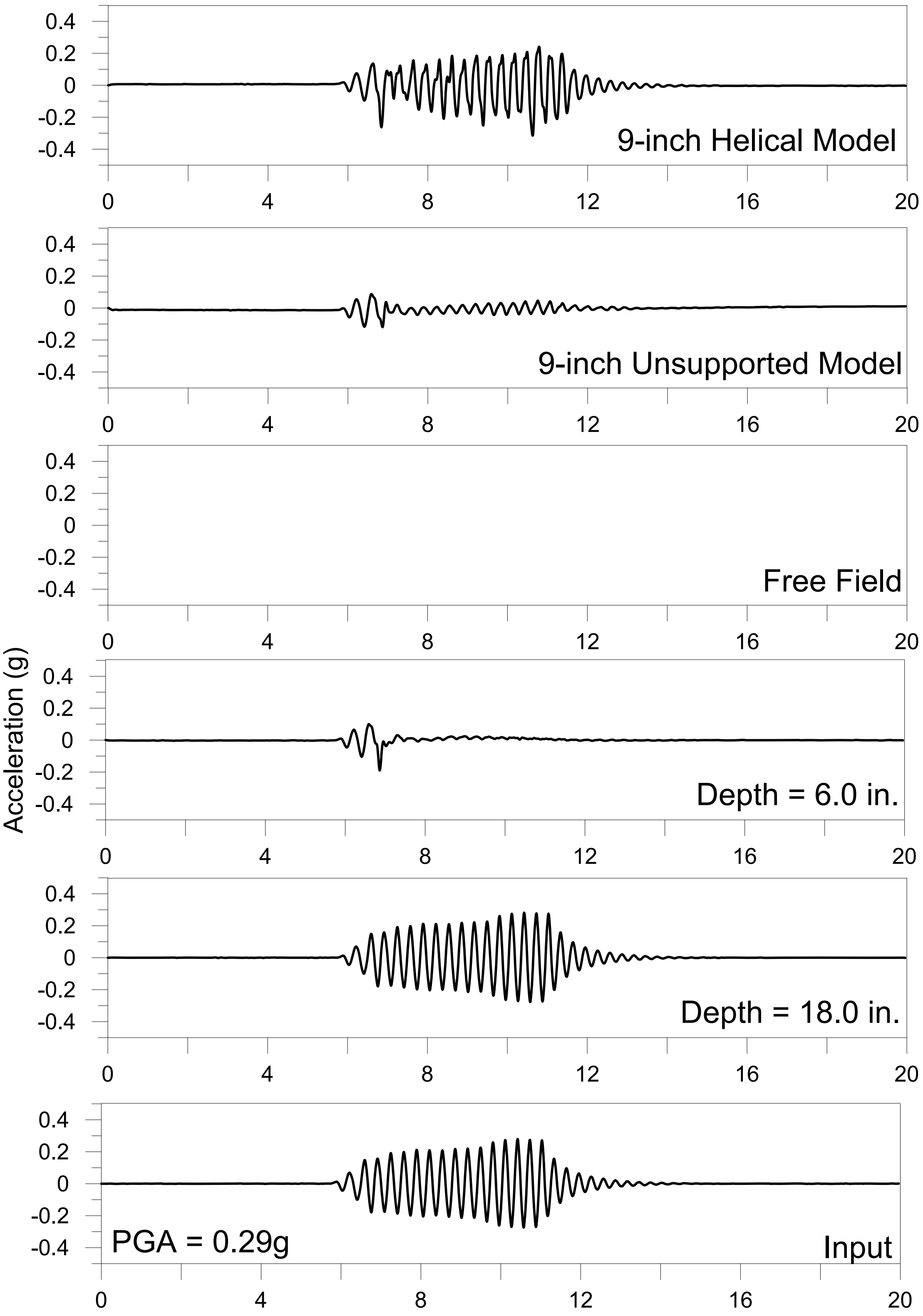

Test #39 (August 4, 2016)

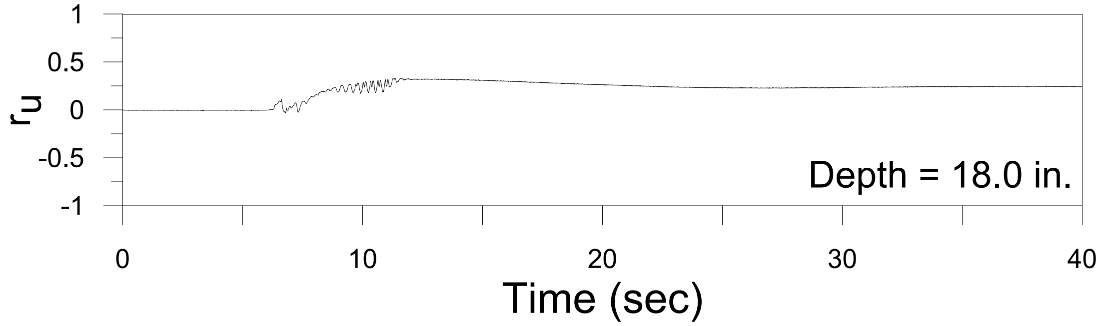

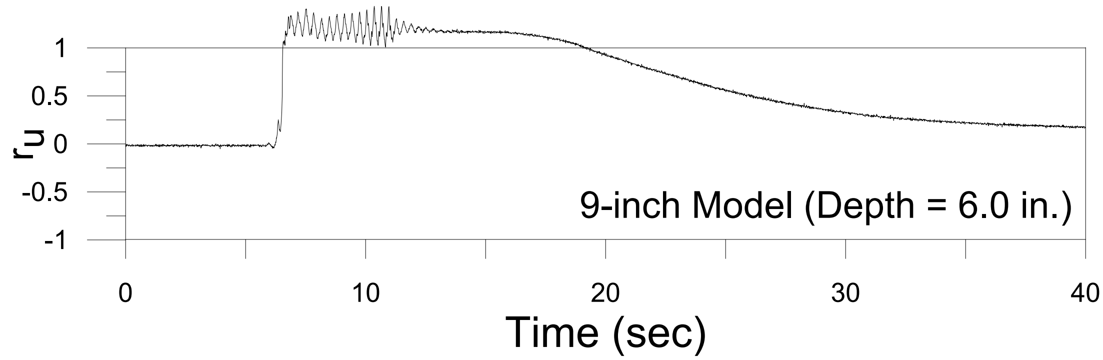

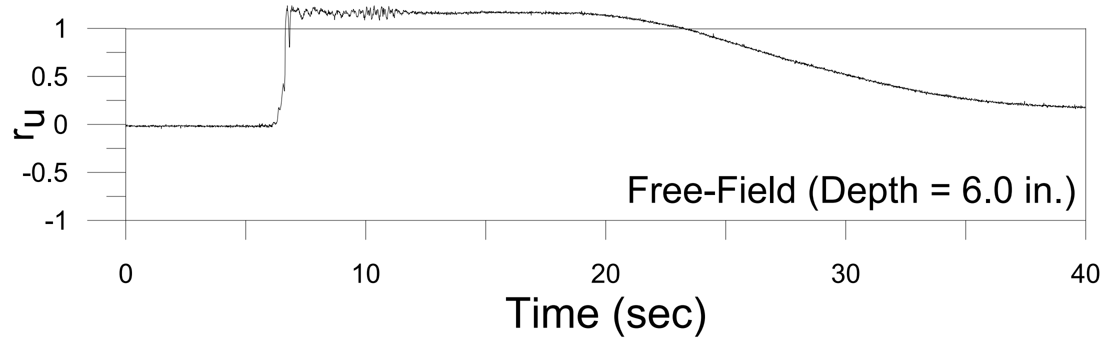

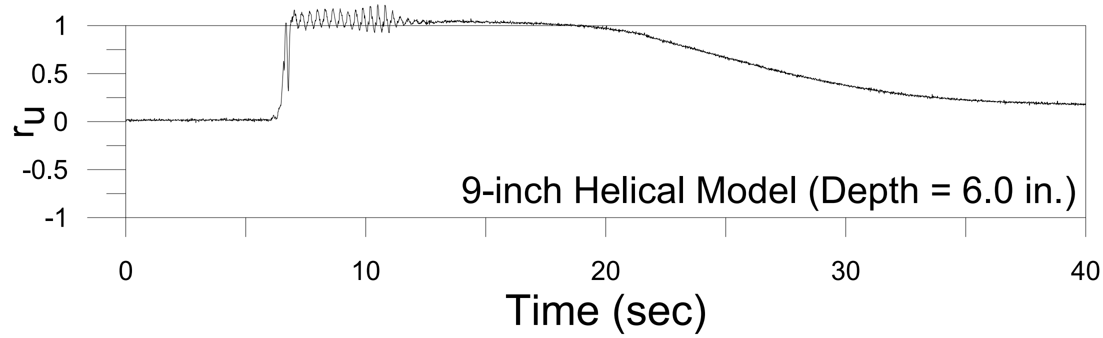

PGA = 0.29g

Test # 39: Ground Motion Characteristics
8/4/2016
PGA: 0.29g

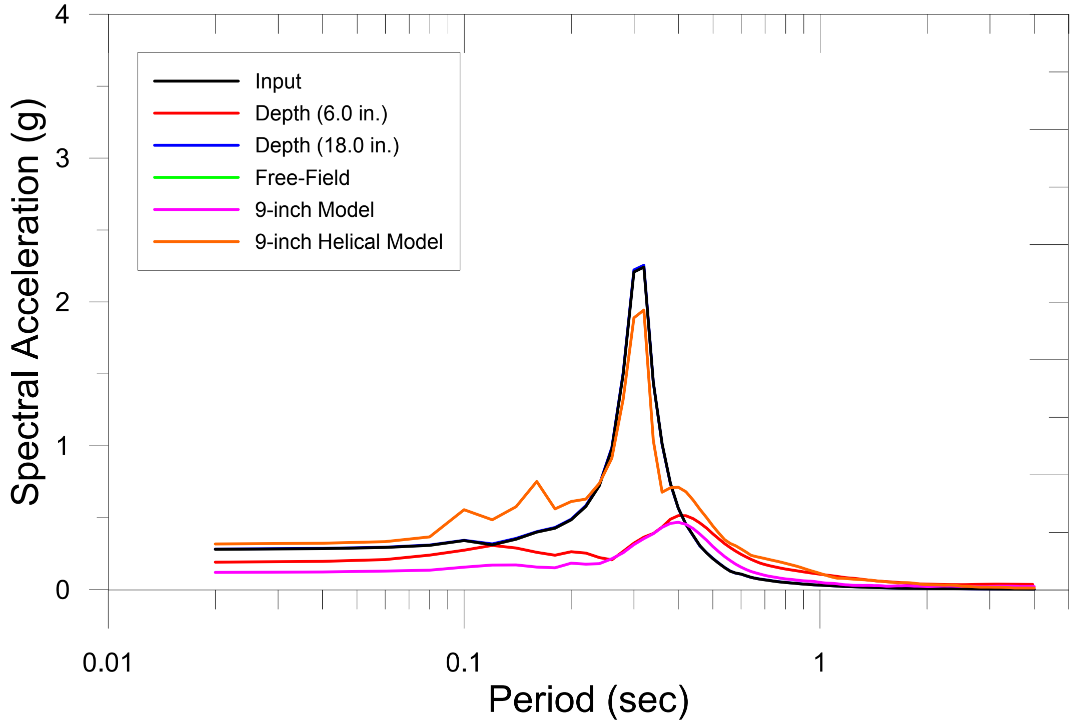

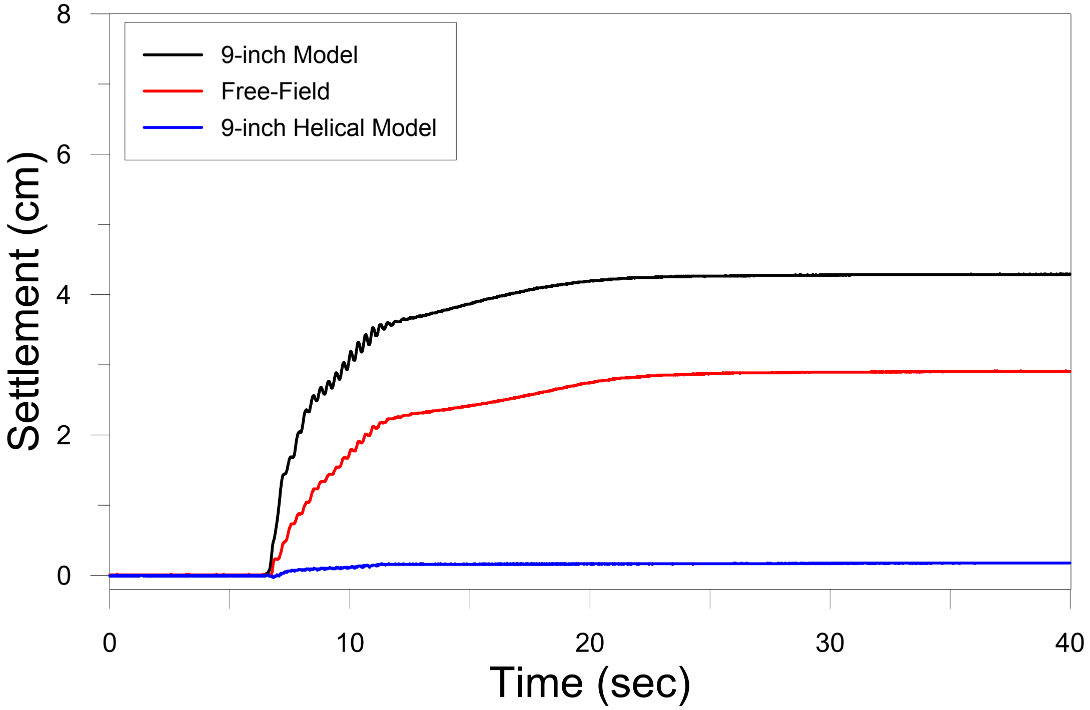

Test # 39: Settlement (cm)
8/4/2016
PGA: 0.29g

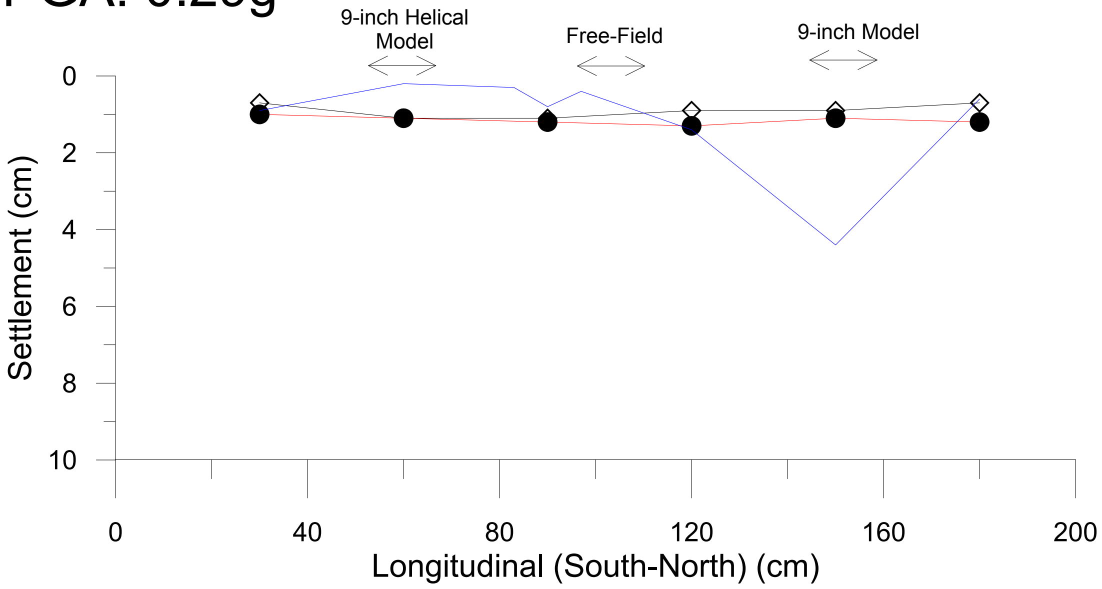

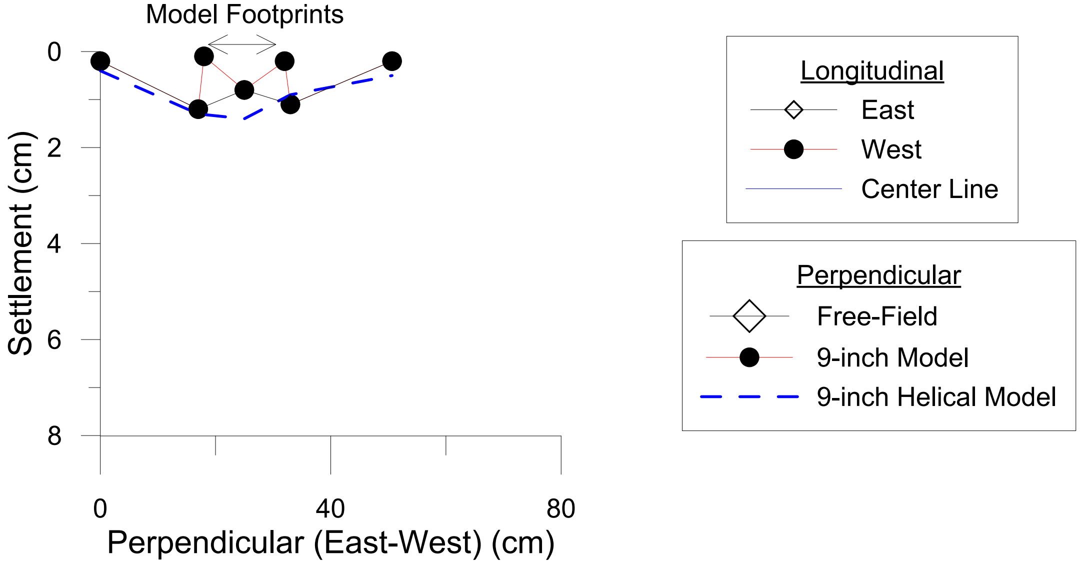

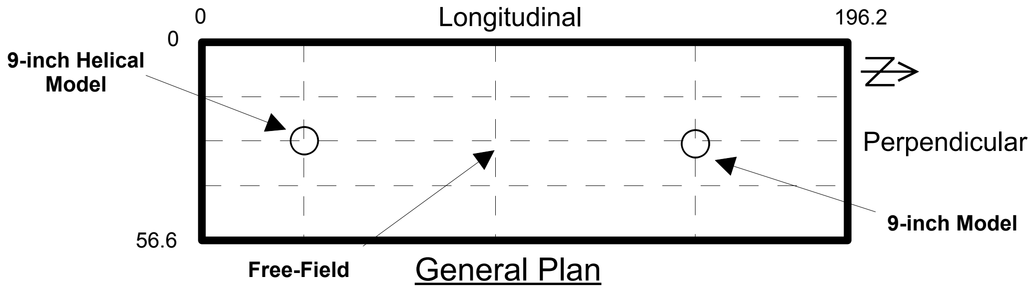

Test #40 (August 9, 2016)

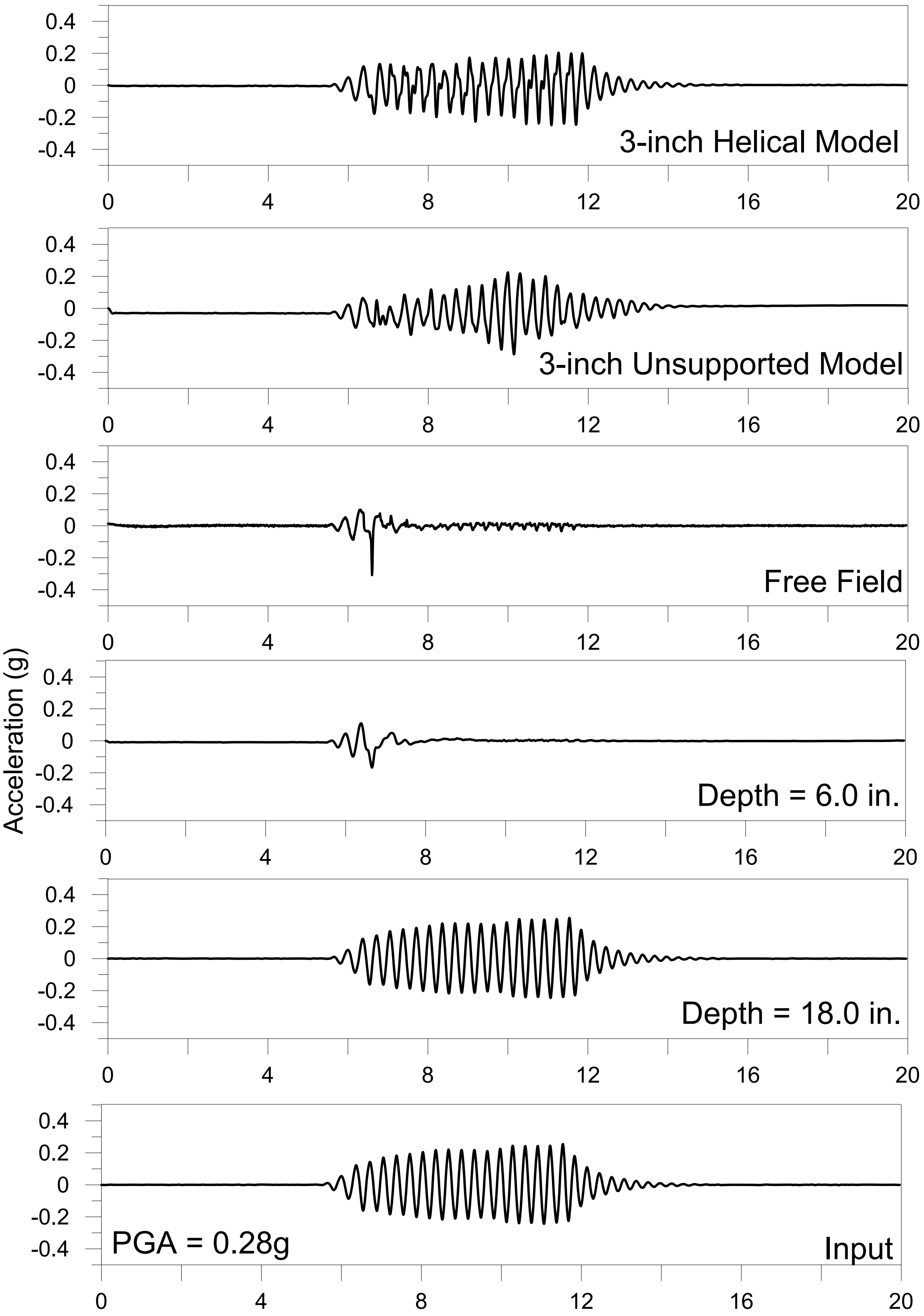

Test #40 (August 9, 2016)

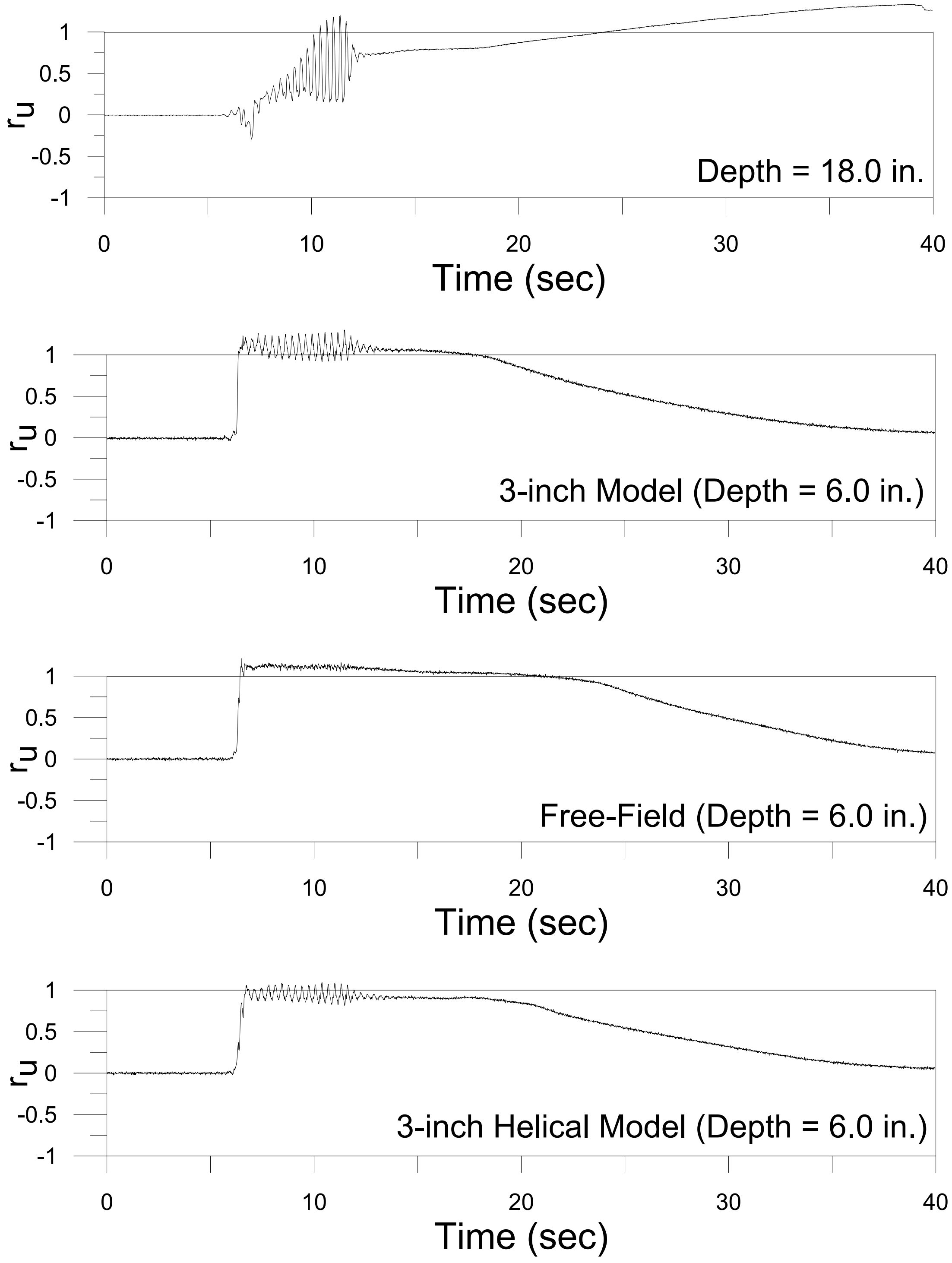

PGA = 0.28g

Test # 40: Ground Motion Characteristics
8/9/2016
PGA: 0.28g

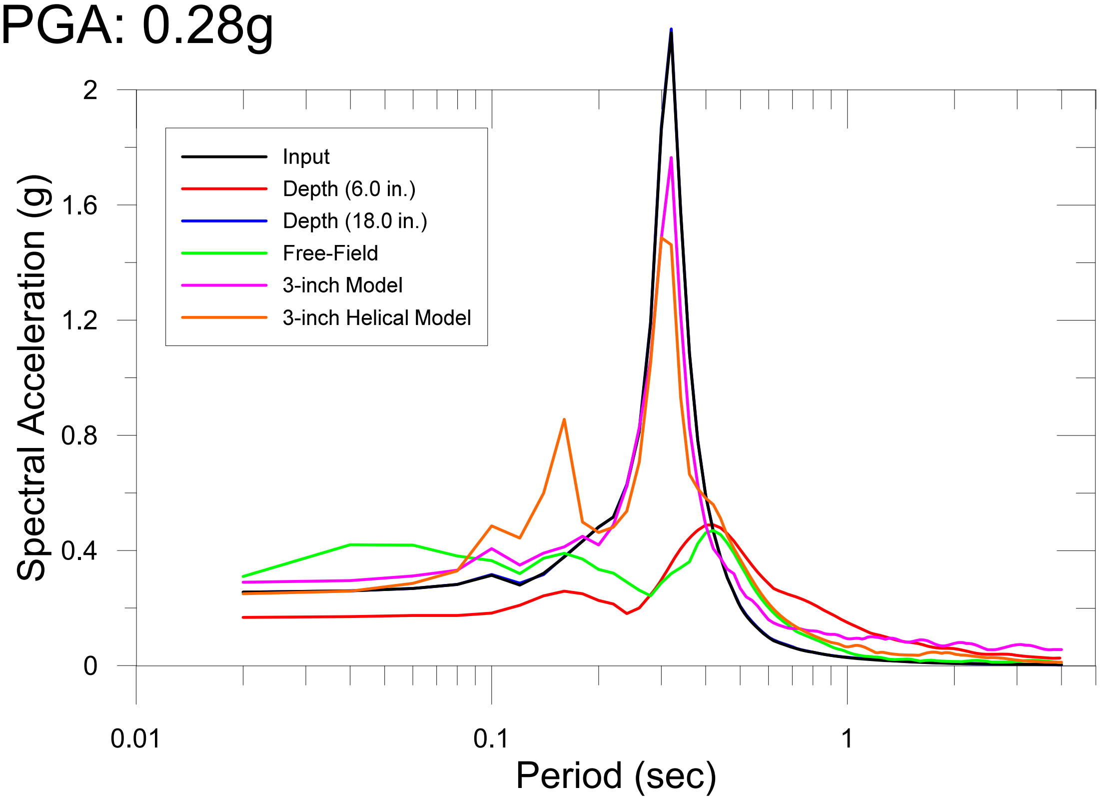

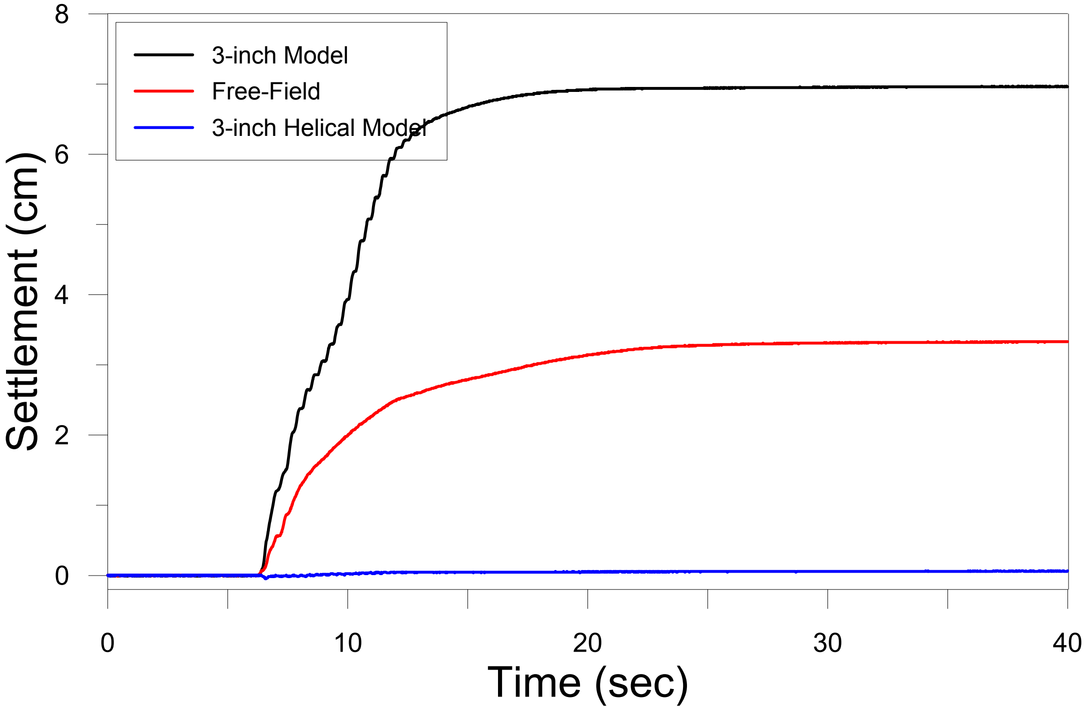

Test # 40: Settlement (cm)
8/9/2016
PGA: 0.28g

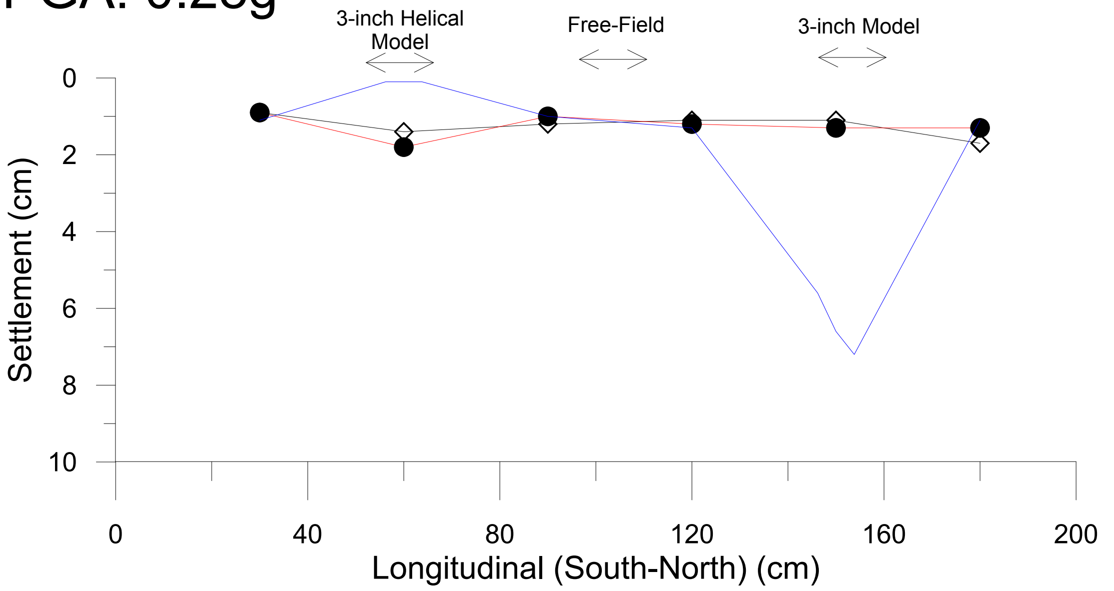

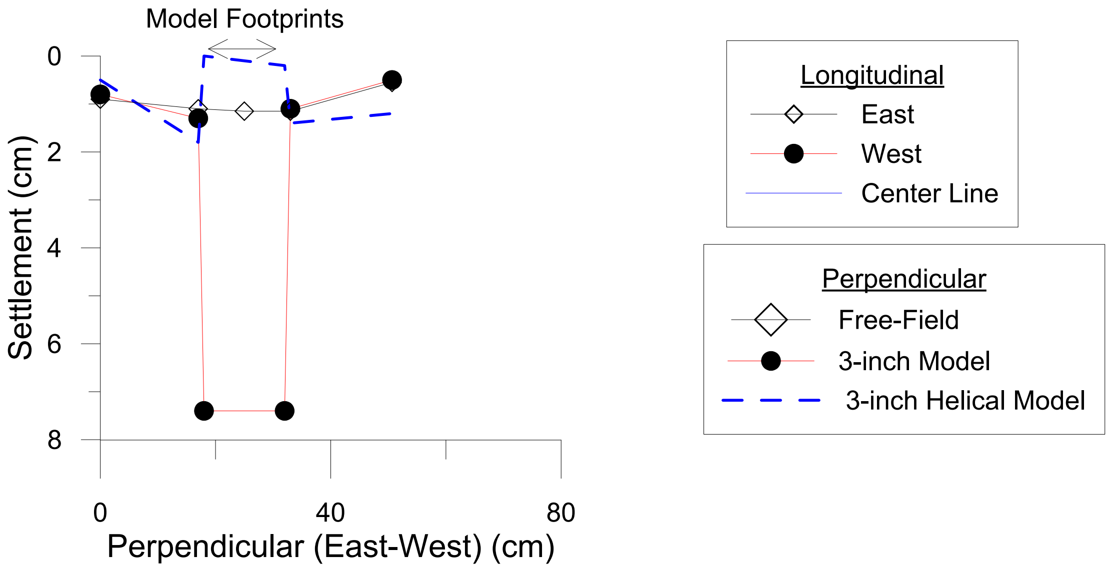

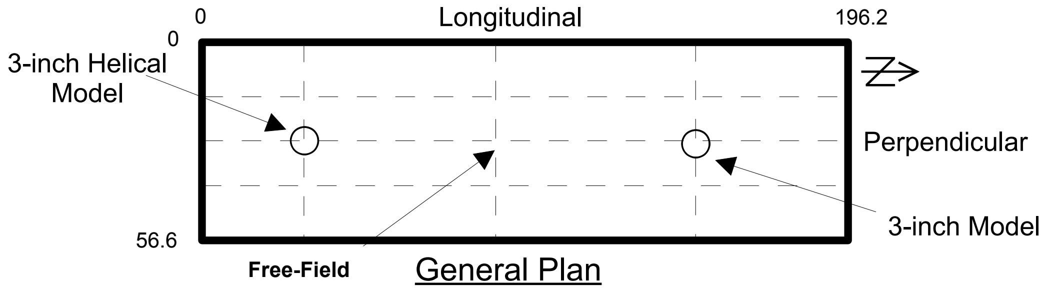

Test #41 (August 17, 2016)

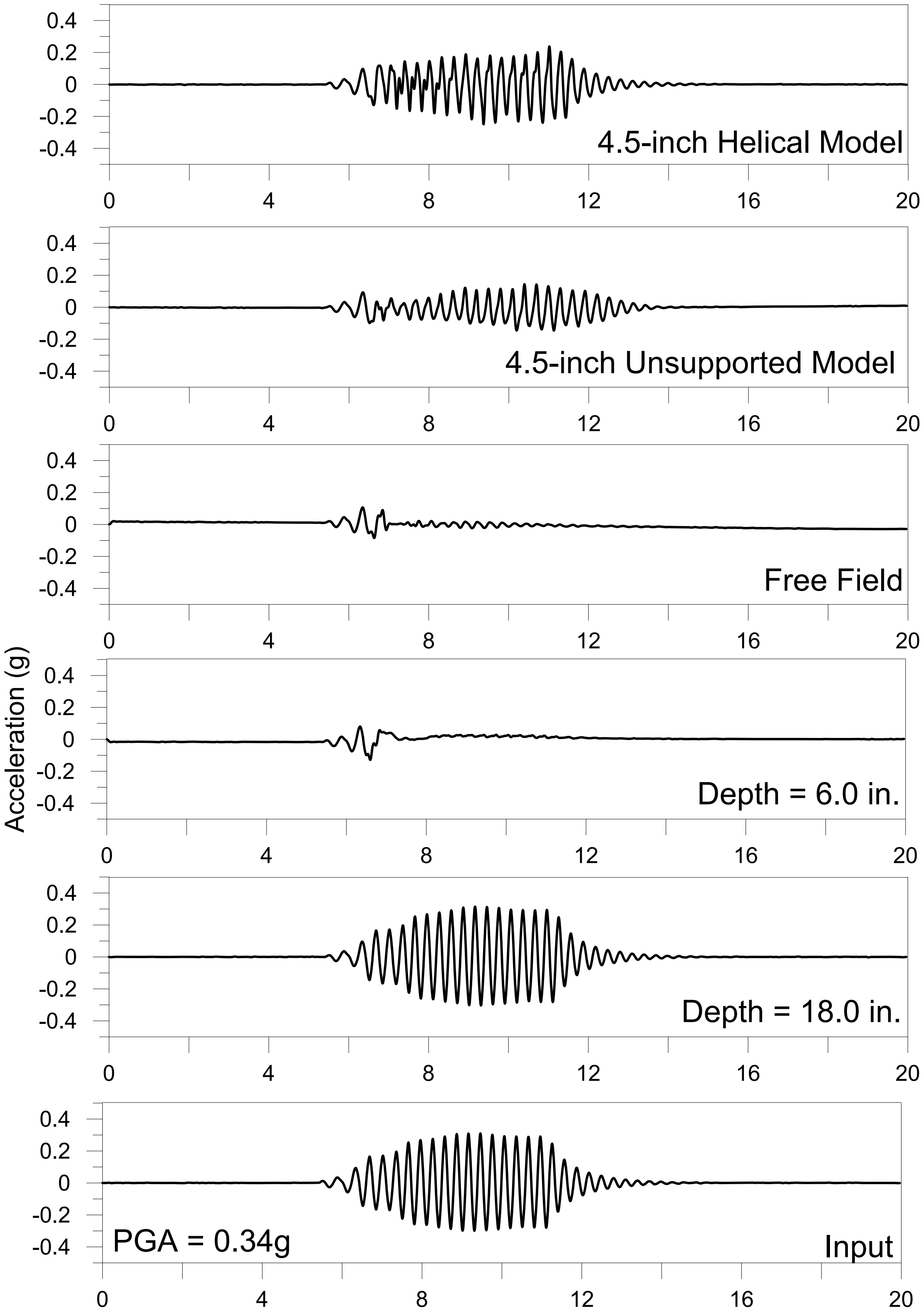

Test #41 (August 17, 2016)

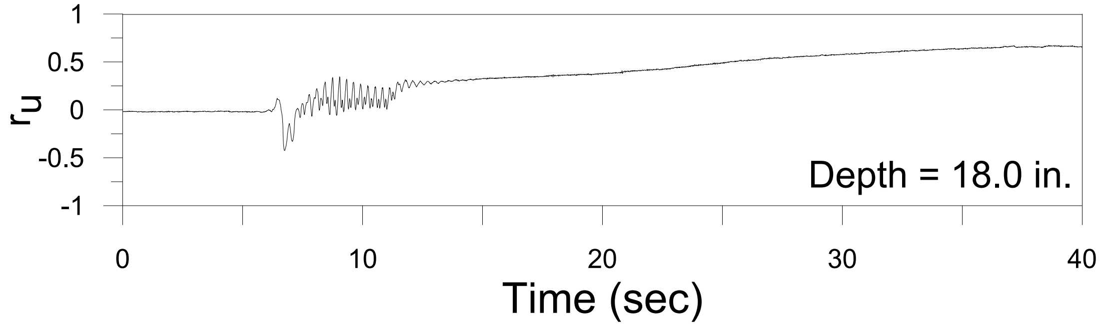

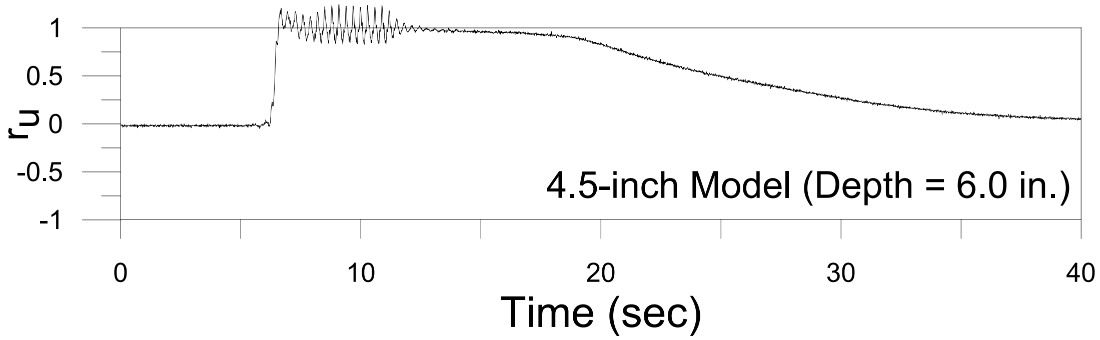

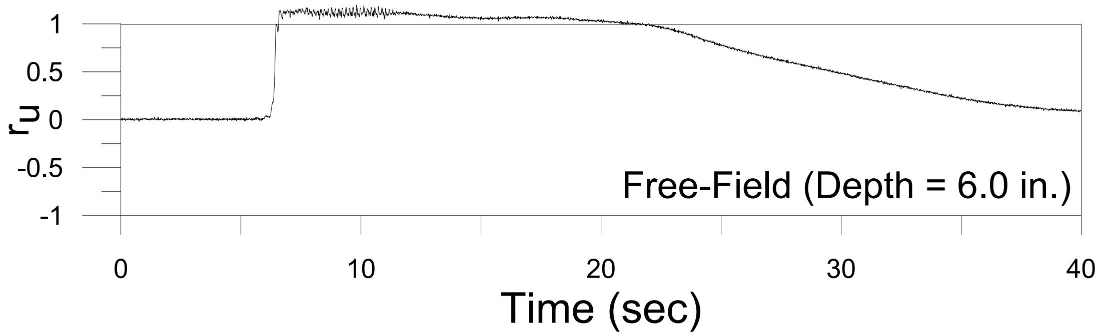

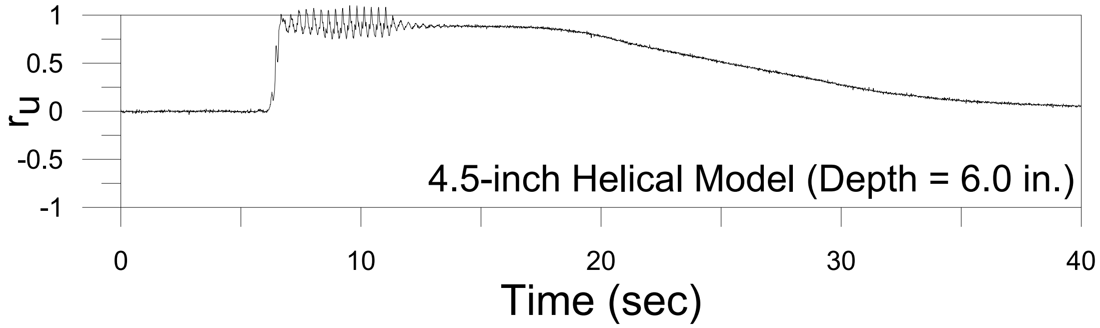

PGA = 0.34g

Test # 41: Ground Motion Characteristics
8/17/2016
PGA: 0.34g

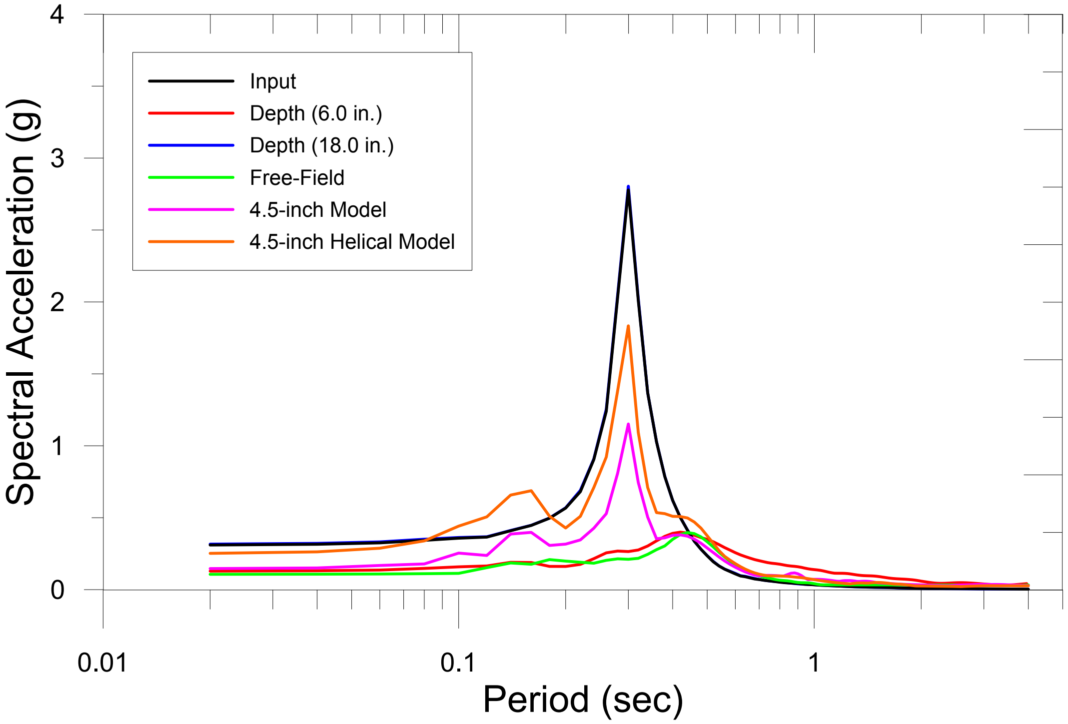

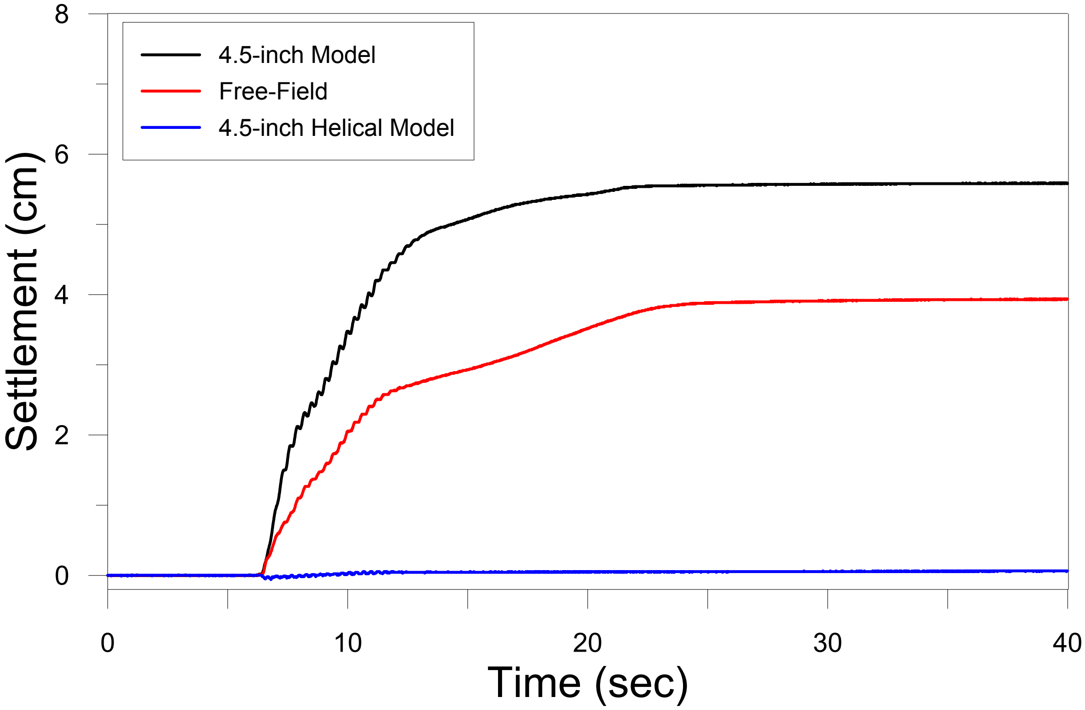

Test # 41: Settlement (cm)
8/17/2016
PGA: 0.34g

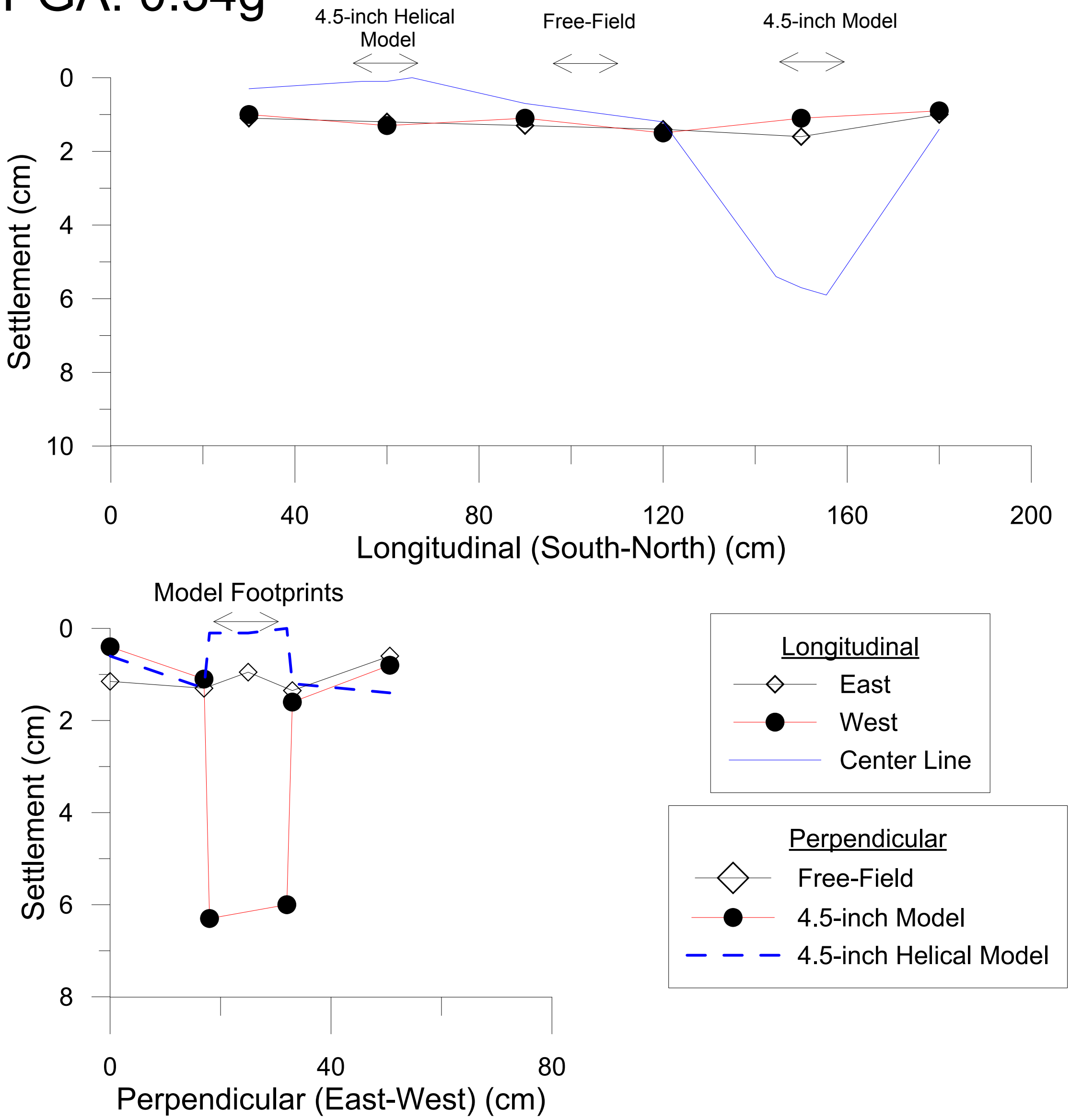

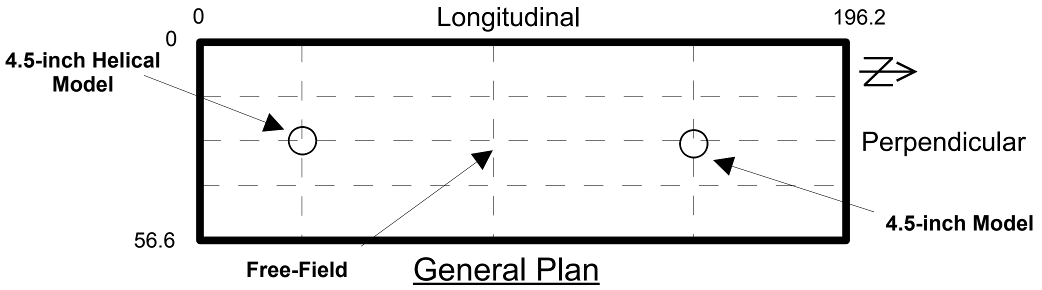

Test #42 (August 27, 2016)

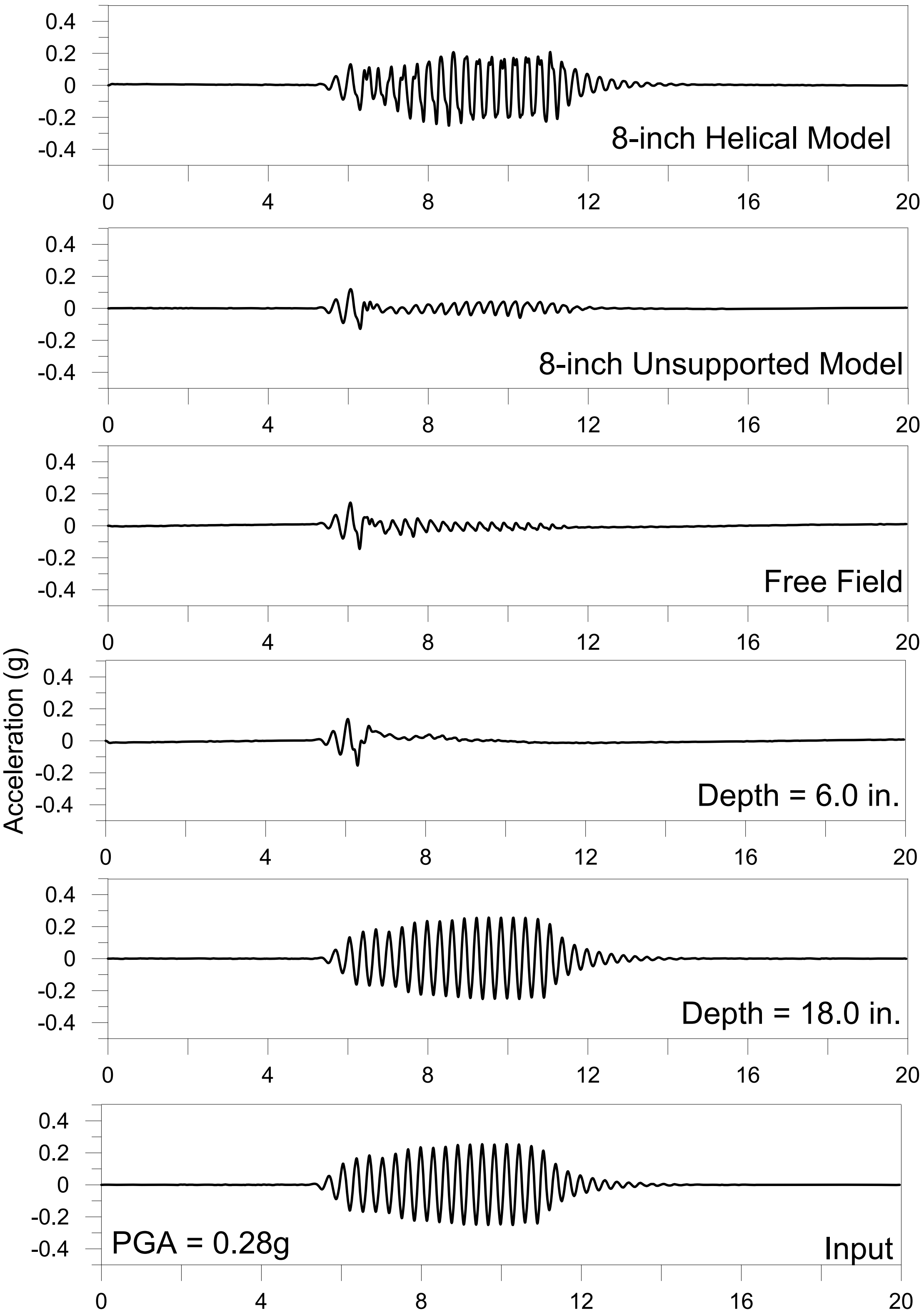

Test #42 (August 27, 2016)

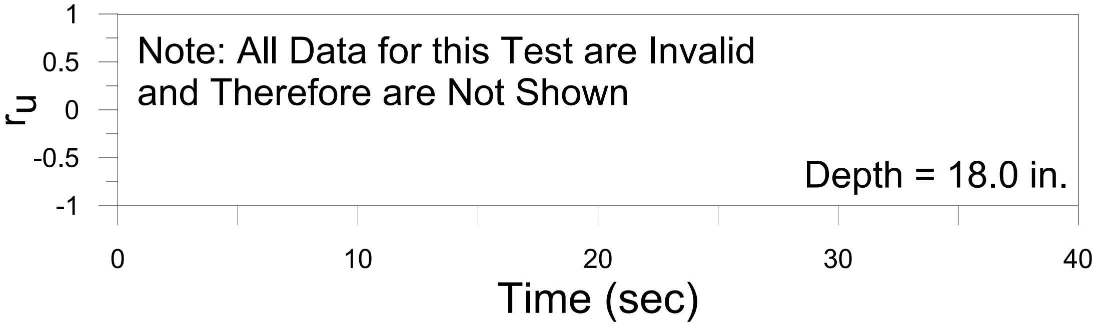

Note: All Data for this Test are Invalid and Therefore are Not Shown

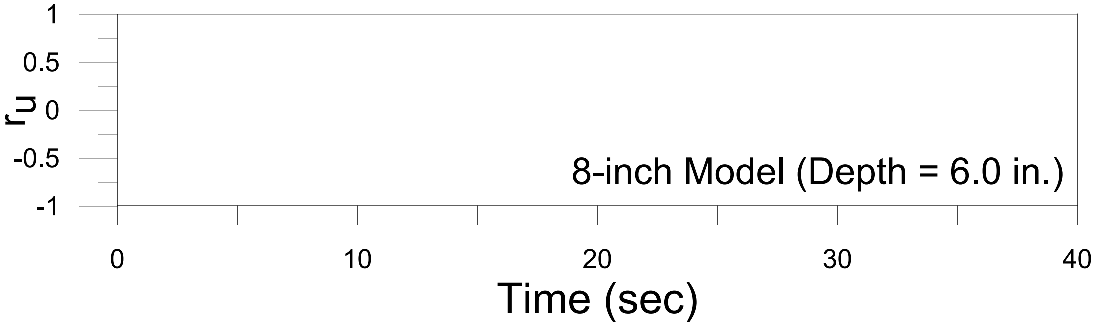

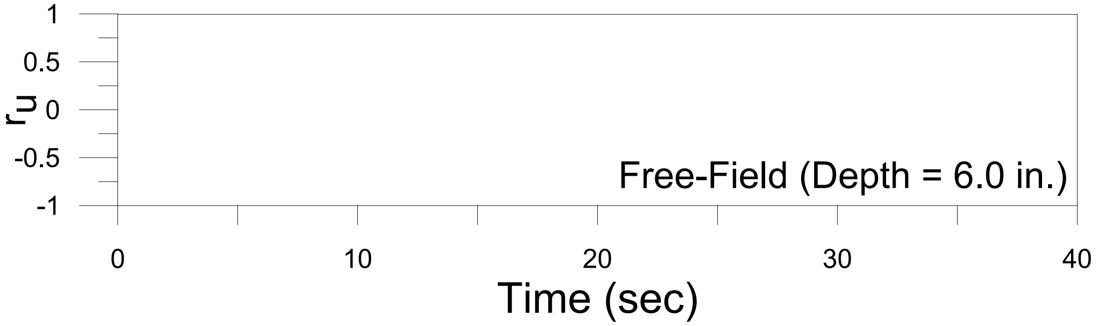

PGA = 0.28g

Test # 42: Ground Motion Characteristics
8/27/2016
PGA: 0.28g

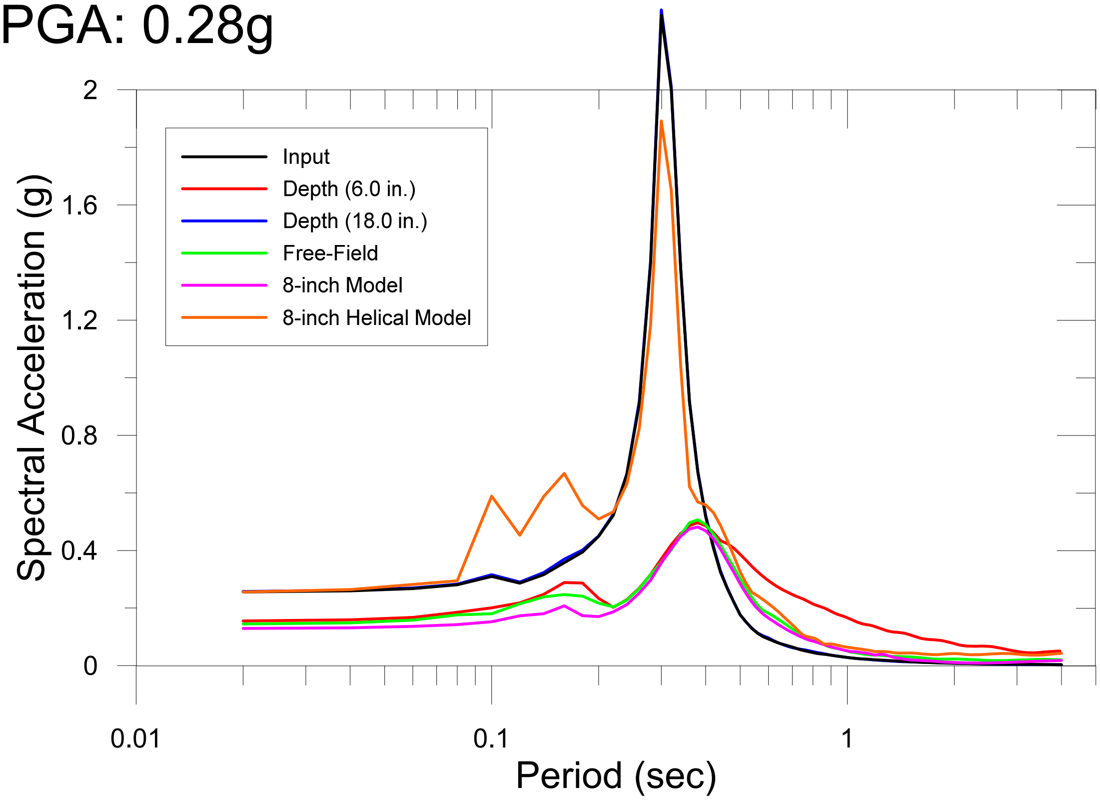

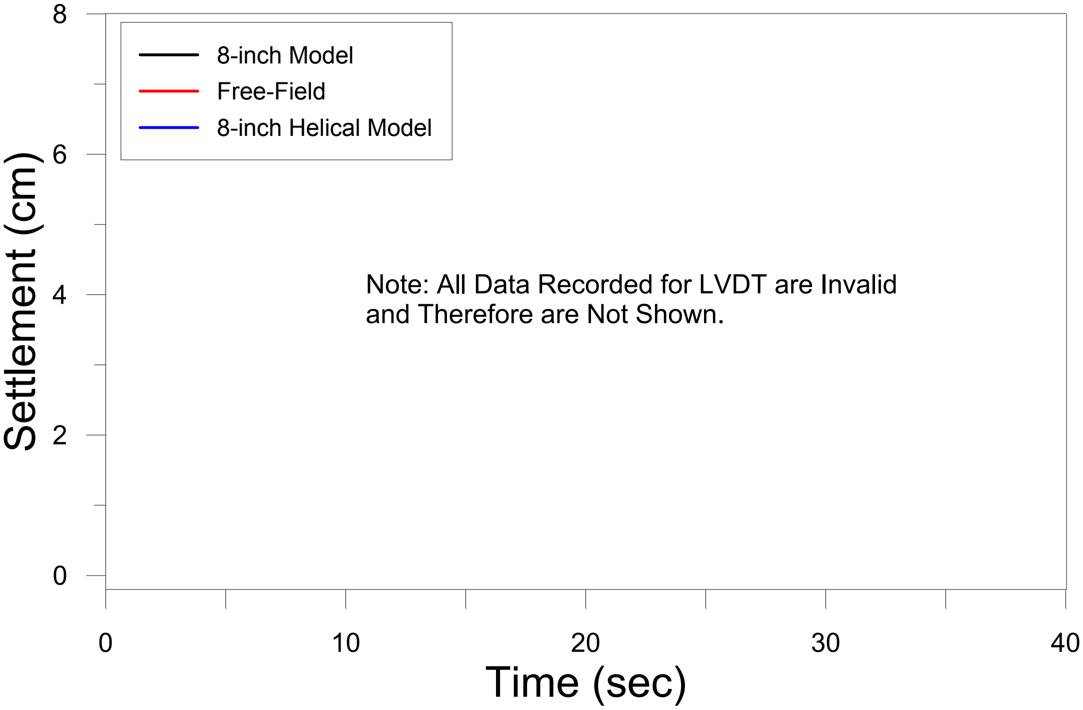

Note: All Data Recorded for LVDT are Invalid and Therefore are Not Shown.

Test # 42: Settlement (cm)
8/27/2016
PGA: 0.28g

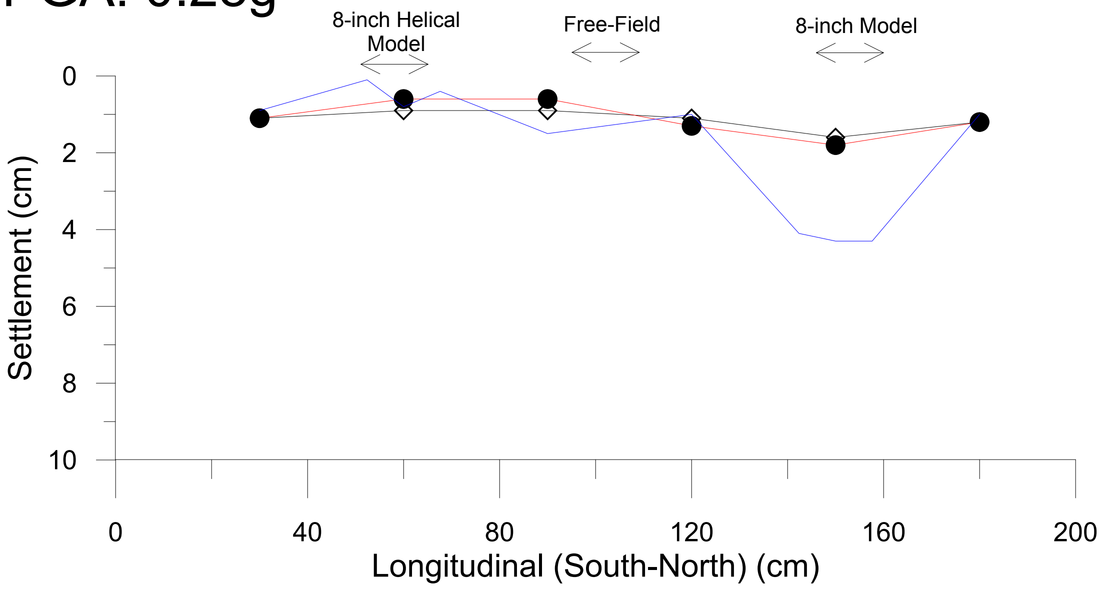

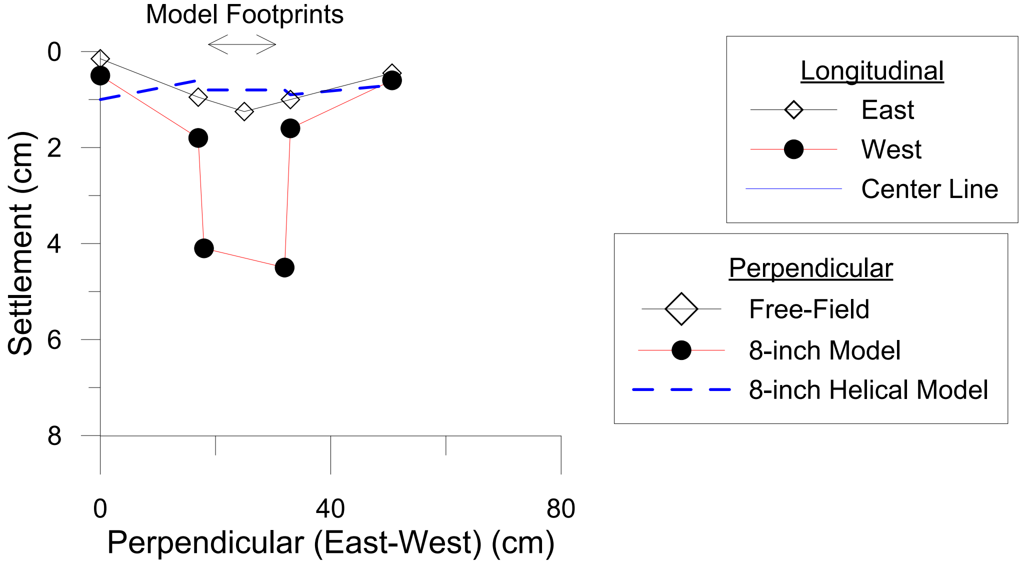

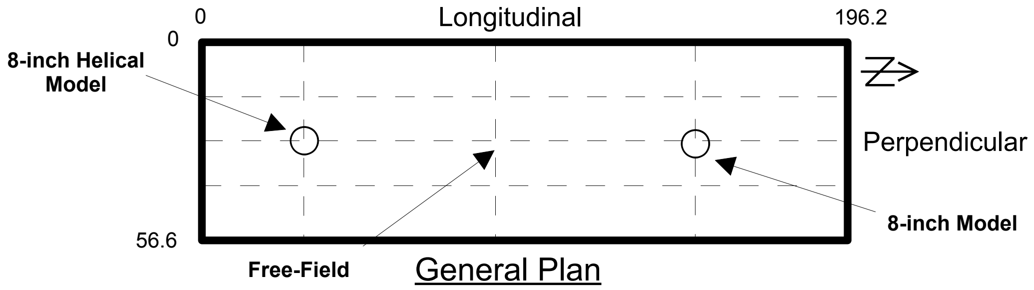

Test #43 (September 9, 2016)

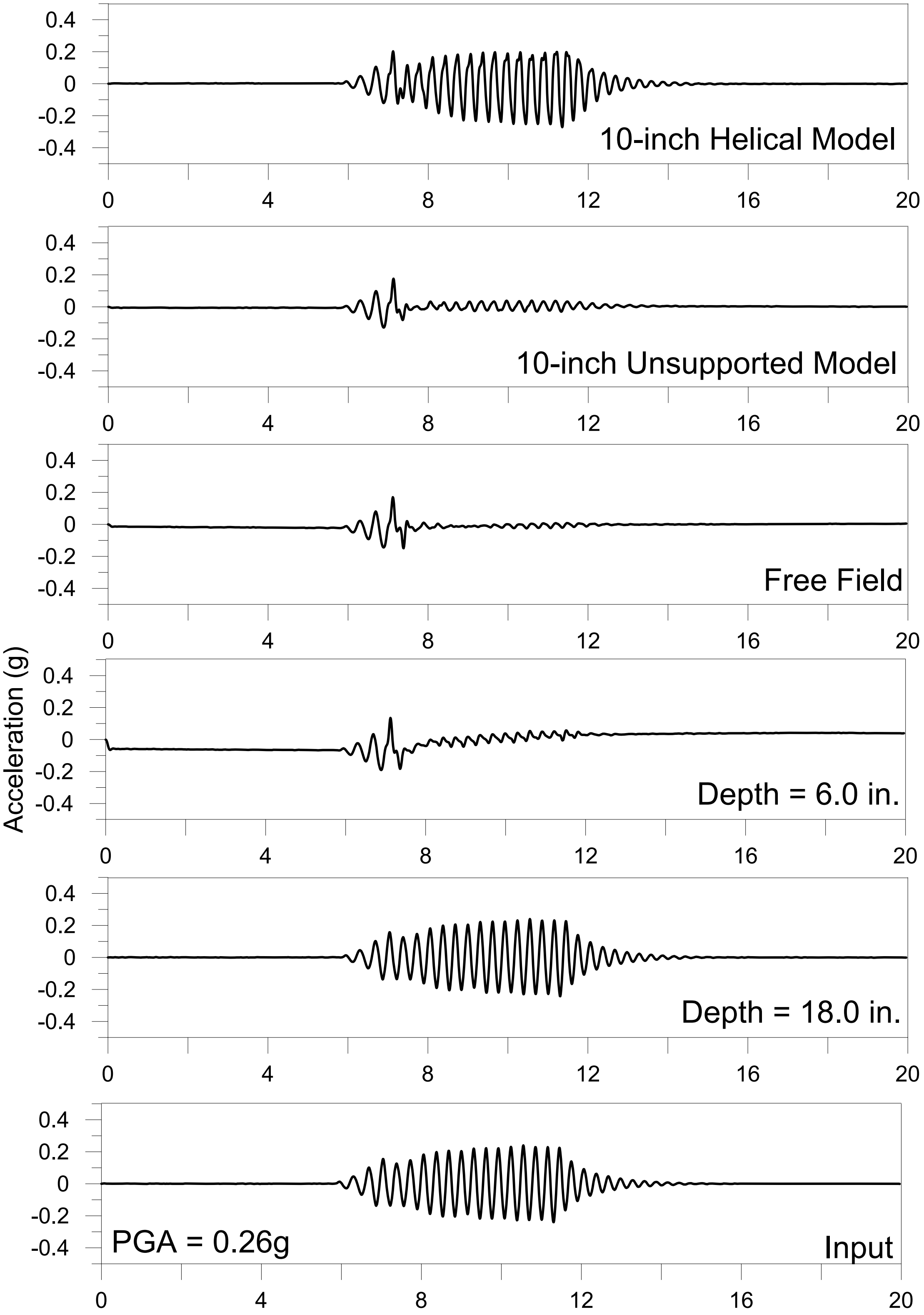

Test #43 (September 9, 2016)

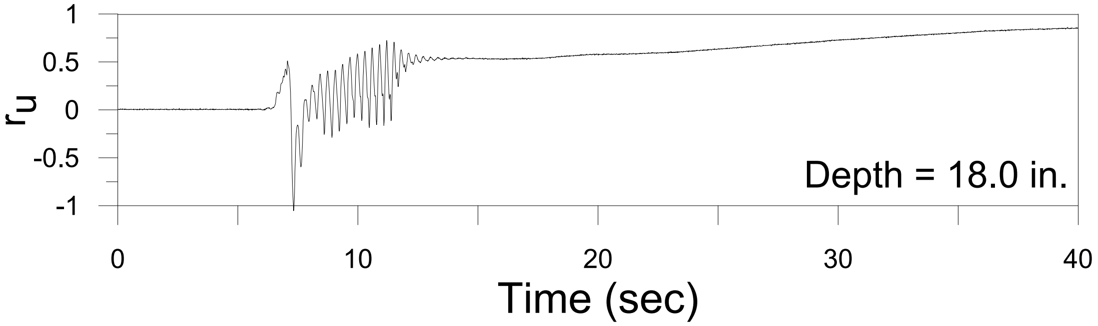

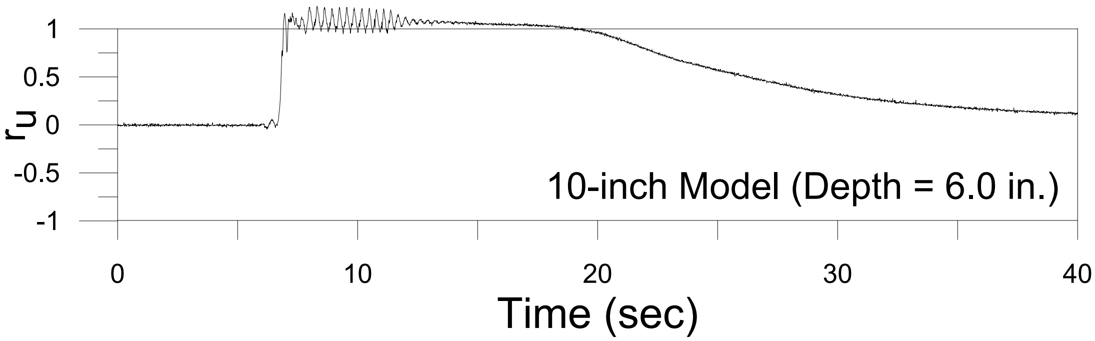

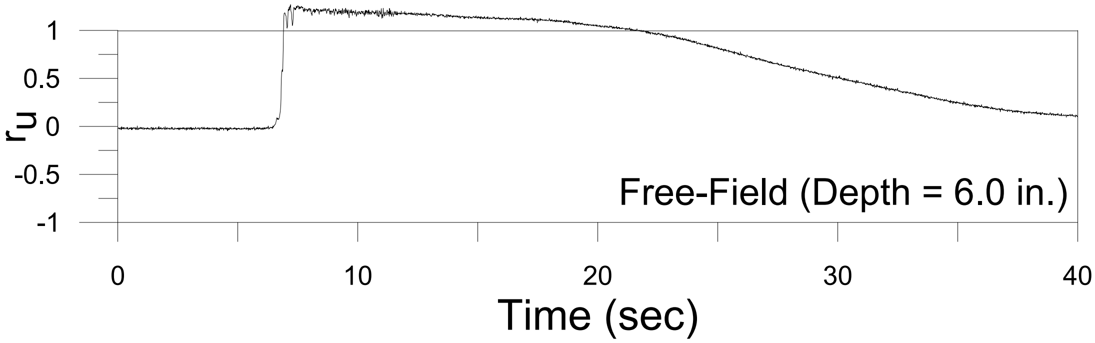

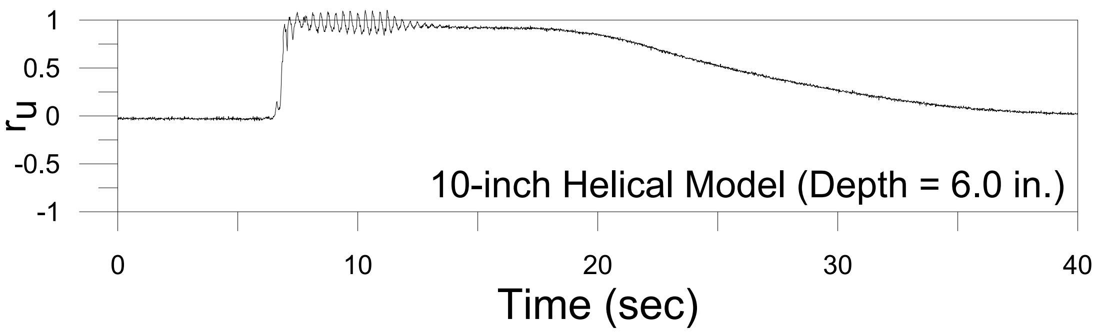

PGA = 0.26g

Test # 43: Ground Motion Characteristics
9/9/2016
PGA: 0.26g

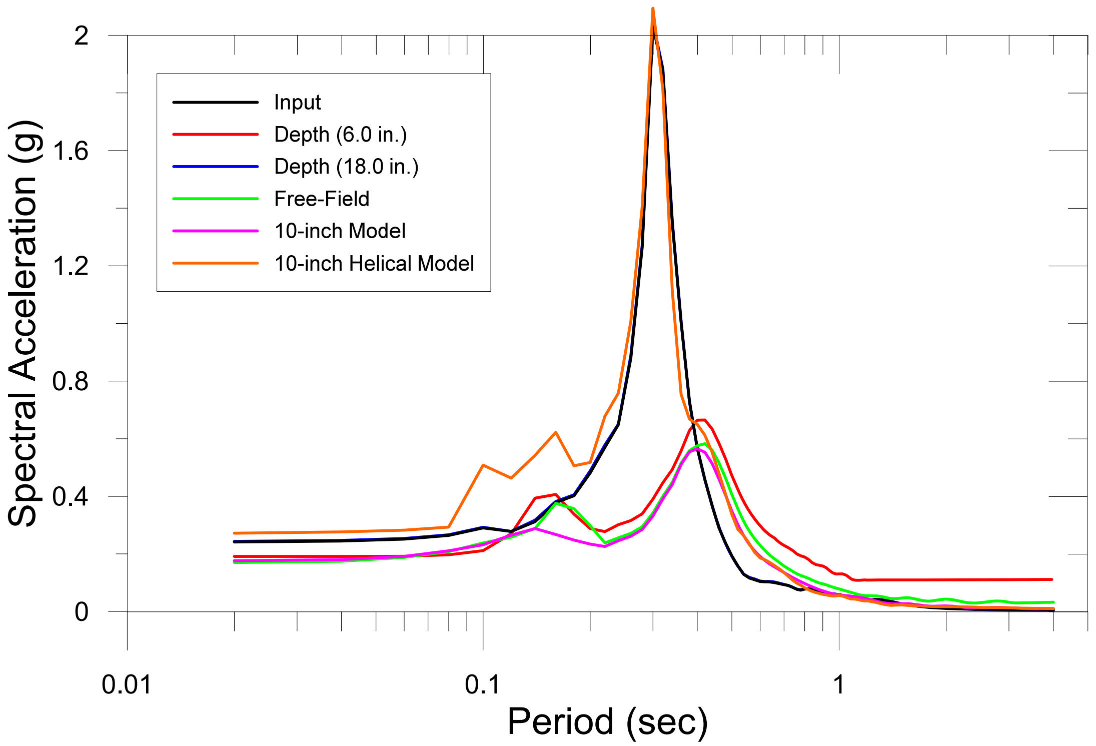

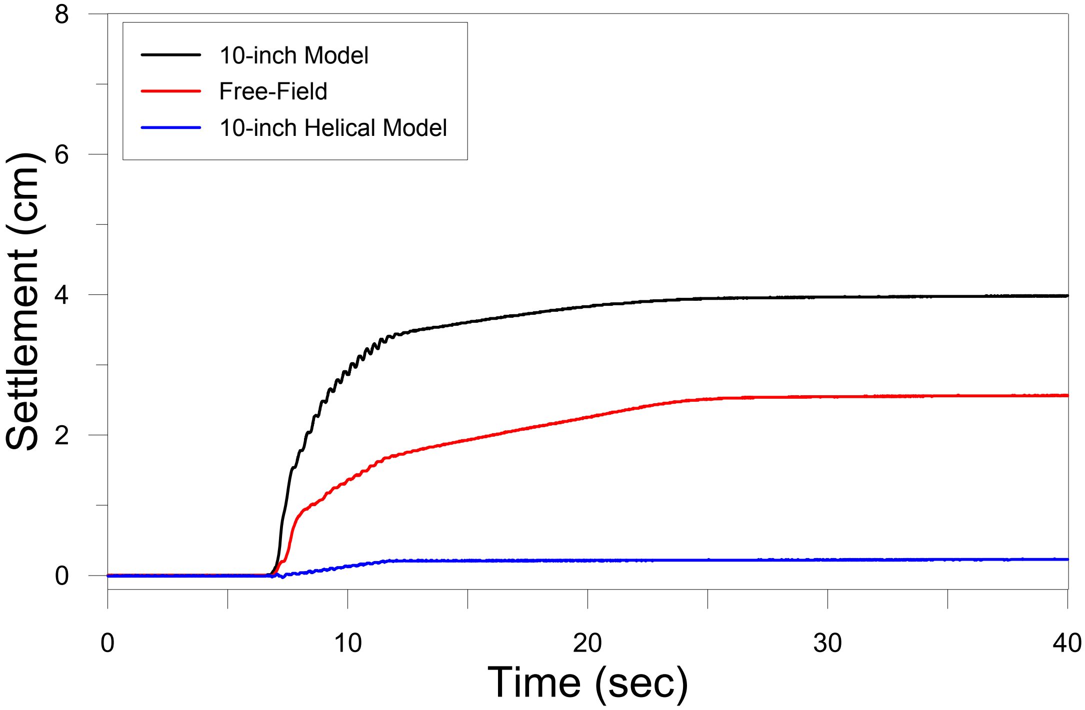

Test # 43: Settlement (cm)
9/9/2016
PGA: 0.26g

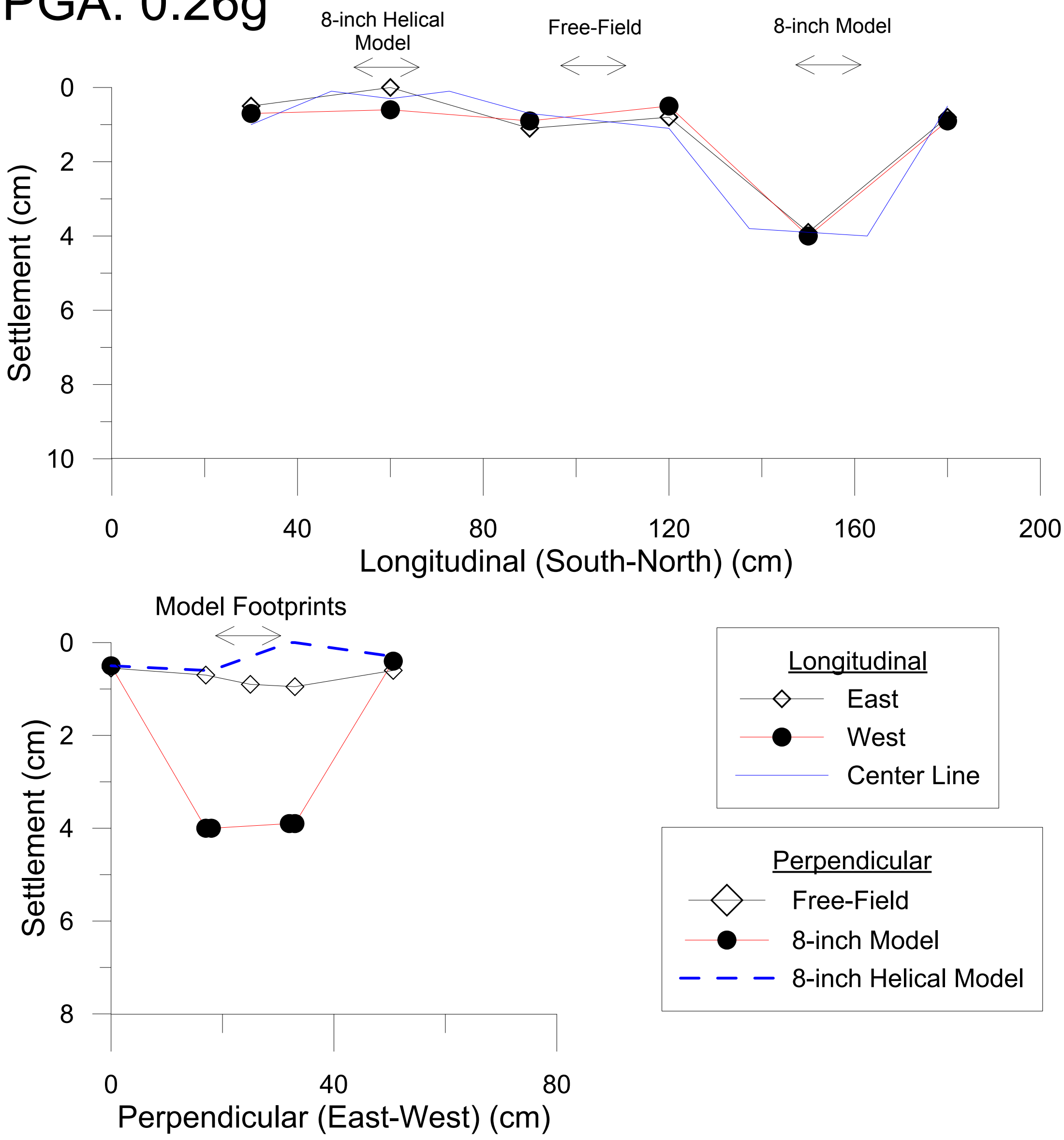

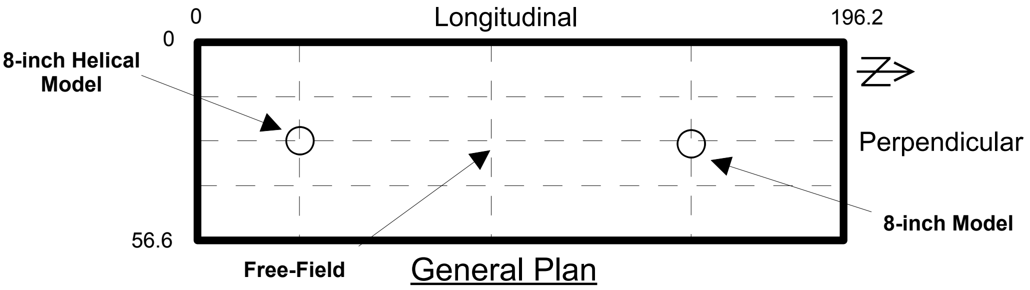

General Plan

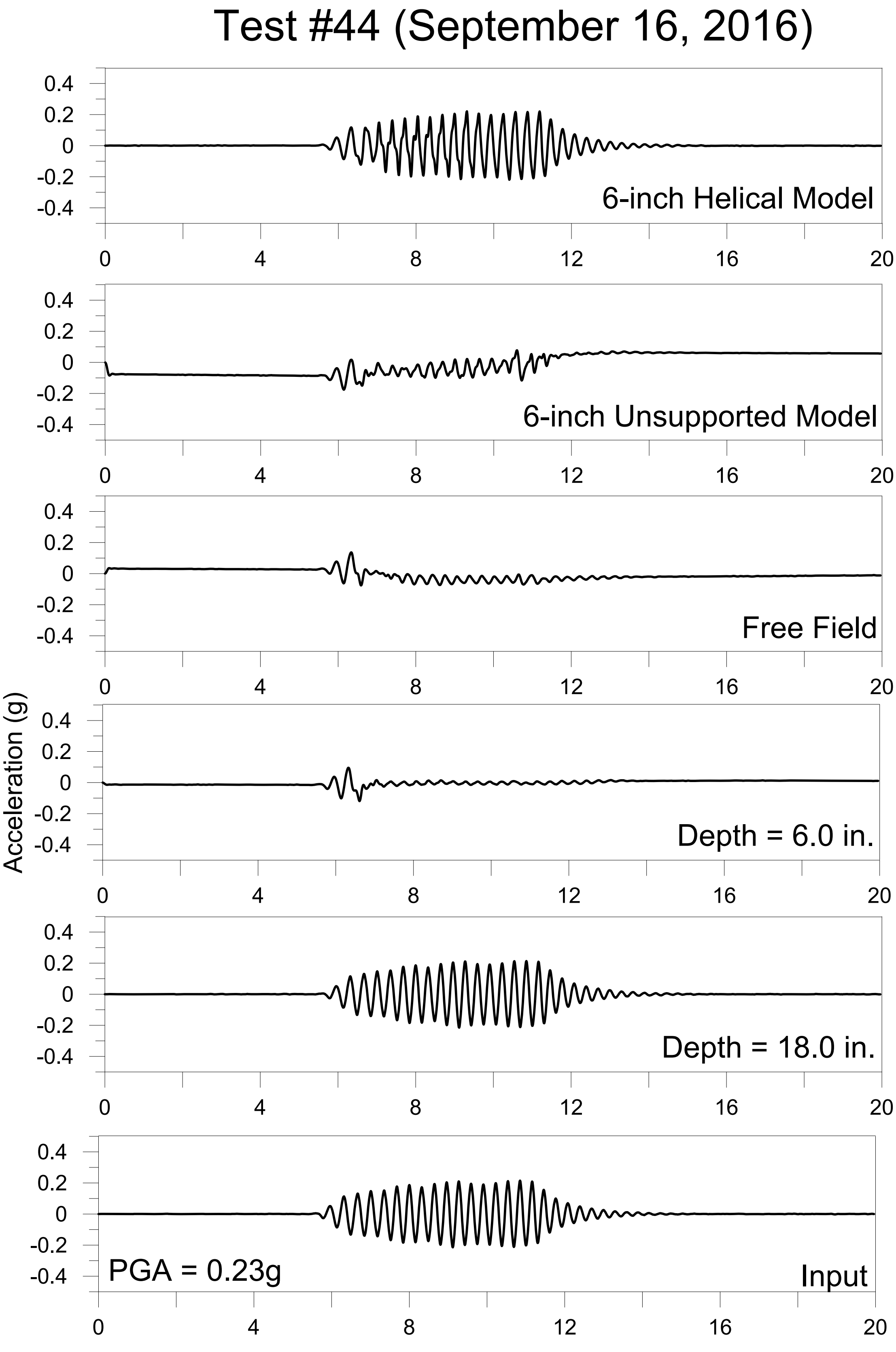
Test #44 (September 16, 2016)
Acceleration (g)
0.4
0.2
0
-0.2
-0.4
0
4
8
12
16
20
6-inch Helical Model
6-inch Unsupported Model
Free Field
Depth = 6.0 in.
Depth = 18.0 in.
PGA = 0.23g
Input

Test #44 (September 16, 2016)

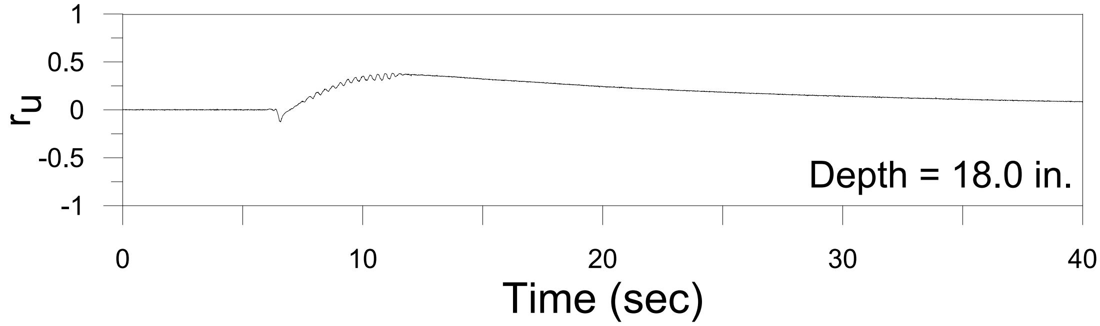

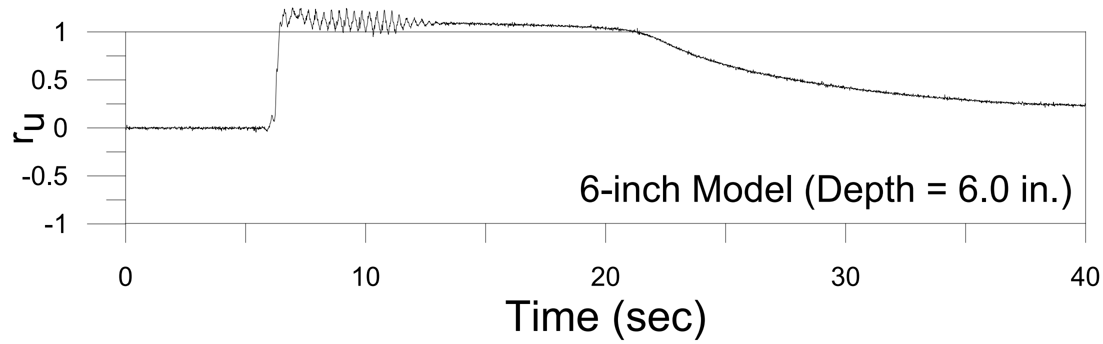

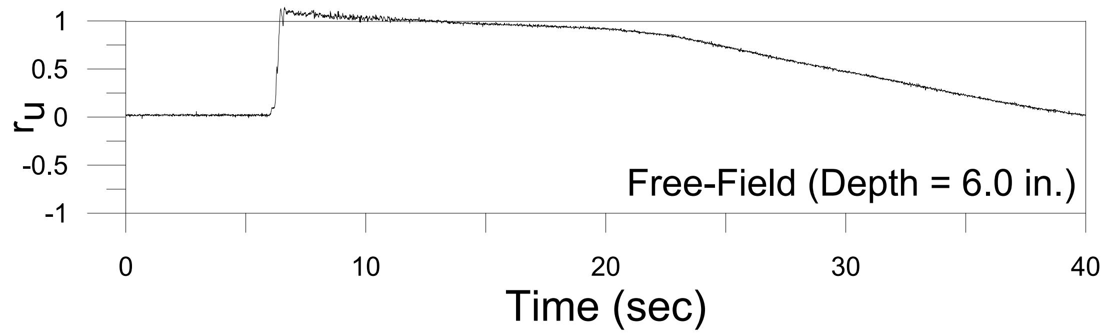

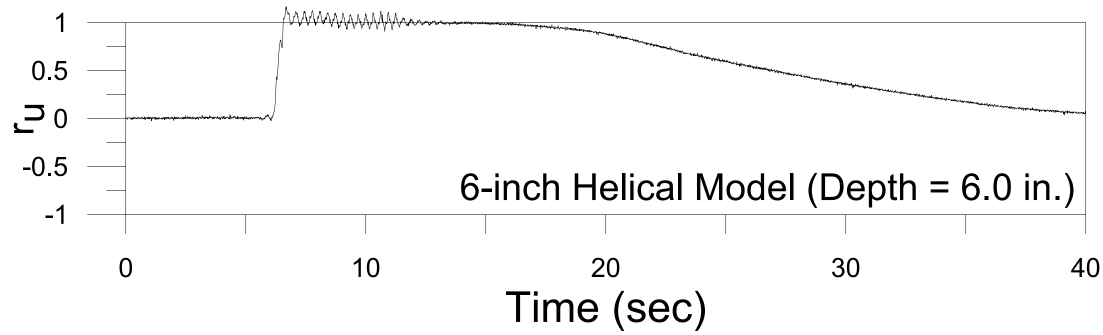

PGA = 0.23g

Test # 44: Ground Motion Characteristics
9/16/2016
PGA: 0.23g

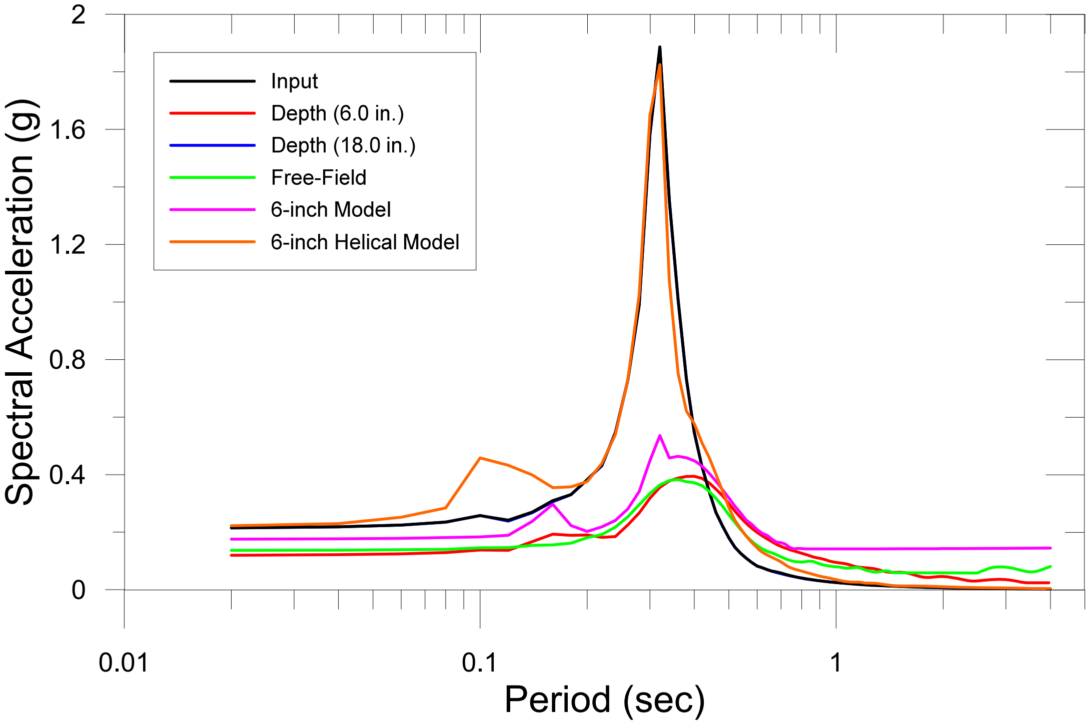

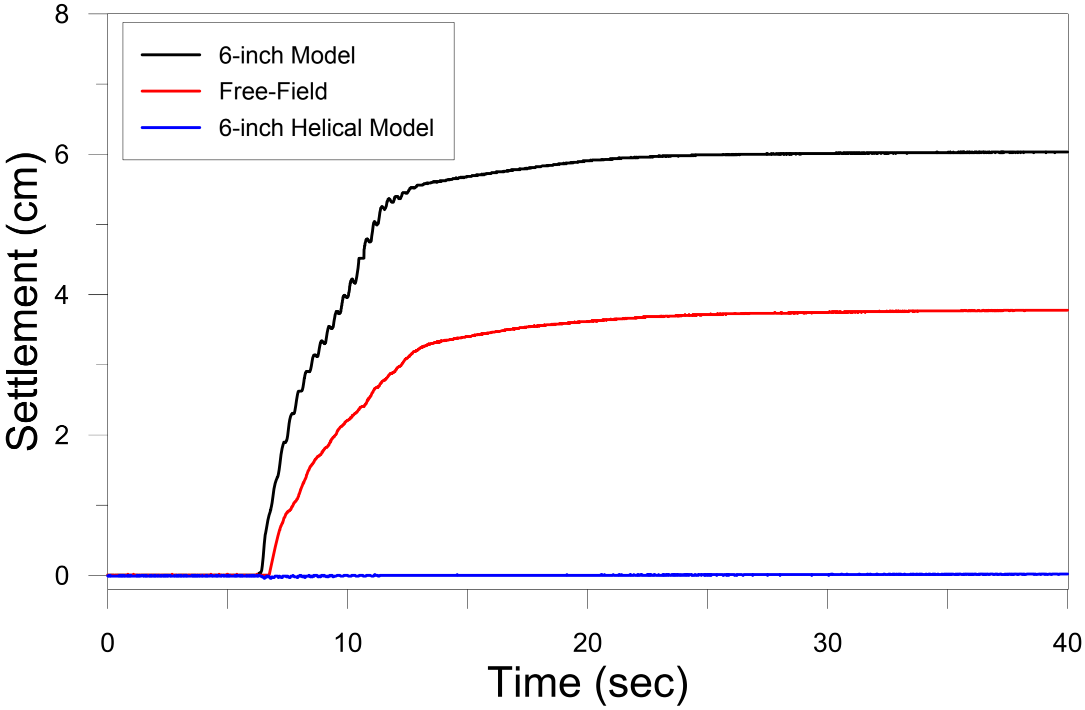

Test # 44: Settlement (cm)
9/16/2016
PGA: 0.23g

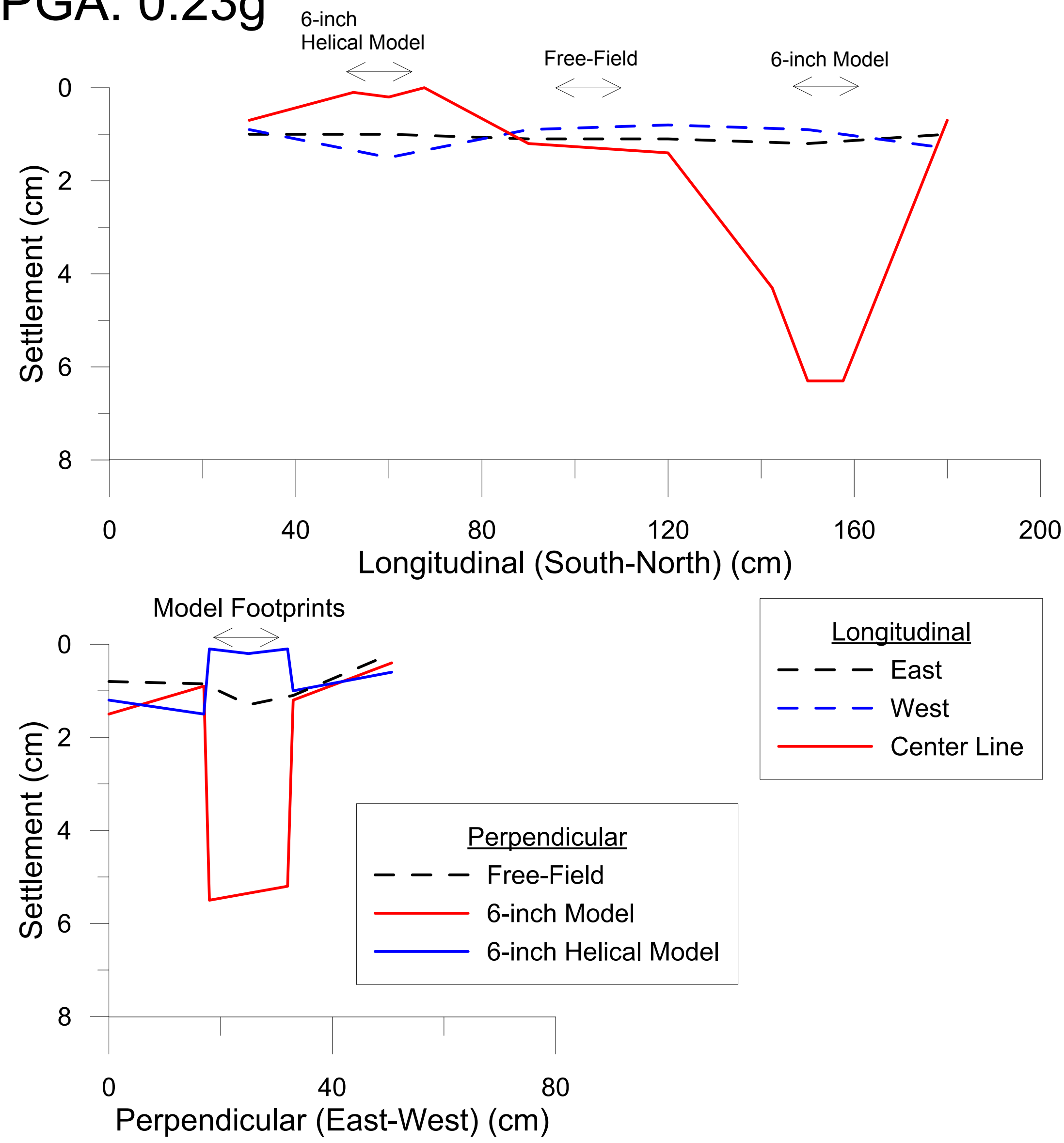

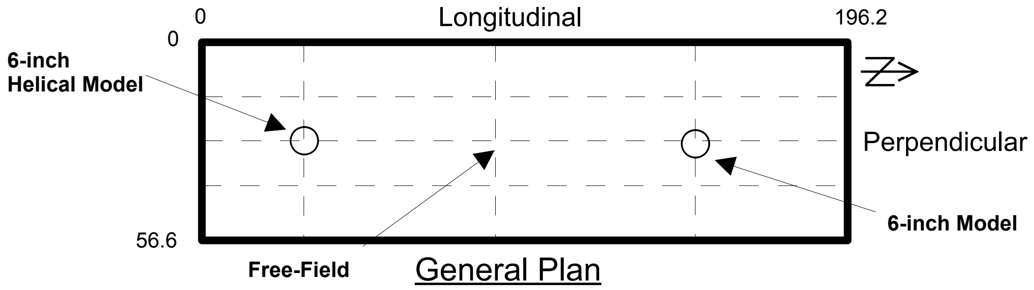

General Plan

Test #45 (September 19, 2016)

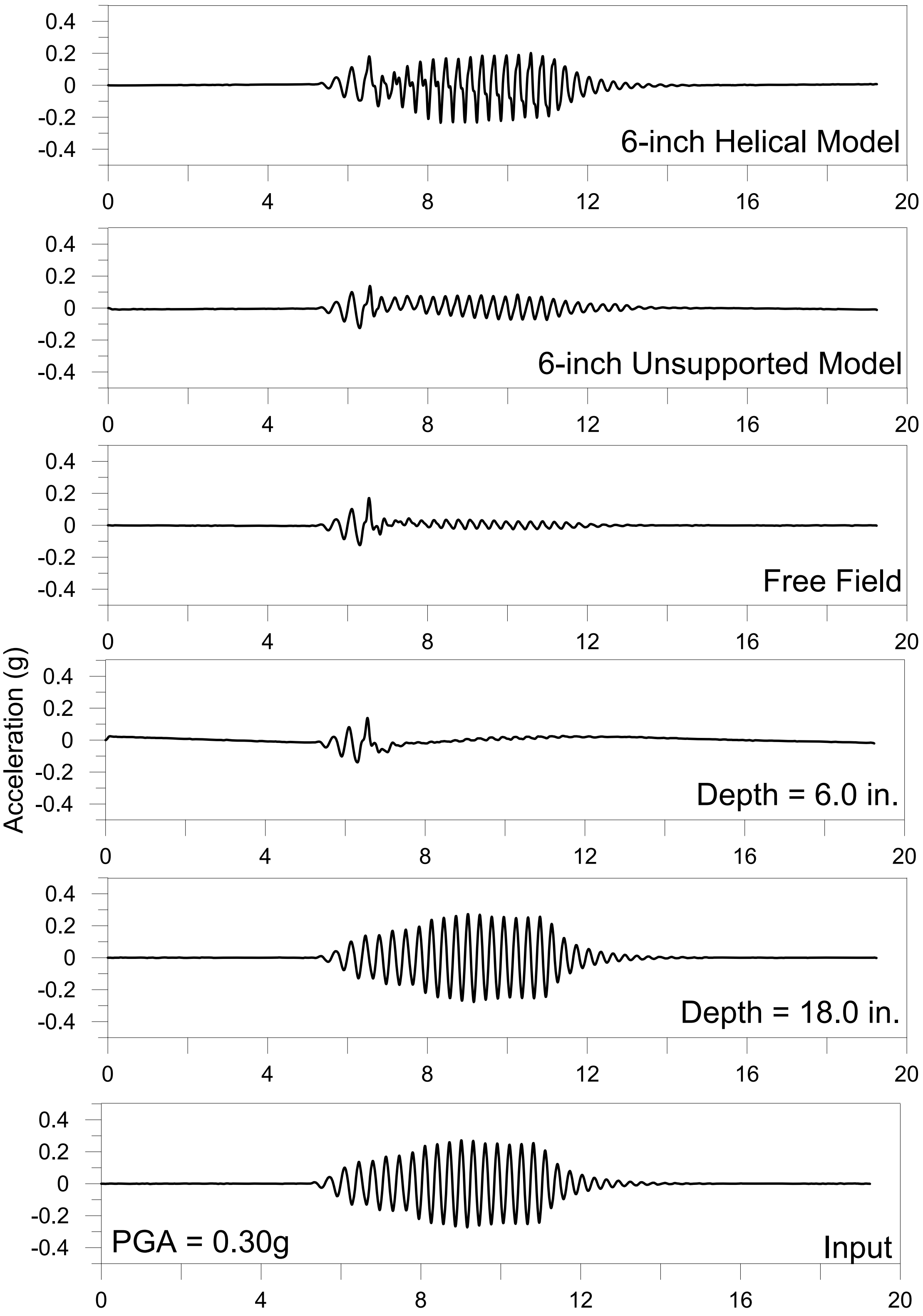

Test #45 (September 19, 2016)

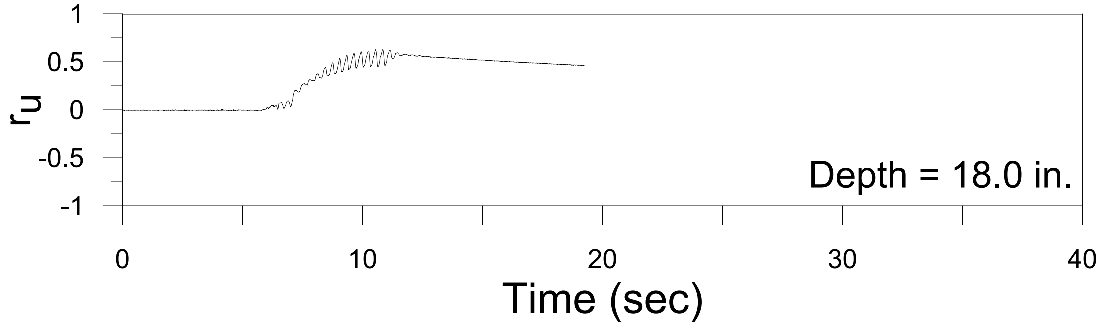

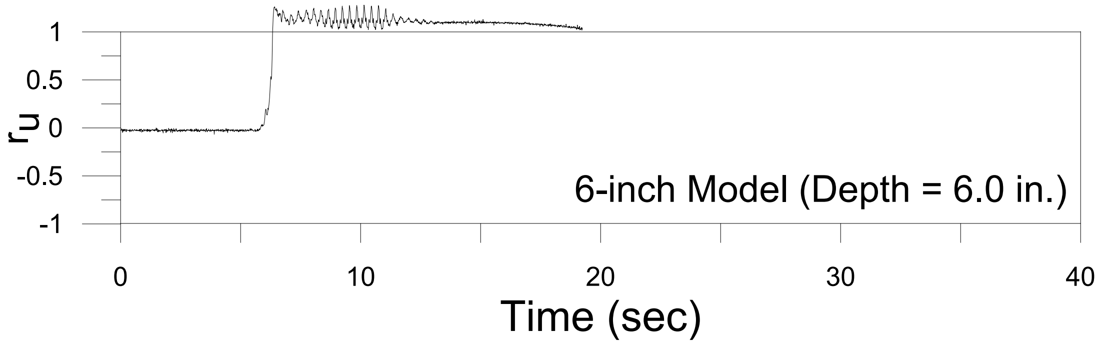

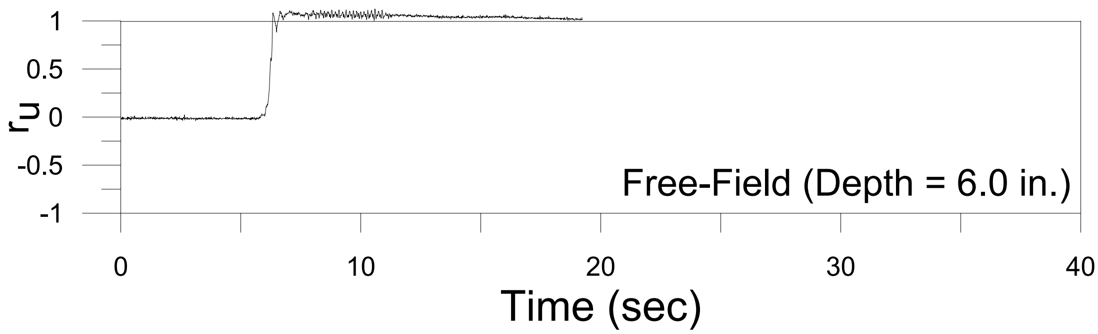

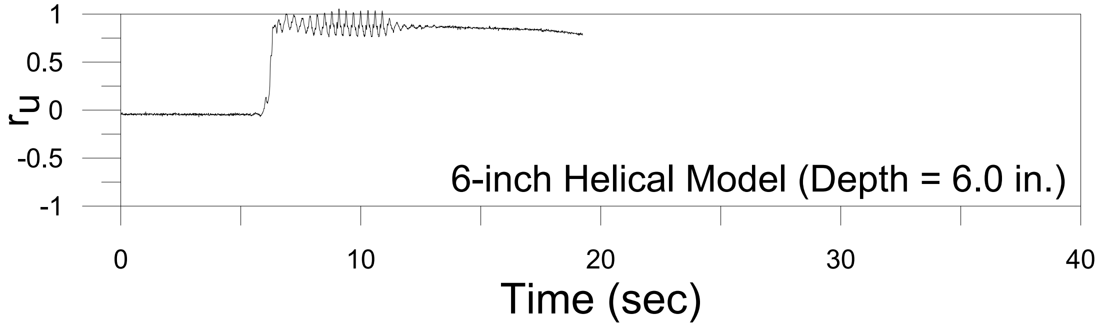

PGA = 0.30g

Test # 45: Ground Motion Characteristics
9/19/2016
PGA: 0.30g

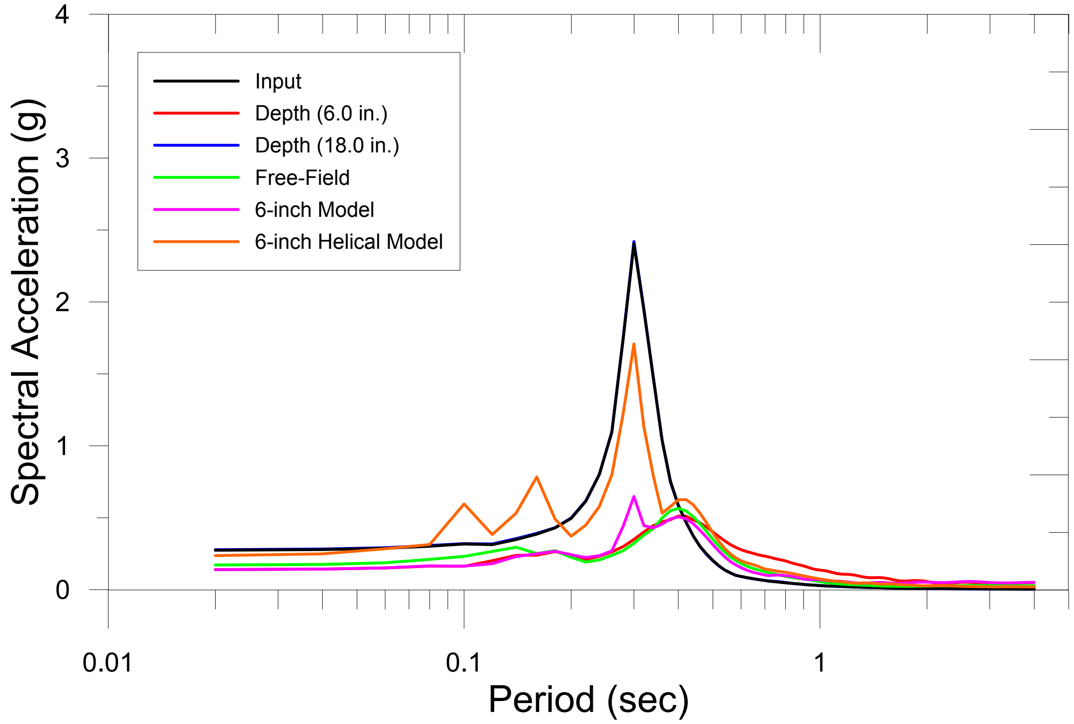

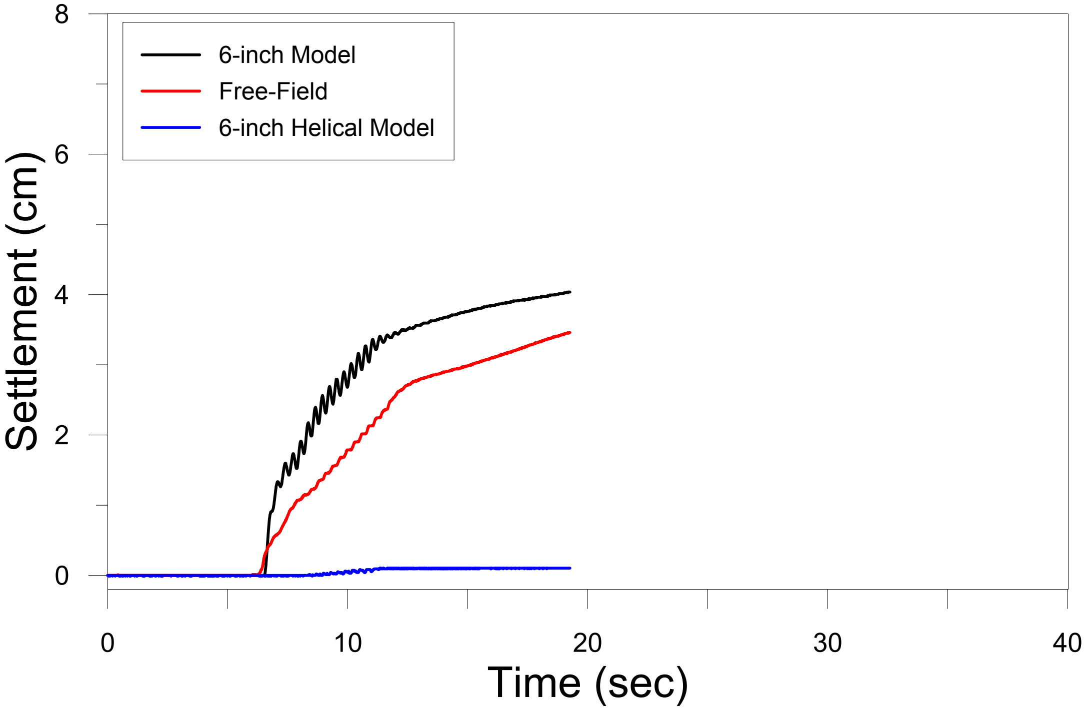

Test # 45: Settlement (cm)
9/19/2016
PGA: 0.30g

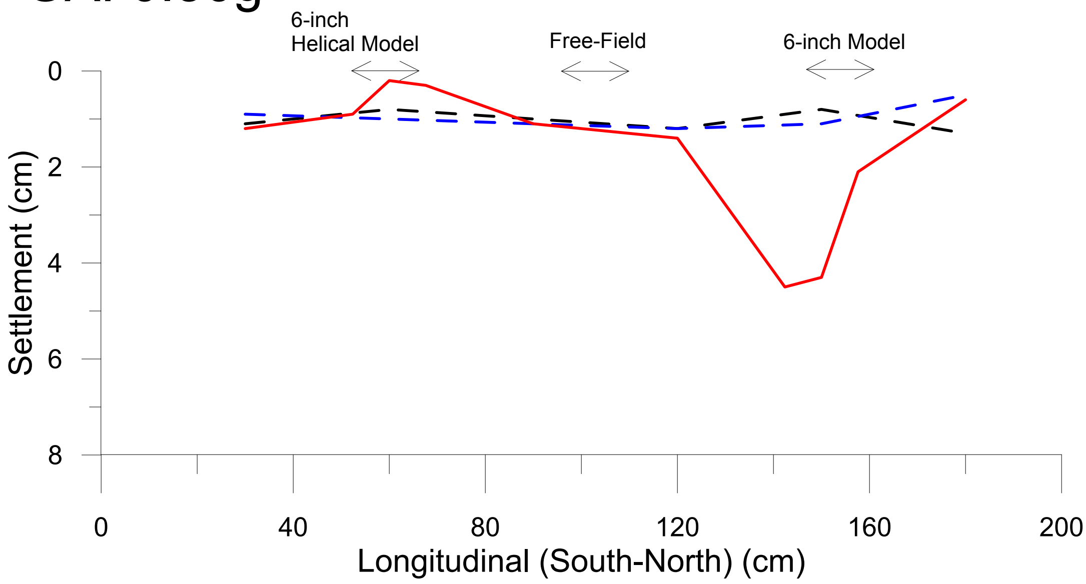

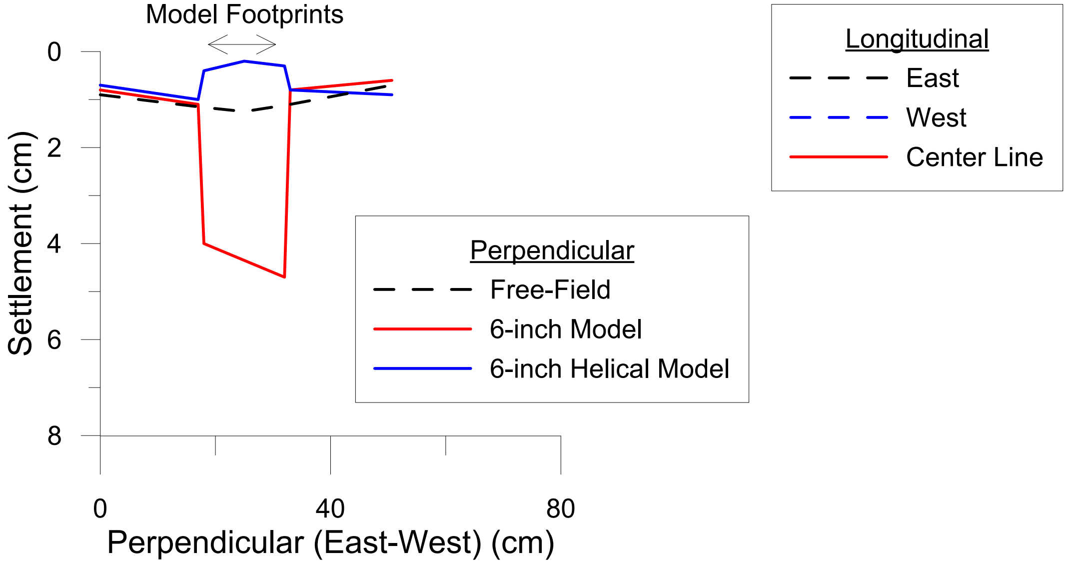

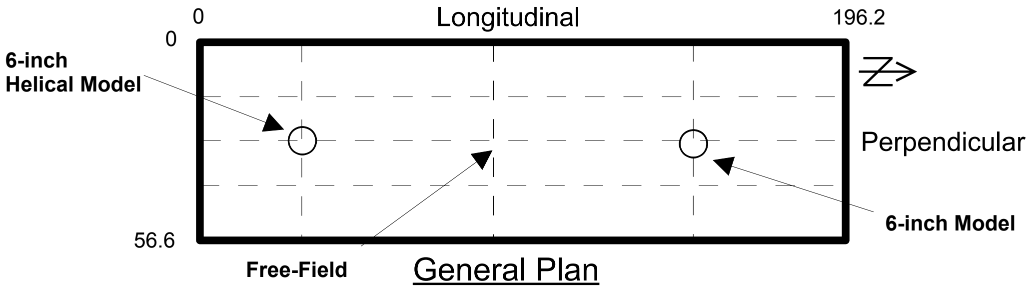

Test #46 (September 23, 2016)

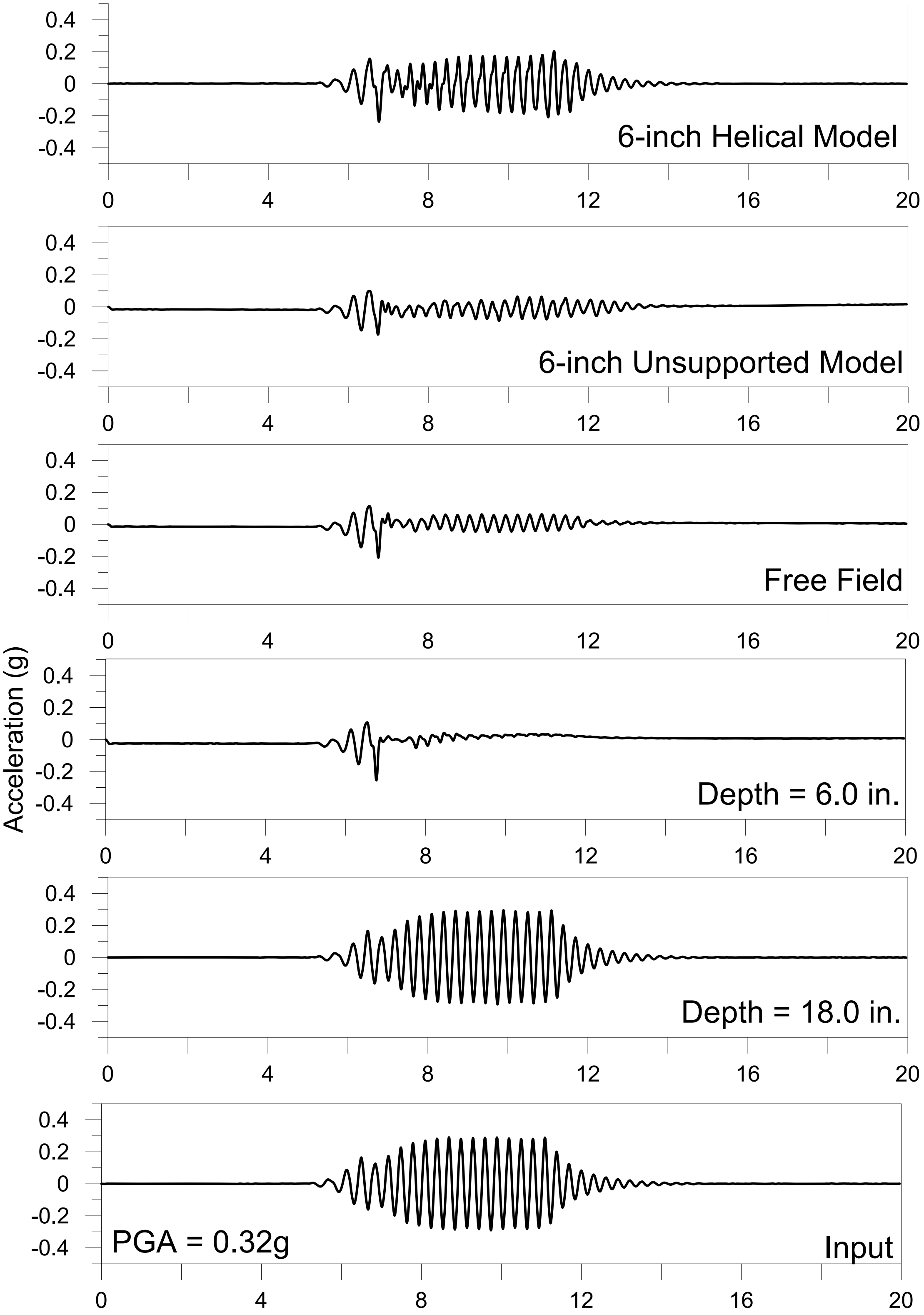

Test #46 (September 23, 2016)

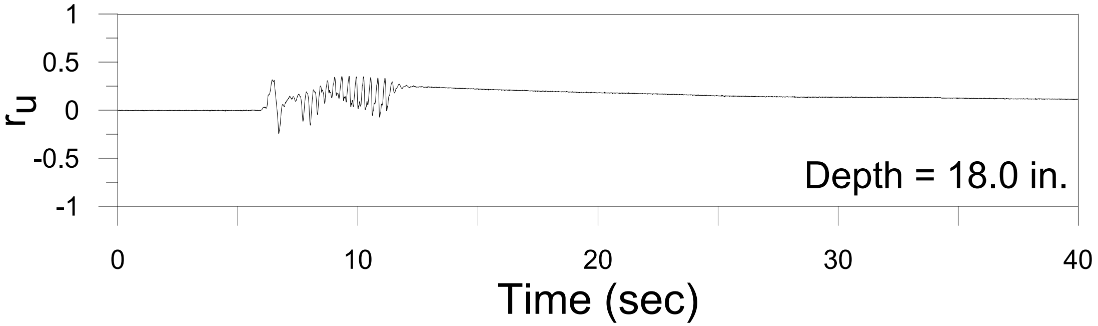

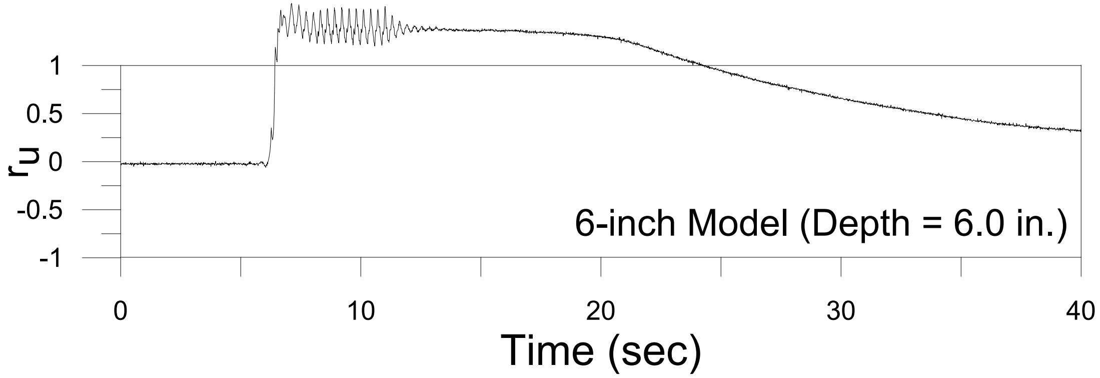

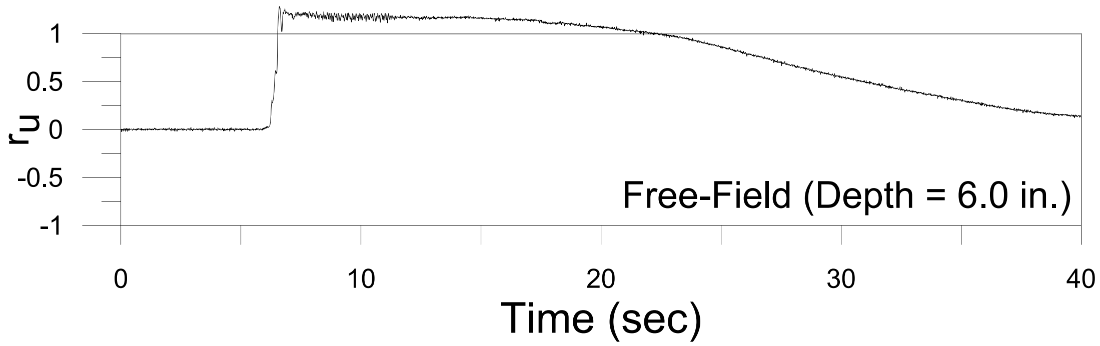

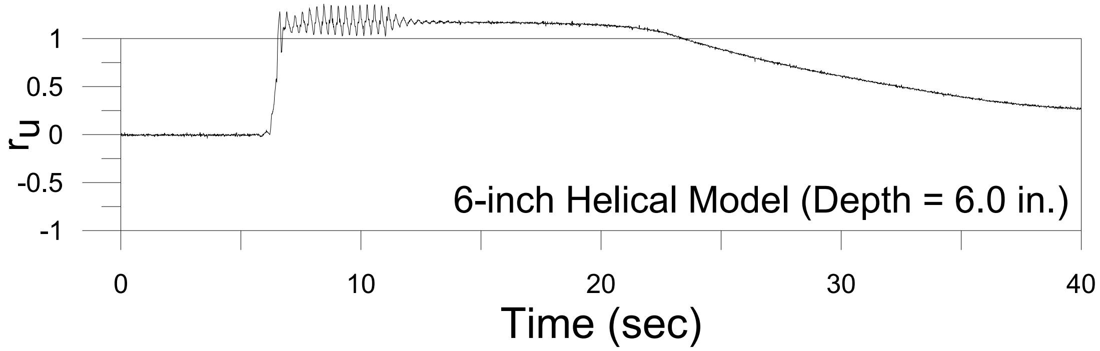

PGA = 0.32g

Test # 46: Ground Motion Characteristics
9/23/2016
PGA: 0.32g

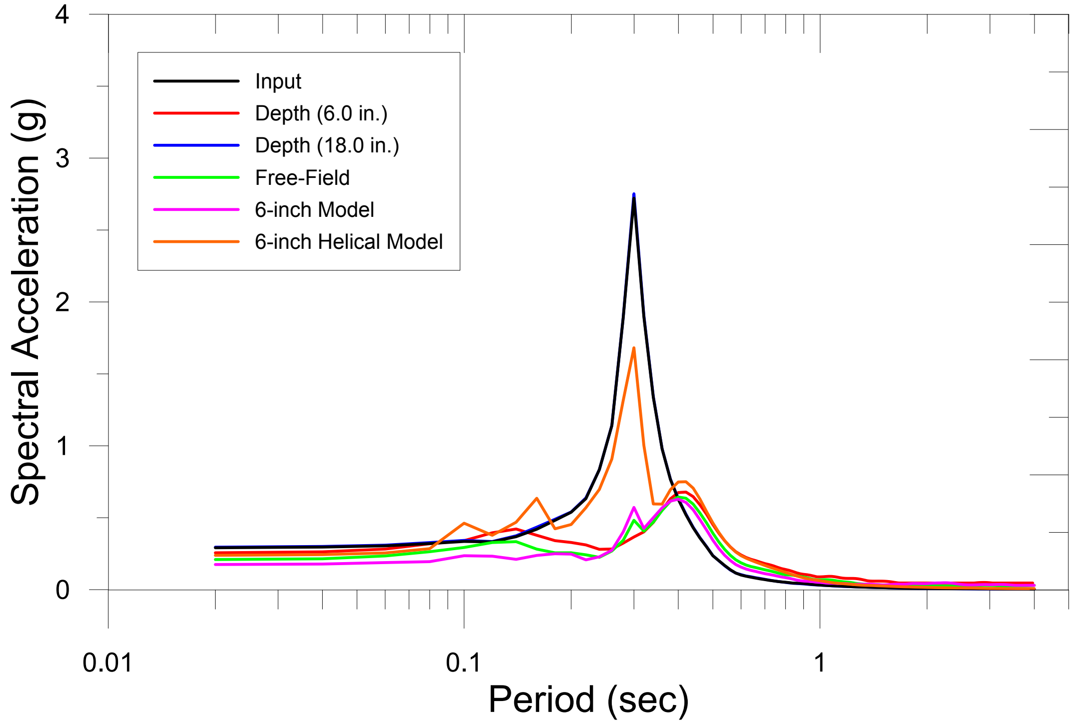

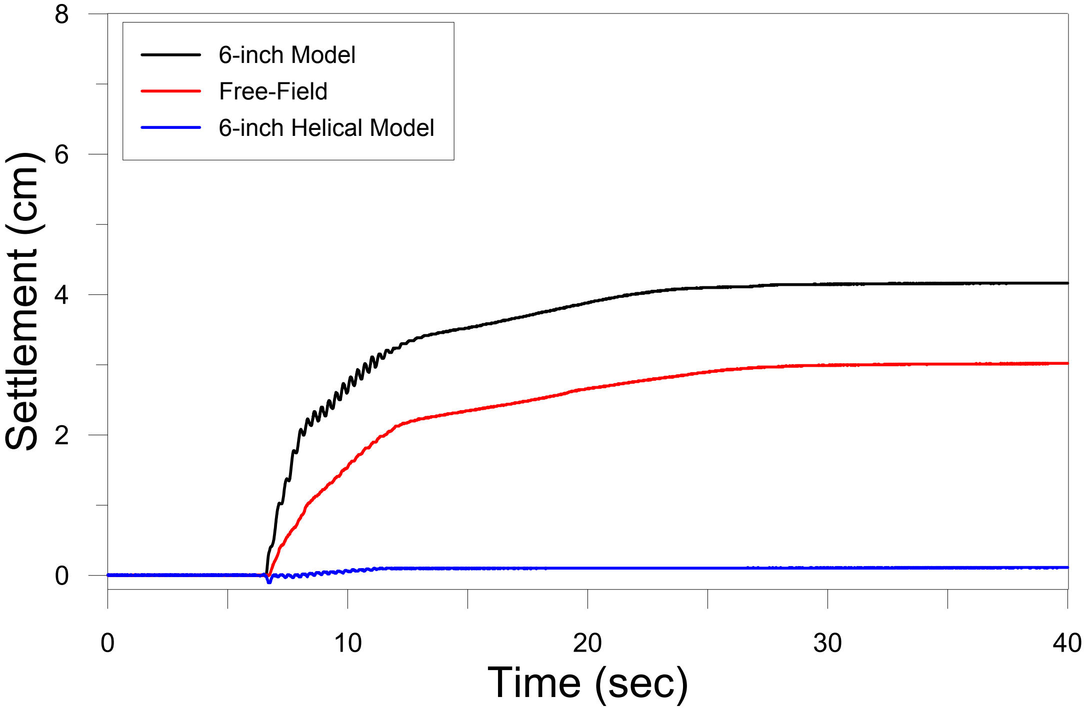

Test # 46: Settlement (cm)
9/23/2016
PGA: 0.32g

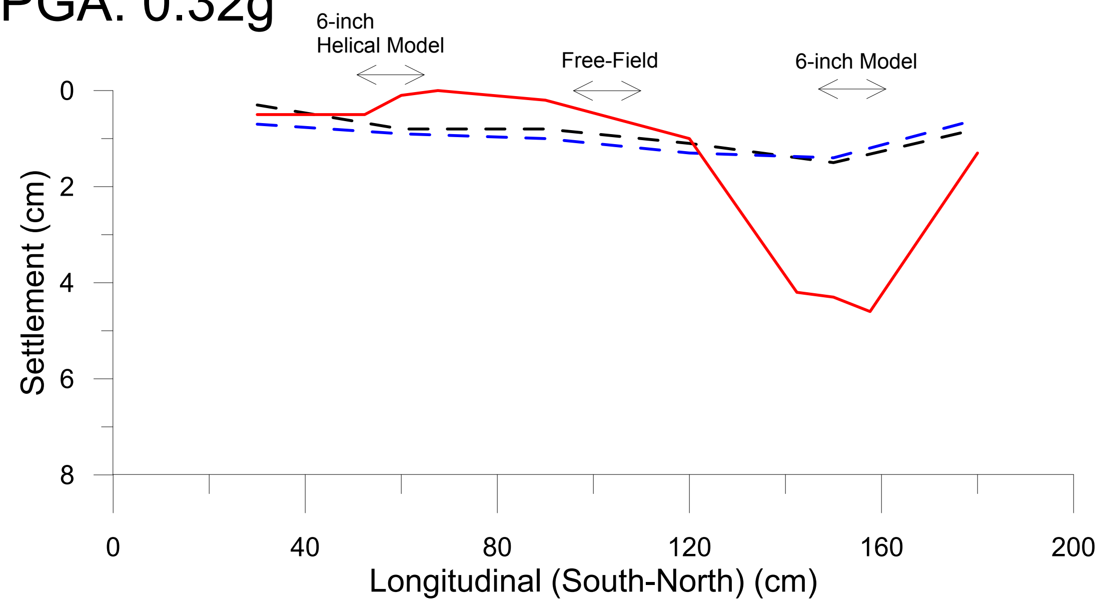

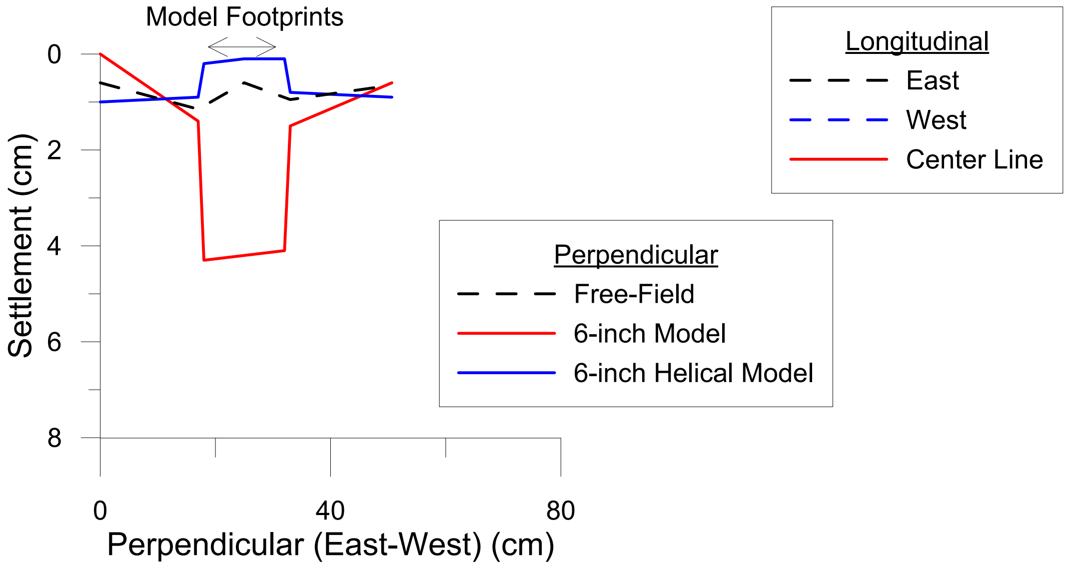

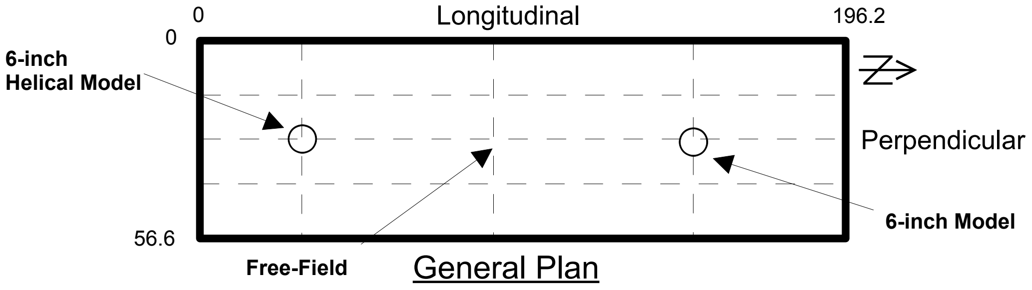

Test #47 (September 26, 2016)

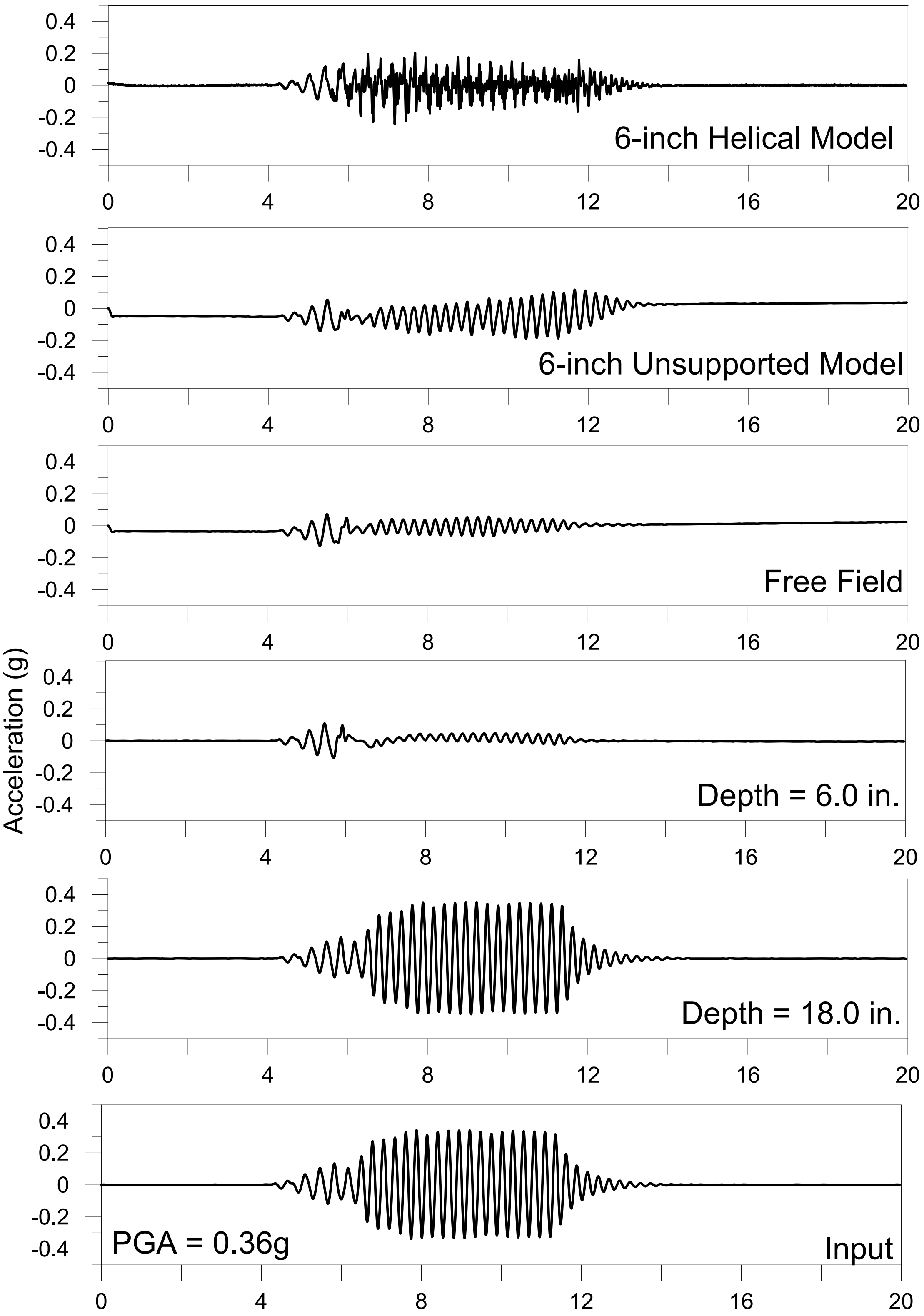

Test #47 (September 26, 2016)

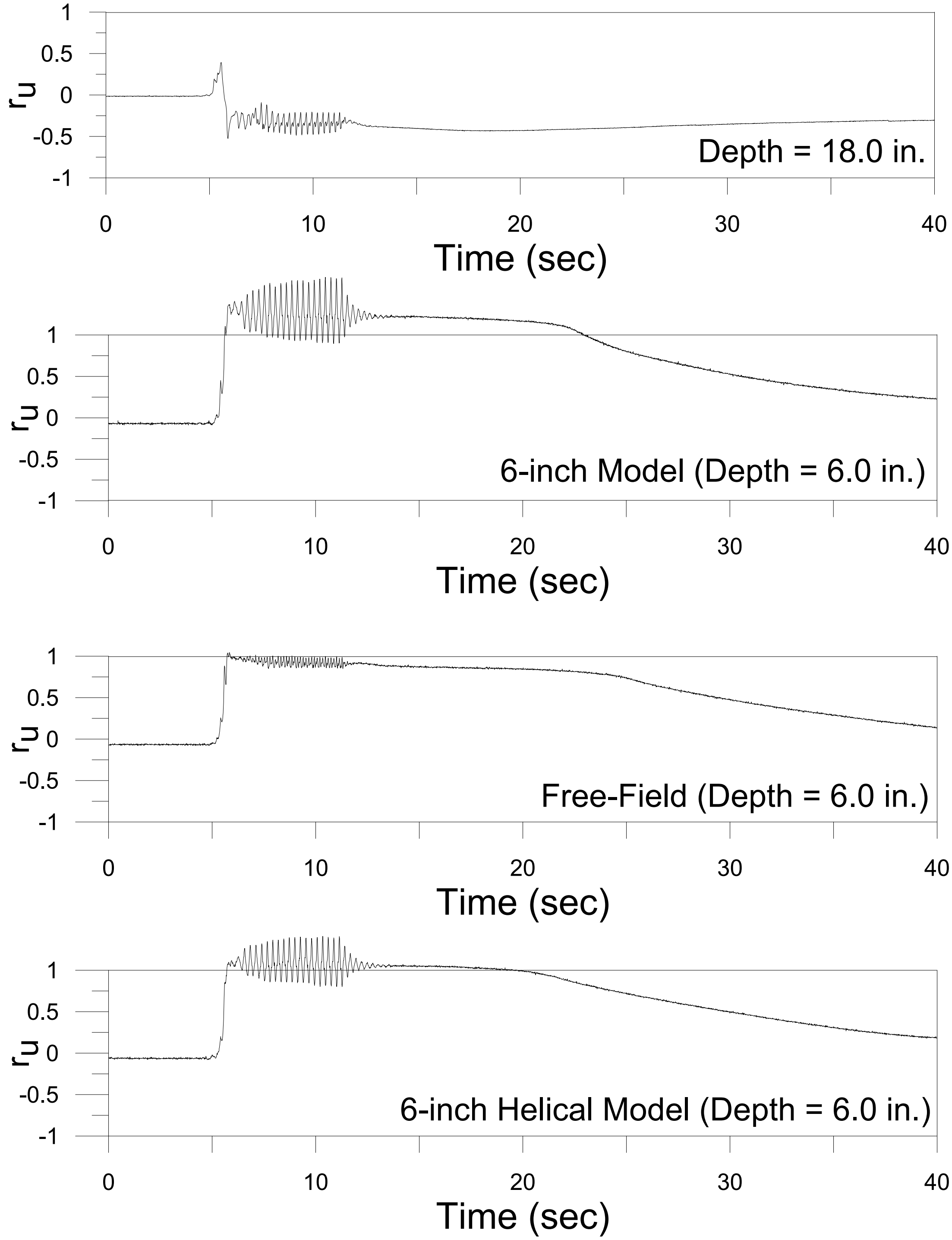

PGA = 0.36g

Test # 47: Ground Motion Characteristics
9/26/2016
PGA: 0.36g

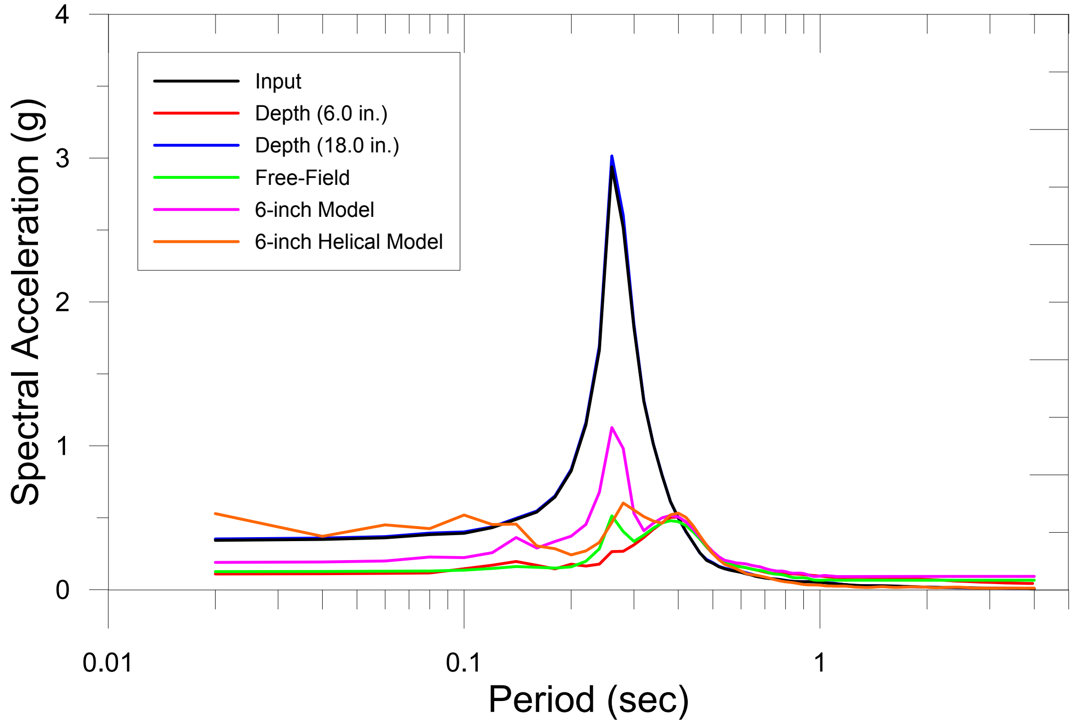

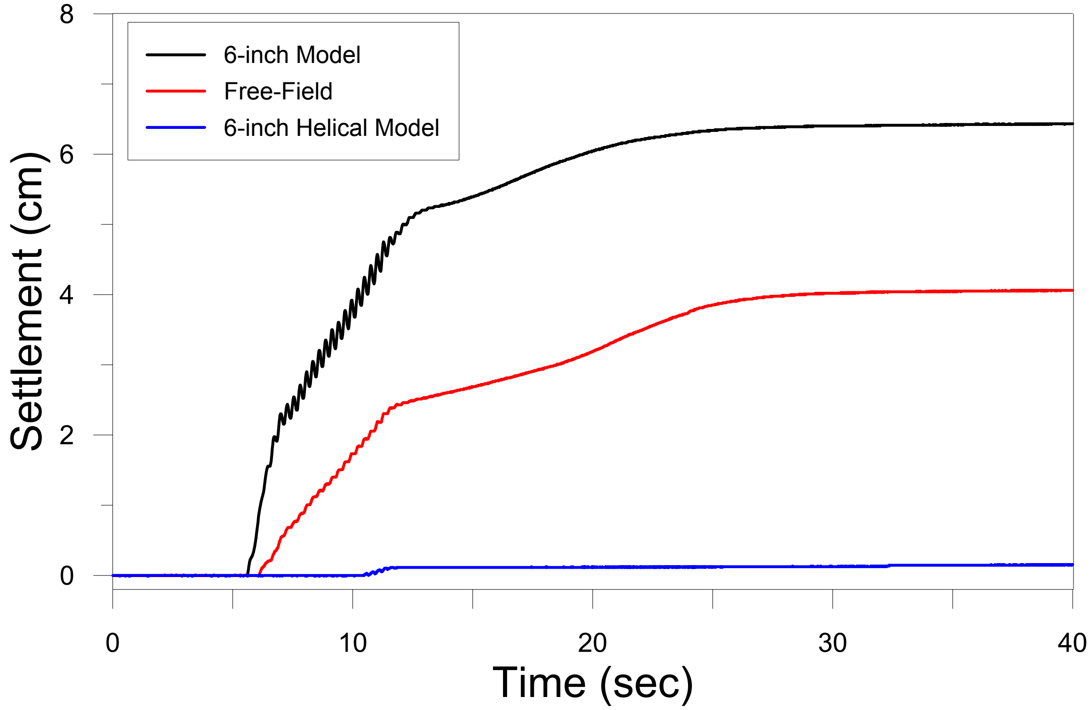

Test # 47: Settlement (cm)
9/26/2016
PGA: 0.36g

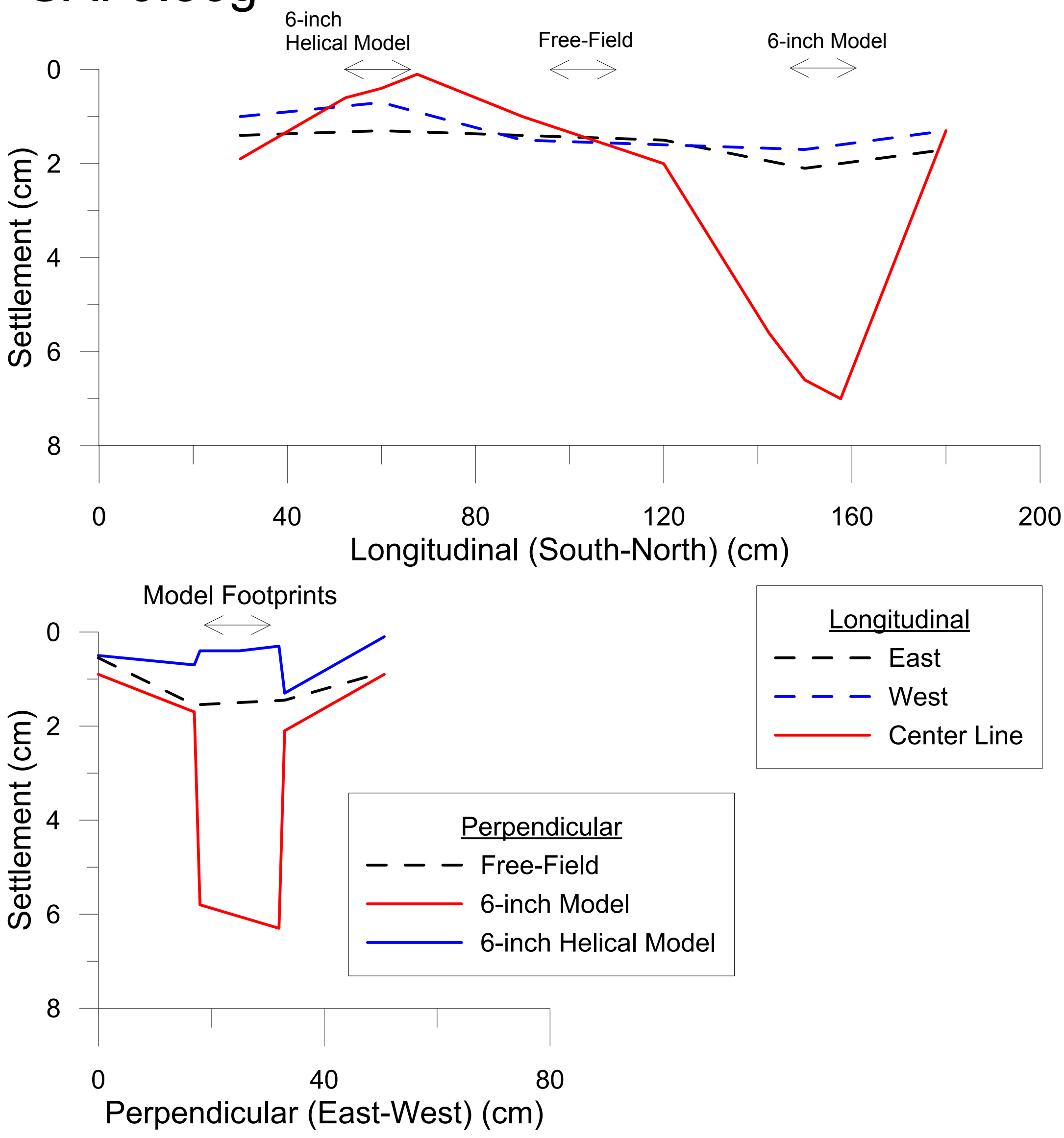

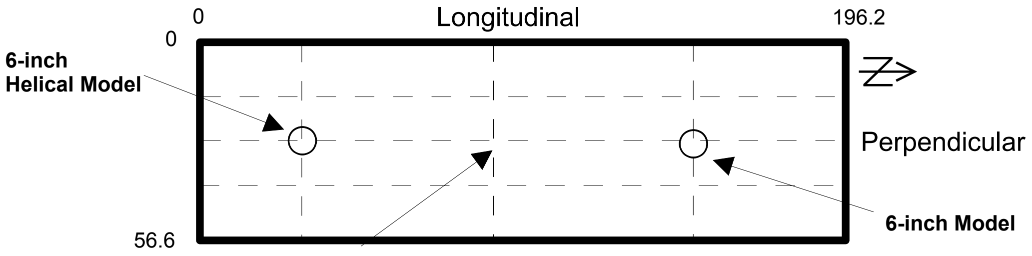

General Plan

Test #48 (September 30, 2016)

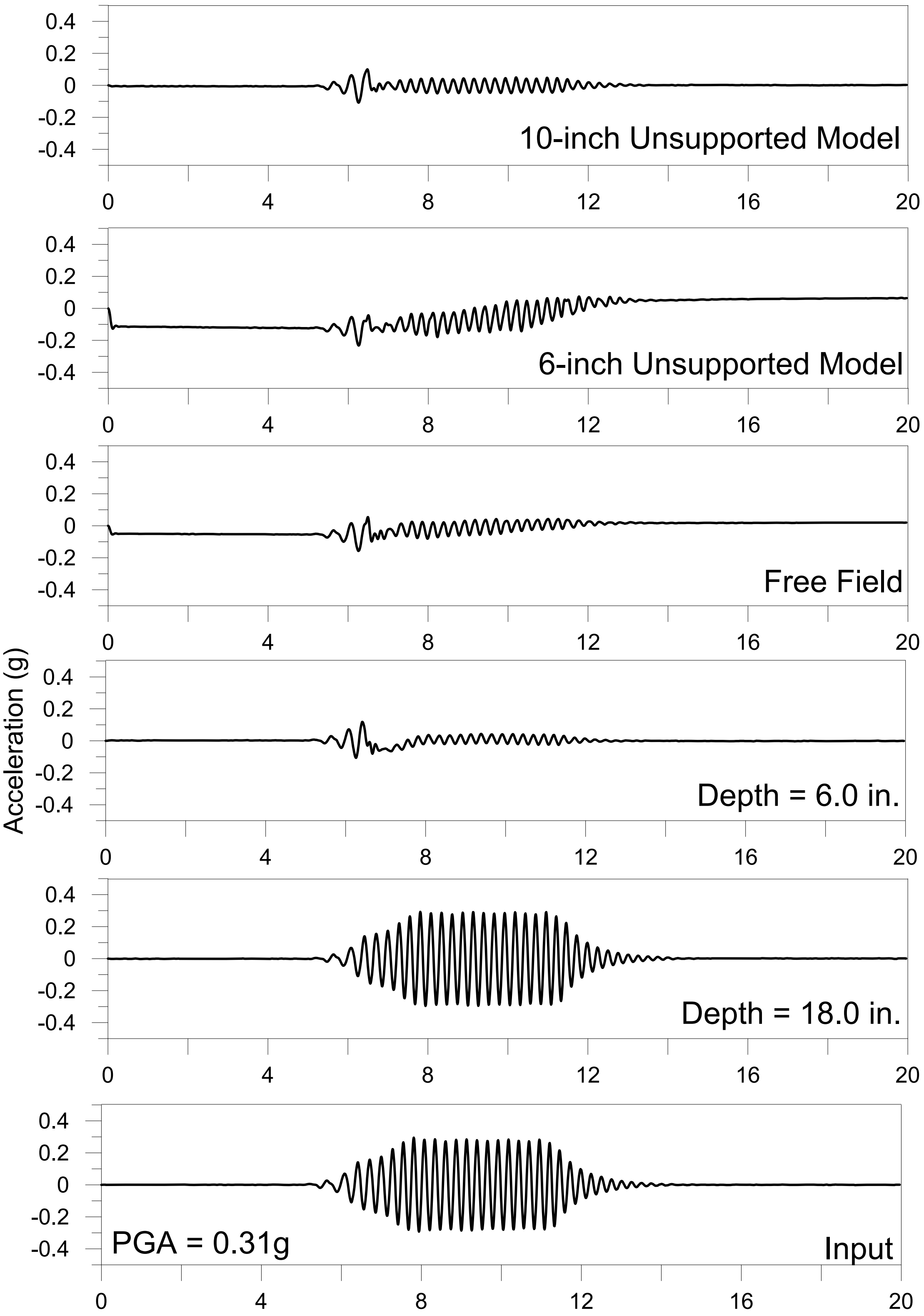

Test #48 (September 30, 2016)

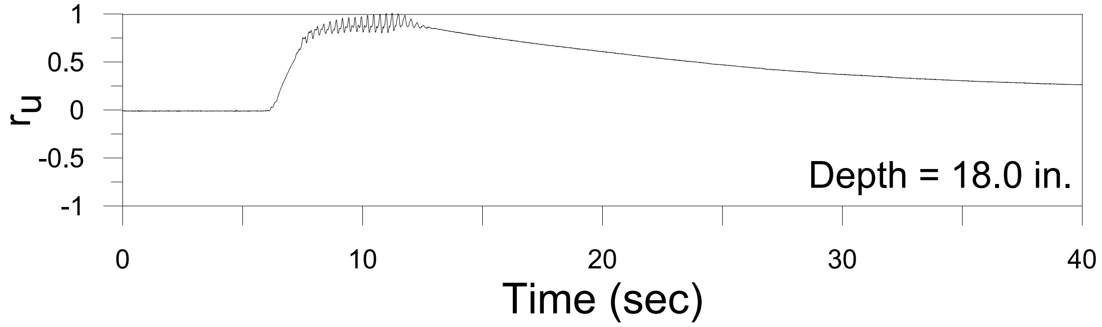

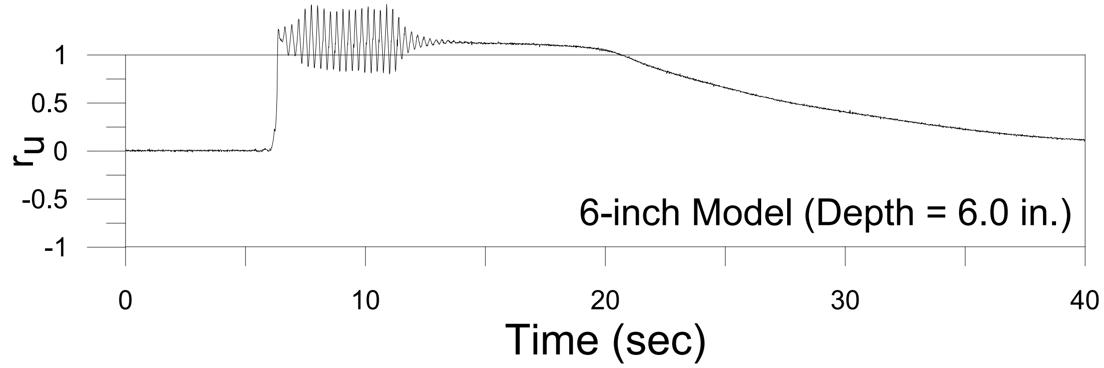

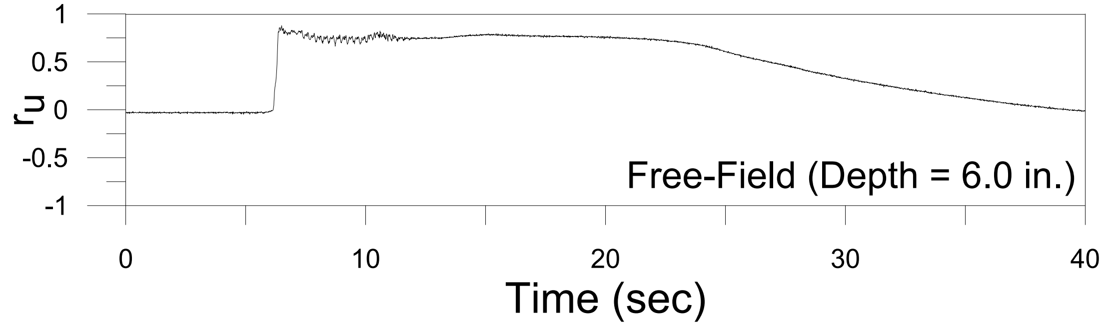

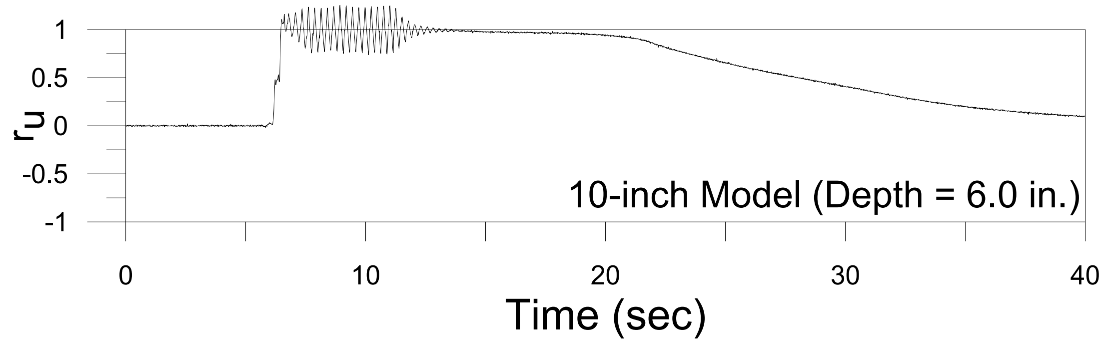

PGA = 0.31g

Test # 48: Ground Motion Characteristics
9/30/2016
PGA: 0.31g

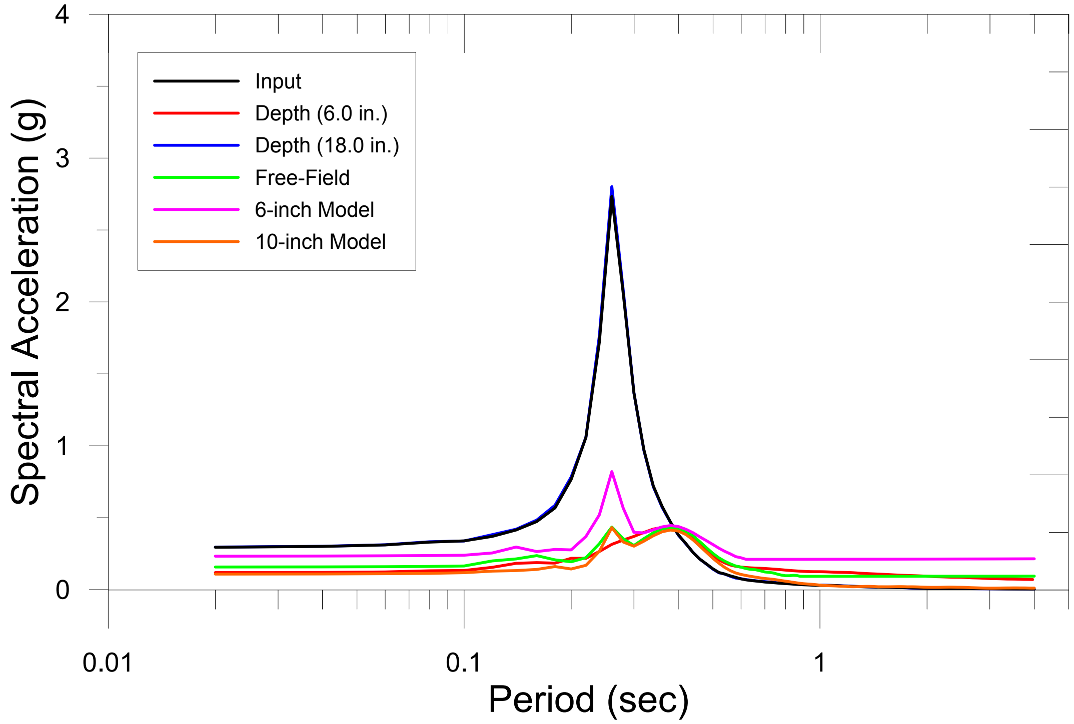

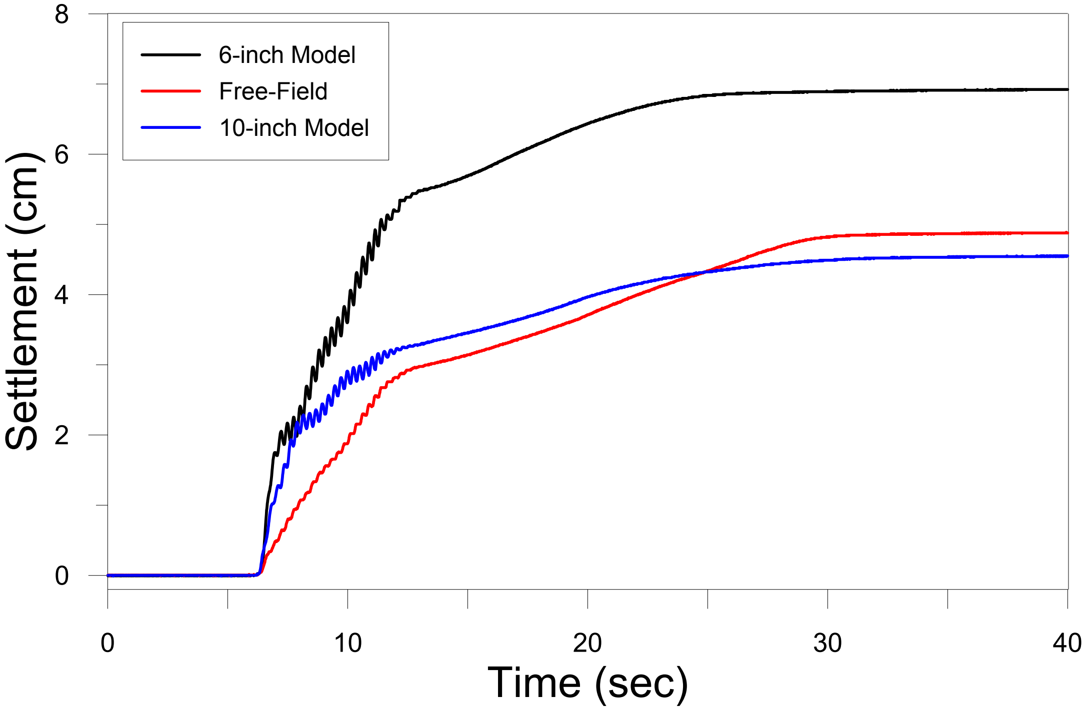

Test # 48: Settlement (cm)
9/30/2016
PGA: 0.31g

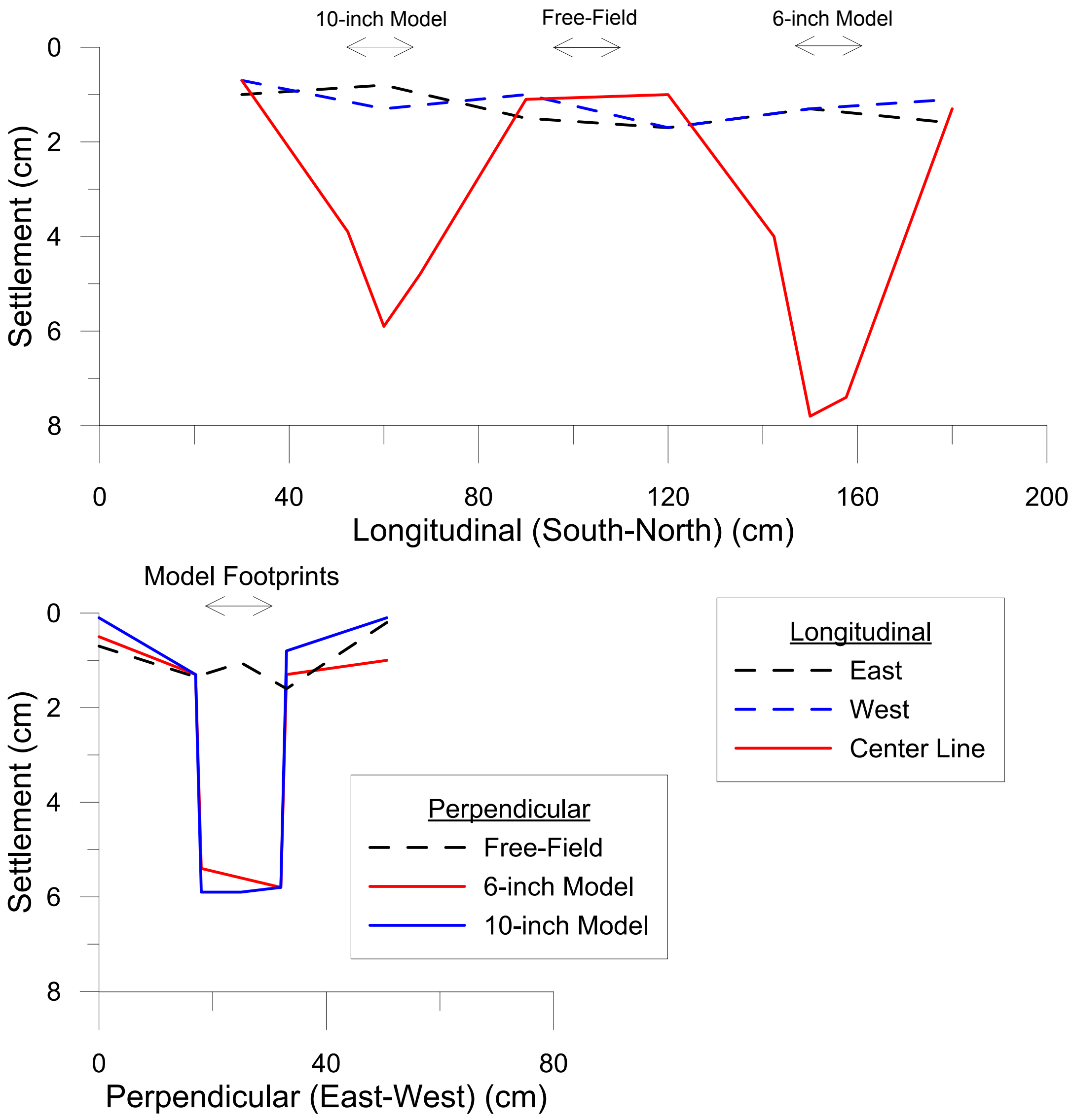

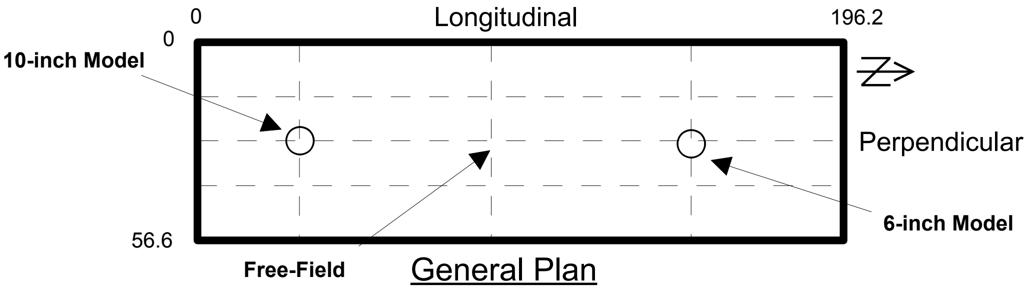

General Plan

Test #49 (October 5, 2016)

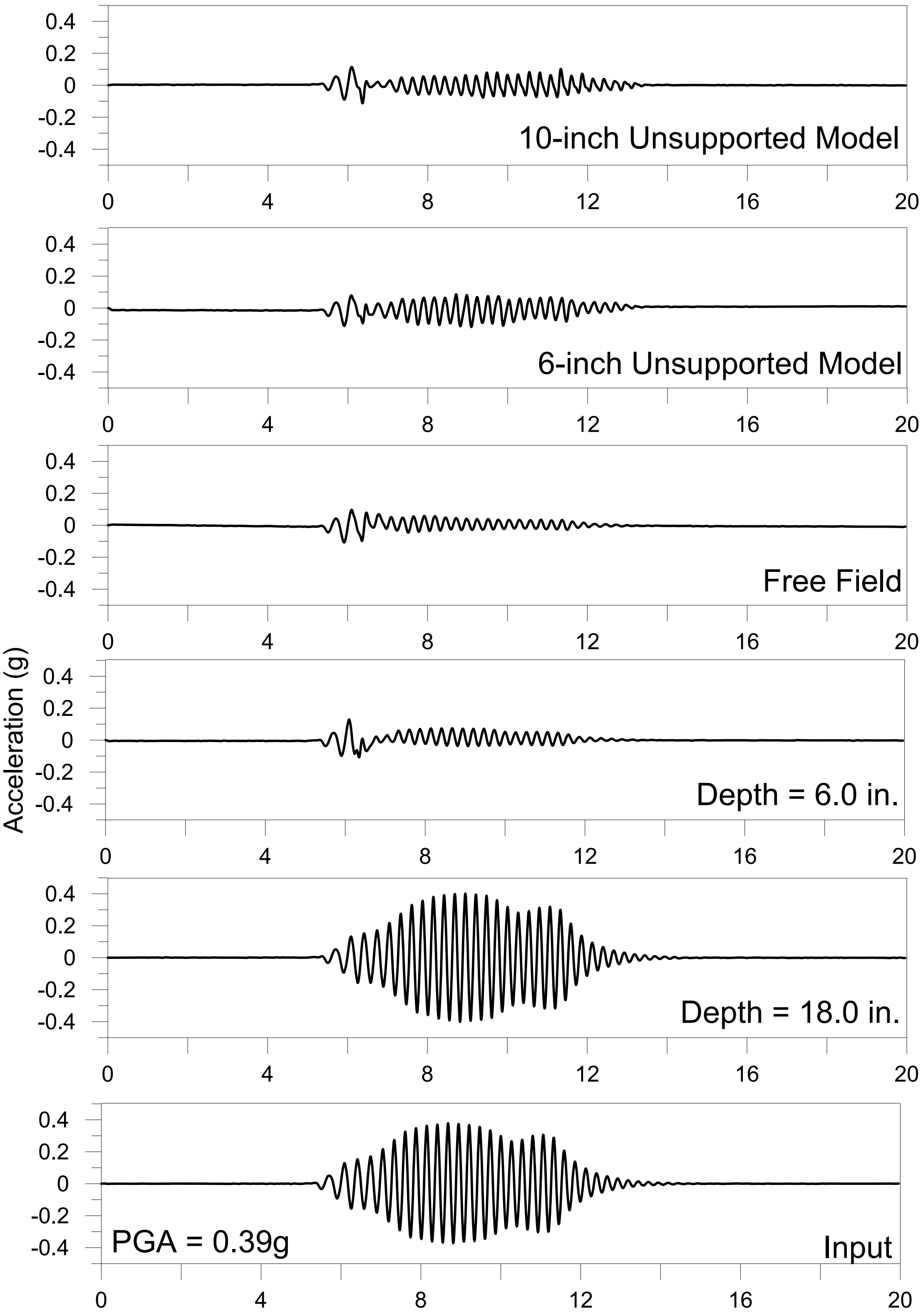

Test #49 (October 5, 2016)

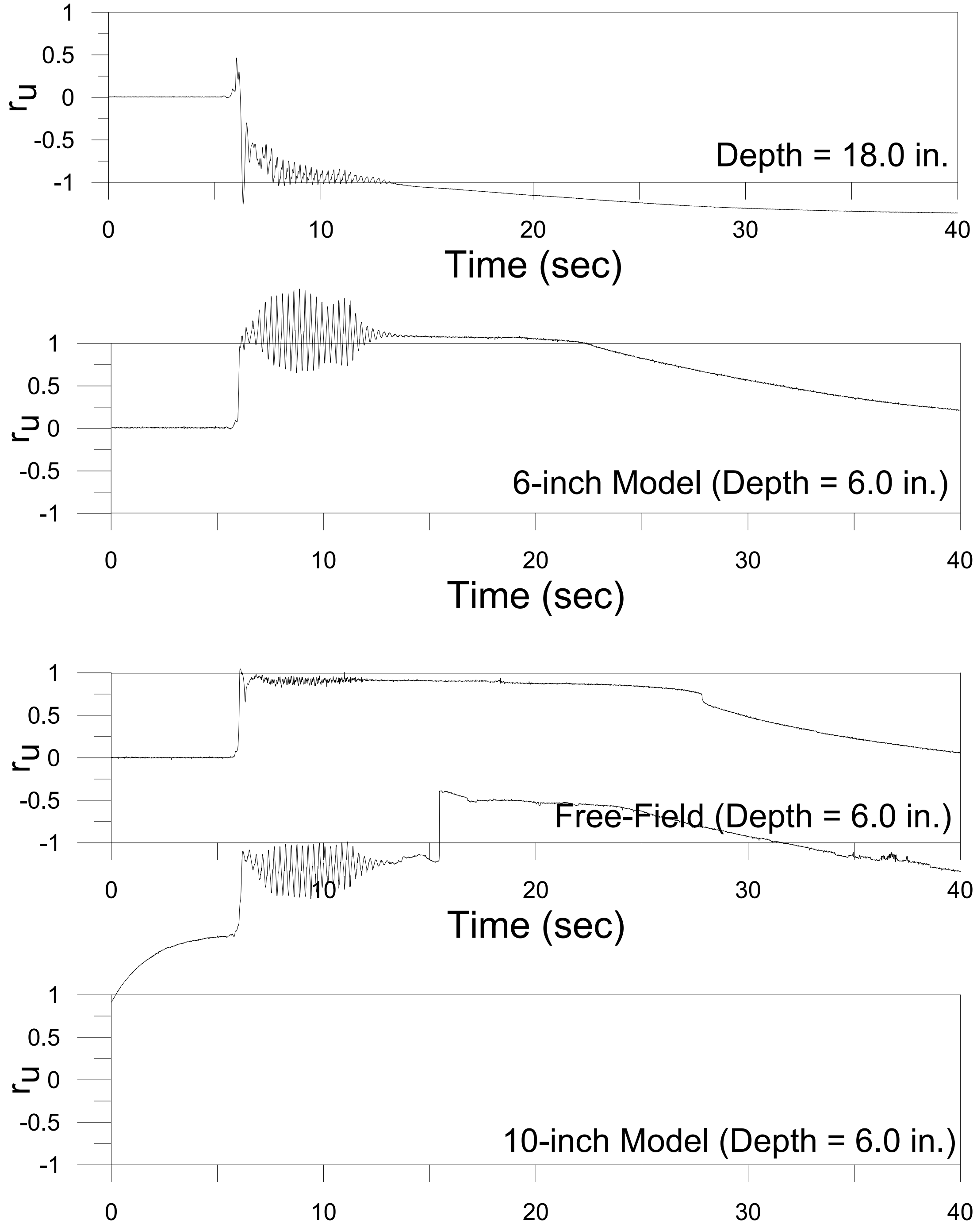

PGA = 0.39g

Test # 49: Ground Motion Characteristics
10/5/2016
PGA: 0.39g

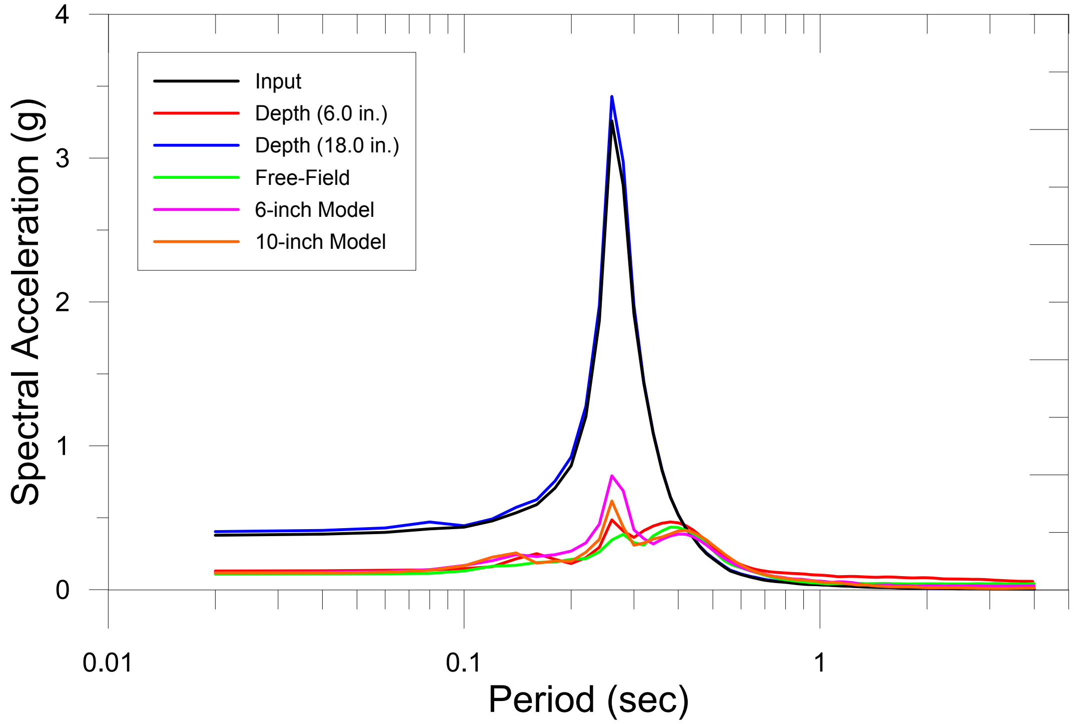

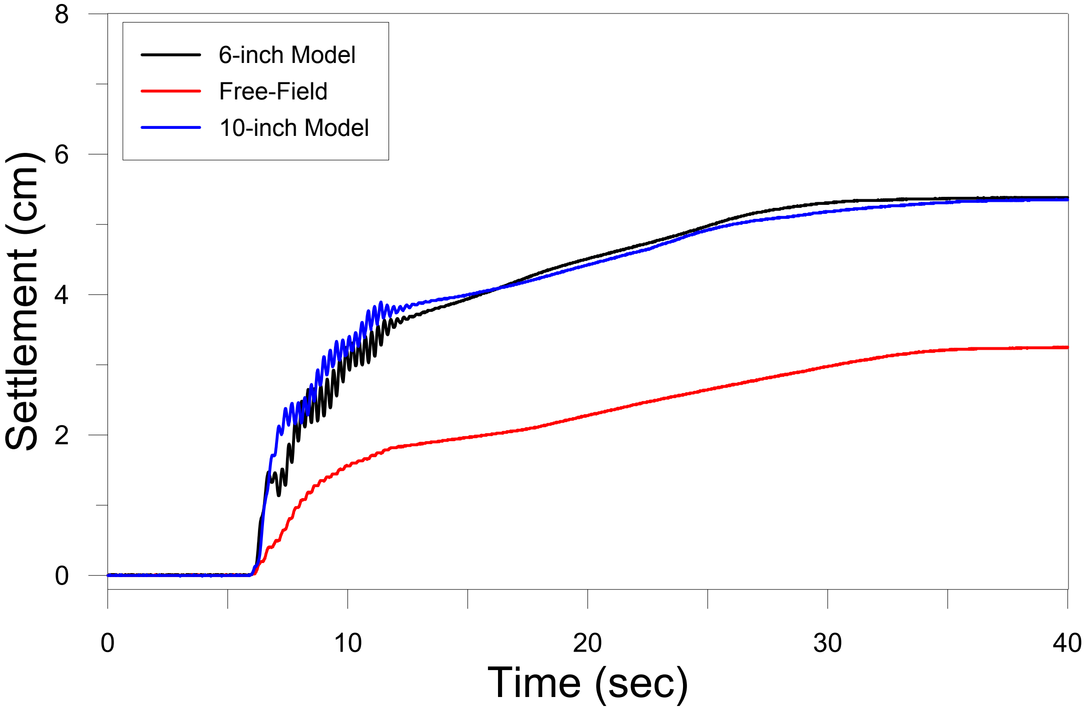

Test # 49: Settlement (cm)
10/5/2016
PGA: 0.39g

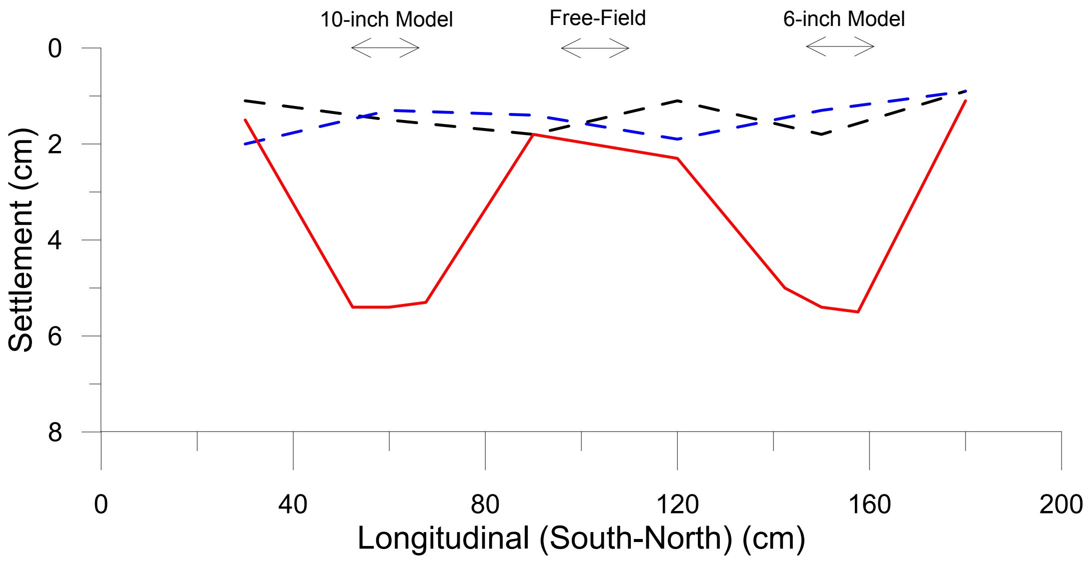

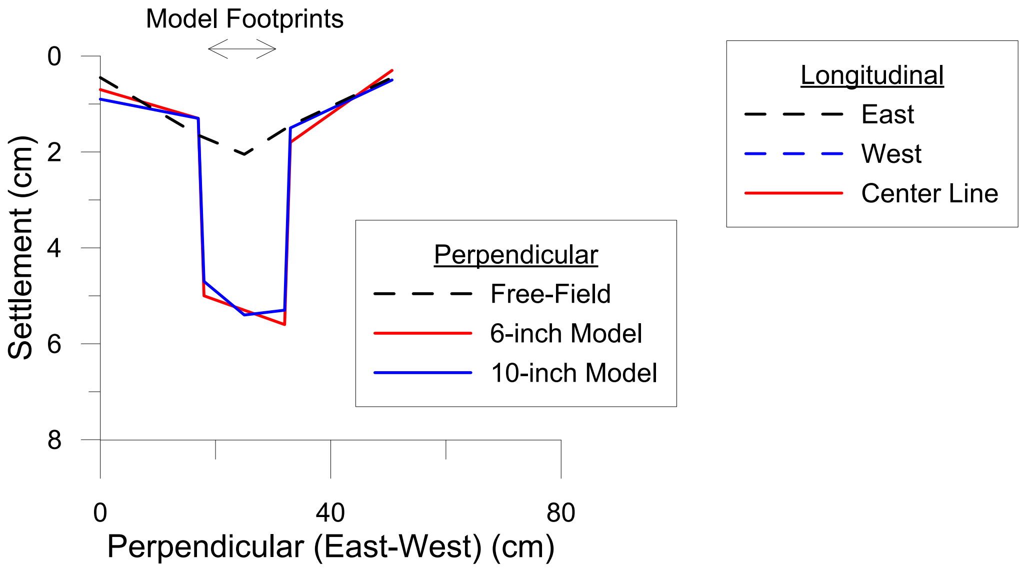

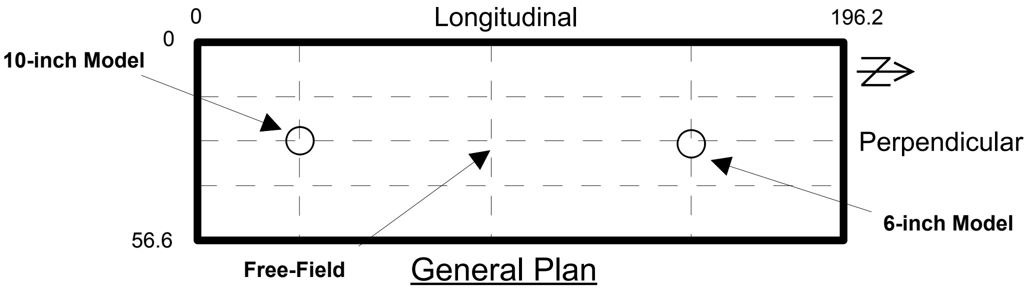

Test #50 (October 14, 2016)

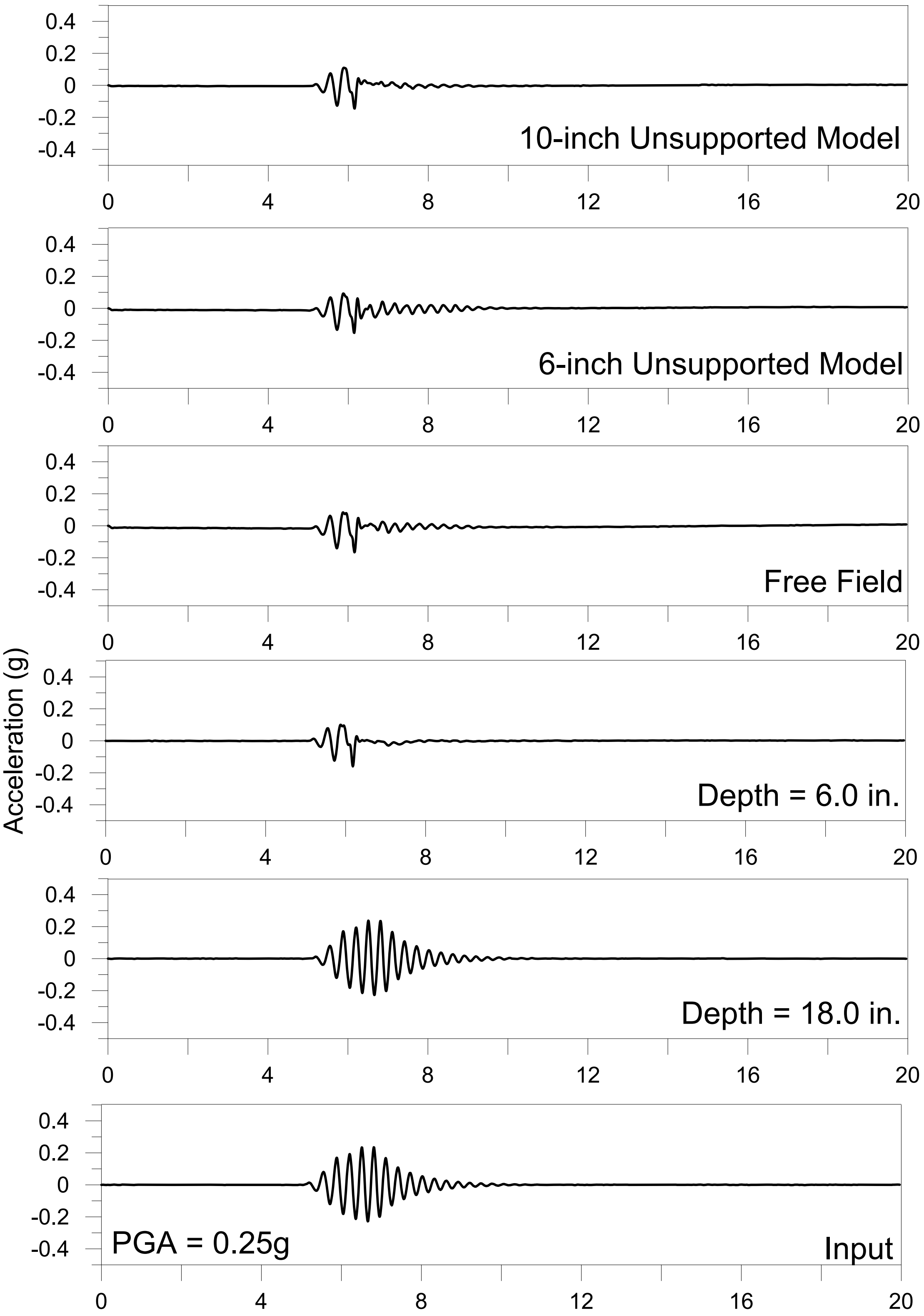

Test #50 (October 14, 2016)

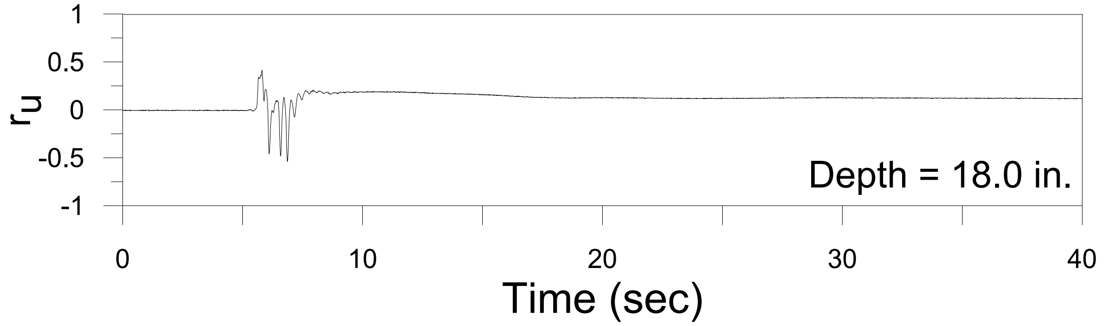

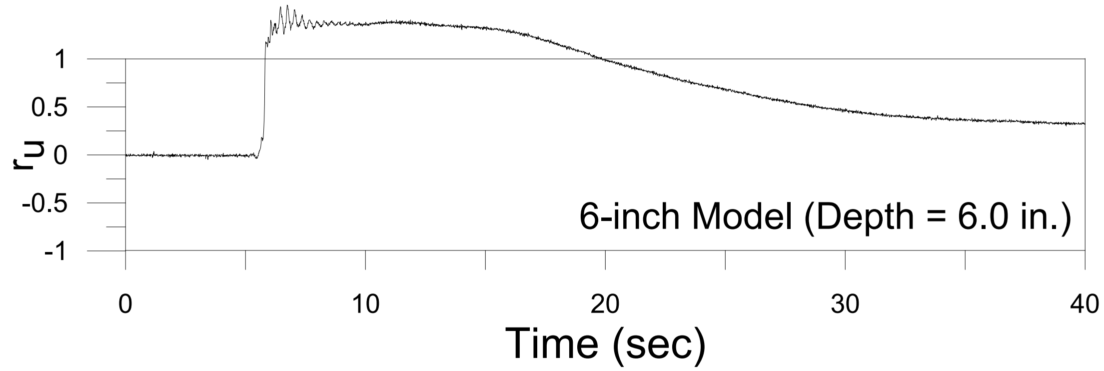

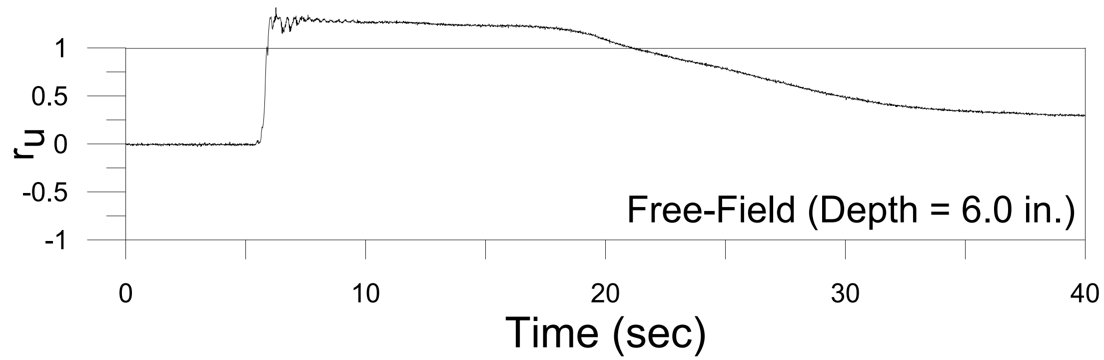

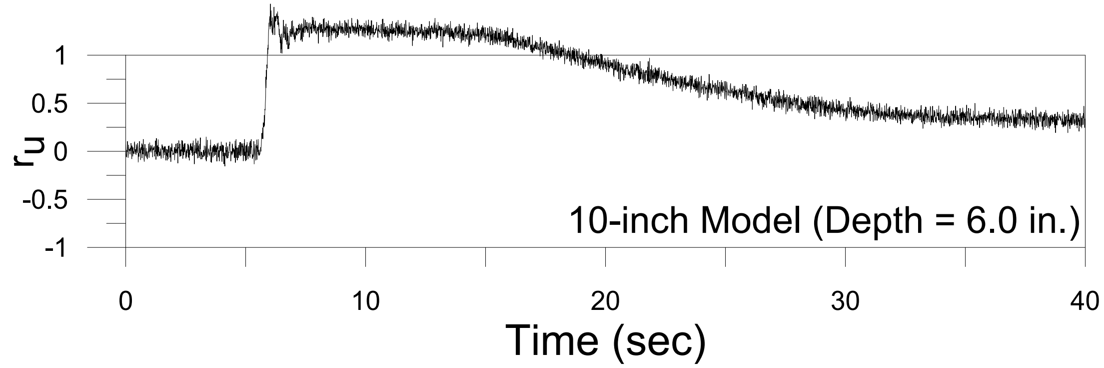

PGA = 0.25g

Test # 50: Ground Motion Characteristics
10/14/2016
PGA: 0.25g

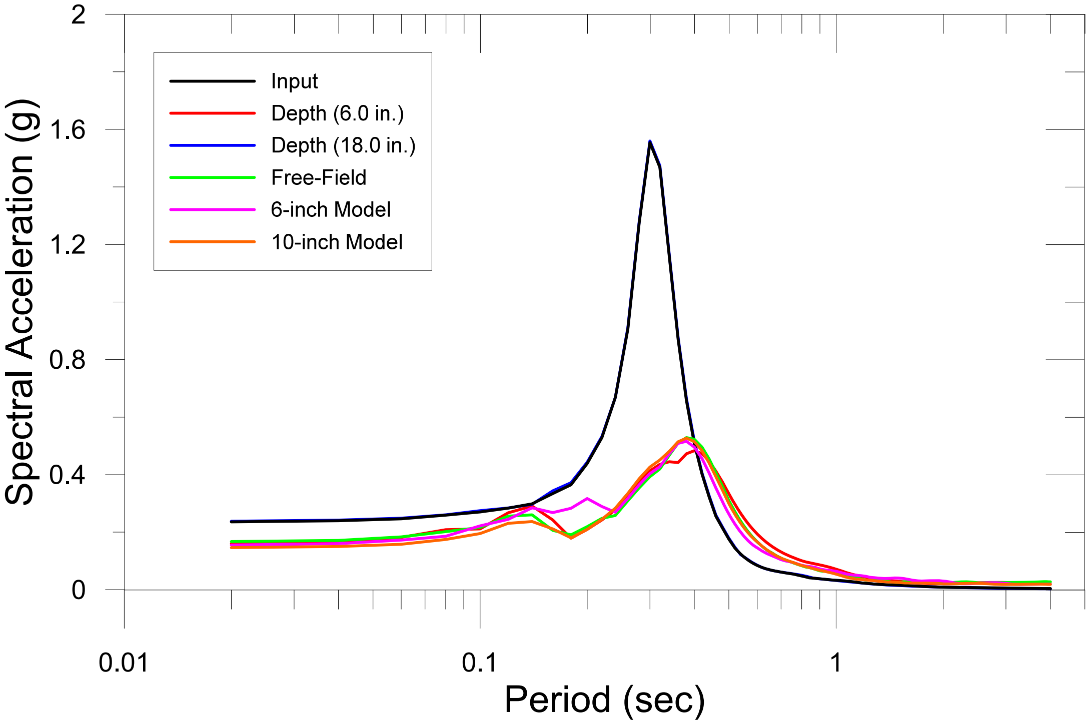

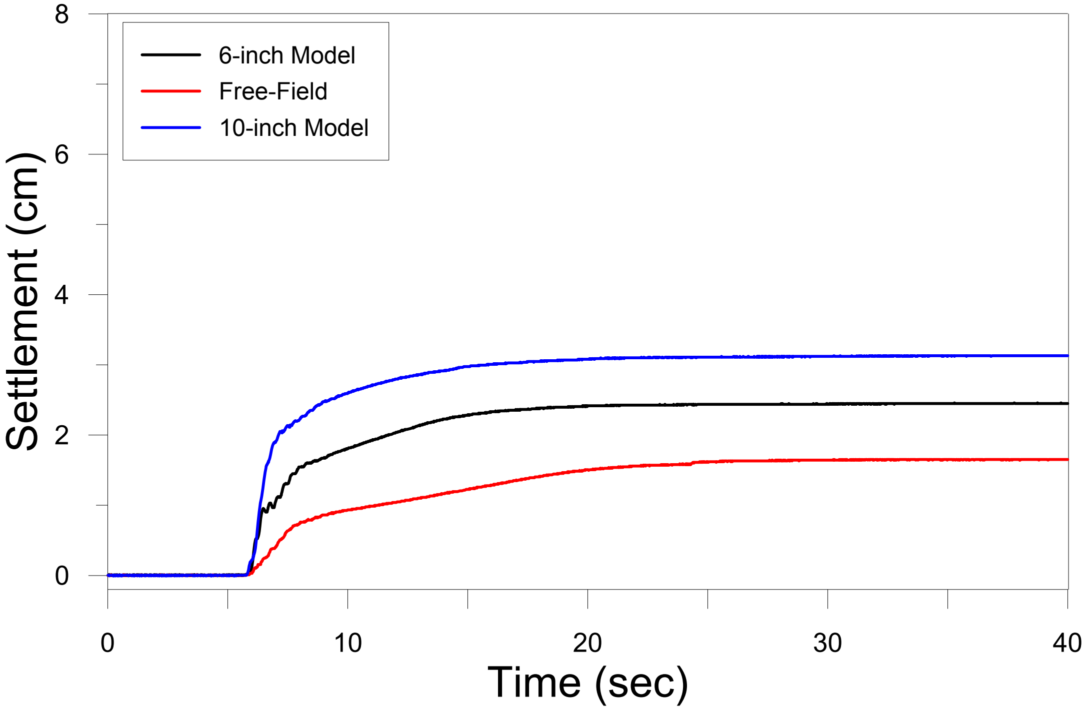

Test # 50: Settlement (cm)
10/14/2016
PGA: 0.25g

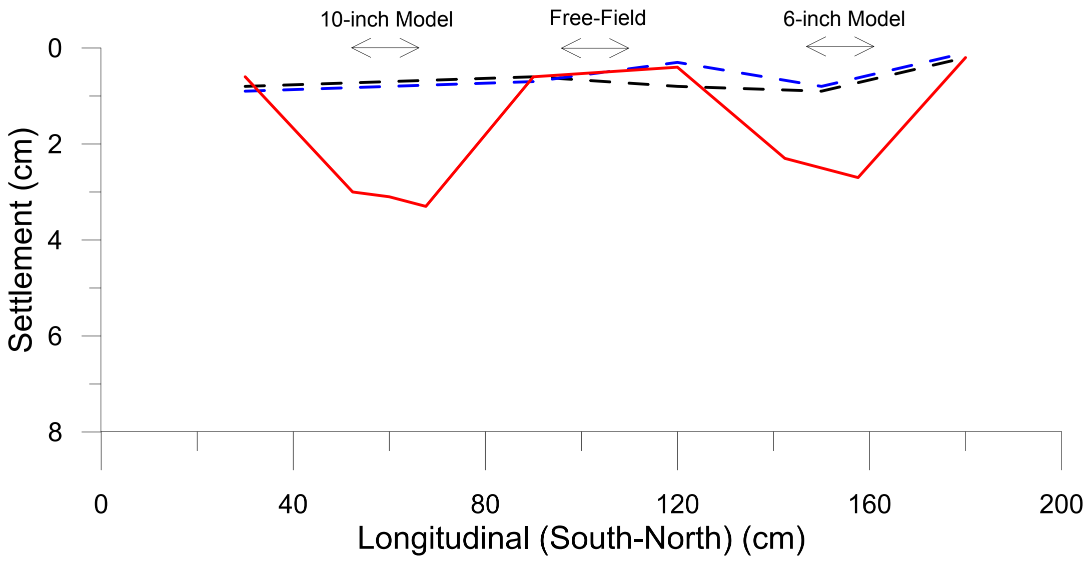

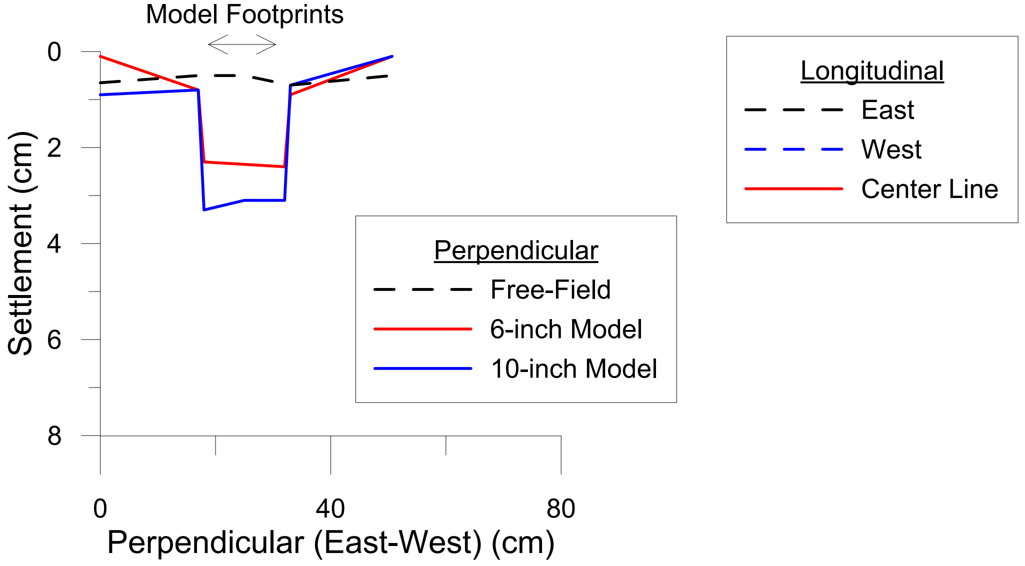

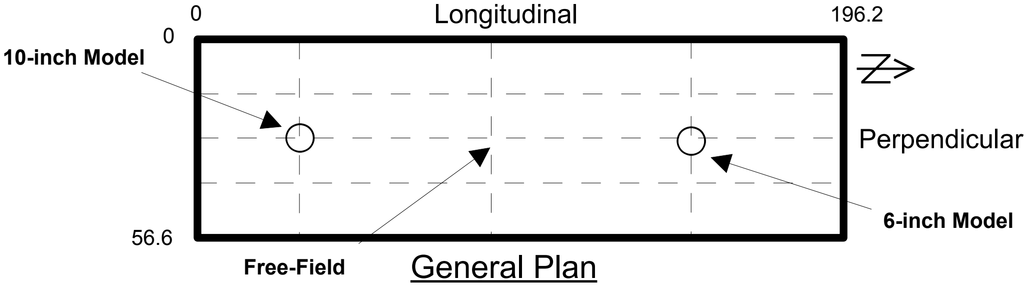

Test #51 (October 21, 2016)

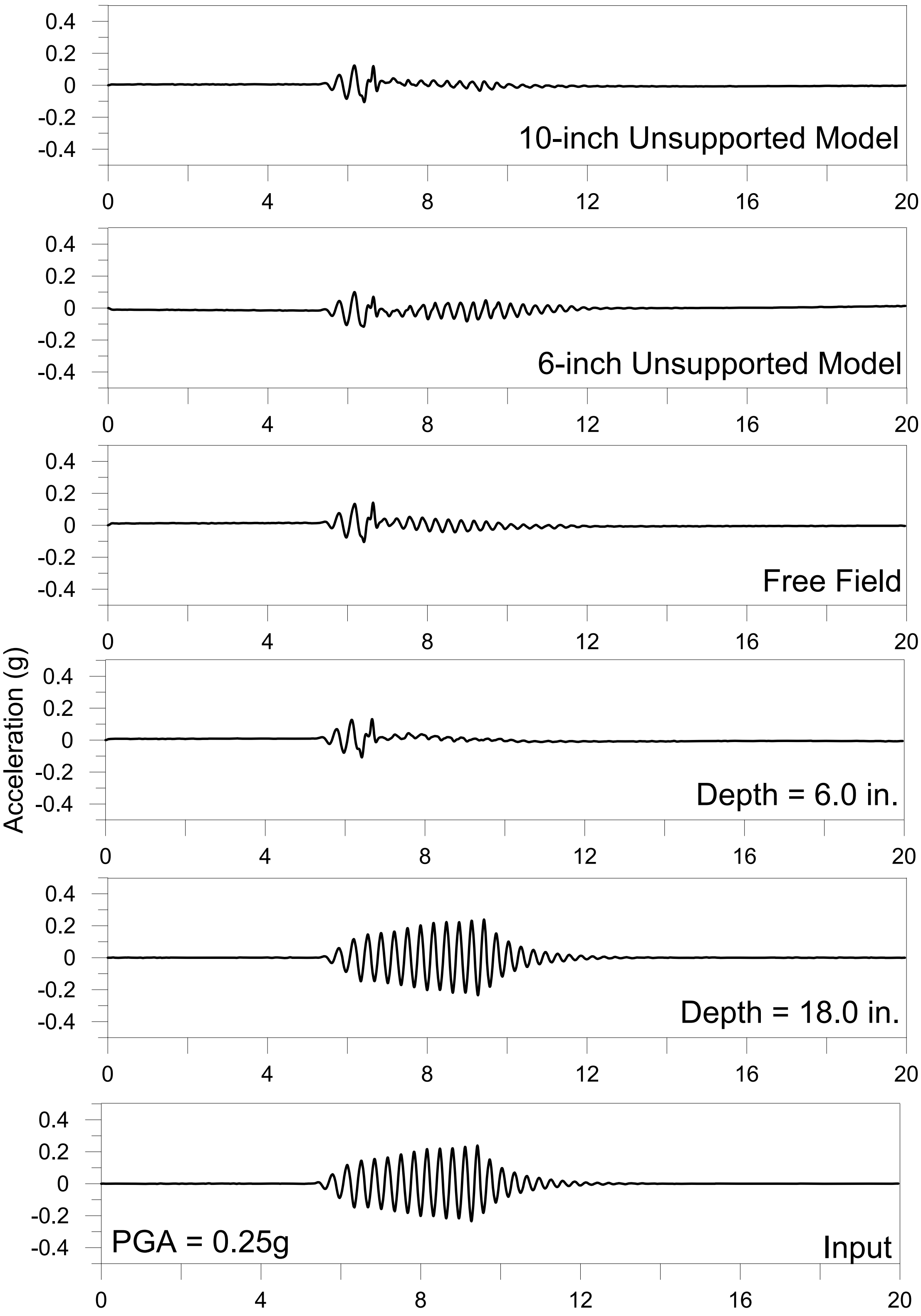

Test #51 (October 21, 2016)

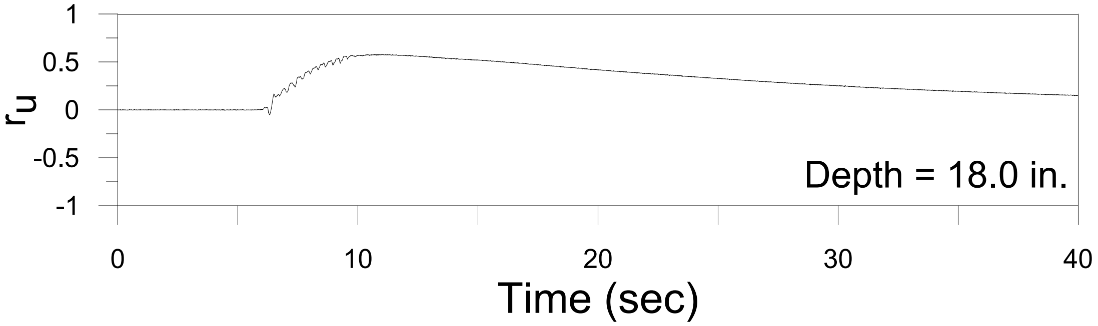

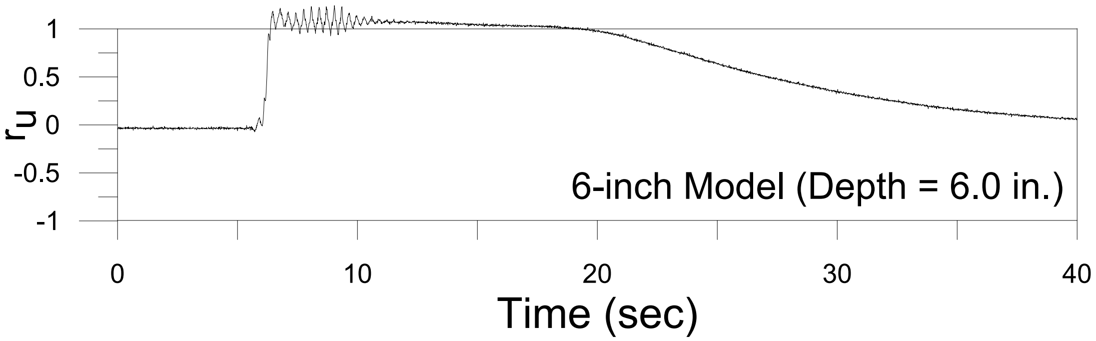

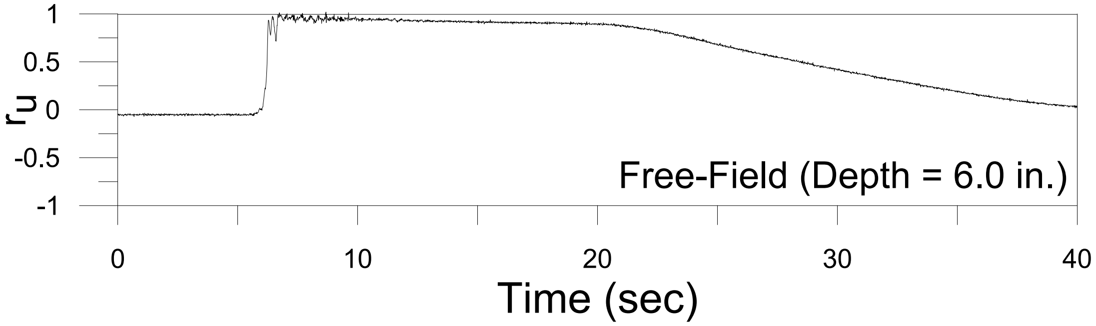

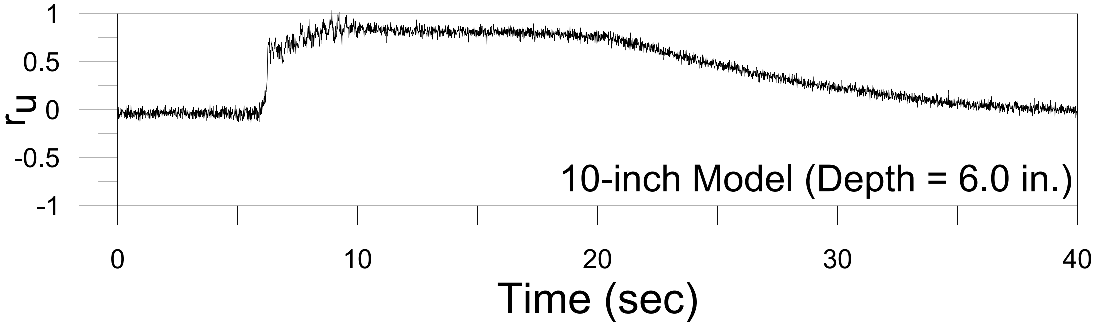

PGA = 0.25g

Test # 51: Ground Motion Characteristics
10/24/2016
PGA: 0.25g

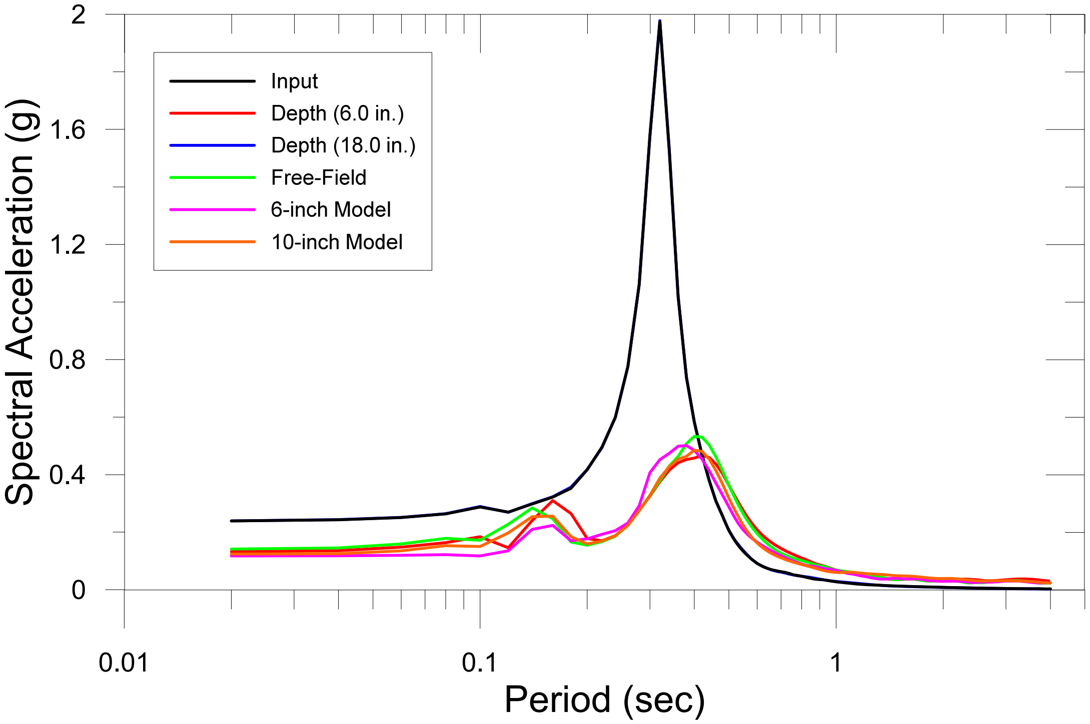

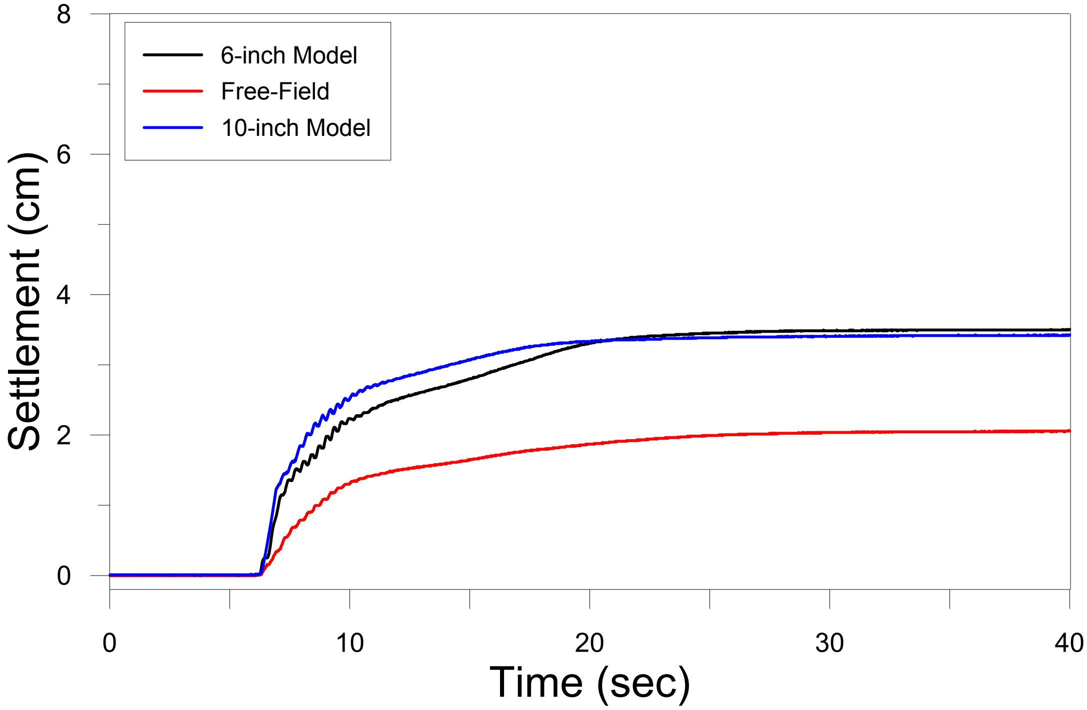

Test # 51: Settlement (cm)
10/21/2016
PGA: 0.25g

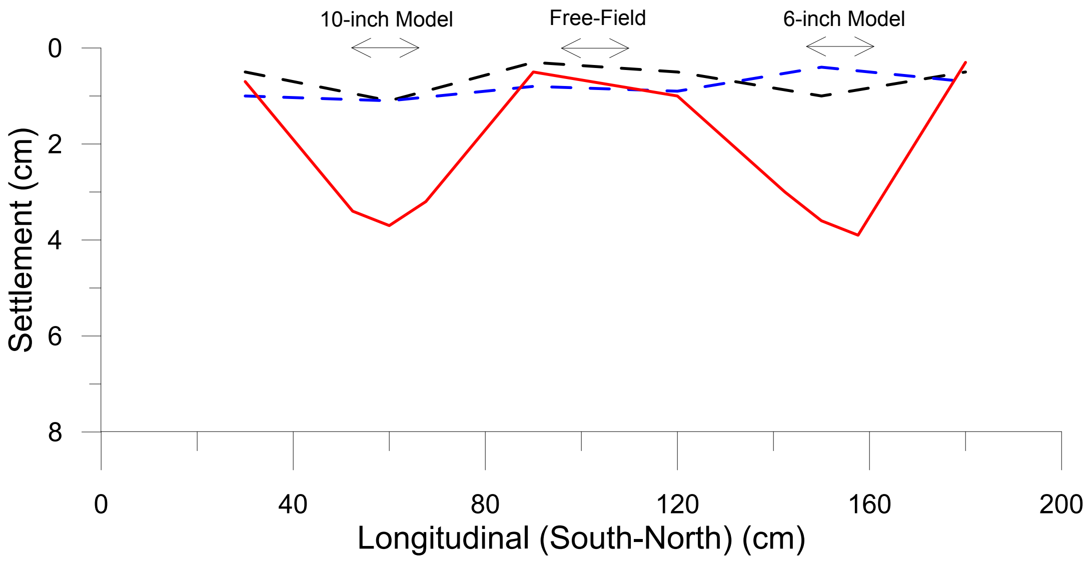

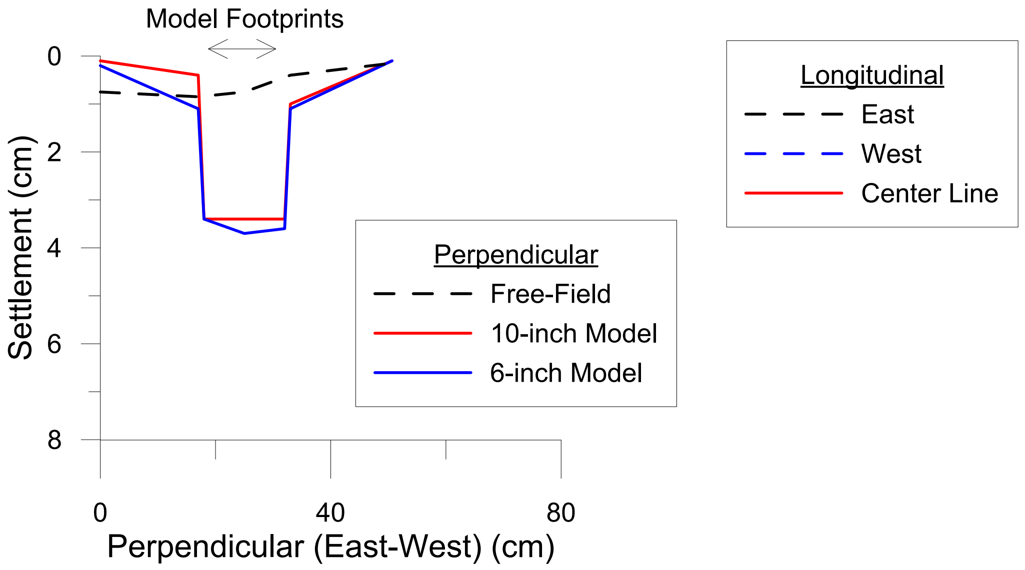

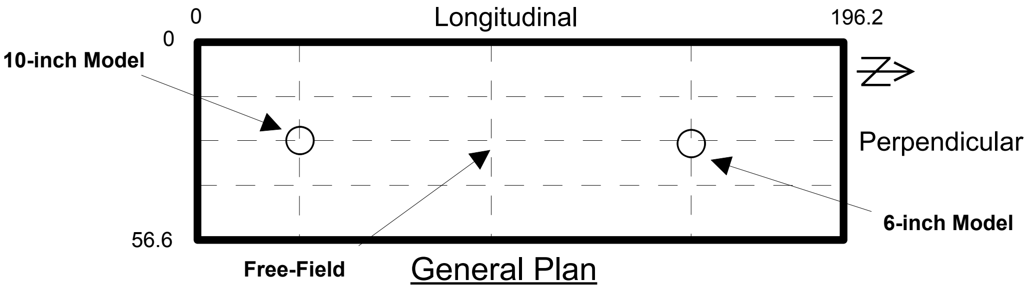

Test #52 (October 24, 2016)

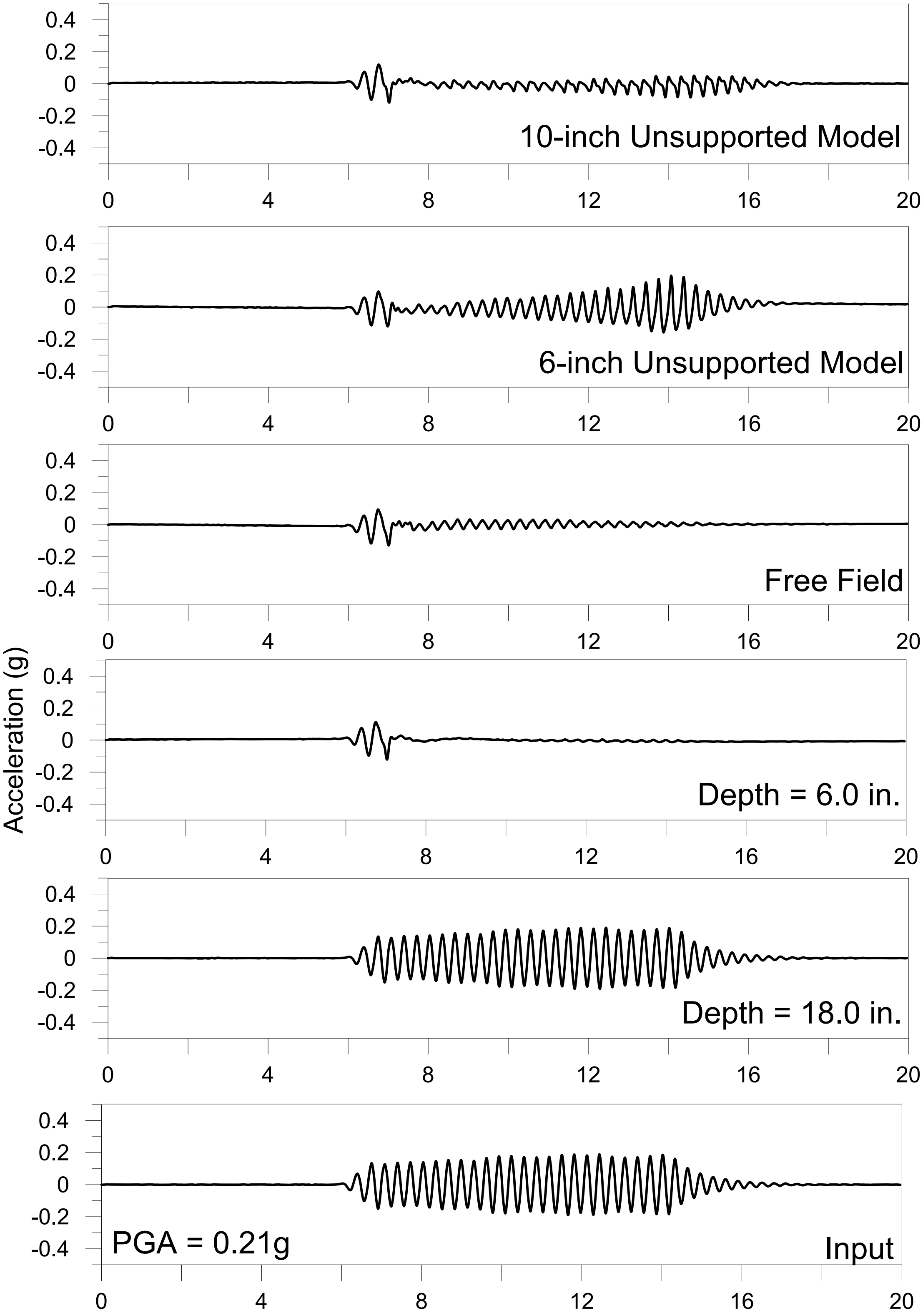

Test #52 (October 24, 2016)

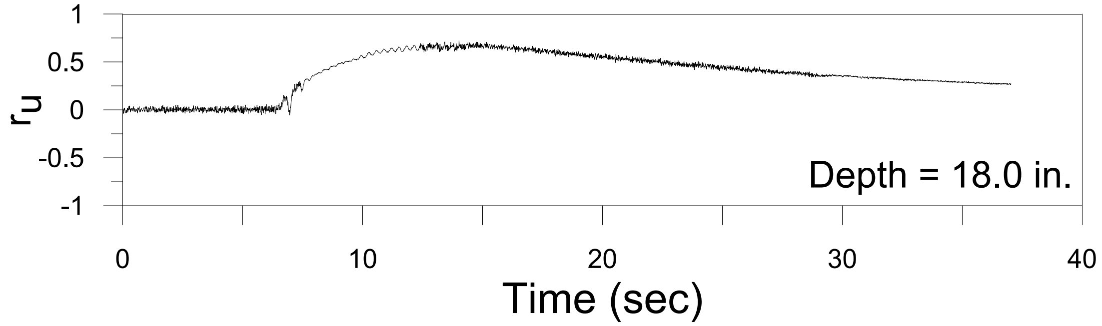

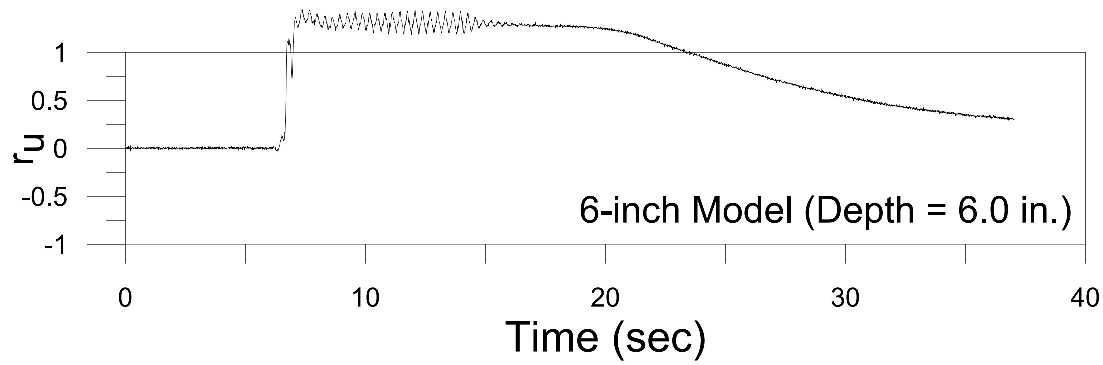

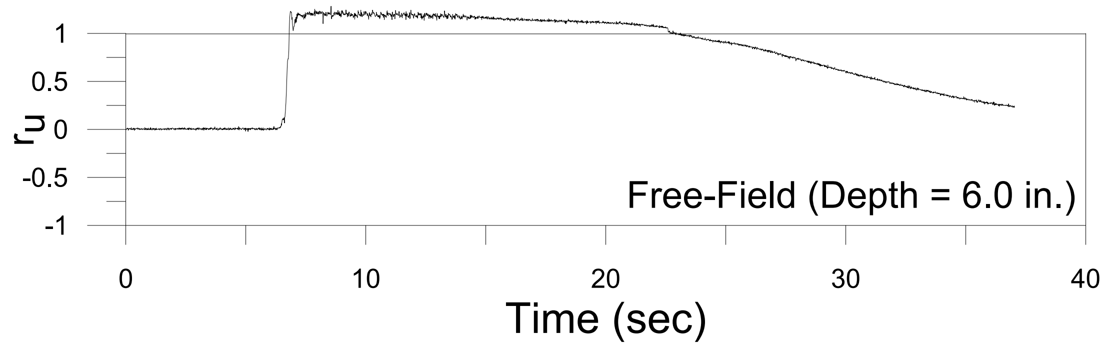

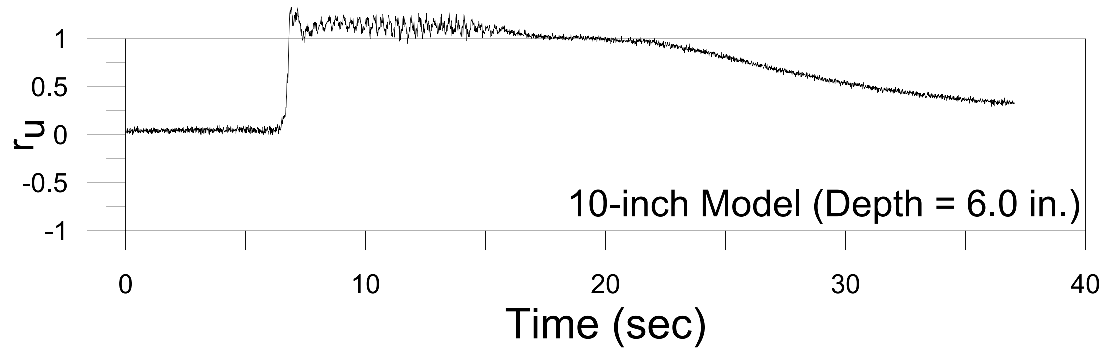

PGA = 0.21g

Test # 52: Ground Motion Characteristics
10/24/2016
PGA: 0.21g

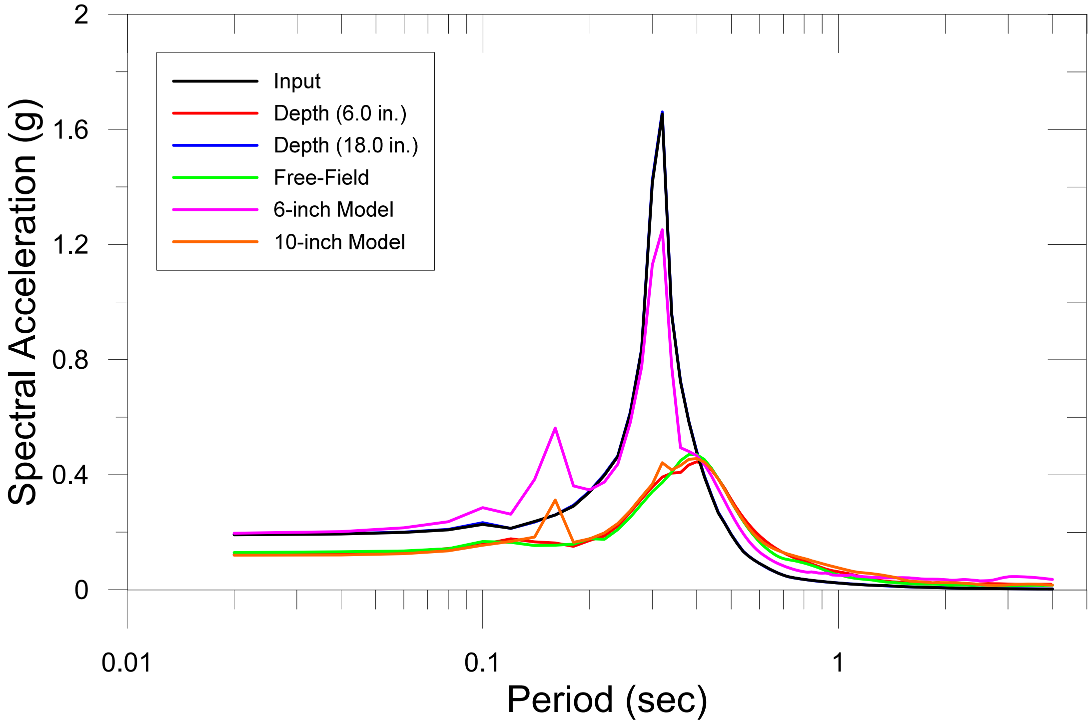

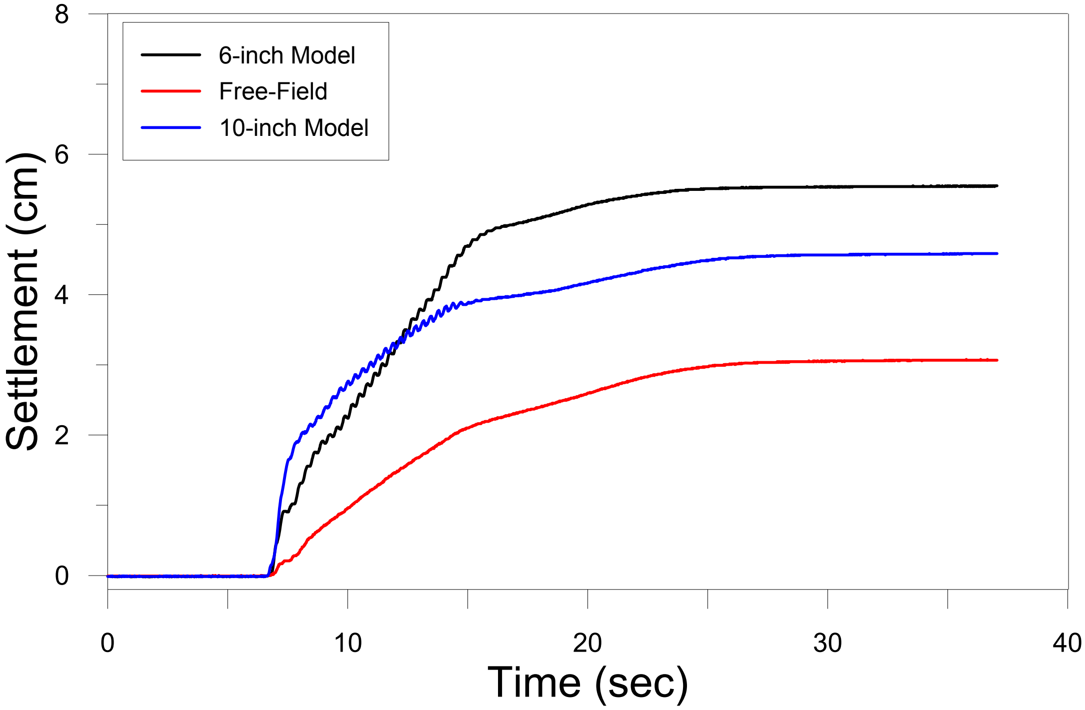

Test # 52: Settlement (cm)
10/24/2016
PGA: 0.21g

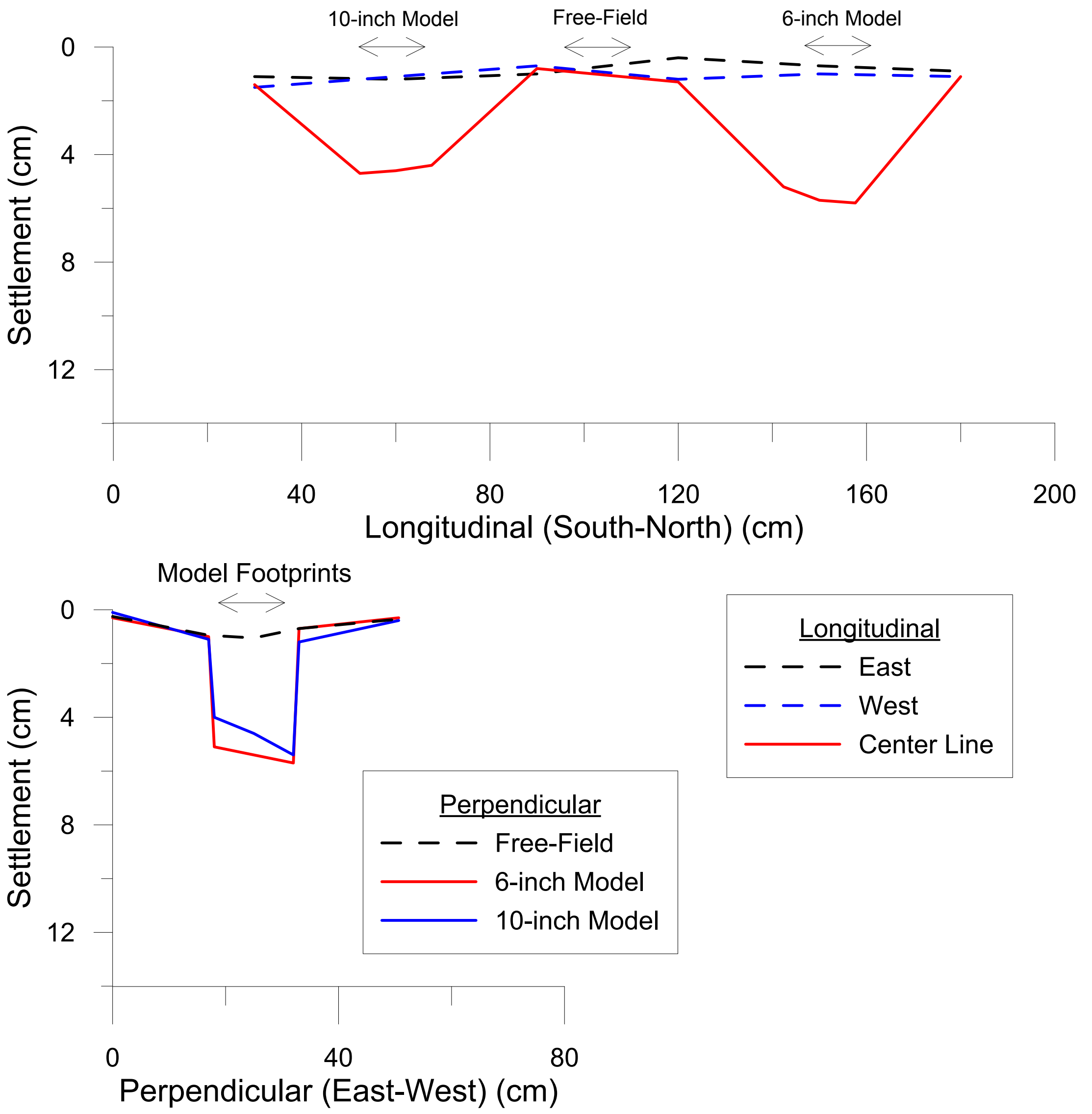

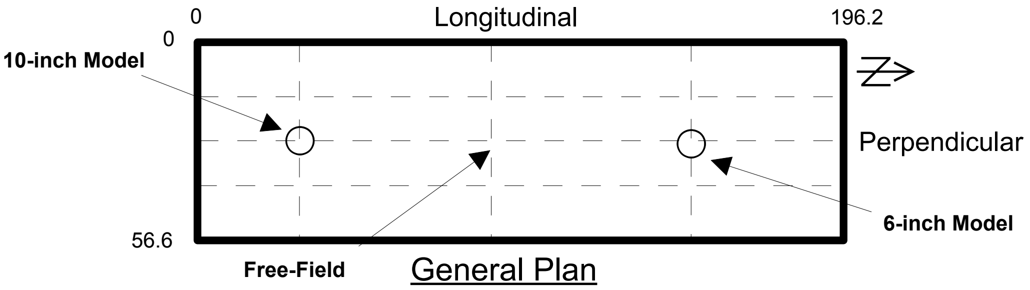

General Plan

Test #53 (October 31, 2016)

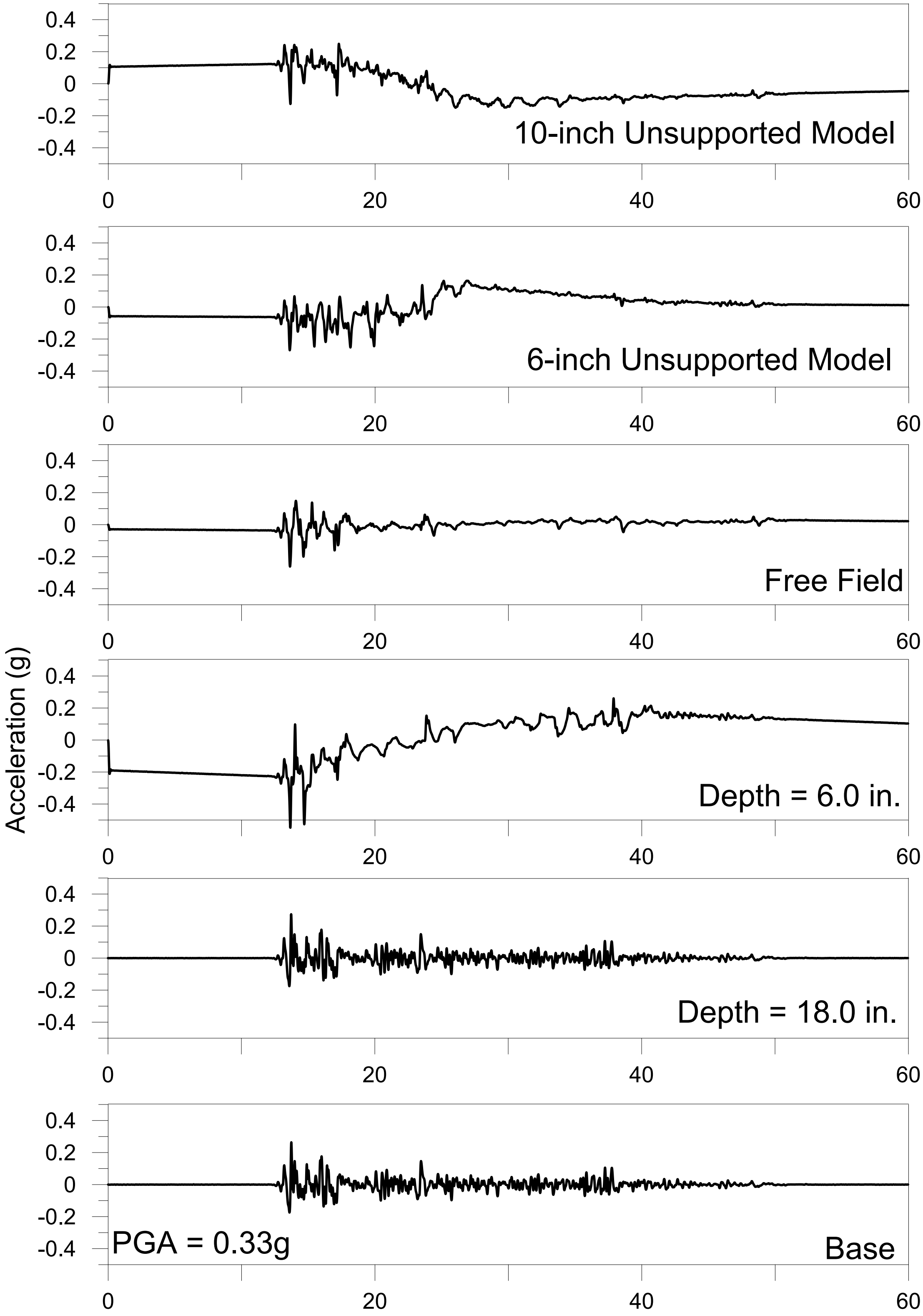

Test #53 (October 31, 2016)

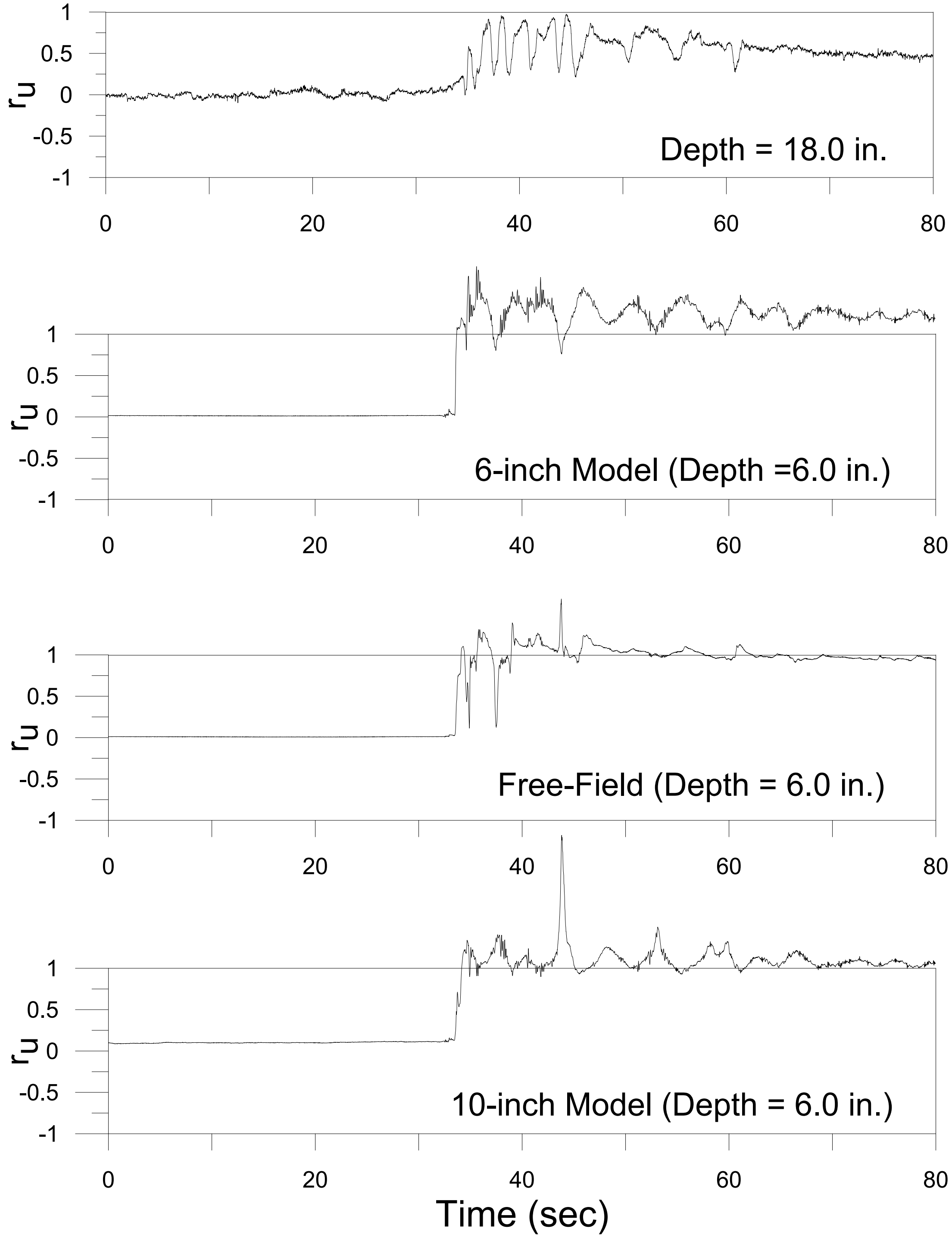

PGA = 0.33g

Test # 53: Ground Motion Characteristics
10/31/2016
PGA: 0.33g

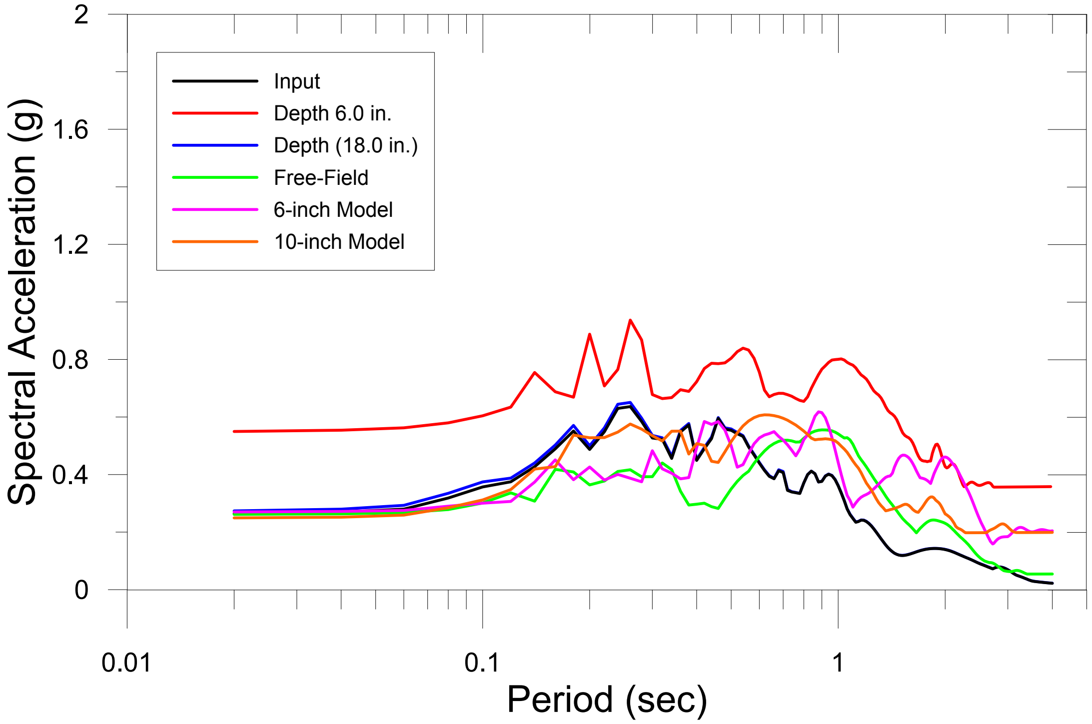

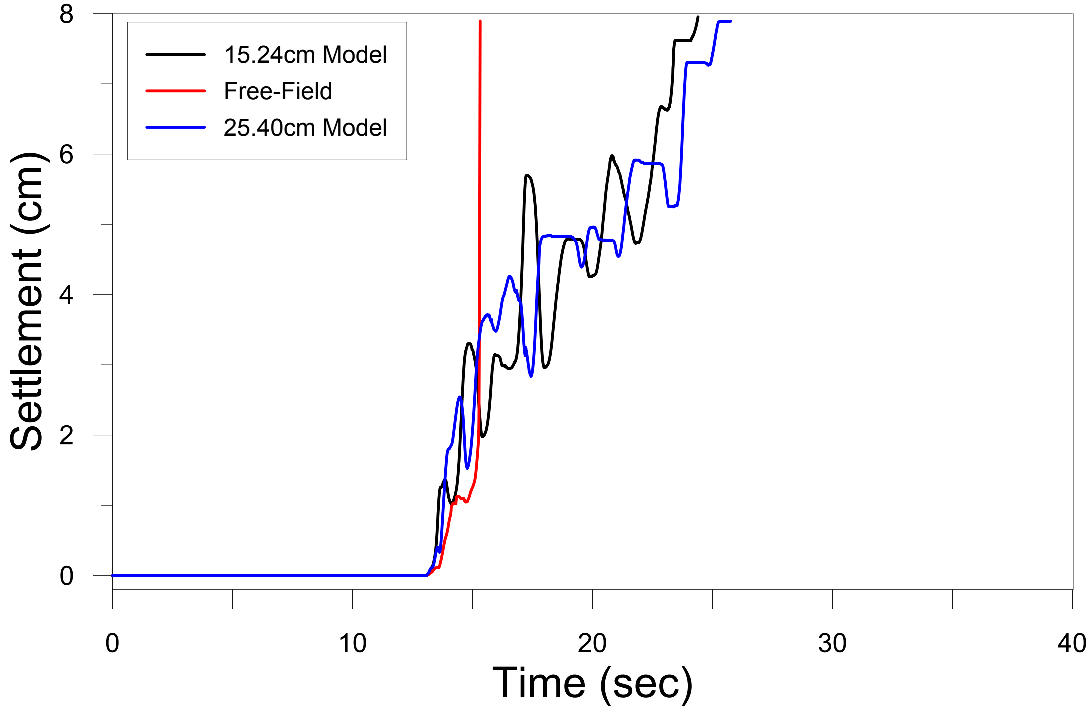

Test # 53: Settlement (cm)
10/31/2016
PGA: 0.33g

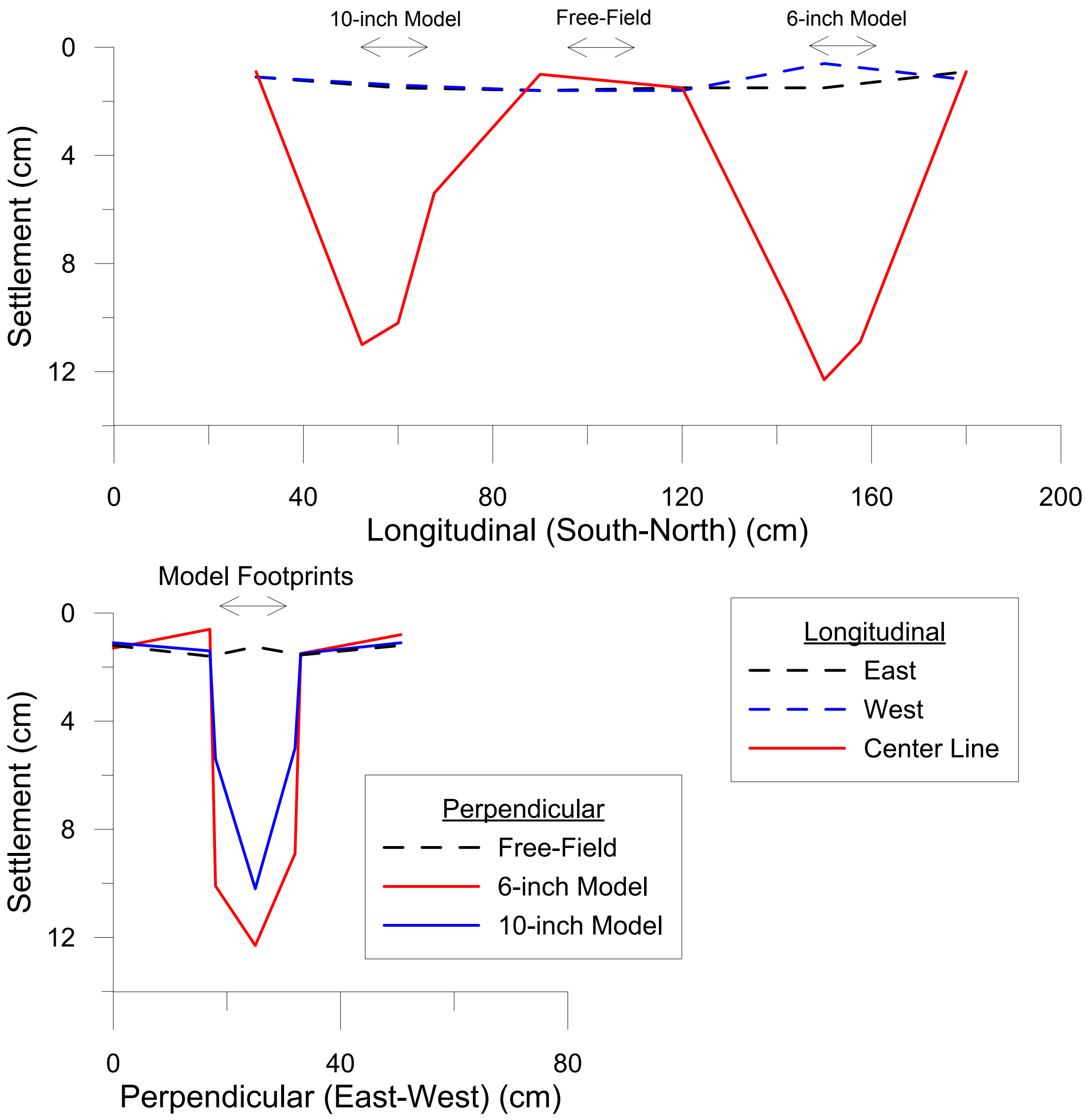

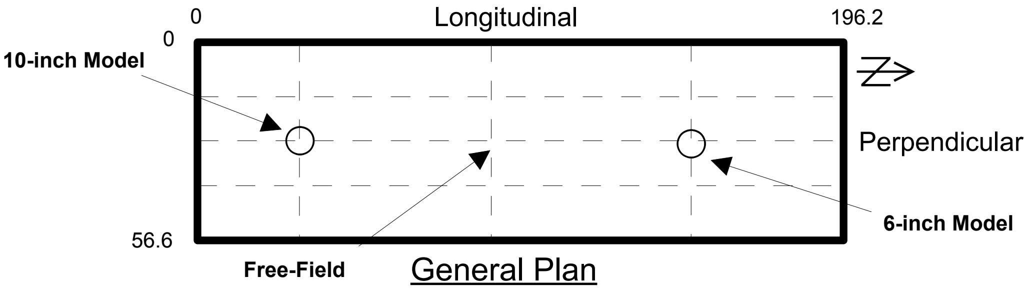

General Plan

Appendix B – Testing Summary Table

Phase	Test #	Date	Soil and Foundation Model Configuration							Instrumentation			Observed Base Parameters		Observed Settlement			Theoretical Settlement (Free-Field)	
			Model Scale Factor	Dr	HL	HD	D_F	Contact Pressure (Unsupported/Supported)	Helical Pier	Accelerometers	Pressure Sensors	LVDT	PGA	Shaking Duration	Free-Field (avg.)	Model Building	LVDT (#1, #2, #3)	Tokimatsu and Seed (1987)	Ishihara and Yoshimine (1992)
				(%)	(ft)	(ft)	(ft)	(psf)	#	#	#	#	(g)	(sec)	(in)	(in)	(in)	(in)	(in)
Phase 1	1	8/12/2015	10	35	1	1	0.75	--	--	--	--	-	0.23	14.50	--	--	--	0.612	0.810
	2	8/20/2015	10	35	1	1	0.75	--	--	--	--	-	0.22	10.05	--	--	--	0.612	0.810
	3	8/25/2015	10	35	1	1	--	--	--	--	--	-	0.44	8.7	--	--	--	0.636	0.870
	4	9/4/2015	10	35	1	1	--	--	--	--	--	-	0.03	15.9	--	--	--	0.492	0.600
	5	9/18/2015	10	35	1	1	0.5	--	--	4	--	-	0.36	4.6	--	--	--	0.636	0.870
	6	9/25/2015	10	35	1	1	0.5	25	--	5	--	-	0.40	7.8	0.961	1.22*	--	0.636	0.870
	7	10/2/2015	10	35	1	1	0.5	--	--	5	--	-	0.44	6	0.602	2.087*	--	0.636	0.870
	8	10/7/2015	10	35	1	1	0.5	--	--	5	--	-	0.38	6.88	0.638	1.953*	--	0.636	0.870
	9	10/30/2015	10	35	1	1	0.75	--	--	5	--	-	0.36	8.35	0.657	1.134*	--	0.636	0.870
Phase 2	10	11/6/2015	20	35	1	1	0.5	--	--	5	--	-	0.31	5.3	0.531	1.354*	--	0.624	0.870
	11	11/13/2015	20	35	0.5	0.5	0.5	--	--	5	--	-	0.30	14.25	0.370	3.567*	--	0.312	0.435
	12	11/20/2015	20	35	0.5	0.5	0.5	--	--	5	--	-	0.33	4.65	0.248	1.252*	--	0.315	0.435
	13	12/1/2015	15	35	0.5	0.5	0.5	--	--	5	1	-	0.30	13.5	0.280	1.205*	--	0.312	0.435
	14	12/8/2015	20	35	0.5	0.5	0.5	--	--	5	1	-	0.20	15.9	0.307	1.795*	--	0.300	0.375
	15	12/11/2015	20	35	0.5	0.5	0.5	--	--	5	--	-	0.16	11.75	0.201	1.173*	--	0.246	0.300
	16	12/15/2015	20	35	0.5	0.5	0.5	--	--	5	--	-	0.17	12.5	0.008	0.039*	--	0.246	0.300
	17	12/18/2015	20	35	0.5	0.5	0.5	--	--	5	--	-	0.17	8.85	0.189	1.323*	--	0.246	0.300
	18	1/5/2016	10	35	0.5	0.5	0.5	13.17	--	5	--	-	0.39	11	0.291	1.323*	--	0.318	0.435
	19	1/8/2016	10	35	0.5	0.5	0.5	13.17	--	5	--	-	0.37	20	0.213	1.008*	--	0.318	0.435
	19.1	1/22/2016	10	35	0.5	0.5	0.5	13.17	--	5	--	-	0.36	6.75	0.224	1.102*	--	0.318	0.450
	19.2	2/5/2016	10	35	0.5	0.5	0.5	13.17	--	5	1	-	0.34	5.75	0.193	1.102*	--	0.315	0.450
	20	1/12/2016	10	35	0.5	0.5	0.5	13.17	--	5	--	-	0.36	6.75	0.173	1.276*	--	0.318	0.450
	21	1/14/2016	10	35	0.5	0.5	0.5	13.17	--	5	--	-	0.37	5.25	0.189	1.26*	--	0.318	0.450
	22	1/20/2016	10	35	0.5	0.5	0.67	12.36	--	5	--	-	0.34	5.75	0.193	1.276*	--	0.315	0.450
	22.1	2/12/2016	10	35	0.5	0.5	0.67	12.36	--	5	1	-	0.34	6.96	0.185	1.339*	--	0.315	0.450
	23	2/19/2016	10	35	0.5	0.5	0.83	12.79	--	5	1	-	0.33	6.85	0.209	1.362*	--	0.315	0.450
	24	2/26/2016	10	35	0.5	0.5	1	12.92	--	5	1	-	0.34	6.01	0.173	1.402*	--	0.315	0.450
	25	3/1/2016	10	35	0.5	0.5	0.25	11.67	--	5	1	-	0.33	6.45	0.220	0.669*	--	0.315	0.450
	26	3/9/2016	10	35	0.5	0.5	0.375	12.05	--	5	1	-	0.37	5.64	0.248	1.205*	--	0.318	0.450
	27	3/16/2016	10	35	0.75	0.25	0.25	12.5	--	5	1	-	0.49	5.36	0.299	0.85*	--	0.399	0.525
	28	3/18/2016	10	35	0.75	0.25	0.375	12.05	--	5	1	-	0.44	5.11	0.323	1.047*	--	0.399	0.525
	29	3/24/2016	10	35	0.75	0.25	0.5	12.59	--	5	1	-	0.5	5.61	0.374	1.323*	--	0.399	0.525
Phase 3	30	4/1/2016	10	35	1	1	0.25	12.2	4	5	1	-	0.3	9.1	0.476	0.055-Helical	--	0.624	0.900
	31	4/20/2016	10	35	1	1	0.5	12.77(12.43)	4	6	1	-	(Note 1)	-	0.406	2.024(0.055)**	--	--	--
	32	5/12/2016	10	35	1	1	0.5	13.2(12.65)	3	6	1	-	0.33	4.46	0.417	1.732(0.055)**	--	0.630	0.900
	33	6/15/2016	10	35	1	1	0.5	12.5	3	6	1	-	0.18	5.73	0.331	1.543(0.004)**	--	0.600	0.600
	34	6/22/2016	10	35	1	1	0.5	12.5	3	6	1	1	0.26	4.65	0.437	2.150(0.087)**	2.35-F.F.	0.618	0.858
	35	7/1/2016	10	35	1	1	0.5	12.5	3	6	4	3	0.14	5.54	0.343	1.835(0.039)**	(1.661 / 0.831 / 0.004)*	0.492	0.600
	36	7/15/2016	10	35	1	1	0.5	12.5	3	6	4	3	0.25	4.93	0.319	1.598(0.016)**	(1.618 / 1.091 / 0.008)*	0.618	0.852
	37	7/22/2016	10	35	1	1	0.5	12.5	3	6	4	3	0.2	5.26	0.358	2.087(0.031)**	(2.098 / 1.350 / 0.008)*	0.600	0.750
	38	7/27/2016	10	35	1	1	0.5	12.5	3	6	4	3	0.26	4.73	0.311	2.457(0.079)**	(2.327 / 1.512 / 0.047)*	0.618	0.858
	39	8/4/2016	10	35	1	1	0.75	--	3	6	4	3	0.29	4.31	0.358	1.693(0.094)**	(1.693 / 1.150 / 0.075)*	0.624	0.900
	40	8/9/2016	10	35	1	1	0.25	13.54(13.8)	3	6	4	3	0.279	5.02	0.413	2.693(0.039)**	(2.752 / 1.323 / 0.035)*	0.624	0.900
	41	8/17/2016	10	35	1	1	0.375	12.58(12.45)	3	6	4	3	0.335	4.25	0.409	2.307(0.024)**	(2.201 / 1.555 / 0.024)*	0.630	0.900
	42	8/27/2016	10	35	1	1	0.67	12.71(12.83)	3	6	4	3	0.276	4.65	0.374	1.677(0.228)**	(Note 2)	0.618	0.900
	43	9/9/2016	10	35	1	1	0.83	12.82(12.84)	3	6	4	3	0.259	4.53	0.346	1.543(0.087)**	(1.571 / 1.012 / 0.094)*	0.618	0.858
	44	9/16/2016	10	25	1	1	0.5	12.5(11.7)	3	6	4	3	0.234	4.78	0.358	2.173(0.039)**	(2.378 / 1.492 / 0.012)*	0.732	0.960
	45	9/19/2016	10	45	1	1	0.5	12.5(11.7)	3	6	4	3	0.298	4.35	0.358	1.543(0.165)**	(1.591 / 1.362 / 0.039)*	0.492	0.780
	46	9/23/2016	10	55	1	1	0.5	12.5(11.7)	3	6	4	3	0.318	4.31	0.319	1.693(0.071)**	(1.642 / 1.193 / 0.047)*	0.396	0.672
	47	9/26/2016	10	35	1.25	0.75	0.5	12.5(11.7)	3	6	4	3	0.356	4.67	0.449	2.465(0.142)**	(2.535 / 1.606 / 0.063)*	0.713	0.975
	48	9/30/2016	10	35	1.50	0.50	0.5 (0.83)	12.5(12.82)	--	6	4	3	0.306	4.47	0.622	2.394(2.071)***	(2.728 / 1.925 / 1.795)*	0.792	1.050
	49	10/5/2016	10	35	1.67	0.33	0.5 (0.83)	12.5(12.82)	--	6	4	3	0.393	4.49	0.673	2.087(2.055)***	(2.126 / 1.287 / 2.122)**	0.851	1.099
	50	10/14/2016	10	35	1	1	0.5 (0.83)	12.5(12.82)	--	6	4	3	0.248	1.83	0.350	0.961(1.244)***	(0.969 / 0.654 / 1.236)**	0.612	0.852
	51	10/21/2016	10	35	1	1	0.5 (0.83)	12.5(12.82)	--	6	4	3	0.254	3.51	0.386	1.362(1.362)***	(1.386 / 0.819 / 1.354)**	0.612	0.852
	52	10/24/2016	10	35	1	1	0.5 (0.83)	12.5(12.82)	--	6	4	3	0.205	7.23	0.496	2.165(1.819)***	(2.185 / 1.213 / 1.811)**	0.600	0.750
Phase 4	53	10/31/2016	10	35	1	1	0.5 (0.83)	12.5(12.82)	--	6	4	3	0.329	24.25	0.752	4.063(2.913)***	(3.551 / 3.693 / 3.591)**	0.630	0.752

Notes: Dr - Relative Density of Liquefiable Layer
HL - Thickness of Liquefiable Layer
HD - Thickness of Non-Liquefiable Layer
D_F - Diameter of Model Foudation
Observed Building Settlement - * Unsupported Foundation, ** Unsupported Foundation(Helical Supported Foundation), *** 0.5ft Unsupported Foundation(0.83ft Unsupported Foundation)
Observed LVDT Settlement - *(Unsupported Foundation / Free-Field / Helical Supported Foundation), **(0.5ft Unsupported Foundation / Free-Field / 0.83ft Unsupported Foundation)
Note (1) - Data Acquisition Malfunction - No Instrument Data Recorded for Test #31, Only Manual Measurements.
Note (2) - Data Acquisition Malfunction - PWP and LVDT lost power to DAQ during testing, Data not Valid, Only Manual Measurements.

Appendix C – Laboratory Notes and Measurements

775-815
4149

Golder Associates
RENO, NEVADA

SUBJECT: Trial Test #1 Shake Table		
PROJECT No.:	PREPARED BY: J. Toth	DATE: 8/11/15
PHASE:	CHK/RVW BY:	SHEET of

lift #1 (~ Dr 60%) need 1075lbs
* assume sand is initial dry

$w(W_s) = W_w$
$w = 5\%$

	Tare (lbs)	Tare + W_s (lbs)	W_w (lbs)
1.	~~0~~	33.324	1.666
2.	~~0~~	22.311	1.115
3.	—	33.079	1.654
4.	—	32.743	1.637
5.	—	32.888	1.644
6.	—	5.485	0.274
7.	—	33.487	1.674
8	—	29.435 - 1.533 = 27.902	1.395
9.	—	33.728	1.686
10.		4.818	0.2409
11.		31.799	1.589
12.		34.815	1.740
13.		34.951	1.748
14.		1.567	0.078
15.		33.032	1.652
16.		32.745	1.637
17.		31.183	1.559
18.		34.464	1.723
19.		33.626	1.6813
20.		32.639	1.632
21.		3.130	0.1565
22.			
23.			
24.		29.330	
25.		34.346	
26.		34.645	
27.		2.374	5.0
28.		33.519	
29.		34.249	
30.	↓	28.155	4.8
		30.968	
		34.701	
		27.250	4.65
		33.406	
		34.293	
		30.661	
		9.731	5.4
		29.122	
		32.786	
		33.824	
		4.978	5.0

GEO 20

Golder Associates
RENO, NEVADA

SUBJECT: Trial Test #1 Shake Table
PROJECT No.:
PREPARED BY: J. Totz
DATE: 8/12/15
PHASE:
CHK/RVW BY:
SHEET of

Liquefiable layer

Ws
31.548
28.766
24.151
34.969
29.852
31.589
31,822
31.713
27.895
29.780
34.680
32.705
29.181
27.652
27.513
28.688

26.988 lbs
32.930
33.644
4.213
33.326
32.785
34.590
33.702
33.839
32.541
31.767
34.964
34.040
34.544
30.981
32.375
12.718
32.696
30.791
34.562
30.662
31.078
34.424 —— 704.16 lbs
27.074
33.120
30.470
25.356
33.554
33.551
3.938
28.707
29.438
33.410

~~field camera & tri-pod~~
~~pipe small diameter~~
~~respirator & extra N-99 face masks~~

* 1/16 plates Order from MSM (3 total)
files from Computer

Labview
C drive

Shakle Table Test #2
Date: 8/19/15

Joseph Toth

tare 1.674 lbs

@ 24%

tare 1.66

	Dense Layer (1075 lbs)			Liquefiable Layer (1025 lbs)
	W_T ~~Ws (lbs)~~	Ww (lbs)		Ws (lbs)
1	34.071	0	1	34.888
2	31.935	0	2	33.408
3	33.403	0	3	33.535
4	29.207	0	4	31.885
5	32.039	0	5	34.923
6	33.616	0	6	29.146
7	34.148	0	7	34.704
8	28.378	0	8	34.735
9	32.896	0	9	33.205
10	100 lb sand dry	0	10	12.037
11	32.876	0	11	32.461
12	31.197	0	12	34.612
13	32.957	0	13	34.449
14	34.119	0	14	34.476
15	33.441	0	15	30.620
16	32.431	0	16	33.891
17	33.872	↓	17	32.407
18	34.800		18	32.017
19	33.575		19	34.291
20	31.475	6.686 lbs	20	34.628
21	34.886	↓	21	34.619
22	34.208		22	34.053
23	34.513		23	29.286
24	29.686	6.66 lbs	24	33.357
25	34.495	↓	25	34.993
26	34.170		26	32.907
27	33.766		27	34.163
28	32.598	6.75 lbs	28	31.827
29	33.656	↓	29	33.819
30	32.707	3.3 lbs	30	32.665

NOTES: ~ 70 lbs of sand already in bottom of soil tank (Dense layer)

Joseph Toth

Shakle Table Test # 3
Date: 8/25/2015

se layer
t in place
m test#2

	Dense Layer		Liquefiable Layer
	Ws (lbs)	Ww (lbs)	Ws (lbs)
1			34.9375
2			34.047
3			34.119
4			34.443
5			34.890
6			33.942
7			34.298
8			34.556
9			34.646
10			34.526
11			33.385
12			34.558
13			34.385
14			33.920
15			32.639
16			34.796
17			31.880
18			34.034
19			33.124
20			33.314
21			33.765
22			34.107
23			34.390
24			34.607
25			32.979
26			33.094
27			33.949
28			33.491
29			33.304
30			28.809

tare = 1.667
target = 10251
for Dr ~ 30%

16.810
32.970
31.498

NOTES: dense layer washed out because plexiglass rub sheet corners lost seal.

848-0952

Shakle Table Test # 4

Date: 9/4/2015

Joseph Toth

		Dense Layer			Liquefiable Layer	
		Ws (lbs)	Ww (lbs)		Ws (lbs)	
5%	1	49.7	2.485	1	51.7	
Js	2	54.5	2.725	2	53.8	
ncludes	3	52.0	2.6 lbs	3	44.0	
tare wt.	4	54.2	2.71	4	11.3	
	5	55.9	2.795	5	55.8	
re= 1.6 lbs	6	58.4	2.92	6	10.4	
	7	59.2	2.96	7	54.6	
	8	55.7	2.785	8	44.6	
	9	61.2	3.06	9	59.5	
	10	60.2	3.01	10	44.4	
12lbs	11	58.6	2.93	11	52.8	
	12	59.6	2.98	12	50.1	
	13	62.0	3.1	13	50.7	583.7
	14	59.7	2.985	14	51.6	
	15	61.0	3.05	15	49.9	
	16	59.8	2.985	16	63.0	
	17	59.0	2.95	17	57.5	
	18	56.6	2.83	18	39.9	
	19	54.9	2.745	19	54.8	
	20	finished	—	20	49.4	
	21			21	54.2	
	22			22	43.8	
	23			23	51.8	515.9
	24			24	35.0 - 6.3 =	1099
	25			25		
	26			26		
	27			27		
	28			28		
	29			29		
	30			30		

NOTES:

Shakle Table Test # 5

Date: 9/17/2015

Joseph Toth

wat
ne = 0lbs

placed
~
5% moisture
n storage
ns

Dense Layer

	Ws (lbs)	Ww (lbs)
1	44.9	
2	51.4	
3	50.3	
4	45.9	
5	51.6	
6	56.3 300.4	
7	52.6	
8	57.1	
9	57.9	
10	52.3	
11	60.9	
12	57.7	
13	56.0 394.5	
14	51.6	
15	54.0	
16	51.3	
17	50.5 207.4	
18	59.3	
19	54.5	
20	56.9	
21	49.1	
22	53.7	
23		
24		
25		
26		
27		
28		
29		
30		

902.3

175.8 lbs @ 5% moisture → 22

Dobri.

Liquefiable Layer

P = 3.2 lbs

	Ws (lbs)	
1	40.5	P
2	45.5	P
3	45.8	P
4	41.5	P
5	43.2	P
6	38.8	P
7	43.6	P
8	42.9	P
9	41.4	P
10	40.9	P
11	42.8	P
12	43.5	P
13	44.1	P
14	36.8	P
15	34.0	P
16	44.0	P
17	54.3	
18	54.2	
19	49.2	
20	41.5	
21	40.4	
22	40.9	
23	59.1	
24	61.5	
25	28.1 - 3.9	
26		
27		
28		
29		
30		

* need to deduct P from Ws

669.3 - 3.
= 618.1 lb
Ws

Total = 1043.4 l

NOTES:

Shakle Table Test # 6

Joseph Toth

Date: 9/24/2015

Dense Layer

		Ws (lbs)	Ww (lbs)	
repared for 5% moisture	1	35 lbs @ 5% moisture		
	2	42.1	2.1	
	3	52.2	2.6	
	4	53.7	~~2.7~~ 2.68	
	5	42.2	2.098	
	6	44.3	2.2	
316.8	7	50.3	2.509	
	8	52.1	2.605	
	9	47.01	2.35	
	10	55.7	2.78	
	11	47.5	2.38	
	12	49.5	2.5	
6.31 299.51	13	47.7	2.4	
	14	52.3 - 3.3 = 49	—	
	15	48.9 - 3.4 = 45.5	—	at 10% moist.
230.9	16	46.2 - 3.3 = 42.9	—	dry Ws = 209.9
	17	50.7 - 3.3 = 47.4	—	
	18	49.4 - 3.3 = 46.1	—	
	19	56.5	2.825	
	20	59.7	2.985	
	21	53.5	2.675	
1055	22	59.01	2.950	
	23			
	24			
	25			
	26			
	27			
	28			
	29			
	30			

Liquefiable Layer

	Ws (lbs)	
1	58.1	
2	54.8	
3	56.9	
4	59.4	
5	58.2	
6	59.8	
7	61.7	
8	61.9	
9	62.9	534 lb
10	61.6	
11	58.1	
12	61.0	
13	60.0	
14	62.1	
15	57.2	894
16	56.5	
17	56.4	
18	18.4	1025.3
19		
20		
21		
22		
23		
24		
25		
26		
27		
28		
29		
30		

NOTES: For Dense layer - Scale zero w/bucket, Δ tare = 0 lbs.

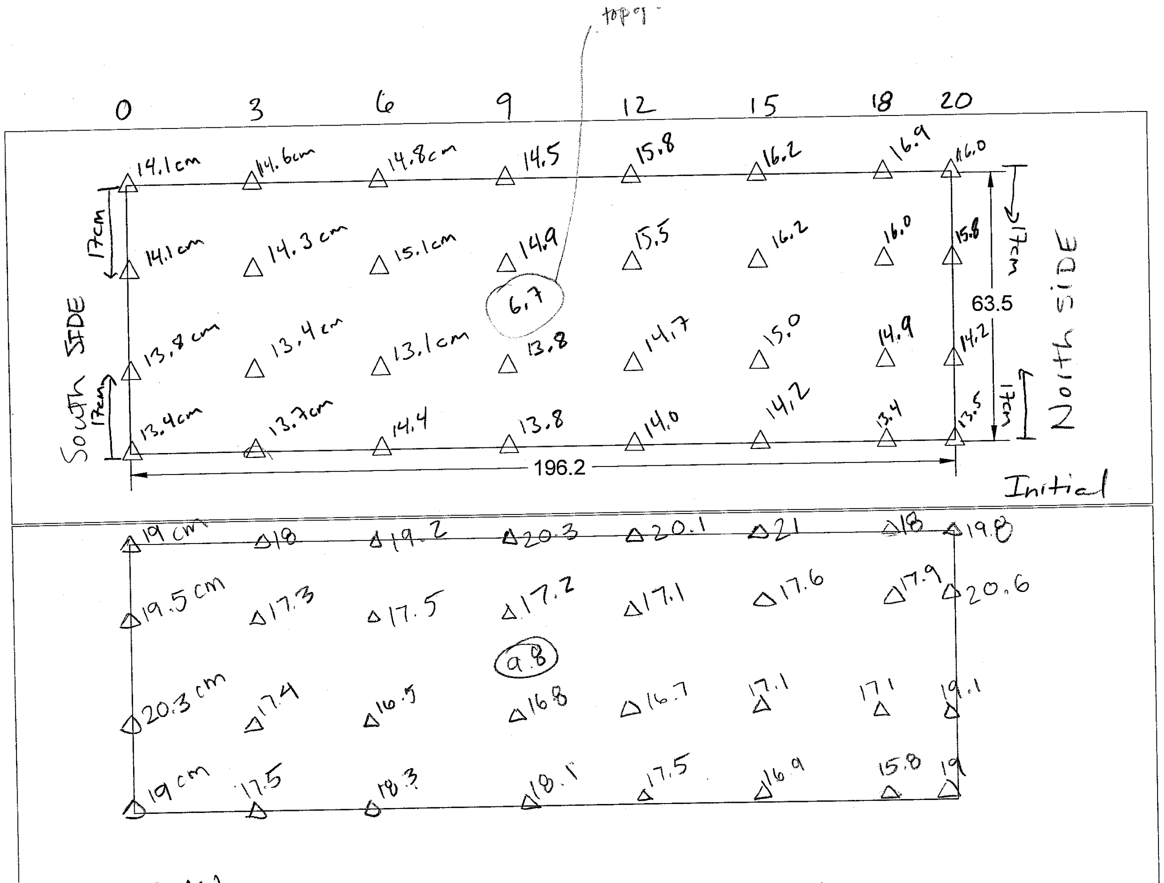

SOIL BOX ~~PROFILE~~ PLAN TEST NO: 6 DATE: 9/25/15 FINAL

● MODEL BUILDING WITH ACCELEROMETER

■ ACCELEROMETER

▲ PORE WATER PRESSURE SENSOR

▼ GROUNDWATER LEVEL

△ SETTLEMENT MEASUREMENT LOCATIONS

NOTES:

JOSEPH TOTH

Joseph Toth

Shakle Table Test # 7

Date: 10/2/2015

Dense Layer

		Ws (lbs)	Ww (lbs)
	1	45.8 - 3.3 =	—
125.2	2	48.6 - 3.3 =	— 116 dry
w≈81.	3	40.7 - 3.3 =	—
116	4	47.5	2.4 lbs
	5	57.4	2.88 lb
	6	53.7	2.68
	7	49.0	2.45
	8	52.6	2.63
	9	52.3	2.62
367.2	10	54.8	2.74
	11	53.2	2.66
	12	55.2	2.76
	13	52.5	2.63
	14	52.1	2.6
	15	53.0	2.65
318.9	16	52.9	2.65
	17	53.1	2.655
	18	50.3	2.52
	19	51.8	2.59
206.6	20	51.4	2.57
109	21	54.5	2.73
	22	14.2	0.71
1077.7lbs	23		
	24		
	25		
	26		
	27		
	28		
	29		
	30		

Liquefiable Layer

	Ws (lbs)	
1	49.7	
2	47.7	
3	~~48.0~~ 48.2	
4	43.8	
5	48.3	
6	50.0	
7	58.0	
8	51.5	
9	53.4	
10	51.0	501.6
11	55.2	
12	50.5	
13	59.4	
14	54.8	721.5
15	56.5	
16	57.4	835.4
17	54.5	
18	46.3	
19	53.4	989.6
20	35.7	
21	18.5	1043
22		
23		
24		
25		
26		
27		
28		
29		
30		

NOTES:

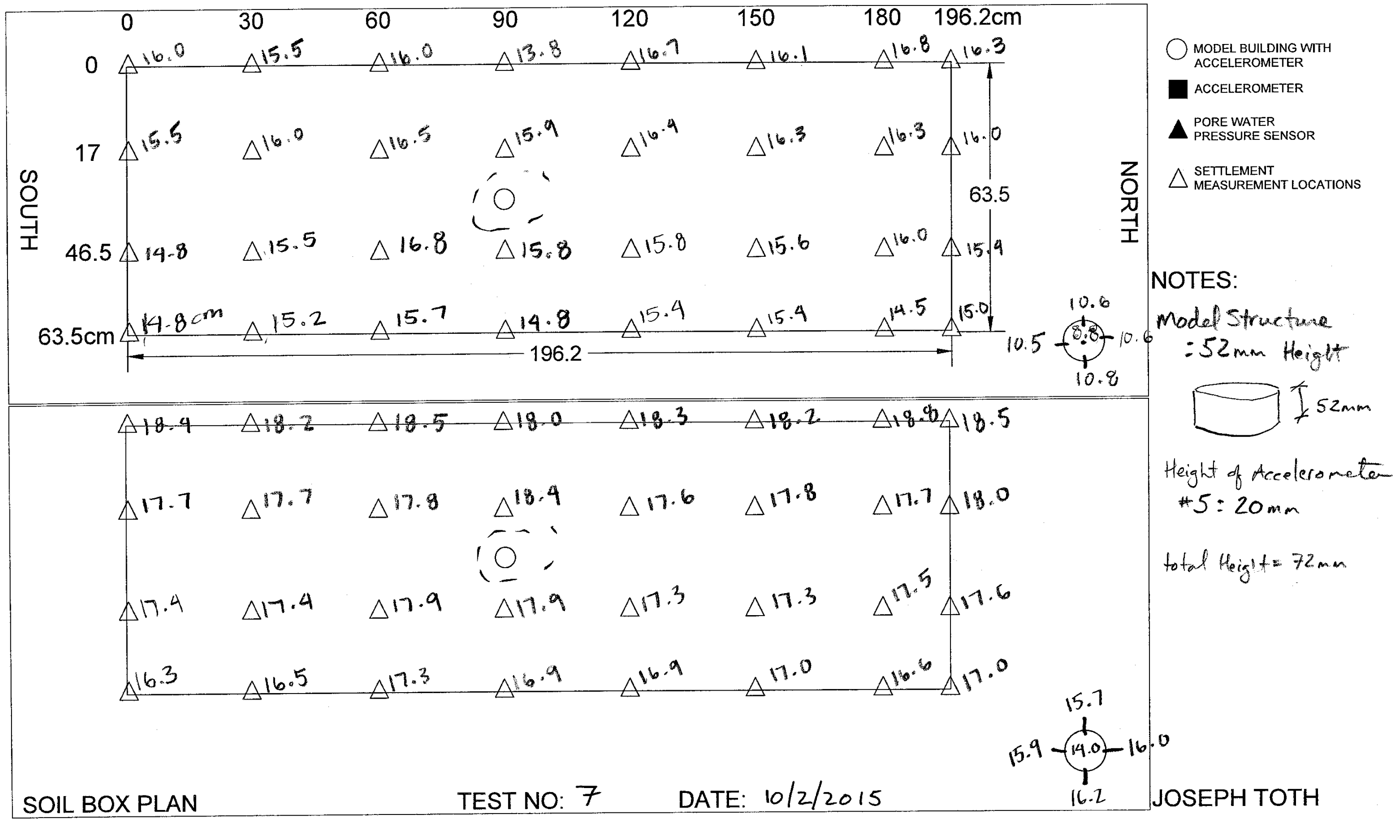

NOTES:

Model Structure
:52mm Height

Height of Accelerometer
#5: 20mm

total Height= 72mm

Joseph Toth

Shakle Table Test # 8

Date: 10/7/2015

Dense Layer

	Ws (lbs)	Ww (lbs)
1	Same layer as Test #7	
2		
3		
4		
5		
6		
7		
8		
9		
10		
11		
12		
13		
14		
15		
16		
17		
18		
19		
20		
21		
22		
23		
24		
25		
26		
27		
28		
29		
30		

Liquefiable Layer

tare = 1.7lbs

	Ws (lbs)	
1	46.0	
2	48.9	
3	45.1	
4	45.5	
5	45.9	
6	51.4	
7	43.3	
8	42.0	
9	44.3	
10	52.5	
11	46.0	
12	52.1	
13	47.5	
14	48.7	
15	53.2	
16	46.3	811.6*
17	52.9	
18	51.9	
19	56.3	
20	44.7	
21	54.0	
22	6.5	1025 lbs
23		
24		
25		
26		
27		
28		
29		
30		

NOTES: large tensile crack developed along east side of container due to pwp b/w lexan and rubsheets

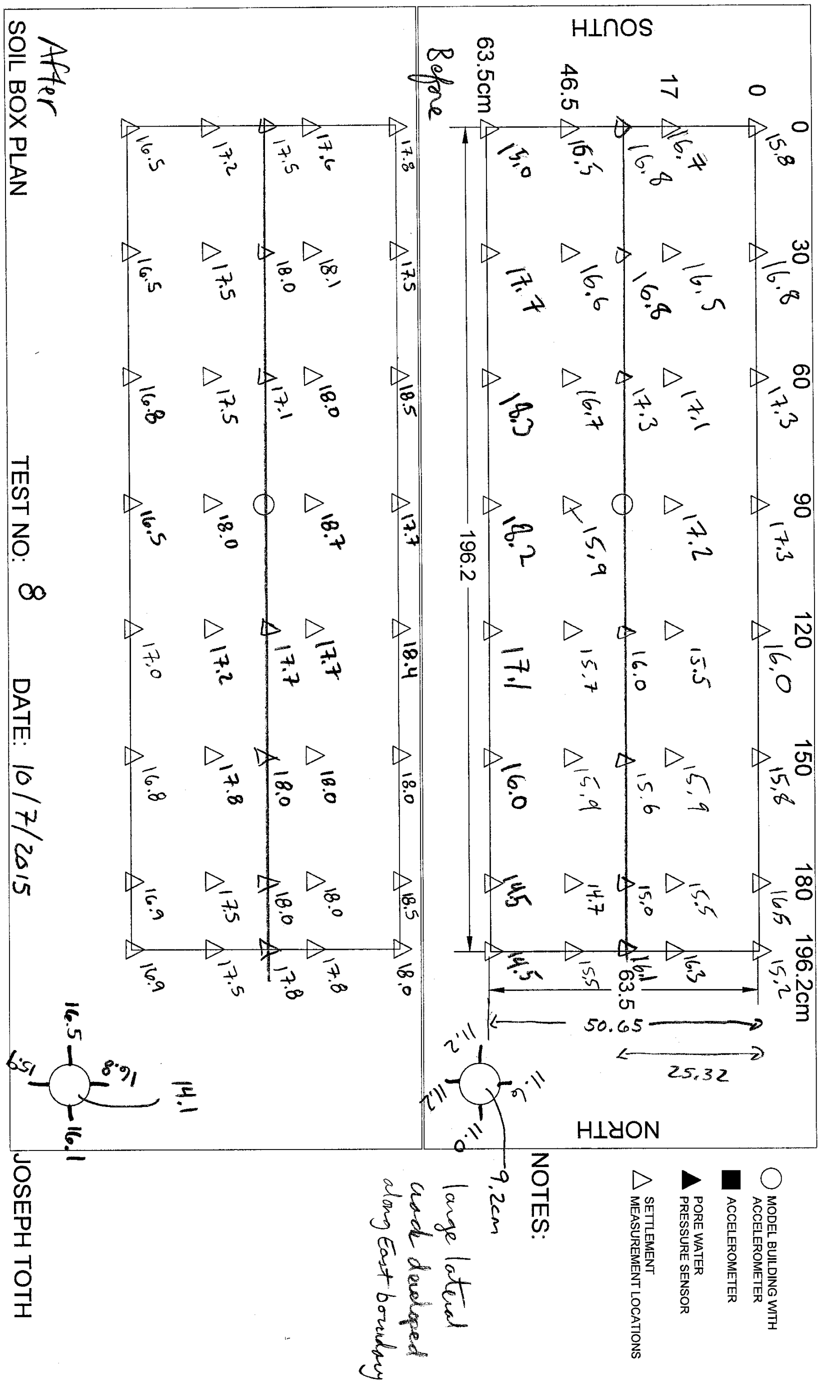

SOIL BOX PLAN

TEST NO: 8

DATE: 10/7/2015

JOSEPH TOTH

NOTES:

large lateral crack developed along East boundary

Joseph Toth

Shakle Table Test # 9

Date: 10/29/2015

Dense Layer

		Ws (lbs)	Ww (lbs)
	1	55.3	2.77
	2	50.6	2.53
	3	53.2	2.66
	4	49.1	2.46
	5	51.6	2.58
	6	56.6	2.83
	7	51.8	2.59
	8	53.2	2.66
	9	55.1	2.76
	10	56.5	2.82
	11	53.9	2.69
	12	53.8	~~226~~ 2.7
695.8	13	55.1	2.76
	14	55.8	2.79
	15	54.1	2.71
	16	51.9	2.60.
911.5	17	53.9	2.7
	18	54.5	2.73
	19	29.8	1.5
	20	Total 995.8lbs	
	21		
	22		
	23		
	24		
	25		
	26		
	27		
	28		
	29		
	30		

Liquefiable Layer

	Ws (lbs)	
1	61.5	
2	60.7	
3	61.6	
4	63.3	
5	61.3	
6	63.7	
7	61.6	433.7 lbs
8	61.4	
9	59.5	
10	61.6	
11	62.6	678.8
12	63.2	
13	61.8	803.8
14	62.2	
15	64.2	
16	14.1	
17	944.3 total	
18		
19		
20		
21		
22		
23		
24		
25		
26		
27		
28		
29		
30		

NOTES: Target weights revised based on foam used to dampen soil motion boundary effects

Dr = 60% → 995 lbs

Dr = 30% → 944 lbs.

12(2Hz) ~ 0.04f
2.5Hz ~ 0.05

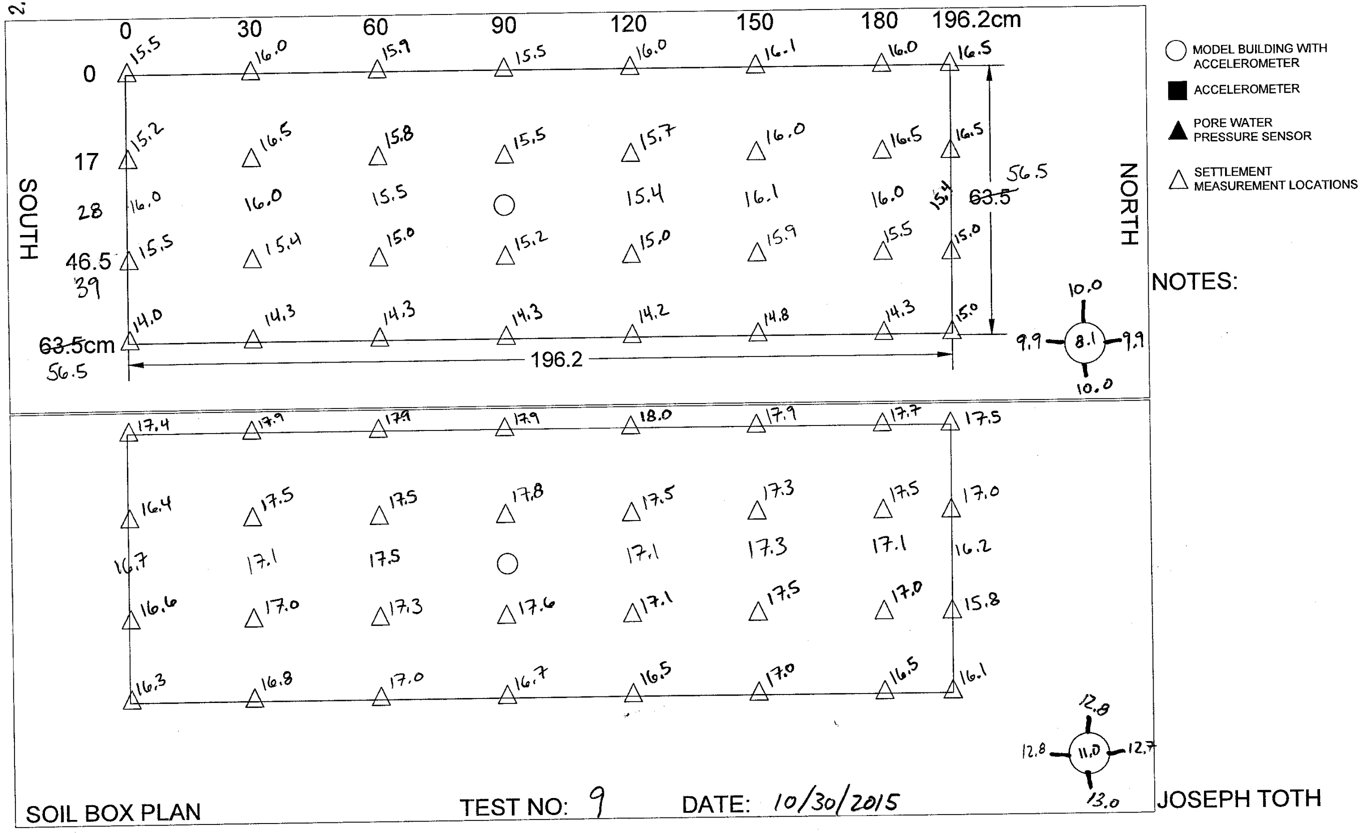

NOTES:

SOIL BOX PLAN TEST NO: 9 DATE: 10/30/2015

JOSEPH TOTH

Shakle Table Test # 10

Date: 11/5/2015

Joseph Toth

Dense Layer

		Ws (lbs)	Ww (lbs)
	1	57.9	2.9
	2	58.8	2.94
	3	60.3	3.07
	4	62.7	3.09
	5	60.6	3.07
	6	62.6	3.16
	7	61.4	3.13
	8	63.2	3.19
	9	62.0	3.14
	10	60.7	3.05
671.6	11	61.4	3.04
	12	62.0	3.2
795.1	13	61.5	3.09
	14	53.9	2.78
	15	53.8	2.64
	16	53.3	2.76
	17	38.9	2.09
	18		
	19		
	20		
	21		
	22		
	23		
	24		
	25		
	26		
	27		
	28		
	29		
	30		

Liquefiable Layer

	Ws (lbs)	
1	41.2	
2	38.4	
3	39.6	
4	39.8	
5	41.1	
6	37.0	
7	39.0	
8	37.1	
9	39.6	
10	37.3	
11	36.9	427lbs
12	37.1	
13	37.2	
14	38.1	
15	38.1	
16	37.1	
17	39.5	654.1
18	38.6	
19	35.6	
20	36.9	
21	37.3	802.5
22	39.5	
23	42.6	884.6
24	34.9	919.5
25	24.6	
26	total 944.1	
27		
28		
29		
30		

NOTES: Dr ~ 60% (995lbs)

30% (944lbs)

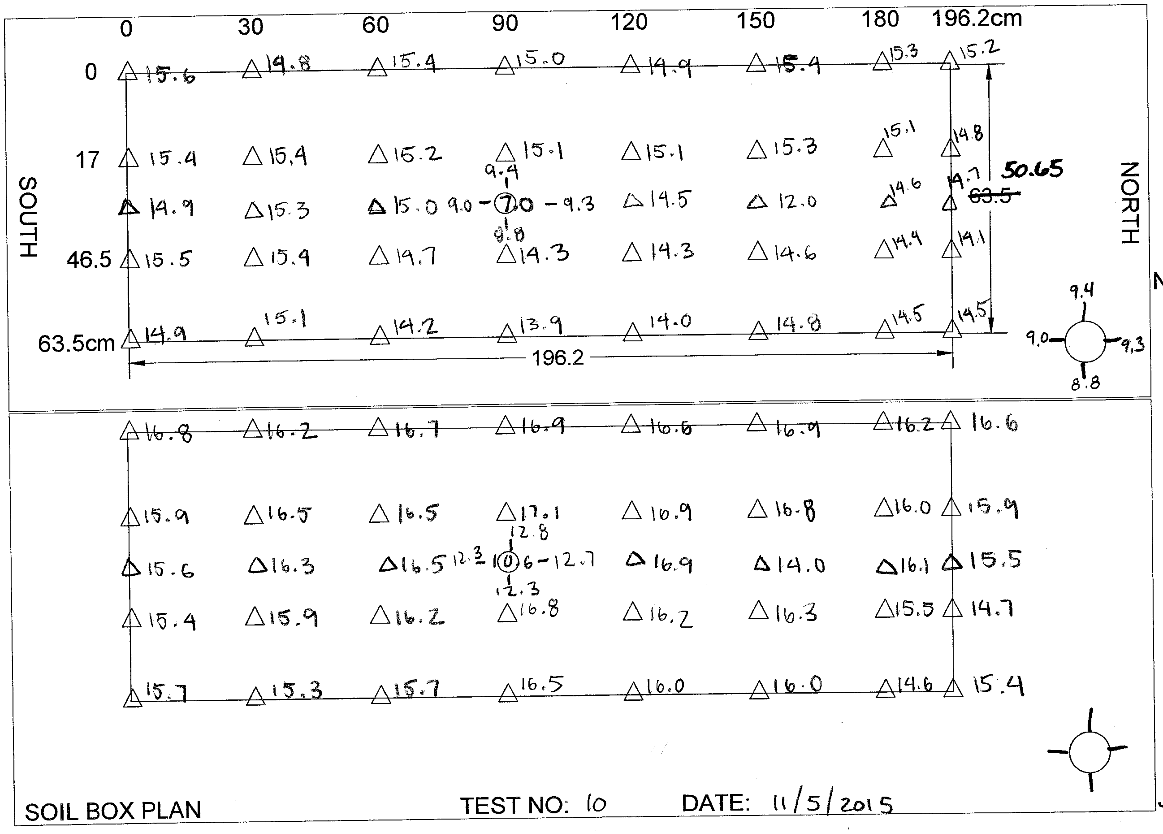

SOIL BOX PLAN TEST NO: 10 DATE: 11/5/2015

○ MODEL BUILDING WITH ACCELEROMETER

■ ACCELEROMETER

▲ PORE WATER PRESSURE SENSOR

△ SETTLEMENT MEASUREMENT LOCATIONS

NOTES:

JOSEPH TOTH

Joseph Toth

Shakle Table Test # 11
Date: 11/12/2015

Dense Layer

		Ws (lbs)	Ww (lbs)
	1	55.9	2.87
	2	60.4	3.11
	3	55.4	2.71
	4	59.2	2.93
291.4	5	60.5	3.09
353.6	6	62.2	3.10
	7	52.6	2.55
	8	62.8	3.14
	9		
	10	469 total	
	11		
	12		
	13		
	14		
	15		
	16		
	17		
	18		
	19		
	20		
	21		
	22		
	23		
	24		
	25		
	26		
	27		
	28		
	29		
	30		

Liquefiable Layer

	Ws (lbs)	
1	41.6	
2	45.2	
3	40.8	
4	41.2	168.8
5	37.1	
6	43.2	
7	37.9	
8	39.2	326.2
9	40.3	
10	43.1	409.6
11	35.4	
12	445 lbs total	
13		
14		
15		
16		
17		
18		
19		
20		
21		
22		
23		
24		
25		
26		
27		
28		
29		
30		

NOTES:
Dense - 469 lbs
Loose - 445 lbs

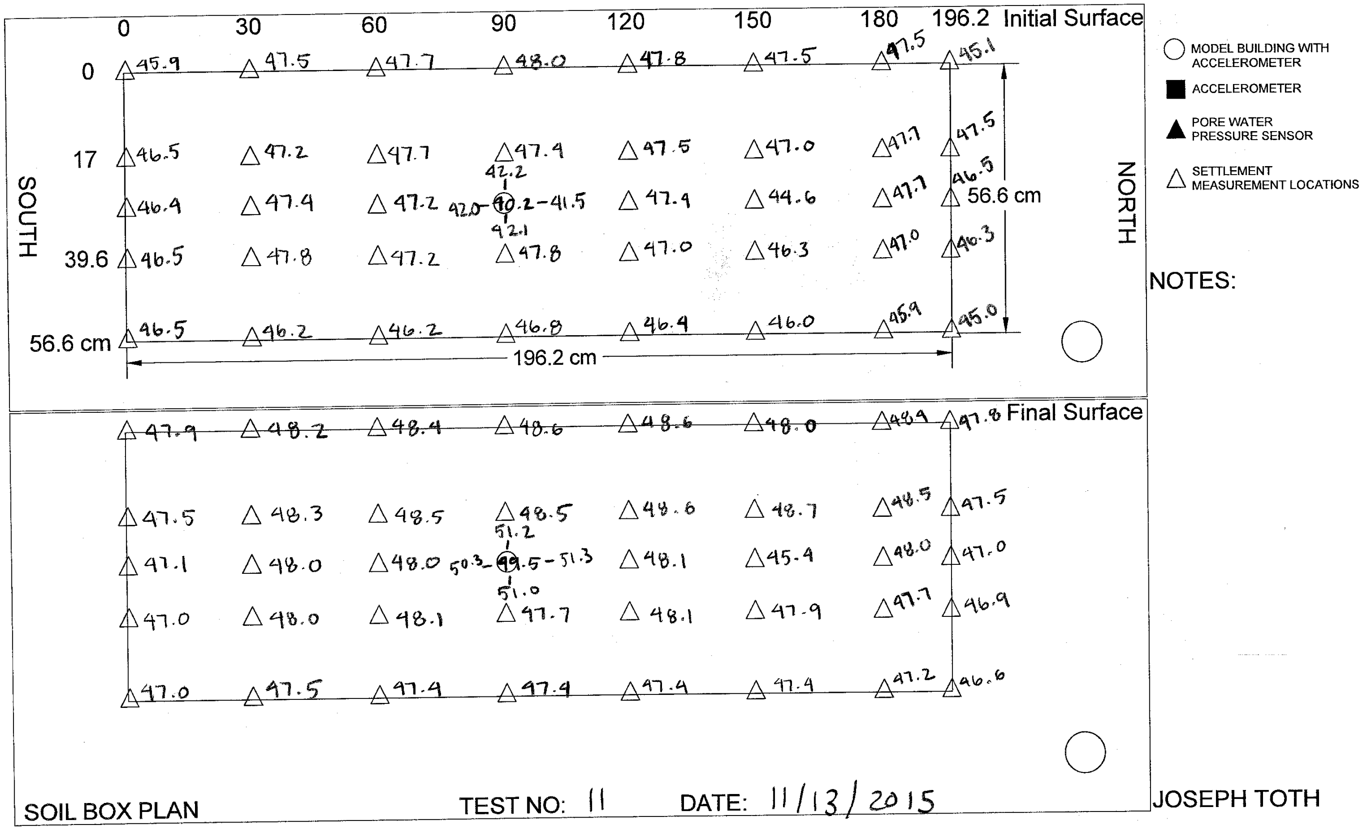

NOTES:

SOIL BOX PLAN

TEST NO: 11

DATE: 11/13/2015

JOSEPH TOTH

Joseph Toth

Shakle Table Test # 12
Date: 11/20/2015

		Dense Layer	
		Ws (lbs)	Ww (lbs)
	1	35.6	1.79
	2	34.1	1.71
	3	36.7	1.84
	4	37.7	1.89
	5	38.5	1.93
	6	38.5	1.93
	7	37.5	1.88
	8	35.2	1.76
	9	37.0	1.85
	10	33.7	1.69
397.1	11	32.6	1.63
	12	37.6	1.88
	13	34.3	1.715
	14		
	15		
	16		
	17		
	18		
	19		
	20		
	21		
	22		
	23		
	24		
	25		
	26		
	27		
	28		
	29		
	30		

	Liquefiable Layer	
	Ws (lbs)	
1	39.5	
2	30.1	
3	37.1	
4	35.7	
5	34.2	
6	36.1	
7	37.5	
8	35.9	
9	36.4	
10	37.6	
11	36.7	— 396.8
12	6.3	
13	41.9	
14		
15		
16		
17		
18		
19		
20		
21		
22		
23		
24		
25		
26		
27		
28		
29		
30		

NOTES: Dense = 469 lbs
Loose = 445 lbs

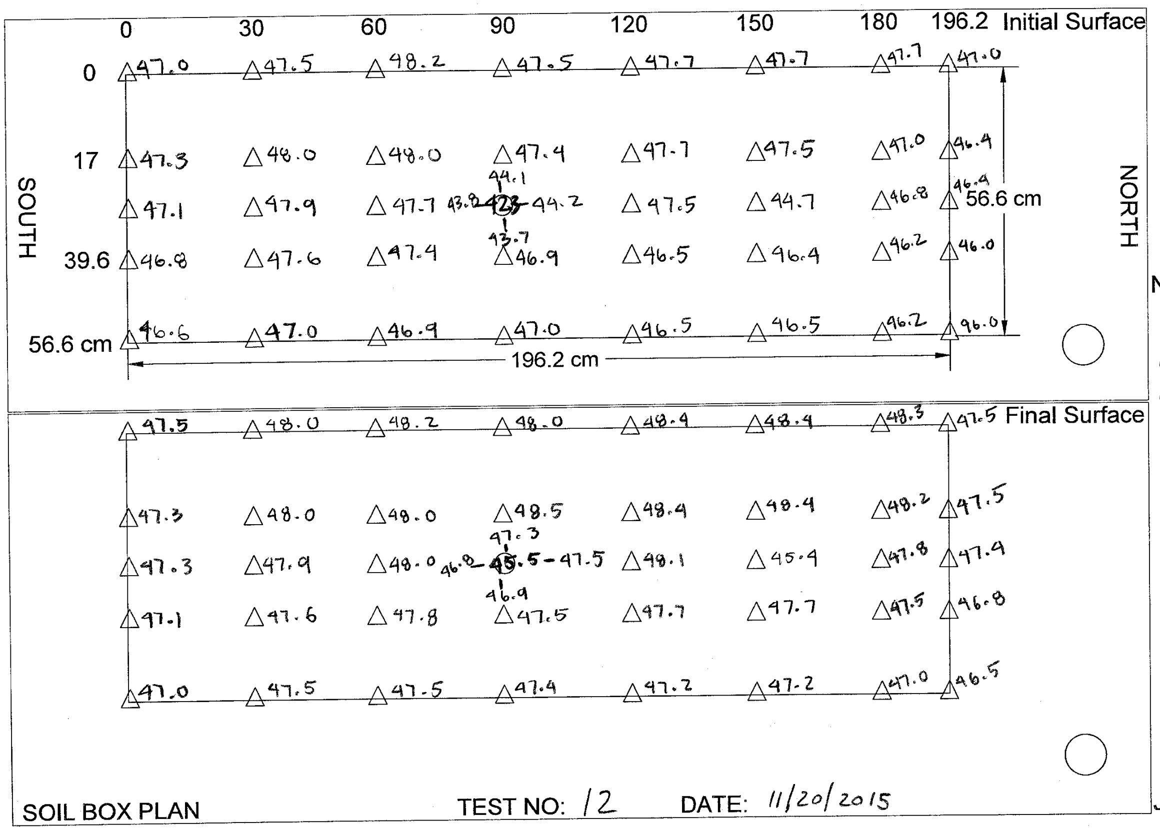

Initial Surface

	0	30	60	90	120	150	180	196.2
0	47.0	47.5	48.2	47.5	47.7	47.7	47.7	47.0
17	47.3	48.0	48.0	47.4	47.7	47.5	47.0	46.4
	47.1	47.9	47.7		47.5	44.7	46.8	46.4
39.6	46.8	47.6	47.4	46.9	46.5	46.4	46.2	46.0
56.6 cm	46.6	47.0	46.9	47.0	46.5	46.5	46.2	46.0

Final Surface

47.5	48.0	48.2	48.0	48.4	48.4	48.3	47.5
47.3	48.0	48.0	48.5	48.4	48.4	48.2	47.5
47.3	47.9	48.0		48.1	45.4	47.8	47.4
47.1	47.6	47.8	47.5	47.7	47.7	47.5	46.8
47.0	47.5	47.5	47.4	47.2	47.2	47.0	46.5

○ MODEL BUILDING WITH ACCELEROMETER

■ ACCELEROMETER

▲ PORE WATER PRESSURE SENSOR

△ SETTLEMENT MEASUREMENT LOCATIONS

NOTES:

Sensor 2 in dense layer possibly damaged.

SOIL BOX PLAN TEST NO: 12 DATE: 11/20/2015

JOSEPH TOTH

Shakle Table Test # 13

Joseph Toth

Date: 12/1/2015

		Dense Layer			Liquefiable Layer	
		Ws (lbs)	Ww (lbs)		Ws (lbs)	
	1	36.3	1.82	1	31.0	
	2	37.0	1.85	2	33.8	
	3	34.3	1.72	3	32.8	
	4	25.8	1.29	4	37.0	
	5	36.5	1.83	5	34.3	
06.9	6	37.0	1.85	6	32.3	
	7	37.7	1.89	7	35.7	236.9
	8	39.9	2.0	8	34.5	
	9	34.9	1.75	9	42.6	
354.2	10	34.8	1.74	10	38.5	
	11	39.8	2.0	11	36.6	
428	12	34.0	1.7	12	36.1	
	13	33.8	1.7	13	18.1	
	14	7.2	0.4	14	5.4	
	15	469 total		15		
	16			16		
	17			17		
	18			18		
	19			19		
	20			20		
	21			21		
	22			22		
	23			23		
	24			24		
	25			25		
	26			26		
	27			27		
	28			28		
	29			29		
	30			30		

NOTES:

Dense - 469 lbs

Loose - 445 lbs

after test add additional 4 inches to liquefiable layers

test at different frequencies.

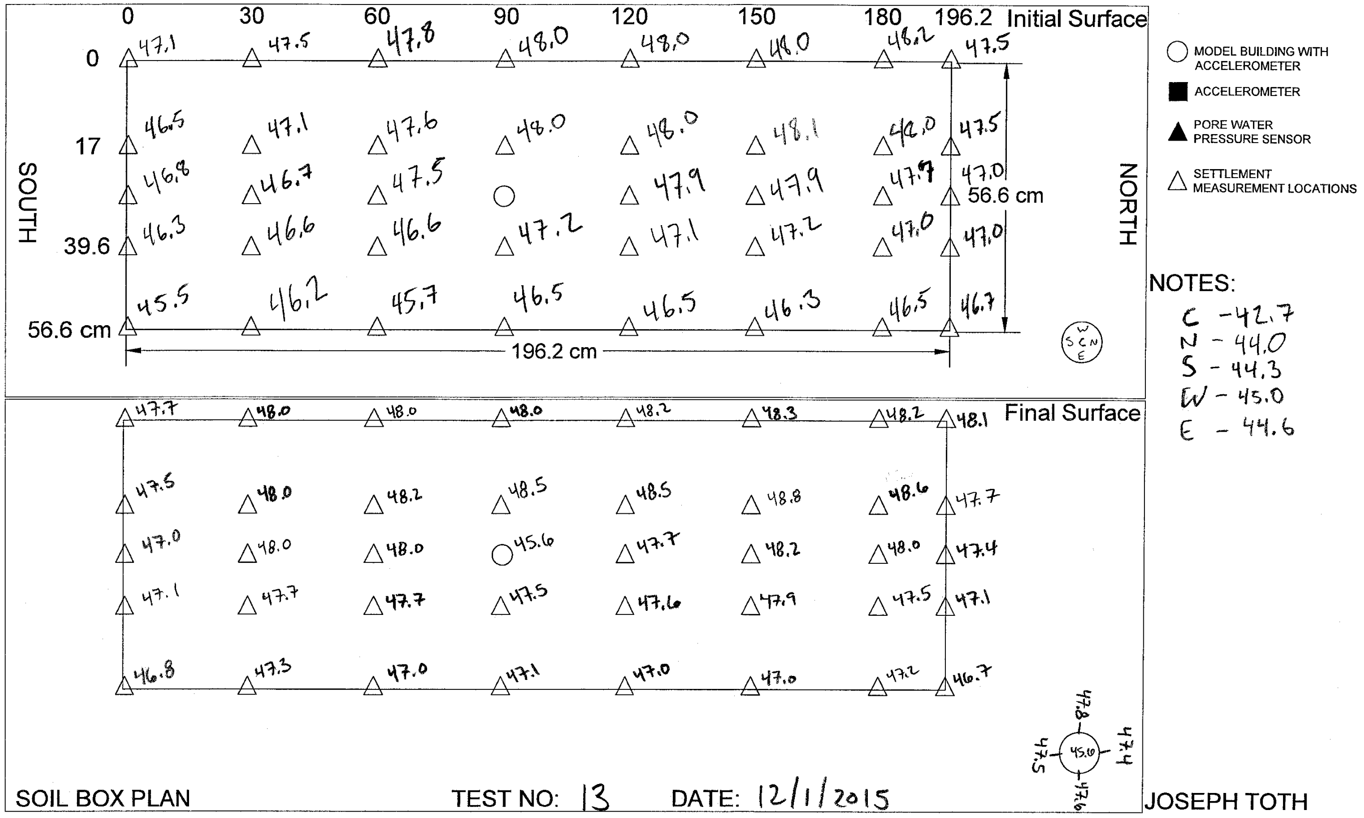

NOTES:

C -42.7
N - 44.0
S - 44.3
W - 45.0
E - 44.6

SOIL BOX PLAN TEST NO: 13 DATE: 12/1/2015

JOSEPH TOTH

Shakle Table Test # 14

Date: 12/8/2015

Joseph Toth

Dense Layer

		Ws (lbs)	Ww (lbs)
	1	39.7	1.99
	2	35.5	1.78
	3	39.7	1.99
155.4	4	40.5	2.03
	5	36.7	1.84
	6	36.5	1.82
272.3	7	43.7	2.19
	8	40.0	2.0
	9	38.5	1.93
388.0	10	37.2	1.86
	11	41.6	2.08
472.8	12	43.2	2.16
	13	36.7	1.84
	14	16.0	0.8
	15	total 525.5 lbs	
	16		
	17		
	18		
	19		
	20		
	21		
	22		
	23		
	24		
	25		
	26		
	27		
	28		
	29		
	30		

Liquefiable Layer

	Ws (lbs)	
1	20.8	
2	43.0	
3	37.2	
4	42.5	143.5
5	37.7	
6	41.4	
7	23.1	
8	37.1	245.1
9	34.6	
10	36.3	
11	37.3	
12	39.8	393.1
13	33.9	
14	30.2	457.2
15	41.3	
16	498.5 total	
17		
18		
19		
20		
21		
22		
23		
24		
25		
26		
27		
28		
29		
30		

NOTES: Dense - 525.6 lbs

Loose - 498.5 lbs

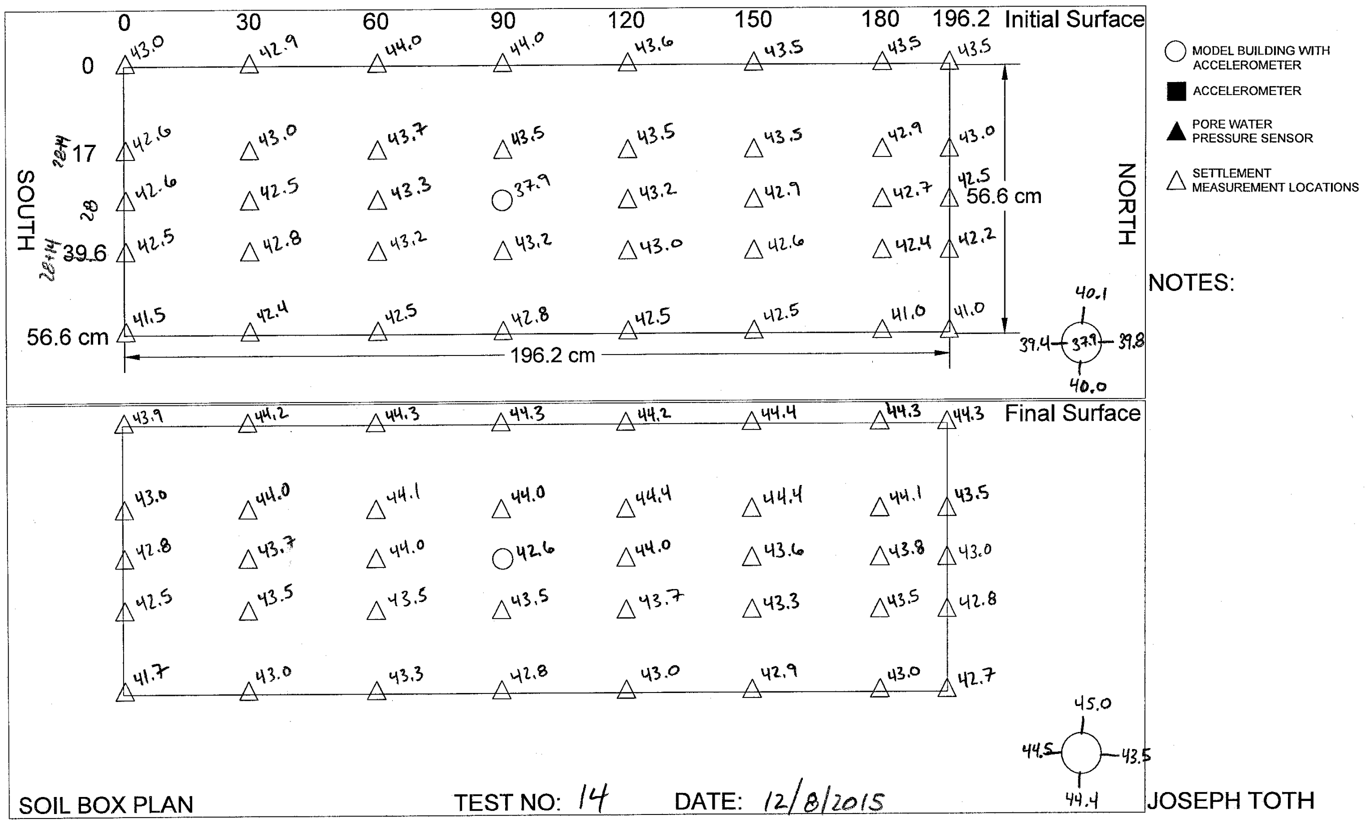

Initial Surface

	0	30	60	90	120	150	180	196.2
0	43.0	42.9	44.0	44.0	43.6	43.5	43.5	43.5
17	42.6	43.0	43.7	43.5	43.5	43.5	42.9	43.0
28	42.6	42.5	43.3	○37.9	43.2	42.9	42.7	42.5
39.6	42.5	42.8	43.2	43.2	43.0	42.6	42.4	42.2
56.6 cm	41.5	42.4	42.5	42.8	42.5	42.5	41.0	41.0

Final Surface

43.9	44.2	44.3	44.3	44.2	44.4	44.3	44.3
43.0	44.0	44.1	44.0	44.4	44.4	44.1	43.5
42.8	43.7	44.0	○42.6	44.0	43.6	43.8	43.0
42.5	43.5	43.5	43.5	43.7	43.3	43.5	42.8
41.7	43.0	43.3	42.8	43.0	42.9	43.0	42.7

NOTES:

SOIL BOX PLAN TEST NO: 14 DATE: 12/8/2015

JOSEPH TOTH

Joseph Toth

Shakle Table Test # 15
Date: 12/11/2015

Dense Layer

		Ws (lbs)	Ww (lbs)
	1	42.8	2.14
	2	36.6	1.83
	3	41.7	2.09
159.8	4	38.7	1.94
	5	35.6	1.78
	6	43.5	2.18
	7	38.2	1.91
313.4	8	36.3	1.82
	9	38.8	1.94
	10	40.8	2.04
434	11	41.0	2.05
	12	39.6	1.98
506.5	13	32.9	1.65
	14	19.1	0.96
	15	total 525.6	
	16		
	17		
	18		
	19		
	20		
	21		
	22		
	23		
	24		
	25		
	26		
	27		
	28		
	29		
	30		

Liquefiable Layer

	Ws (lbs)	
1	12.6	
2	37.5	
3	38.4	
4	40.3	
5	37.7	166.5
6	39.3	
7	39.8	
8	37.8	
9	35.1	318.5
10	40.5	
11	40.6	399.7
12	35.3	
13	36.4	471.4
14	27.1	
15	total 498.5	
16		
17		
18		
19		
20		
21		
22		
23		
24		
25		
26		
27		
28		
29		
30		

NOTES:
Loose - 498.5 lbs
Dense - 525.6 lbs

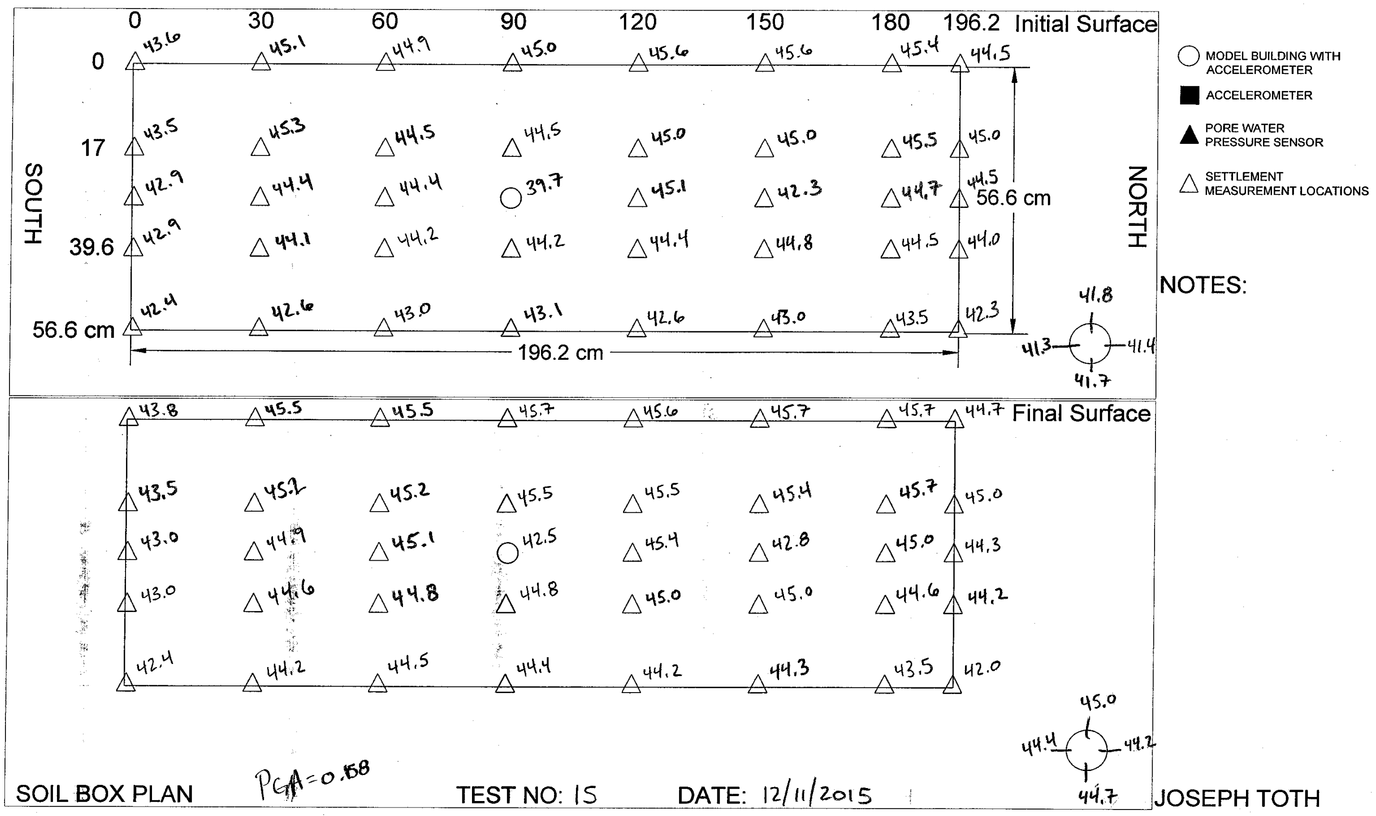

SOIL BOX PLAN PGA=0.58 TEST NO: 15 DATE: 12/11/2015 JOSEPH TOTH

Shakle Table Test # Test #16
Date: 12/15/2015

Joseph Toth

Dense Layer

		Ws (lbs)	Ww (lbs)
	1	40.5	2.03
	2	34.1	1.71
	3	38.8	1.94
150.5	4	37.1	1.86
	5	36.3	1.82
	6	38.3	1.92
	7	43.7	2.19
310.3	8	41.5	2.08
	9	38.8	1.94
	10	37.6	1.88
	11	38.9	1.95
467.4	12	41.8	2.09
510	13	42.6	2.13
	14	15.6	0.8
	15	525.6 total	
	16		
	17		
	18		
	19		
	20		
	21		
	22		
	23		
	24		
	25		
	26		
	27		
	28		
	29		
	30	525.6 total	

Liquefiable Layer

	Ws (lbs)	
1	36.8	
2	39.7	
3	36.6	113.1
4	37.5	
5	26.3	
6	41.0	
7	38.6	256.5
8	39.5	
9	41.7	337.7
10	38.9	
11	41.9	418.5
12	40.7	459.2
13	39.3	
14	498.5 total	
15		
16		
17		
18		
19		
20		
21		
22		
23		
24		
25		
26		
27		
28		
29		
30	498.5 total	

NOTES:

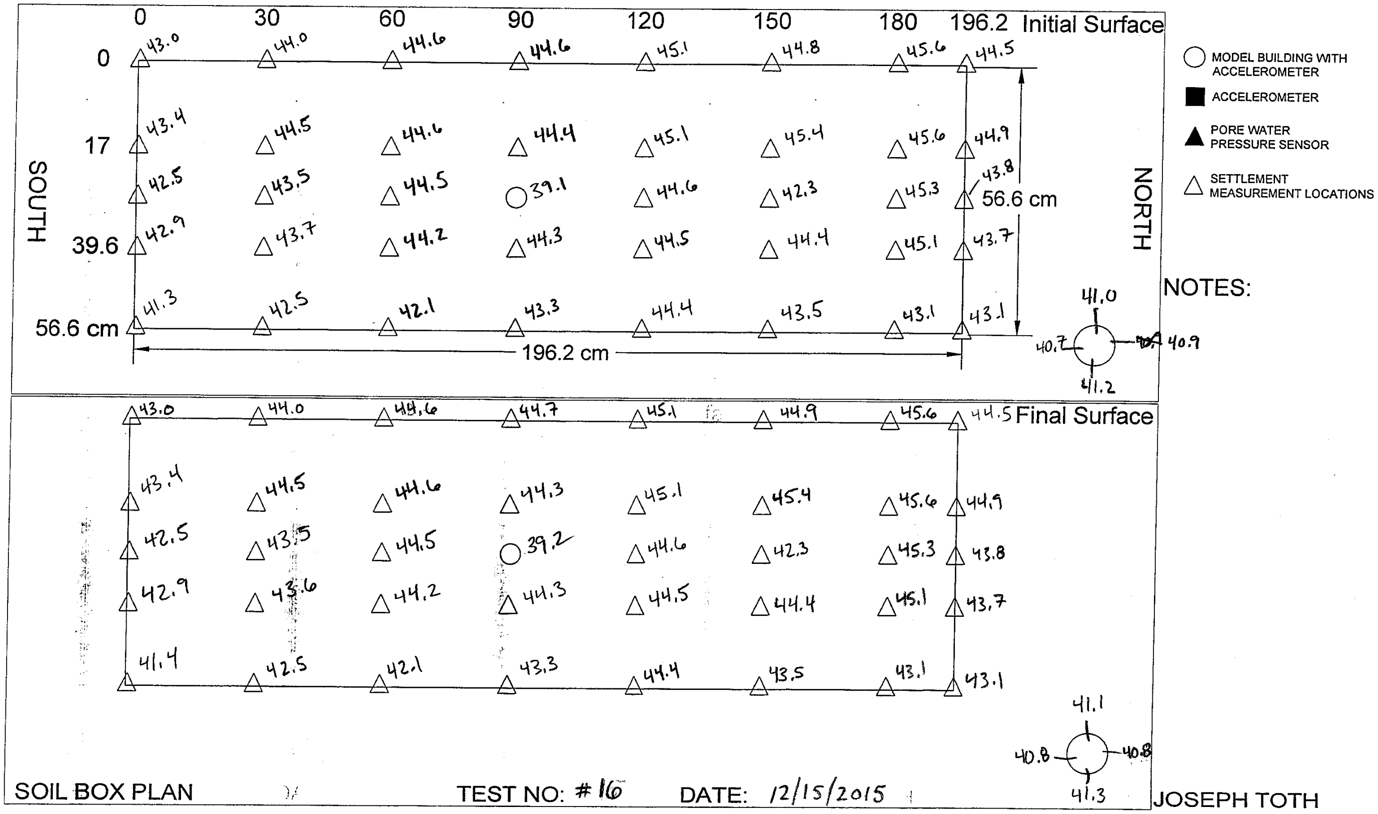

Initial Surface

	0	30	60	90	120	150	180	196.2
0	43.0	44.0	44.6	44.6	45.1	44.8	45.6	44.5
17	43.4	44.5	44.6	44.4	45.1	45.4	45.6	44.9
	42.5	43.5	44.5	○ 39.1	44.6	42.3	45.3	43.8
39.6	42.9	43.7	44.2	44.3	44.5	44.4	45.1	43.7
56.6 cm	41.3	42.5	42.1	43.3	44.4	43.5	43.1	43.1

Final Surface

43.0	44.0	44.6	44.7	45.1	44.9	45.6	44.5
43.4	44.5	44.6	44.3	45.1	45.4	45.6	44.9
42.5	43.5	44.5	○ 39.2	44.6	42.3	45.3	43.8
42.9	43.6	44.2	44.3	44.5	44.4	45.1	43.7
41.4	42.5	42.1	43.3	44.4	43.5	43.1	43.1

SOIL BOX PLAN TEST NO: # 16 DATE: 12/15/2015

JOSEPH TOTH

Shakle Table Test # 17

Joseph Toth

Date: 12/18/2015

		Dense Layer			Liquefiable Layer	
		Ws (lbs)	Ww (lbs)		Ws (lbs)	
	1	35.7	1.79	1	35.3	
	2	35.6	1.78	2	37.9	
108.0	3	36.7	1.84 –	3	38.0	111.2
	4	37.0	1.85 –	4	33.9	
	5	37.1	1.86 –	5	35.5	
221.2	6	39.1	1.96 –	6	39.4	
	7	37.6	1.88 –	7	36.2	256.2
	8	34.3	1.72 –	8	39.6	
329.9	9	36.8	1.84 –	9	36.0	331.8
	10	36.2	1.81 –	10	35.0	
402.3	11	36.2	1.81 –	11	35.6	402.4
	12	34.9	1.75 –	12	33.8	
	13	35.9	1.80 –	13	35.0	471.2
511.5	14	38.4	1.92 –	14	27.3	
	15	14.1	0.71	15	498.5 total	
	16	525.6 total		16		
	17			17		
	18			18		
	19			19		
	20			20		
	21			21		
	22			22		
	23			23		
	24			24		
	25			25		
	26			26		
	27			27		
	28			28		
	29			29		
	30	525.6 lbs		30	498.5 lbs	

NOTES:

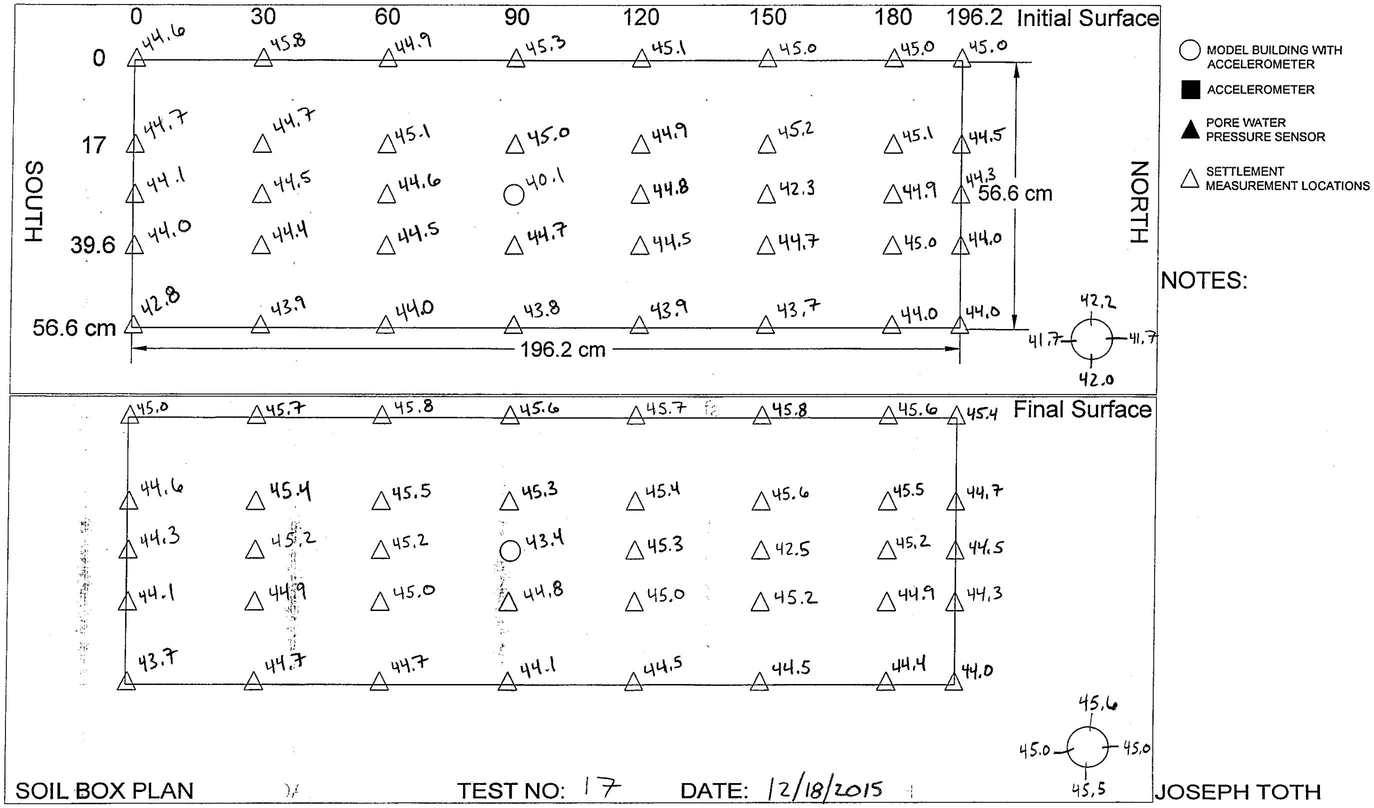

NOTES:

SOIL BOX PLAN TEST NO: 17 DATE: 12/18/2015

JOSEPH TOTH

Shakle Table Test # 18

Date: 1/4/2016

Joseph Toth

Dense Layer

		Ws (lbs)	Ww (lbs)
	1	37.2	1.86 —
	2	38.6	1.93 —
	3	40.8	2.04 —
	4	36.4	1.82 —
	5	40.4	2.02 —
	6	36.2	1.81 —
265.7 —	7	36.1	1.81 —
302.1 —	8	36.4	1.82 —
	9	39.0	1.95 —
	10	36.6	1.83 —
	11	35.7	1.79 —
453.9 —	12	40.5	2.03 —
	13	32.4	1.62
	14	37.0	1.85
	15	2.3	0.12
	16	525.6 total	
	17		
	18		
	19		
	20		
	21		
	22		
	23		
	24		
	25		
	26		
	27		
	28		
	29		
	30	525.6 lbs	

Liquefiable Layer

	Ws (lbs)	
1	42.1	
2	41.6	
3	38.8	
4	33.7	
5	34.4	
6	38.8	
7	38.6	
8	37.2	— 305.2
9	40.2	
10	39.3	
11	39.3	
12	41.9	— 465.9
13	32.6	
14		
15	498.5 total	
16		
17		
18		
19		
20		
21		
22		
23		
24		
25		
26		
27		
28		
29		
30	498.5 lbs	

NOTES:

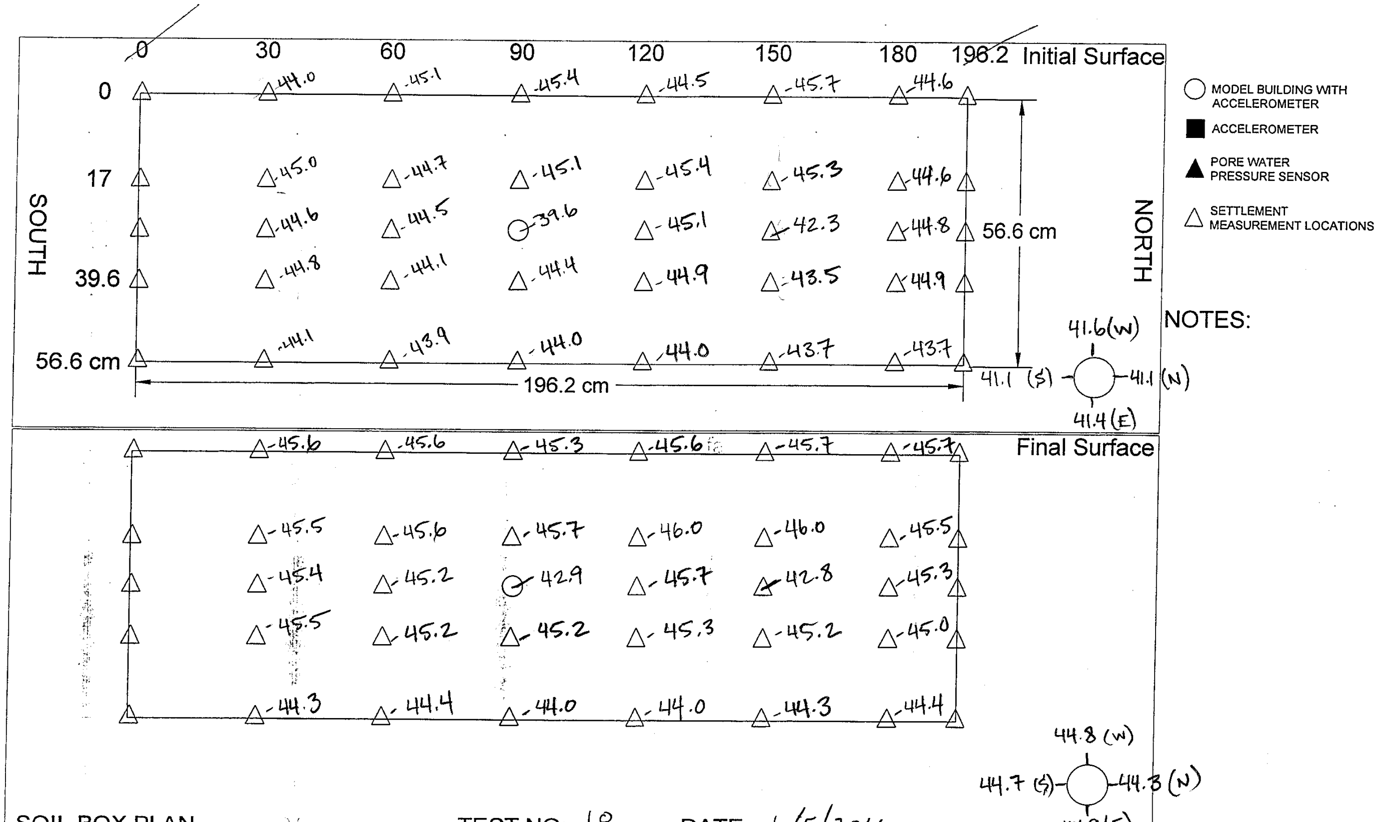

NOTES:

SOIL BOX PLAN TEST NO: 18 DATE: 1/5/2016

JOSEPH TOTH

Shakle Table Test # 19 SF= 20, 6in layer, 6in-footing

Date: 1/8/2015

Joseph Toth

		Dense Layer			Liquefiable Layer	
		Ws (lbs)	Ww (lbs)		Ws (lbs)	
	1	30.8	1.54	1	35.7	
	2	31.7	1.59	2	39.0	
	3	30.5	1.53	3	38.6	
	4	33.4	1.67	4	38.2	
	5	35.0	1.75	5	37.4	
	6	37.3	1.87	6	38.0	
	7	31.8	1.59	7	33.8	
	8	32.1	1.61	8	35.9	
	9	36.8	1.84	9	39.6	— 336.2 lb
336.4 —	10	37.0	1.85	10	37.3	
	11	39.1	1.96	11	38.2	
	12	30.7	1.54	12	37.4	— 449.1
	13	28.6	1.43	13	37.8	
473.8 —	14	39.0	1.95	14	11.6	
502.8 —	15	29.0	1.45	15	—— total	
	16	22.8	1.14	16		
	17			17		
	18			18		
	19			19		
	20			20		
	21			21		
	22			22		
	23			23		
	24			24		
	25			25		
	26			26		
	27			27		
	28			28		
	29	525.6 lbs		29	498.5 lbs	
	30			30		

NOTES: SF-20

6in footing (13.5psf)

No pwp sensor

26sec to 46sec
46 to 56 (cool down)

0.37g

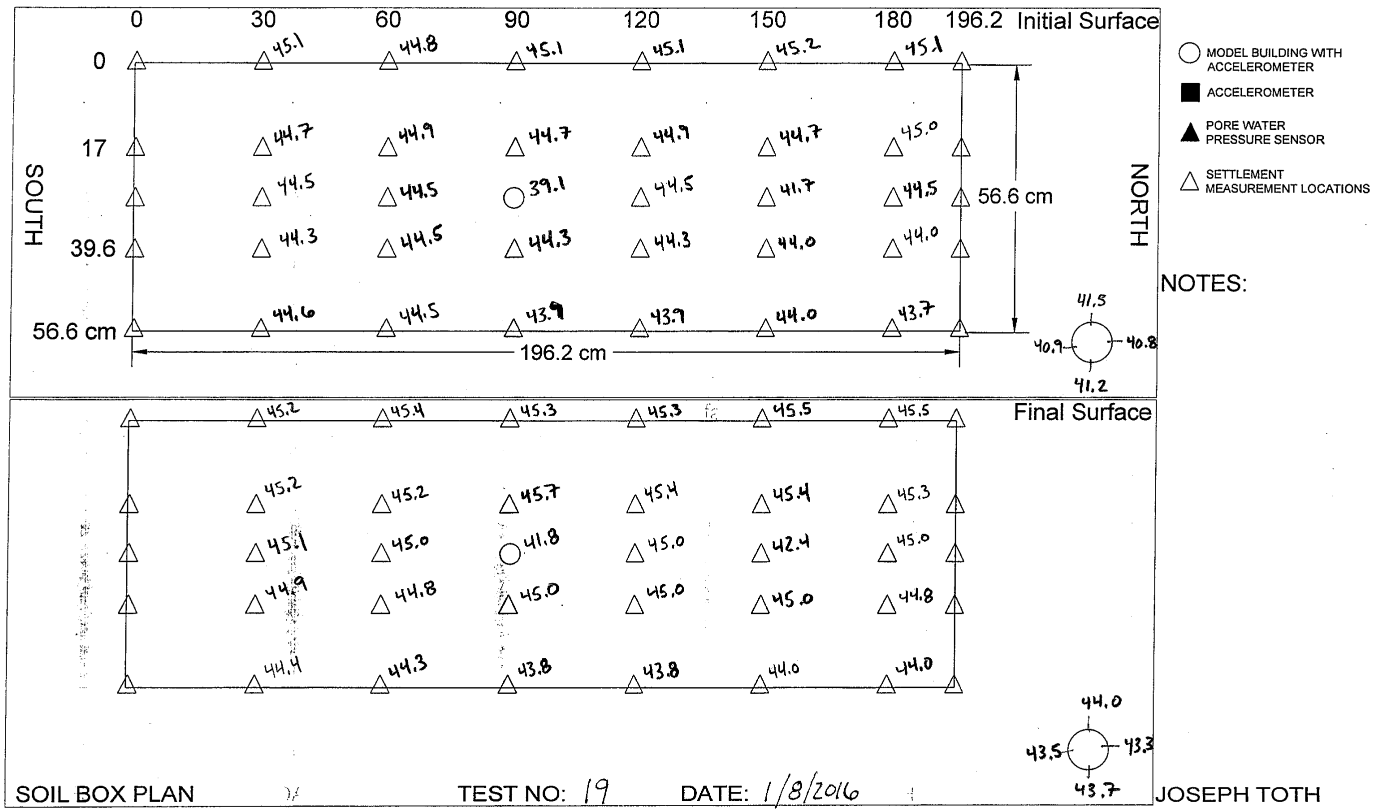

Shakle Table Test # 19.1

Joseph Toth

Date: 1/22/2016

		Dense Layer			Liquefiable Layer	
		Ws (lbs)	Ww (lbs)		Ws (lbs)	
	1	43.8	2.19	1	45.2	
	2	39.5	1.98	2	35.5	
	3	42.0	2.1	3	42.2	
	4	39.6	1.98	4	32.3	
	5	40.6	2.03	5	39.7	
	6	39.6	1.98	6	40.4	
	7	39.6	1.98	7	42.1	
324.4	8	39.7	1.98	8	39.9	317.3
	9	43.0	2.15	9	41.3	
	10	38.9	1.95	10	37.3	395.9
	11	44.8	2.24	11	39.2	
491.7	12	40.6	2.03	12	39.9	475.0
	13	33.9	1.70	13	23.5	
	14	525.6 total		14	498.5 total	
	15			15		
	16			16		
	17			17		
	18			18		
	19			19		
	20			20		
	21			21		
	22			22		
	23			23		
	24			24		
	25			25		
	26			26		
	27			27		
	28			28		
	29	525.6 lbs		29	498.5 lbs	
	30			30		

NOTES:

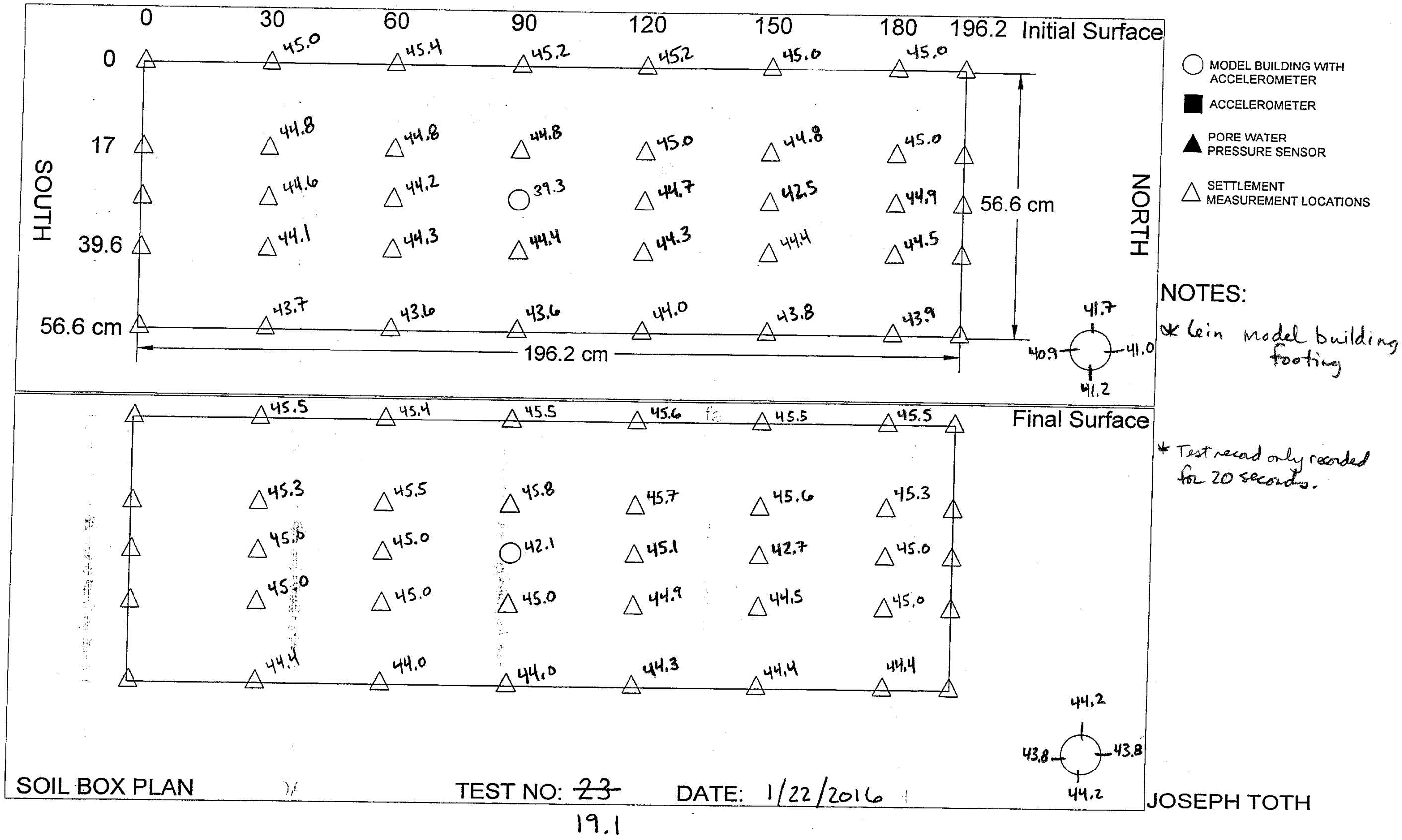

NOTES:

* 6in model building footing

* Test read only recorded for 20 seconds.

SOIL BOX PLAN

TEST NO: ~~23~~ 19.1

DATE: 1/22/2016

JOSEPH TOTH

Shakle Table Test # 19.2
Date: 2/5/2016

Joseph Toth

		Dense Layer			Liquefiable Layer	
		Ws (lbs)	Ww (lbs)		Ws (lbs)	
	1	36.7	1.84	1	41.9	
	2	43.9	2.20	2	44.8	
	3	43.7	2.19	3	44.1	
	4	38.9	1.95	4	42.5	
204.5	5	41.3	2.07 ✓	5	30.6	
	6	42.8	2.14 ✓	6	41.4	245.3
	7	37.9	1.90 ✓	7	42.2	
	8	42.8	2.14 ✓	8	~~40.7~~ 40.6	
	9	43.3	2.17 ✓	9	40.1	
	10	42.3	2.12 ✓	10	43.1	
456.8	11	43.2	2.16 ✓	11	44.7	456.0
	12	40.4	2.02 ✓	12	40.3	
	13	26.1	1.31 ✓	13		
	14			14		
	15	523.3 total		15	496.3 total	
	16			16		
	17			17		
	18			18		
	19			19		
	20			20		
	21			21		
	22			22		
	23			23		
	24			24		
	25			25		
	26			26		
	27			27		
	28			28		
	29	523.3 lbs		29	496.3	
	30			30		

NOTES:

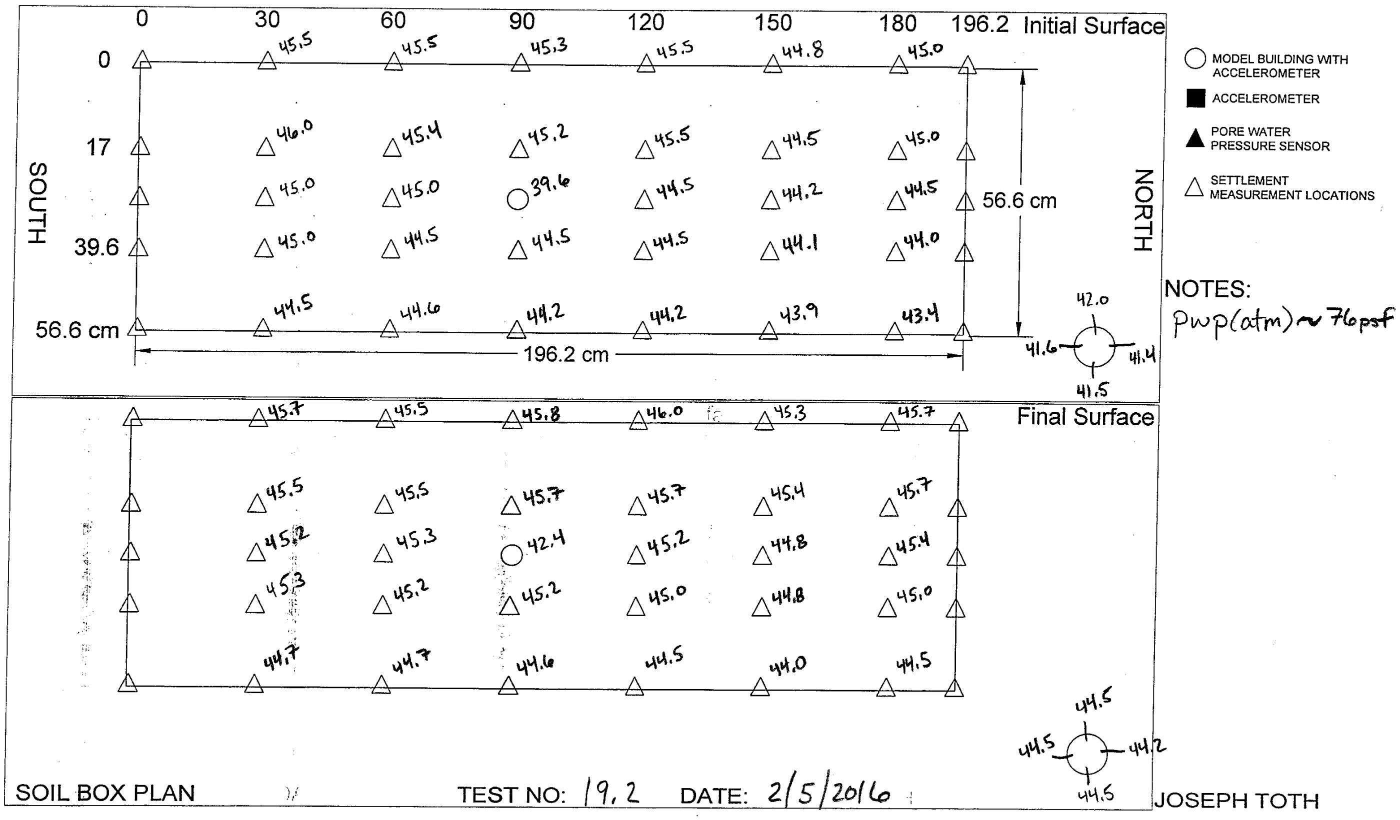

NOTES:
Pwp(atm) ~ 76psf

SOIL BOX PLAN TEST NO: 19.2 DATE: 2/5/2016

JOSEPH TOTH

Shakle Table Test # 20

Date: 1/12/2016

Joseph Toth

		Dense Layer		Liquefiable Layer	
		Ws (lbs)	Ww (lbs)	Ws (lbs)	
	1	41.1	2.10 ✓	41.8	
	2	34.9	1.75 ✓	38.0	
	3	41.1	2.10 ✓	39.4	
	4	37.3	1.87 ✓	39.3	
	5	35.8	1.79 ✓	38.7	
	6	40.9	2.05 ✓	39.2	
	7	41.5	2.08 ✓	38.8	275.2
	8	38.7	1.94 ✓	37.8	
	9	37.5	1.88 ✓	37.4	
389.6	10	40.8	2.04 ✓	40.2	
	11	36.8	1.84 ✓	36.8	427.4
469.4	12	43.0	2.15 ✓	4.9	432.3
	13	39.1	1.96 ✓	37.0	
	14	17.1	0.86 ✓	29.2	
	15	525.6		498.5	
	16				
	17				
	18				
	19				
	20				
	21				
	22				
	23				
	24				
	25				
	26				
	27				
	28				
	29	525.6 lbs		498.5 lbs	
	30				

NOTES:

Scale = 20

6in footing (13.5psf)

No pwp sensor

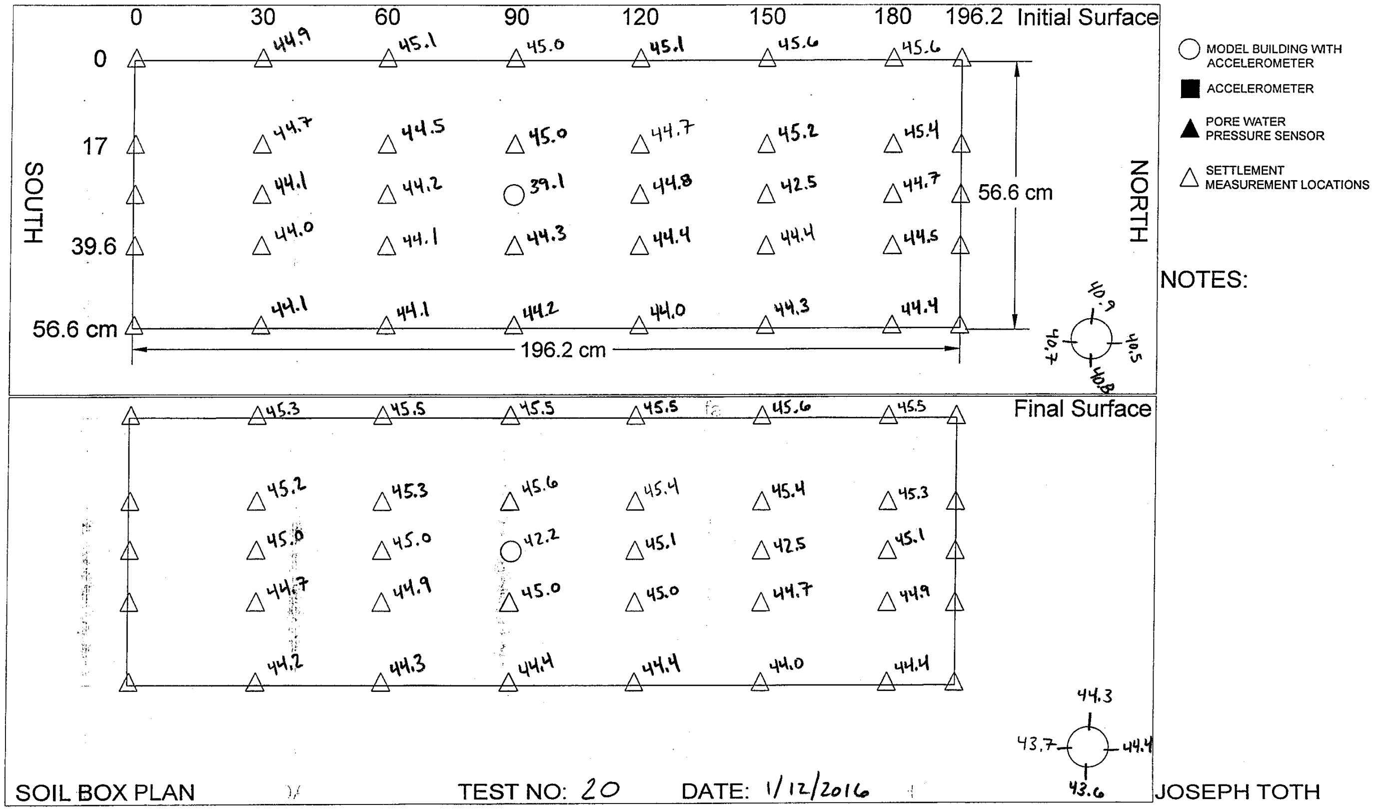
0
30
60
90
120
150
180
196.2
Initial Surface
0
17
39.6
56.6 cm
SOUTH
NORTH
44.9
45.1
45.0
45.1
45.6
45.6
44.7
44.5
45.0
44.7
45.2
45.4
44.1
44.2
39.1
44.8
42.5
44.7
44.0
44.1
44.3
44.4
44.4
44.5
44.1
44.1
44.2
44.0
44.3
44.4
56.6 cm
196.2 cm
40.9
40.7
40.5
40.8
Final Surface
45.3
45.5
45.5
45.5
45.6
45.5
45.2
45.3
45.6
45.4
45.4
45.3
45.0
45.0
42.2
45.1
42.5
45.1
44.7
44.9
45.0
45.0
44.7
44.9
44.2
44.3
44.4
44.4
44.0
44.4
44.3
43.7
44.4
43.6
○ MODEL BUILDING WITH ACCELEROMETER
■ ACCELEROMETER
▲ PORE WATER PRESSURE SENSOR
△ SETTLEMENT MEASUREMENT LOCATIONS
NOTES:
SOIL BOX PLAN
TEST NO: 20
DATE: 1/12/2016
JOSEPH TOTH

Joseph Toth

Shakle Table Test # 21
Date: 1/15/2016

Dense Layer

		Ws (lbs)	Ww (lbs)
	1	37.6	1.88
	2	39.0	1.95
	3	39.0	1.95
	4	39.6	1.98
	5	32.5	1.63
228.2	6	40.5	2.03
	7	37.8	1.89
	8	39.7	1.99
	9	38.0	1.9
	10	37.5	1.88
	11	37.9	1.89
457.0	12	37.9	1.89
	13	36.4	1.82
	14	32.2	1.61
	15		
	16	525.6	
	17		
	18		
	19		
	20		
	21		
	22		
	23		
	24		
	25		
	26		
	27		
	28		
	29		
	30	525.6 lbs	

Liquefiable Layer

	Ws (lbs)	
1	45.9	
2	32.2	
3	40.0	
4	36.2	
5	37.7	192.0
6	33.8	
7	40.1	265.9
8	35.7	
9	38.0	
10	39.4	379.0
11	24.1	
12	37.2	
13	29.5	
14	28.7	
15		
16	498.5	
17		
18		
19		
20		
21		
22		
23		
24		
25		
26		
27		
28		
29		
30	498.5 lbs	

NOTES:

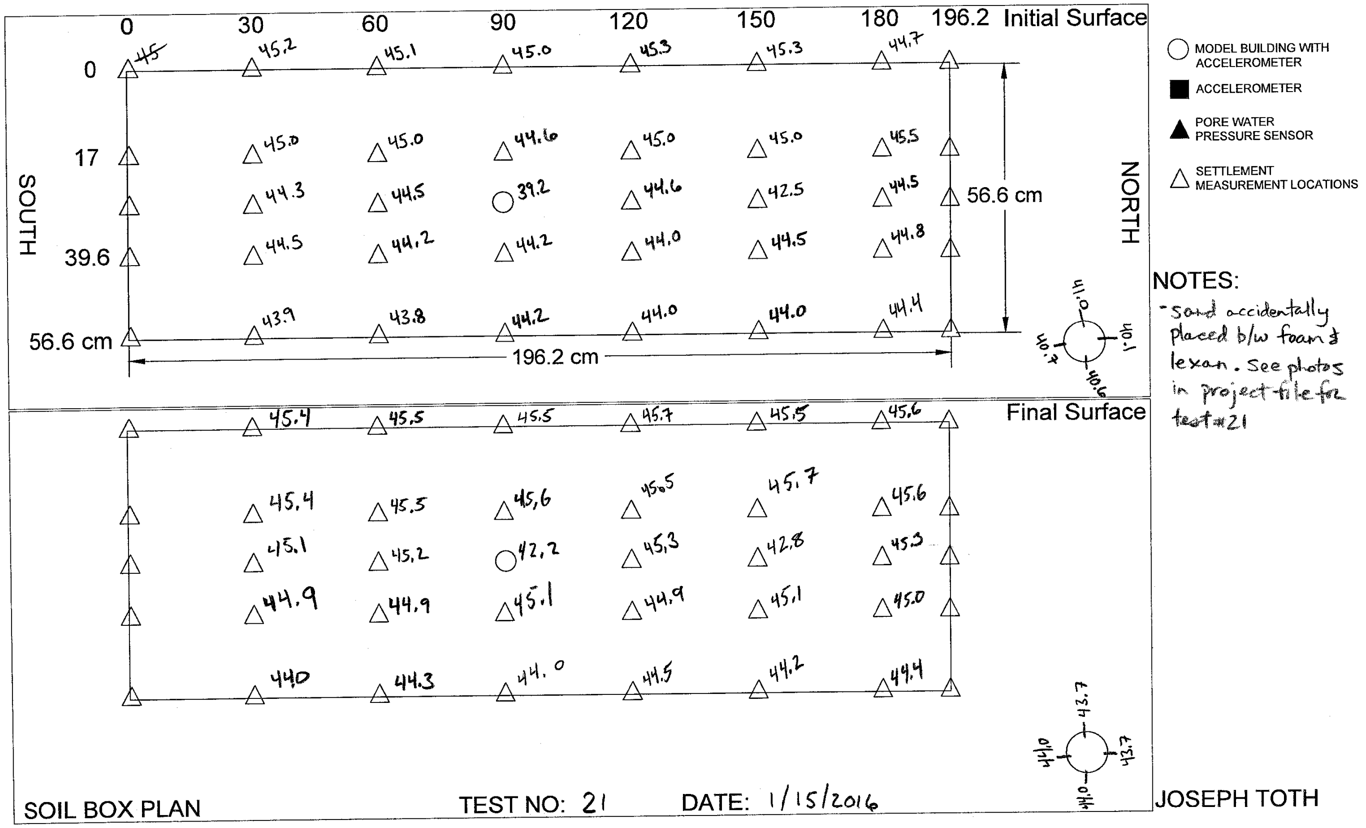

SOIL BOX PLAN TEST NO: 21 DATE: 1/15/2016

JOSEPH TOTH

NOTES:

- Sand accidentally placed b/w foam & lexan. See photos in project file for test #21

Shakle Table Test # 22

Joseph Toth

Date: 1/20/2016

		Dense Layer			Liquefiable Layer	
		Ws (lbs)	Ww (lbs)		Ws (lbs)	
	1	39.6	1.98 ✓	1	28.3	
	2	39.5	1.98 ✓	2	40.1	
	3	39.7	1.99 ✓	3	37.1	
	4	38.3	1.92 ✓	4	39.4	
	5	40.3	2.02 ✓	5	34.2	
	6	41.3	2.07 ✓	6	41.7	
	7	34.0	1.7 ✓	7	37.0	
	8	38.8	1.94 ✓	8	42.1	
	9	39.6	1.98 ✓	9	40.0	339.9
	10	40.2	2.01 ✓	10	39.7	
431.1	11	39.8	1.99 ✓	11	35.4	
	12	36.2	1.81 ✓	12	42.6	
507.8	13	40.5	2.03 ✓	13	29.7	487.3
	14	17.8	0.89 ✓	14	11.2	
	15	525.6 total		15	498.5 total	
	16			16		
	17			17		
	18			18		
	19			19		
	20			20		
	21			21		
	22			22		
	23			23		
	24			24		
	25			25		
	26			26		
	27			27		
	28			28		
	29			29		
	30	525.6 lbs		30	498.5 lbs	

NOTES:

8in diameter footing

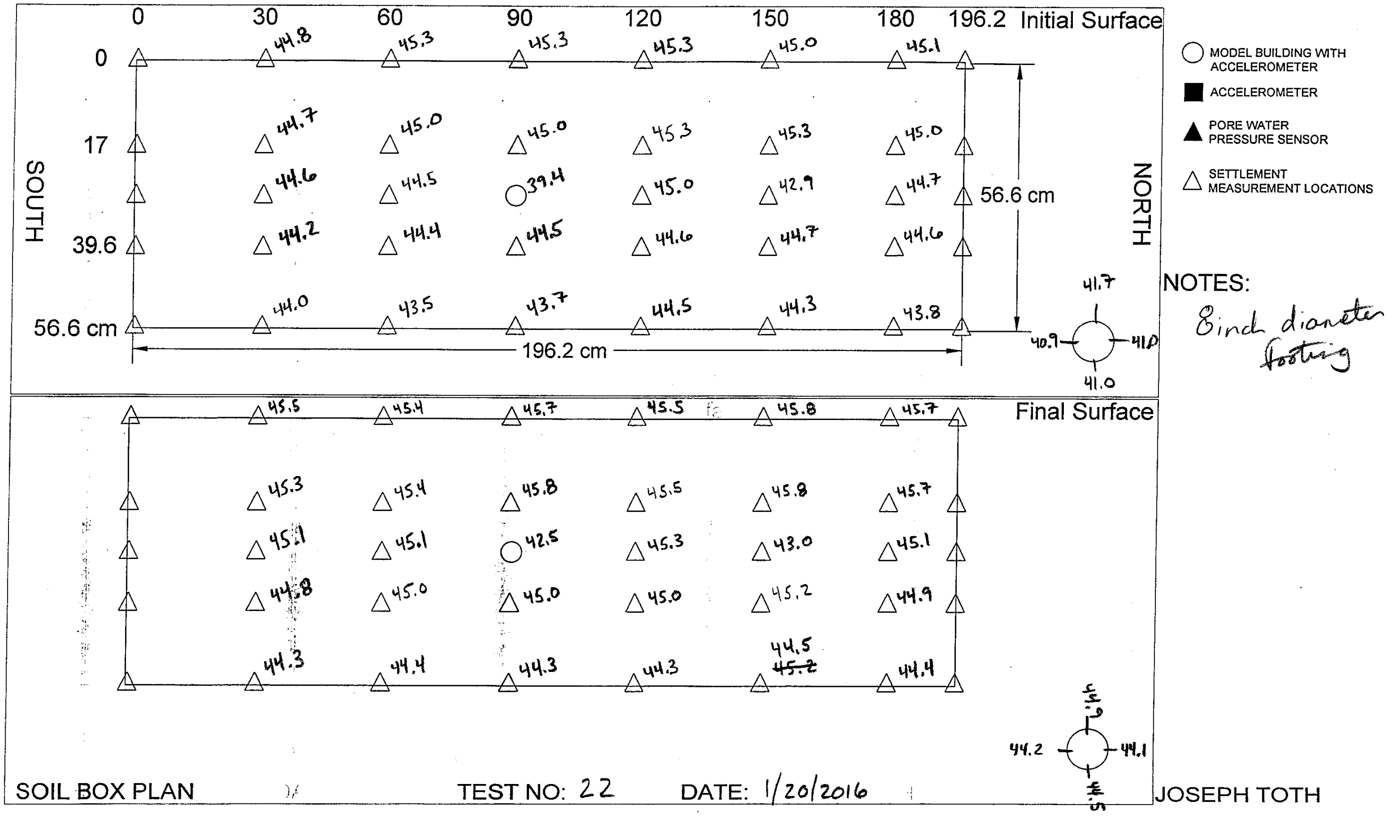

NOTES:
8 inch diameter footing

SOIL BOX PLAN

TEST NO: 22

DATE: 1/20/2016

JOSEPH TOTH

Shakle Table Test # 22.1

Date: 2/12/16

Joseph Toth

		Dense Layer			Liquefiable Layer	
		Ws (lbs)	Ww (lbs)		Ws (lbs)	
	1	41.8	2.09	1	43.6	
	2	44.1	2.21	2	44.6	
	3	43.5	2.18	3	43.7	
	4	43.4	2.17 ✓	4	42.8	
	5	37.6	1.88 ✓	5	42.1	
	6	41.7	2.09 ✓	6	40.8	
	7	40.1	2.01 ✓	7	37.3	
326.0	8	33.8	1.69 ✓	8	41.3	
	9	40.2	2.01 ✓	9	46.5	
	10	43.6	2.18 ✓	10	37.7	
453.1	11	43.3	2.17 ✓	11	39.7	460.1
	12	44.5	2.23 ✓	12	36.2	
	13	25.7	1.29 ✓	13		
	14			14		
	15			15		
	16			16		
	17			17		
	18			18		
	19			19		
	20			20		
	21	523.3 lbs		21	496.3 lbs	
	22			22		
	23			23		
	24			24		
	25			25		
	26			26		
	27			27		
	28			28		
	29			29		
	30			30		

NOTES: 8 in footing

1 pwp sensor (3in)

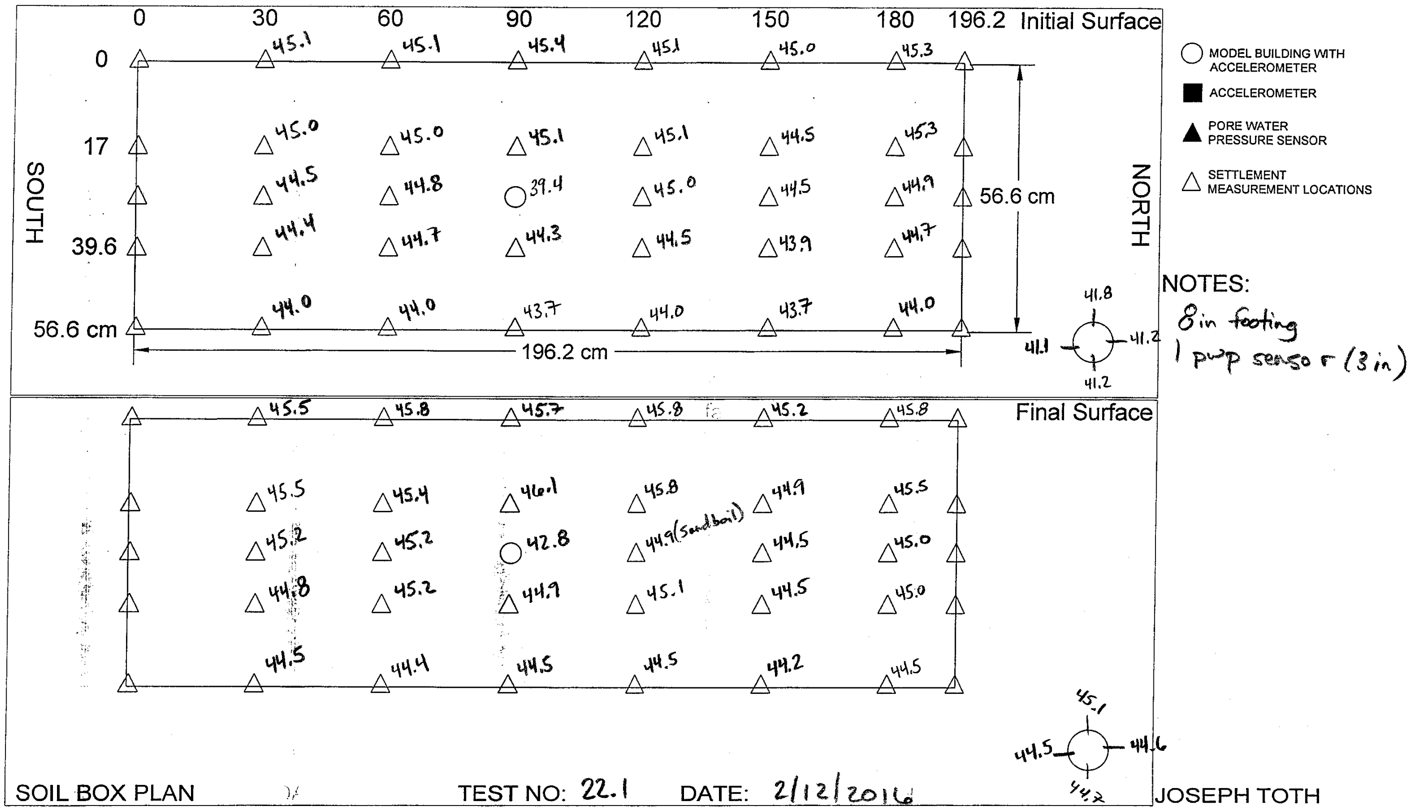

NOTES:

8 in footing

1 pwp sensor (3 in)

Shakle Table Test # 23

Date: 2/19/2016

Joseph Toth

		Dense Layer			Liquefiable Layer	
		Ws (lbs)	Ww (lbs)		Ws (lbs)	
	1	42.0	2.1	1	38.6	
	2	43.9	2.20	2	40.6	
	3	44.7	2.24 ✓	3	42.6	
	4	44.4	2.22 ✓	4	37.6	
	5	41.2	2.06 ✓	5	40.5	
	6	43.4	2.17 ✓	6	42.8	
	7	41.8	2.09 ✓	7	43.7	
	8	41.8	2.09 ✓	8	44.8	
	9	42.3	2.12 ✓	9	42.2	
	10	33.6	1.68 ✓	10	41.1	414.5
	11	41.5	2.08 ✓	11	41.1	
503.2	12	42.6	2.13 ✓	12	40.7	496.3
	13	20.1	1.01 ✓	13		
	14	523.3		14	496.3 lbs	
	15			15		
	16			16		
	17			17		
	18			18		
	19			19		
	20	523.3 lbs		20	496.3 lbs	
	21			21		
	22			22		
	23			23		
	24			24		
	25			25		
	26			26		
	27			27		
	28			28		
	29			29		
	30			30		

NOTES: 10 inch footing

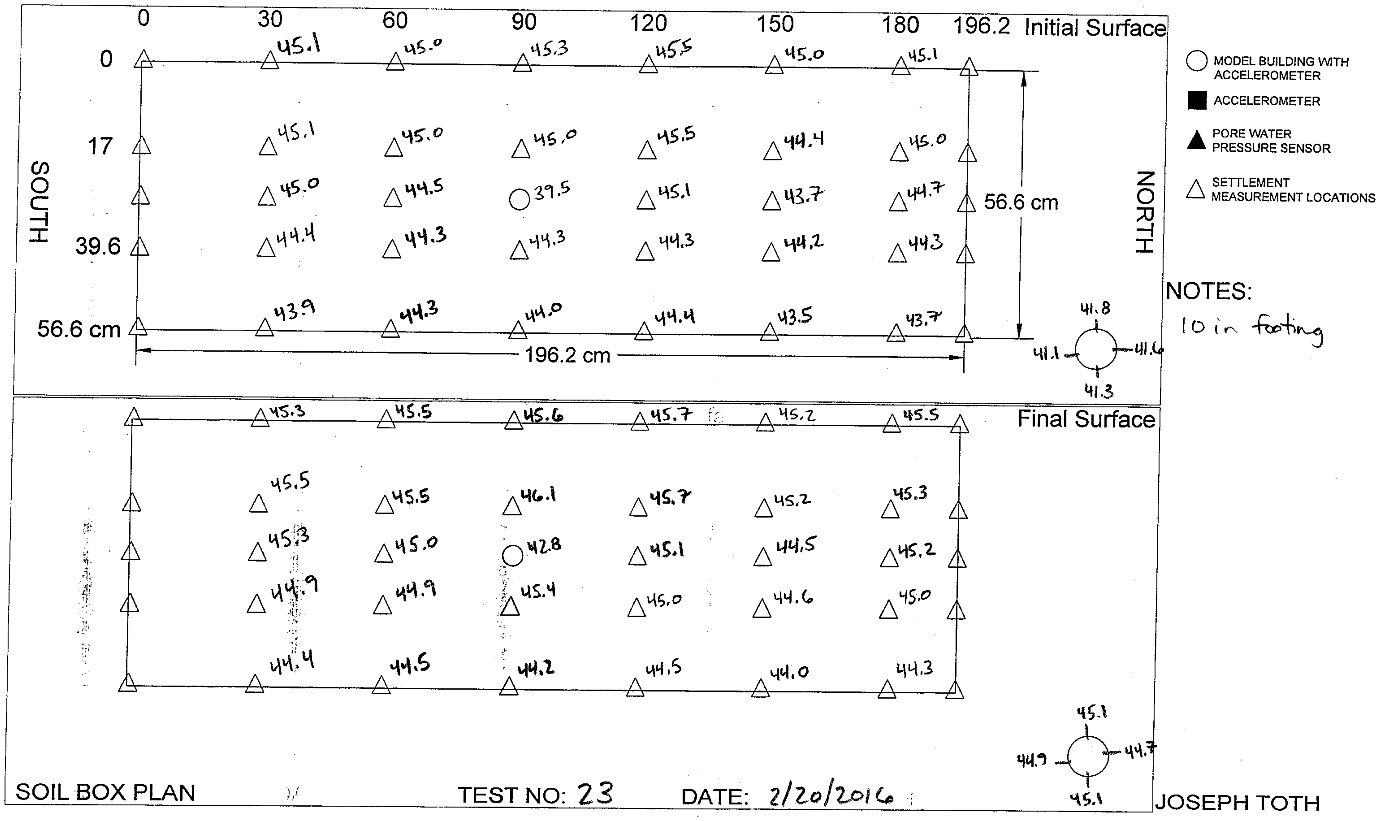

NOTES:
10 in footing

SOIL BOX PLAN TEST NO: 23 DATE: 2/20/2016

JOSEPH TOTH

Shakle Table Test # 24
Date: 2/26/16

Joseph Toth

		Dense Layer			Liquefiable Layer	
		Ws (lbs)	Ww (lbs)		Ws (lbs)	
	1	43.6	2.18	1	42.0	
	2	41.7	2.09.	2	44.8	
	3	37.9	1.90	3	41.0	
	4	38.0	1.9	4	43.2	
	5	43.6	2.18	5	45.4	
	6	41.1	2.06	6	40.2	256.6
	7	44.6	2.23	7	41.1	
333.6	8	43.1	2.16	8	43.3	
	9	39.6	1.98	9	37.5	378.5
	10	43.9	2.20	10	39.8	
458.6	11	41.5	2.08	11	45.7	
	12	36.0	1.8	12	32.3	
	13	28.7	1.44	13	496.3	
	14	523.3		14		
	15			15		
	16			16		
	17			17		
	18			18		
	19			19		
	20			20		
	21			21		
	22			22		
	23			23		
	24			24		
	25			25		
	26			26		
	27			27		
	28	523.3 lbs		28	496.3 lbs	
	29			29		
	30			30		

NOTES: 12in footing → 12.9psf

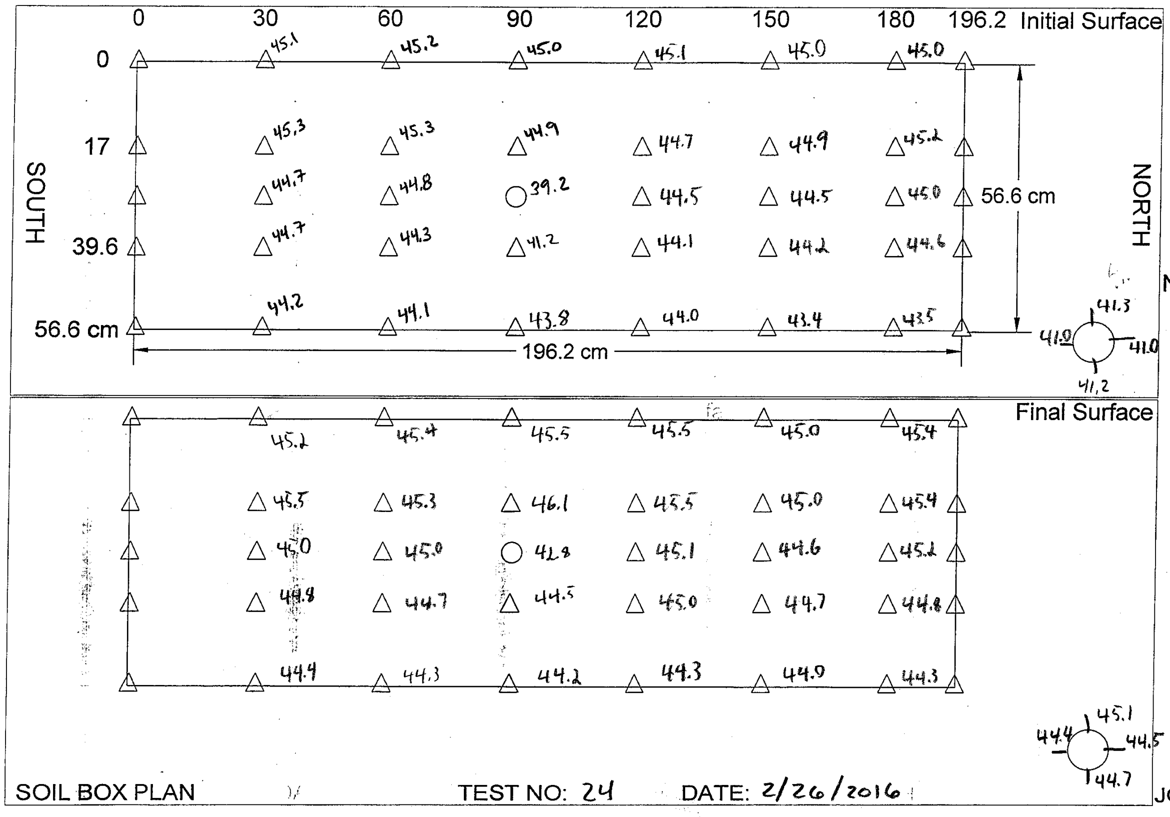

SOIL BOX PLAN TEST NO: 24 DATE: 2/26/2016

JOSEPH TOTH

○ MODEL BUILDING WITH ACCELEROMETER

■ ACCELEROMETER

▲ PORE WATER PRESSURE SENSOR

△ SETTLEMENT MEASUREMENT LOCATIONS

NOTES:

12in footing

Shakle Table Test # 25

Joseph Toth

Date: 3/2/2016

		Dense Layer			Liquefiable Layer	
		Ws (lbs)	Ww (lbs)		Ws (lbs)	
	1	42.2	2.11	1	41.0	
	2	44.5	2.23	2	41.1	
	3	41.7	2.09	3	43.6	
	4	36.0	1.8	4	43.1	
	5	40.2	2.01 ✓	5	39.8	
	6	37.8	1.89 ✓	6	38.3	
	7	44.7	2.24 ✓	7	38.0	
	8	41.8	2.09 ✓	8	44.1	
	9	42.2	2.11 ✓	9	42.2	
415.0—	10	43.9	2.20 ✓	10	44.8	
	11	33.0	1.65 ✓	11	40.2	— 456.2
489.6	12	41.6	2.08 ✓	12	40.1	
	13	33.7	1.69 ✓	13		
	14	523.3		14		
	15			15		
	16			16		
	17			17		
	18			18		
	19			19		
	20			20		
	21			21		
	22			22		
	23			23		
	24			24		
	25			25		
	26			26		
	27			27		
	28			28		
	29	523.3 lbs		29	496.3 lbs	
	30			30		

NOTES: 3in footing

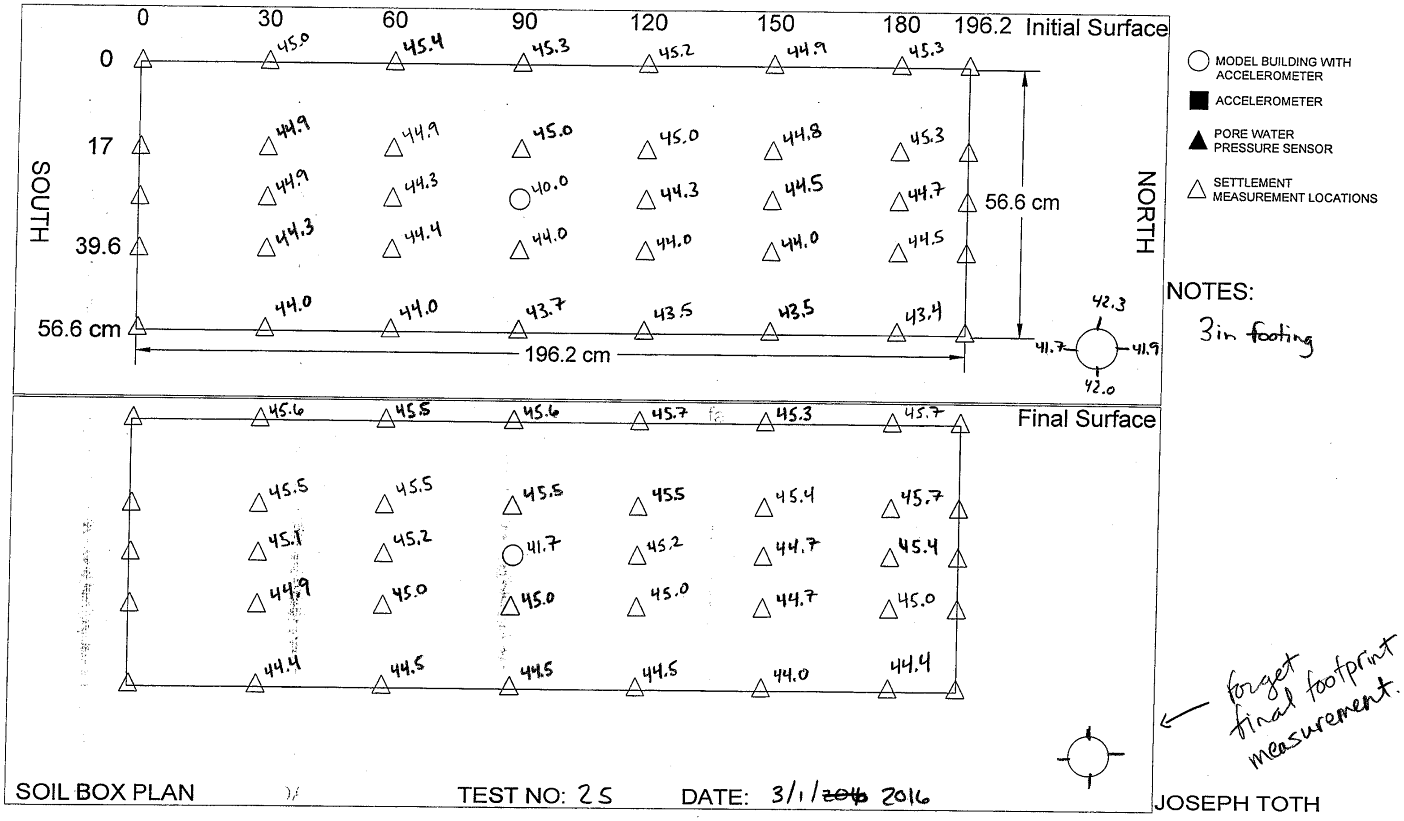

SOIL BOX PLAN

TEST NO: 2S

DATE: 3/1/~~2016~~ 2016

NOTES:

3in footing

JOSEPH TOTH

← forget final footprint measurement.

Shakle Table Test # 26

Date: 3/9/2016

Joseph Toth

		Dense Layer			Liquefiable Layer
		Ws (lbs)	Ww (lbs)		Ws (lbs)
	1	29.0	1.45	1	42.7
	2	42.9	2.15	2	40.7
	3	28.2	1.41	3	42.4
	4	40.5	2.03	4	45.9
	5	43.5	2.18	5	47.9
	6	45.5	2.28	6	47.1
	7	42.8	2.14	7	47.0
	8	45.8	2.29	8	47.8
	9	44.3	2.22	9	43.8
	10	43.4	2.17	10	47.1
451.4	11	45.5	2.28	11	43.9
	12	45.9	2.30	12	
	13	26.0	1.3	13	496.3 lbs
	14	523.3		14	
	15			15	
	16			16	
	17			17	
	18			18	
	19			19	
	20			20	
	21			21	
	22			22	
	23			23	
	24			24	
	25			25	
	26			26	
	27	523.3 lbs		27	496.3 lbs
	28			28	
	29			29	
	30			30	

NOTES: 4.5in footing

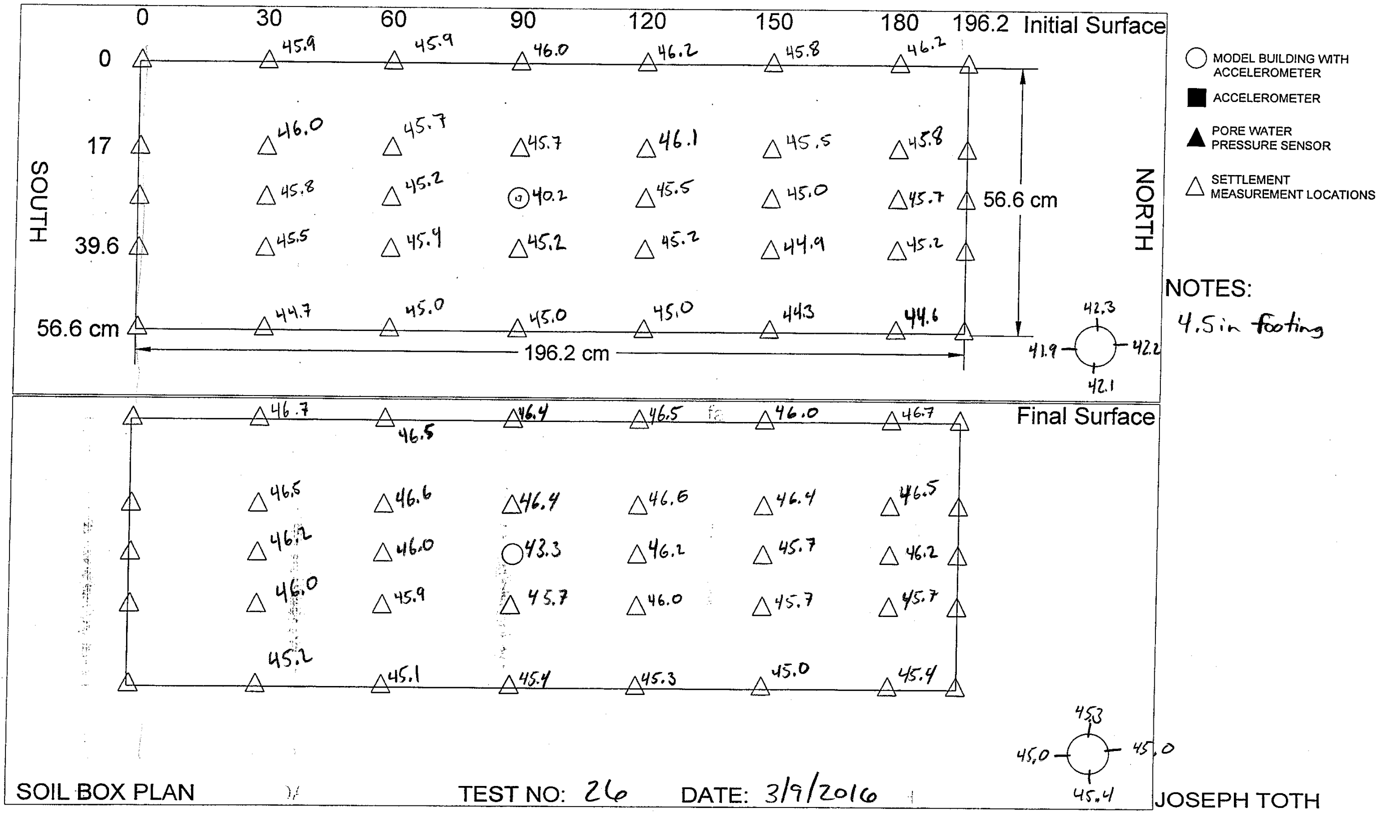

NOTES:
4.5 in footing

SOIL BOX PLAN TEST NO: 26 DATE: 3/9/2016

JOSEPH TOTH

Shakle Table Test # 27 Joseph Toth

Date: 3/15/2016

	Dense Layer			Liquefiable Layer	
	Ws (lbs)	**Ww (lbs)**		**Ws (lbs)**	
1	43.8	2.19	1	37.6	
2	43.6	2.18	2	37.8	
3	38.6	1.93	3	43.8	
4	43.0	2.15	4	38.4	
5	44.5	2.23	5	40.2	
6	43.1	2.16	6	41.6	
7	5.1	0.26	7	40.1	
8			8	41.6	
9			9	42.1	
10			10	42.1	
11			11	37.8	
12			12	43.4	
13			13	41.9	
14			14	42.7	
15			15	44.3	615.4
16			16	39.6	
17			17	42.9	697.9
18			18	37.4	
19			19	9.2	
20			20		
21			21		
22	261.7 lbs		22		
23			23		
24			24	744.5 lbs	
25			25		
26			26		
27			27		
28			28		
29			29		
30			30		

NOTES:

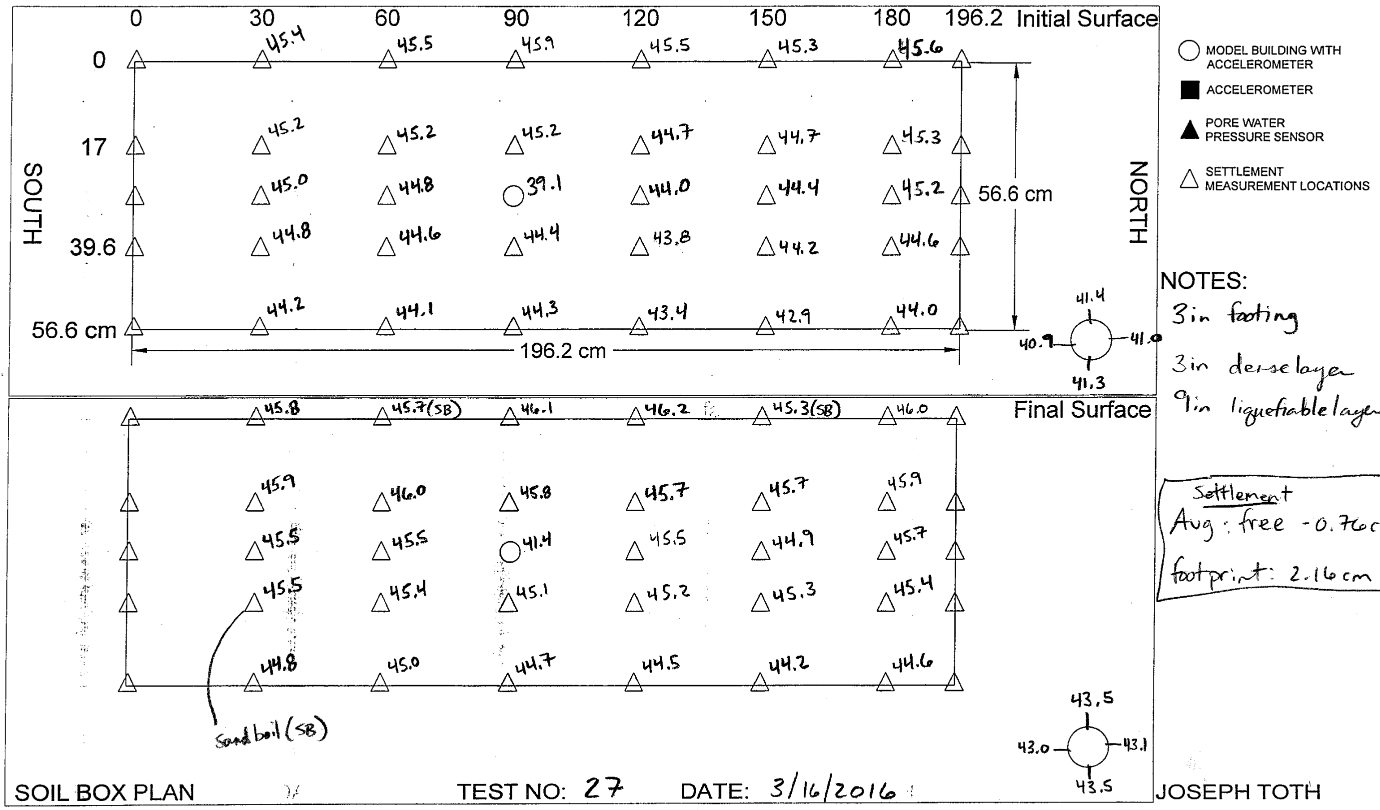

NOTES:

3in footing

3in dense layer

9in liquefiable layer

Settlement

Avg: free -0.76cm

footprint: 2.16cm

SOIL BOX PLAN TEST NO: 27 DATE: 3/16/2016

JOSEPH TOTH

Shakle Table Test # 28

Date: 3/18/16

Joseph Toth

		Dense Layer			Liquefiable Layer	
		Ws (lbs)	Ww (lbs)		Ws (lbs)	
	1	42.1	2.11	1	45.1	
	2	39.9	1.99	2	42.1	
	3	42.2	2.11	3	47.1	
	4	42.7	2.14	4	44.3	
	5	40.0	2.0	5	41.6	
250.3	6	43.4	2.17	6	41.6	
	7	11.3	0.57	7	44.1	
	8			8	37.1	
	9			9	40.0	
	10			10	44.2	
	11			11	38.5	
	12			12	38.9	463.0
	13			13	31.9	
	14			14	42.9	
	15			15	38.4	
	16			16	42.0	618.2
	17			17	41.2	
	18			18	39.3	698.7
	19			19	41.9	
	20			20	3.9	
	21			21	744.5 ~~0~~	
	22			22		
	23			23		
	24			24		
	25			25		
	26			26		
	27	2261.6		27	744.5	
	28			28		
	29			29		
	30			30		

NOTES: 4.5in footing

9in Liq. Layer

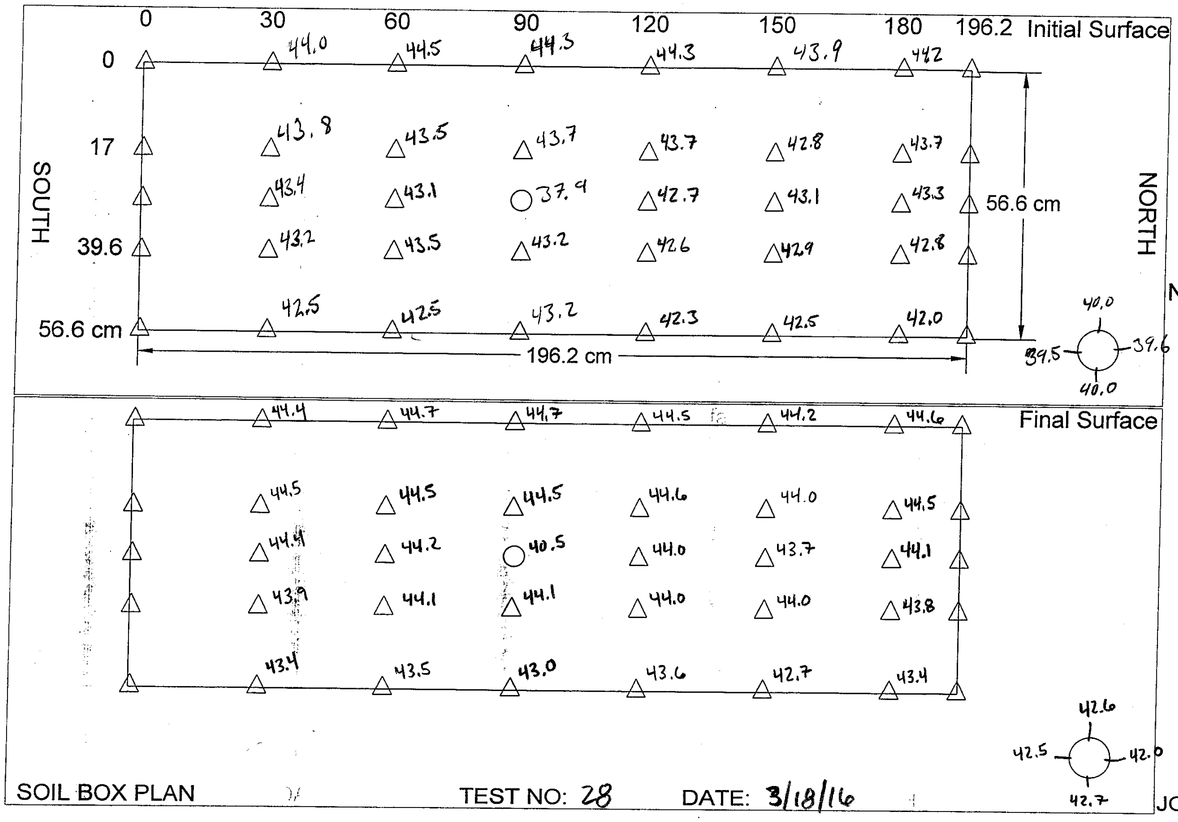

SOIL BOX PLAN TEST NO: 28 DATE: 3/18/16

JOSEPH TOTH

○ MODEL BUILDING WITH ACCELEROMETER

■ ACCELEROMETER

▲ PORE WATER PRESSURE SENSOR

△ SETTLEMENT MEASUREMENT LOCATIONS

NOTES:

4.5in footing

Shakle Table Test # 29

Joseph Toth

Date: 3/24/16

		Dense Layer			Liquefiable Layer	
		Ws (lbs)	Ww (lbs)		Ws (lbs)	
	1	29.7	1.49	1	38.3	
	2	40.8	2.04	2	42.1	
	3	44.4	2.22	3	44.6	
	4	45.3	2.27	4	44.5	
	5	43.6	2.18	5	41.1	
244.9 –	6	41.1	2.06	6	43.3	
	7	16.8	0.84	7	45.9	
	8	0		8	44.3	
	9			9	38.2	
	10			10	42.9	
	11			11	43.8	
	12			12	40.8	– 509.8
	13			13	41.9	
	14			14	45.2	
	15			15	42.0	– 638.9
	16			16	44.0	
	17			17	40.9	
	18			18	20.7	
	19			19	0	
	20			20		
	21			21		
	22			22		
	23			23		
	24			24		
	25			25		
	26			26		
	27			27		
	28	261.7 lbs	—	28	744.5 lbs	
	29			29		
	30			30		

NOTES: 6 in footing 2.472 lbs

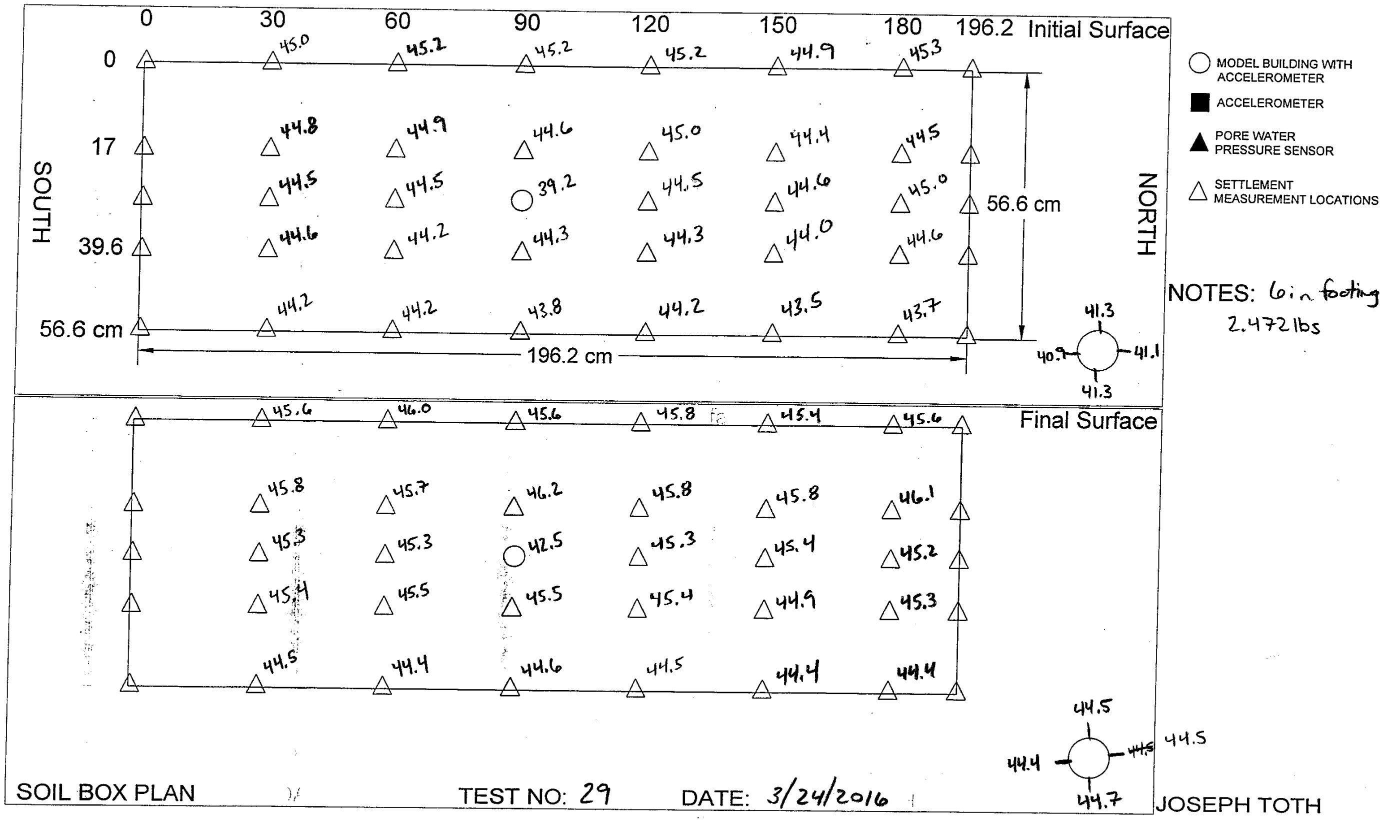

NOTES: 6 in footing
2.472 lbs

SOIL BOX PLAN

TEST NO: 29

DATE: 3/24/2016

JOSEPH TOTH

Shakle Table Test # 30

Joseph Toth

Date: 4/1/2016

		Dense Layer			Liquefiable Layer	
		Ws (lbs)	Ww (lbs)		Ws (lbs)	
	1	44.1	2.21	1	40.3	
	2	40.6	2.03	2	36.8	
	3	42.4	2.12	3	33.7	
	4	25.8	1.29	4	38.8	
	5	42.4	2.12	5	40.0	
	6	41.9	2.10	6	36.7	
	7	43.1	2.16	7	44.6	
	8	41.5	2.08	8	42.1	
	9	39.7	1.99 ✓	9	40.2	
	10	43.0	2.15 ✓	10	37.5	
	11	44.6	2.23 ✓	11	38.0	
	12	41.2	2.06 ✓	12	40.8	
	13	41.7	2.09 ✓	13	40.8	
	14	42.1	2.11 ✓	14	42.6	
	15	43.3	2.17 ✓	15	40.9	
659.6	16	42.2	2.11 ✓	16	40.1	
	17	41.0	2.05 ✓	17	43.6	
	18	45.4	2.27 ✓	18	39.4	
	19	42.2	2.11 ✓	19	37.8	754.7
	20	44.8	2.24 ✓	20	40.8	
	21	43.5	2.18 ✓	21	38.4	
	22	43.5	2.18 ✓	22	37.9	
	23	40.2	2.01 ✓	23	40.2	
	24	45.1	2.23 ✓	24	41.1	
1046.6	25	41.3	2.07 ✓	25	39.6	992.7
	26			26		
	27			27		
	28			28		
	29			29		
	30	1046.6 lbs		30	992.7 lbs	

NOTES: 3in footing w/ helical piles to 17in depth – single helix 1.2 in (12 in prototype) diame

W = 0.599 lbs ~ 12.2 psf

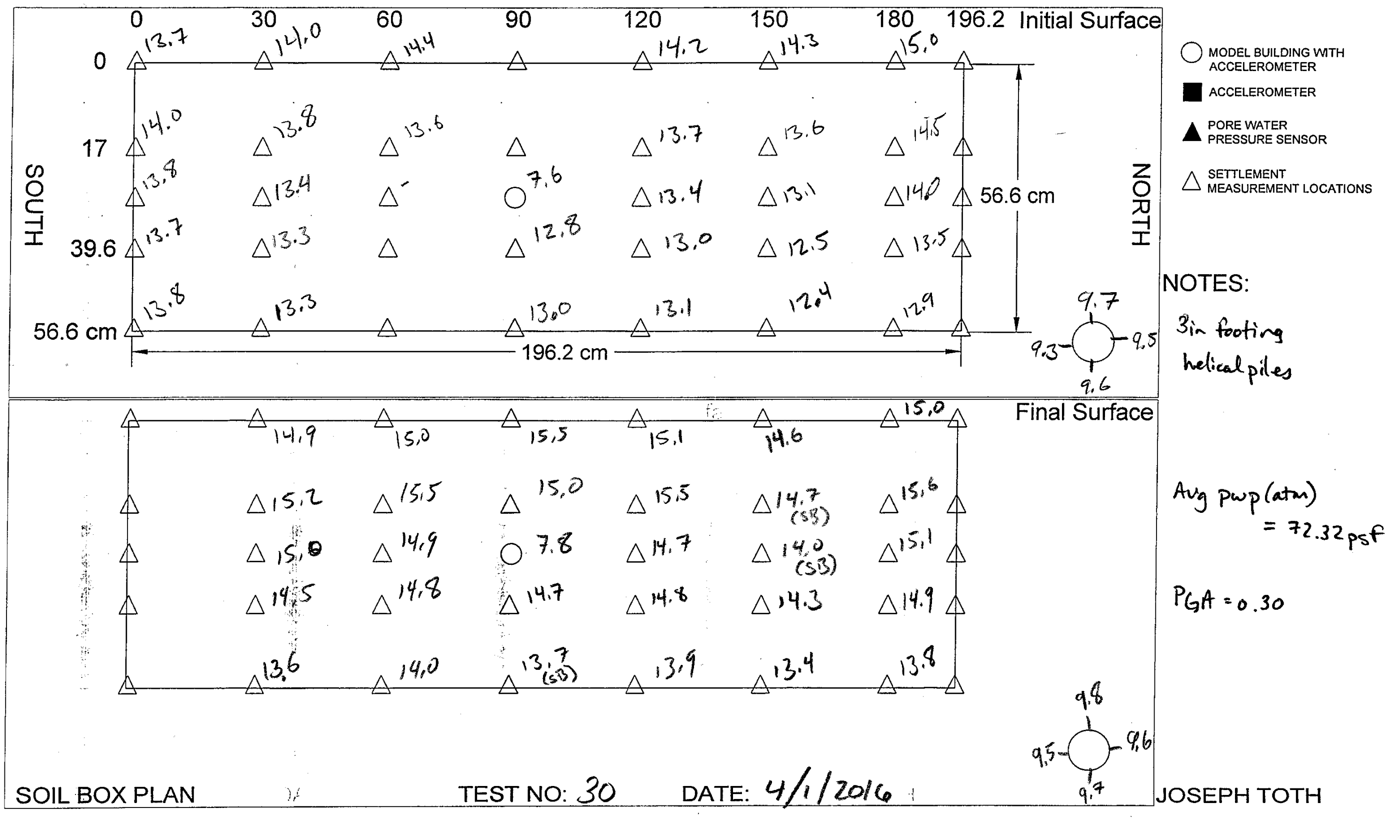

NOTES:

3in footing
helical piles

Avg pwp (atm)
= 72.32 psf

PGA = 0.30

SOIL BOX PLAN TEST NO: 30 DATE: 4/1/2016

JOSEPH TOTH

Shakle Table Test # 31

Date: 4/20/2016

Joseph Toth

		Dense Layer		Liquefiable Layer	
		Ws (lbs)	Ww (lbs)	Ws (lbs)	
	1	52.9	2.65	64.9	
	2	56.2	2.81	59.6	
	3	58.6	2.93	55.8	
	4	61.2	3.06	58.1	— 238.4
	5	60.9	3.05	35.5	
	6	61.9	3.09	25.6	
	7	61.1	3.05	59.8	
473.7 —	8	60.9	3.05	60.3	
	9	59.7	2.99	57.4	
	10	60.8	3.04	53.6	
	11	55.8	2.79	58.1	
681.3 —	12	31.7	1.59	56.4	
	13	60.8	3.04	56.3	
	14	62.0	3.09	53.2	— 754.6
	15	64.0	3.2	58.8	
931.3 —	16	63.2	3.16	60.5	— 873.9
	17	60.3	3.02	58.9	
1046.6 —	18	55.0	2.75	49.6	— 982.4
	19			10.3	
	20	— 1046.6	—	~~20~~ 992.7 —	
	21				
	22				
	23				
	24				
	25				
	26				
	27				
	28				
	29	1046.6 lbs	—	992.7 —	
	30				

NOTES:

6 in footing - helical = 2.441 lbs

6 in unsupported = 2.508 lbs

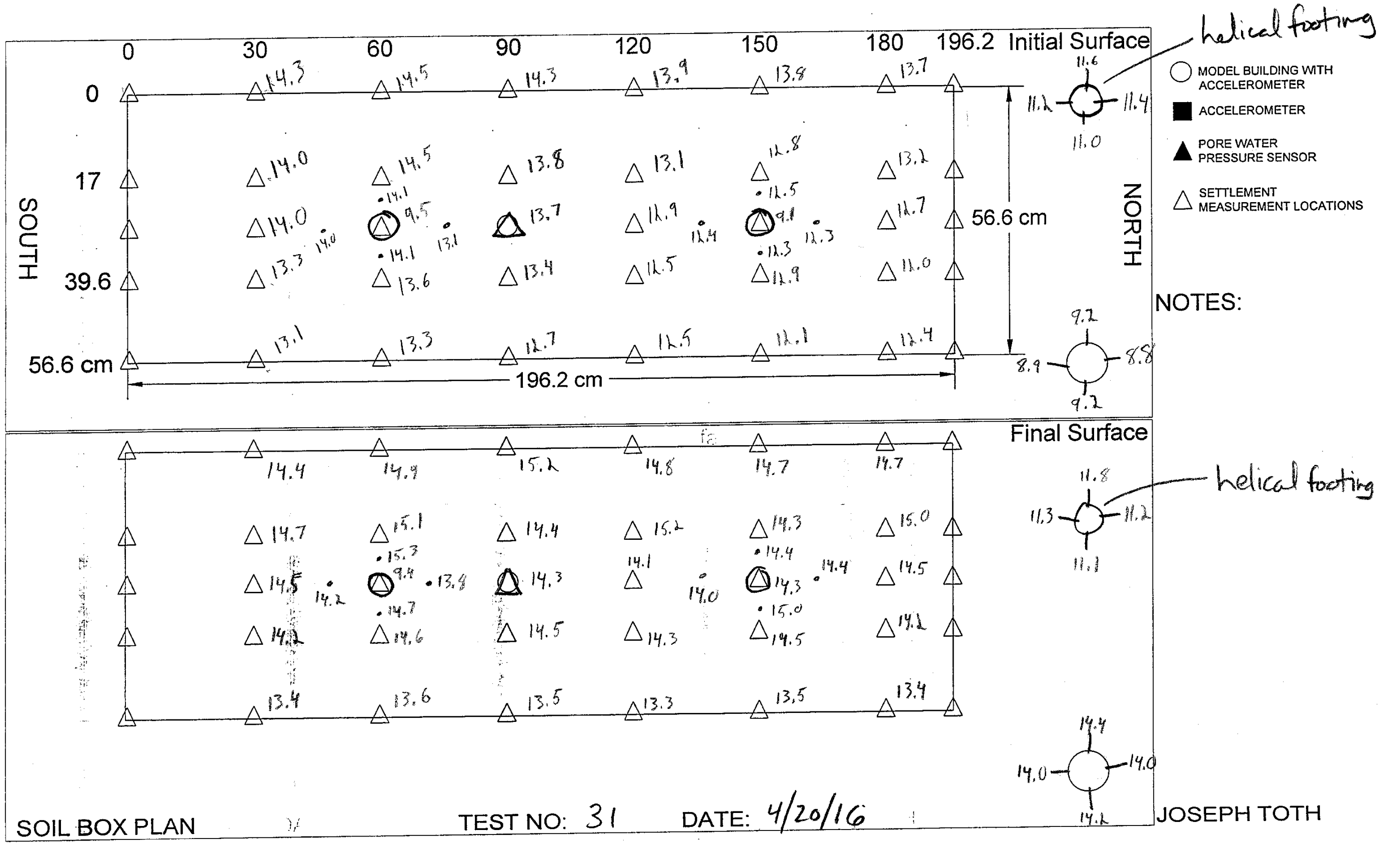

SOIL BOX PLAN TEST NO: 31 DATE: 4/20/16

JOSEPH TOTH

Shakle Table Test # 32

Date: 5/12/2016

Joseph Toth

Dense Layer

		Ws (lbs)	Ww (lbs)
	1	58.4	2.92
	2	58.4	2.92
	3	59.3	2.97
	4	59.4	2.97
291.4 —	5	55.9	2.80
	6	55.7	2.79
	7	55.3	2.77
	8	58.5	2.93
	9	52.9	2.65
	10	55.6	2.78
	11	56.4	2.82
	12	38.8	1.94
	13	53.5	2.68
771.9 —	14	53.8	2.69
	15	51.0	2.55
877.7	16	54.8	2.74
	17	51.4	2.57
	18	52.0	2.6
1033 —	19	51.9	2.6
	20	13.6	0.7
	21		
	22	1046.6	—
	23		
	24		
	25		
	26		
	27		
	28		
	29	1046.6 lbs	
	30		

Liquefiable Layer

	Ws (lbs)	
1	50.3	
2	51.9	
3	50.3	
4	15.3	— 167.8
5	54.9	
6	51.2	— 273.9
7	47.0	— 320.9
8	62.4	
9	59.3	— 442.6
10	60.9	
11	59.6	
12	58.1	
13	63.1	
14	64.0	— 748.3
15	56.2	
16	59.5	— 864
17	55.4	— 919.4
18	49.7	
19	22.6	
20	1.0	
21		
22		
23		
24		
25		
26		
27		
28		
29	992.7 lbs	
30		

NOTES:

TEST NO: 32 **DATE:** 5/12/2016 **JOSEPH TOTH**

Initial (cm)	0	30	45	60	75	90	120	135	150	165	180	196.2
0	-	14.4	-	14.4	-	13.2	14.7	-	14.4	-	14.7	-
14.5	-	14.1	-	14.3	-	14.0	14.1	-	14.0	-	14.5	-
18	-	-	-	14.4	-	-	-	-	13.9	-	-	-
28	-	13.8	13.2		13.5	13.7	13.7	13.3		13.4	14.0	-
39	-	-	-	13.8	-	-	-	-	13.1	-	-	-
42.5	-	13.6	-	13.8	-	13.5	13.6	-	13.1	-	13.5	-
56.6	-	13.2	-	13.0	-	12.8	13.9	-	12.6	-	13.5	-

Final (cm)	0	30	45	60	75	90	120	135	150	165	180	196.2
0	-	14.8	-	15.5	-	15.3	15.5	-	14.9	-	15.1	-
14.5	-	15.2	-	15.4	-	15.3	15.7	-	14.8	-	15.0	-
18	-	-	-	15.4	-	-	-	-	15.0	-	-	-
28	-	14.8	14.3		14.5	14.4	14.9	14.5		14.2	15.0	-
39	-	-	-	15.0	-	-	-	-	15.0	-	-	-
42.5	-	14.9	-	14.8	-	14.9	15.0	-	14.8	-	14.8	-
56.6	-	13.4	-	13.7	-	14.0	14.0	-	13.5	-	14.0	-

NOTES: 5.75in footing - 3 helical piers 120° pattern

W = 2.282lbs Contact Pressure = 12.65 psf

W unsupport = 2.592 lbs = 13.2 psf.

Initial (cm)	BUILDING FOOTPRINT	HELICAL BUILDING FOOTPRINT
NORTH	10.5	11.0
EAST	10.3	11.3
SOUTH	10.4	11.0
WEST	11.0	11.4
CENTER	—	9.3

Final (cm)	BUILDING FOOTPRINT	HELICAL BUILDING FOOTPRINT
NORTH	15.0	10.8
EAST	14.5	11.0
SOUTH	14.5	11.0
WEST	15.5	11.5
CENTER	—	9.2

Shakle Table Test # 33

Date: 6/15/2016

Joseph Toth

$w = \frac{Mw}{Ms}$

Dense Layer

		Ws (lbs)	Ww (lbs)
	1	59.2	2.96
lry wt. x .05	2	51.0	2.55
	3	55.1	2.755
	4	49.3	2.465
	5	53.4	2.67
	6	51.7	2.585
	7	53.8	2.69
	8	49.2	2.46
	9	56.2	2.81
	10	54.3	2.715
	11	49.7	2.485
	12	49.9	2.495
.15 lbs	13	54.0	2.70
	14	51.1	2.555
789.0	15	51.1	2.555
	16	53.2	2.66
	17	50.9	2.545
	18	51.4	2.57
	19	51.5	2.575
	20	53.4	2.67
	21		
	22		
	23		
	24		
	25		
	26		
	27		
	28	1046.6 lbs	
	29		
	30		

Liquefiable Layer

	Ws (lbs)	
1	46.0	
2	32.9	
3	51.9	
4	46.4	
5	53.8	231
6	46.3	
7	53.8	
8	32.2	
9	51.5	
10	50.0	464.8
11	47.4	
12	49.3	
13	49.2	
14	49.4	— 660.1
15	51.8	
16	14.3	
17	31.5	
18	36.8	795.5
19	11.2	
20	37.4	
21	32.5	
22	38.9	915.5
23	57.0	
24	20.2	
25		
26		
27		
28	992.7 lbs	
29		
30		

NOTES: helical footing (5.875)" w = 2.263 lbs → 12.16 psf

unsupported footing (6in) w = 2.472 lbs → 13.13 psf

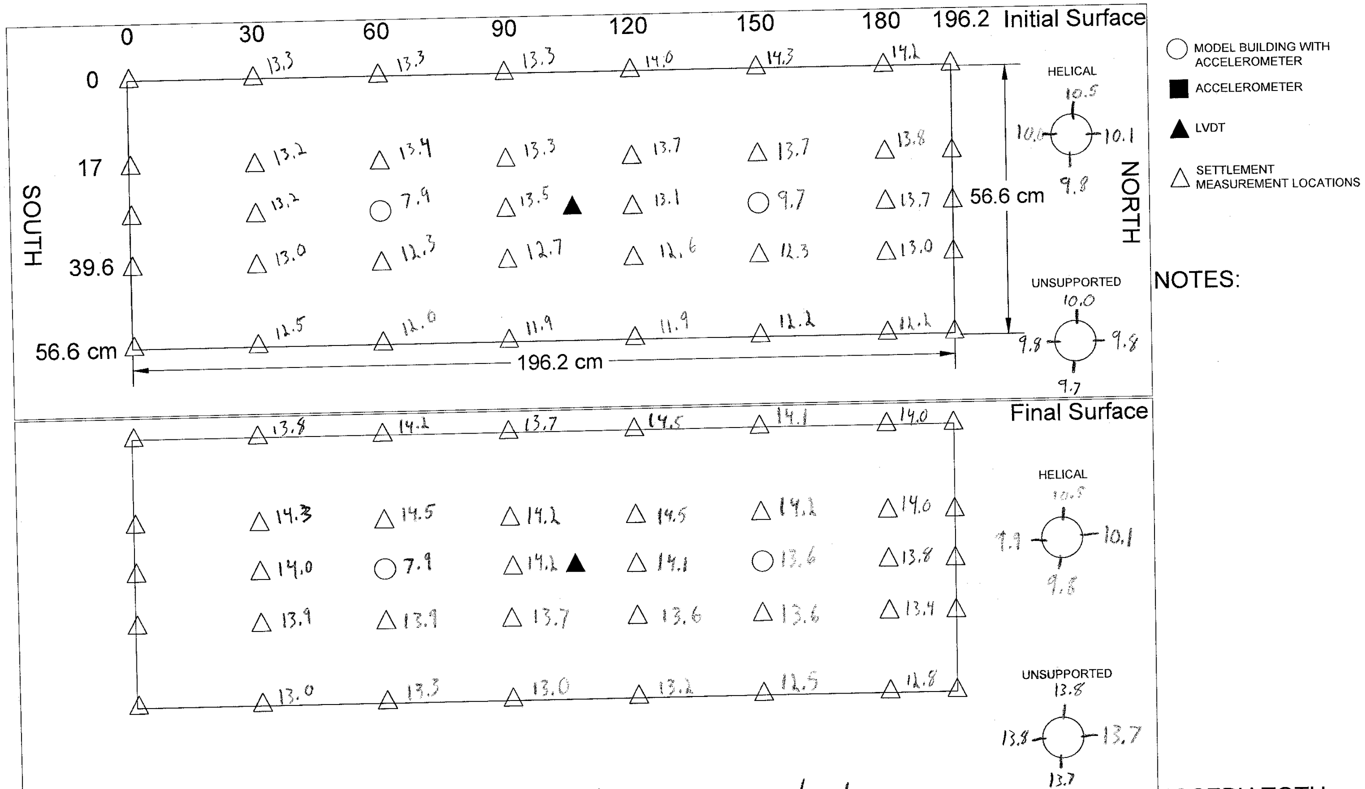

NOTES:

SOIL BOX PLAN TEST NO: 33 DATE: 6/15/2016 top of accelerometer: 11.7

JOSEPH TOTH

Shakle Table Test # 34

Date: 6/22/2016

Joseph Toth

Dense Layer

		Ws (lbs)	Ww (lbs)
	1	55.4	2.77
	2	54.8	2.74
	3	49.5	2.48
	4	52.1	2.61
267.1	5	56.3	2.82
	6	58.6	2.93
	7	56.6	2.83
	8	53.4	2.67
	9	52.1	2.61
544.1	10	56.3	2.82
	11	53.5	2.675
	12	55.5	2.775
	13	54.4	2.72
	14	51.6	2.58
812.6	15	53.5	2.675
	16	53.0	2.65
	17	51.3	2.57
967.2	18	50.3	2.52
1021	19	53.8	2.69
	20	25.6	1.28
	21		
	22		
	23		
	24		
	25		
	26		
	27		
	28		
	29	1046.6 lbs	
	30		

Liquefiable Layer

	Ws (lbs)	
1	21.0	
2	41.1	
3	41.3	103.4
4	43.8	
5	45.7	
6	42.2	
7	39.6	274.7
8	40.6	
9	39.6	
10	59.1	
11	57.7	471.7
12	58.8	
13	57.0	
14	57.9	645.4
15	55.1	700.5
16	53.7	
17	52.6	
18	52.3	859.1
19	54.9	
20	47.9	961.
21	30.9	
22		
23		
24		
25		
26		
27		
28		
29	992.7 lbs	
30		

NOTES:

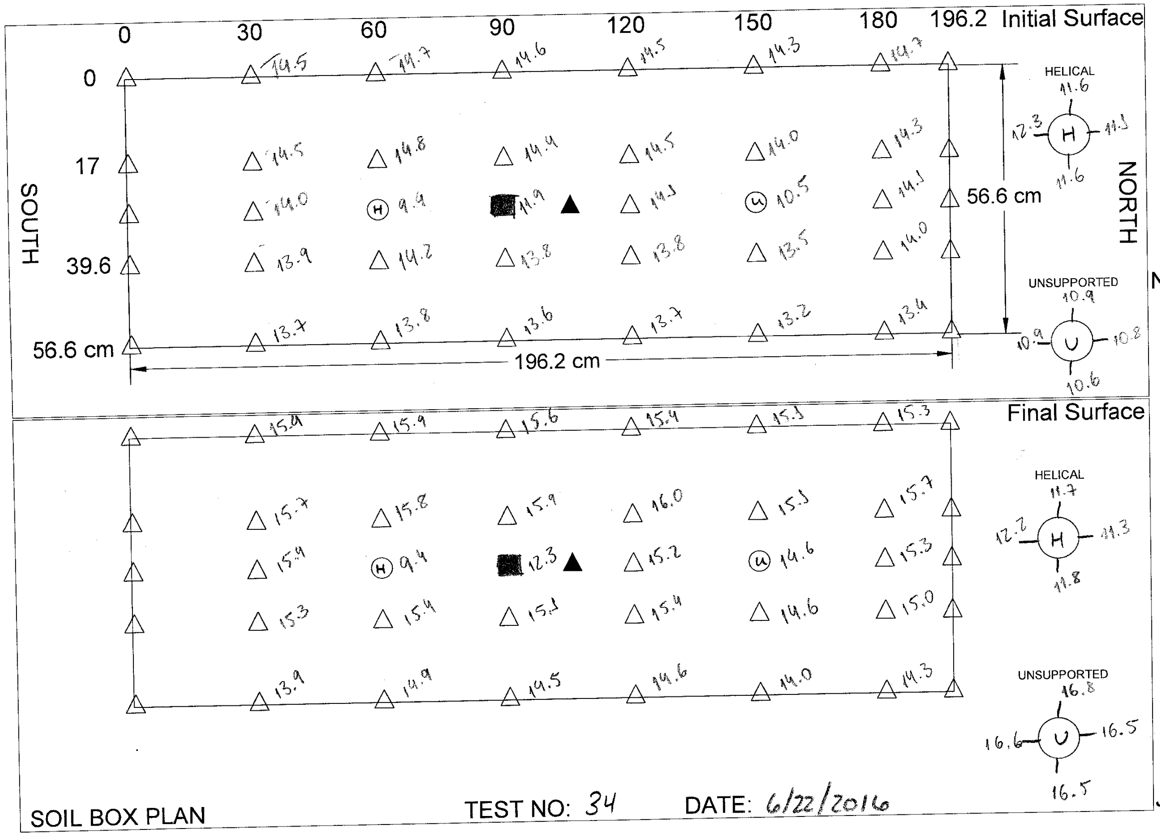

○ MODEL BUILDING WITH ACCELEROMETER

■ ACCELEROMETER (top)

▲ LVDT

△ SETTLEMENT MEASUREMENT LOCATIONS

NOTES:

Coin footings

SOIL BOX PLAN TEST NO: 34 DATE: 6/22/2016

JOSEPH TOTH

Shakle Table Test # 35

Date: 6/30/2016

Joseph Toth

		Dense Layer			Liquefiable Layer	
		Ws (lbs)	Ww (lbs)		Ws (lbs)	
	1	38.2	1.91	1	62.3	
	2	39.3	1.97	2	56.7	
	3	36.8	1.84	3	61.3	
	4	41.3	2.07	4	59.7	
155.6	5	37.4	1.87	5	59.8	299.8
	6	41.9	2.10	6	34.6	
	7	38.2	1.91	7	36.9	
	8	41.1	2.06	8	38.0	409.3
314.2	9	39.4	1.97	9	39.5	
	10	38.9	1.95	10	36.6	
	11	36.6	1.82	11	41.0	
	12	40.3	2.02	12	39.2	
	13	37.7	1.89	13	39.1	604.7
	14	36.0	1.80	14	36.3	
	15	39.5	1.98	15	38.6	
582.6	16	36.7	1.84	16	38.4	
	17	38.6	1.93	17	39.1	757.1
	18	39.4	1.97	18	57.0	
	19	39.6	1.98	19	57.9	
781.6	20	44.7	2.24	20	57.7	
	21	40.0	2.00	21	55.7	985.4
	22	40.1	2.01	22	7.3	
	23	43.2	2.16	23		
943.3	24	38.4	1.92	24		
	25	36.8	1.84	25		
1015.9	26	35.8	1.79	26		
	27	30.7	1.54	27		
	28			28		
	29			29		
	30	1046.6 lbs		30	992.7 lbs	

NOTES:

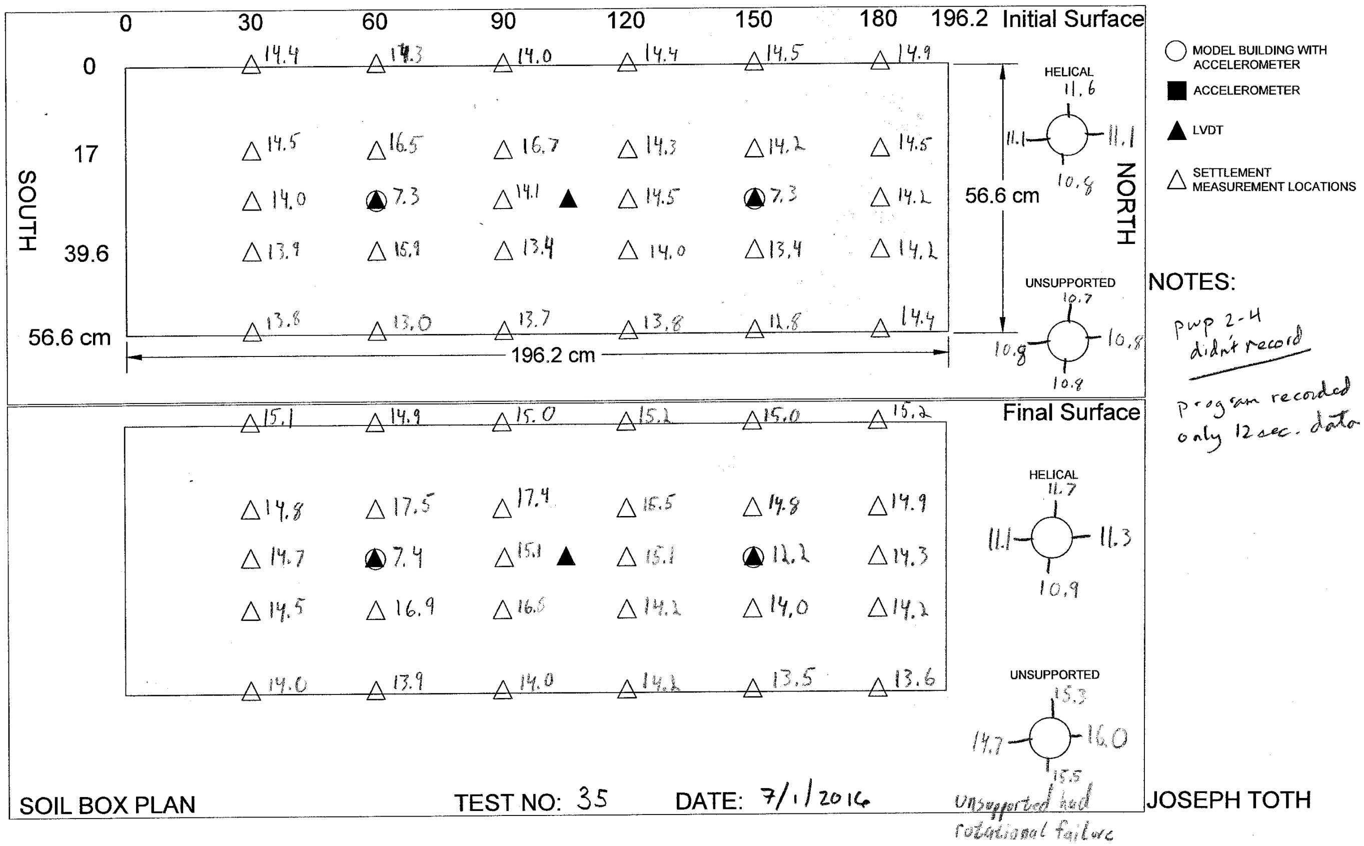

Initial Surface

	30	60	90	120	150	180
0	14.4	14.3	14.0	14.4	14.5	14.9
17	14.5	16.5	16.7	14.3	14.2	14.5
	14.0	7.3	14.1	14.5	7.3	14.2
39.6	13.9	15.9	13.4	14.0	13.4	14.2
56.6 cm	13.8	13.0	13.7	13.8	11.8	14.4

Final Surface

15.1	14.9	15.0	15.2	15.0	15.2
14.8	17.5	17.4	15.5	14.8	14.9
14.7	7.4	15.1	15.1	12.2	14.3
14.5	16.9	16.5	14.2	14.0	14.2
14.0	13.9	14.0	14.2	13.5	13.6

Unsupported had rotational failure

SOIL BOX PLAN TEST NO: 35 DATE: 7/1/2016

JOSEPH TOTH

NOTES:

pwp 2-4 didn't record

program recorded only 12 sec. data

Shakle Table Test # 36
Date: 7/15/2016

Joseph Toth

		Dense Layer			Liquefiable Layer	
		Ws (lbs)	Ww (lbs)		Ws (lbs)	
	1	40.5	2.03	1	62.4	
	2	35.7	1.79	2	59.8	
	3	38.2	1.91	3	58.3	
	4	36.4	1.82	4	60.5	241.0
	5	38.7	1.94	5	63.6	
	6	47.8	2.39	6	64.1	
281.3	7	44.0	2.2	7	60.5	
	8	34.6	1.73	8	61.9	491.1
	9	40.4	2.02	9	64.4	
	10	37.9	1.90	10	57.6	
	11	40.2	2.01	11	63.2	
	12	39.9	2.0	12	64.6	740.9
	13	35.3	1.77	13	62.0	
549.6	14	40.0	2.0	14	63.9	
	15	38.3	1.92	15	61.4	928.2
	16	39.2	1.96	16	58.5	
	17	35.0	1.75	17	6.0	
	18	37.7	1.89	18		
	19	40.6	2.03	19		
	20	35.0	1.75	20		
816.7	21	41.3	2.07	21		
	22	42.5	2.13	22		
	23	36.9	1.85	23		
	24	39.2	1.96	24		
975.7	25	40.4	2.02	25		
	26	46.9	2.35	26		
	27	24.0	1.2	27		
	28			28		
	29			29		
	30	1046.6 lbs		30	992.7 lbs	

NOTES:

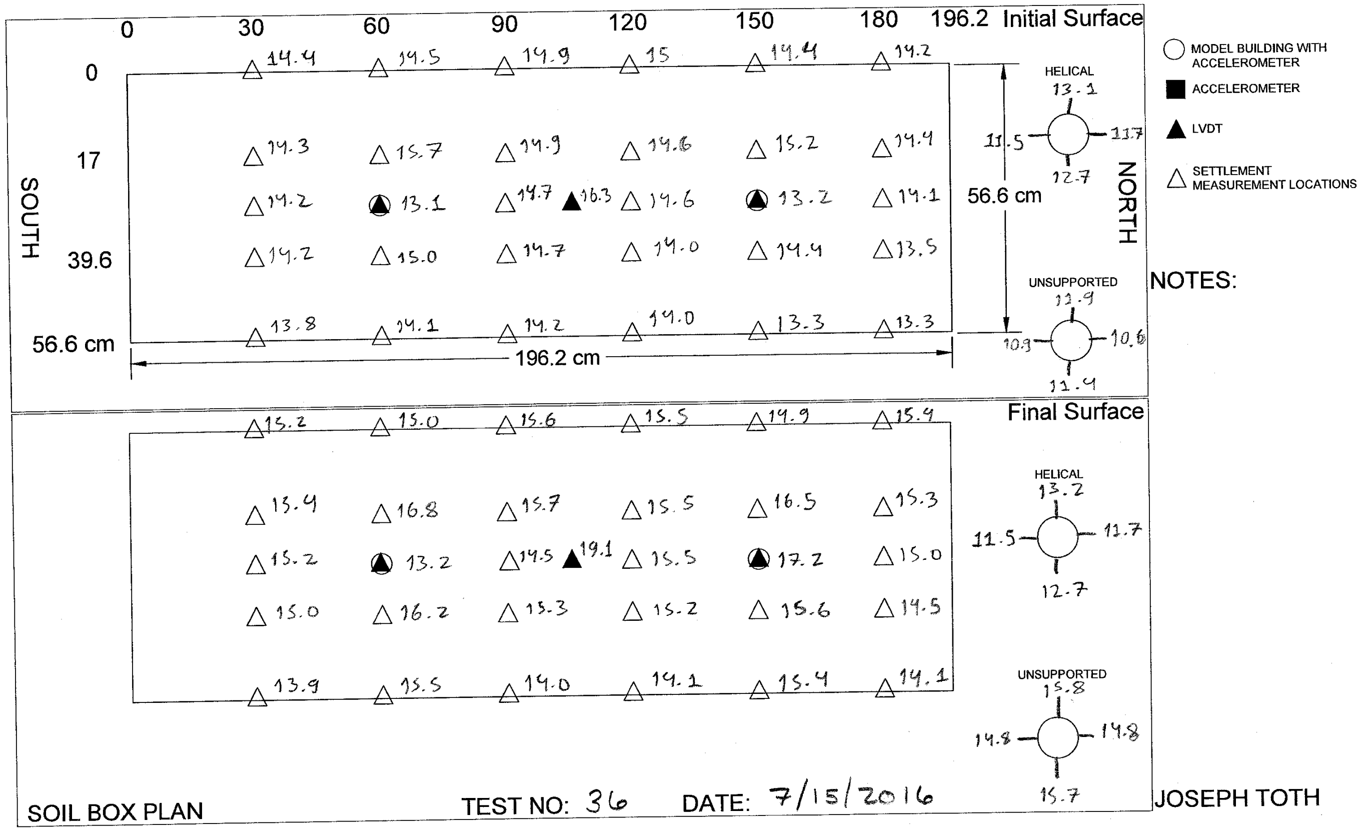
Initial Surface
0
30
60
90
120
150
180
196.2
0
17
39.6
56.6 cm
SOUTH
NORTH
14.4
14.5
14.9
15
14.4
14.2
14.3
15.7
14.9
14.6
15.2
14.4
14.2
13.1
14.7
16.3
14.6
13.2
14.1
14.2
15.0
14.7
14.0
14.4
13.5
13.8
14.1
14.2
14.0
13.3
13.3
196.2 cm
56.6 cm
HELICAL
13.1
11.5
11.7
12.7
UNSUPPORTED
11.9
10.3
10.6
11.4
Final Surface
15.2
15.0
15.6
15.5
14.9
15.4
15.4
16.8
15.7
15.5
16.5
15.3
15.2
13.2
14.5
19.1
15.5
17.2
15.0
15.0
16.2
15.3
15.2
15.6
14.5
13.9
15.5
14.0
14.1
15.4
14.1
HELICAL
13.2
11.5
11.7
12.7
UNSUPPORTED
15.8
14.8
14.8
15.7
○ MODEL BUILDING WITH ACCELEROMETER
■ ACCELEROMETER
▲ LVDT
△ SETTLEMENT MEASUREMENT LOCATIONS
NOTES:
SOIL BOX PLAN
TEST NO: 36
DATE: 7/15/2016
JOSEPH TOTH

Shakle Table Test # 7/21/2016
Date: 37

Joseph Toth

		Dense Layer			Liquefiable Layer	
		Ws (lbs)	Ww (lbs)		Ws (lbs)	
	1	41.0	2.05	1	61.5	
	2	40.6	2.03	2	57.3	
	3	41.4	2.07	3	61.5	
	4	38.1	1.90	4	58.0	
	5	41.6	2.08	5	60.9	
	6	37.6	1.88	6	62.6	
	7	34.5	1.73	7	59.7	– 421.5
	8	44.4	2.22	8	54.9	
	9	42.4	2.12	9	55.7	– 532.1
	10	35.7	1.79	10	56.8	
	11	40.6	2.03	11	54.4	– 643.3
	12	34.9	1.75	12	56.5	
	13	35.3	1.77	13	52.7	– 752.5
	14	32.7	1.64	14	57.5	– 810.0
	15	41.3	2.07	15	53.8	
	16	41.0	2.05	16	57.0	– 920.8
	17	42.1	2.11	17	50.0	
703.8	18	38.7	1.94	18	21.9	
	19	37.3	1.87	19		
	20	39.2	1.96	20		
	21	37.4	1.87	21		
856.6	22	38.9	1.95	22		
	23	40.2	2.0	23		
934.7	24	37.9	1.90	24		
	25	34.3	1.72	25		
	26	~~37~~ 37.5	1.88	26		
	27	40.1	2.01	27		
	28	1046.6		28	992.7	
	29			29		
	30			30		

NOTES: 6in footing

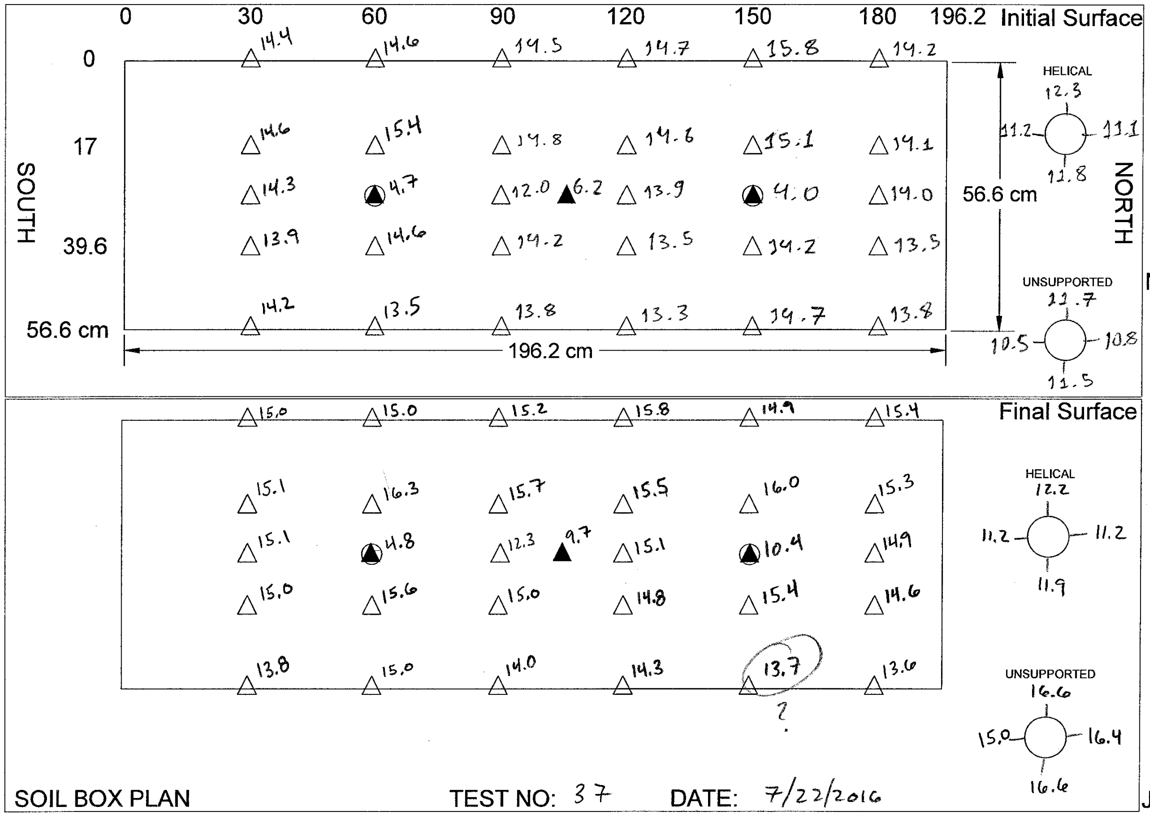

SOIL BOX PLAN TEST NO: 37 DATE: 7/22/2016

○ MODEL BUILDING WITH ACCELEROMETER

■ ACCELEROMETER

▲ LVDT

△ SETTLEMENT MEASUREMENT LOCATIONS

NOTES:

problems installing footing onto helical piles,

grind down piles to smaller diameter

fix pwp #4

JOSEPH TOTH

Shakle Table Test # 38

Joseph Toth

Date: 7/26/2016

		Dense Layer			Liquefiable Layer	
		Ws (lbs)	Ww (lbs)		Ws (lbs)	
	1	39.4	1.97	1	62.6	
	2	36.7	1.84	2	54.8	
	3	41.2	2.06	3	58.7	
	4	38.6	1.93	4	58.3	– 234.4
	5	37.3	1.87	5	59.0	
	6	33.3	1.67	6	58.4	
	7	43.0	2.15	7	55.9	— 407.7
	8	37.9	1.90	8	57.2	– 464.9
	9	38.4	1.92	9	57.5	
	10	41.6	2.08	10	58.6	
	11	41.1	2.06	11	57.1	
	12	38.6	1.93	12	57.8	– 695.9
	13	32.5	1.63	13	56.9	
	14	33.2	1.66	14	58.7	– 811.5
	15	39.5	1.98	15	58.2	
	16	42.7	2.14	16	57.3	– 927.0
	17	37.9	1.90	17	62.7	
	18	38.9	1.95	18	3.0	
	19	36.4	1.82	19	—	
	20	38.5	1.93	20		
	21	38.8	1.94	21		
	22	39.0	1.95	22		
	23	36.1	1.81	23		
921.5 —	24	40.9	2.05	24		
	25	42.0	2.1	25		
	26	39.7	1.99	26		
	27	36.8	1.84	27		
	28	6.6	0.33	28		
	29			29		
	30	1046.6 lbs	—	30	992.7 lbs	

NOTES:

6 in footings.

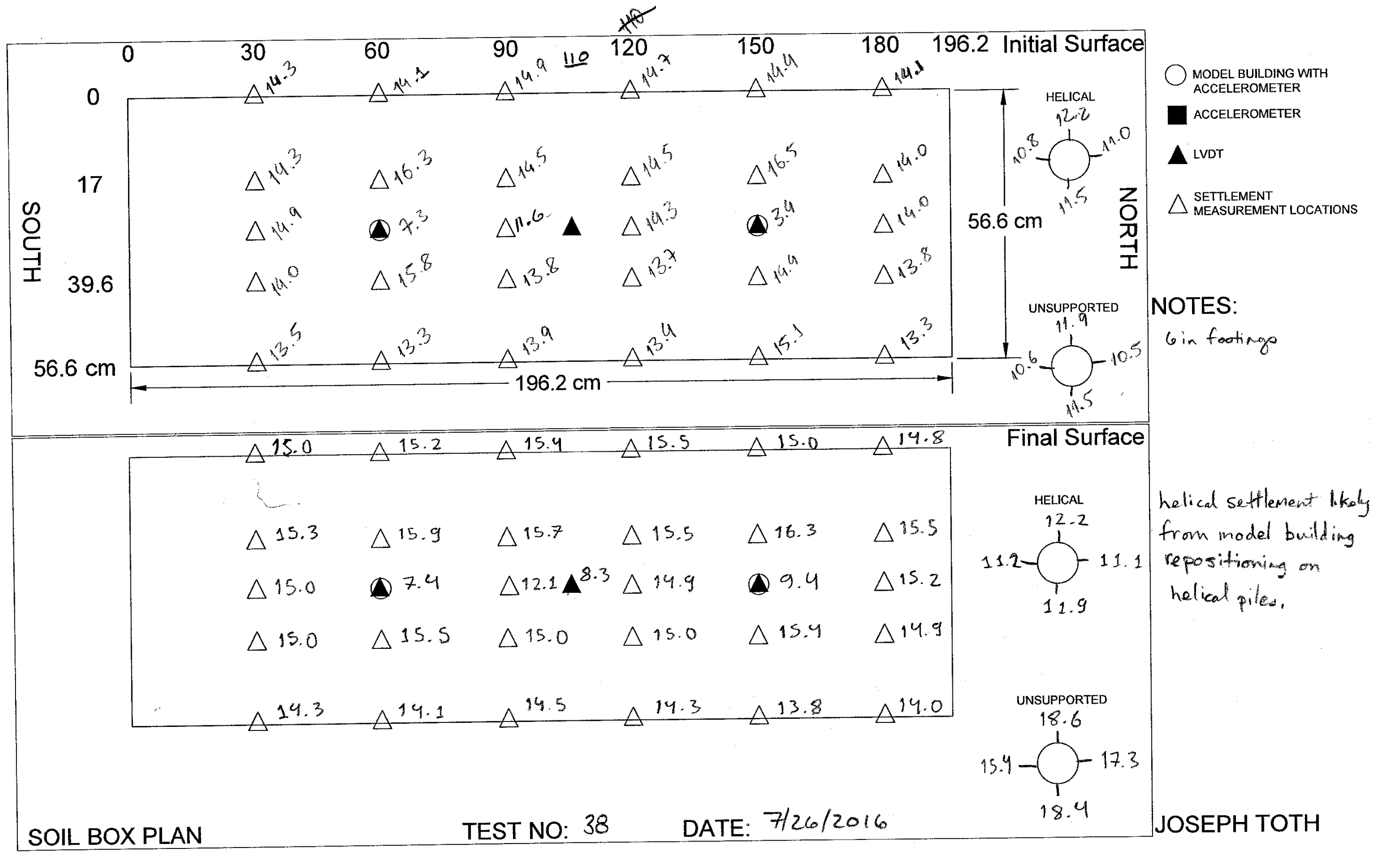

NOTES:

6 in footings

helical settlement likely from model building repositioning on helical piles.

SOIL BOX PLAN

TEST NO: 38

DATE: 7/26/2016

JOSEPH TOTH

Shakle Table Test # 39
Date: 8/4/2016

Joseph Toth

		Dense Layer			Liquefiable Layer	
		Ws (lbs)	Ww (lbs)		Ws (lbs)	
	1	38.2	1.91	1	34.2	
	2	41.1	2.05.	2	20.0	
	3	39.8	1.99	3	57.3	
	4	42.7	2.14	4	55.4	
	5	39.3	1.97	5	61.8	
	6	38.4	1.92	6	55.8	
	7	37.4	1.87	7	56.2	– 340.7
	8	42.5	2.13	8	57.2	
	9	36.9	1.85	9	55.6	
	10	40.4	2.02	10	58.9	– 512.4
	11	40.4	2.02	11	60.2	
	12	37.4	1.87	12	62.4	— 635.0
	13	37.4	1.87	13	50.8	
	14	35.4	1.77	14	56.3	
	15	38.5	1.93	15	56.3	
	16	37.2	1.86	16	62.0	
	17	38.4	1.92	17	55.0	– 915.4
	18	40.8	2.04	18	56.4	
	19	40.2	2.01	19	20.9	
	20	37.9	1.90	20	0	
	21	43.5	2.18	21		
	22	39.4	1.97	22		
	23	37.9	1.90	23		
939.4 →	24	38.4	1.92	24		
	25	32.2	~~2.04~~ 1.61	25		
	26	40.1	2.01	26		
	27	34.9	1.75	27		
	28	0		28		
	29			29		
	30	1046.6		30	992.7	

NOTES:

8 inch footings

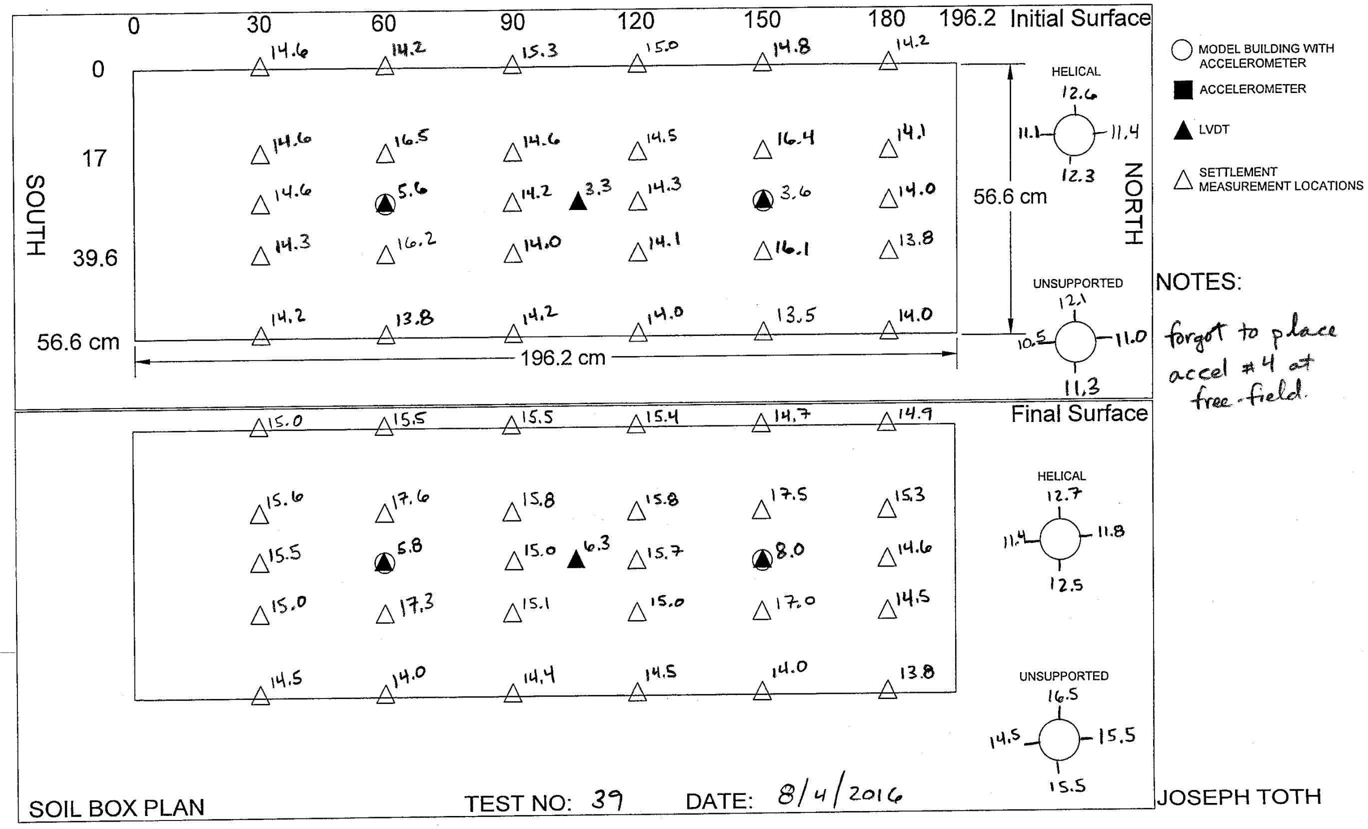

NOTES:

forgot to place accel #4 at free-field.

SOIL BOX PLAN

TEST NO: 39

DATE: 8/4/2016

JOSEPH TOTH

Shakle Table Test # 40

Date: 8/9/2016

Joseph Toth

		Dense Layer			Liquefiable Layer	
		Ws (lbs)	Ww (lbs)		Ws (lbs)	
	1	40.8	2.04	1	39.7	
	2	41.3	2.07	2	31.7	71.4
	3	39.1	1.96	3	54.9	
	4	41.8	2.09	4	51.4	
	5	35.7	1.79	5	61.1	
	6	42.2	2.11	6	57.8	
	7	41.7	2.09	7	58.7	
	8	40.5	2.03	8	61.0	
	9	41.0	2.05	9	58.6	419.9
	10	42.0	2.10	10	59.6	
	11	40.5	2.03	11	57.2	
	12	43.5	2.18	12	60.0	
	13	39.7	1.99	13	59.2	
	14	41.0	2.05	14	58.3	
	15	37.2	1.86	15	56.2	-825.4
	16	38.9	1.95	16	59.4	
	17	39.9	2.00	17	59.1	
	18	39.8	1.99	18	48.8	
	19	37.3	1.87	19		
	20	41.4	2.07	20		
847.6	21	42.3	2.12	21		
	22	40.0	2.00	22		
	23	38.3	1.92	23		
	24	39.0	1.95	24		
	25	42.3	2.12	25		
	26	39.4	1.97	26		
	27			27		
	28			28		
	29			29		
	30	1046.6 lbs		30	992.7 lbs	

NOTES:

Helical = 0.679 lbs ≈ 13.8 Psf

3 inch footings

unsupp = 0.665 lbs ≈ 13.54 psf

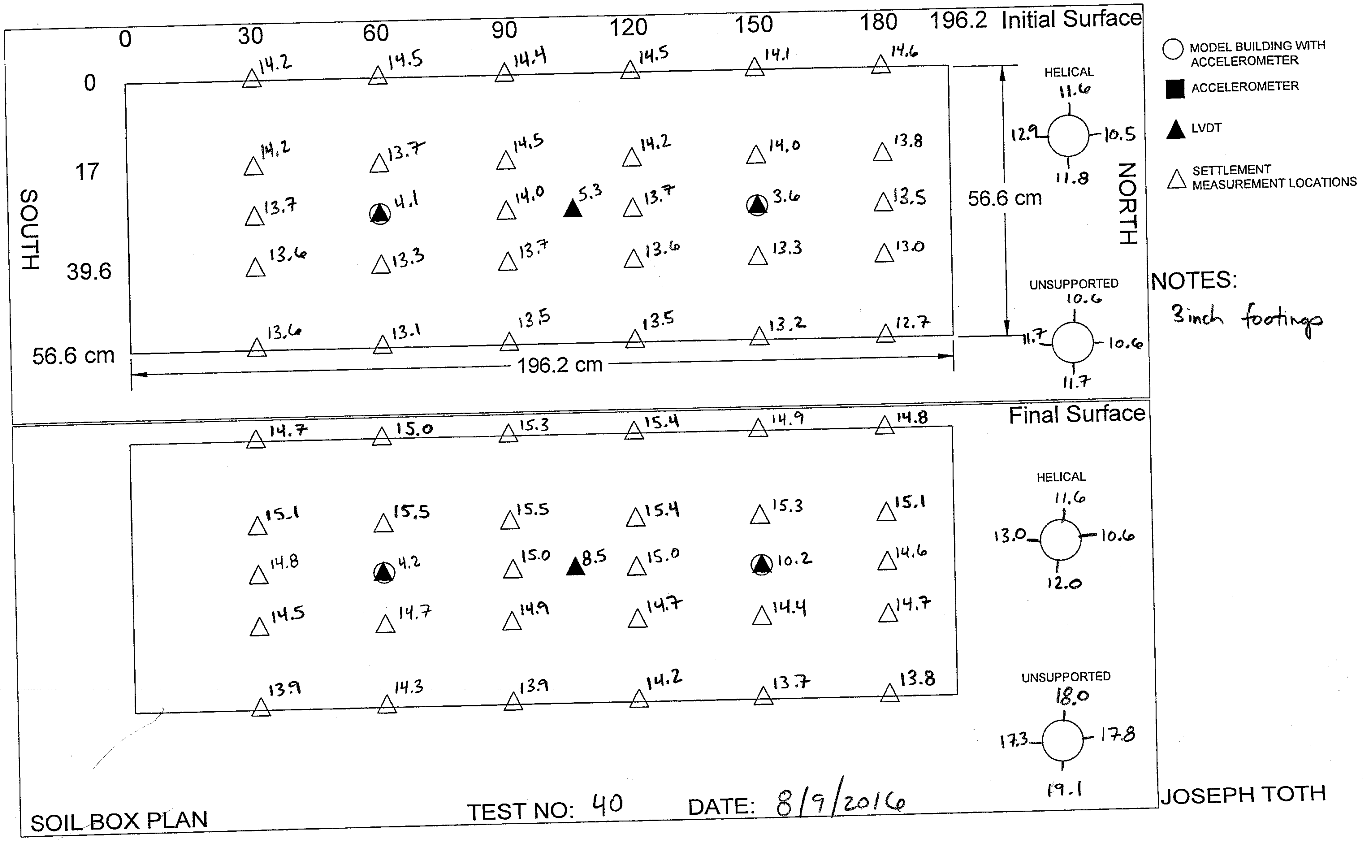

NOTES:
3inch footings

SOIL BOX PLAN

TEST NO: 40

DATE: 8/9/2016

JOSEPH TOTH

Joseph Toth

Shakle Table Test # 41
Date: 8/17/2016

Dense Layer

		Ws (lbs)	Ww (lbs)
	1	32.9	1.65
	2	24.9	1.25
	3	17.6	0.88
	4	41.1	2.06
	5	41.6	2.08
	6	43.5	2.18
	7	37.3	1.87
	8	39.4	1.97
	9	43.2	2.16
	10	42.7	2.14
	11	43.0	2.15
452.3	12	45.1	2.26
	13	41.3	2.07
	14	42.4	2.12
	15	43.4	2.17
	16	43.9	2.20
	17	44.7	2.24
	18	44.0	2.20
	19	41.6	2.08
	20	42.6	2.13
832.5	21	36.3	1.82
	22	36.9	1.85
	23	39.8	1.99
	24	36.9	1.85
	25	39.5	1.98
1031.4	26	45.8	2.29
	27	15.2	0.76
	28	0	
	29		
	30	1046.6 lbs	

Liquefiable Layer

	Ws (lbs)	
1	29.9	
2	15.0	
3	61.4	
4	63.4	
5	61.9	
6	62.6	
7	60.3	354.5
8	61.2	
9	62.0	
10	62.8	
11	61.8	
12	60.0	662.3
13	60.2	
14	59.9	
15	57.8	
16	59.4	
17	60.1	
18	33.0	
19	0	
20		
21		
22		
23		
24		
25		
26		
27		
28		
29		
30	992.7 lbs	

NOTES: 4.325 in footing helical = 1.267 lbs

unsupp = 1,280 lbs
~~4.25~~ in footings
4.375

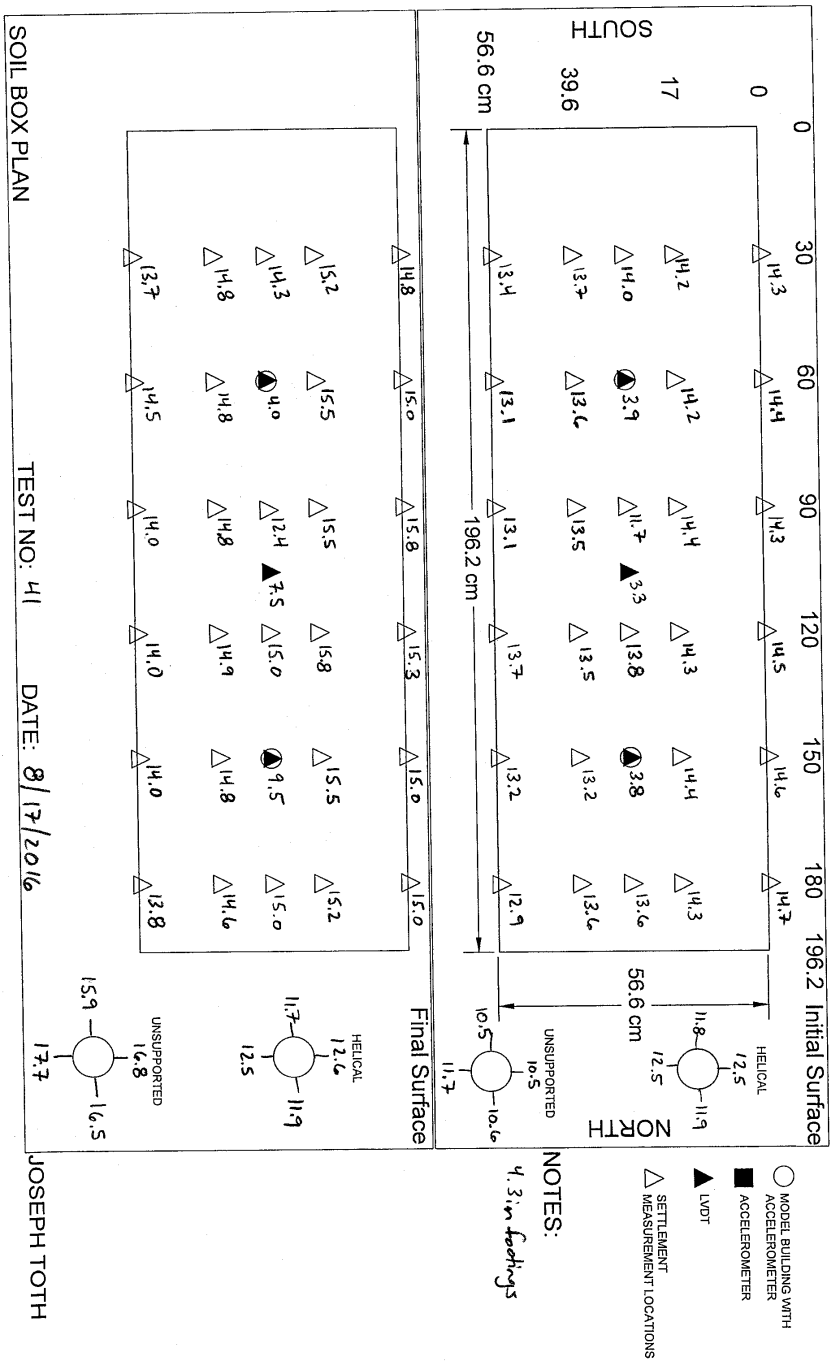

NOTES:

4.3 in footings

SOIL BOX PLAN

TEST NO: 41

DATE: 8/17/2016

JOSEPH TOTH

Joseph Toth

Shakle Table Test # 42
Date: 8/27/16

		Dense Layer		Liquefiable Layer	
		Ws (lbs)	Ww (lbs)	Ws (lbs)	
	1	39.7	1.99	64.3	
	2	44.4	2.22	52.6	
	3	41.8	2.09	55.1	
	4	44.8	2.24	51.9	
	5	39.7	1.99	52.9	– 276.8
	6	42.7	2.14	57.6	
	7	40.6	2.03	56.5	
	8	39.2	1.95	54.4	
	9	44.4	2.22	57.3	
	10	42.4	2.12	58.8	– 561.4
	11	40.9	2.05	56.8	
	12	39.5	1.98	54.1	
	13	41.3	2.12	57.1	
	14	41.5	2.08	56.1	
	15	41.1	2.06	58.0	– 843.5
	16	43.9	2.20	54.3	
	17	41.1	2.06	35.5	
	18	40.2	2.01	56.1	– 989.3
	19	39.0	1.95	3.4	
	20	42.1	2.11		
	21	42.4	2.12		
	22	41.6	2.08		
	23	43.1	2.16		
999.3 –	24	41.1	2.06		
	25	47.3	2.37		
	26				
	27				
	28				
	29				
	30	1046.6		992.7	

NOTES: 8 inch footings Helical - 4.524 lbs unsupp - 4.483 lbs

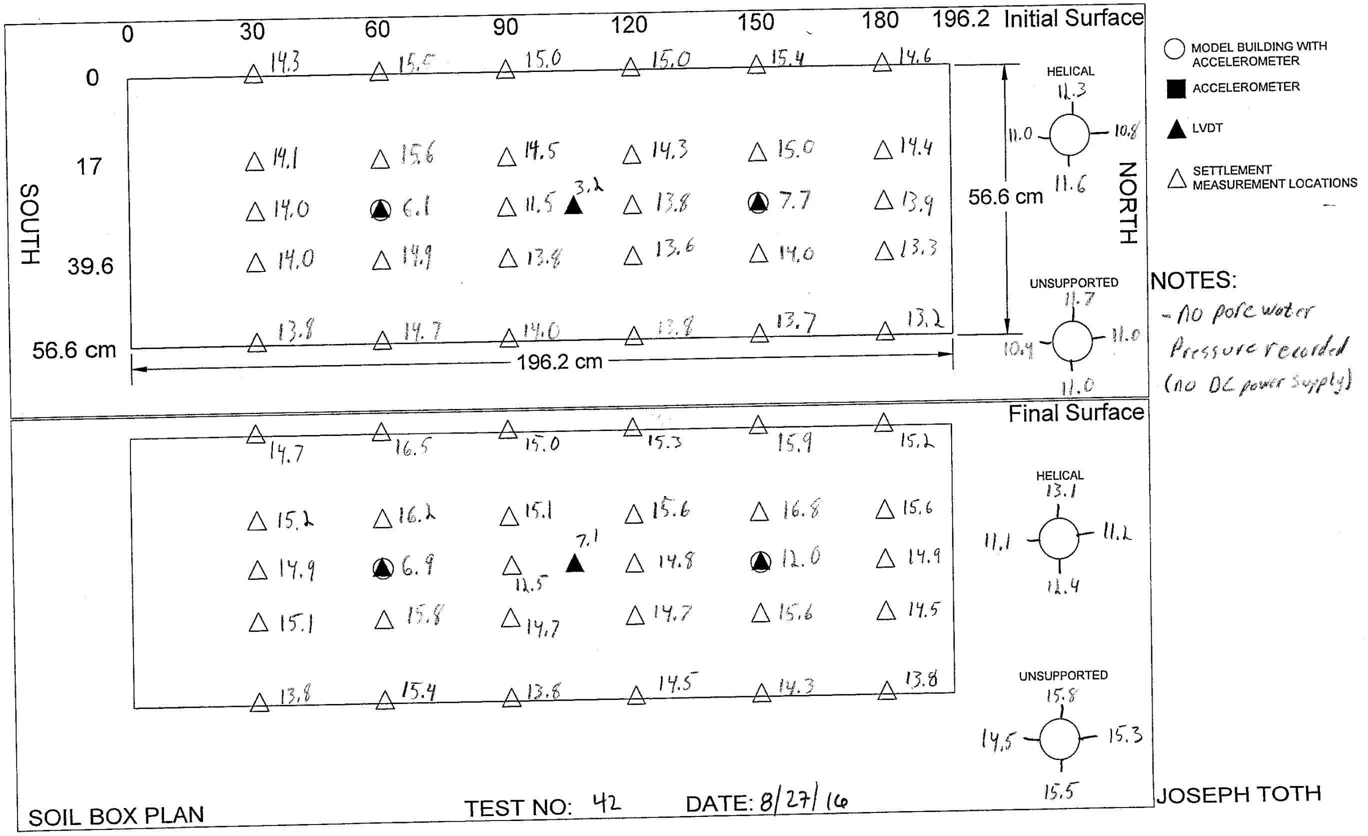

NOTES:
- No pore water
Pressure recorded
(no DC power supply)

Joseph Toth

Shakle Table Test # 43

Date: ~~8/28/2016~~ 9/9/2016

Dense Layer

		Ws (lbs)	Ww (lbs)
	1	53.6	2.68
	2	60.9	3.05
	3	55.1	2.76
	4	56.9	2.85
288.4	5	61.7	3.09
	6	55.4	2.77
	7	56.3	2.82
	8	57.1	2.86
	9	62.1	3.11
575.5	10	56.4	2.82
	11	55.0	2.75
	12	56.5	2.83
	13	58.8	2.94
	14	56.1	2.81
856.6	15	54.7	2.74
	16	54.7	2.74
	17	57.7	2.89
	18	55.2	2.76
	19	22.4	1.12
	20		
	21		
	22		
	23		
	24		
	25		
	26		
	27		
	28		
	29	Dr = 70 %	
	30	1046.6	

Liquefiable Layer

	Ws (lbs)	
1	36.3	
2	41.5	
3	39.4	
4	39.6	
5	38.9	
6	33.0	
7	38.5	
8	42.1	
9	43.8	
10	42.9	
11	41.1	
12	43.3	
13	44.4	
14	43.9	
15	42.7	
16	42.1	
17	43.9	
18	38.9	
19	41.8	
20	35.5	
21	44.1	857.6
22	40.2	
23	40.1	
24	41.3	979.2
25	13.5	992.7
26		
27		
28		
29	Dr = 35 %	
30	992.7	

NOTES:

10 in footing helical = 7.005 lbs

unsupp = 6.995 lbs

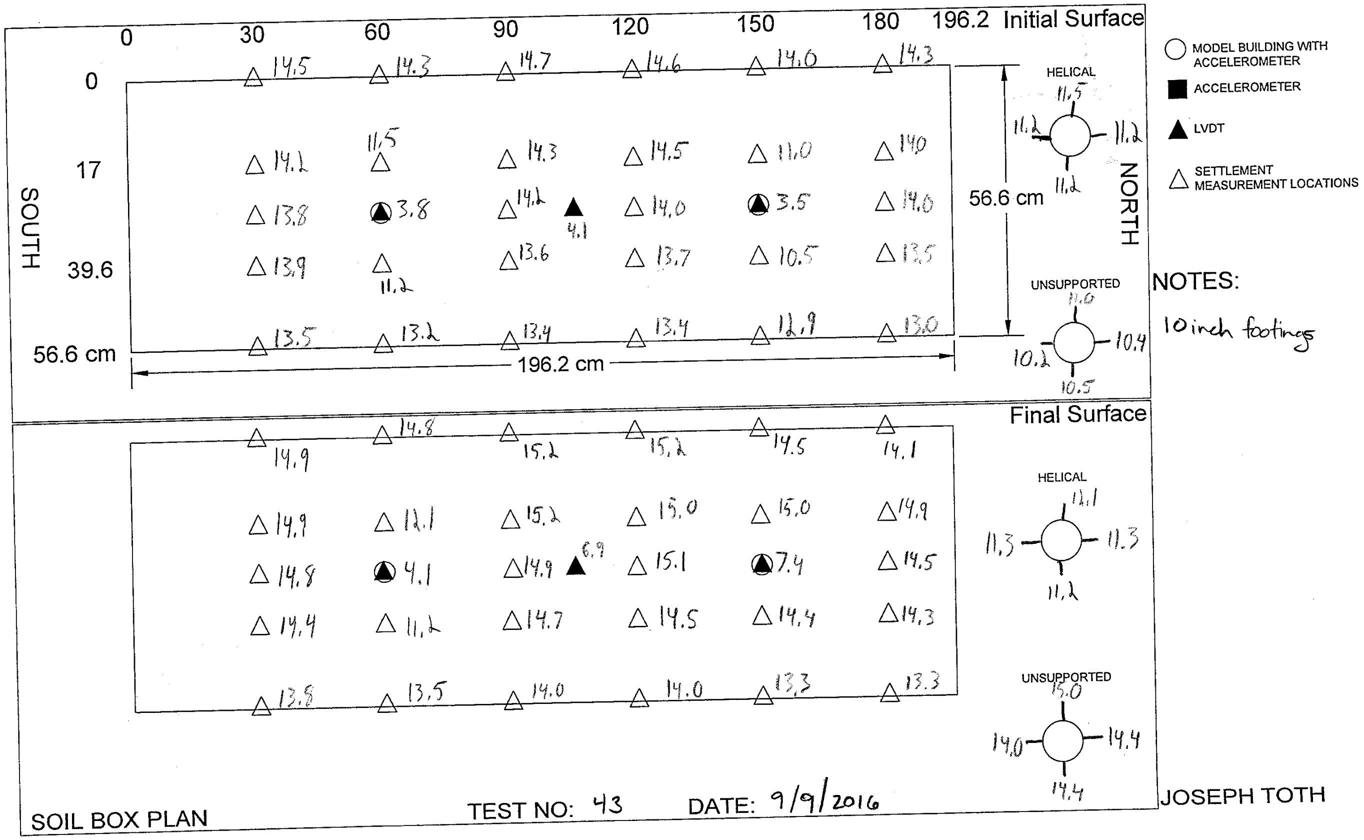

SOIL BOX PLAN

TEST NO: 43

DATE: 9/9/2016

NOTES:

10 inch footings

JOSEPH TOTH

Shakle Table Test # 44

Joseph Toth

Date: 9/16/2016

		Dense Layer			Liquefiable Layer	
		Ws (lbs)	Ww (lbs)		Ws (lbs)	
	1	39.9	2.00	1	46.4	
	2	43.0	2.15	2	45.7	
	3	41.0	2.05	3	44.1	
	4	48.1	2.41	4	47.9	
	5	43.5	2.18	5	53.2	
	6	44.6	2.23	6	42.1	
	7	48.1	2.40	7	44.7	
	8	38.2	1.91	8	41.6	
	9	42.6	2.13	9	46.1	
	10	41.9	2.10	10	41.4	– 453.2
	11	45.2	2.26	11	39.3	
	12	42.2	2.11	12	38.2	
	13	39.7	1.99	13	37.0	
	14	43.9	2.20	14	37.2	
	15	41.3	2.07	15	37.9	– 642.8
	16	42.1	2.11	16	29.4	
	17	44.0	2.20	17	29.7	
	18	41.0	2.05	18	31.0	
	19	41.3	2.07	19	32.3	
	20	42.3	2.12	20	26.8	– 792
891.7	21	37.9	1.90	21	35.2	
	22	41.7	2.09	22	30.3	
	23	45.6	2.28	23	31.3	
1021.2	24	42.2	2.11	24	30.8	
	25	25.4	1.27	25	29.3	– 948.9
	26			26	27.4	
	27			27		
	28			28		4.2
	29	Dr = 70 %		29	Dr = 20 %	980.5
	30	1046.6 lbs		30	976.3 lbs	

NOTES: 6 in footings Dr = 20%, liquefiable layer H_L = 12 in H_D = 12 in

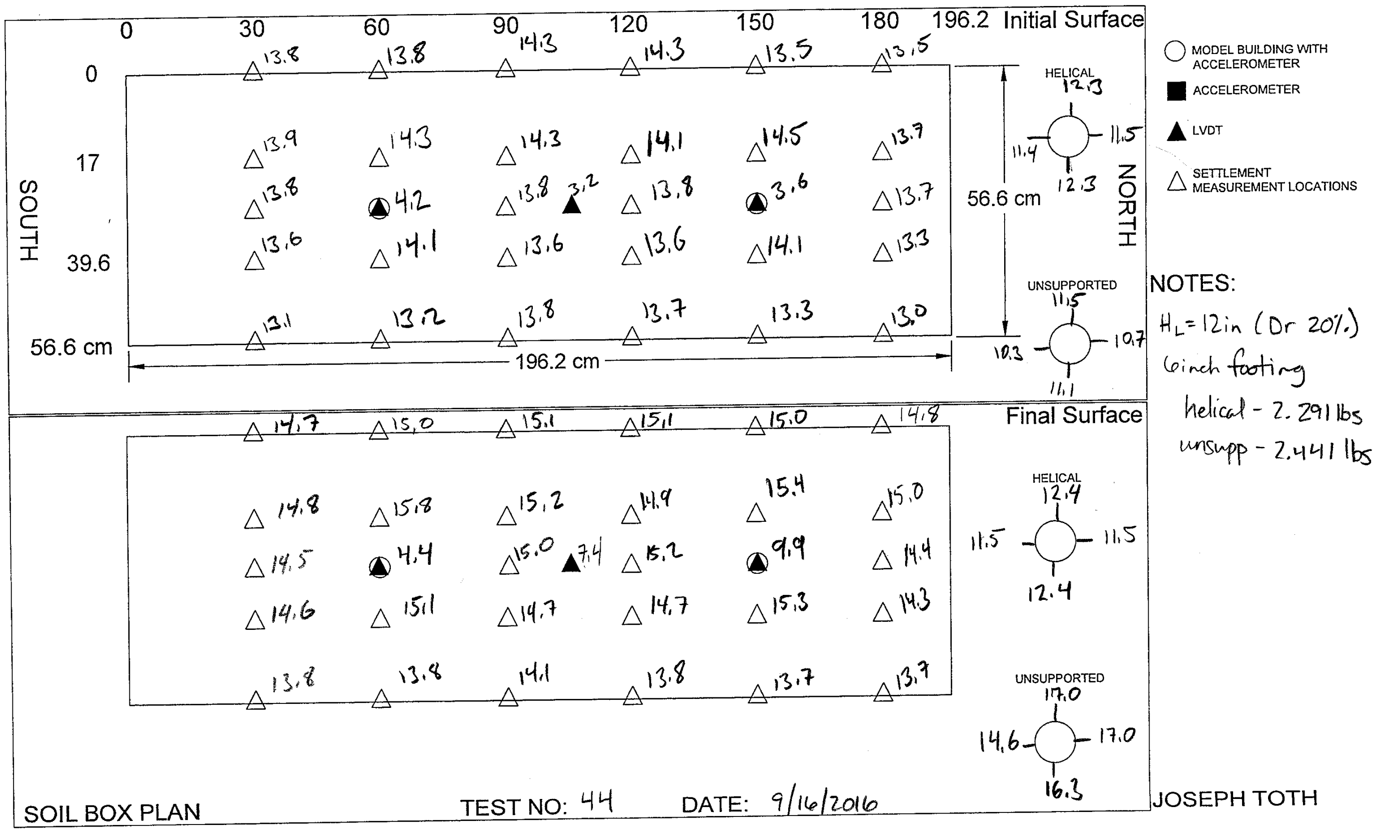
0
30
60
90
120
150
180
196.2
Initial Surface
0
17
39.6
56.6 cm
SOUTH
NORTH
196.2 cm
56.6 cm
13.8
13.8
14.3
14.3
13.5
13.5
13.9
14.3
14.3
14.1
14.5
13.7
13.8
4.2
13.8
3.2
13.8
3.6
13.7
13.6
14.1
13.6
13.6
14.1
13.3
13.1
13.2
13.8
13.7
13.3
13.0
HELICAL
12.3
11.4
11.5
12.3
UNSUPPORTED
11.5
10.3
10.7
11.1
Final Surface
14.7
15.0
15.1
15.1
15.0
14.8
14.8
15.8
15.2
14.9
15.4
15.0
14.5
4.4
15.0
7.4
15.2
9.9
14.4
14.6
15.1
14.7
14.7
15.3
14.3
13.8
13.8
14.1
13.8
13.7
13.7
HELICAL
12.4
11.5
11.5
12.4
UNSUPPORTED
17.0
14.6
17.0
16.3
SOIL BOX PLAN
TEST NO: 44
DATE: 9/16/2016
JOSEPH TOTH
○ MODEL BUILDING WITH ACCELEROMETER
■ ACCELEROMETER
▲ LVDT
△ SETTLEMENT MEASUREMENT LOCATIONS
NOTES:
H_L = 12in (Dr 20%)
6inch footing
helical - 2.291 lbs
unsupp - 2.441 lbs

Shakle Table Test # ~~44~~ 45

Joseph Toth

Date: 9/19/2016

	Dense Layer			Liquefiable Layer	
	Ws (lbs)	Ww (lbs)		Ws (lbs)	
1	43.3	2.17	1	57.3	
2	42.1	2.11	2	60.0	
3	41.3	2.07	3	60.1	
4	40.2	2.01	4	59.2	
5	43.0	2.15	5	61.3	
6	44.0	2.20	6	61.7	
7	43.6	2.18	7	61.4	
8	43.1	2.16	8	59.8	
9	43.3	2.17	9	60.2	
10	38.6	1.93	10	63.3	- 604.3
11	38.9	1.95	11	58.1	
12	43.0	2.15	12	60.4	
13	40.9	2.05	13	58.3	
14	40.6	2.03	14	61.1	
15	40.7	2.04	15	59.5	— 901.7
16	42.4	2.12	16	60.6	
17	40.5	2.03	17	45.3	
18	42.4	2.12	18		
19	40.3	2.03	19		
20	39.5	1.98	20		
21	38.2	1.91	21		
22	37.8	1.89	22		
23	40.3	2.02	23		
24	41.0	2.05	24		
25	21.3	1.07	25		
26	36.1	1.81	26		
27			27		
28	Dr = 70%		28	Dr = ~~40%~~ 45%	
29			29		
30	1046.6 lbs		30	1007.6 ~~1010.0 lbs~~	

NOTES: benchmark Cein footings

Dr = 40% H$_L$ = 12in

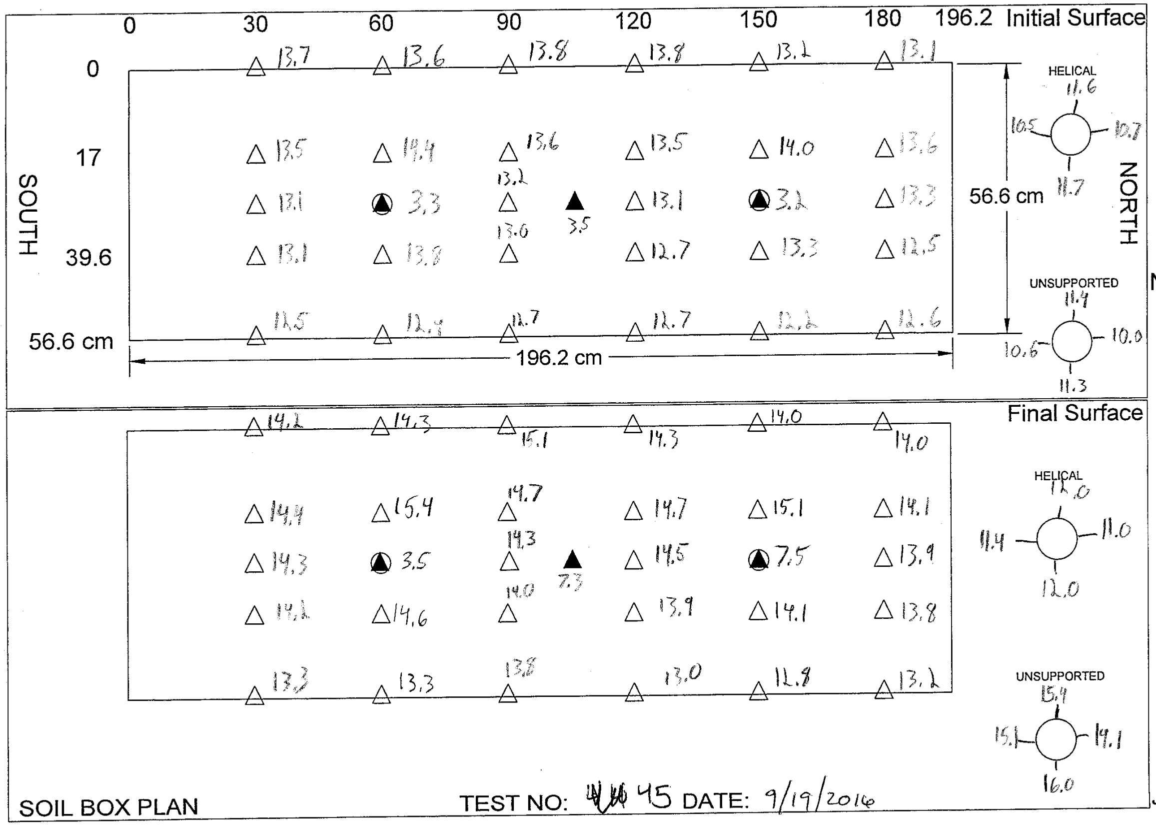

TEST NO: 45 DATE: 9/19/2016

NOTES:

6in footing benchmark

H_L = 12 in

Dr of H_L = ~~40%~~ 35 45%

helical = 2.291 lbs

Unsupp = 2.441 lbs

* helical pile likely broken helix on installation

* settlement likely from broken pile and/or poor connection

JOSEPH TOTH

* Puncture failure

Joseph Toth

Shakle Table Test # 46
Date: 9/23/2016

		Dense Layer			Liquefiable Layer	
		Ws (lbs)	Ww (lbs)		Ws (lbs)	
	1	40.8	2.04	1	56.8	
	2	41.9	2.10	2	62.4	
	3	44.5	2.23	3	56.7	
	4	42.2	2.11	4	61.6	
	5	39.3	1.97	5	61.7	- 299.2
	6	42.2	2.11	6	56.4	
	7	38.7	1.94	7	60.9	
	8	46.8	2.34	8	60.9	
	9	40.7	2.04	9	57.4	
	10	43.0	2.15	10	57.9	- 592.7
	11	47.4	2.37	11	58.6	
	12	44.8	2.24	12	58.1	
	13	43.2	2.16	13	59.7	
	14	40.6	2.03	14	58.9	
	15	41.7	2.09	15	59.1	- 887.1
	16	46.2	2.31	16	60.2	
	17	44.5	2.23	17	60.3	
	18	42.3	2.12	18	14.9	
	19	45.7	2.29	19		
	20	36.2	1.81	20		
	21	42.5	2.13	21		
	22	40.3	2.02	22		
	23	44.5	2.23	23		
1021.8	24	41.8	2.09	24		
	25	24.8	1.24	25		
	26			26		
	27			27		
	28			28		
	29			29		
	30	1046.6		30	1022.5	

NOTES: Dr = 70 % Dr = ~~50%~~ 55 %

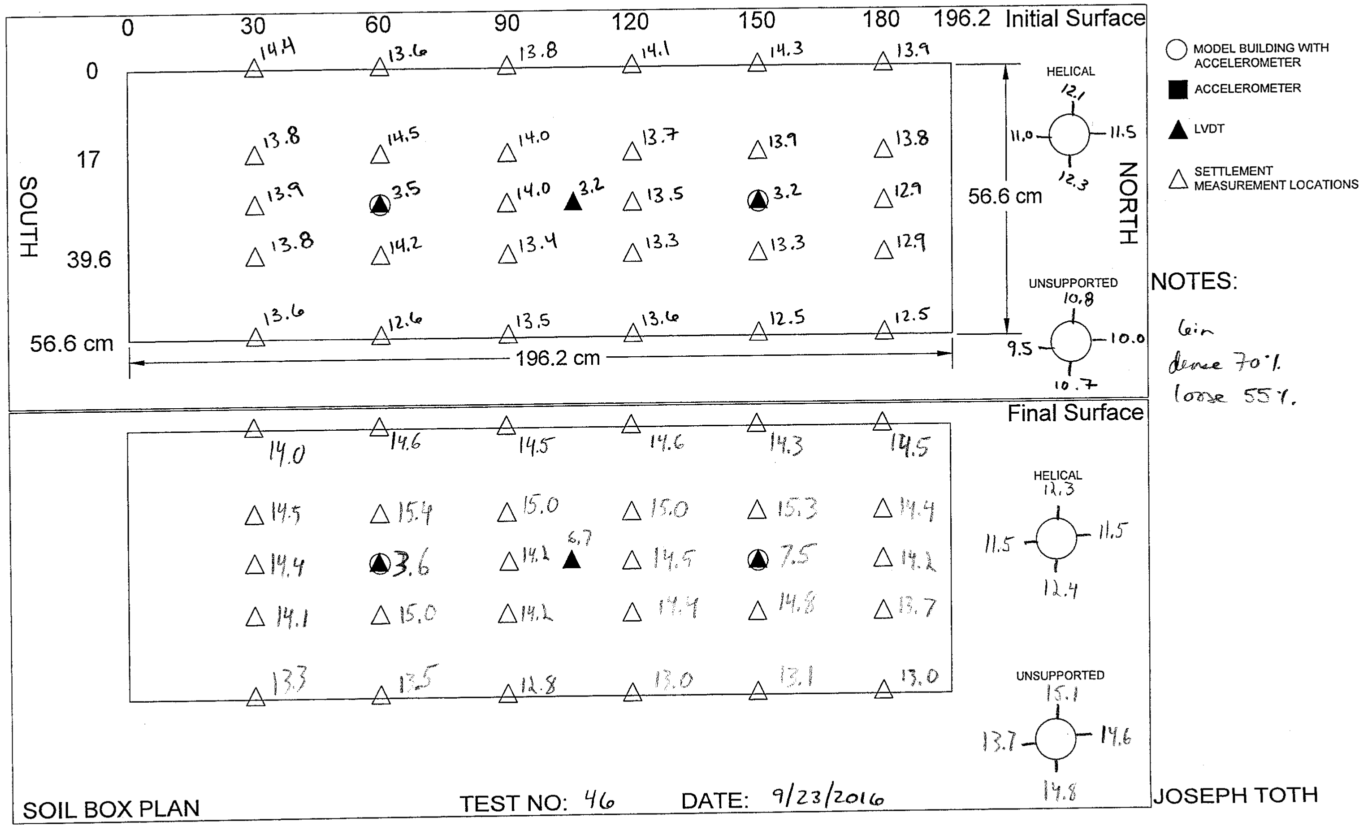

NOTES:

6in
dense 70%
loose 55%

SOIL BOX PLAN

TEST NO: 46

DATE: 9/23/2016

JOSEPH TOTH

Shakle Table Test # 47
Date: 9/26/2016

Joseph Toth

		Dense Layer			Liquefiable Layer	
		Ws (lbs)	Ww (lbs)		Ws (lbs)	
	1	41.2	2.06 ✓	1	42.0	
	2	47.9	2.40 ✓	2	22.1	
	3	44.6	2.23 ✓	3	42.9	
	4	48.2	2.41 ✓	4	40.0	
	5	46.0	2.30 ✓	5	43.2	
	6	40.3	2.02 ✓	6	45.8	
	7	44.0	2.20 ✓	7	44.9	280.8
	8	46.2	2.31 ✓	8	63.5	
	9	43.1	2.16 ✓	9	58.8	
	10	39.4	1.97 ✓	10	55.4	
	11	45.6	2.28 ✓	11	58.6	
	12	44.8	2.24 ✓	12	62.9	580
574.5	13	43.2	2.16 ✓	13	60.2	
	14	42.8	2.14 ✓	14	62.8	
	15	43.2	2.16 ✓	15	60.5	
	16	46.9	2.35 ✓	16	59.5	
749.9	17	42.5	2.13 ✓	17	59.1	882.1
	18	35.1	1.76 ✓	18	59.2	
	19		0	19	55.6	
	20			20	62.1	
	21			21	59.6	
	22			22	58.1	
	23			23	64.2	
	24			24	0	
	25			25		
	26			26		
	27			27		
	28			28		
	29			29		
	30	785.0 lbs		30	1240.9 lbs	

NOTES:

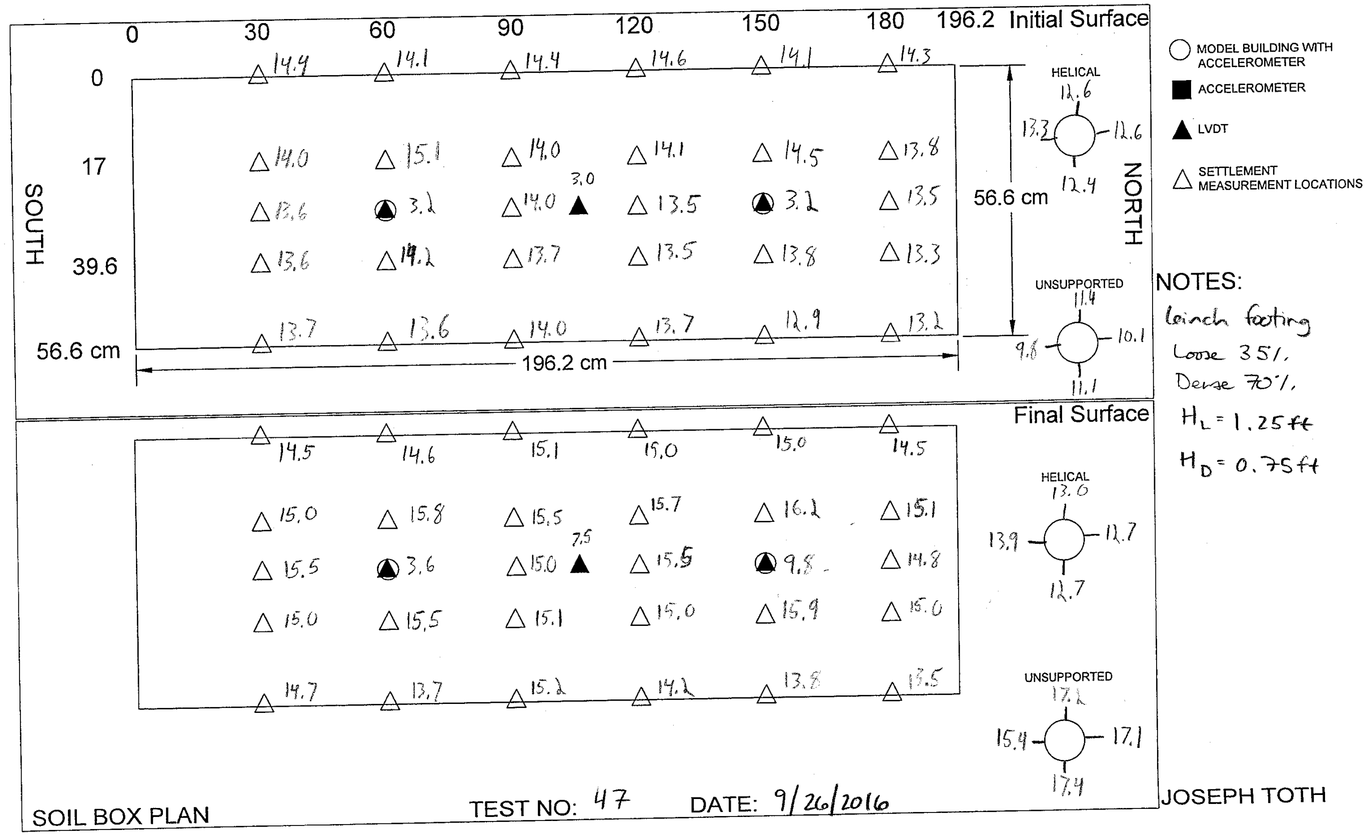

SOIL BOX PLAN

TEST NO: 47

DATE: 9/26/2016

NOTES:

6inch footing

Loose 35%

Dense 70%

$H_L = 1.25 ft$

$H_D = 0.75 ft$

JOSEPH TOTH

Shakle Table Test # 48

Date: 9/30/2016

Joseph Toth

Dense Layer

		Ws (lbs)	Ww (lbs)
	1	31.0	1.55
	2	38.2	1.91
	3	41.0	2.05
	4	42.9	2.15
	5	17.3	0.87
	6	26.5	1.33
	7	42.1	2.11
	8	39.0	1.95
	9	41.6	2.08
	10	37.7	1.89
	11	42.6	2.13
441.2 –	12	41.3	2.07
	13	45.3	2.27
	14	36.8	1.84
	15		
	16		
	17		
	18		
	19		
	20		
	21		
	22		
	23		
	24		
	25		
	26		
	27		
	28		
	29		
	30	523.3 lbs	

Liquefiable Layer

	Ws (lbs)	
1	41.6	
2	37.8	
3	38.4	
4	39.8	
5	38.4	
6	37.9	
7	37.8	
8	42.4	
9	36.1	
10	43.0	
11	41.1	
12	40.6	
13	40.9	
14	38.6	
15	41.2	– 595.6
16	59.7	
17	64.2	*
18	58.8	
19	62.3	
20	62.7	
21	61.2	
22	59.7	
23	59.6	
24	61.8	
25	61.9	– 1207.5
26	56.6	
27	61.7	
28	63.5	
29	61.9	– 1451.2
30	37.8 lbs	

NOTES: 1489.0 lbs

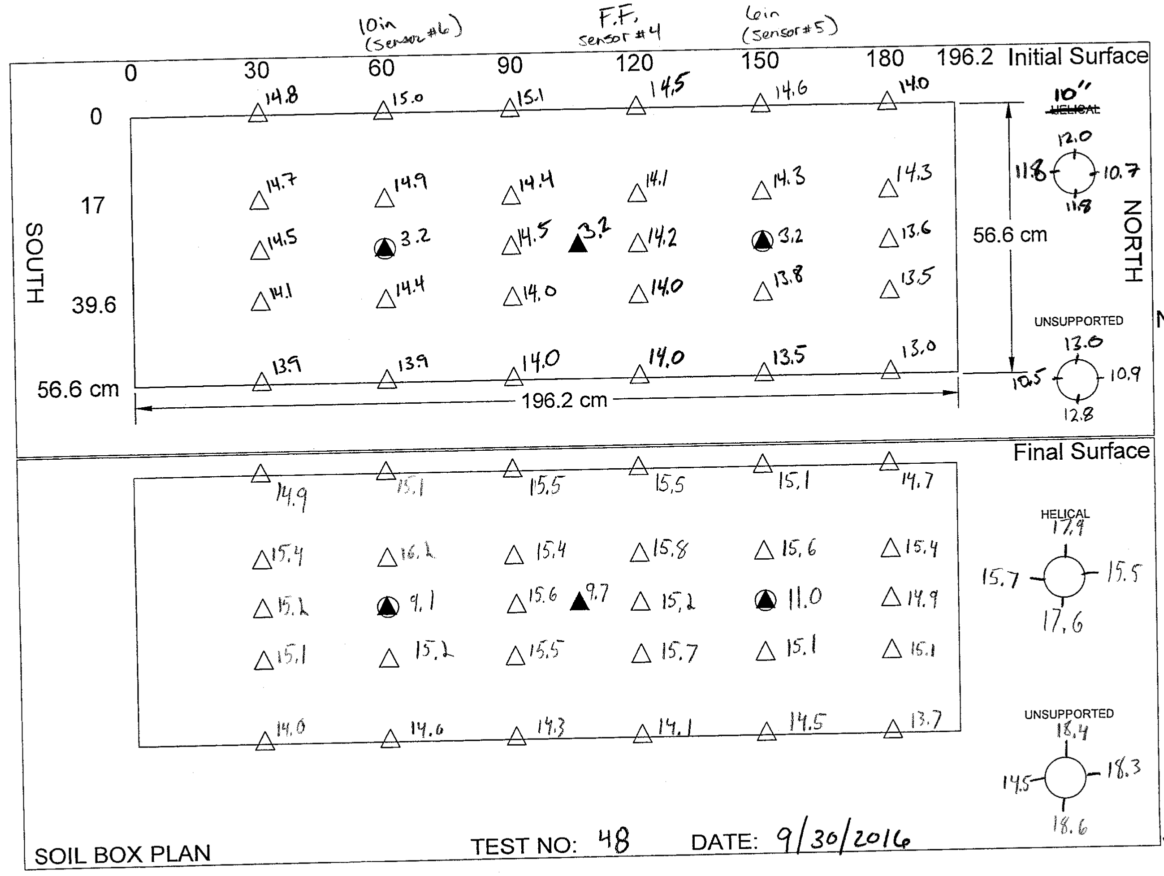

SOIL BOX PLAN TEST NO: 48 DATE: 9/30/2016

○ MODEL BUILDING WITH ACCELEROMETER
■ ACCELEROMETER
▲ LVDT
△ SETTLEMENT MEASUREMENT LOCATIONS

NOTES:
Unsupp. No helices
6in footing & 10in feet
H_L = 1.5 (35%)
H_D = 0.5 (70%)
no initial line of profile

rotational failure

JOSEPH TOTH

Joseph Toth

Shakle Table Test # 49

Date:

Dense Layer

	Ws (lbs)	Ww (lbs)
1	36.2	1.81
2	24.3	1.22
3	37.1	1.86
4	36.0	1.80
5	39.5	1.98
6	42.6	2.13
7	41.0	2.05
8	39.7	1.99
9	39.7	1.99
10	12.8	0.64
11	0	
12		
13		
14		
15		
16		
17		
18		
19		
20		
21		
22		
23		
24		
25		
26		
27		
28		
29		
30	348.9 lbs	

Liquefiable Layer

	Ws (lbs)		
1	18.7	41.0	
2	41.8	45.0	
3	44.7	40.5	
4	41.5	44.2	
5	40.1	37.7	
6	42.4	40.9	
7	40.6	45.4	
8	45.3	39.1	
9	35.4	40.1	724.4
10	58.1		
11	57.7		
12	60.0		
13	58.7		
14	59.3		1018.2
15	63.7		
16	65.7		
17	60.8		
18	63.9		
19	61.7		1334.0
20	59.1		
21	59.0		
22	63.2		
23	60.7		
24	61.6		1637.6
25	17.3		
26	0		
27			
28			
29			
30	1654.9 lbs		

NOTES:

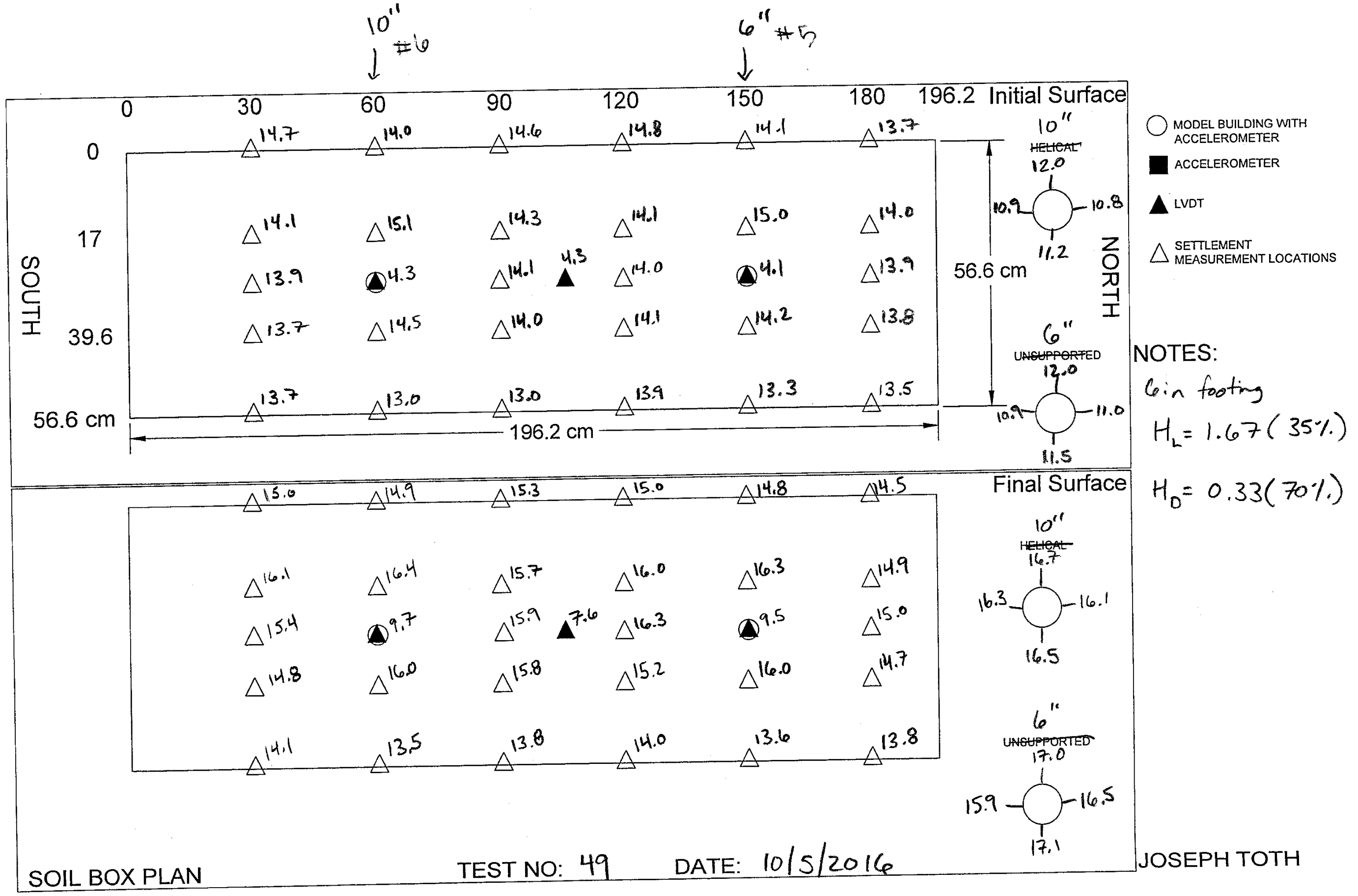

SOIL BOX PLAN

TEST NO: 49 DATE: 10/5/2016

JOSEPH TOTH

NOTES:

6 in footing

$H_L = 1.67$ (35%)

$H_D = 0.33$ (70%)

Shakle Table Test # 50

Date: 10/13/2016

Joseph Toth

		Dense Layer		Liquefiable Layer	
		Ws (lbs)	Ww (lbs)	Ws (lbs)	
	1	42.9	2.15	64.1	
	2	38.5	1.93	60.2	
	3	37.3	1.87	62.6	
	4	42.2	2.11	60.3	
	5	34.8	1.74	60.2	- 307.4
	6	45.4	2.27	62.0	
	7	40.4	2.02	62.1	
	8	45.7	2.29	61.3	
	9	40.5	2.03	60.2	
	10	42.6	2.13	61.3	614.3
	11	39.0	1.95	61.9	
	12	41.9	2.10	60.7	
	13	36.4	1.82	62.0	
	14	43.8	2.19	53.7	
	15	37.4	1.87	64.5	917.1
	16	45.3	2.27	60.5	
	17	39.2	1.96	15.1	
	18	37.6	1.88	0	
	19	37.7	1.89		
811.0	20	42.4	2.12		
	21	40.6	2.03		
	22	38.6	1.93		
	23	42.9	2.15		
	24	33.3	1.67		
1006.4	25	40.0	2		
	26	35.5	1.78		
	27	4.7	0.24		
	28	0			
	29				
	30	1046.6 lbs		992.7	

NOTES:

Dr = 35 & 70%. 12in & 12in layer Thickness

10 in footing (sensor #6) 6in footing (sensor #5)

2 second shaking duration

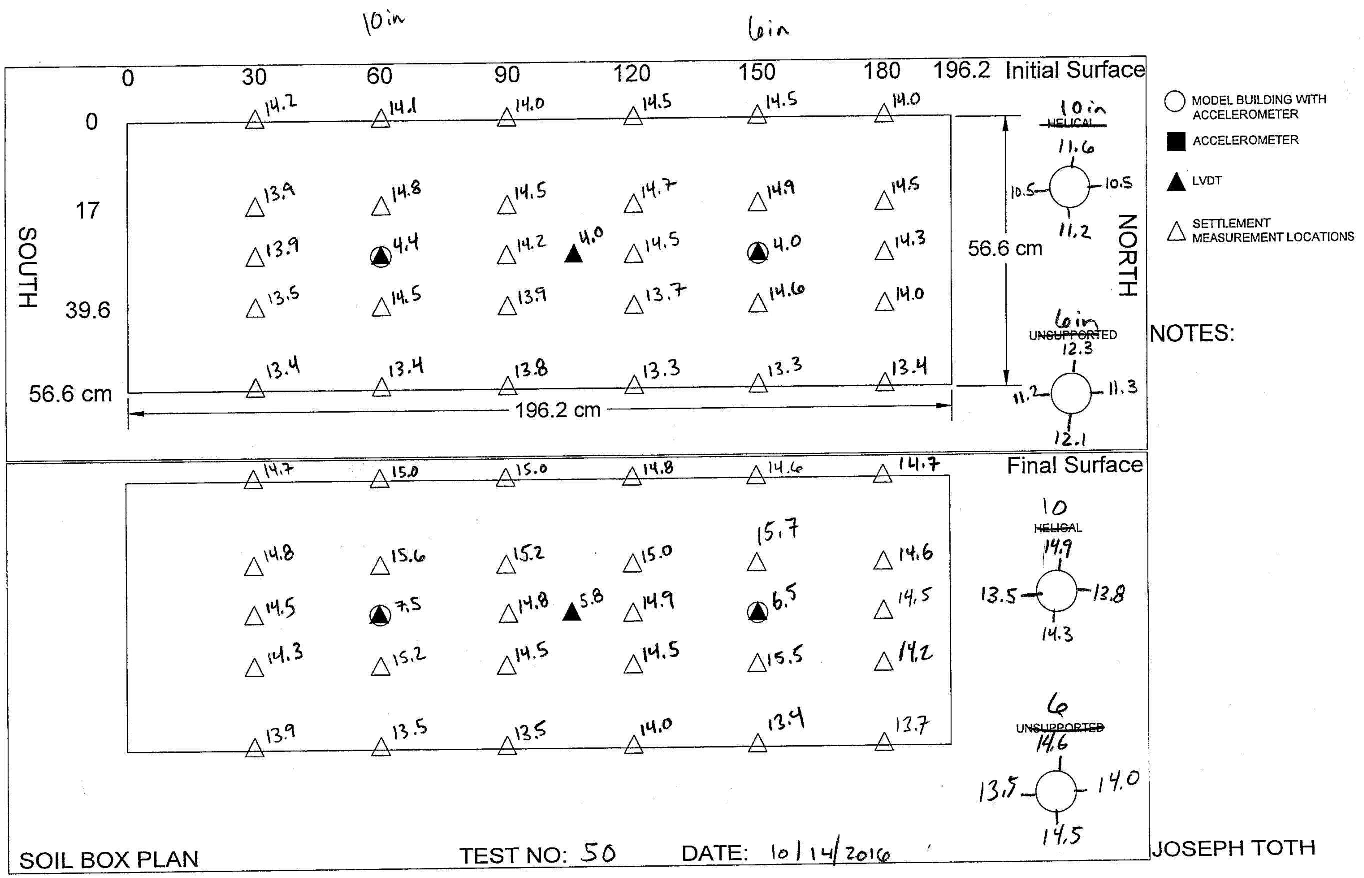
10in
6in
0
30
60
90
120
150
180
196.2
Initial Surface
0
17
39.6
56.6 cm
SOUTH
NORTH
14.2
14.1
14.0
14.5
14.5
14.0
13.9
14.8
14.5
14.7
14.9
14.5
13.9
4.4
14.2
4.0
14.5
4.0
14.3
13.5
14.5
13.9
13.7
14.6
14.0
13.4
13.4
13.8
13.3
13.3
13.4
196.2 cm
56.6 cm
10 in
~~HELICAL~~
11.6
10.5
10.5
11.2
6in
~~UNSUPPORTED~~
12.3
11.2
11.3
12.1
Final Surface
14.7
15.0
15.0
14.8
14.6
14.7
14.8
15.6
15.2
15.0
15.7
14.6
14.5
7.5
14.8
5.8
14.9
6.5
14.5
14.3
15.2
14.5
14.5
15.5
14.2
13.9
13.5
13.5
14.0
13.9
13.7
10
~~HELICAL~~
14.9
13.5
13.8
14.3
6
~~UNSUPPORTED~~
14.6
13.5
14.0
14.5
○ MODEL BUILDING WITH ACCELEROMETER
■ ACCELEROMETER
▲ LVDT
△ SETTLEMENT MEASUREMENT LOCATIONS
NOTES:
SOIL BOX PLAN
TEST NO: 50
DATE: 10/14/2016
JOSEPH TOTH

Joseph Toth

Shakle Table Test # 51

Date: 10/21/2016

Dense Layer

	Ws (lbs)	Ww (lbs)
1	41.8	2.09
2	39.5	1.98
3	42.6	2.13
4	36.7	1.84
5	38.5	1.93
6	38.6	1.93
7	39.5	1.98
8	45.4	2.27
9	37.6	1.88
10	42.1	2.11
11	40.1	2.01
12	42.5	2.13
13	39.7	1.99
14	43.5	2.18
15	43.4	2.17
16	42.7	2.14
17	39.8	1.99
18	43.8	2.19
19	43.3	2.17
20	43.7	2.19
21	40.2	2.01
22	45.1	2.25
23	44.3	2.22
24	40.6	2.03
25	43.0	2.15
26	8.7	0.44
27	0	
28		
29		
30	1046.6 lbs	

Liquefiable Layer

	Ws (lbs)	
1	38.2	
2	44.5	
3	39.2	
4	38.9	
5	20.7	
6	64.1	
7	60.6	
8	57.7	
9	63.1	
10	57.5	– 484.5
11	62.5	
12	62.2	
13	63.5	
14	57.3	
15	59.4	– 789.4
16	60.2	
17	64.0	
18	57.1	– 970.7
19	22.0	
20	0	
21		
22		
23		
24		
25		
26		
27		
28		
29		
30	992.7 lbs	

NOTES:

HL = 1 ft (35%) HD = 1 ft (70%)

10in unsupp footing (sensor #6)

6in " " (sensor #5)

4 sec shaking duration

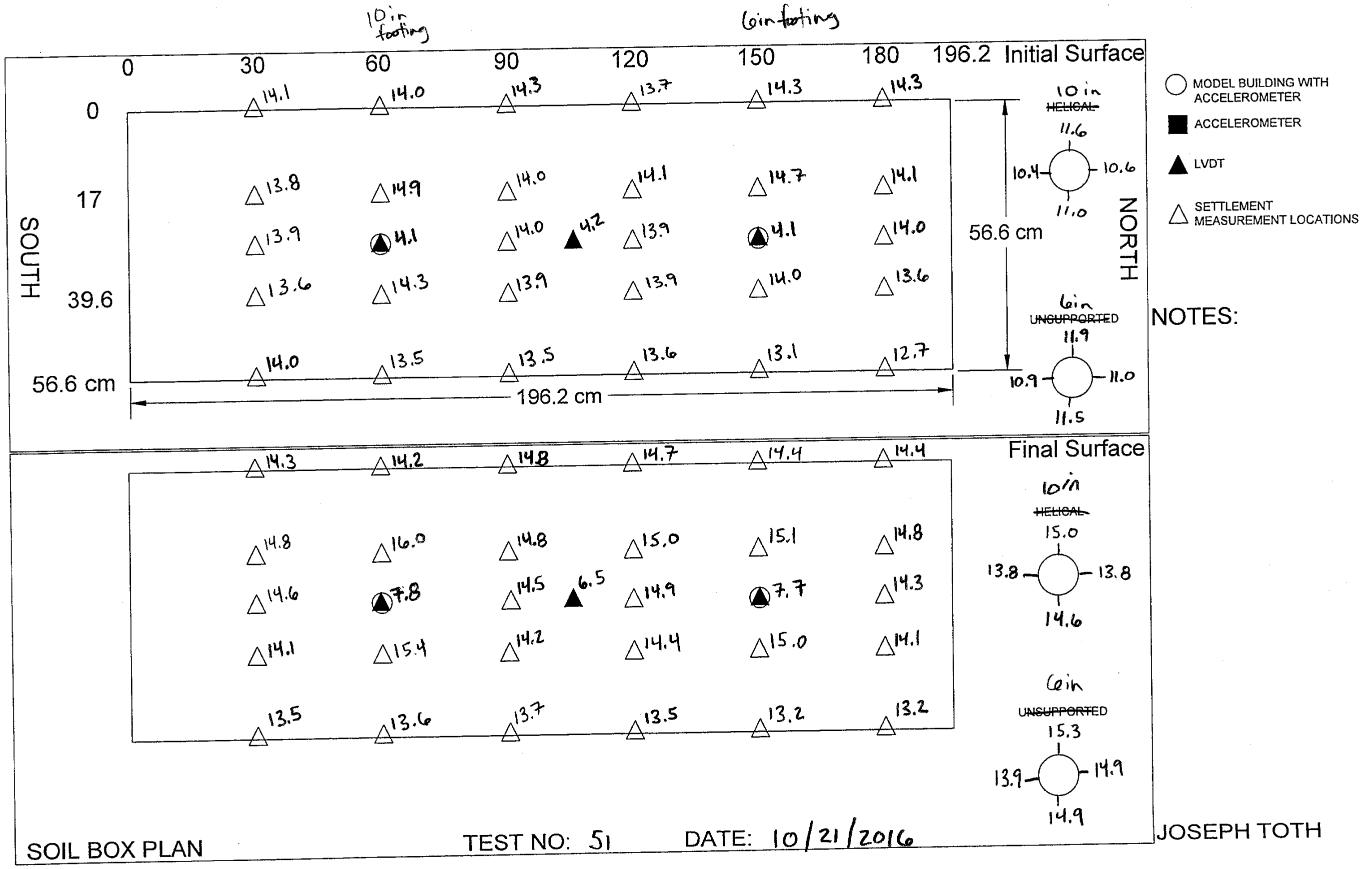

SOIL BOX PLAN

TEST NO: 51

DATE: 10/21/2016

JOSEPH TOTH

Shakle Table Test # 52 Joseph Toth

Date: 10/24/2016

$r_u = \frac{\sigma_u}{\sigma_v'}$

	Dense Layer			Liquefiable Layer	
	Ws (lbs)	Ww (lbs)		Ws (lbs)	
1	28.7	1.44	1	61.2	
2	40.2	2.01	2	63.5	
3	49.9	2.50	3	64.1	
4	42.7	2.14	4	61.9	
5	42.7	2.14	5	64.0	– 314.7
6	40.6	2.03	6	62.0	
7	46.5	2.33	7	62.4	
8	42.4	2.12	8	61.8	
9	41.2	2.06	9	64.3	
10	45.3	2.27	10	64.3	— 629.5
11	43.6	2.18	11	64.3	
12	42.7	2.14	12	63.8	
13	45.7	2.29	13	65.1	
14	42.7	2.14	14	62.5	
15	39.6	1.98	15	63.5	— 948.7
16	46.7	2.34	16	44.0	
17	44.8	2.24	17	0	
18	44.9	2.25	18		
19	43.3	2.17	19		
20	40.7	2.04	20		
21	43.3	2.17	21		
22	42.1	2.11	22		
23	41.1	2.06	23		
24	38.3	1.92	24		
25	26.9	1.35	25		
26		0	26		
27			27		
28			28		
29			29		
30	1046.6 lbs		30	992.7 lbs	

NOTES:

HL = 1ft (35%) HD = 1ft (70%)

10in unsupp footing (sensor #6)

6in " " (sensor #5)

8 sec shaking duration

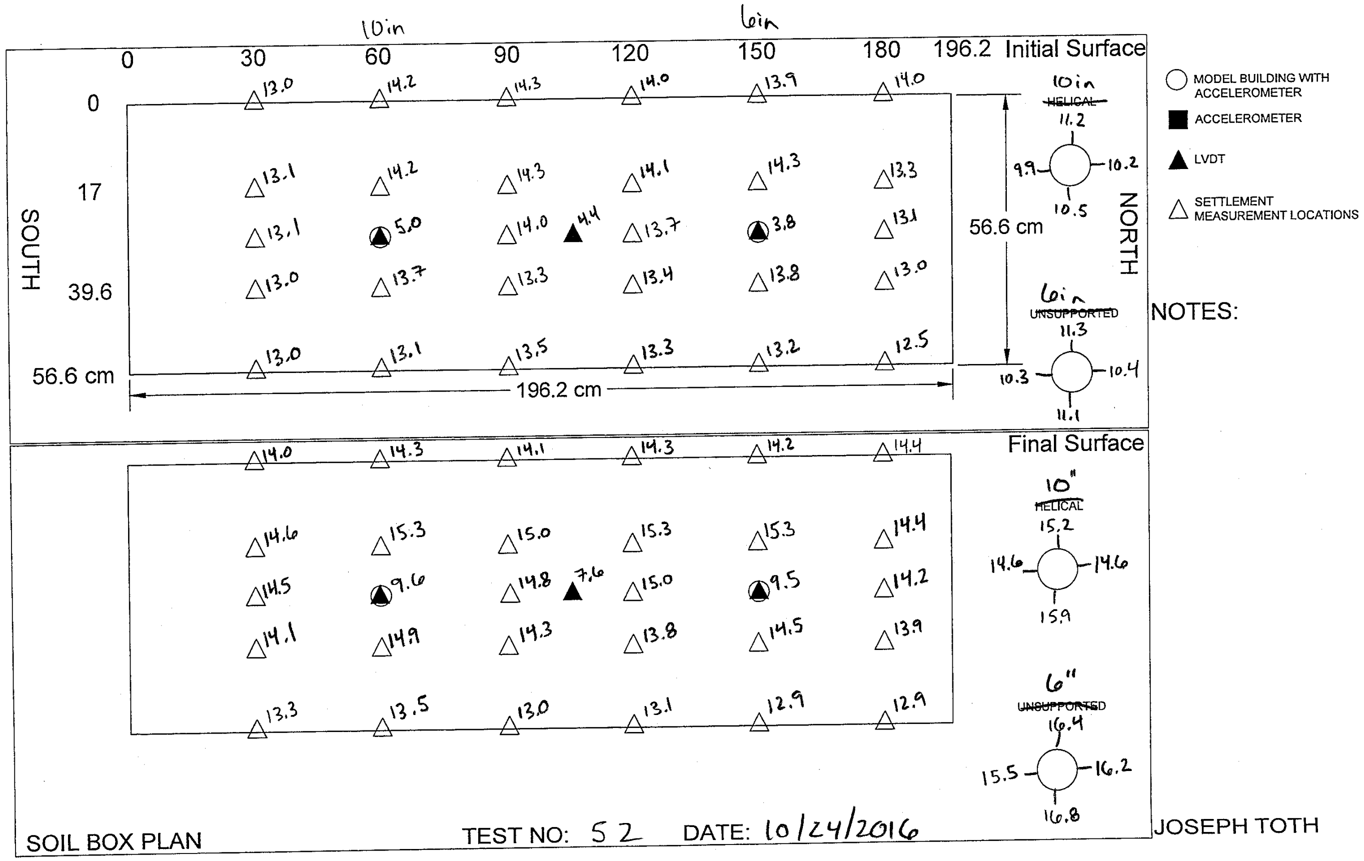

NOTES:

SOIL BOX PLAN

TEST NO: 52

DATE: 10/24/2016

JOSEPH TOTH

Shakle Table Test # 53

Date: 10/31/2016

Joseph Toth

		Dense Layer			Liquefiable Layer	
		Ws (lbs)	Ww (lbs)		Ws (lbs)	
	1	41.0	2.05	1	58.0	
	2	42.0	2.10	2	60.2	
	3	48.0	2.40	3	56.2	
	4	43.0	2.15	4	56.7	
	5	45.1	2.26	5	58.8	289.9
	6	40.5	2.03	6	56.9	
	7	38.9	1.95	7	55.4	402.2
	8	42.7	2.14	8	55.3	
	9	43.1	2.16	9	53.2	
	10	43.6	2.18	10	52.4	
	11	42.2	2.11	11	50.0	
	12	41.9	2.10	12	57.3	
	13	44.1	2.21	13	54.7	725.1
	14	38.3	1.92	14	52.4	
	15	40.1	2.01	15	51.2	
	16	41.2	2.06	16	56.7	
	17	41.7	2.09	17	58.6	944.0
	18	40.5	2.03	18	48.7	
	19	39.7	1.99	19		
	20	44.9	2.25	20		
	21	41.9	2.10	21		
	22	42.4	2.12	22		
	23	44.3	2.22	23		
1010.8	24	39.7	1.99	24		
	25	35.8	1.79	25		
	26			26		
	27			27		
	28			28		
	29	1046.6		29	992.7 lbs	
	30			30		

NOTES:

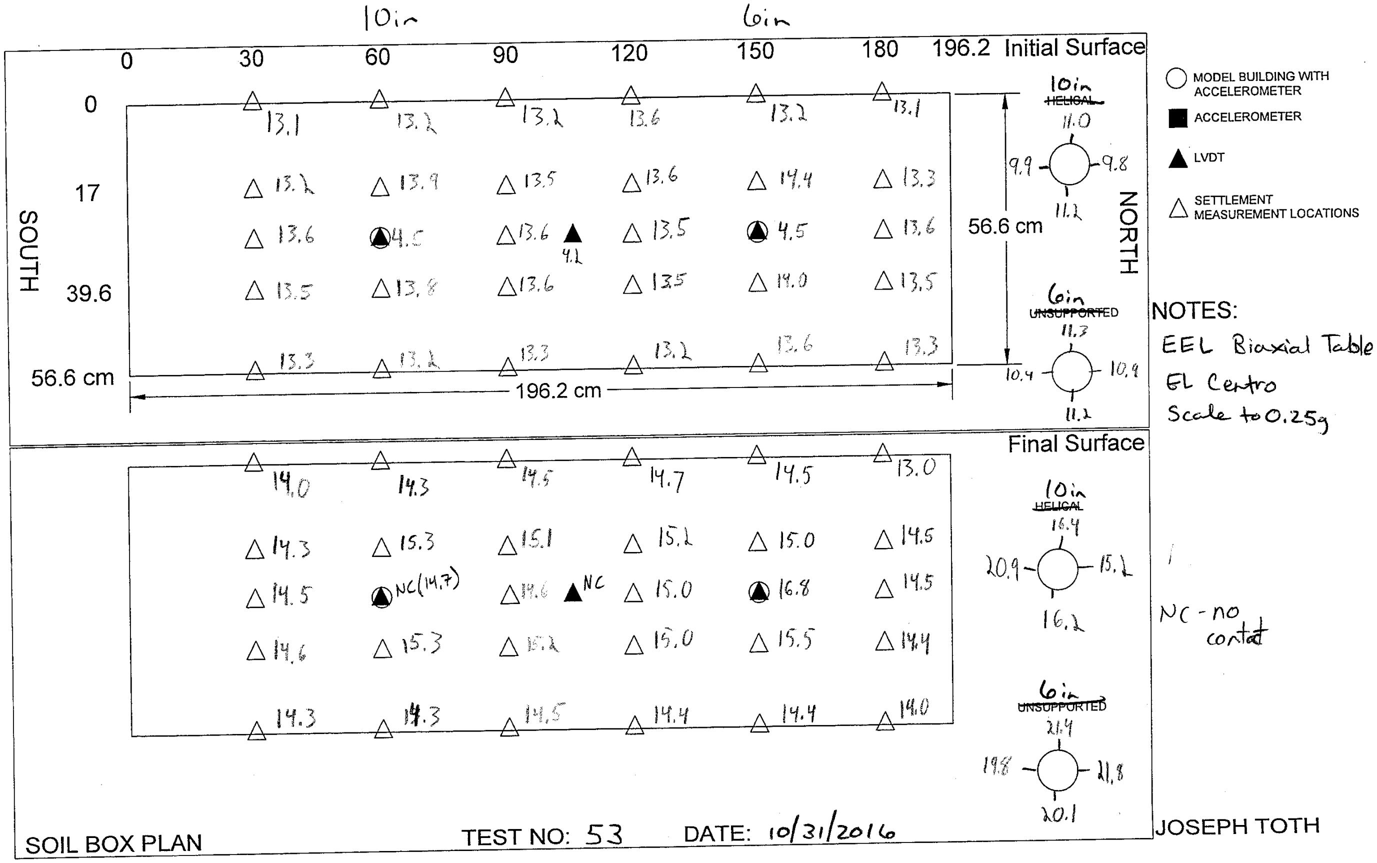

NOTES:
EEL Biaxial Table
EL Centro
Scale to 0.25g

NC - no contact

SOIL BOX PLAN

TEST NO: 53

DATE: 10/31/2016

JOSEPH TOTH